Fracture mechanics

ME 524

University of Tennessee Knoxville (UTK) /

University of Tennessee Space Institute (UTSI)

Reza Abedi

Disclaimer

- The content of this presentation are produced by R. Abedi and also taken from several sources, particularly from the fracture mechanics presentation by **Dr. Vinh Phu Nguyen** nvinhphu@gmail.com Monash University (formerly at University of Adelaide and Ton Duc Thang University)

Other sources

Books:

- T. L. Anderson, Fracture Mechanics: Fundamentals and Applications, 3rd Edition, CRC Press, USA, 2004
- S. Murakami, Continuum Damage Mechanics, Springer Netherlands, Dordrecht, 2012.
- L.B. Freund, Dynamic Fracture Mechanics, Cambridge University Press, 1998.
- B. Lawn, Fracture of Brittle Solids, Cambridge University Press, 1993.
- M.F. Kanninen and C.H. Popelar, Advanced Fracture Mechanics, Oxford Press, 1985.
- R.W. Hertzberg, Deformation & Fracture Mechanics of Engineering Materials. John Wiley & Sons, 2012.

Course notes:

- V.E. Saouma, Fracture Mechanics lecture notes, University of Colorado, Boulder.
- P.J.G. Schreurs, Fracture Mechanics lecture notes, Eindhoven University of Technology (2012).
- A.T. Zender, Fracture Mechanics lecture notes, Cornell University.
- L. Zhigilei, http://people.virginia.edu/~lz2n/mse209/index.html
  MSE 2090: Introduction to Materials Science Chapter 8, Failure

Outline

- Brief recall on mechanics of materials
  - stress/strain curves of metals, concrete
- Introduction
- Linear Elastic Fracture Mechanics (LEFM)
  - Energy approach (Griffith, 1921, Orowan and Irwin 1948)
  - Stress intensity factors (Irwin, 1960s)
- LEFM with small crack tip plasticity
  - Irwin's model (1960) and strip yield model
  - Plastic zone size and shape
- Elastic-Plastic Fracture Mechanics
  - Crack tip opening displacement (CTOD), Wells 1963
  - J-integral (Rice, 1958)
- Dynamic Fracture Mechanics

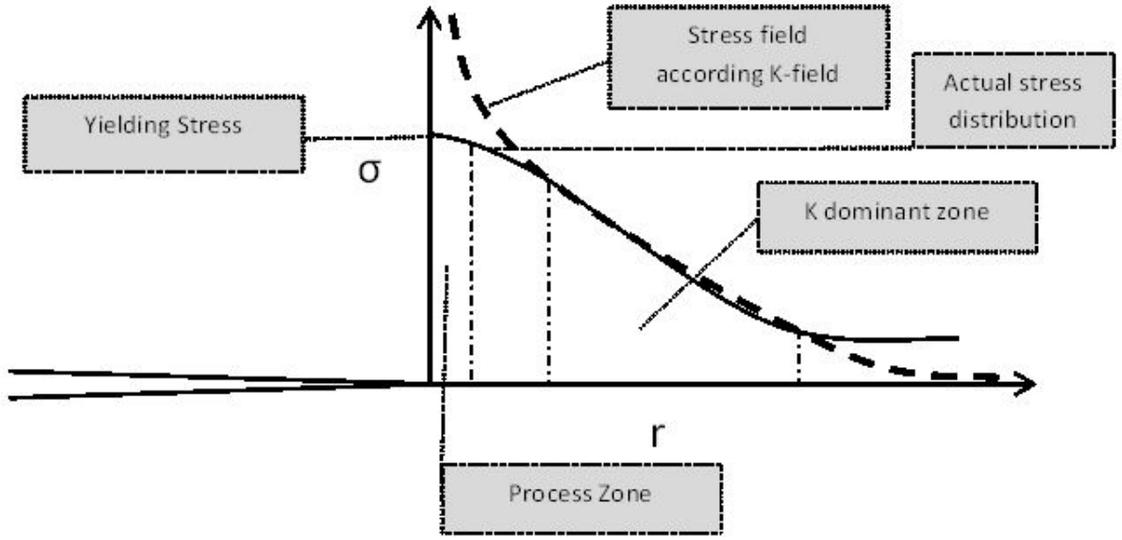

Source: Sheiba, Olson, UT Austin

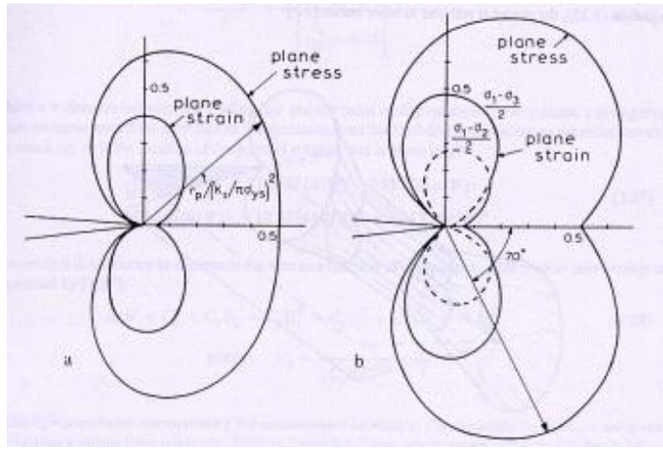

Source: Farkas, Virgina

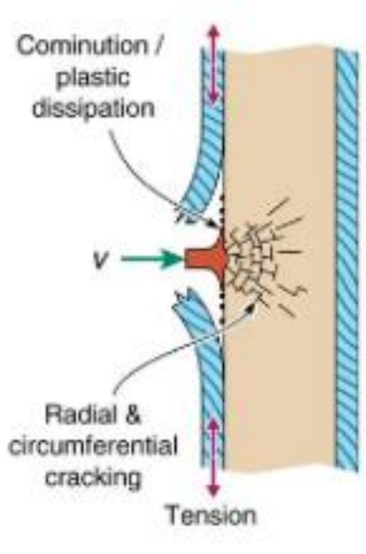

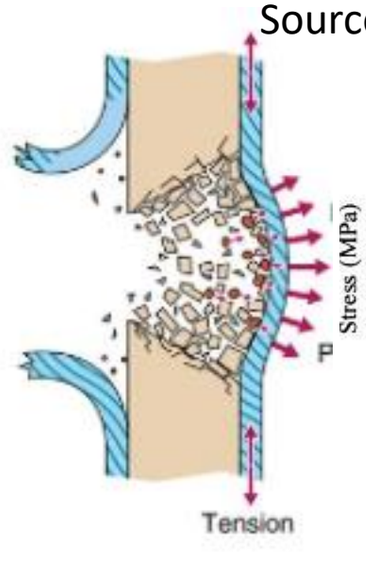

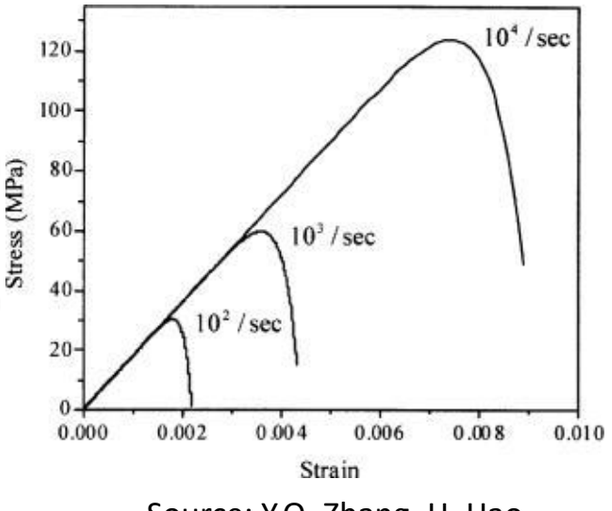

Source: Y.Q. Zhang, H. Hao, J. Appl Mech (2003)

Outline (cont.)

Fatigue
- Fatigue crack propagation & life prediction
- Paris law

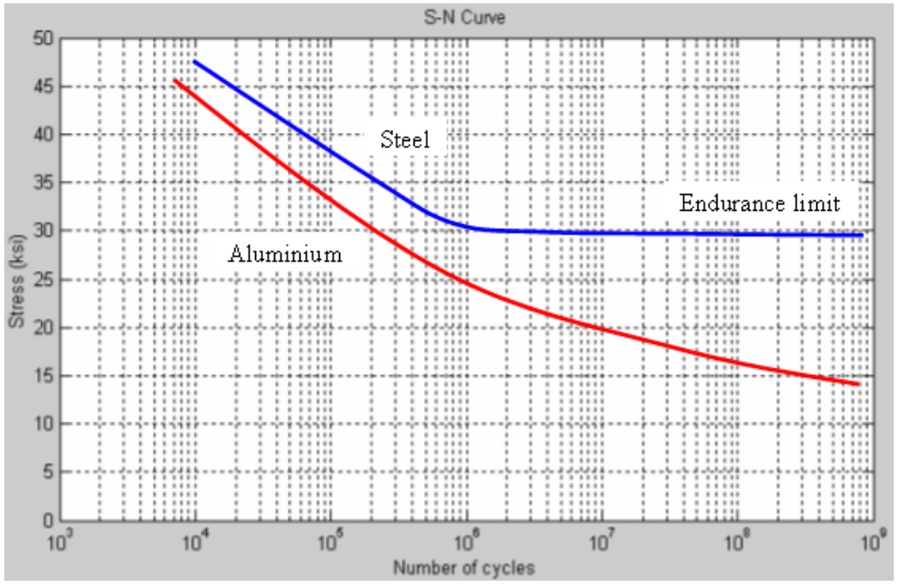

wikipedia

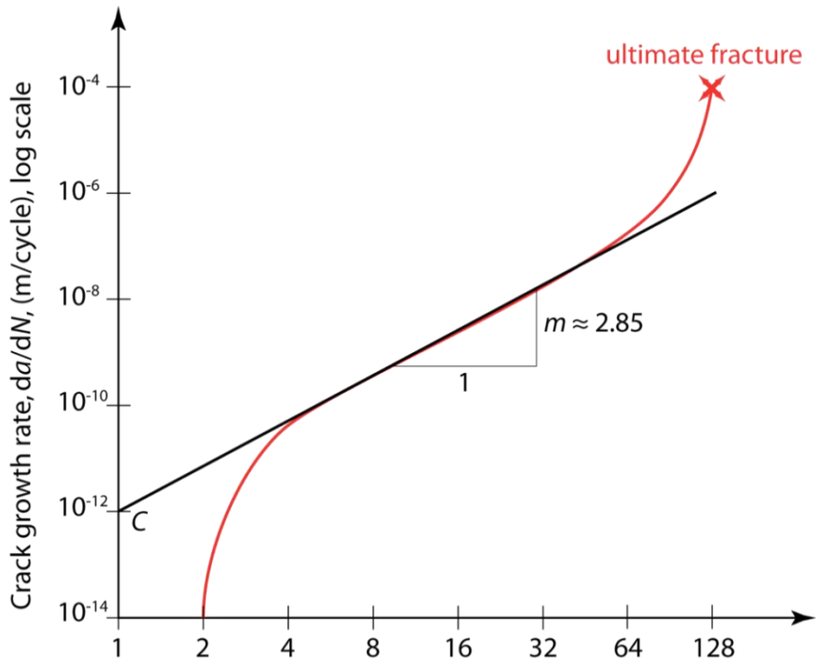

Ductile versus Brittle Fracture
- Stochastic fracture mechanics
- Microcracking and crack branching in brittle fracture

Brittle Fracture

quippy documentation (www.jrkermode.co.uk)

Ductile Fracture

DynamicFractureBifurcation PMMA
Murphy 2006

Outline (cont.)

- Computational fracture mechanics
  - FEM aspects:
    - Isoparametric singular elements
    - Calculation of LEFM/EPFM Integrals
    - Adaptive meshing, XFEM

- Cohesive crack model (Hillerborg, 1976)
- Continuum Damage Mechanics
  - size effect (Bazant)

Singular Element

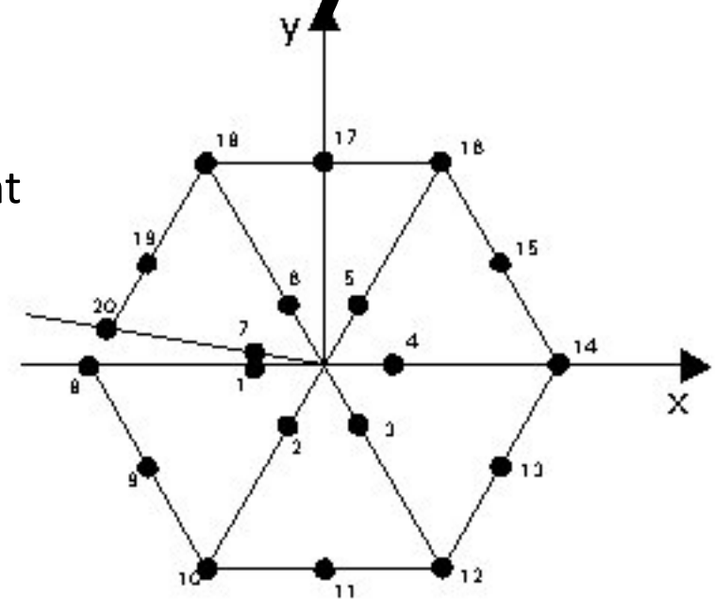

http://www.fgg.uni-lj.si/~/pmoze/ESDEP/master/toc.htm

Cracks in FEM

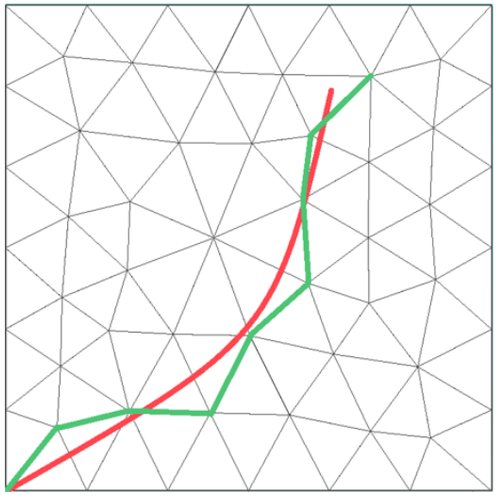

Adaptive mesh

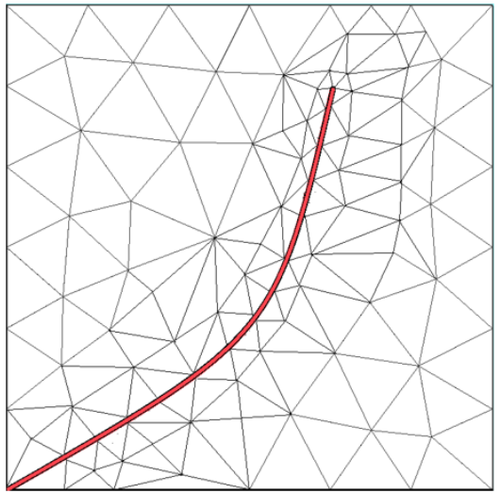

XFEM

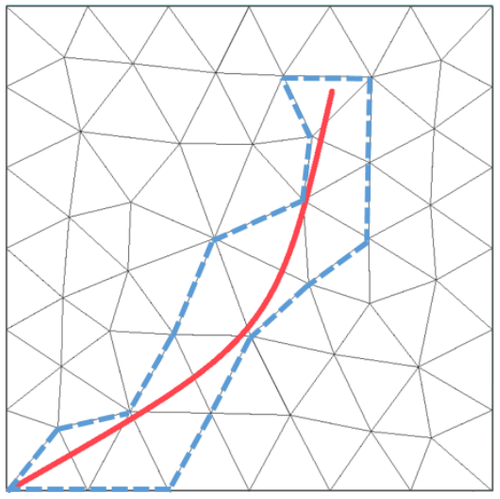

bulk damage

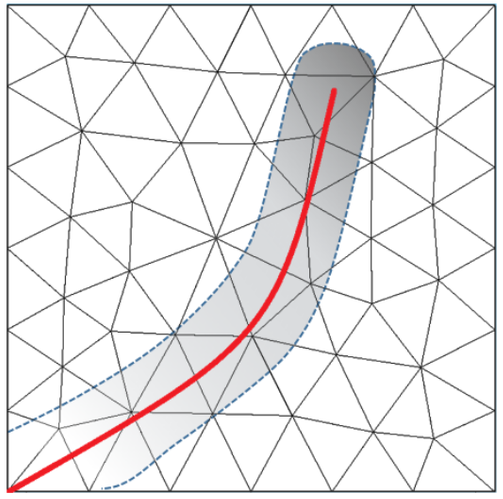

P. Clarke UTSI

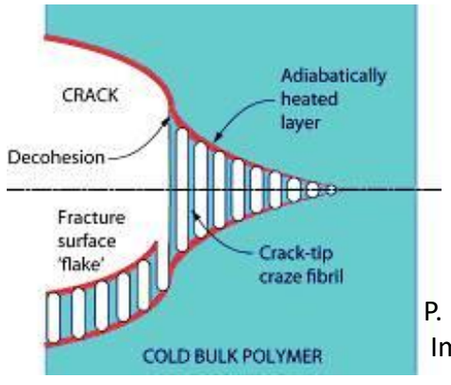

Cohesive Zone

P. Leevers
Imperical College

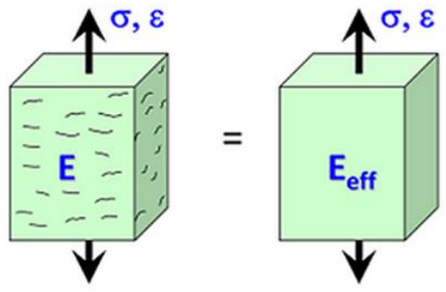

underwood.faculty.asu.edu

Introduction

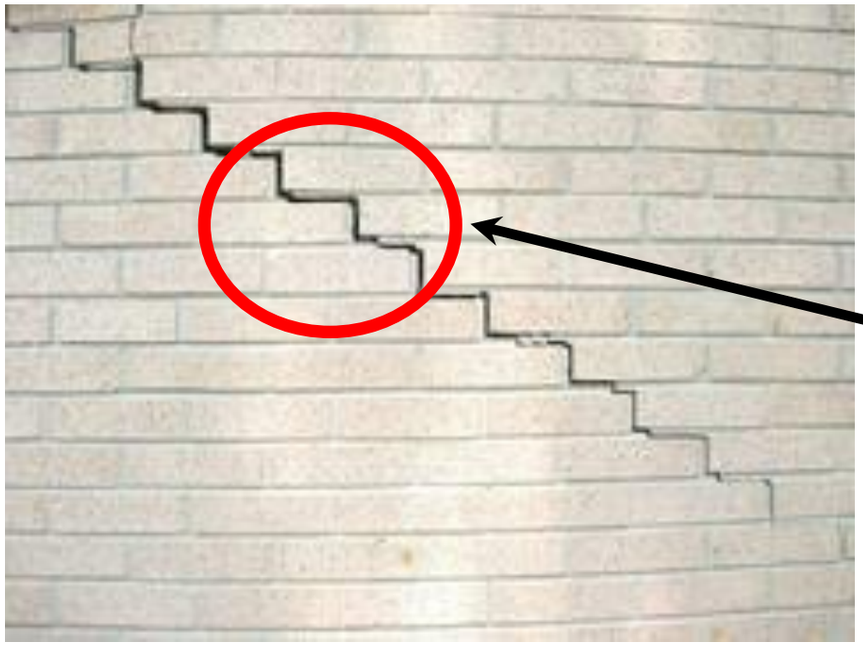

Cracks: ubiquitous !!!

Definitions

- Crack, Crack growth/propagation
- A **fracture** is the (local) separation of an object or material into two, or more, pieces under the action of stress.
- Fracture mechanics is the field of mechanics concerned with the study of the propagation of cracks in materials. It uses methods of analytical solid mechanics to calculate the driving force on a crack and those of experimental solid mechanics to characterize the material's resistance to fracture (Wiki).

Objectives of FM

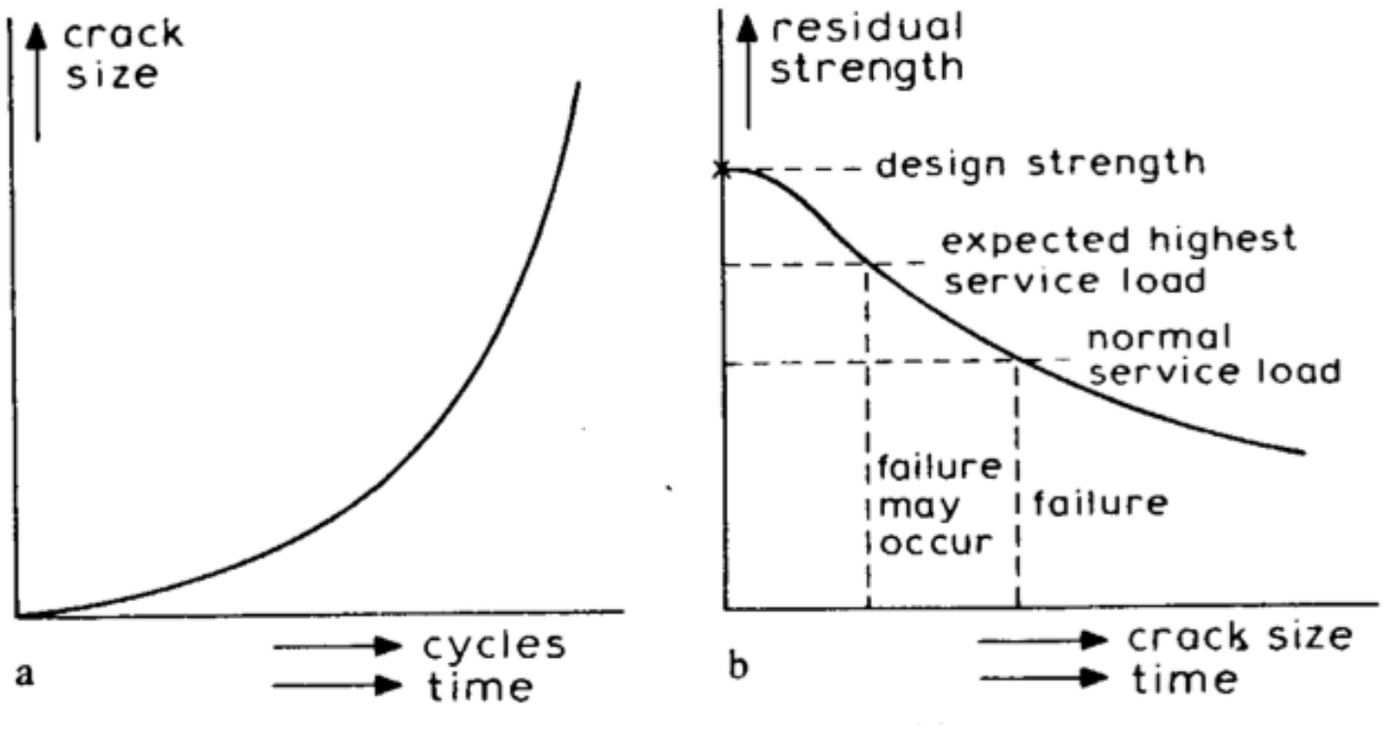

- What is the residual strength as a function of crack size?
- What is the critical crack size?
- How long does it take for a crack to grow from a certain initial size to the critical size?

Approaches to fracture

- Stress analysis
- Energy methods
- Computational fracture mechanics

covered in the course

- Micromechanisms of fracture (eg. atomic level)
- Experiments
- Applications of Fracture Mechanics

Design philosophies

- Safe life

  The component is considered to be free of defects after fabrication and is designed to remain defect-free during service and withstand the maximum static or dynamic working stresses for a certain period of time. If flaws, cracks, or similar damages are visited during service, the component should be discarded immediately.

- Damage tolerance

  The component is designed to withstand the maximum static or dynamic working stresses for a certain period of time even in presence of flaws, cracks, or similar damages of certain geometry and size.

New Failure analysis

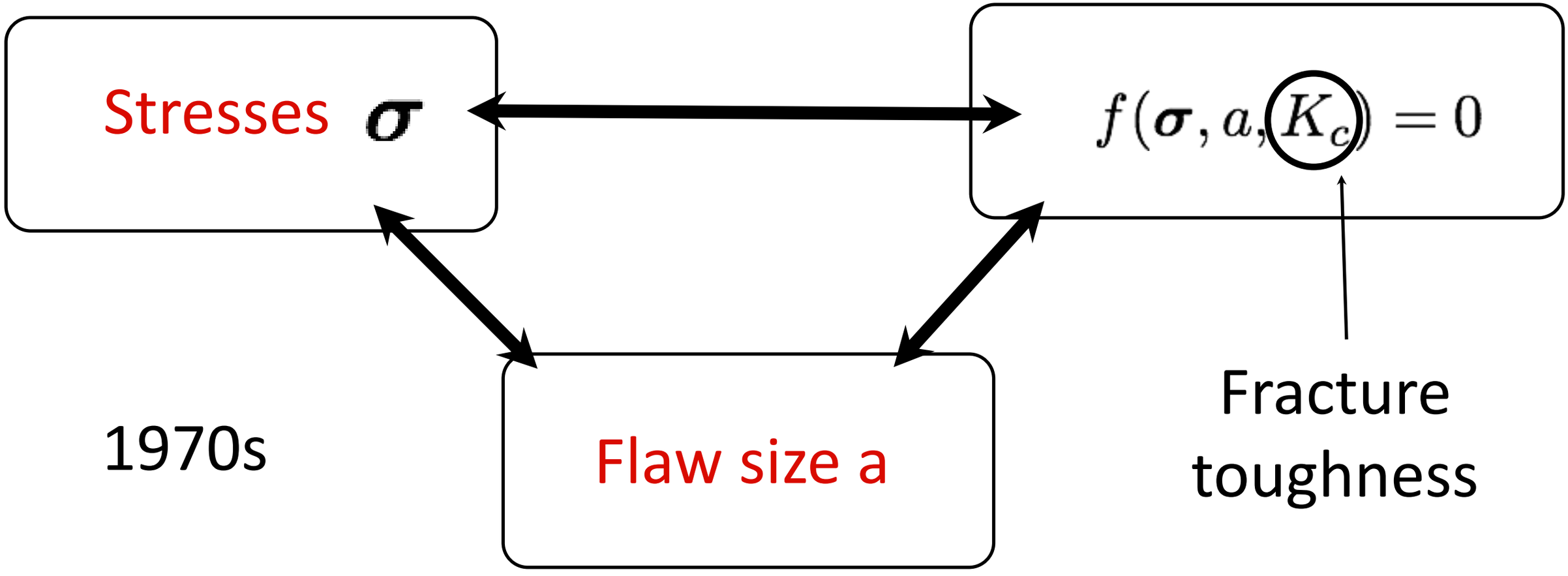

Fracture Mechanics (FM)

- FM plays a vital role in the design of every critical structural or machine component in which durability and reliability are important issues (aircraft components, nuclear pressure vessels, microelectronic devices).

- has also become a valuable tool for material scientists and engineers to guide their efforts in developing materials with improved mechanical properties.

1. Preliminaries
2. History

Indicial notation

a 3D vector

$$\mathbf{x} = \{x_1, x_2, x_3\}$$

$$||\mathbf{x}|| = \sqrt{x_1^2 + x_2^2 + x_3^2}$$

two times repeated index=sum,
summation/dummy index

$$\sigma_{xx}\epsilon_{xx} + \sigma_{xy}\epsilon_{xy} + \sigma_{yx}\epsilon_{yx} + \sigma_{yy}\epsilon_{yy}$$

$$\frac{\partial \sigma_x}{\partial x} + \frac{\partial \tau_{xy}}{\partial y} = 0, \quad \frac{\partial \sigma_y}{\partial y} + \frac{\partial \tau_{xy}}{\partial x} = 0$$

$$\sigma_{xx}n_x + \sigma_{xy}n_y = t_x$$

$$\sigma_{yx}n_x + \sigma_{yy}n_y = t_y$$

$$i = 1, 2, 3$$

$$||\mathbf{x}|| = \sqrt{x_i x_i}$$

$$||\mathbf{x}|| = \sqrt{x_k x_k}$$

$$\sigma_{ij}\epsilon_{ij}$$

$$\sigma_{ij,j} = 0$$

i: **free index** (appears precisely once in each side of an equation)

$$\sigma_{ij}n_j = t_i$$

$\boldsymbol{\sigma} : \boldsymbol{\epsilon}$ tensor notation

Engineering/matrix notation

$$\mathbf{x} = \begin{bmatrix} x_1 \\ x_2 \\ x_3 \end{bmatrix}$$

$$||\mathbf{x}|| = \mathbf{x}^{\mathrm{T}}\mathbf{x}$$

$$||\mathbf{x}|| = \sqrt{x_i x_i}$$

Voigt notation

$$\boldsymbol{\sigma} = \begin{bmatrix} \sigma_{xx} \\ \sigma_{yy} \\ \sigma_{xy} \end{bmatrix} \quad \boldsymbol{\epsilon} = \begin{bmatrix} \epsilon_{xx} \\ \epsilon_{yy} \\ 2\epsilon_{xy} \end{bmatrix}$$

$$\boldsymbol{\sigma}^{\mathrm{T}}\boldsymbol{\epsilon} = \sigma_{ij}\epsilon_{ij}$$

$$\sigma_{ij}\epsilon_{ij}$$

$$\boldsymbol{\sigma} = \begin{bmatrix} \sigma_{xx} & \sigma_{xy} \\ \sigma_{xy} & \sigma_{yy} \end{bmatrix}$$

$$\boldsymbol{\epsilon} = \begin{bmatrix} \epsilon_{xx} & \epsilon_{xy} \\ \epsilon_{xy} & \epsilon_{yy} \end{bmatrix}$$

Stress/strain curve

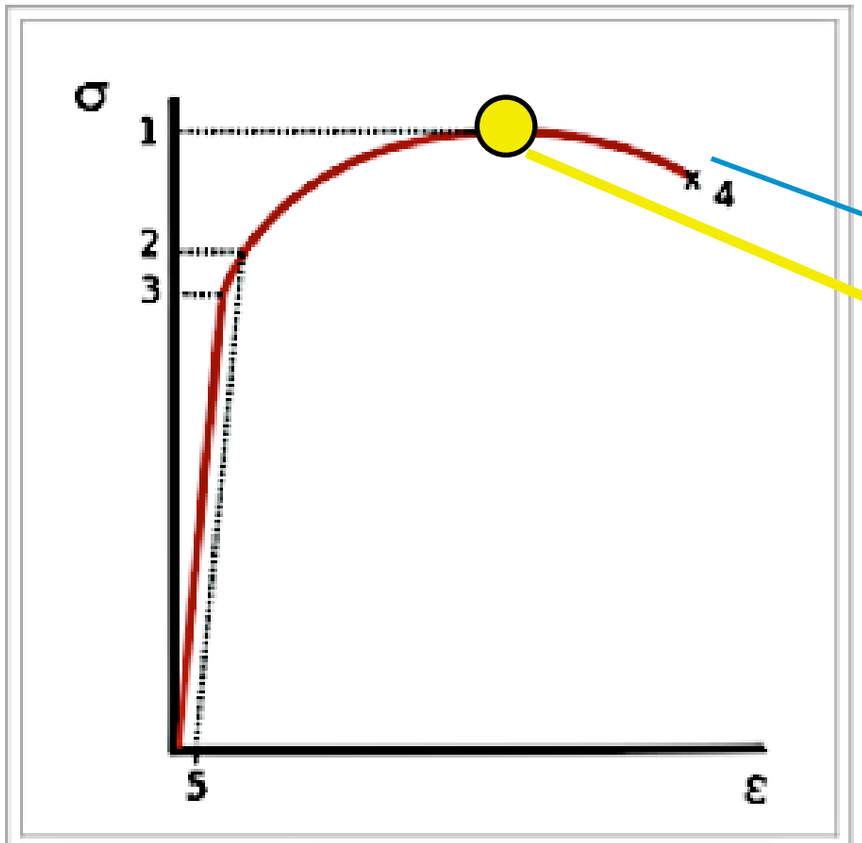

Stress vs. Strain curve typical of aluminum
1. Ultimate strength
2. Yield strength
3. Proportional limit stress
4. Fracture
5. Offset strain (typically 0.2%)

Wikipedia

fracture

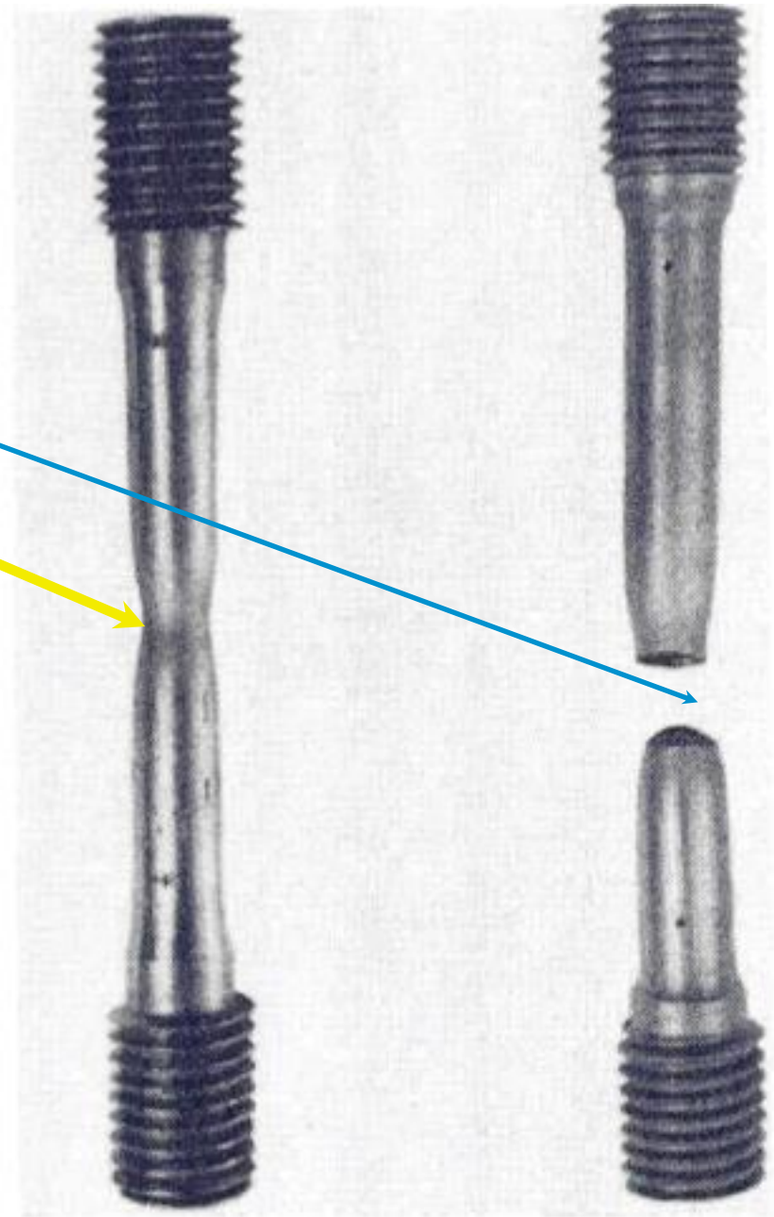

necking=decrease of cross-sectional area due to plastic deformation

1: ultimate tensile strength

Principal stresses

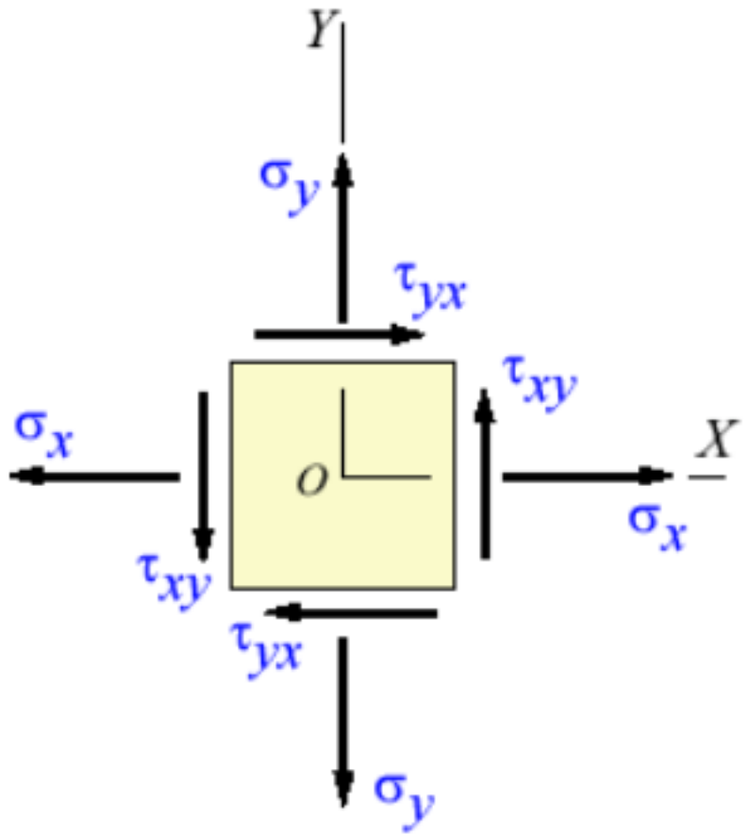

Stresses in given coordinate system

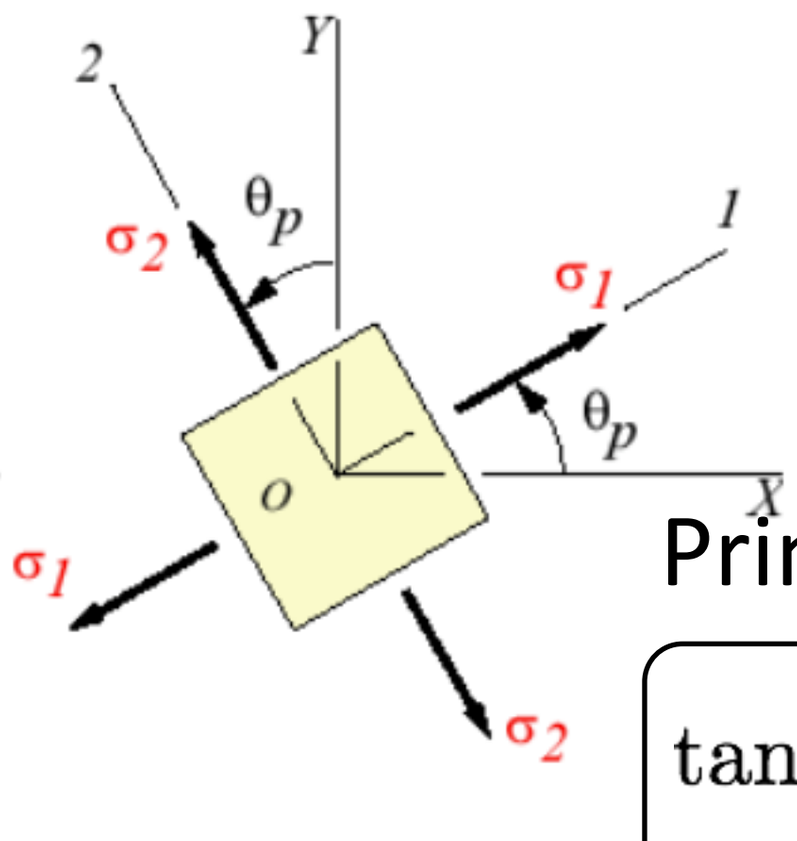

Principal stresses

Principal direction

$$\tan 2\theta_p = \frac{2\tau_{xy}}{\sigma_{xx} - \sigma_{yy}}$$

Principal stresses are those stresses that act on principal surface. Principal surface here means the surface where components of shear-stress is zero.

$$\sigma_1, \sigma_2 = \frac{\sigma_{xx} + \sigma_{yy}}{2} \pm \sqrt{\left(\frac{\sigma_{xx} - \sigma_{yy}}{2}\right)^2 + \tau_{xy}^2}$$

Material classification / Tensile test

Elastic

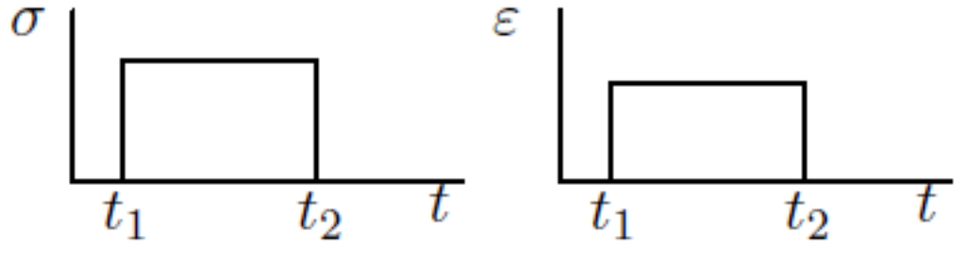

Visoelastic

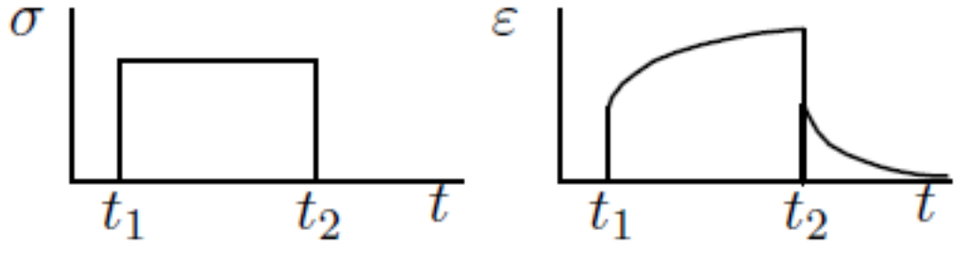

Elastic-Plastic

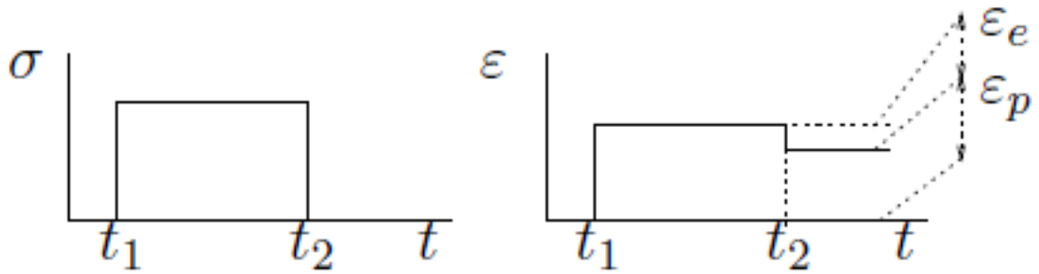

Visoplastic

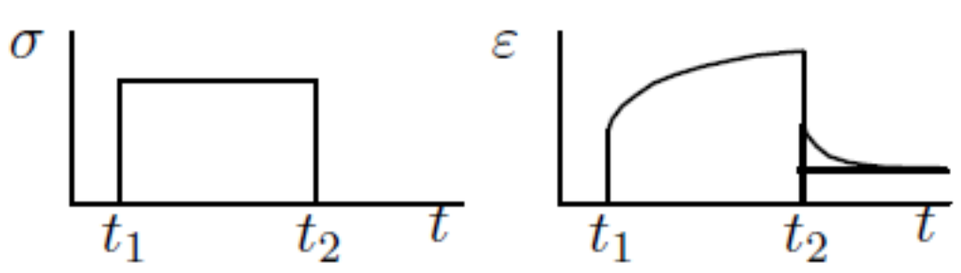

Strain energy density

Poisson's ratio

$$u = \frac{1}{2E}(\sigma_x^2 + \sigma_y^2 + \sigma_z^2) - \frac{\nu}{E}(\sigma_x\sigma_y + \sigma_y\sigma_z + \sigma_z\sigma_x) + \frac{1}{2\mu}(\tau_{xy}^2 + \tau_{yz}^2 + \tau_{zx}^2)$$

Plane problems

$$\mu = \frac{E}{2(1+\nu)}$$ shear modulus

$$u = \frac{1}{4\mu}\left[\frac{\kappa+1}{4}(\sigma_x^2 + \sigma_y^2) - 2(\sigma_x\sigma_y - \tau_{xy}^2)\right]$$

Kolosov coefficient

$$\kappa = \begin{cases} 3 - 4\nu & \text{plane strain} \\ \dfrac{3-\nu}{1+\nu} & \text{plane stress} \end{cases}$$

3.1 Fracture modes
3.2 Ductile fracture

Fracture

Fracture: separation of a body into pieces due to stress, at temperatures below the melting point.

Steps in fracture:

- crack formation
- crack propagation

Depending on the ability of material to undergo plastic deformation before the fracture two fracture modes can be defined - **ductile or brittle**

Lecture source:

Prof. Leonid Zhigilei, http://people.virginia.edu/~lz2n/mse209/index.html

- **Ductile fracture** - most metals (not too cold):
  - ➢ Extensive plastic deformation ahead of crack
  - ➢ Crack is "stable": resists further extension unless applied stress is increased
- **Brittle fracture** - ceramics, ice, cold metals:
  - ➢ Relatively little plastic deformation
  - ➢ Crack is "unstable": propagates rapidly without increase in applied stress

Ductile fracture is preferred in most applications

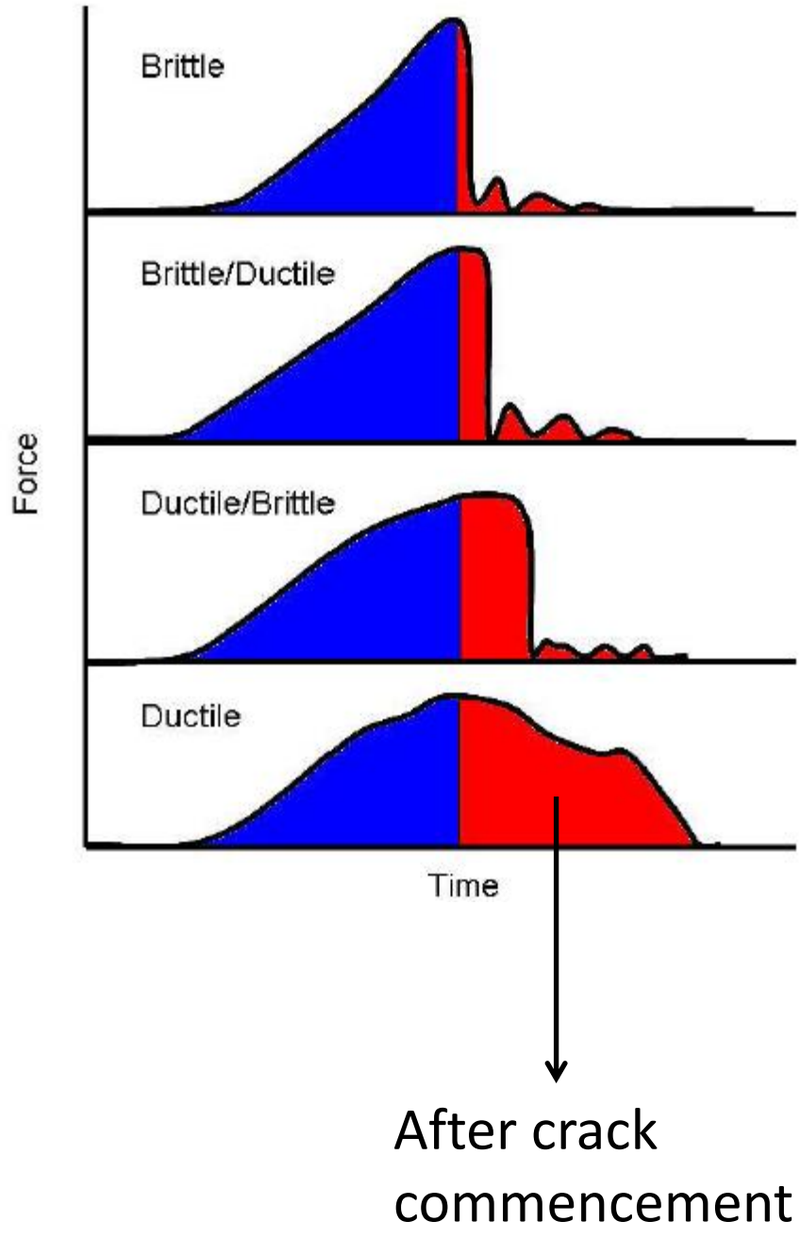

Lecture source:

Prof. Leonid Zhigilei, http://people.virginia.edu/~lz2n/mse209/index.html

Brittle vs. Ductile Fracture

- **Ductile materials** - extensive plastic deformation and energy absorption ("toughness") before fracture
- **Brittle materials** - little plastic deformation and low energy absorption before fracture

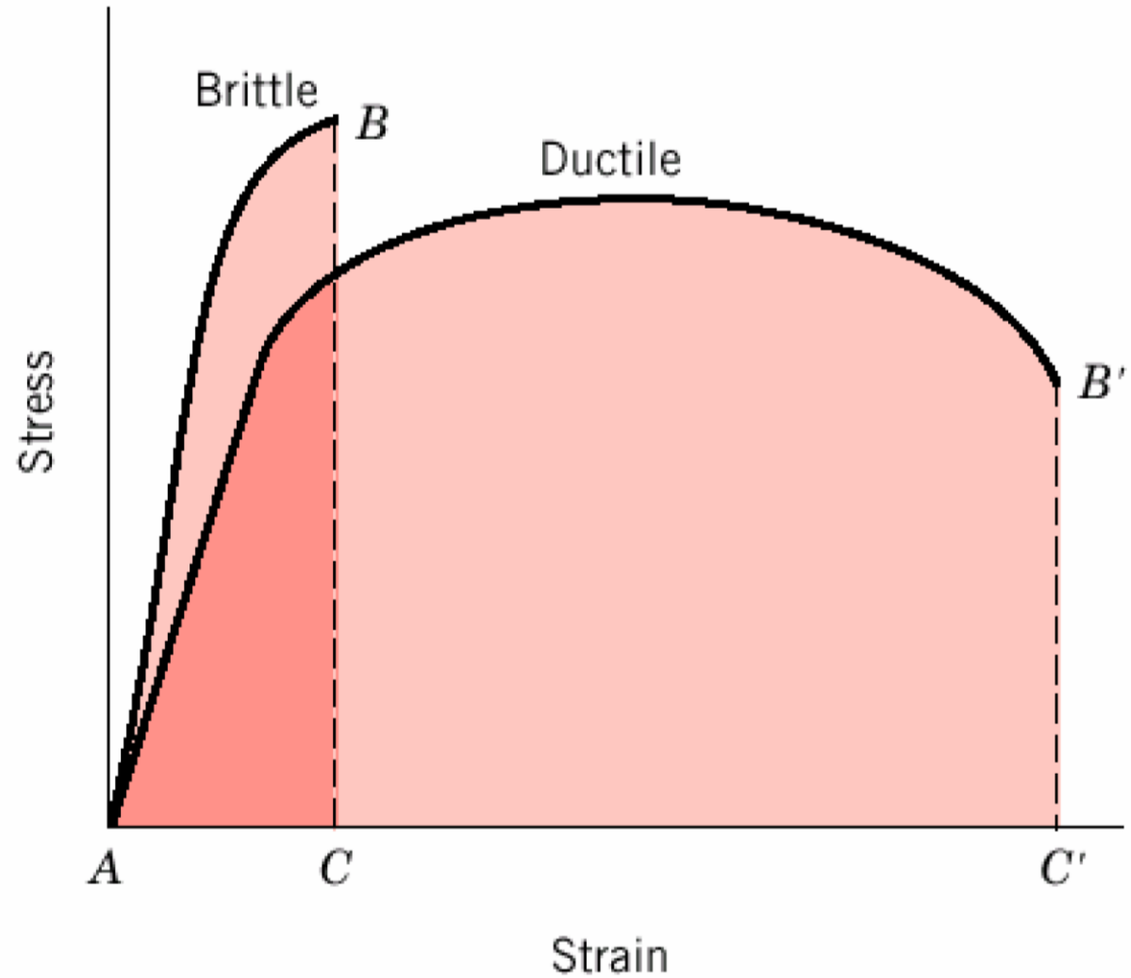

Lecture source:

Prof. Leonid Zhigilei, http://people.virginia.edu/~lz2n/mse209/index.html

Brittle vs. Ductile Fracture

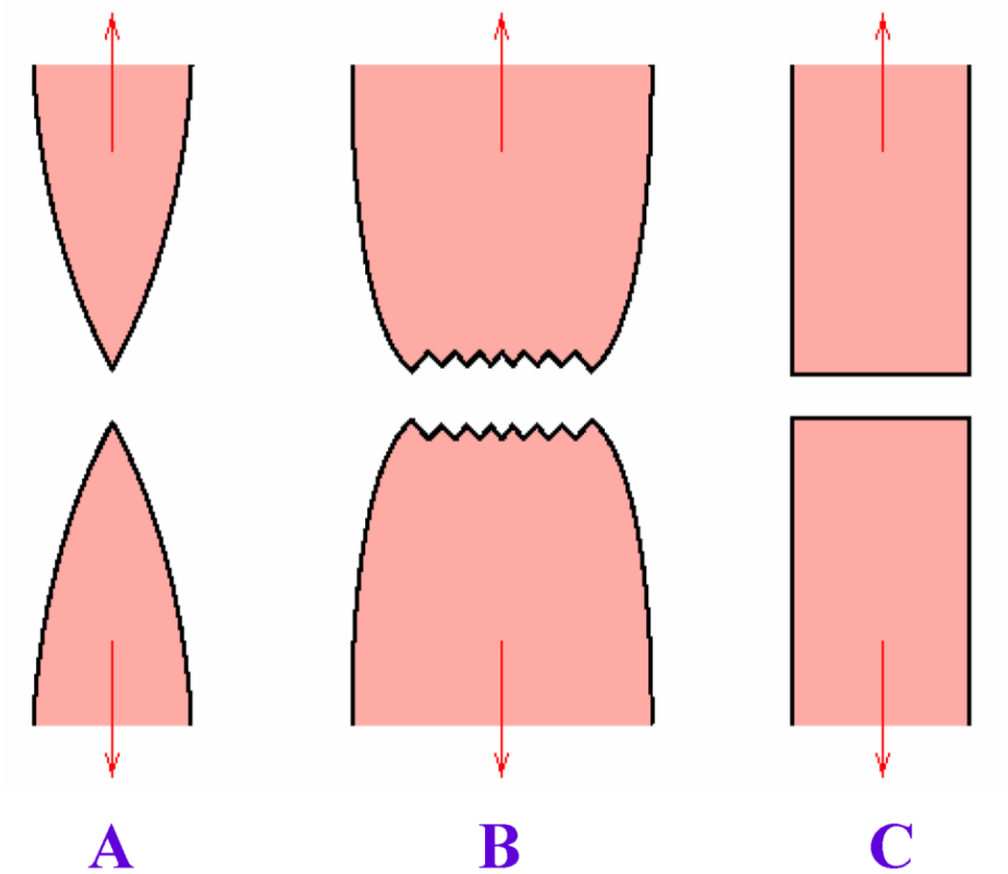

A. **Very ductile**, soft metals (e.g. Pb, Au) at room temperature, other metals, polymers, glasses at high temperature.

B. **Moderately ductile fracture**, typical for ductile metals

C. **Brittle fracture,** cold metals, ceramics.

Lecture source:

Prof. Leonid Zhigilei, http://people.virginia.edu/~lz2n/mse209/index.html

Fracture Types

Shearing

- Applied stress =>
- Dislocation generation and motion =>
- Dislocations coalesce at grain boundaries =>
- Forming voids =>
- Voids grow to form macroscopic cracks
- Macroscropic crack growth lead to fracture

Plastic deformation (ductile material)

Dough-like or conical features

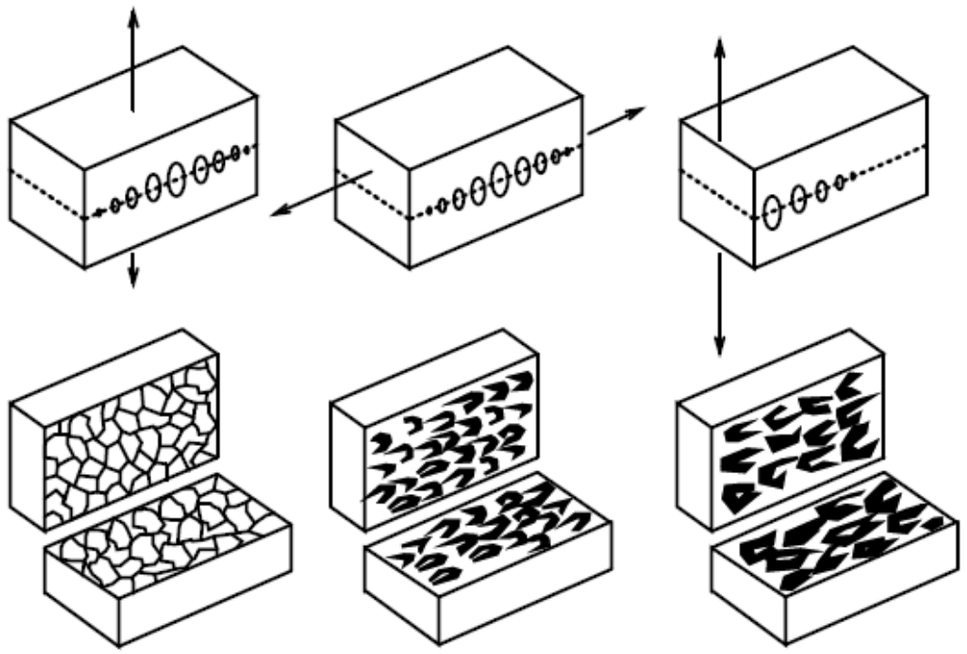

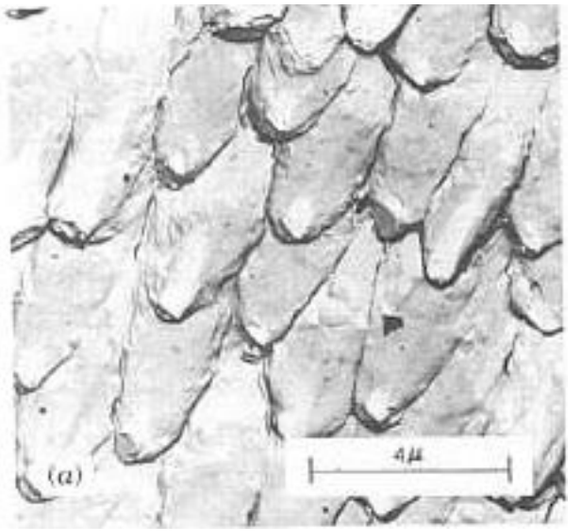

Ductile Fracture (Dislocation Mediated)

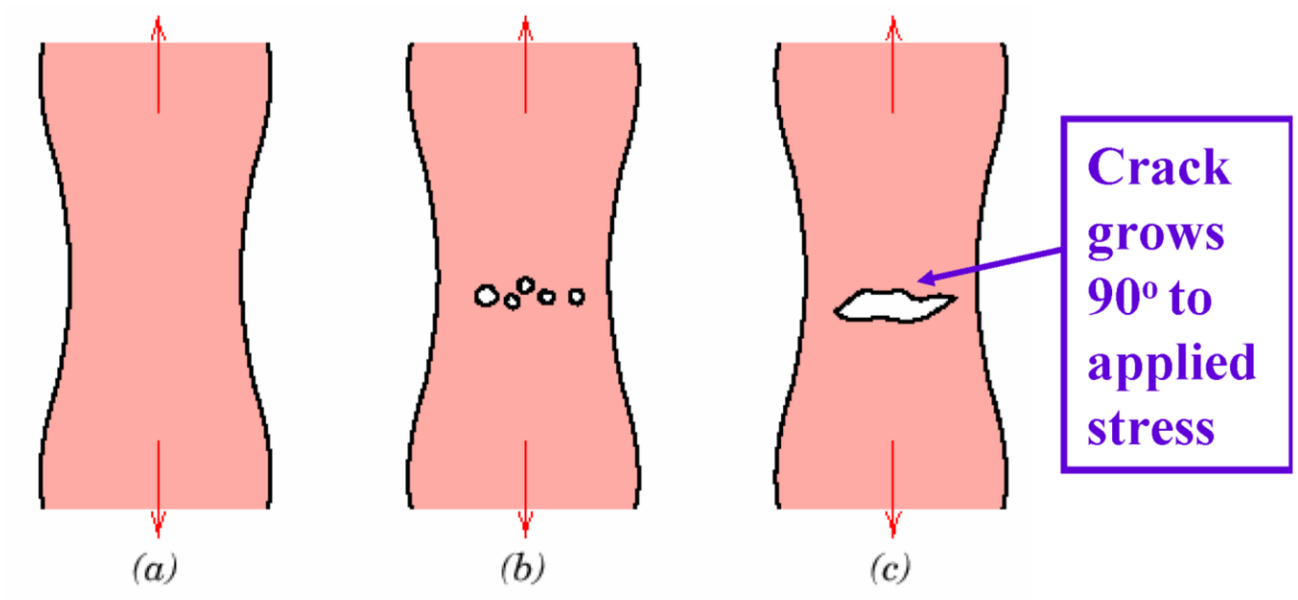

(a) Necking

(b) Formation of microvoids

(c) Coalescence of microvoids to form a crack

(d) Crack propagation by shear deformation

(e) Fracture

Lecture source:

Prof. Leonid Zhigilei, http://people.virginia.edu/~lz2n/mse209/index.html

Ductile Fracture

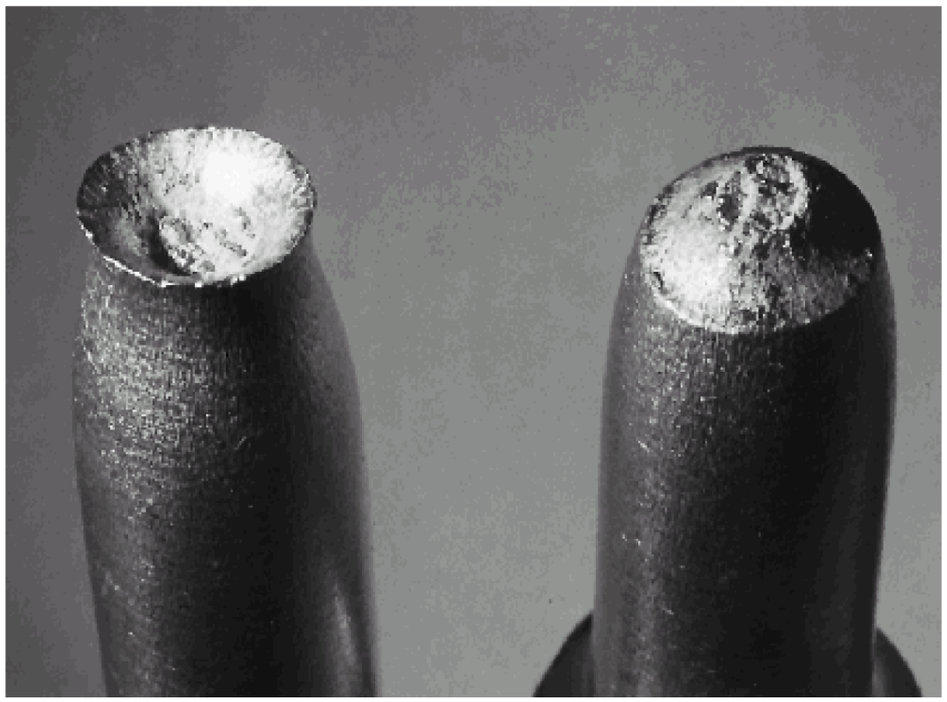

(Cup-and-cone fracture in Al)

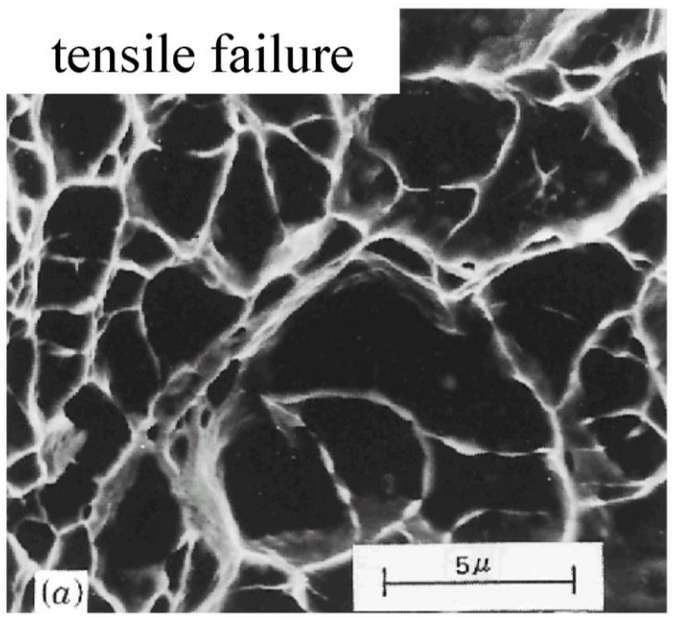

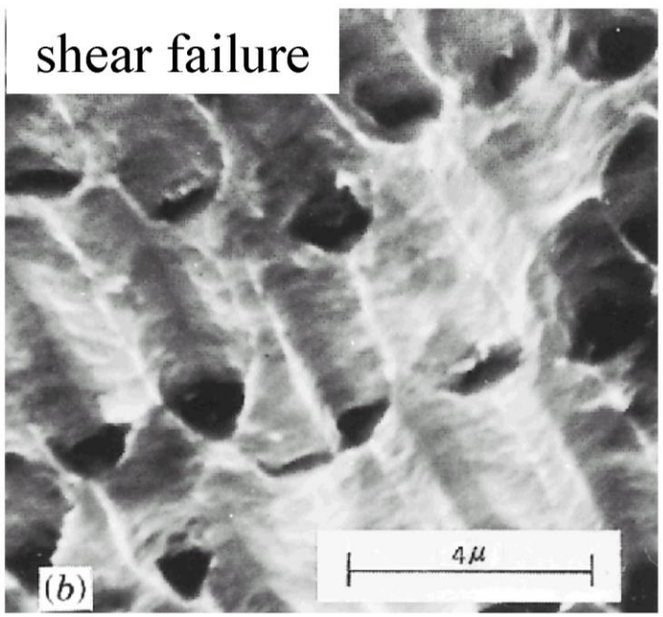

Scanning Electron Microscopy: *Fractographic* studies at high resolution. Spherical "dimples" correspond to microvoids that initiate crack formation.

Lecture source:

Prof. Leonid Zhigilei, http://people.virginia.edu/~lz2n/mse209/index.html

MSE 2090: Introduction to Materials Science Chapter 8, Failure

Brittle Fracture (Limited Dislocation Mobility)

- No appreciable plastic deformation
- Crack propagation is very fast
- Crack propagates nearly perpendicular to the direction of the applied stress
- Crack often propagates by cleavage - breaking of atomic bonds along specific crystallographic planes (cleavage planes).

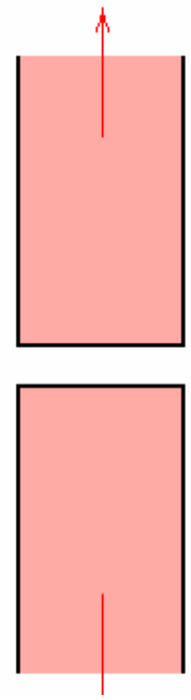

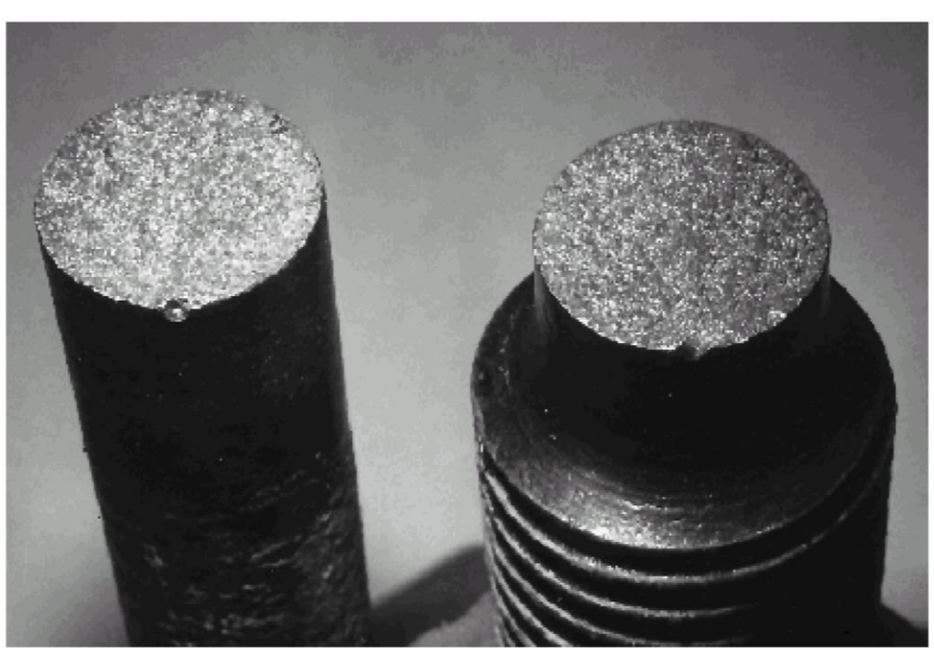

Brittle fracture in a mild steel

Lecture source:

Prof. Leonid Zhigilei, http://people.virginia.edu/~lz2n/mse209/index.html

Brittle Fracture

A. Transgranular fracture: Fracture cracks pass through grains. Fracture surface have faceted texture because of different orientation of cleavage planes in grains.

B. Intergranular fracture: Fracture crack propagation is along grain boundaries (grain boundaries are weakened or embrittled by impurities segregation etc.)

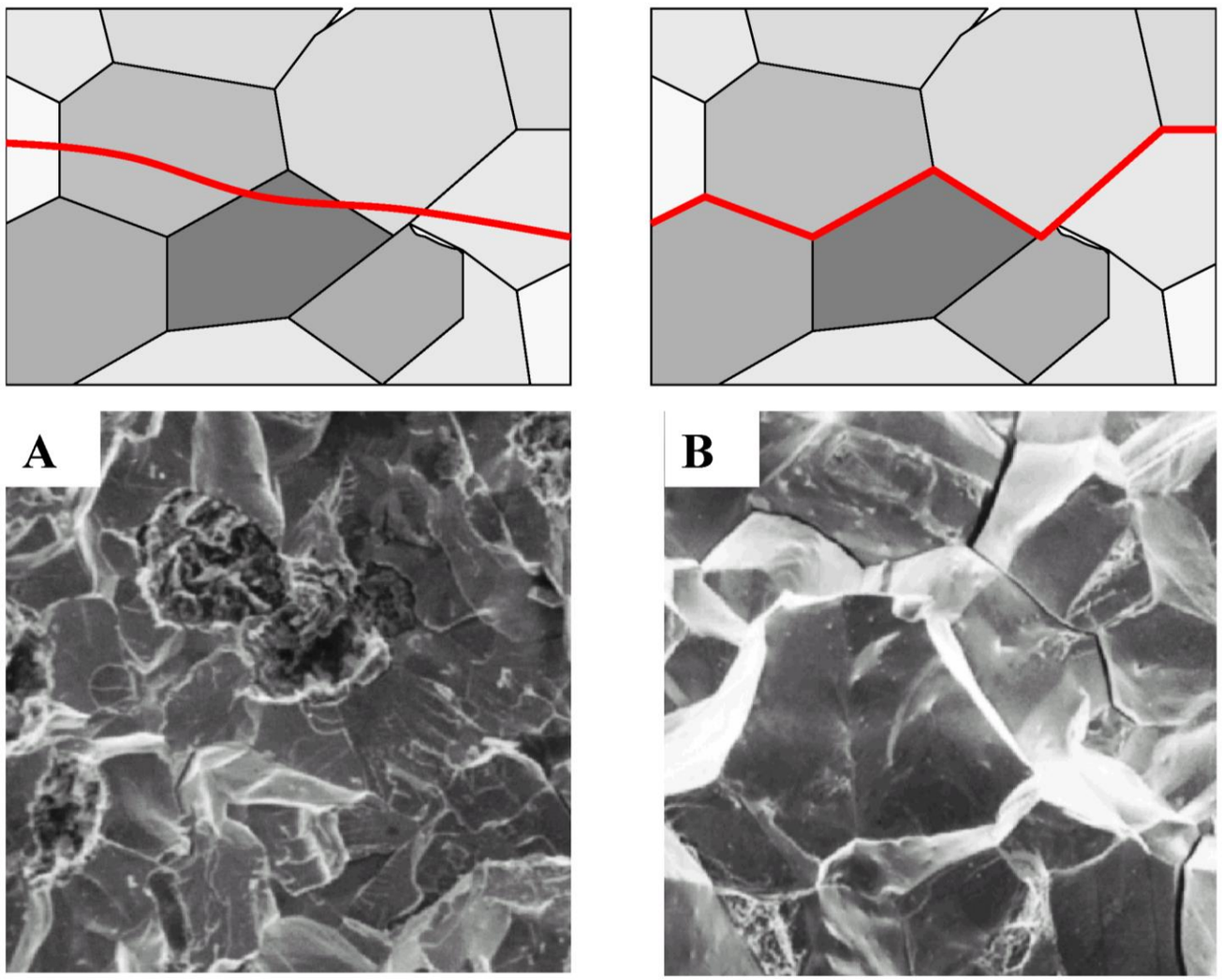

Lecture source:

Prof. Leonid Zhigilei, http://people.virginia.edu/~lz2n/mse209/index.html

Fracture Types

Cleavage

mostly brittle

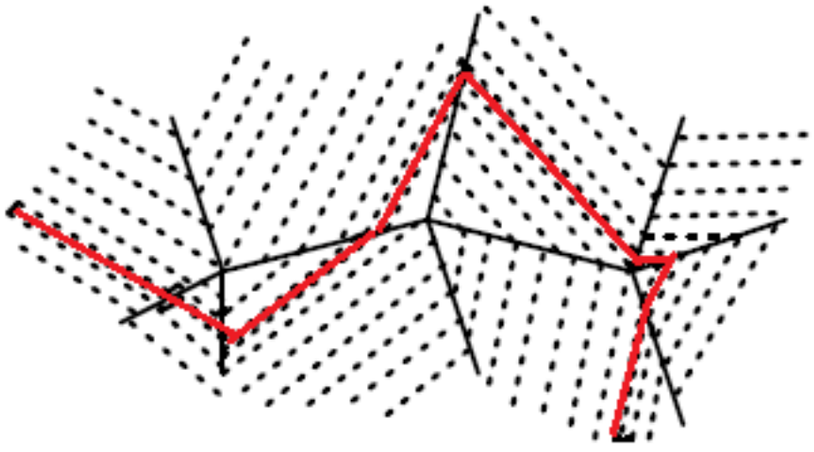

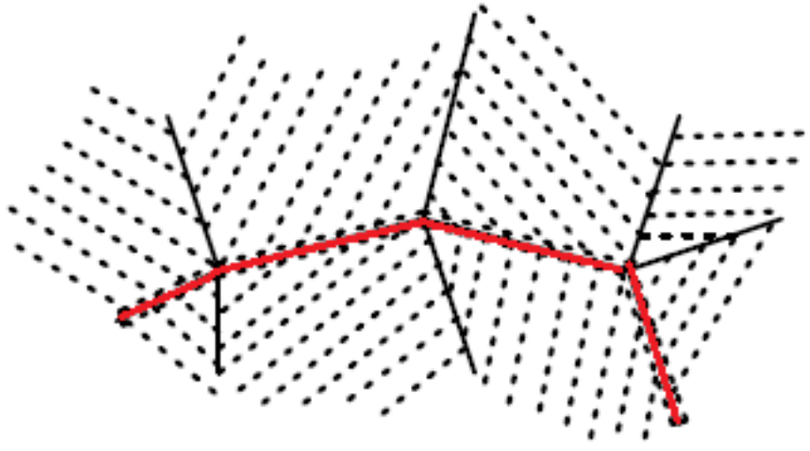

intra-granulair

(or transgranular)

split atom bonds

inter-granulair

between grain boundaries

Fatigue

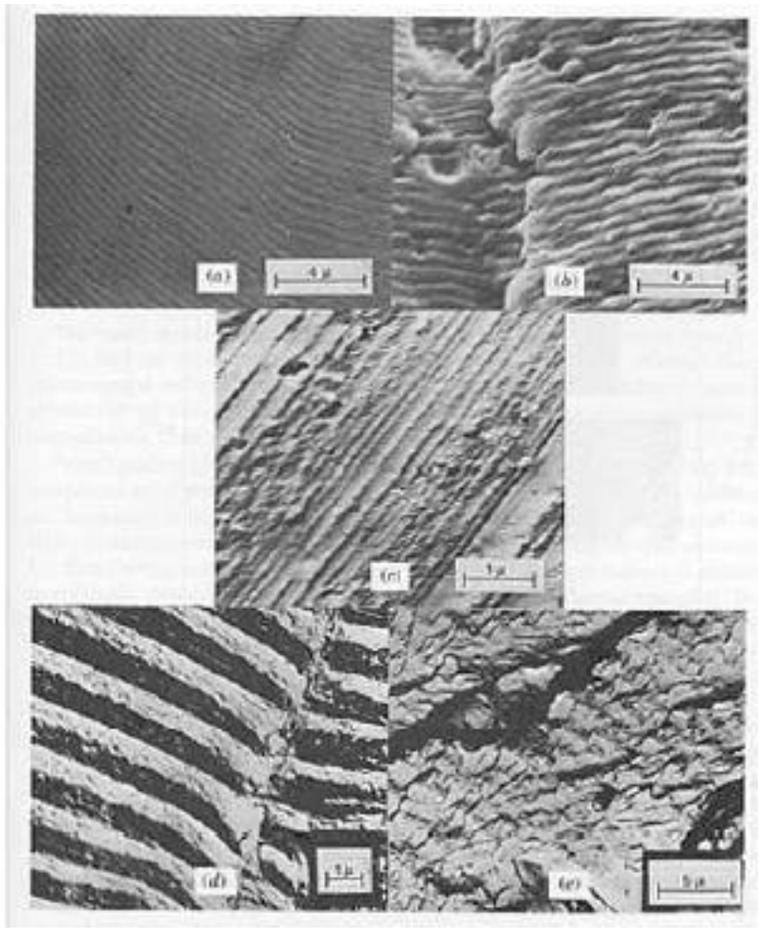

- Cracks grow a very short distance every time

Clam shell structures mark the location of crack tip after each individual cyclic loading

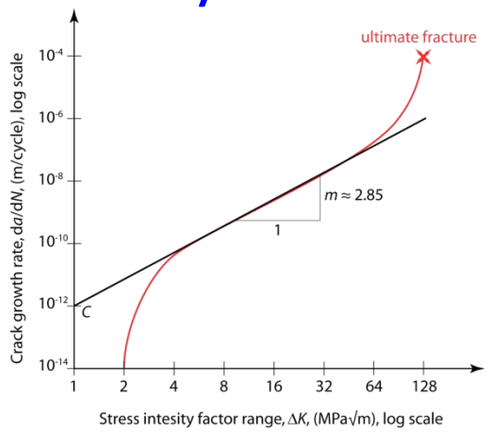

Fracture Types

- Delamination (De-adhesion)

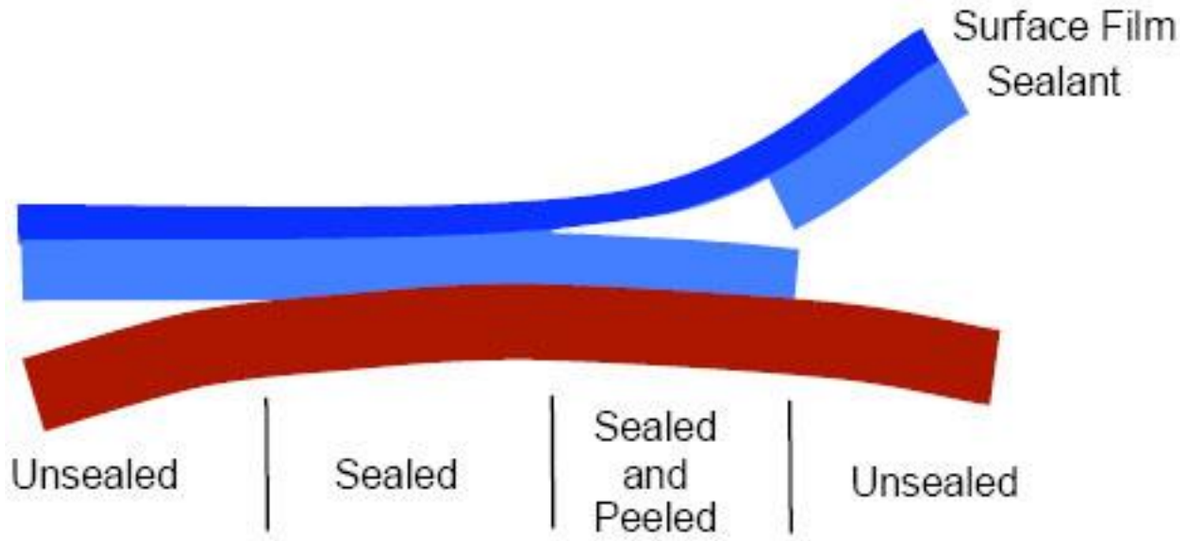

- Crazing

- Common for polymers
- sub-micormeter voids initiate

stress whitening because of light reflection from crazes

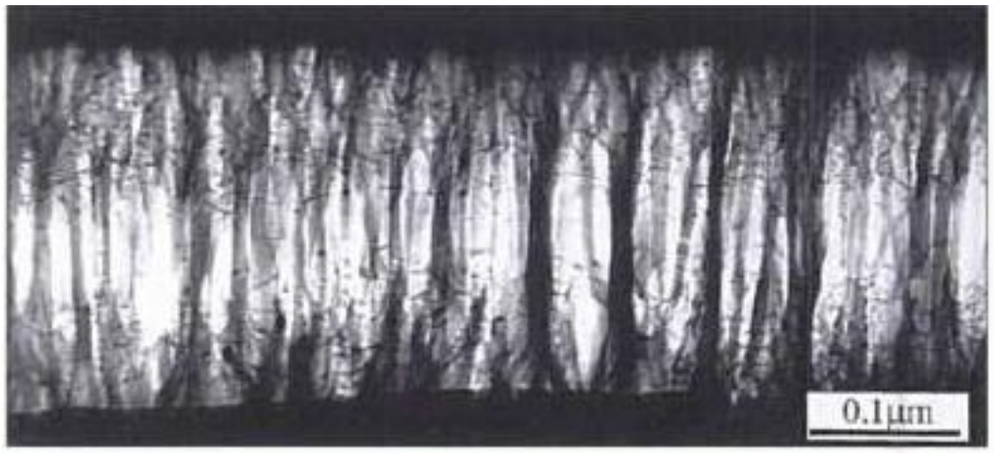

3.3 Ductile to brittle transition

Ductile-to-brittle transition

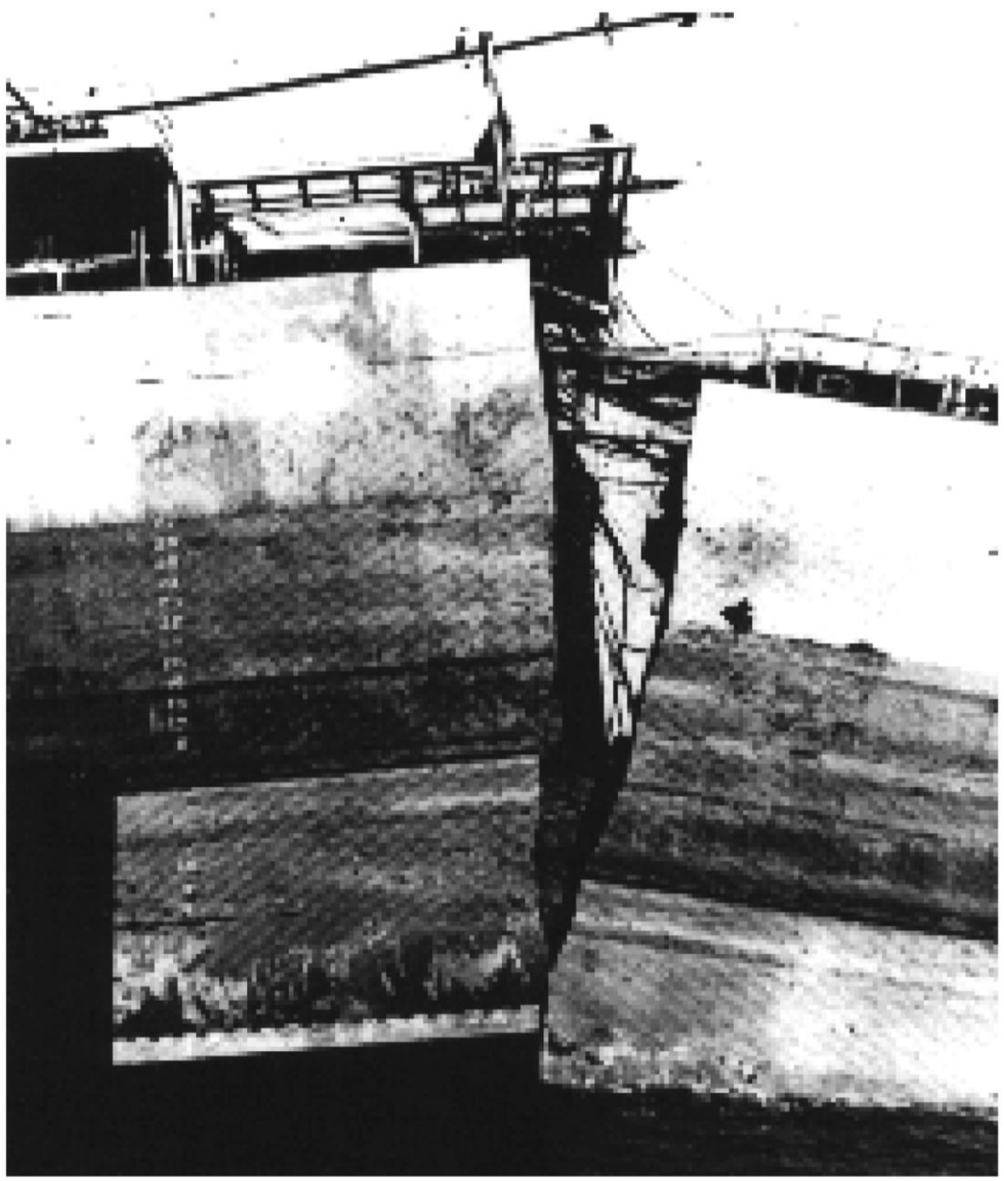

Low temperatures can severely embrittle steels. The Liberty ships, produced in great numbers during the WWII were the first all-welded ships. A significant number of ships failed by catastrophic fracture. Fatigue cracks nucleated at the corners of square hatches and propagated rapidly by brittle fracture.

Lecture source:

Prof. Leonid Zhigilei, http://people.virginia.edu/~lz2n/mse209/index.html

MSE 2090: Introduction to Materials Science Chapter 8, Failure

Charpy v-notch test

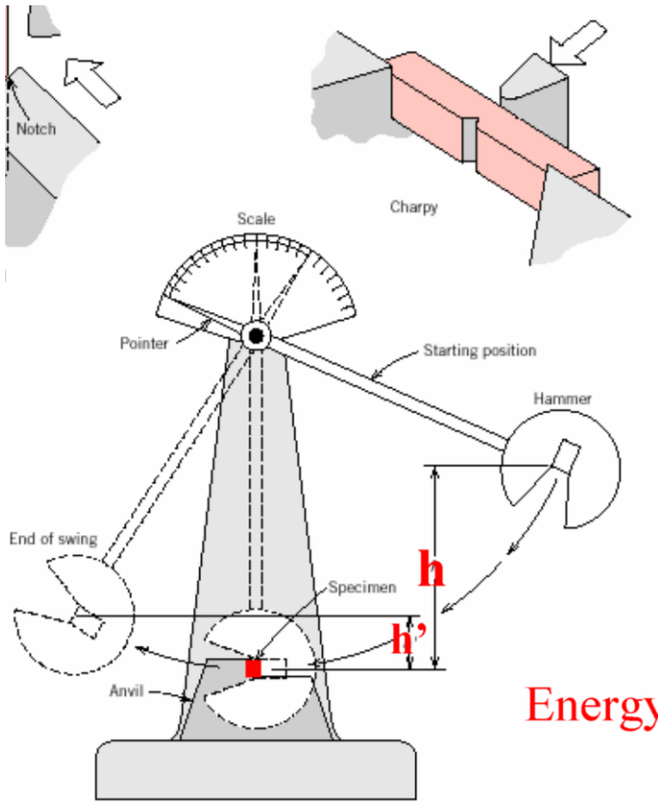

Charpy

Energy ~ h - h'

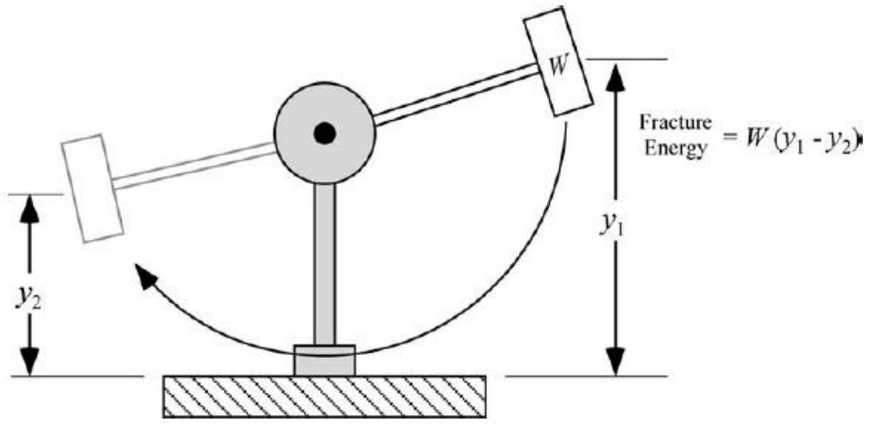

Influence of temperature on Cv

Brittle Fracture

Ductile Fracture

quippy documentation (www.jrkermode.co.uk)

fcc (hcp) metals

low strength

bcc metals
Be, Zn, ceramics

high strength metals
Al, Ti alloys

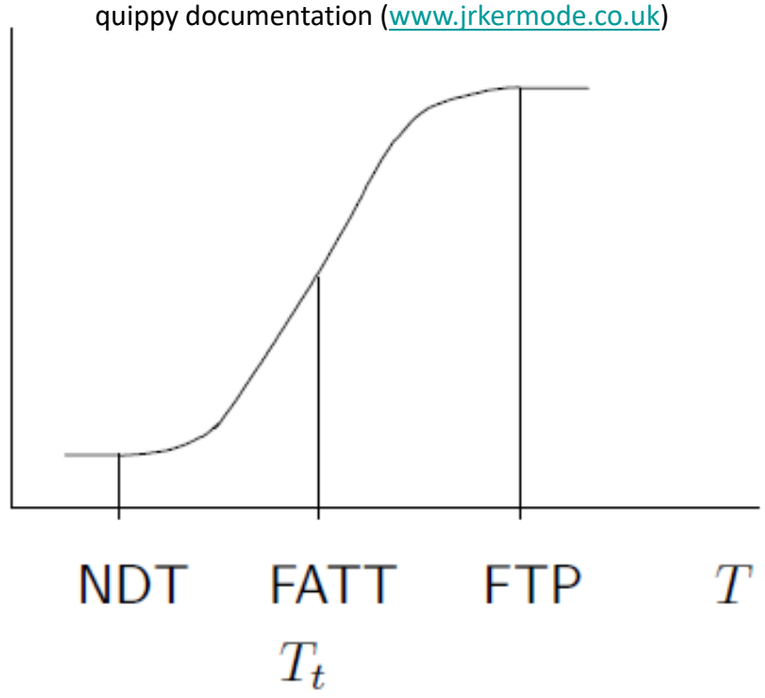

1. Temperature Effects

Temperature decrease => Ductile material can become brittle

- BCC metals: Limited dislocation slip systems at low T =>
- Impact energy drops suddenly over a relatively narrow temperature range around DBTT.
  - Ductile to brittle transition temperature (DBTT) or
  - Nil ductility transition temperature (T_0)
- FCC and HCP metals remain ductile down to very low temperatures
- Ceramics, the transition occurs at much higher temperatures than for metals

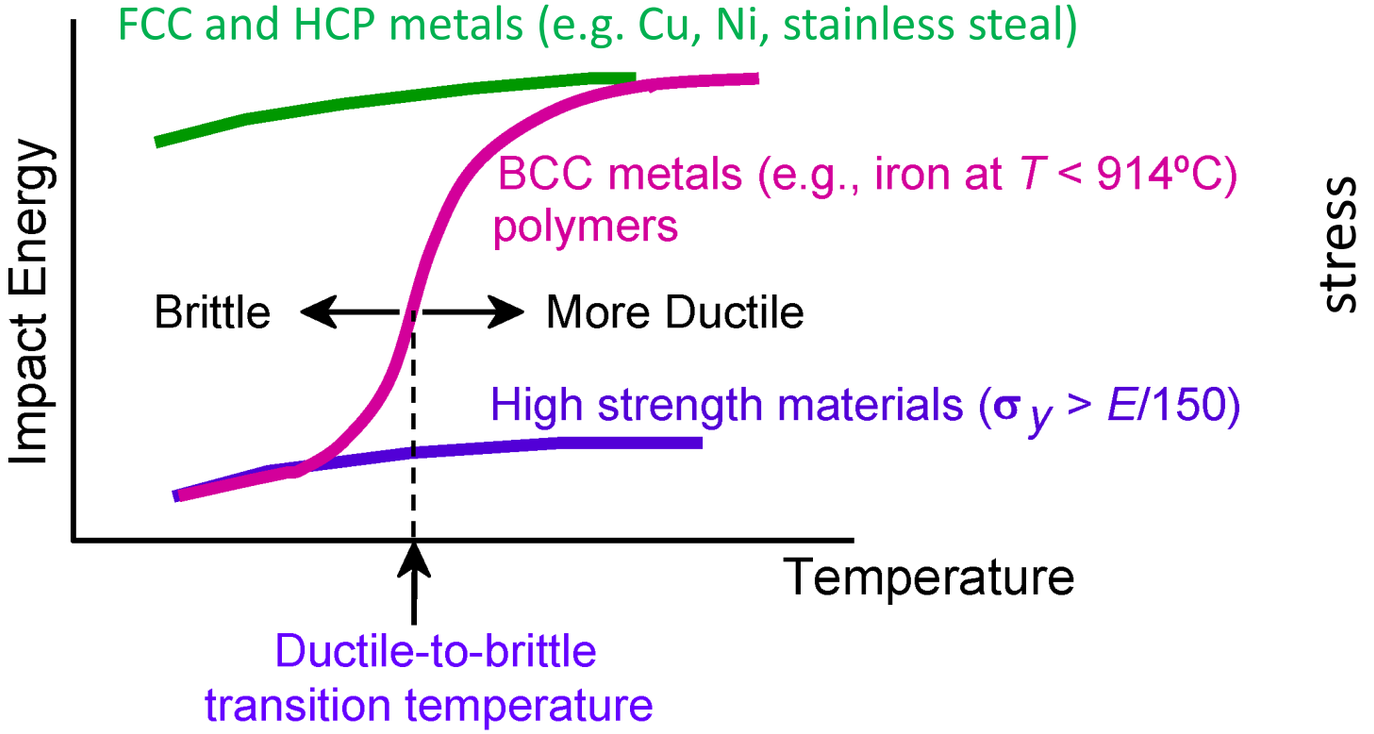

stress

strain

- Titanic in the icy water of Atlantic (BCC)
- Steel structures are every likely to fail in winter

Fracture surfaces of tested specimens

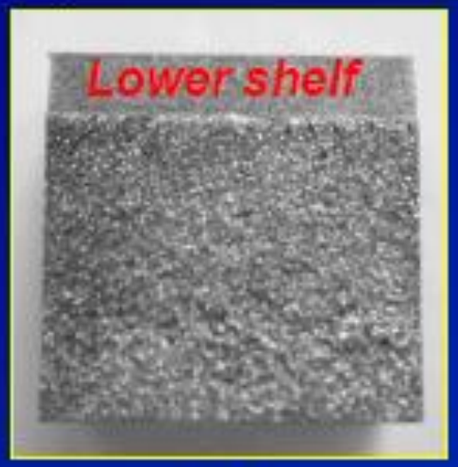

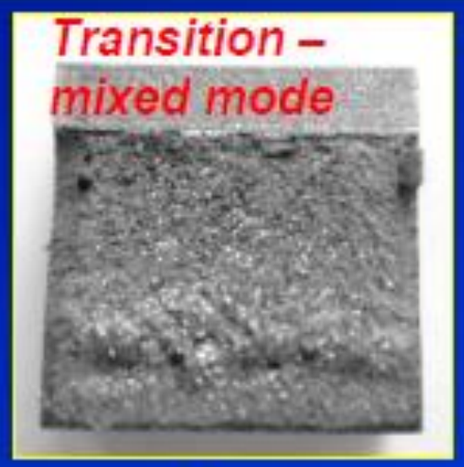

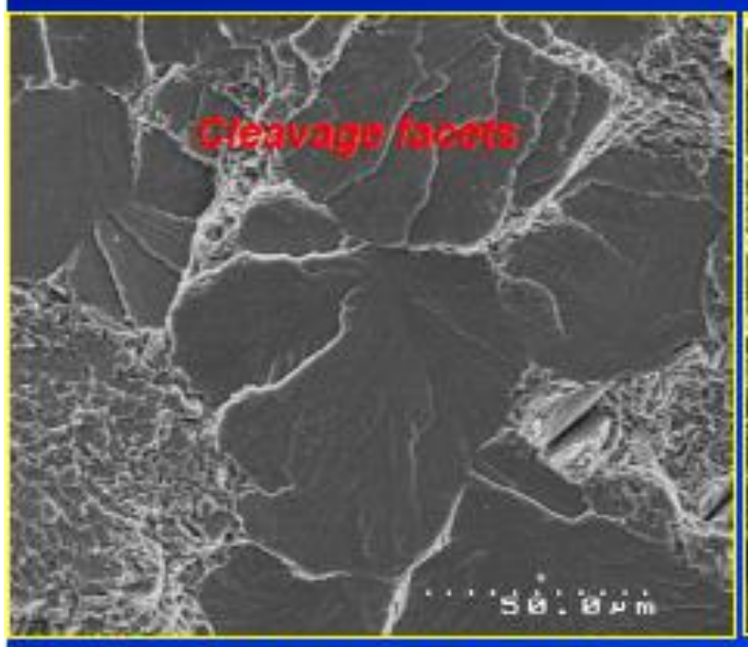

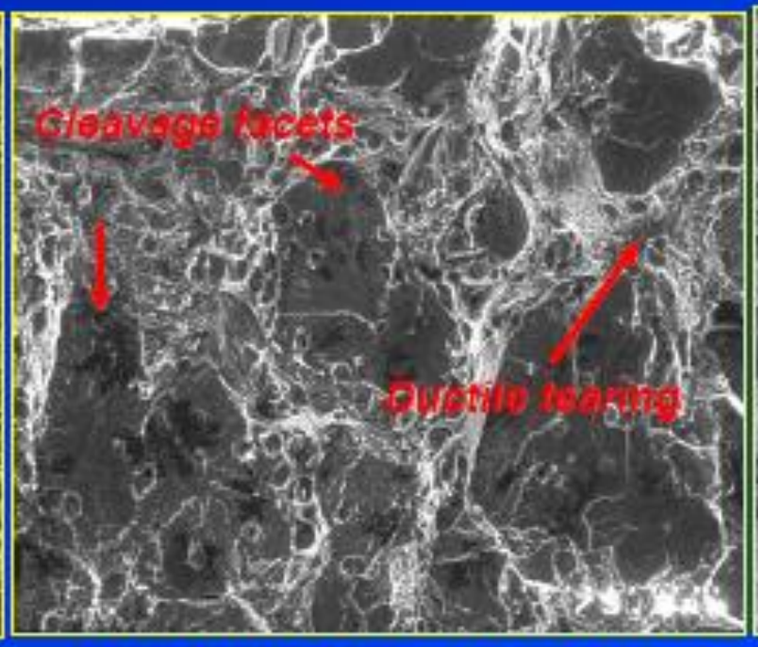

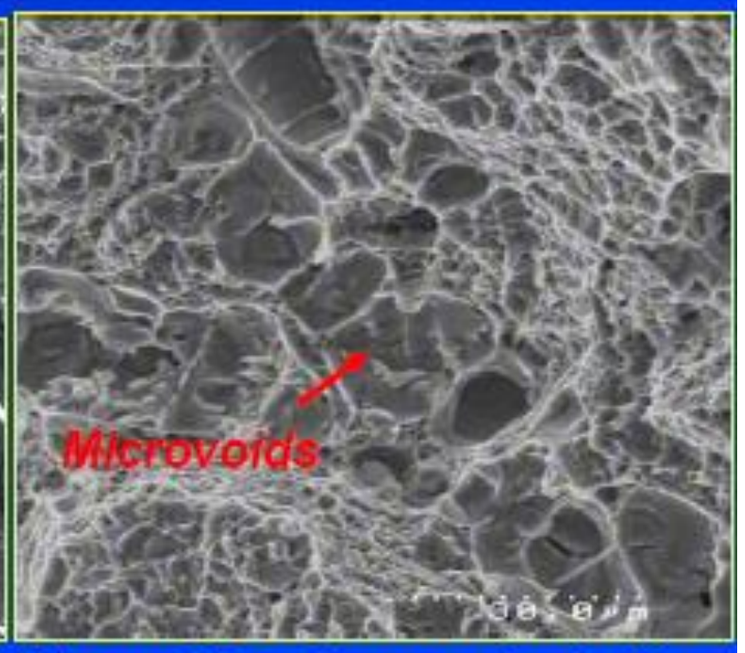

Brittle fracture

Mixed mode of brittle and ductile failures

Microvoid coalescence in ductile failure

Suranaree University of Technology Tapany Udomphol May-Aug 2007

Source: Tapany Udomphol, Suranaree University of Technology
http://eng.sut.ac.th/metal/images/stories/pdf/14_Brittle_fracture_and_impact_testing_1-6.pdf

2. Impurities and alloying effect on DBTT

- Alloying usually increases DBTT by inhibiting dislocation motion. They are generally added to increase strength or are (an unwanted) outcome of the processing
- For steal P, S, Si, Mo, O increase DBTT while Ni, Mg decease it.

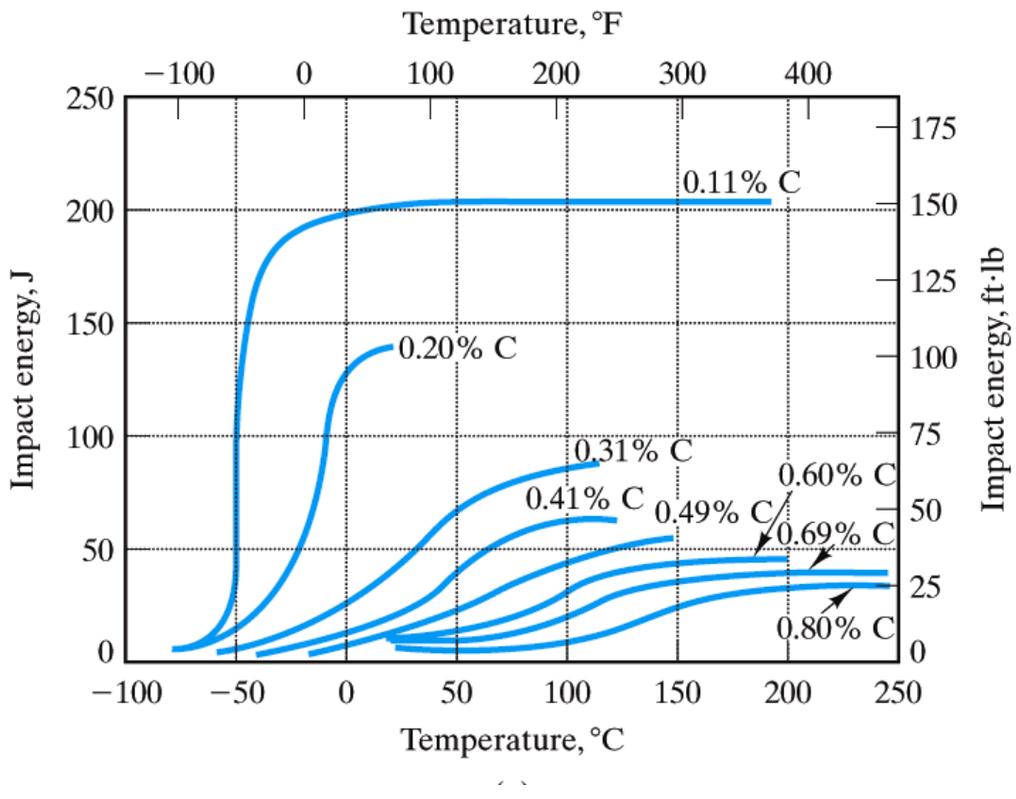

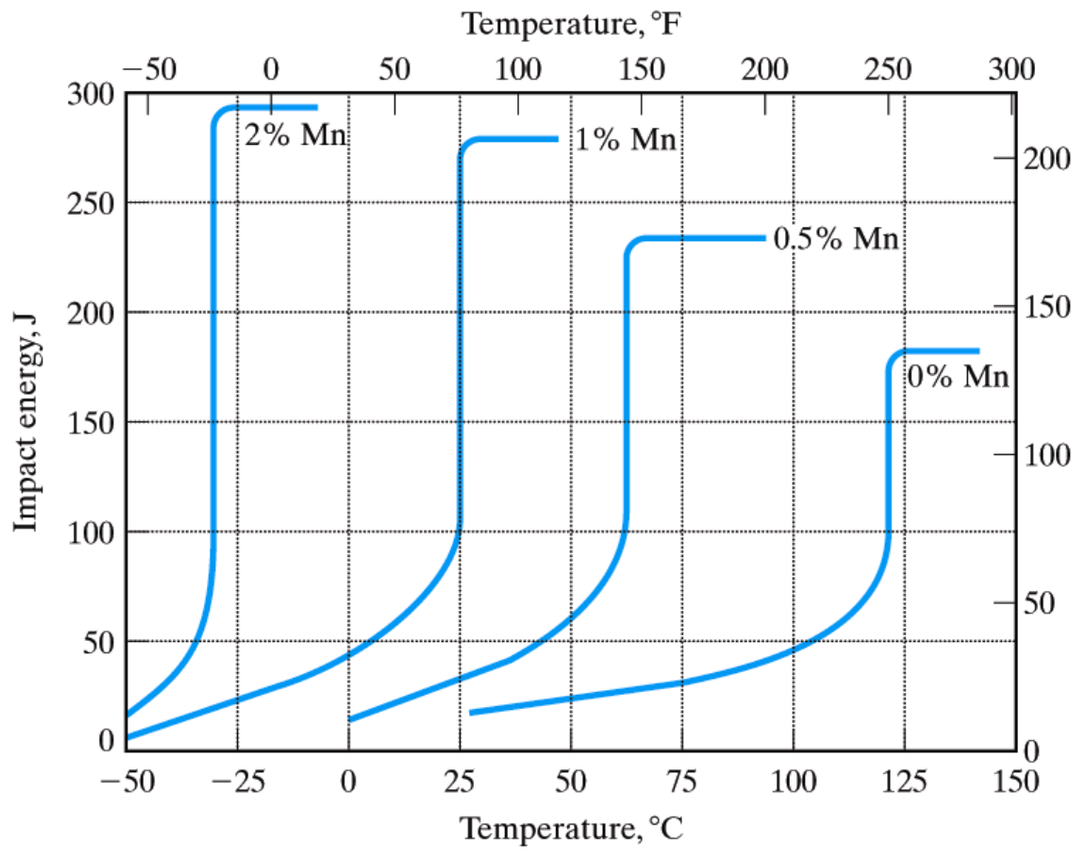

Decrease of DBTT by Mg: formation of manganese-sulfide (MnS) and consumption of some S. It has some side effects

3. Radiation embrittlement through DBTT

- Energetic particles (such as neutron or fission fragments) => knocking atoms out of natural lattice positions changing material property
- T_0 corresponds to K_{JC} = 100 MPa$\sqrt{m}$
- Wallin Master Curve model:
  K-T shifts to right by ΔT_o
  by irradiation

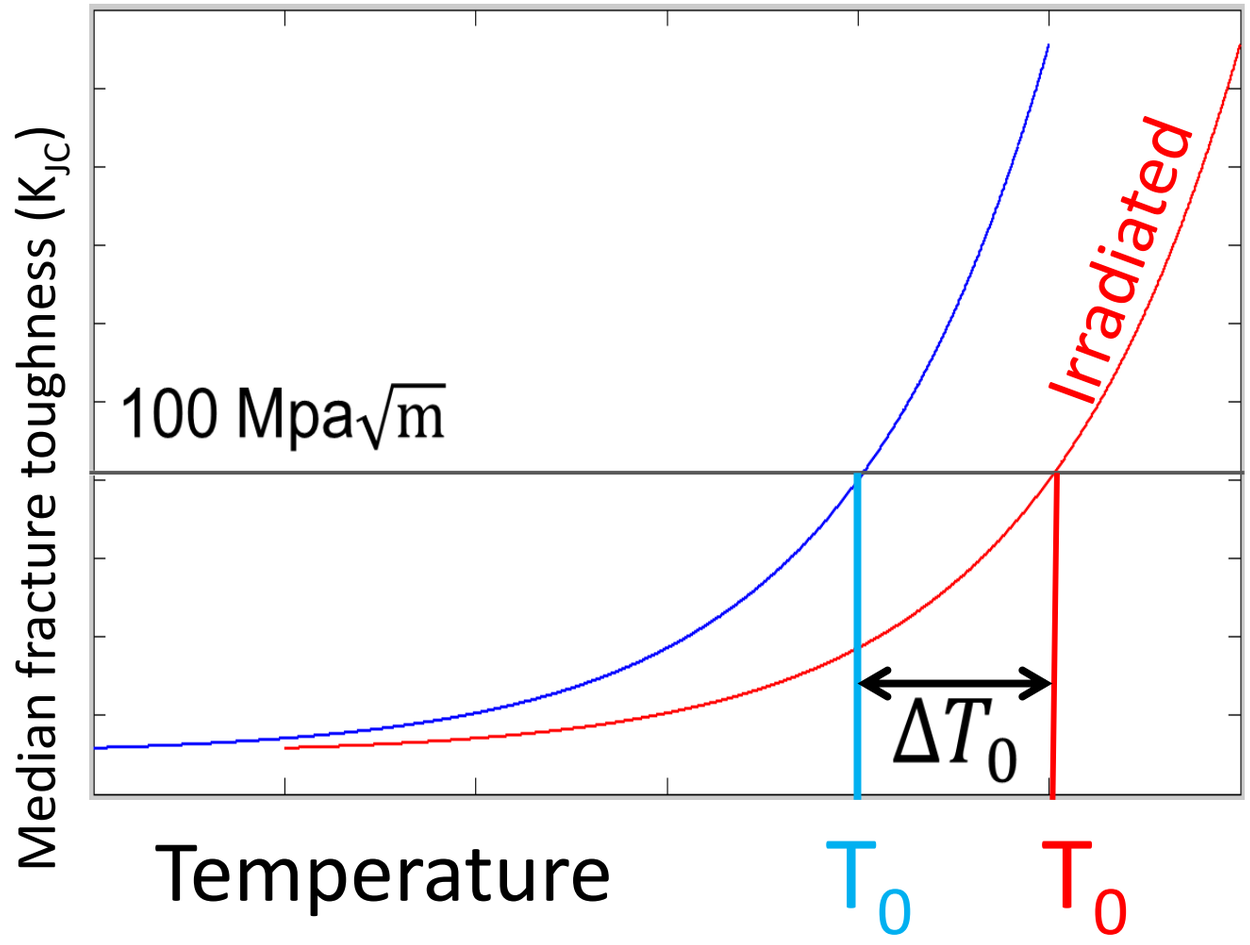

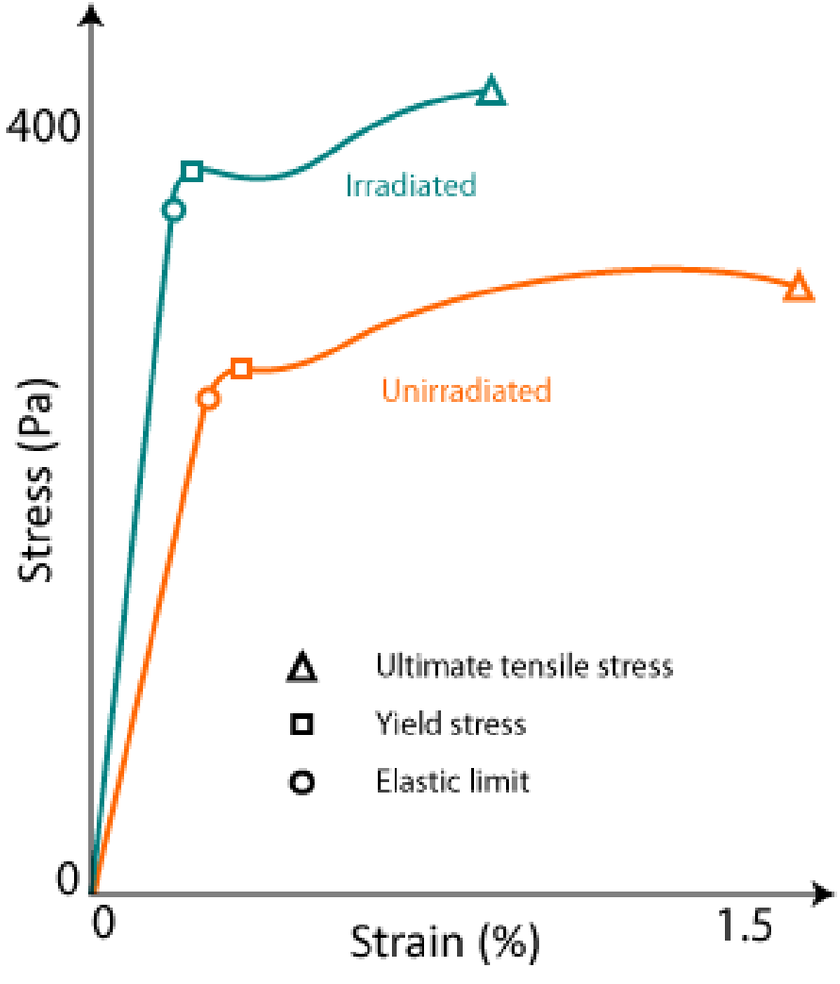

Irradiation effect:

1. **Strengthening**
2. **More brittle**

3. Radiation embrittlement through DBTT

Wallin's Master Curve
Irradiation inceases T_0

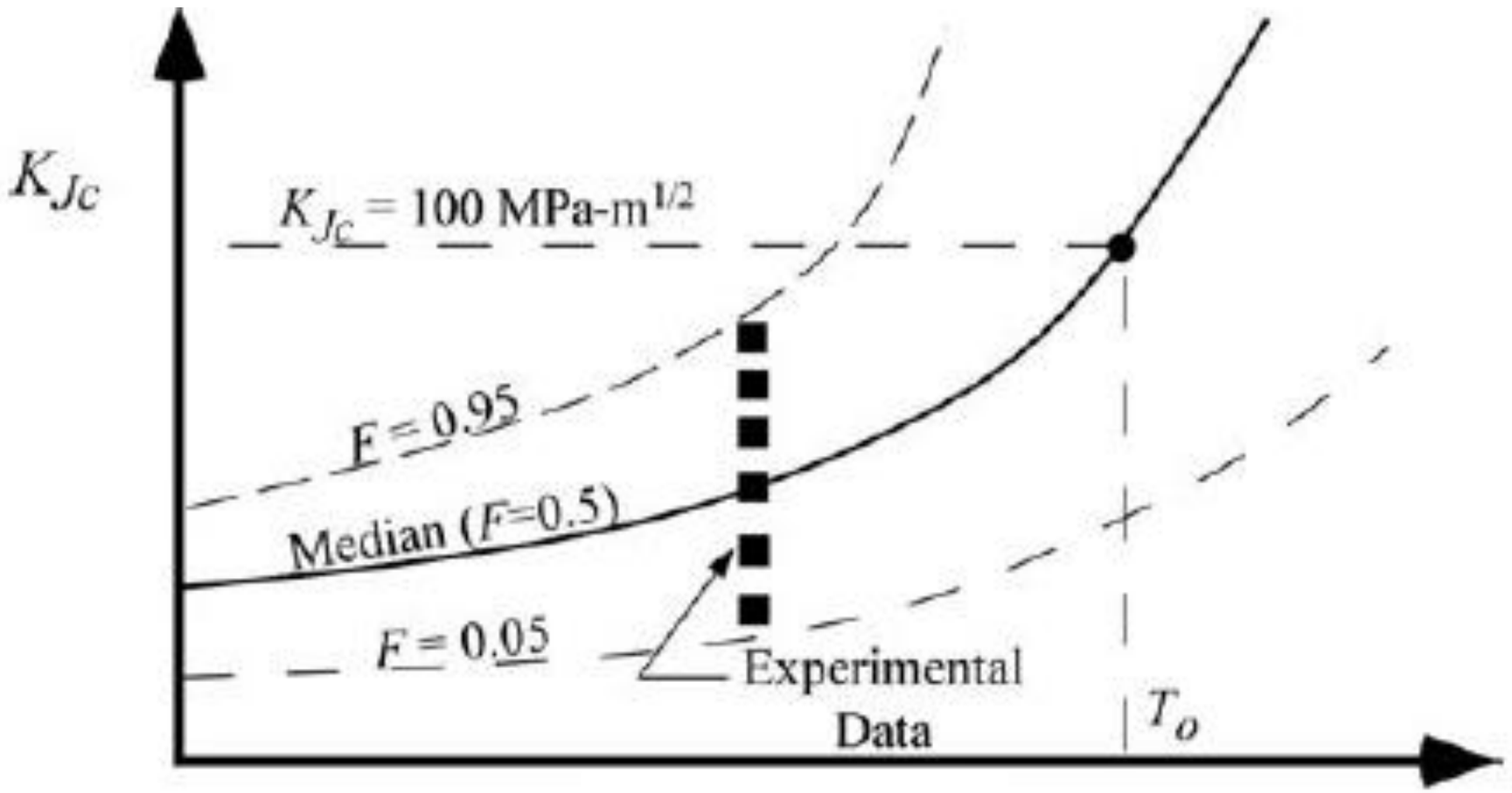

$$T - T_0$$

$$K_{Jc(med)} = 30 + 70\exp[0.019(T - T_0)], \text{MPa}\sqrt{\text{m}}$$

4. Hydrogen embrittlement through DBTT

- Hydrogen in alloys drastically reduces ductility in most important alloys:
  - nickel-based alloys and, of course, both ferritic and austenitic steel
  - Steel with an ultimate tensile strength of less than 1000 Mpa is almost insensitive
- A very common mechanism in Environmentally assisted cracking (EAC):
  - High strength steel, aluminum, & titanium alloys in aqueous solutions is usually driven by hydrogen production at the crack tip (i.e., the cathodic reaction)
  - Different from previously thought anodic stress corrosion cracking(SCC)
- Reason (most accepted)
  - Reduces the bond strength between metal atoms => easier fracture.

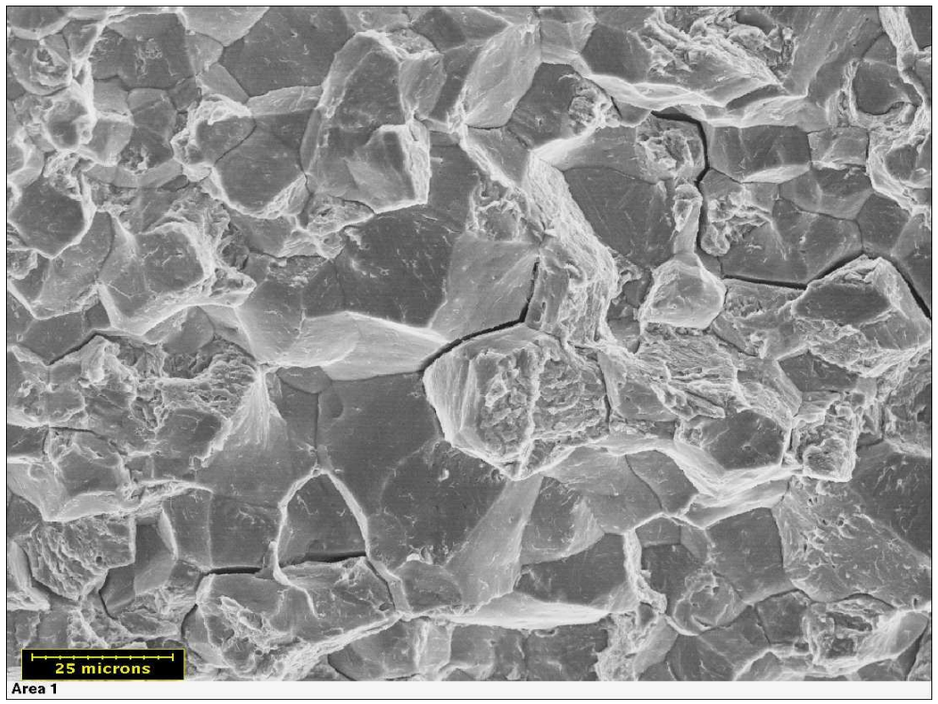

Grains

Polycrystalline material:
Composed of many small crystals or grains

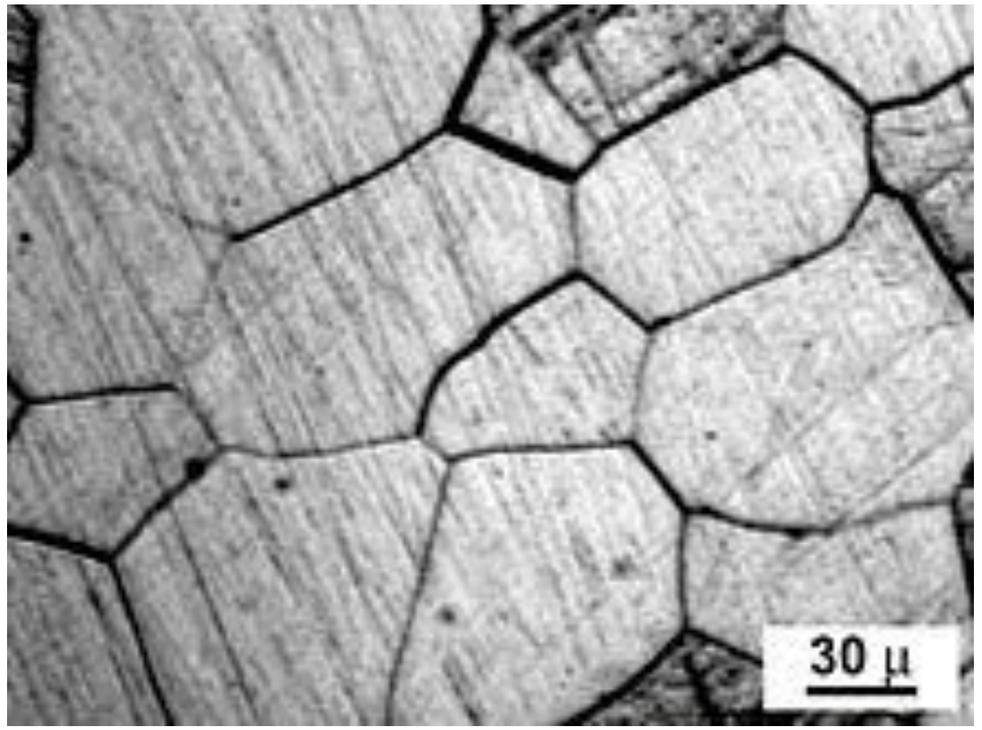

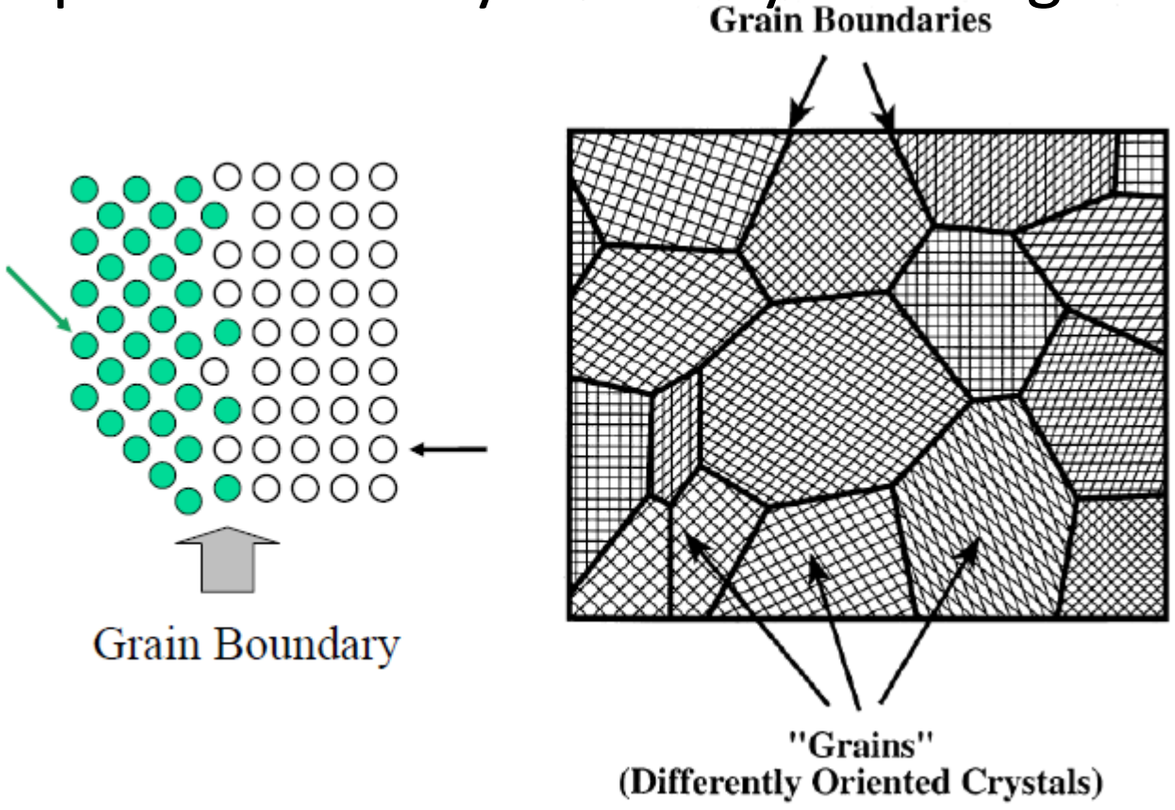

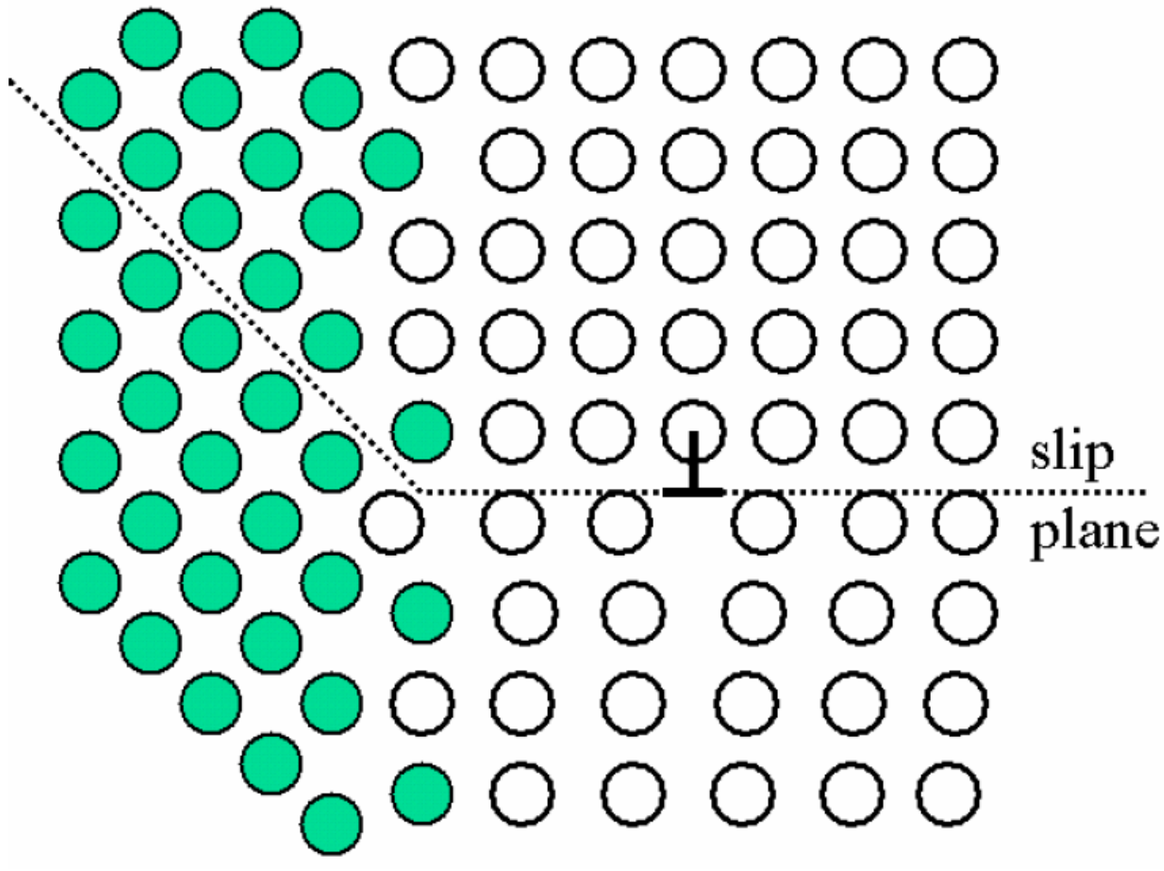

Grain boundary barrier to dislocation motion:
High angle grain boundaries block slip and harden the material

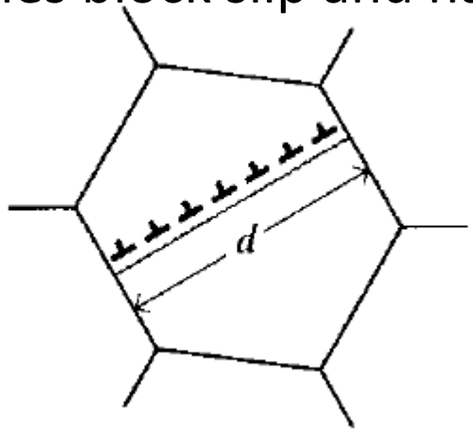

5. Grain size

- In BCC metals, brittle fracture can be initiated by dislocation glide within a crystalline grain
- Yield stress depends on grain size (Hall-Petch law)

$$\sigma_y = \sigma_0 + \frac{k_y}{\sqrt{d}}$$

- Dislocation pile-up acts as crack with size ≈d =>
- Stress to cause brittle fracture is

$$\sigma_f = \frac{k_f}{\sqrt{d}},\ k_f = \sqrt{\frac{EG_c}{\pi}}$$

- Left size: small d ($d < d_{cr}$)
  $\sigma_y < \sigma_f$ ⇨ Ductile fracture
- Right side: large ($d > d_{cr}$)
  $\sigma_y < \sigma_f$ ⇨ Britle fracture

- **Small grain size =>**
  1. Lower DBTT (more ductile)
  2. Increases thoughness

⇨

DUCTILITY & STRENGH INCREASE SIMULTANEOUSLY!!!!
ONLY STRENGTHING MECHANISM THAT IMPROVES DUCTILITY

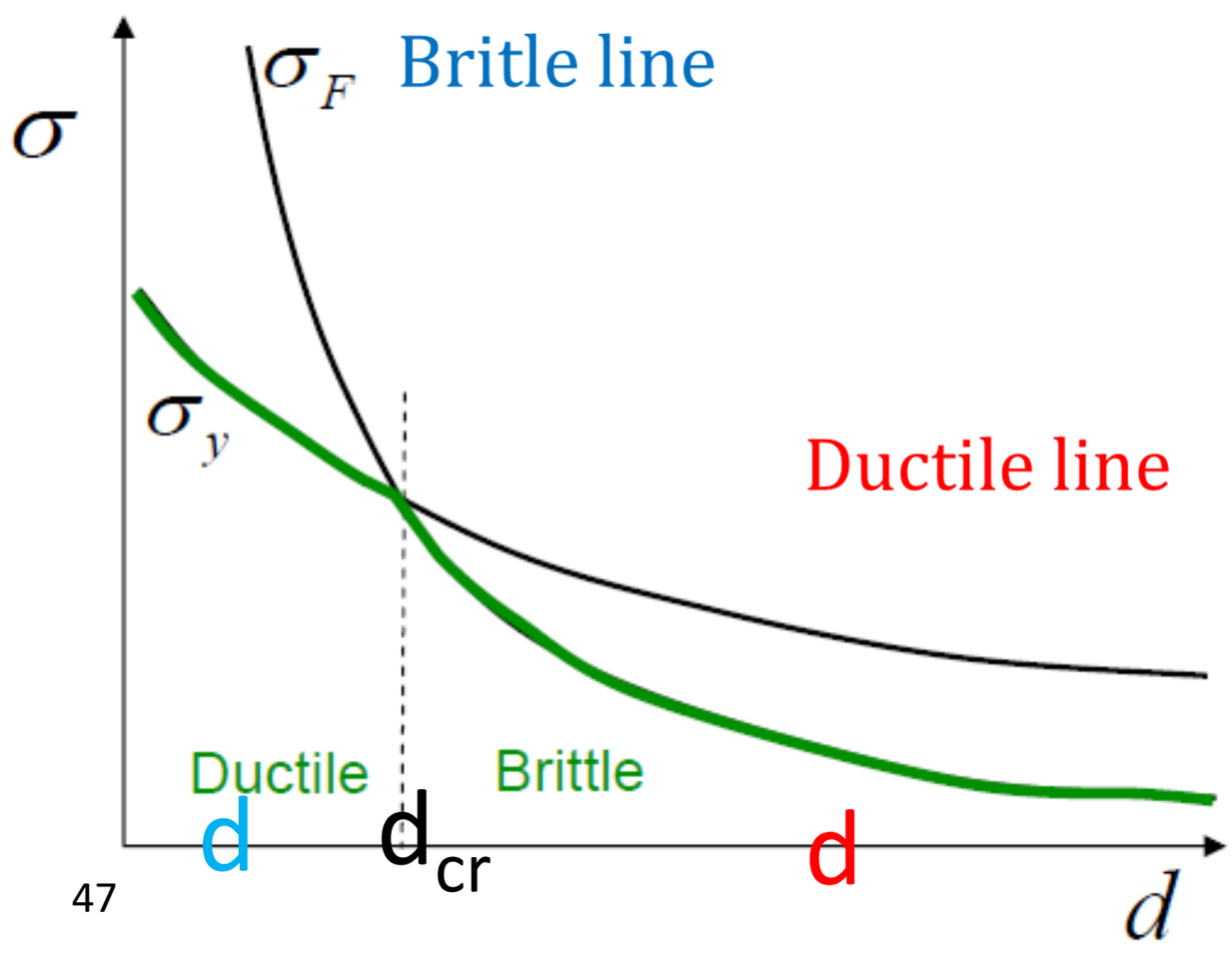

Lowering Grain size

- **Small grain size =>**
  1. Lower DBTT (more ductile)
  2. Increases thoughness

⇨

DUCTILITY & STRENGH INCREASE SIMULTANEOUSLY!!!!
ONLY STRENGTHING MECHANISM THAT IMPROVES DUCTILITY

- **Grain boundaries have higher energies (surface energy) ⇨**
  Grains tend to diffuse and get larger to lower the energy

- Heat treatments that provide grain refinement such as air cooling, recrystallisation during hot working help to lower transition temperature.

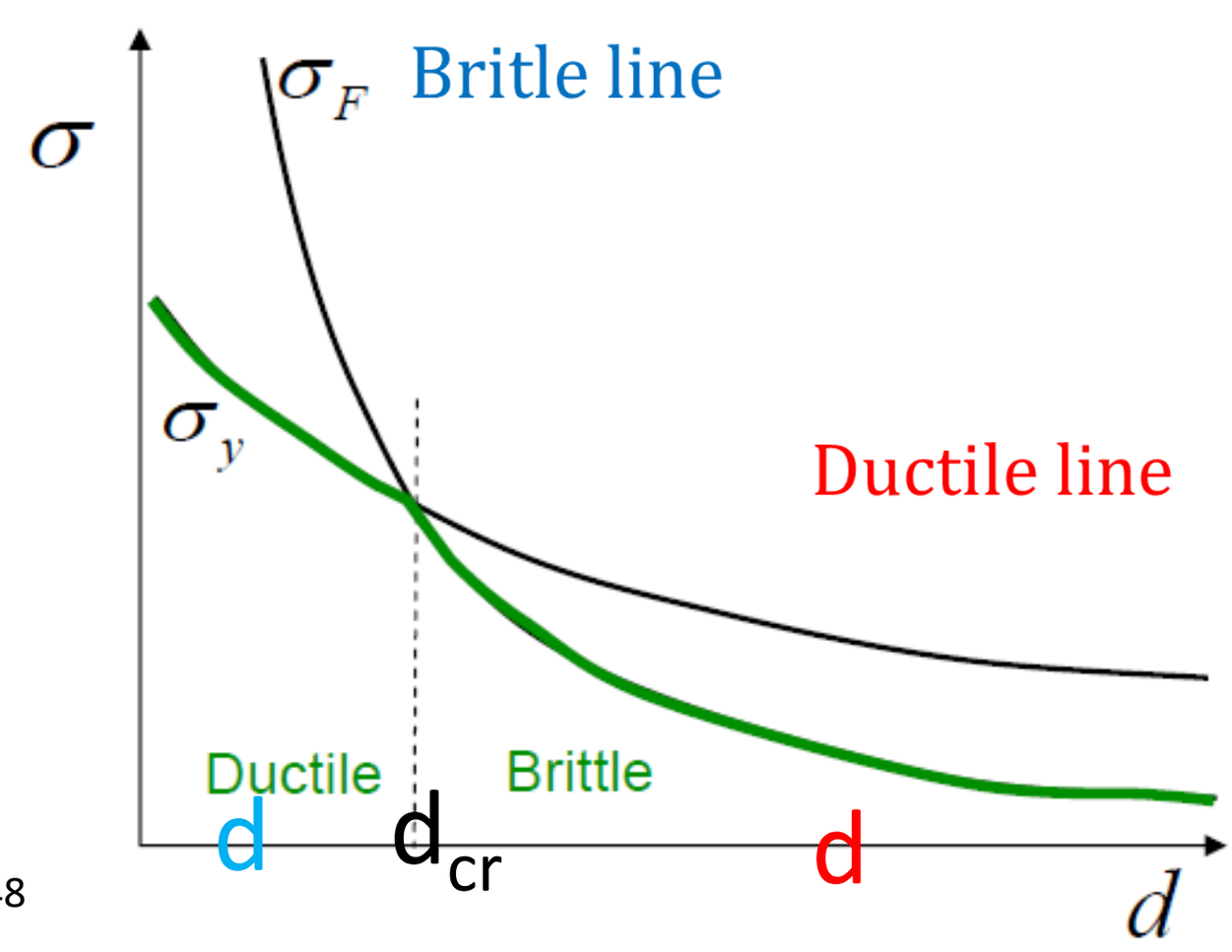

DBTT relation to grain size analysis

T ↘: T →T − ΔT

1. σ_y↗ $(\sigma_y = a_0 + \frac{k_y}{\sqrt{d}}, a_0 = Be^{-\beta T})$

2. $\sigma_f = \frac{1}{d}\sqrt{\frac{EG_c}{\pi}}$ ↘ because G_c↘

dcr ↘ ⇨
material becomes more brittle

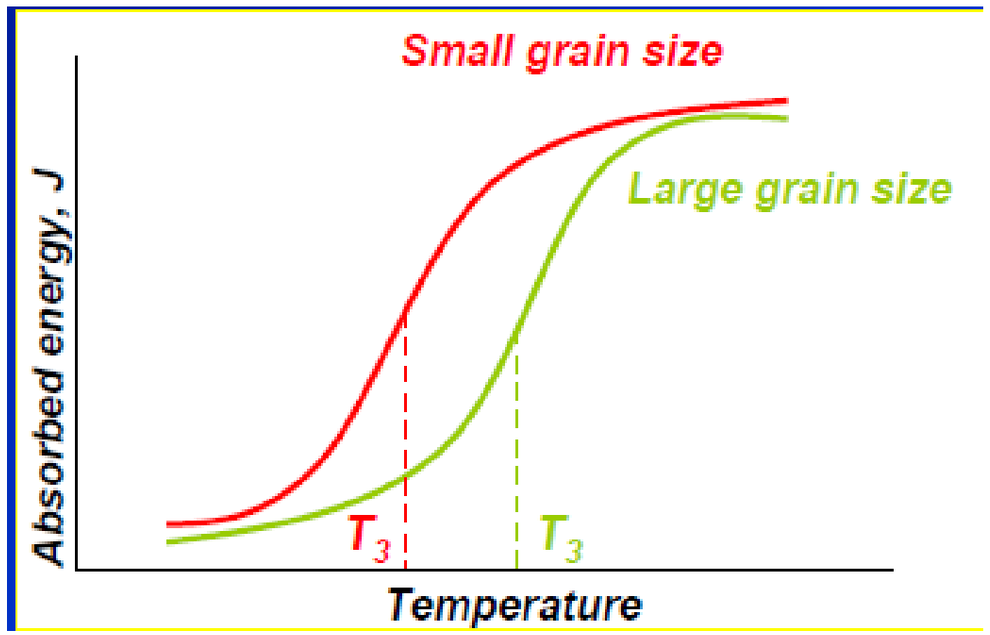

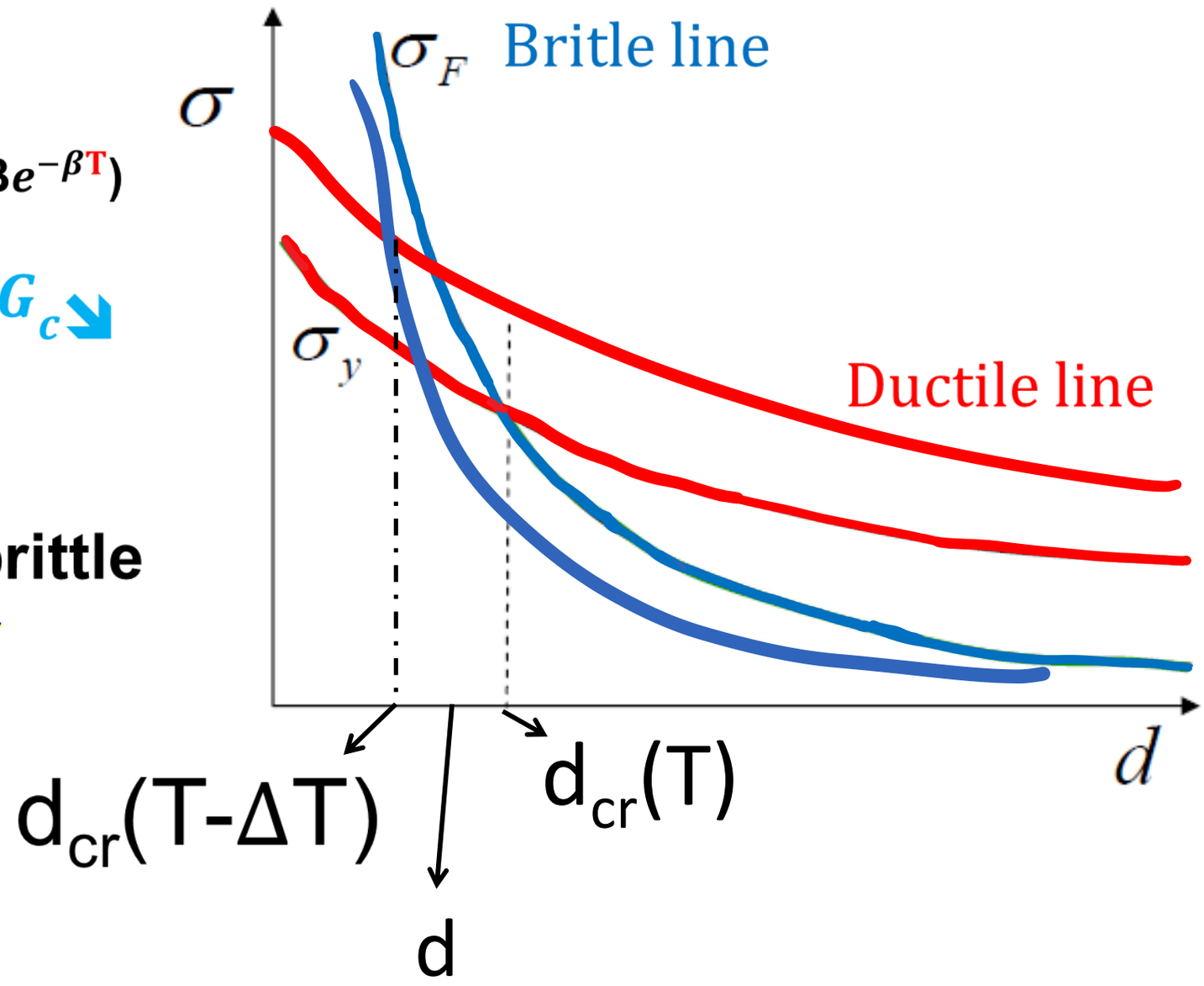

Example:
Consider sample grain size d shown

- At T it is in ductile mode
- At T − ΔT it is in ductile mode

6.Size effect and embrittlement

- Experiment tests: scaled versions of real structures
- The result, however, depends on the size of the specimen that was tested
- From experiment result to engineering design: knowledge of size effect required

- The size effect is defined by comparing the nominal strength (nominal stress at failure) σ_N of geometrically similar structures of different sizes.
- Classical theories (elastic analysis with allowable stress): cannot take size effect into account
- LEFM: strong size effect

- Size effect is crucial in concrete structures (dam, bridges), geomechanics (tunnels): laboratory tests are small
- Size effect is less pronounced in mechanical and aerospace engineering the structures or structural components can usually be tested at full size.

geometrically similar structures of different sizes

$$\sigma_N = \frac{c_N P}{bD}$$

b is thickness

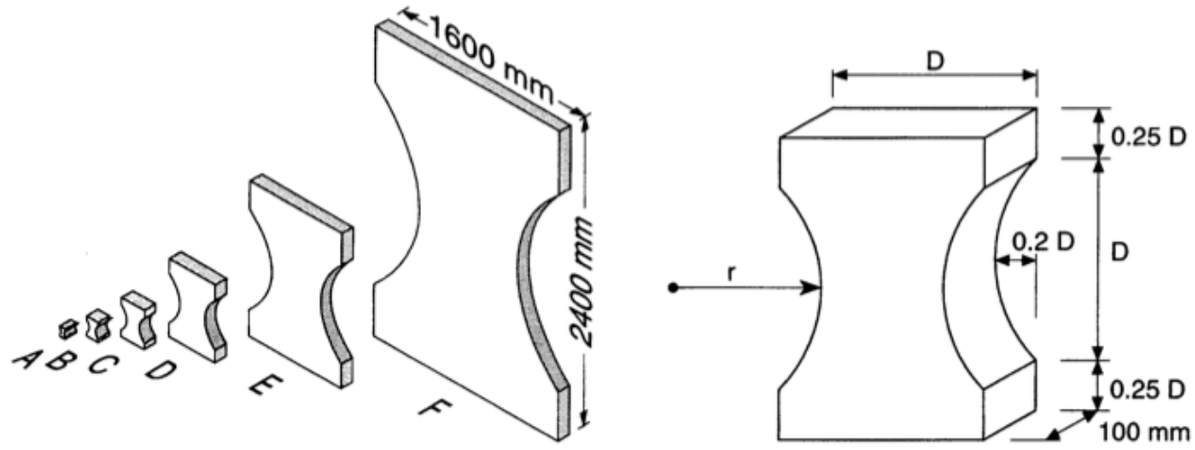

Fig. 1. Specimens with sizes in a scale range of 1:32 and specimen proportions.

type	A	B	C	D	E	F
D [mm]	50	100	200	400	800	1600
r [mm]	36.25	72.5	145	290	580	1160

Structures and tests

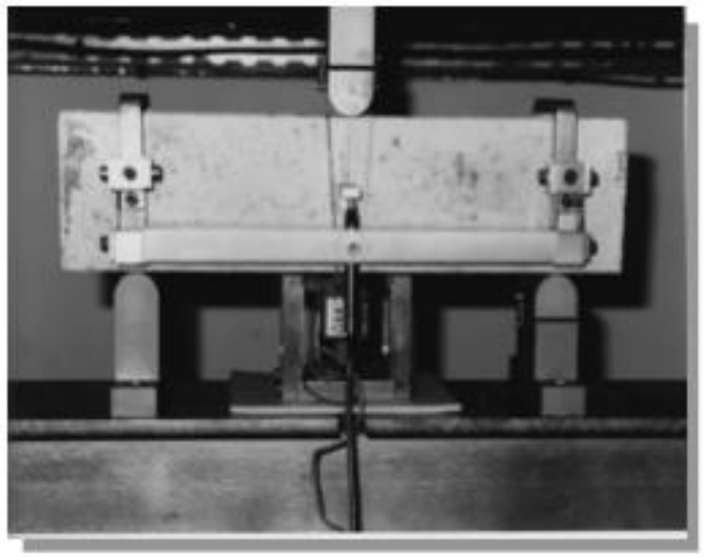

Usual lab tests (10 cm)

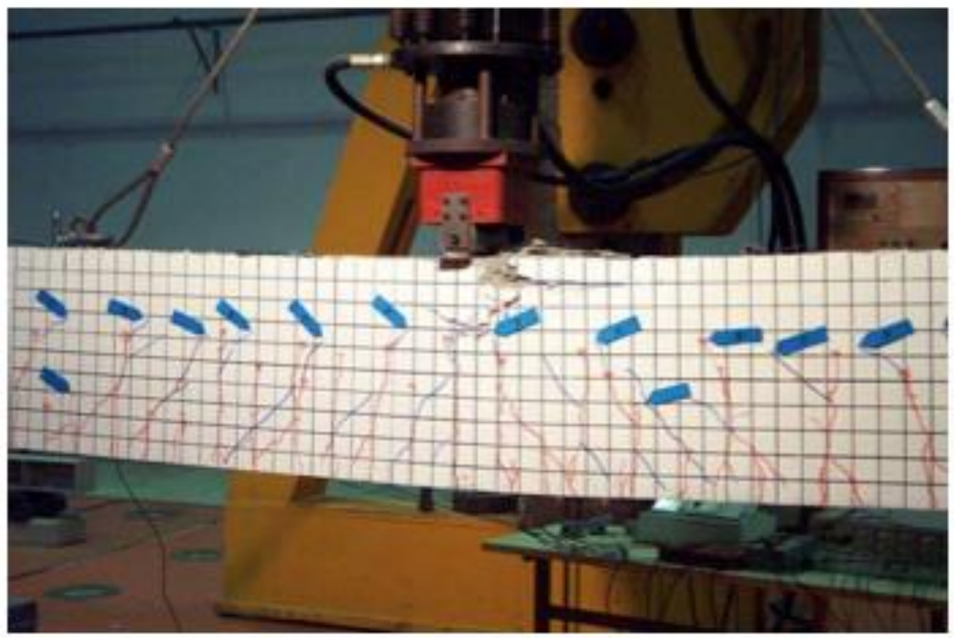

Unusual lab tests (1m)

"Usual" structures (10m)

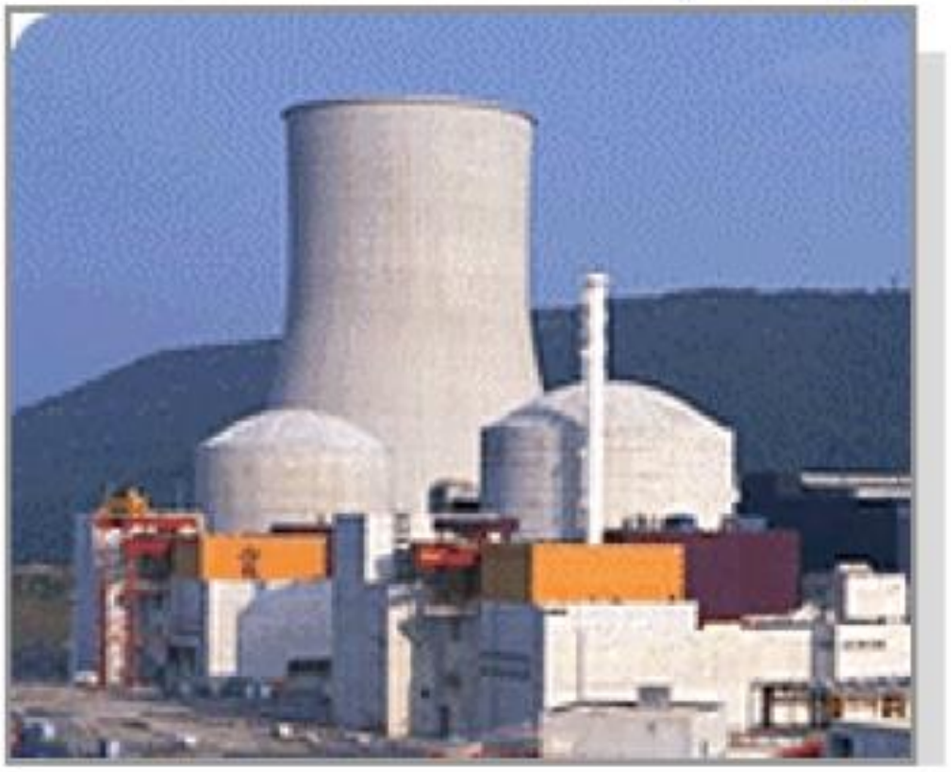

Size effect (cont.)

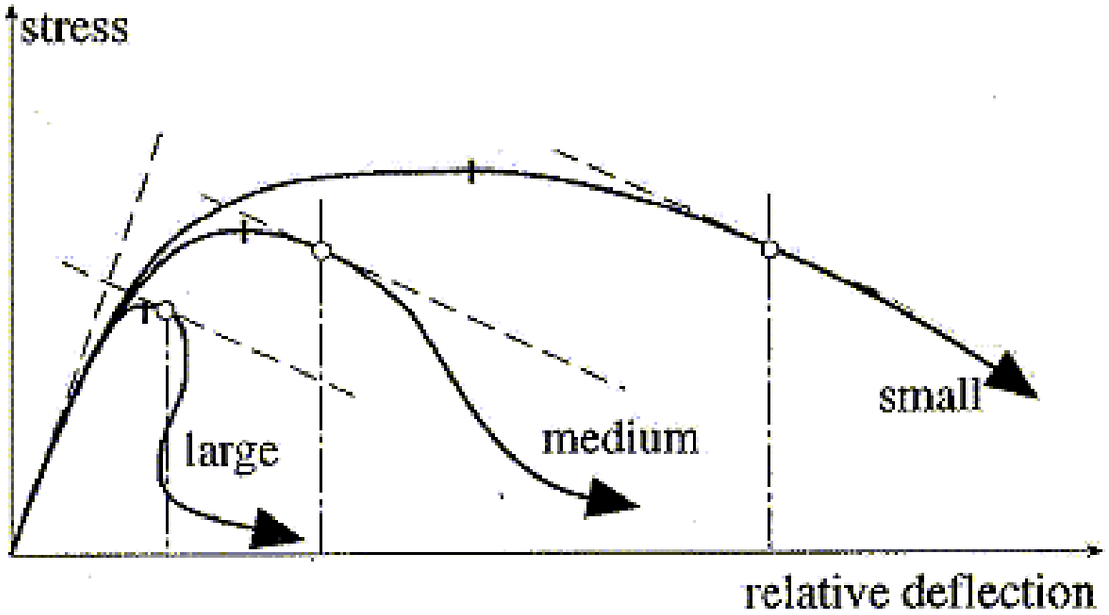

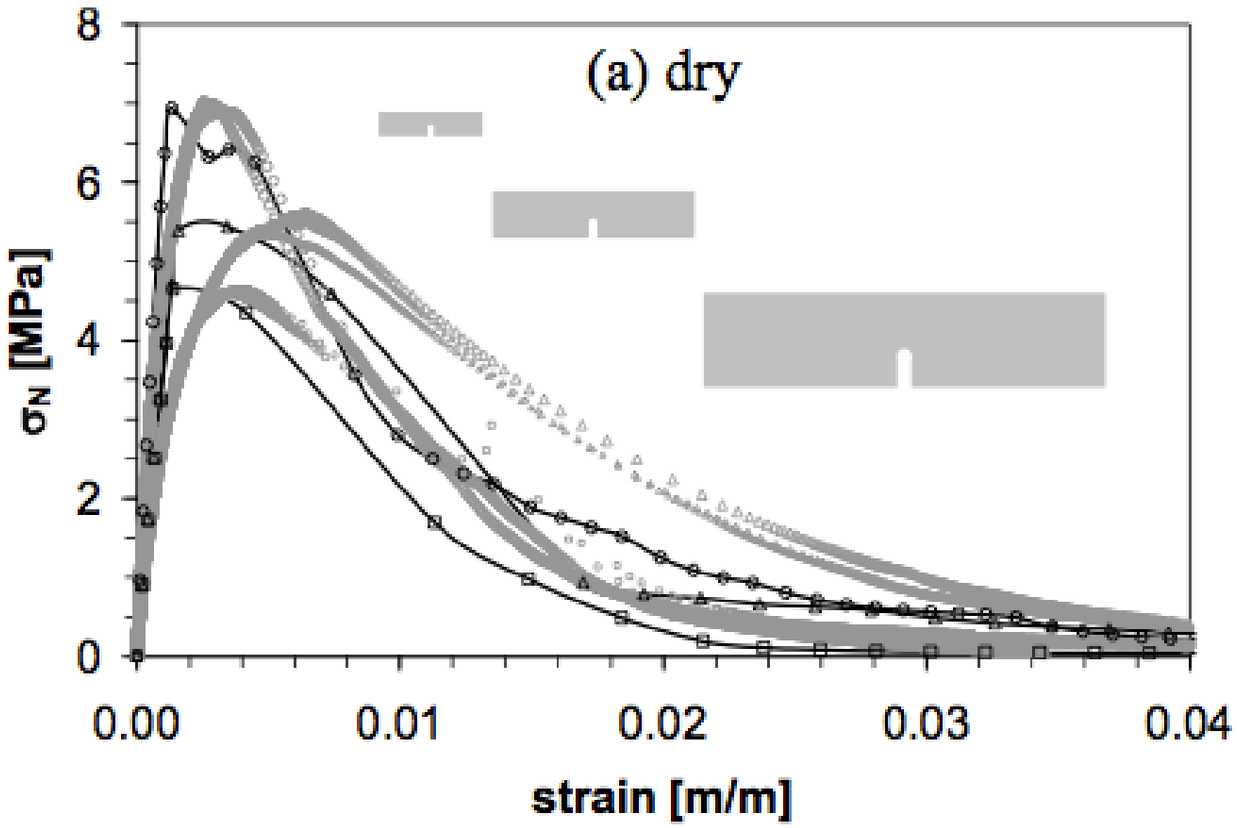

1. Large structures are softer than small structures.
2. A large structure is more brittle and has a lower strength than a small structure.

Size effect

$$\sigma_N = f_t = f_t(D)^0$$

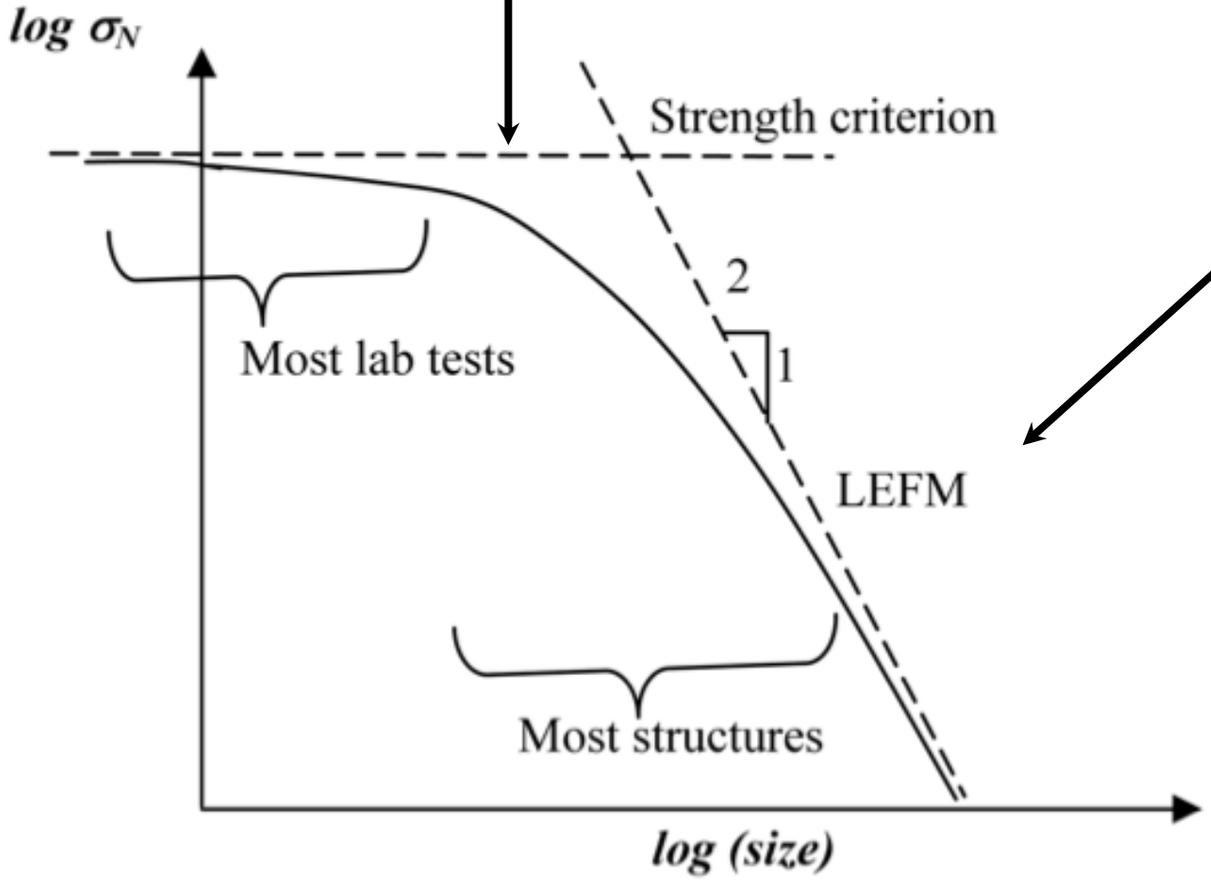

$$\sigma_N = \frac{K_{Ic}}{\sqrt{\pi a}} = \frac{K_{Ic}}{\sqrt{\pi c_N D}}$$

Larger size ⇨
More brittle

For very small structures the curve approaches the horizontal line and, therefore, the failure of these structures can be predicted by a strength theory. On the other hand, for large structures the curve approaches the inclined line and, therefore, the failure of these structures can be predicted by LEFM.

Bazant's size effect law

$$(\sigma_N)_u = A f_t \left(1 + \frac{W}{B}\right)^{-1/2} \tag{14.8}$$

where

$(\sigma_N)_u$ = Nominal stress at failure of a structure of specific shape and loading condition.

W = Characteristic length of the structure.

A, B = Positive constants that depend on the fracture properties of the material and on the shape of the structure, but not on the size of the structure.

f_t = Tensile strength of the material introduced for dimensional purposes.

7. Rate effects on ductility

- Same materials that show temperature toughness sensitivity (BCC metals) show high rate effect
- Polymers are highly sensitive to strain rate (especially for T > glass transition temperature)
- Strain rate ↗
  1. Strength ↗
  2. Ductility ↘

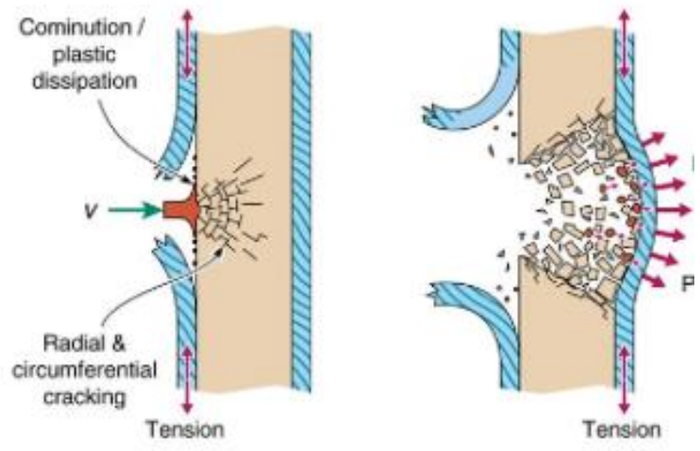

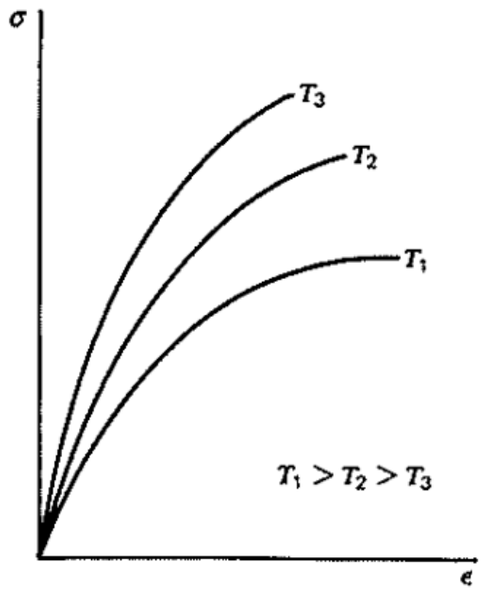

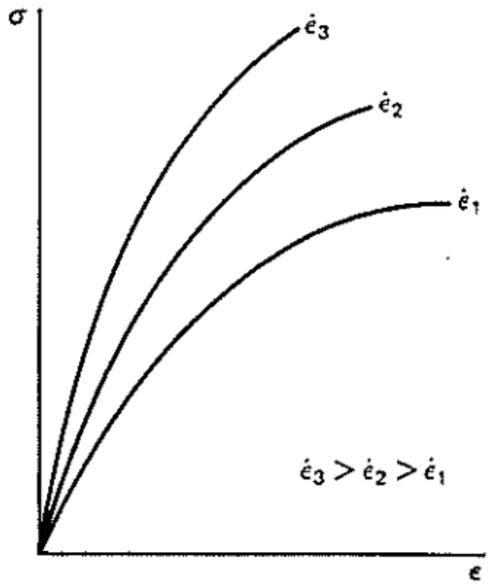

Strain rate ↗ similar to T ↘

Plastic

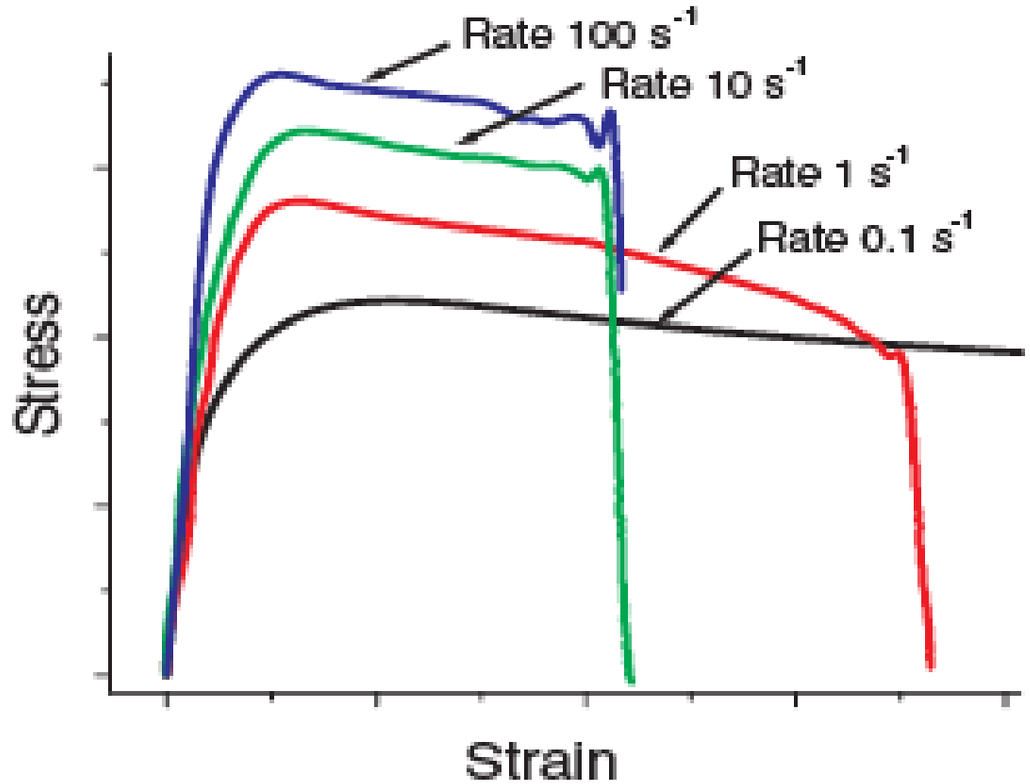

Strain rate effects on Impact toughness

Strain rate ↗ ⇨

DBTT ↗ (more brittle in impact)

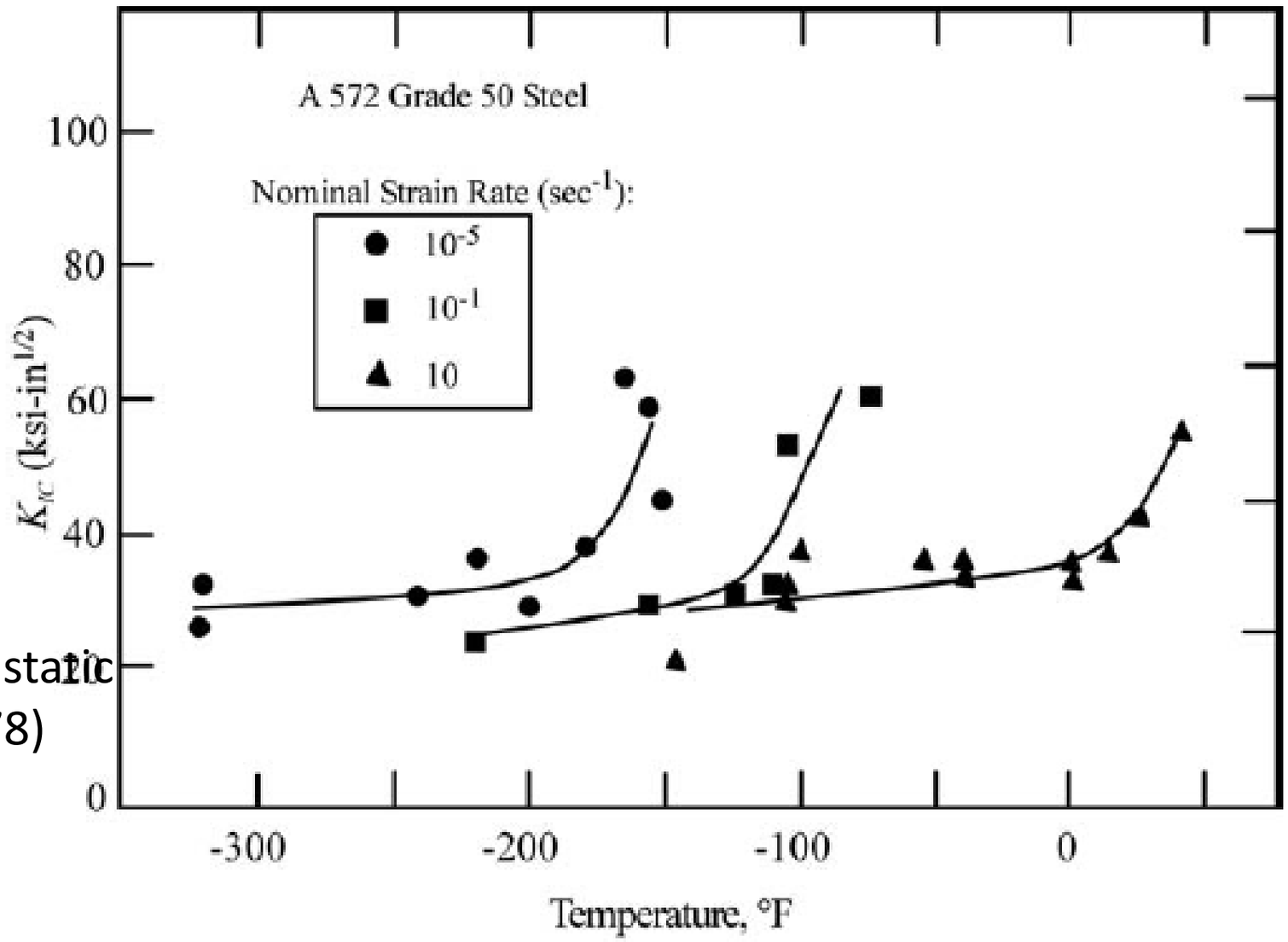

Ki Computed using quasistatic relations (Anderson p.178)

FIGURE 4.5 Effect of loading rate on the cleavage fracture toughness of a structural steel. Taken from Barsom, J.M., "Development of the AASHTO Fracture Toughness Requirements for Bridge Steels." *Engineering Fracture Mechanics,* Vol. 7, 1975, pp. 605–618.

Strain rate effects on crack resistance

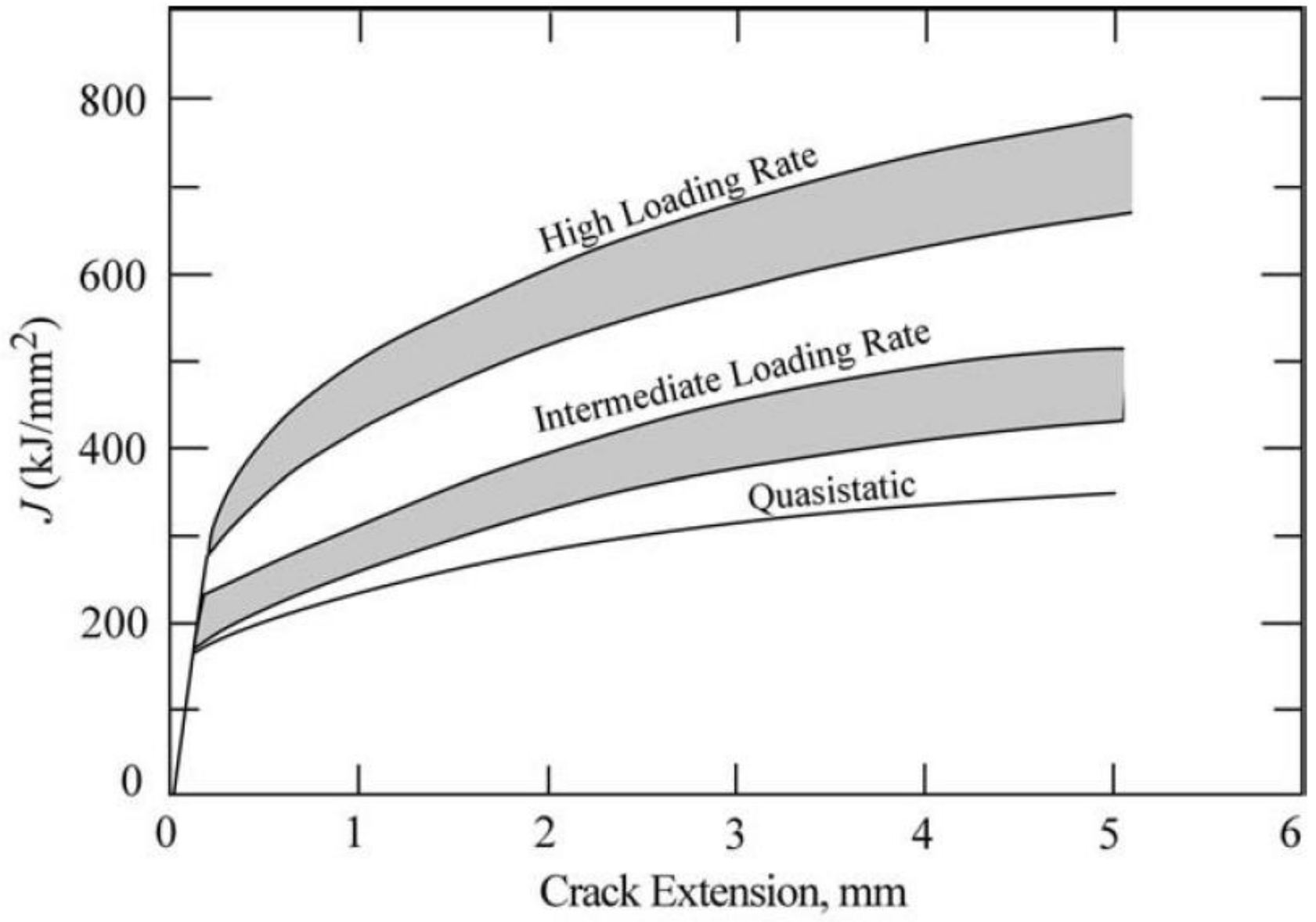

- Strain rate ↗
- J ↗ (upper shelf of toughness; opposite to impact toughness):
  - Ductile fracture of metals is primarily strain controlled.
  - J integral is elevated by high strain rates

Crack speed effect on dynamic crack propagation resistance

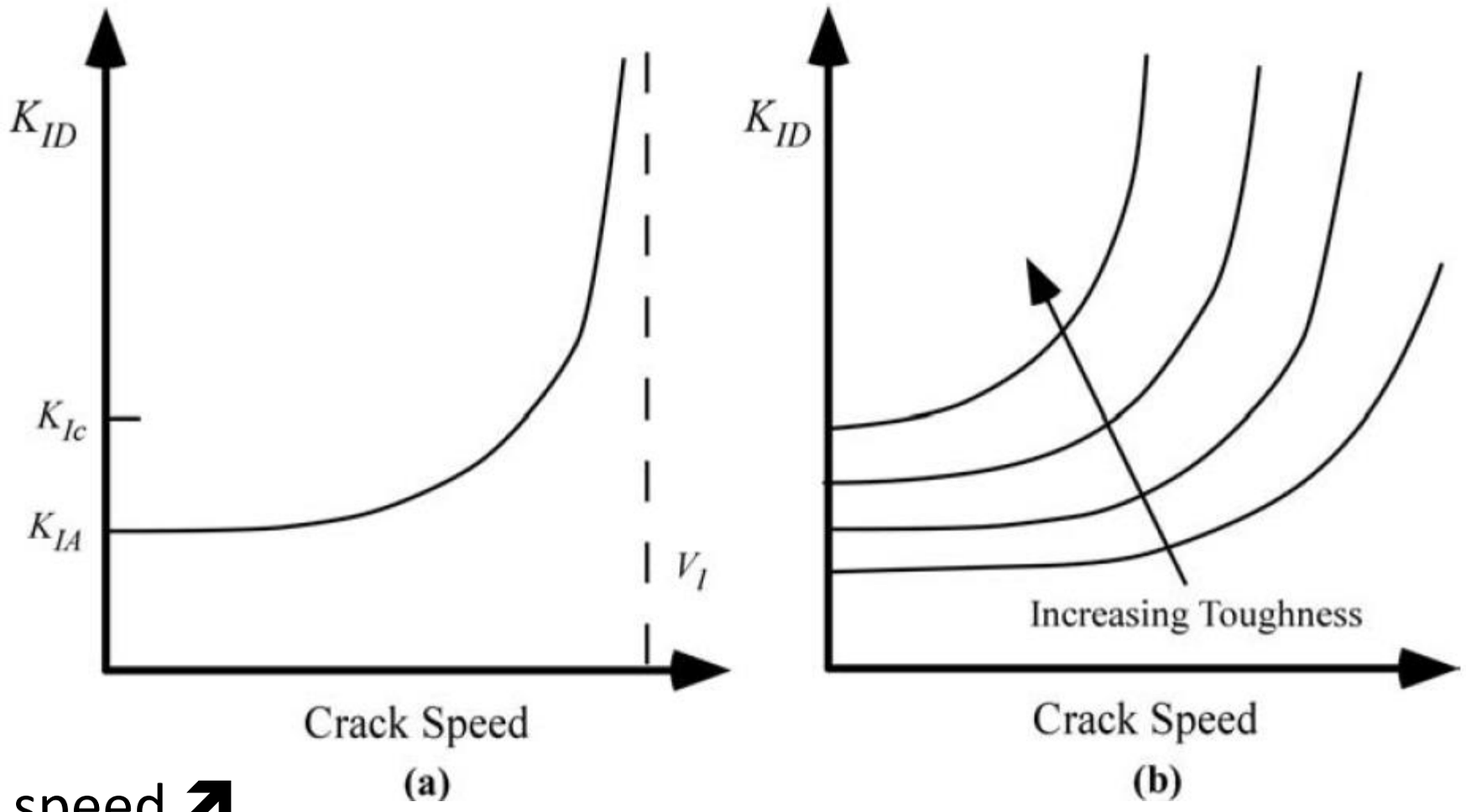

- Strain speed ↗
- K_{ID} ↗ (Insensitive at low speeds, quick increase approaching V_I)
- Increasing toughness makes K_{ID} more sensitive and grow faster

$$K_{ID} = \frac{K_{IA}}{1 - \left(\frac{V}{V_I}\right)^m}$$

8. Triaxial stress and confinement

Effect of specimen thickness

• ***Larger specimen size*** (in-service components) provides higher constraint → ***more brittle***.

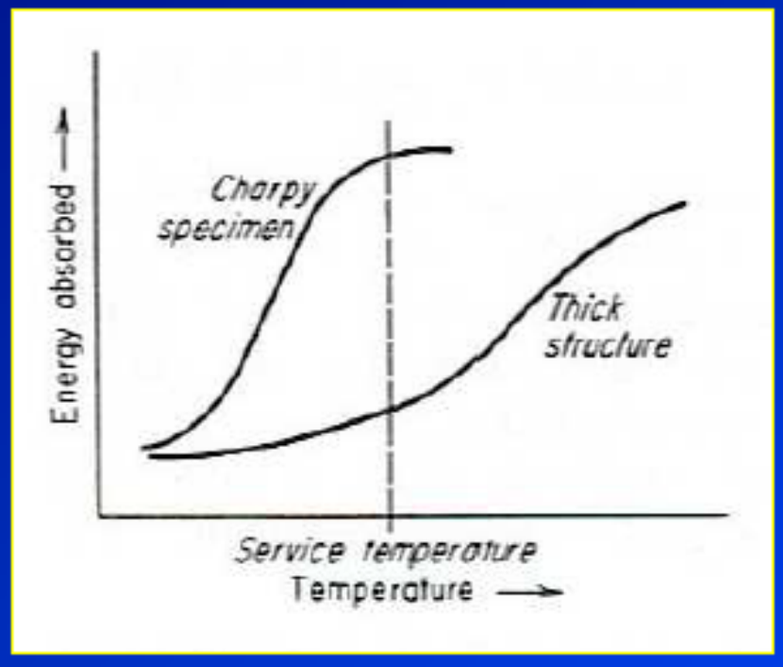

Effect of section thickness on transition temperature

If large size specimens are used, the transition temperature will increase.

Large scale tests

Source: Tapany Udomphol, Suranaree University of Technology
http://eng.sut.ac.th/metal/images/stories/pdf/14_Brittle_fracture_and_impact_testing_1-6.pdf

Ductile to brittle transition

Often hardening (increasing strength) reduces ductility

Phenomena affecting ductile/brittle response

1. T (especially for BCC metals and ceramics)
2. Impurities and alloying
3. Radiation
4. Hydrogen embrittlement
5. Grain size
6. Size effect
7. Rate effect
8. Confinement and triaxial stress state

Decreasing grain size is the only mechanism that hardens and promotes toughness

4. Linear Elastic Fracture Mechanics (LEFM)

4.1Griffith energy approach

Atomistic view of fracture

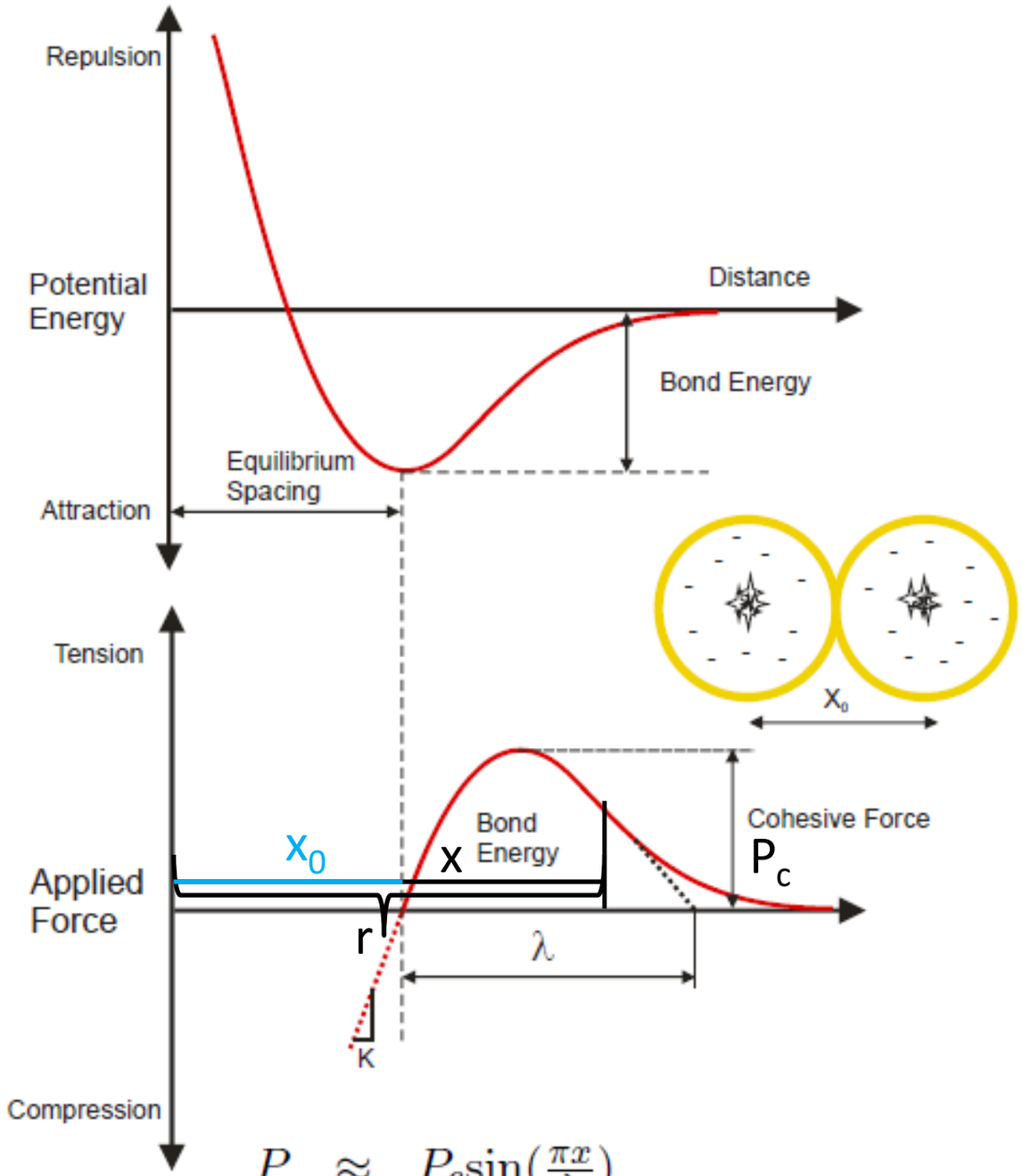

$$\mathbf{P} = -\frac{\partial \Pi_a}{\partial \mathbf{r}} \quad \Rightarrow \quad P = \frac{\partial \Pi_a}{\partial r} \text{ (1D)}$$

- P: Force between atoms (tensile positive cancels - sign)
- Position r: Distance from other atom
- x_0: Equilibrium position, $P = \frac{\partial \Pi_a}{\partial r} = 0$
- Displacement $x = r - x_0$.
- λ: Length scale where atomistic force is too small.
- P_c: Max force at $\frac{\partial^2 \Pi_a}{\partial r^2} = 0$.

$$\left.\begin{array}{l} \text{Atomistic:} \\ x_0 \\ \lambda \\ P_c \end{array}\right\} \Rightarrow \left\{\begin{array}{l} \text{Continuum:} \\ E \\ \gamma_c \text{(surface energy)} \end{array}\right.$$

$$\left.\begin{array}{rcl} P & \approx & P_c \sin(\frac{\pi x}{\lambda}) \\ \sigma & = & \frac{nP}{A} \\ \epsilon & = & \frac{x}{x_0} \\ n & = & \text{No. atoms in cross section area } A \end{array}\right\} \Rightarrow \begin{array}{rcl} \sigma_c & = & \frac{nP_c}{A} \\ \sigma & = & \sigma_c \sin(\frac{\pi \epsilon x_0}{\lambda}) \end{array}$$

Atomistic view of fracture

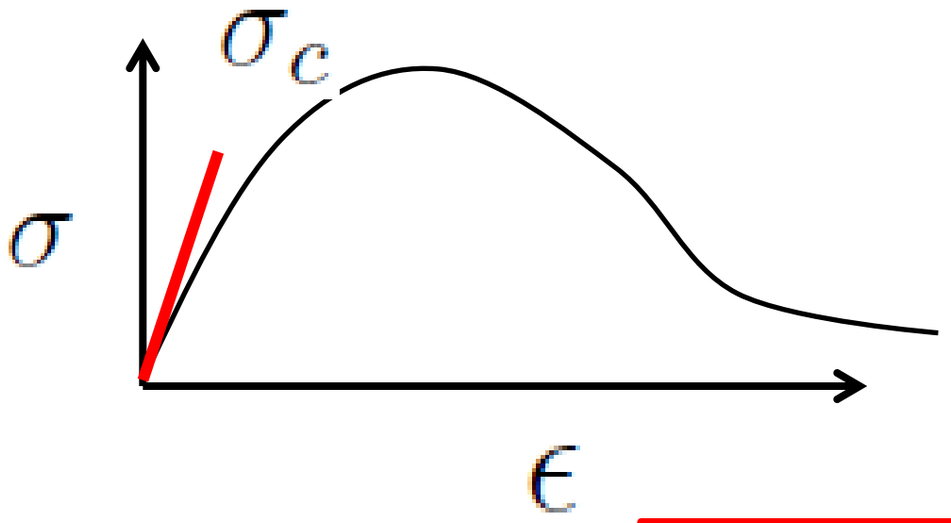

$$E = \frac{\partial \sigma}{\partial \epsilon}|_{\epsilon=0} = \sigma_c \frac{\pi x_0}{\lambda} \quad \Rightarrow \boxed{\sigma_c = \frac{E}{\pi}\frac{\lambda}{x_0} \approx \frac{E}{\pi}}$$

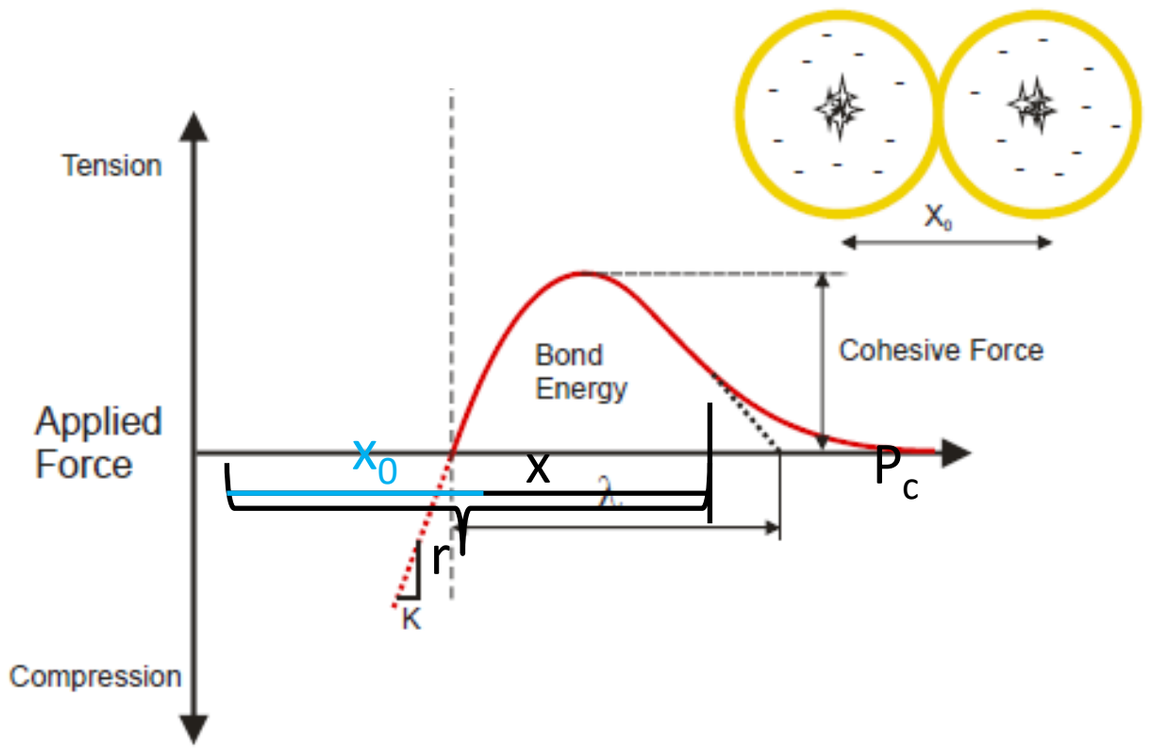

This is not realistic! For steel $\sigma_c \approx 250\text{MPa}$, $E = 200\text{GPa}$

Finally to compute surface energy γ_s:

$$W_s = \Sigma \int_0^\lambda P_i \mathrm{d}x = n \int_0^\lambda P_c \sin(\frac{\pi x}{\lambda}) = 2n\lambda P_c \ /\pi \Rightarrow (5)$$

$$\gamma_s = \frac{1}{2}\frac{W_s}{A} = \left(\frac{nP_c}{A}\right)\frac{\lambda}{\pi} \quad \Rightarrow \sigma_c = \sqrt{\frac{E\gamma_s}{x_0}} \qquad (6)$$

- W_s work of separation fo area section A
- Compare $\gamma_s = \frac{W_s}{A}$ with $\sigma = \frac{\Sigma P_i}{A}$
- Factor $\frac{1}{2}$: fracture generates two surfaces.

Summary

$$\boxed{\sigma_c = \frac{E}{\pi}\frac{\lambda}{x_0} \approx \frac{E}{\pi} \qquad \sigma_c = \sqrt{\frac{E\gamma_s}{x_0}}}$$

Cause: Stress Concentration!

Stress concentration

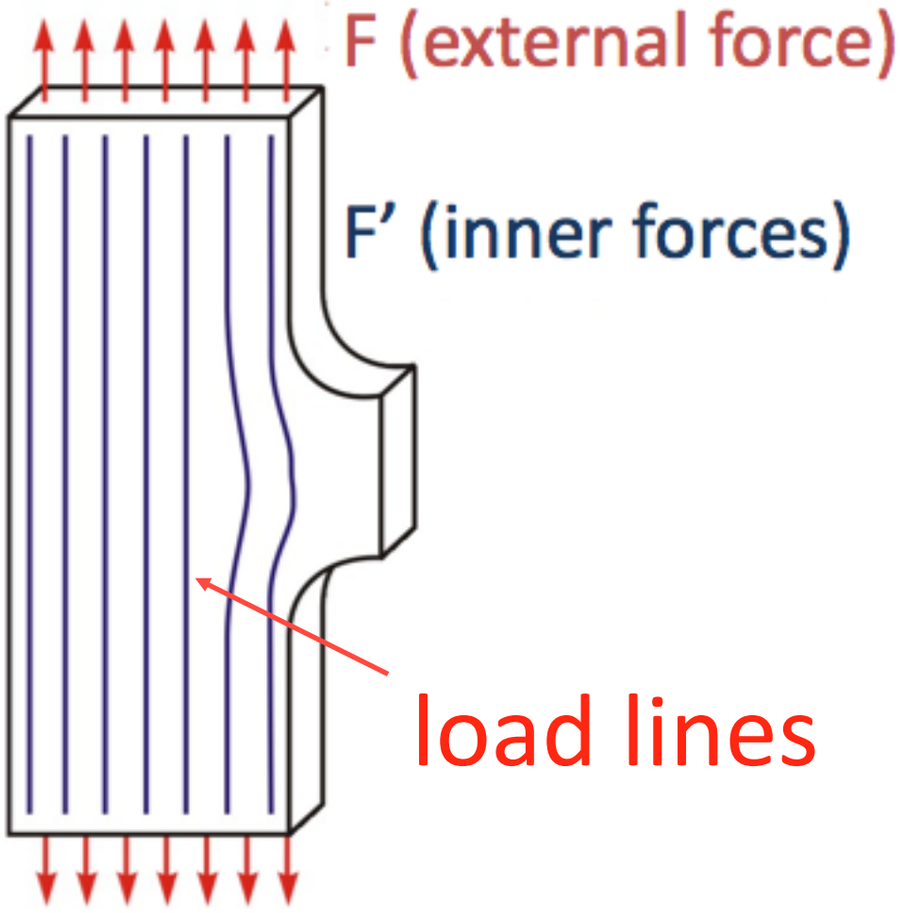

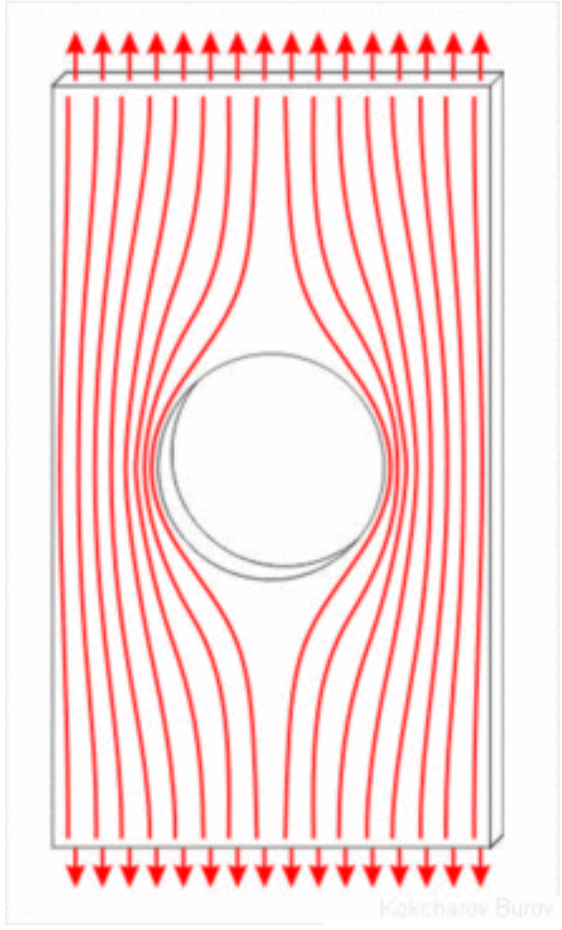

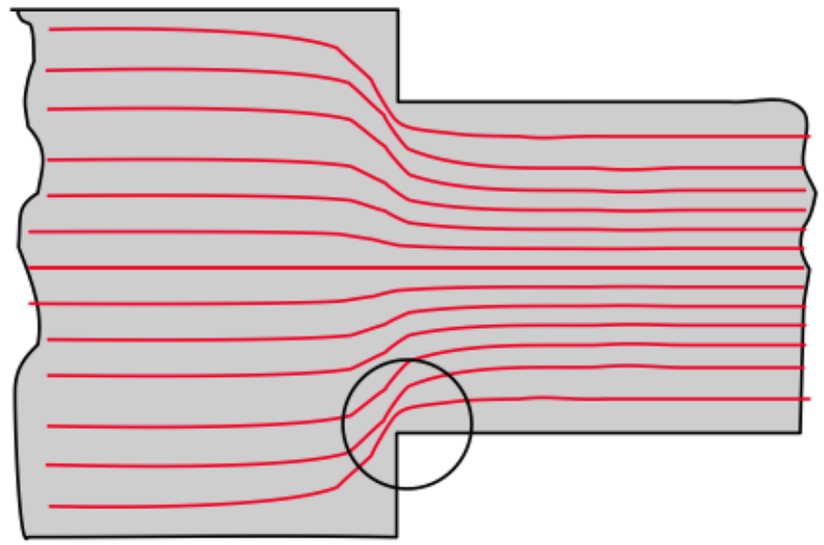

Geometry discontinuities: holes, corners, notches, cracks etc: stress concentrators/risers

Stress concentration (cont.)

uniaxial

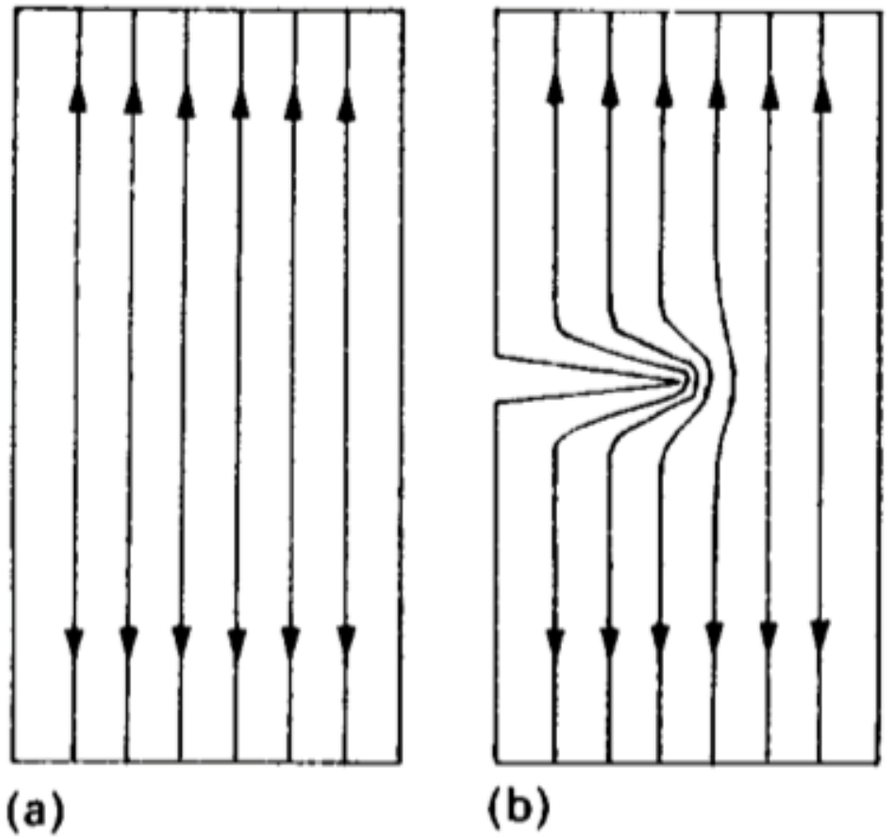

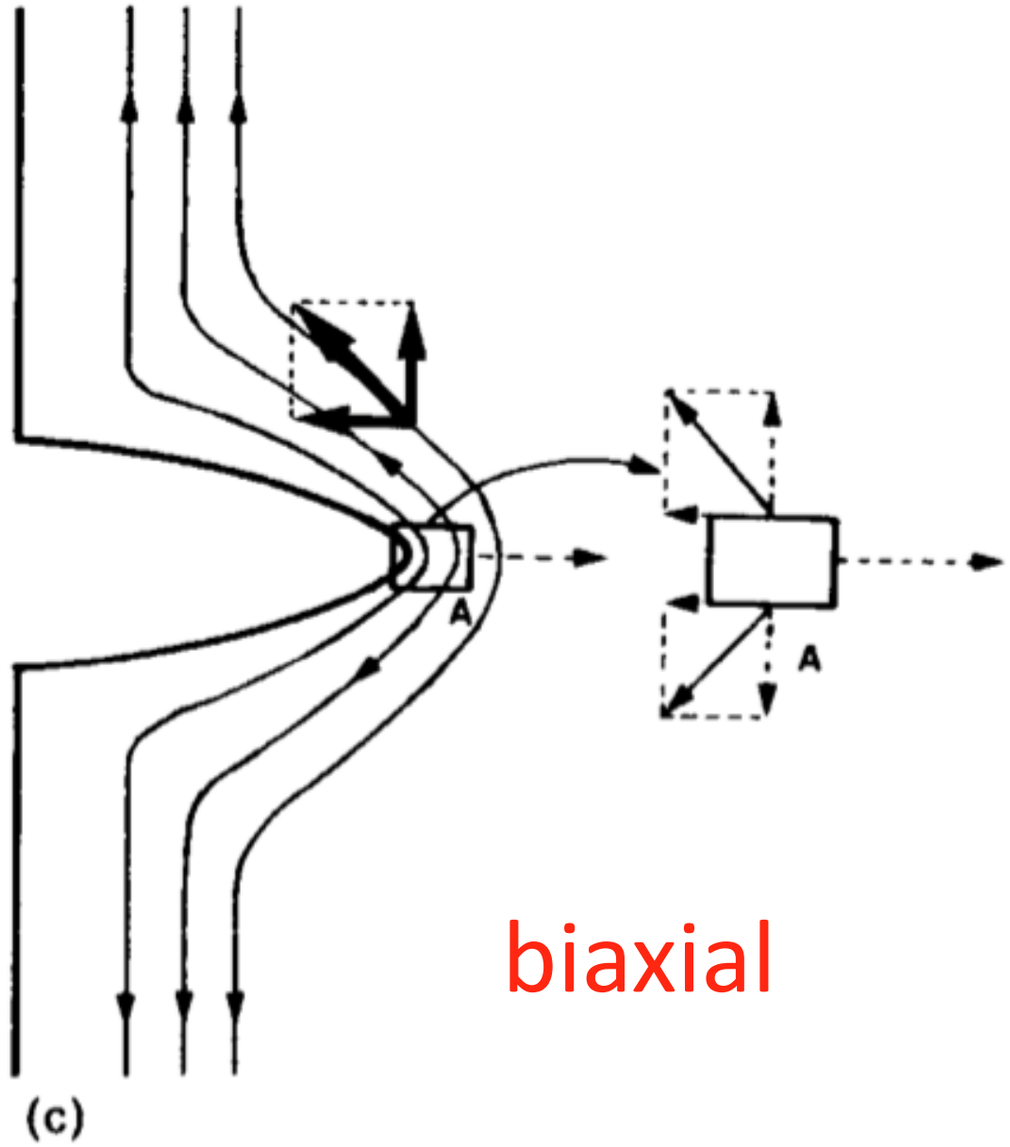

biaxial

Elliptic hole

Inglis, 1913, theory of elasticity

$$\sigma_A = \sigma\left(1 + \frac{2a}{b}\right)$$

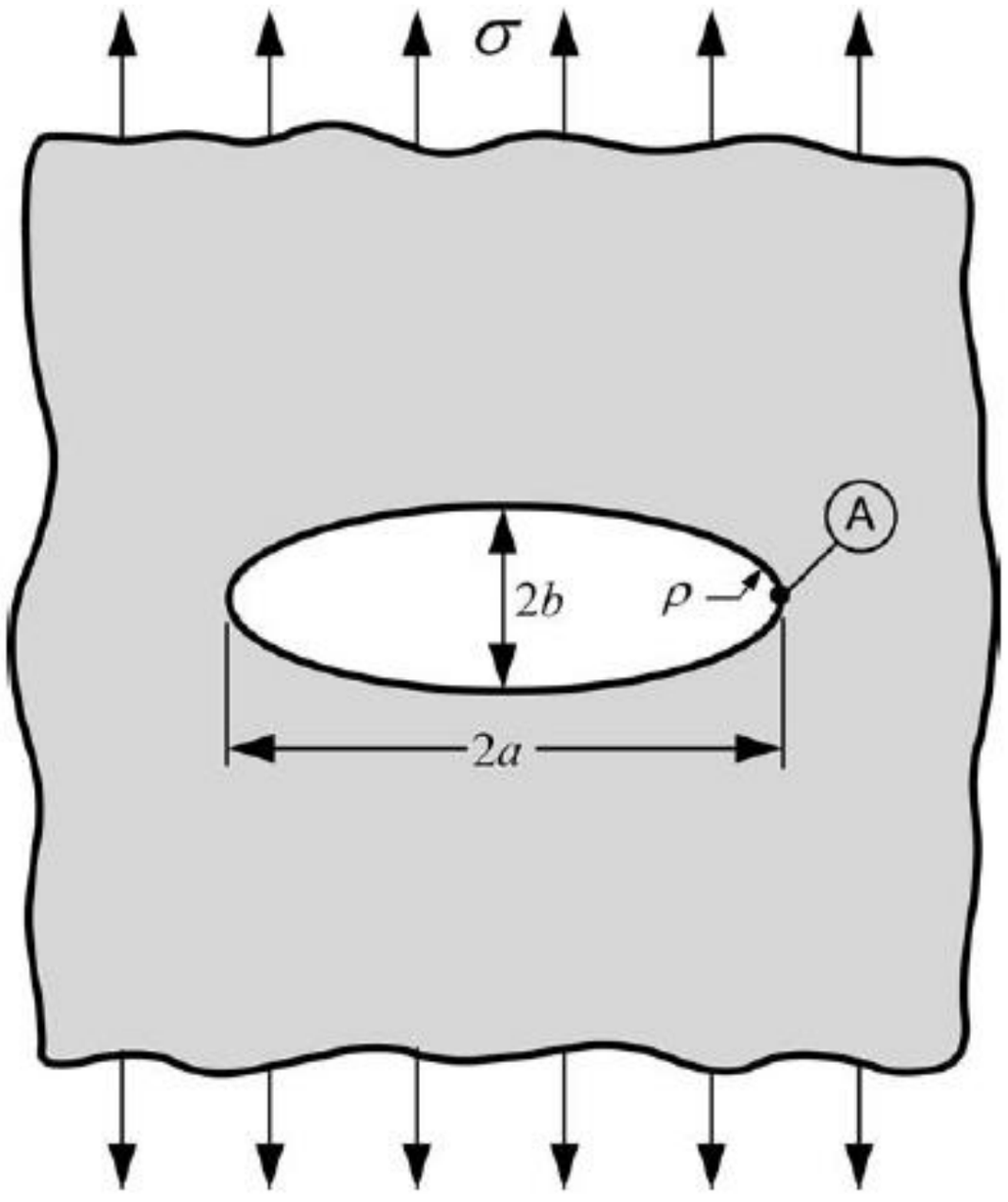

radius of curvature

$$\rho = \frac{b^2}{a}$$

$$\sigma_A = \sigma\left(1 + 2\sqrt{\frac{a}{\rho}}\right)$$

!!! ∞

stress concentration factor [-]

$$K = \frac{\sigma_A}{\sigma} = 1 + \frac{2a}{b}$$

Griffith's work (brittle materials)

FM was developed during WWI by English aeronautical engineer A. A. Griffith to explain the following observations:

- The stress needed to fracture bulk glass is around 100 MPa
- The theoretical stress needed for breaking atomic bonds is approximately 10,000 MPa
- experiments on glass fibers that Griffith himself conducted: the fracture stress increases as the fiber diameter decreases

=> Hence the uniaxial tensile strength, which had been used extensively to predict material failure before Griffith, could not be a specimen-independent material property.

Griffith suggested that the low fracture strength observed in experiments, as well as the size-dependence of strength, was due to the presence of **microscopic flaws** in the bulk material.

Griffith's size effect experiment

TABLE 1.1. Strength of glass fibers according to Griffith's experiments.

Diameter (10^{-3} in)	Breaking stress (lb/in^2)	Diameter (10^{-3} in)	Breaking stress (lb/in^2)
40.00	24 900	0.95	117 000
4.20	42 300	0.75	134 000
2.78	50 800	0.70	164 000
2.25	64 100	0.60	185 000
2.00	79 600	0.56	154 000
1.85	88 500	0.50	195 000
1.75	82 600	0.38	232 000
1.40	85 200	0.26	332 000
1.32	99 500	0.165	498 000
1.15	88 700	0.130	491 000

"the weakness of isotropic solids... is due to the presence of discontinuities or flaws... The effective strength of technical materials could be increased 10 or 20 times at least if these flaws could be eliminated."

Fracture stress: discrepancy between theory and experiment

$$\sigma_{th} = \sqrt{\frac{E\gamma}{a_0}}$$

	a_0 [m]	E [GPa]	σ_{th} [GPa]	σ_b [MPa]	σ_{th}/σ_b
glass	$3 * 10^{-10}$	60	14	170	82
steel	10^{-10}	210	45	250	180
silica fibers	10^{-10}	100	31	25000	1.3
iron whiskers	10^{-10}	295	54	13000	4.2
silicon whiskers	10^{-10}	165	41	6500	6.3
alumina whiskers	10^{-10}	495	70	15000	4.7
ausformed steel	10^{-10}	200	45	3000	15
piano wire	10^{-10}	200	45	2750	16.4

Cause of discrepancy:
1. Stress approach

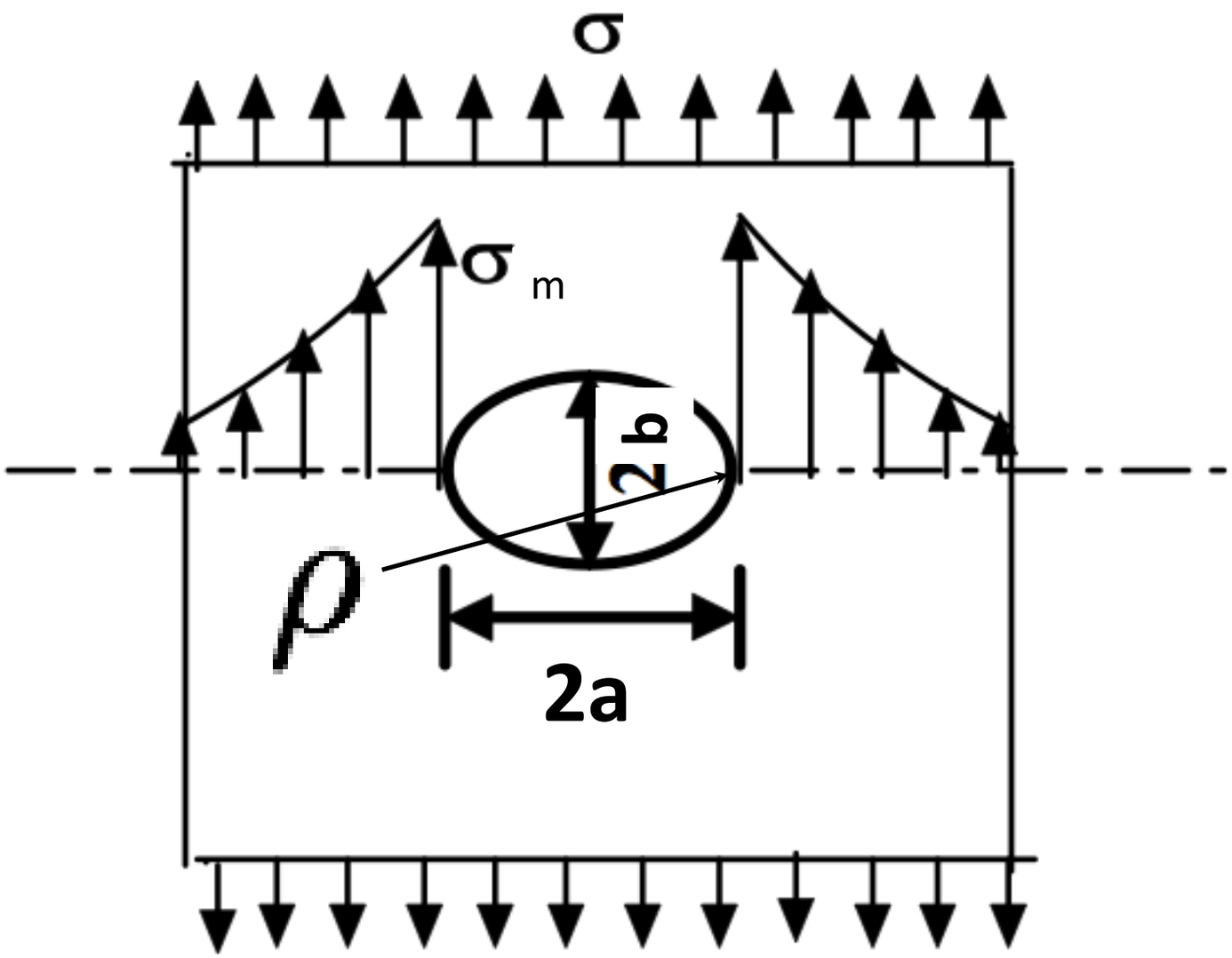

- For a large domain $(L, W \ll a)$, crack length $2a$, & radius of curvature $\rho \ll a$:

$$\sigma_m = \sigma\left(1 + 2\sqrt{\frac{a}{\rho}}\right) \approx 2\sigma\sqrt{\frac{a}{\rho}}$$

- For *effective remote stress at failure* $\sigma = \sigma_f$, σ_m is equal to atomistic based σ_c:

$$\sigma_c = 2\sigma_f\sqrt{\frac{a}{\rho}} \qquad \sigma_f = \sqrt{\frac{E\gamma_s}{4a}\frac{\rho}{x_0}}$$

- If we assume the crack is sharp at atomistic level $\rho \approx x_0$ we get,

$$\sigma_f = \sqrt{\frac{E\gamma_s}{4a}}$$

Atomistic: $\sigma_c = \sqrt{\frac{E\gamma_s}{x_0}}$ $\Leftrightarrow$ Continuum with sharp crack $2a$: $\sigma_f = \sqrt{\frac{E\gamma_s}{4a}} \Rightarrow$

$$\frac{\sigma_f}{\sigma_c} = \sqrt{\frac{x_0}{4a}}$$

Griffith's verification experiment

- Glass fibers with artificial cracks (much larger than natural crack-like flaws), tension tests

	Crack Length, $2a$ mm	Measured Strength, σ_f MPa	$\sigma_f\sqrt{a}$ MPa$\sqrt{\text{m}}$
sample 1	3.8	6.0	0.26
sample 2	6.9	4.3	0.25
sample 3	13.7	3.3	0.27
sample 4	22.6	2.5	0.27

(Data from the Griffith experiment)

$$\sigma_f = \sqrt{\frac{E\gamma_s}{4a}}$$

$$\sigma_f\sqrt{a} = \sqrt{\frac{E\gamma_s}{4}} = \text{const.}$$

4.1.3. Cause of discrepancy:

2. Energy approach

Energy balance during crack growth

kinetic energy

external work

$$\dot{W} = \dot{U}_e + \dot{U}_p + \dot{U}_k + \dot{U}_\Gamma$$

surface energy

internal strain energy

All changes with respect to time are caused by changes in crack size:

$$\frac{\partial(\cdot)}{\partial t} = \frac{\partial(\cdot)}{\partial a}\frac{\partial a}{\partial t}$$

Energy equation is rewritten:

$$\frac{\partial W}{\partial a} = \frac{\partial U_e}{\partial a} + \frac{\partial U_p}{\partial a} + \frac{\partial U_\Gamma}{\partial a}$$

slow process

It indicates that the work rate supplied to the continuum by the applied loads is equal to the rate of the elastic strain energy and plastic strain work plus the energy dissipated in crack propagation

Potential energy $\Pi = U_e - W$

$$-\frac{\partial \Pi}{\partial a} = \frac{\partial U_p}{\partial a} + \frac{\partial U_\Gamma}{\partial a}$$

Brittle materials: no plastic deformation

$$-\frac{\partial \Pi}{\partial a} = \frac{\partial U_\Gamma}{\partial a}$$

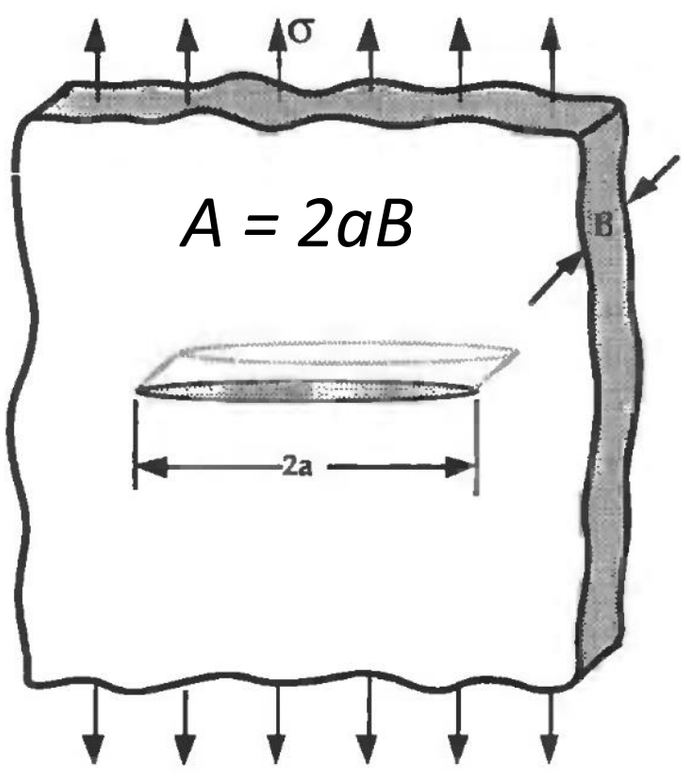

Griffith's through-thickness crack

γ_s is energy required to form a unit of new surface

[J/m2=N/m] $$-\frac{\partial \Pi}{\partial A} = 2\gamma_s$$ (two new material surfaces)

Inglis' solution $$\Pi(a) - \Pi(0) = -\frac{\pi \sigma^2 a^2 B}{E}$$

$$-\frac{\partial \Pi}{\partial A} = \frac{\pi \sigma^2 a}{E} \rightarrow \frac{\pi \sigma^2 a}{E} = 2\gamma_s \rightarrow \sigma_f = \sqrt{\frac{2E\gamma_s}{\pi a}}$$

(linear plane stress, constant load)

Comparison of stress & energy approaches

Stress approach:
Stress Concentration

$$\sigma_f = 0.5\sqrt{\frac{E\gamma_s}{a}}$$

Energy approach:
Griffith

$$\sigma_f = \sqrt{\frac{2}{\pi}}\sqrt{\frac{E\gamma_s}{a}} \approx 0.8\sqrt{\frac{E\gamma_s}{a}}$$

Energy equation for ductile materials

Plane stress

$$\sigma_c = \sqrt{\frac{2E\gamma_s}{\pi a}}$$

Griffith (1921), ideally brittle solids

$$\sigma_c = \sqrt{\frac{2E(\gamma_s + \gamma_p)}{\pi a}}$$

Irwin, Orowan (1948), metals

γ_p plastic work per unit area of surface created

$\gamma_p \gg \gamma_s$

$\gamma_p \approx 10^3 \gamma_s$ (metals)

Generalization of Energy equation

$$\sigma_f = \sqrt{\frac{2Ew_f}{\pi a}}$$

- w_f: Fracture energy from plastic, viscoelastic, or viscoplastic effects
- w_f can also be influenced by crack meandering and branching
- Caution: If nonlinear displacement regions are large enough this equation is not accurate as it is based on linear elastic solution ($\Pi = \Pi_0 - \frac{\pi\sigma^2 a^2 B}{E}$)

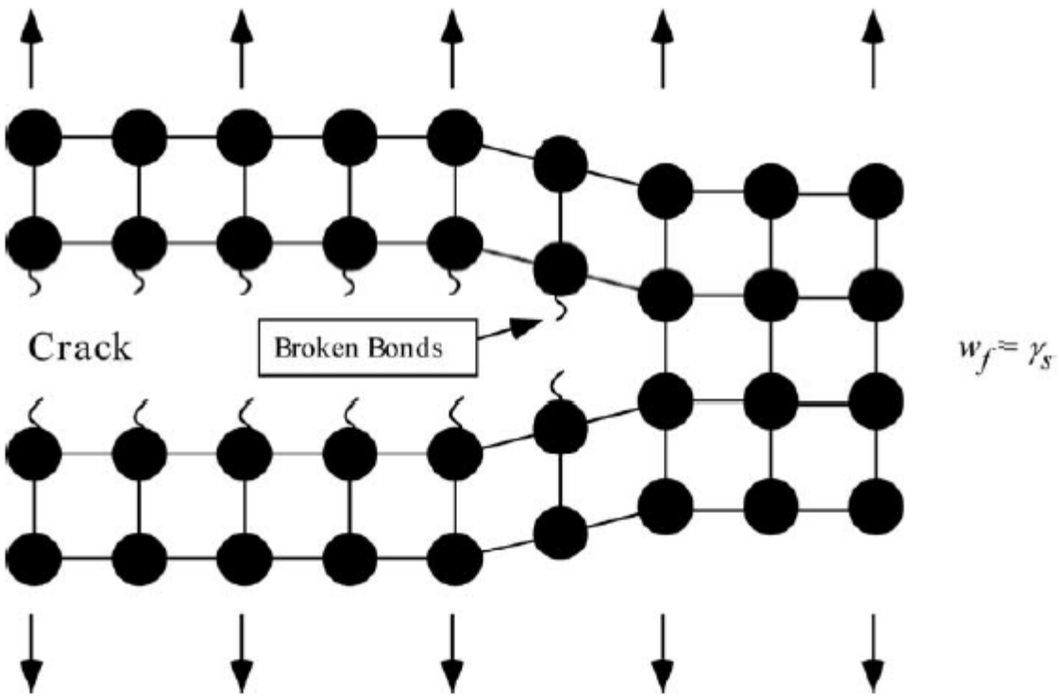

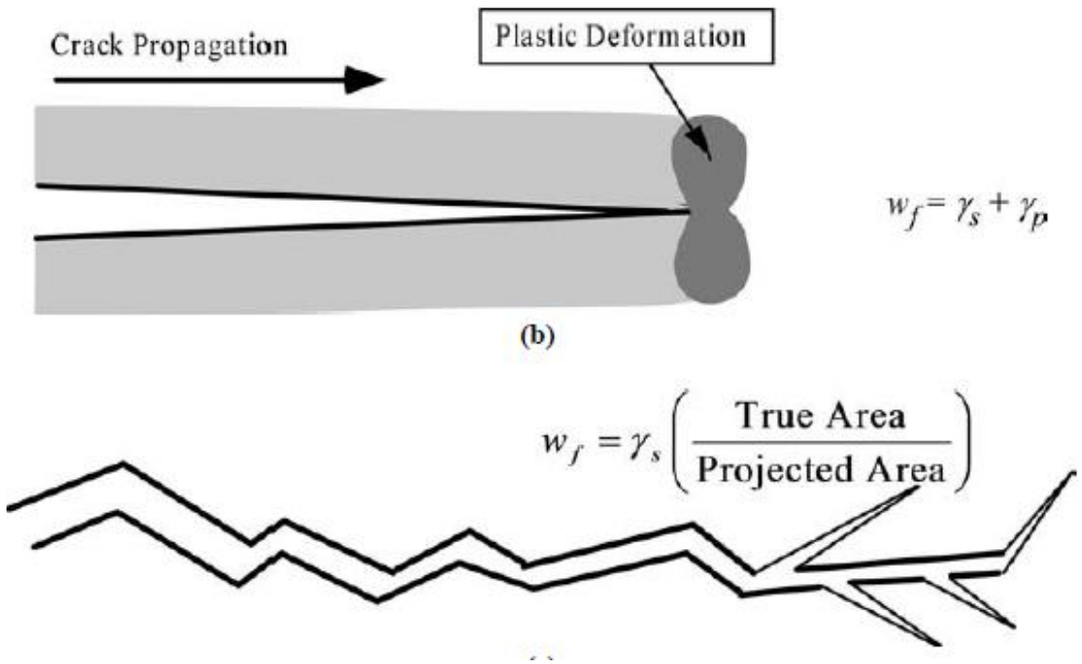

Energy release rate

Irwin 1956 $G \equiv -\frac{d\Pi}{dA}$ a.k.a Crack extension force
Crack driving force

G: Energy released during fracture per unit of newly created fracture surface area

$G = 2w_f$

the resistance of the material that must be overcome for crack growth

energy available for crack growth (crack driving force)

Energy release rate [failure criterion] $G \geq G_c$

fracture energy, considered to be a material property (independent of the applied loads and the geometry of the body).

Strain energy density

Consider a linear elastic bar of stiffness k, length L, area A, subjected to a force F, the work is

$$W = \int_0^u F du = \int_0^u k u du = \frac{1}{2} k u^2 = \frac{1}{2} F u$$

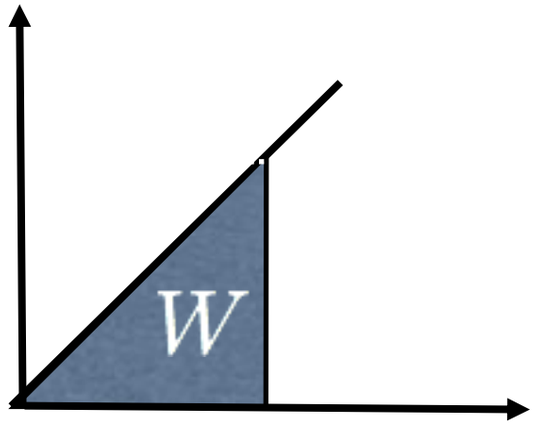

This work will be completely stored in the structure in the form of strain energy. Therefore, the external work and strain energy are equal to one another

$$\boxed{U = W = \frac{1}{2} F u}$$

In terms of stress/strain

$$\boxed{U = \frac{1}{2} F u = \frac{1}{2} \frac{F}{A} \frac{u}{L} AL}$$

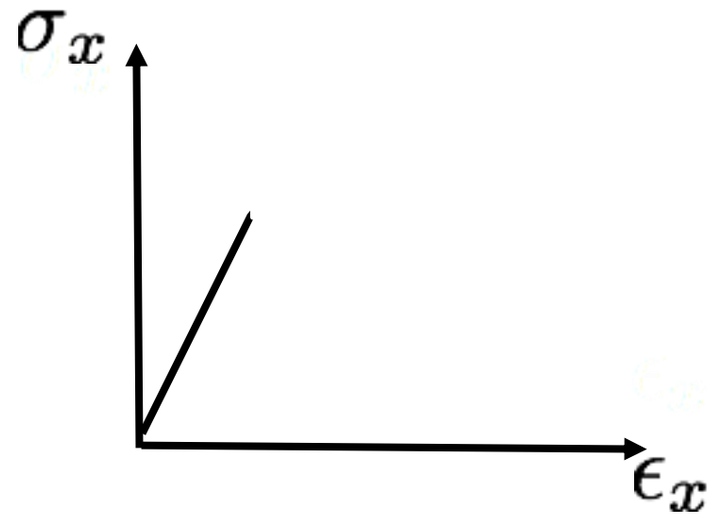

Strain energy density

$$u = \frac{1}{2} \sigma_x \epsilon_x \longrightarrow \boxed{u = \int \sigma_x d\epsilon_x}$$

$[\mathrm{J/m^3}]$

Strain energy density

Poisson's ratio

$$u = \frac{1}{2E}(\sigma_x^2 + \sigma_y^2 + \sigma_z^2) - \frac{\nu}{E}(\sigma_x\sigma_y + \sigma_y\sigma_z + \sigma_z\sigma_x) + \frac{1}{2\mu}(\tau_{xy}^2 + \tau_{yz}^2 + \tau_{zx}^2)$$

Plane problems

$$\mu = \frac{E}{2(1+\nu)}$$ shear modulus

$$u = \frac{1}{4\mu}\left[\frac{\kappa+1}{4}(\sigma_x^2 + \sigma_y^2) - 2(\sigma_x\sigma_y - \tau_{xy}^2)\right]$$

Kolosov coefficient

$$\kappa = \begin{cases} 3 - 4\nu & \text{plane strain} \\ \dfrac{3-\nu}{1+\nu} & \text{plane stress} \end{cases}$$

Evaluation of G

Given: A point load - displacement system with a crack and two data points:

- Load P_1, displacement u_1, & crack length a_1
- Load P_2, displacement u_2, & crack length $a_2 = a_1 + \Delta a$ (small Δa)

Goal: Compute G

Notation:

- W_{12}: External work from n_1 to n_2
- W_{o1} External work that would have happened through elastic (or almost elastic) deformation with fixed crack length from 0 to n_1.
- W_{o2} Similar to W_{o1}

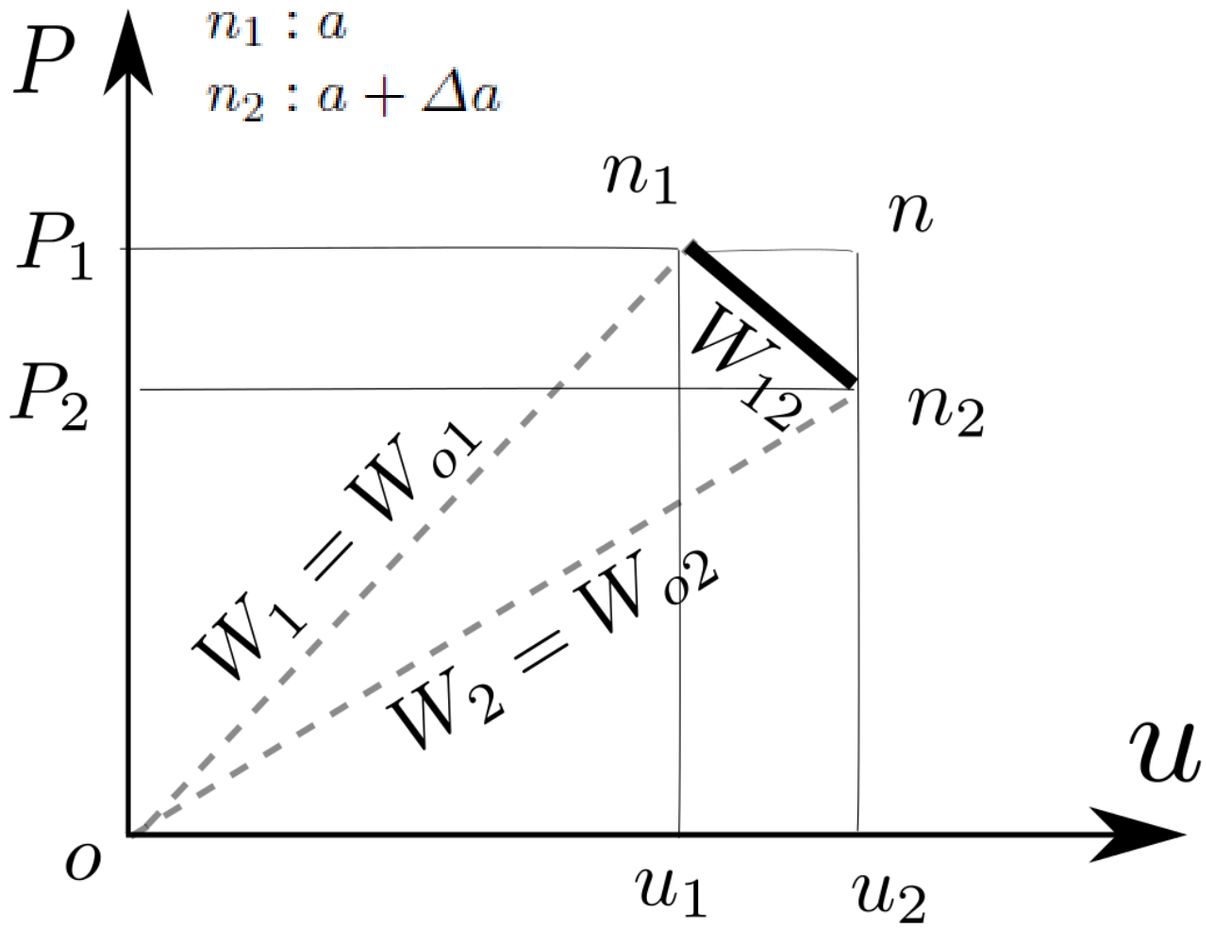

Evaluation of G

Questions:

- What is the value of $W_1 = W_{o1}$?
- For two paths from o to 2 (02 and 012) can we write:

  $W_{o2} = W_{o1} + W_{12} \quad \Rightarrow \quad W_{12} = W_{o2} - W_{o1}$?

  Explain.
- How G is calculated from the figure?

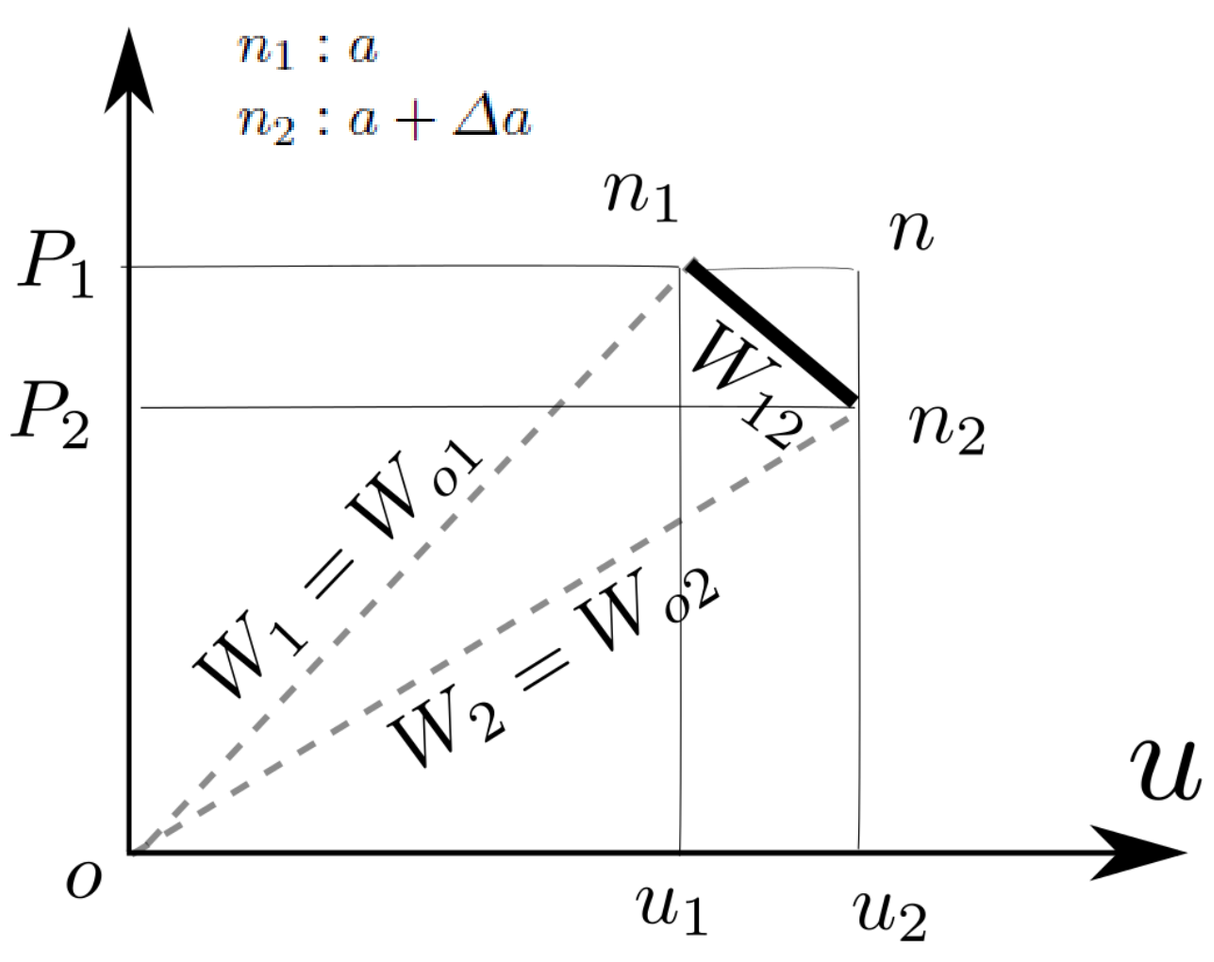

Evaluation of G

- What is the value of $W_1 = W_{o1}$?

$$W_1 = W_{o1} = \frac{1}{2} P_1 u_1 = U_{e1}$$

Linear system for fixed crack length a from o to n_1.

- For two paths from o to 2 (02 and 012) can we write:

$$W_{o2} = W_{o1} + W_{12} \quad \Rightarrow \quad W_{12} = W_{o2} - W_{o1}?$$

No. Because this is a dissipative mechanism between n_1 and n_2 due to crack growth and work is path dependent.

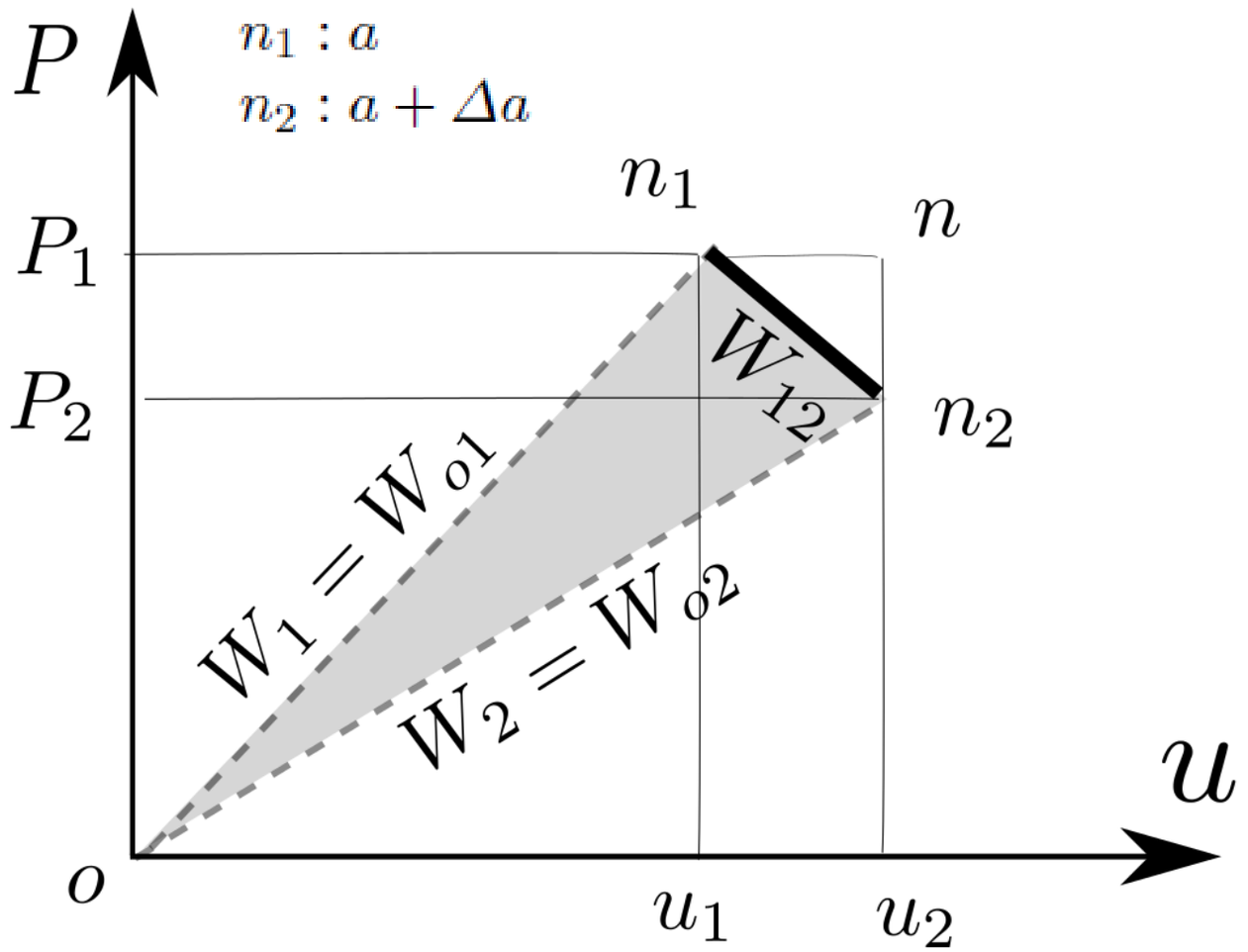

Evaluation of G

$$
\begin{aligned}
G &= -\frac{\mathrm{d}\Pi}{\mathrm{d}A} = -\frac{\mathrm{d}(U_e - W)}{\mathrm{d}Ba} \\
&\approx -\frac{1}{B\Delta a}\left(\Delta U_e - \Delta W\right)
\end{aligned}
$$

$$
\begin{aligned}
\Delta U_e &= U_{e2} - U_{e1} \\
&= W_{o2} - W_{o1} \quad \text{why?} \\
&= \frac{1}{2}(P_2 u_2 - P_1 u_1)
\end{aligned}
$$

$$
\begin{aligned}
\Delta W &= W_1 2 \\
&= \int_{u_1}^{2_2} P \mathrm{d}u \\
&\approx \frac{P_1 + P_2}{2}(u_2 - u_1)
\end{aligned}
$$

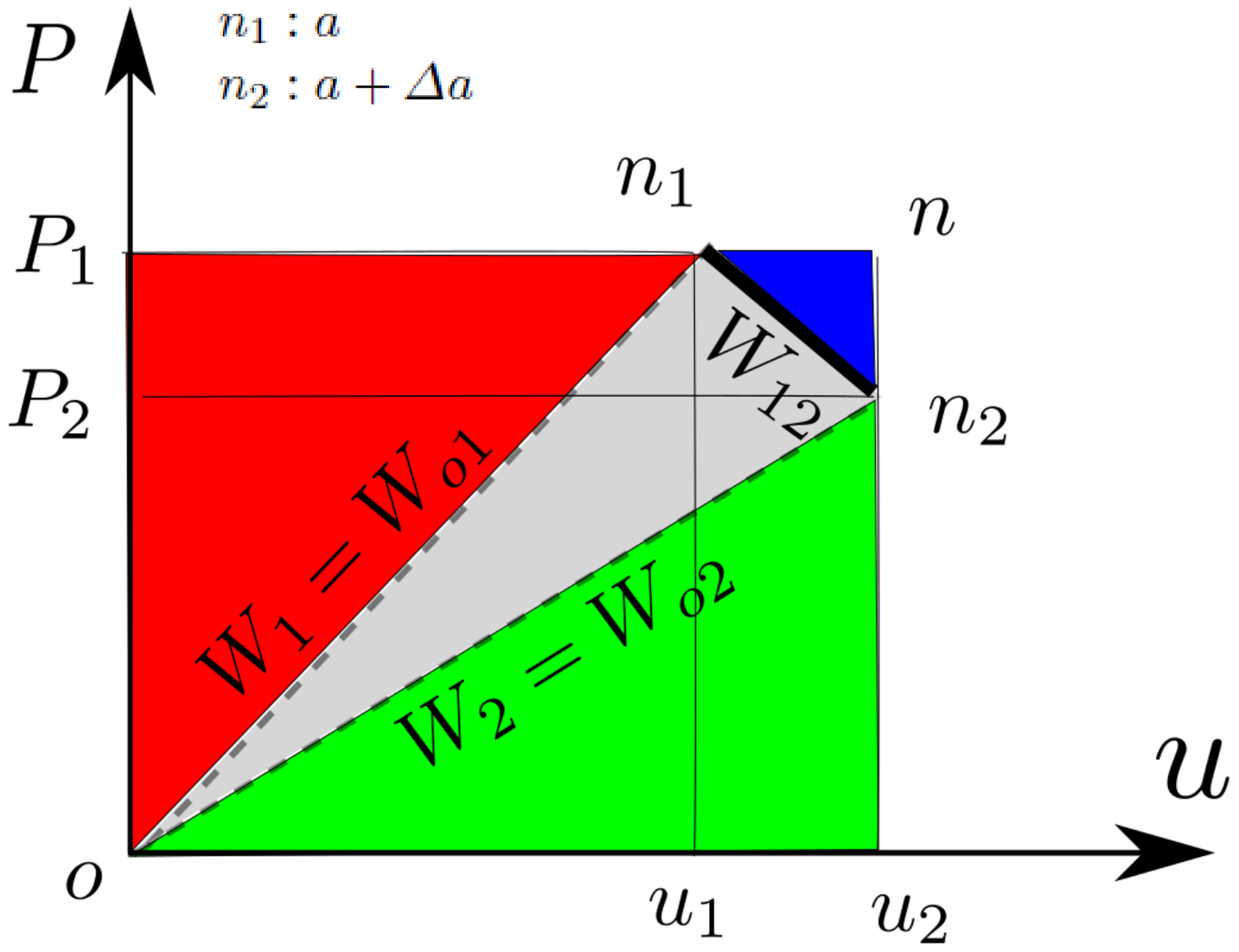

$$
\begin{aligned}
G &= \frac{1}{B\Delta a}\left(P_1 u_2 - \frac{P_1 u_1}{2} - \frac{P_2 u_2}{2} - \frac{(P_1 - P_2)(u_2 - u_1)}{2}\right) \\
&= \frac{\text{Grey area}}{B\Delta a}
\end{aligned}
$$

G from experiments

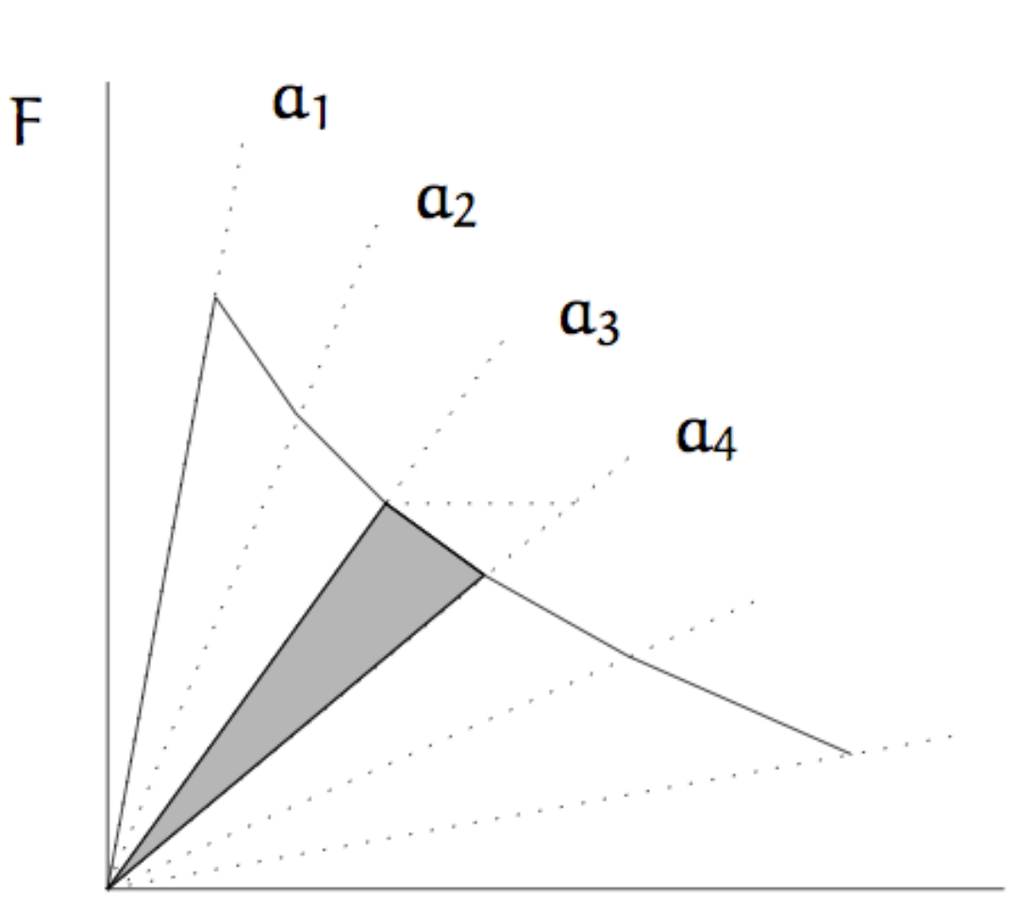

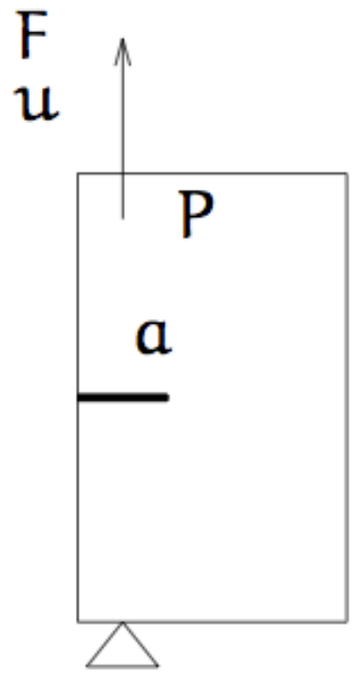

$$G(a_3) = \frac{1}{B}\frac{\text{shaded area}}{a_4 - a_3}$$

G from experiment

a_1: OA, triangle OAC=U

a_2: OB, triangle OBC=U

B: thickness

$$\Pi = U_e - W$$

$$G \equiv -\frac{d\Pi}{dA}$$

Fixed grips

$$\Delta U_e = -\frac{1}{2}(P_1 - P_2)u$$

$$\Delta W = 0 \quad \Rightarrow$$

$$G = \frac{1}{B\Delta a}\frac{1}{2}(P_1 - P_2)u$$

$$G = \frac{1}{B}\frac{(OAB)}{\Delta a}$$

Crack can grow from A to B or we obtain OA, OB with two different tests with different a values.

$W = 0$

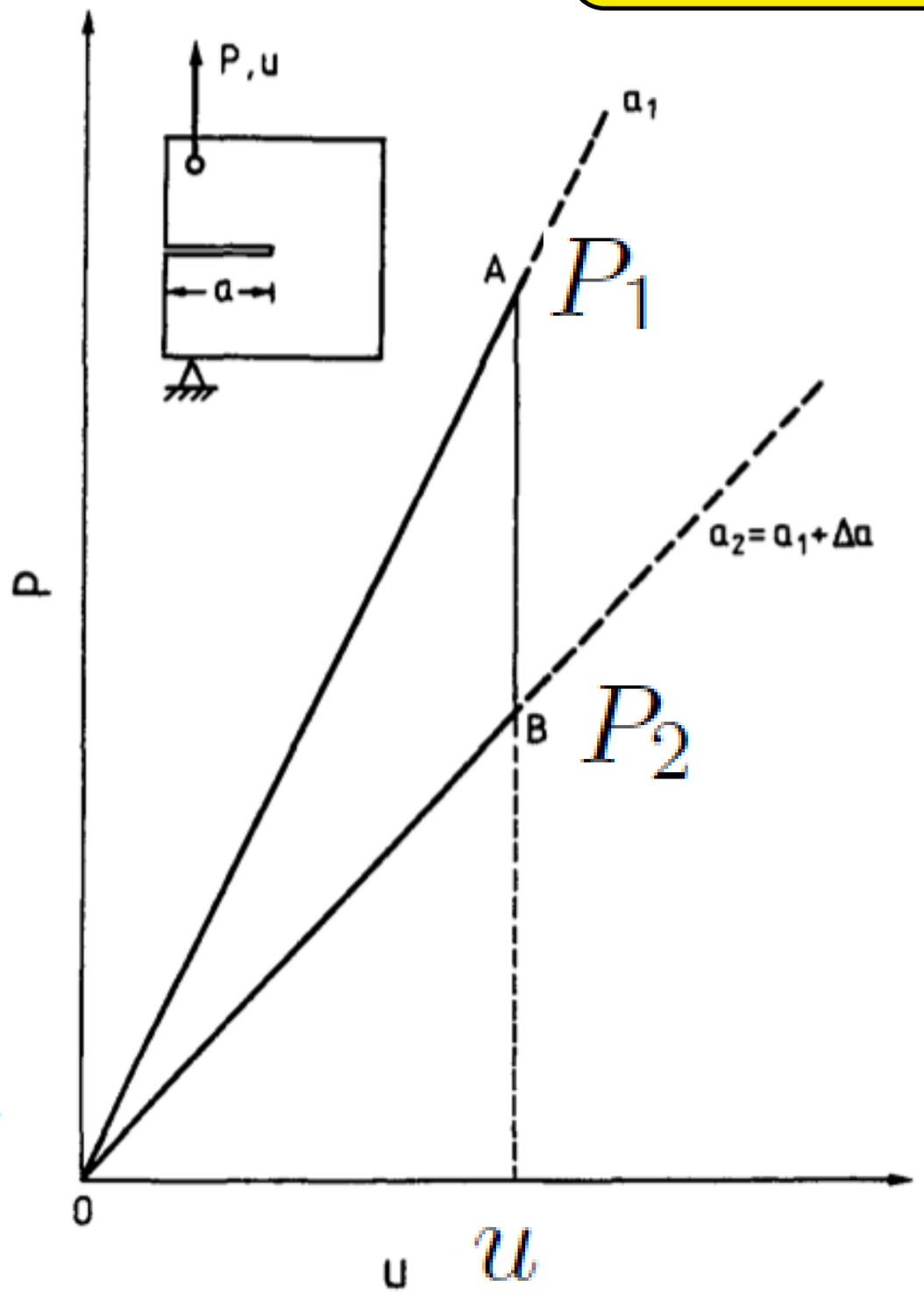

G from experiment

a_1: OA, triangle OAC=U

a_2: OB, triangle OBC=U

B: thickness

$$\Pi = U_e - W$$

$$G \equiv -\frac{d\Pi}{dA}$$

Dead loads

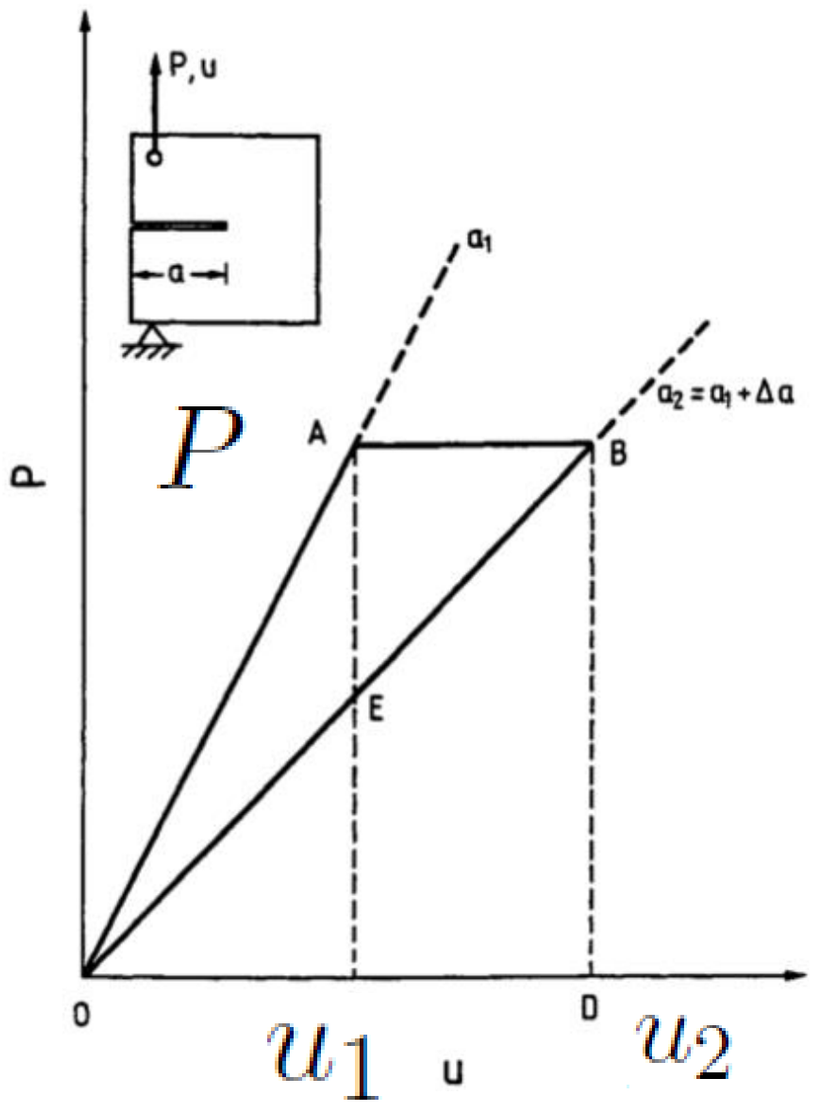

$$\Delta U_e = \frac{1}{2} P(u_2 - u_1),$$

$$\Delta W = P(u_2 - u_1) \quad \Rightarrow$$

$$G = \frac{1}{B\Delta a}\frac{1}{2} P(u_2 - u_1)$$

OAB=ABCD-(OBD-OAC)

$$G = \frac{1}{B}\frac{(OAB)}{\Delta a}$$

Crack can grow from A to B or we obtain OA, OB with two different tests with different a values.

G in terms of compliance

$$C = \frac{u}{P}$$

inverse of stiffness

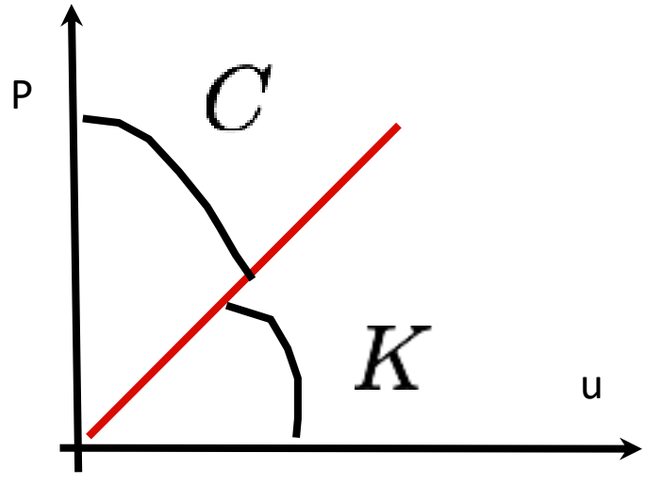

Fixed grips

$$dU_e = U_e(a + da) - U_e(a)$$

$$= \frac{1}{2}(P + dP)u - \frac{1}{2}Pu$$

$$= \frac{1}{2}dPu$$

$$G = -\frac{1}{2B}u\frac{dP}{da}$$

$$G = \frac{1}{2B}\frac{u^2}{C^2}\frac{dC}{da} = \frac{1}{2B}P^2\frac{dC}{da}$$

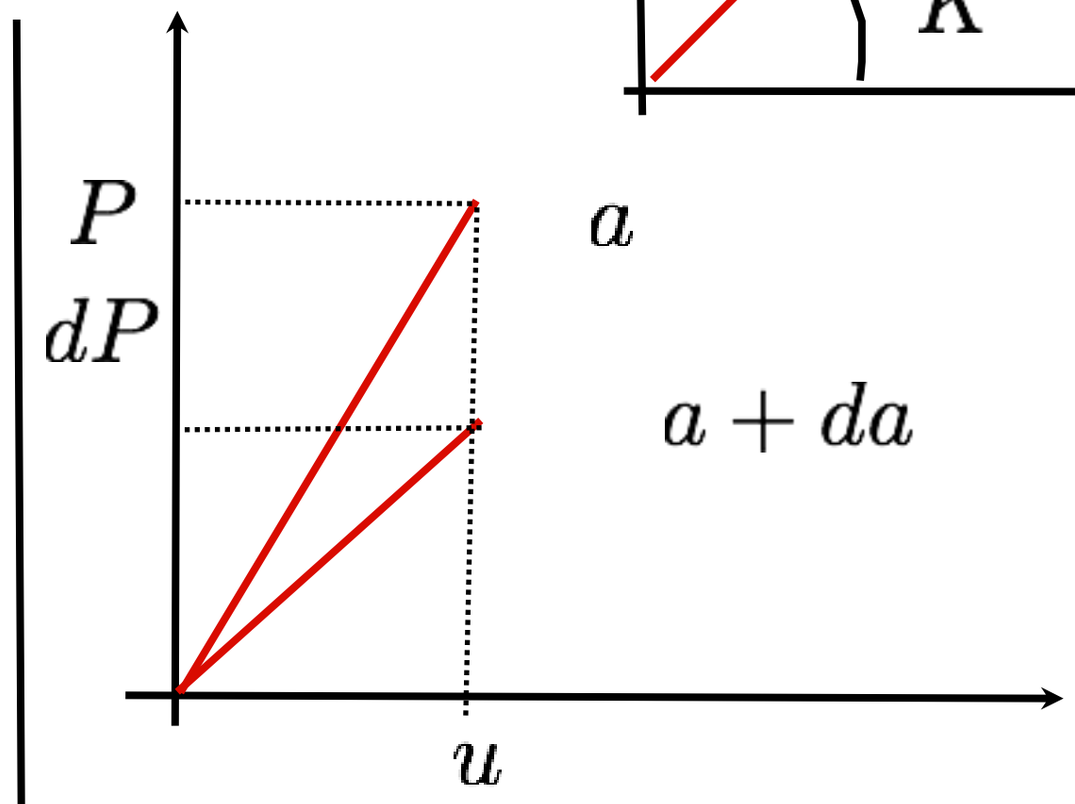

$$dA = Bda$$

$$G = \frac{dW - dU_e}{dA}$$

G in terms of compliance

$$C = \frac{u}{P}$$

inverse of stiffness

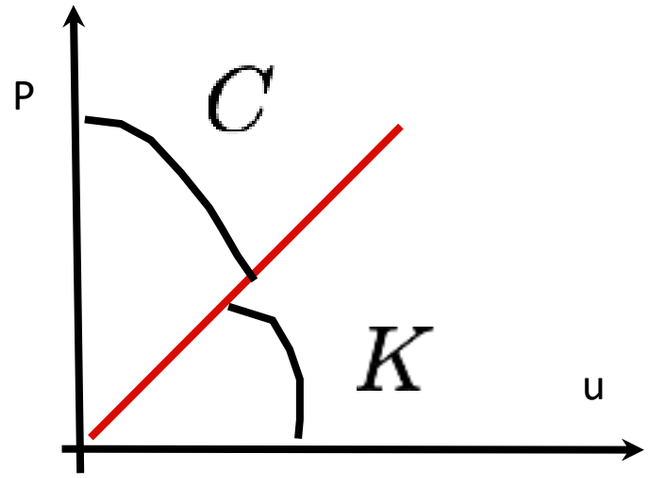

Fixed load

$$dU_e = \frac{1}{2}P(u+du) - \frac{1}{2}Pu$$

$$= \frac{1}{2}Pdu$$

$$dW = Pdu$$

$$G = \frac{1}{2B}P\frac{du}{da}$$

$$G = \frac{1}{2B}P^2\frac{dC}{da}$$

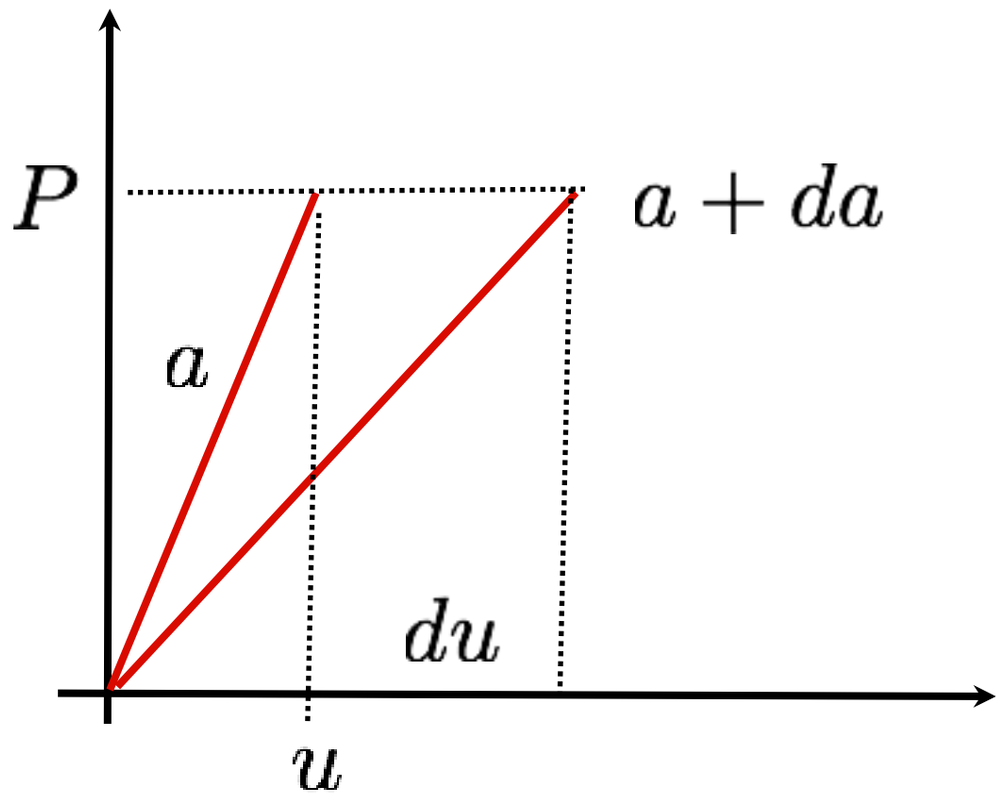

$$G = \frac{dW - dU_e}{dA}$$

G in terms of compliance

Fixed grips

$$G = \frac{1}{2B}\frac{u^2}{C^2}\frac{dC}{da} = \frac{1}{2B}P^2\frac{dC}{da}$$

Fixed loads

$$G = \frac{1}{2B}P^2\frac{dC}{da}$$

Strain energy release rate is identical for fixed grips and fixed loads.

Strain energy release rate is proportional to the differentiation of the compliance with respect to the crack length.

Crack extension resistance curve (R-curve)

Irwin

$$G \equiv -\frac{d\Pi}{dA} = \frac{dU_\Gamma}{dA} + \frac{dU_p}{dA}$$

$$R \equiv \frac{dU_\Gamma}{dA} + \frac{dU_p}{dA}$$

$$G = R$$

Resistance to fracture increases with growing crack size in elastic-plastic materials.

$$R = R(a)$$ Irwin

Stable crack growth: fracture resistance of thin specimens is represented by a curve not a single parameter.

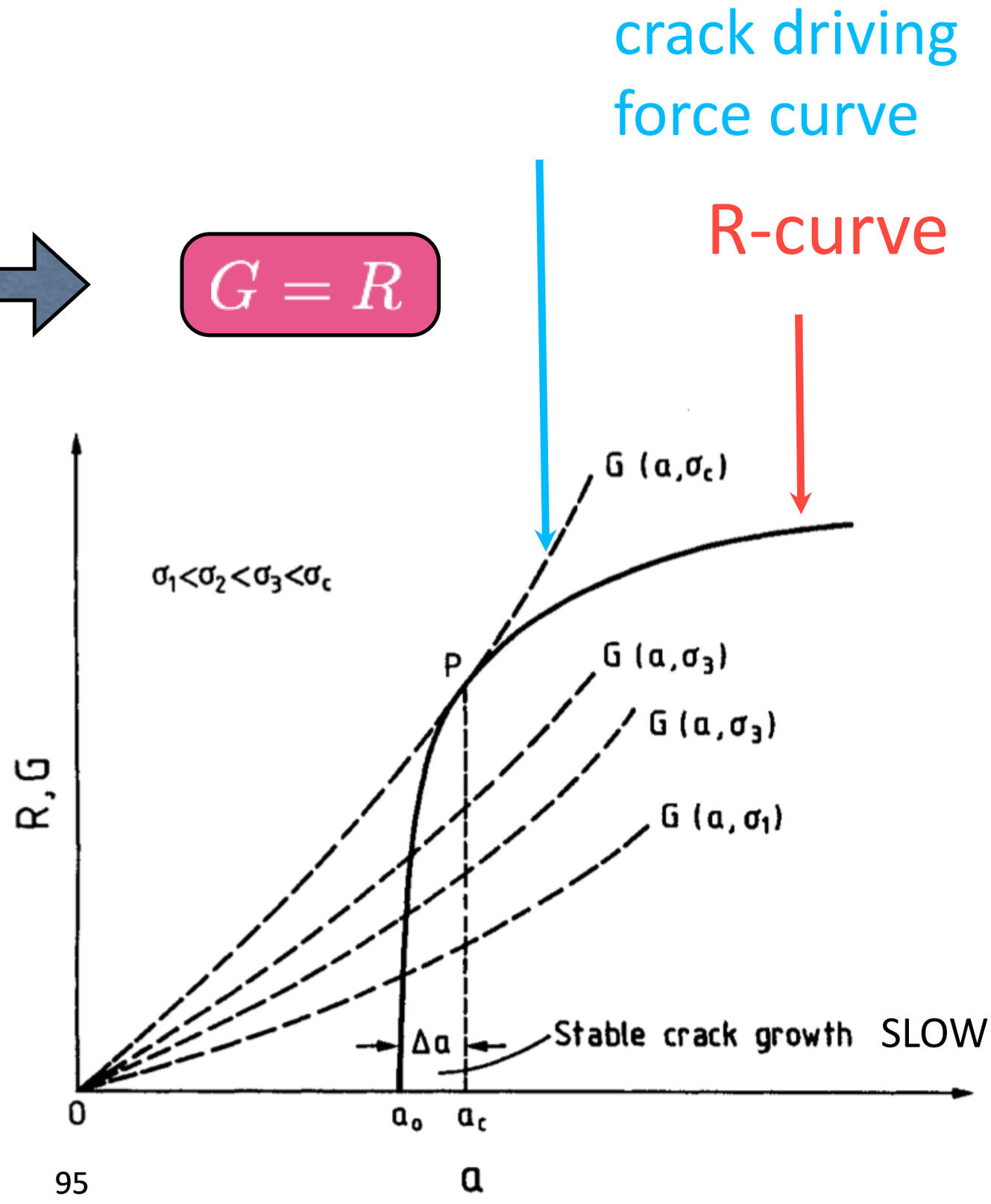

R-curve shapes

flat R-curve
(ideally brittle materials)

$$G = \frac{\pi\sigma^2 a}{E}$$

rising R-curve
(ductile metals)

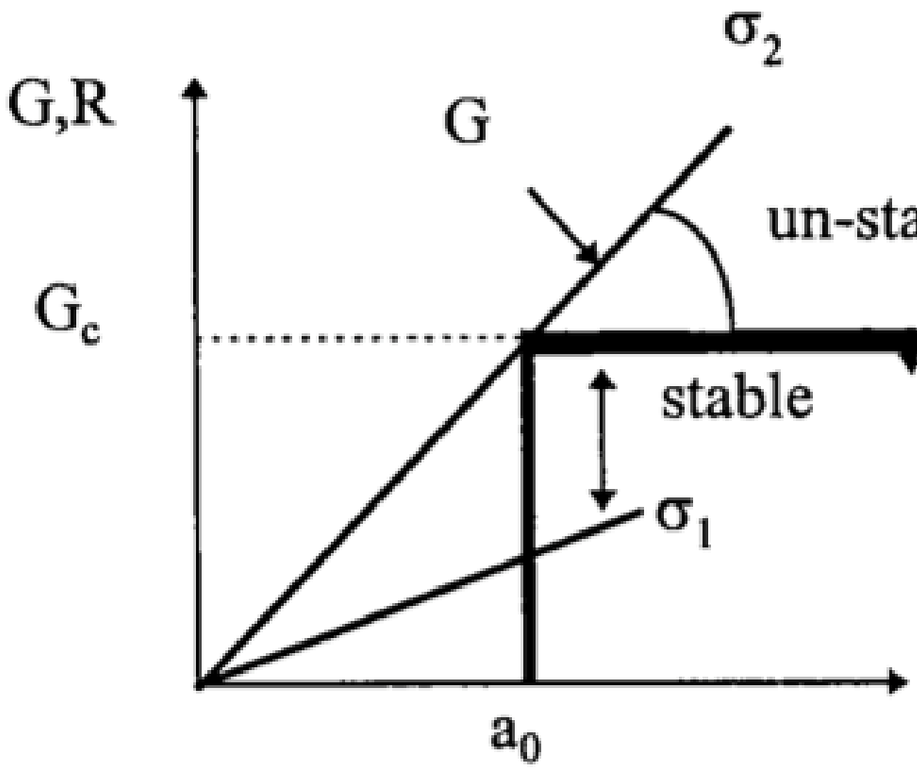

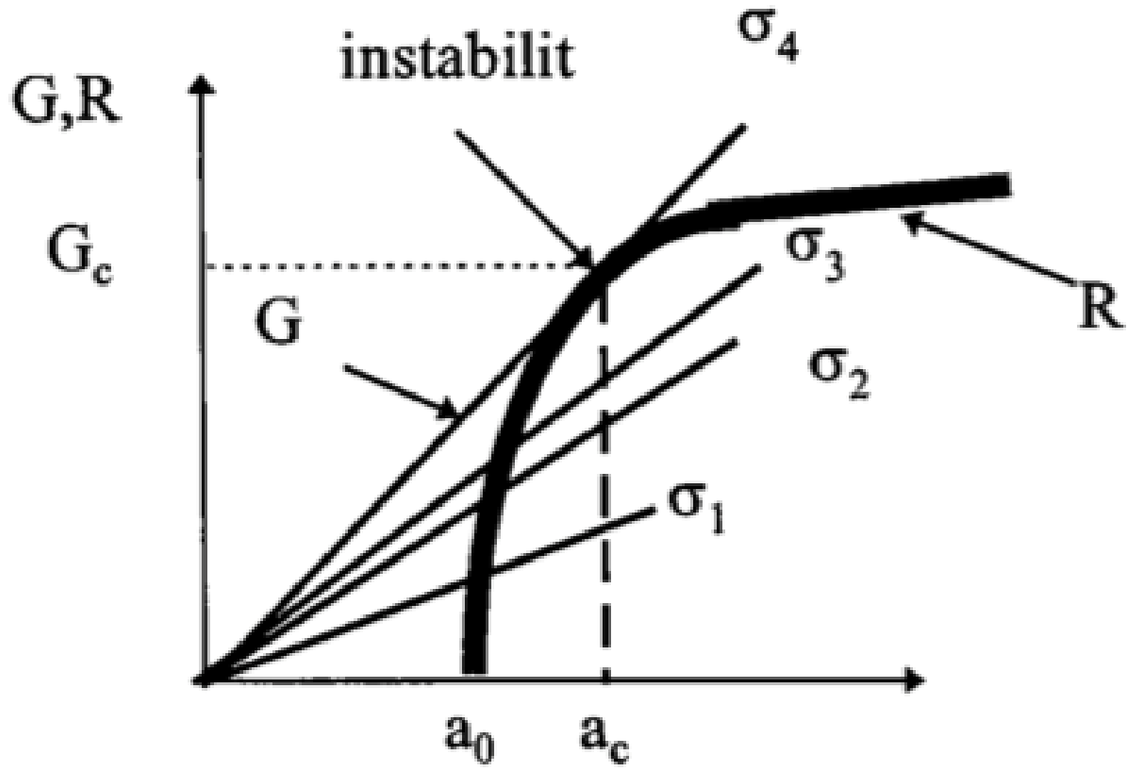

slope

$$G = R, \quad \frac{dG}{da} \leq \frac{dR}{da}$$

stable crack growth

crack grows then stops, only grows further if there is an increase of applied load

Double cantilever beam (DCB) example

$$\frac{\Delta}{2} = \frac{P a^3}{3 E I}$$

$$C = \frac{\Delta}{P} = \frac{2 a^3}{3 E I}$$

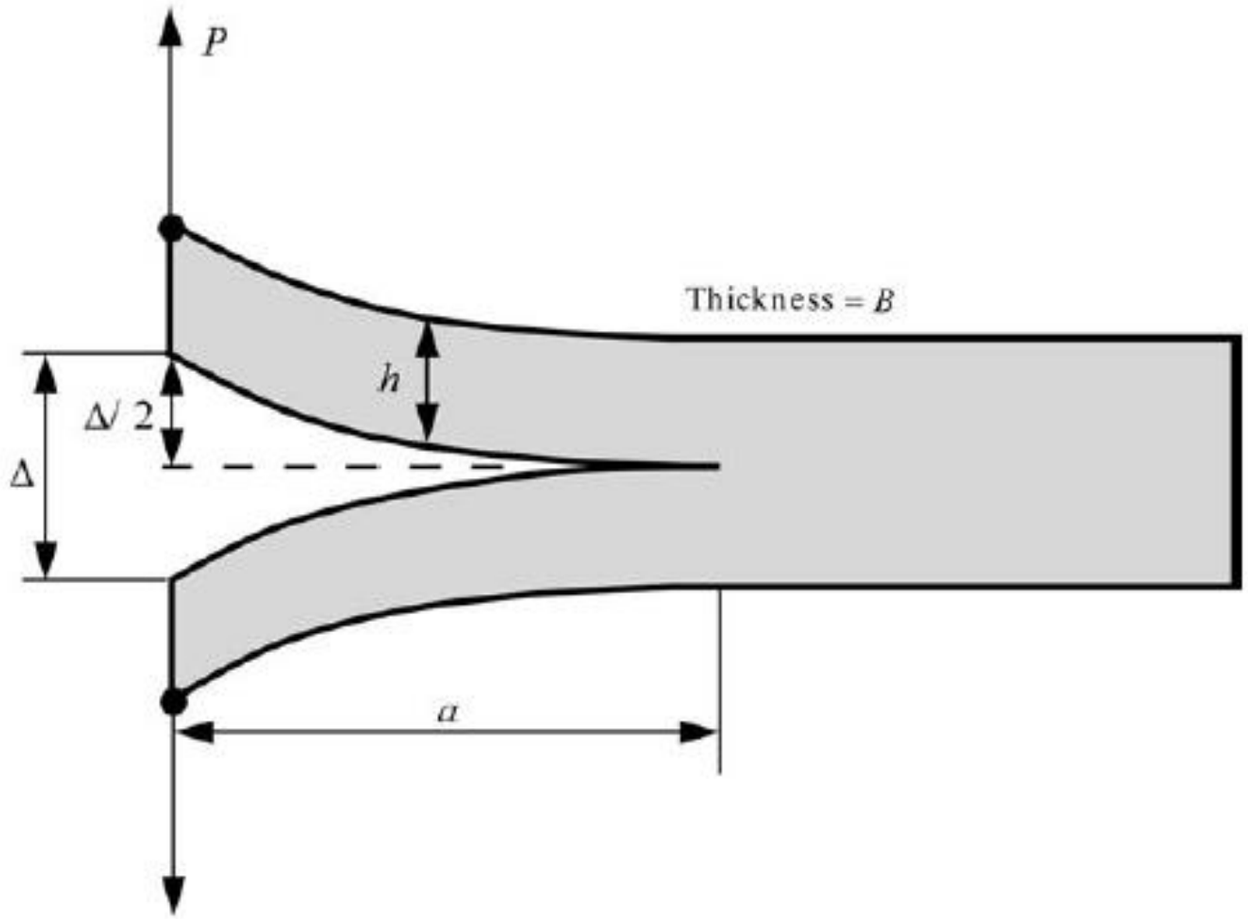

$$G = \frac{P^2}{2B}\frac{\mathrm{d}C}{\mathrm{d}a} = \frac{P^2 a^2}{BEI}$$

Double cantilever beam (DCB) example: load control

$$G = \frac{P^2 a^2}{BEI} \quad \Rightarrow$$

$$\left(\frac{d\mathcal{G}}{da}\right)_P = \frac{2P^2 a}{BEI} = \frac{2\mathcal{G}}{a}$$

$$\frac{d\mathcal{G}}{da} > \frac{dR}{da}$$

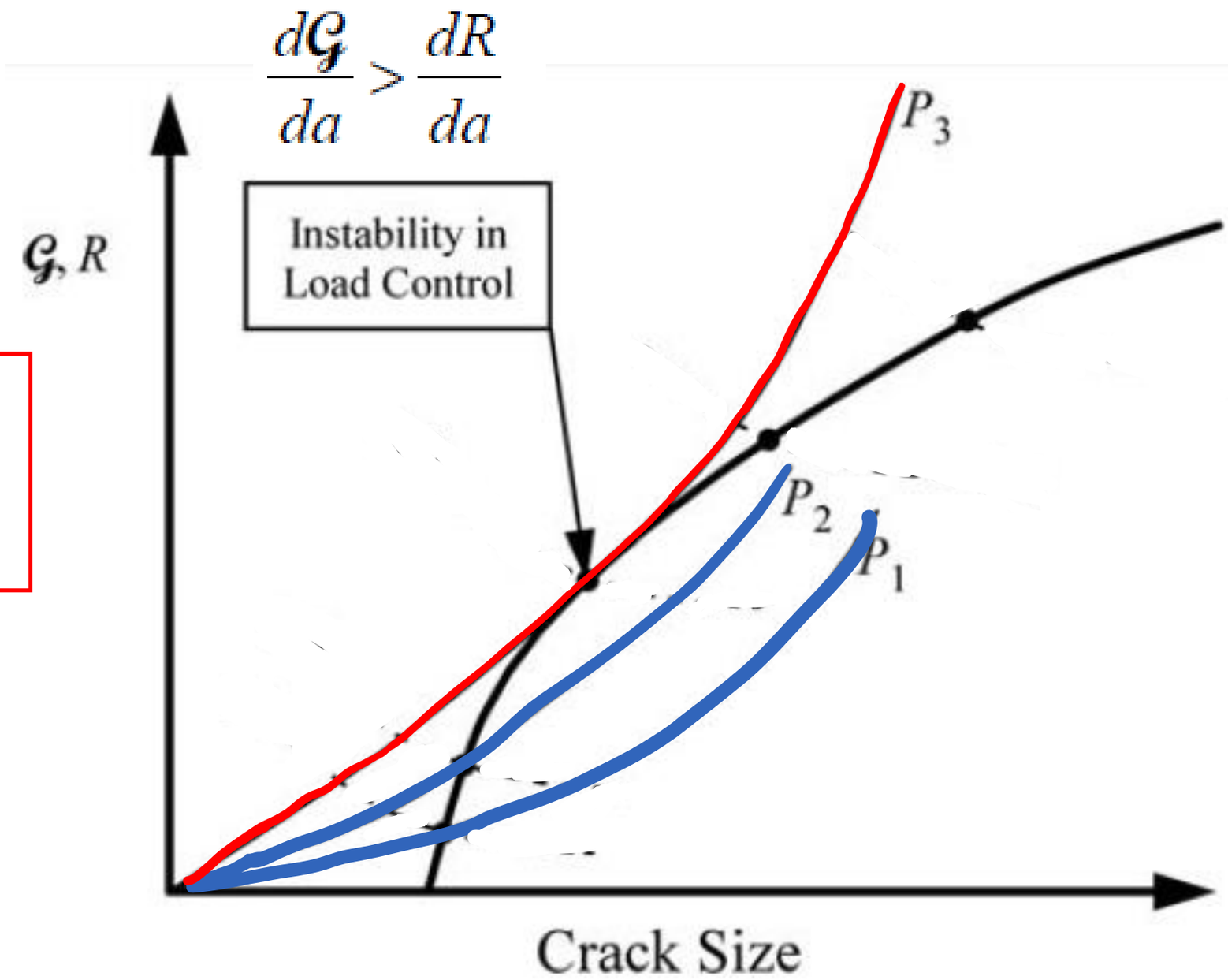

Double cantilever beam (DCB) example: displacement control

$$G = \frac{P^2 a^2}{BEI}, P = \frac{\Delta}{C} \quad \Rightarrow$$

$$G = \frac{9}{4}\frac{\Delta^2}{EIa^4}$$

$$\left(\frac{d\mathcal{G}}{da}\right)_{\Delta} = -\frac{9\Delta^2 EI}{Ba^5} = -\frac{4\mathcal{G}}{a}$$

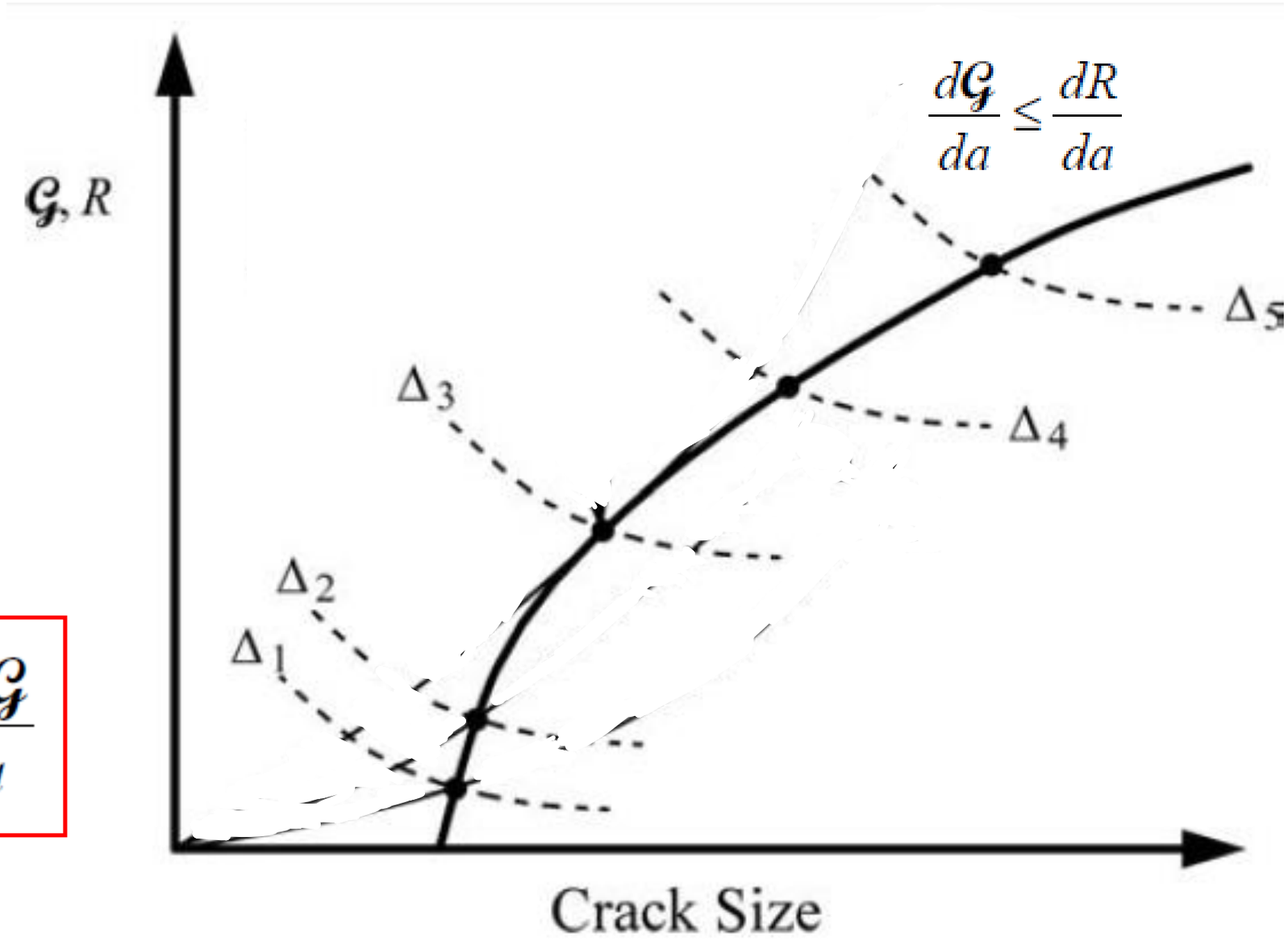

Example

The following data were obtained from a series of tests conducted on precracked specimens of thickness 1 mm.

Crack length a(mm)	Critical load P(kN)	Critical displacement u(mm)
30.0	4.00	0.40
40.0	3.50	0.50
50.5	3.12	0.63
61.6	2.80	0.78
71.7	2.62	0.94
79.0	2.56	1.09

where P and u are the critical load and displacement at crack growth. The load-displacement record for all crack lengths is linearly elastic up to the critical point.

Determine the critical value of the strain energy release rate $G_c = R$ from: (a) the load-displacement records, and (b) the compliance-crack length curve.

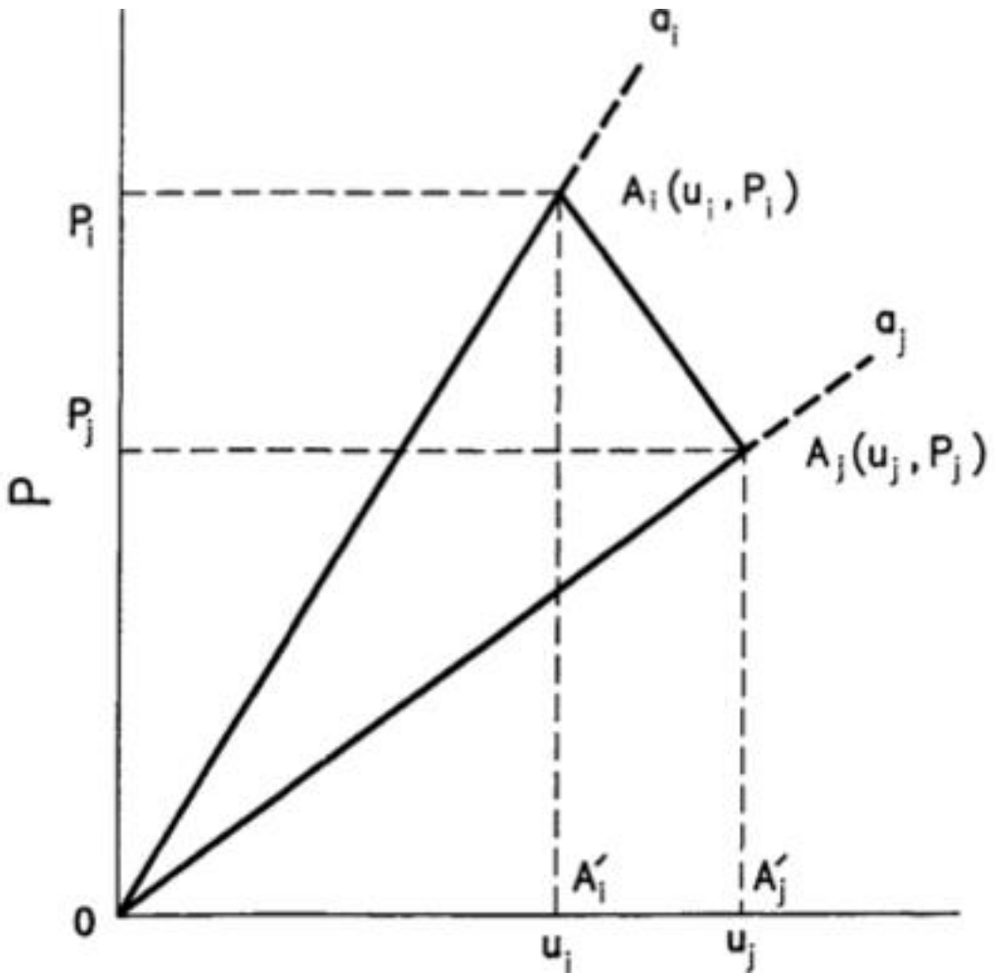

$$(OA_iA_j) = (OA_iA_i') + (A_iA_i'A_j'A_j) - (OA_jA_j')$$

or

$$(OA_iA_j) = \frac{1}{2}P_iu_i + \frac{1}{2}(P_i + P_j)(u_j - u_i) - \frac{1}{2}P_ju_j$$

$$G = \frac{1}{2B}\frac{OA_iA_j}{a_j - a_i} = \frac{P_iu_j - P_ju_i}{2B(a_j - a_i)}$$

Area	OA_1A_2	OA_2A_3	OA_3A_4	OA_4A_5	OA_5A_6
$G_c = R(\mathrm{kJ/m^2})$	30.0	30.7	30.2	29.1	30.8

Gc for different crack lengths are almost the same: flat R-curve.

For the determination of $G_c = R$ from the compliance-crack length curve we first determine the following values of compliance $C = u/P$ for the various crack lengths

a(mm)	30.0	40.0	50.5	61.6	71.7	79.0
$C(\times 10^{-7}$ m/N)	1.00	1.43	2.02	2.79	3.59	4.26

$P = 4$ kN

$$\frac{\mathrm{d}C}{\mathrm{d}a} = \frac{(1.43 - 1.00) \times 10^{-7}\ \mathrm{m/N}}{10 \times 10^{-3}\ \mathrm{m}} = 4.3 \times 10^{-6}\ \mathrm{N}^{-1}$$

and

$$G_c = R = \frac{(4 \times 10^3)^2\ \mathrm{N}^2 \times (4.3 \times 10^{-6}\ \mathrm{N}^{-1})}{2 \times 10^{-3}\ \mathrm{m}} = 34.4\ \mathrm{kJ/m}^2\ .$$

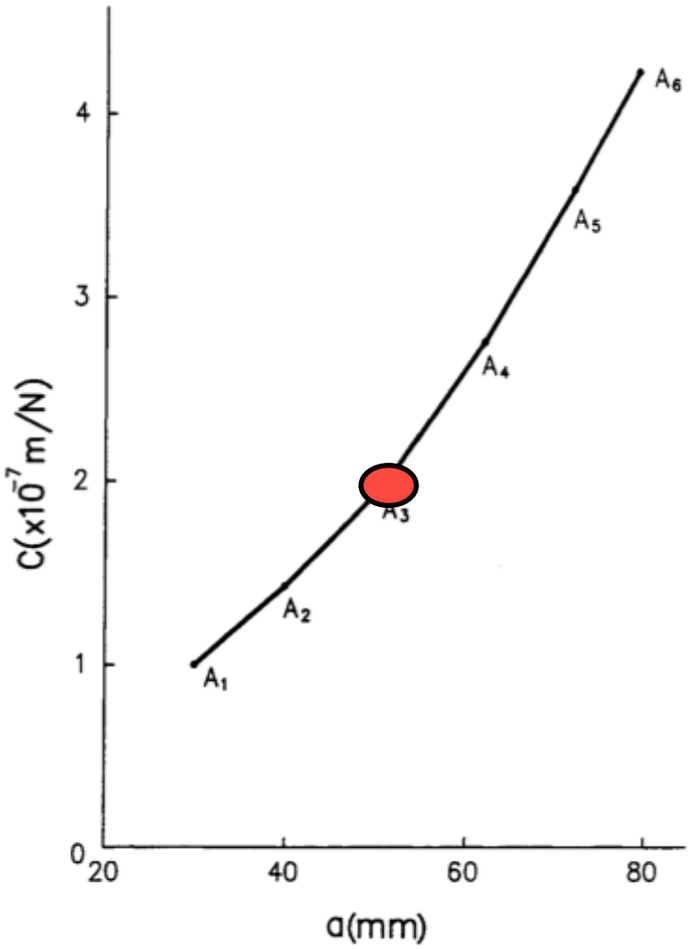

a(mm)	30.0	40.0	50.5	61.6	71.7	79.0
$G_c = R$(kJ/m^2)	34.4	30.4	31.2	29.2	29.7	30.0

For the crack lengths a_2, a_3, a_4 and a_5, $\mathrm{d}C/\mathrm{d}a$ can be determined as the mean value of the left and right derivatives of C. For example, for the crack length $a = 50.5$ mm, we have

$$P = 3.12\ \mathrm{kN}$$

$$\left(\frac{\mathrm{d}C}{\mathrm{d}a}\right)_l = \frac{(2.02 - 1.43) \times 10^{-7}\ \mathrm{m/N}}{10.5 \times 10^{-3}\ \mathrm{m}} = 5.6 \times 10^{-6}\ \mathrm{N}^{-1}$$

$$\left(\frac{\mathrm{d}C}{\mathrm{d}a}\right)_r = \frac{(2.77 - 2.02) \times 10^{-7}\ \mathrm{m/N}}{11.1 \times 10^{-3}\ \mathrm{m}} = 6.8 \times 10^{-6}\ \mathrm{N}^{-1}$$

4.2. Stress solutions, Stress Intensity Factor K (SIF)

Elastodynamics Boundary value problem

Kinematics

displacement u

velocity v

acceleration a

strain ε

$$\epsilon_{ij} = \frac{1}{2}(u_{i,j} + u_{j,i}) \Rightarrow \begin{cases} \epsilon_{11} = u_{1,1} \\ \epsilon_{12} = \frac{1}{2}(u_{1,2} + u_{2,1}) \\ \epsilon_{22} = u_{2,2} \end{cases}$$

Kinetics

stress $\boldsymbol{\sigma} = \sigma_{ij} = \begin{bmatrix} \sigma_{11} & \sigma_{12} & \sigma_{13} \\ \sigma_{21} & \sigma_{22} & \sigma_{23} \\ \sigma_{31} & \sigma_{32} & \sigma_{33} \end{bmatrix}$

traction $\mathbf{T} = \sigma n$

linear momentum p

body force b

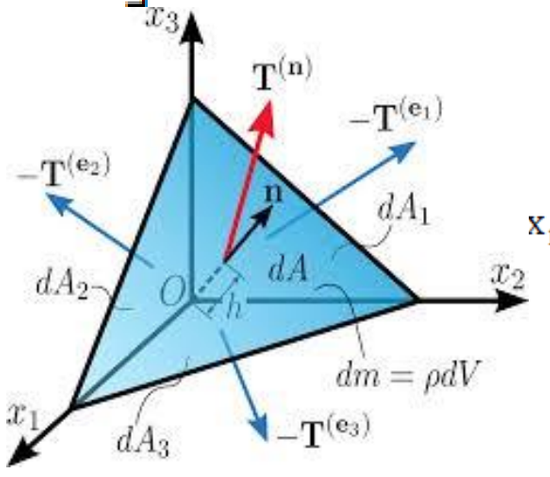

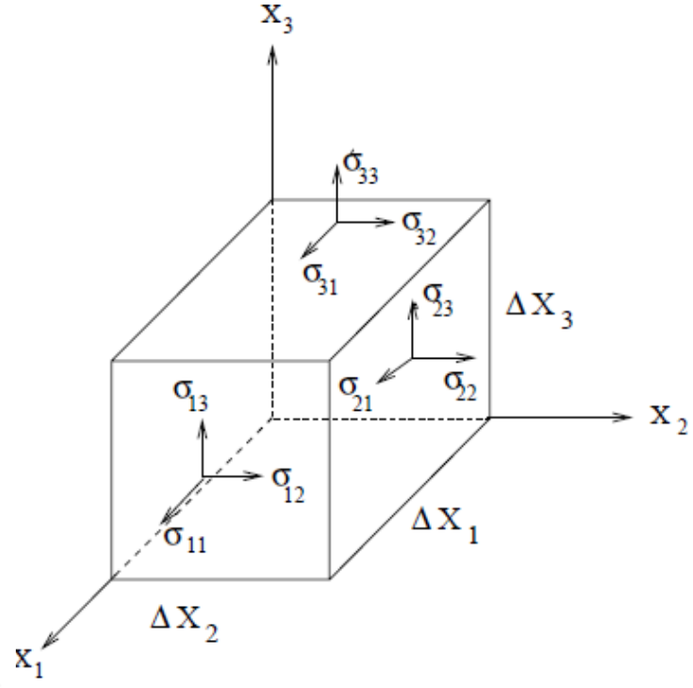

Elastostatics Boundary value problem

Constitutive equation

Hook's law

Isotropic

3D

$$\sigma_{ij} = D_{ijkl}\varepsilon_{kl} \qquad i,j,k,l = 1,2,3$$

$$T_{ij} = \lambda\delta_{ij}E_{kk} + 2\mu E_{ij} \qquad \text{or} \qquad \mathbf{T} = \lambda\mathbf{I}_E + 2\mu\mathbf{E}$$

2D (plane strain)

$$\begin{Bmatrix} \sigma_{xx} \\ \sigma_{yy} \\ \sigma_{zz} \\ \tau_{xy} \end{Bmatrix} = \frac{E}{(1+\nu)(1-2\nu)} \begin{bmatrix} (1-\nu) & \nu & 0 \\ \nu & (1-\nu) & 0 \\ \nu & \nu & 0 \\ 0 & 0 & \frac{1-2\nu}{2} \end{bmatrix} \begin{Bmatrix} \varepsilon_{xx} \\ \varepsilon_{yy} \\ \gamma_{xy} \end{Bmatrix}$$

2D (plane stress)

$$\begin{Bmatrix} \sigma_{xx} \\ \sigma_{yy} \\ \tau_{xy} \end{Bmatrix} = \frac{1}{1-\nu^2} \begin{bmatrix} 1 & \nu & 0 \\ \nu & 1 & 0 \\ 0 & 0 & \frac{1-\nu}{2} \end{bmatrix} \begin{Bmatrix} \varepsilon_{xx} \\ \varepsilon_{yy} \\ \gamma_{xy} \end{Bmatrix}$$

$$p = \rho\mathbf{v}$$

Balance of linear momentum

$$\nabla.\sigma + \rho\mathbf{b} = \dot{p} \qquad \text{or} \qquad \sigma_{ij,j} + \rho b_j = \rho\ddot{u}_i$$

- Static: $\dot{\mathbf{p}} = 0$
- No body force $\mathbf{b} = 0$

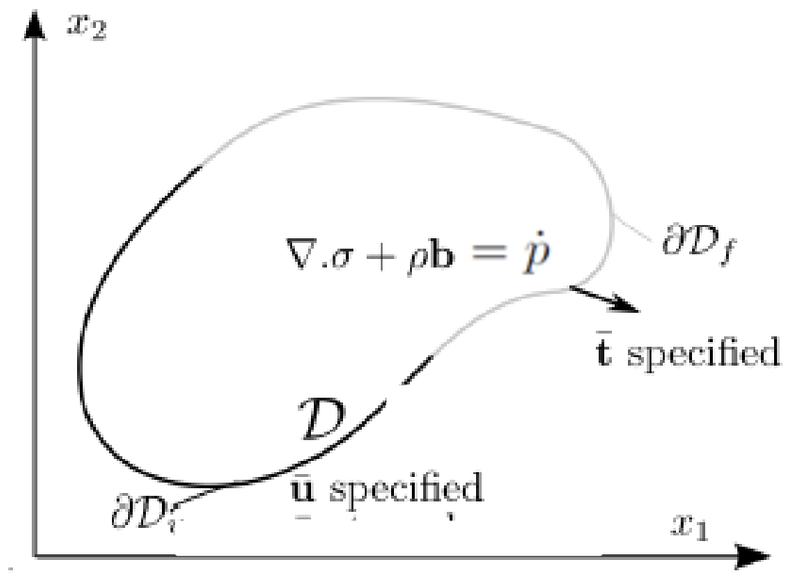

Displacement approach

$$\sigma_{ij,j} = 0$$

$$\sigma_{ij} = \frac{E}{1+\nu}\left(\varepsilon_{ij} + \frac{\nu}{1-2\nu}\,\delta_{ij}\varepsilon_{kk,j}\right)$$

$$\frac{E}{1+\nu}\left(\varepsilon_{ij,j} + \frac{\nu}{1-2\nu}\,\delta_{ij}\varepsilon_{kk,j}\right) = 0$$

$$\varepsilon_{ij} = \tfrac{1}{2}\left(u_{i,j} + u_{j,i}\right)$$

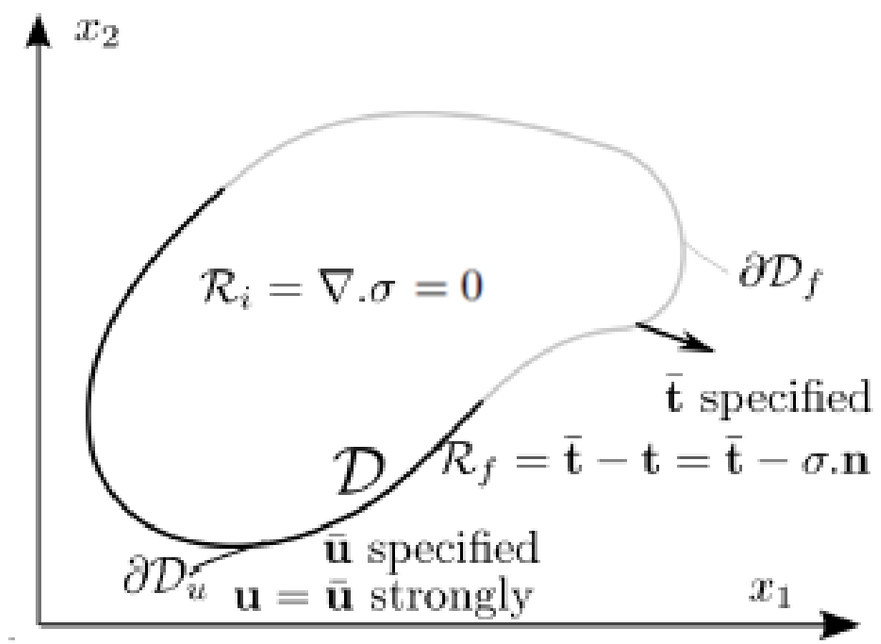

$$(\lambda+\mu)\nabla\nabla.\mathbf{u} + \mu\nabla.\nabla\mathbf{u} = 0 \quad \text{or} \quad (\lambda+\mu)u_{j,ji} + \mu u_{i,jj} = 0$$

BC's

PDE + BC for $\mathbf{u} \Rightarrow \epsilon \Rightarrow \sigma$

Stress function approach

What are Airy stress function approach?

Use of stress function ⇨

Balance of linear momentum is automatically satisfied (no body force, static)

$$\psi(x_1, x_2) \quad \rightarrow \quad \sigma_{ij} = -\psi_{,ij} + \delta_{ij}\psi_{,kk} \quad \rightarrow \quad \sigma_{ij,j} = 0$$

How do we obtain strains and displacements?

Strain: compliance *e.g.* $\varepsilon_{ij} = \frac{1+\nu}{E}(\sigma_{ij} - \nu\delta_{ij}\sigma_{kk})$

Displacements: Integration of $\epsilon_{ij} = \frac{1}{2}(u_{i,j} + u_{j,i})$

Can we always obtain u by integration? No

3 displacements (unknowns)
6 strains (equations)

Need to satisfy strain compatibility condition(s)

$$\frac{\partial^2 \varepsilon_{ik}}{\partial x_j \partial x_j} + \frac{\partial^2 \varepsilon_{jj}}{\partial x_i \partial x_k} - \frac{\partial^2 \varepsilon_{jk}}{\partial x_i \partial x_j} - \frac{\partial^2 \varepsilon_{ij}}{\partial x_j \partial x_k} = 0.$$

Stress function approach

$$\left.\begin{array}{l} \varepsilon_{ij} = \dfrac{1+\nu}{E}\{-\psi_{,ij} + (1-\nu)\delta_{ij}\psi_{,kk}\} \\ \\ 2\varepsilon_{12,12} - \varepsilon_{11,22} - \varepsilon_{22,11} = 0 \end{array}\right\}$$

$$2\psi_{,1122} + \psi_{,2222} + \psi_{,1111} = 0 \qquad \rightarrow$$

$$\left.\begin{array}{l} (\psi_{,11} + \psi_{,22})_{,11} + (\psi_{,11} + \psi_{,22})_{,22} = 0 \\ \\ \text{Laplace operator} \quad : \quad \nabla^2 = \dfrac{\partial^2}{\partial x_1^2} + \dfrac{\partial^2}{\partial x_2^2} = (\ )_{11} + (\ )_{22} \end{array}\right\} \rightarrow$$

$$\left.\begin{array}{l} \text{bi-harmonic equation} \qquad \nabla^2(\nabla^2\psi) = \nabla^4\psi = 0 \\ \text{BC's} \end{array}\right\}$$

Stress function approach:

$$N \Rightarrow \sigma \Rightarrow \epsilon \Rightarrow \mathbf{u}$$

Displacement approach:

$$\text{PDE} + \text{BC for } \mathbf{u} \Rightarrow \epsilon \Rightarrow \sigma$$

- Generally no need to solve biharmonic function: Extensive set of functions from complex analysis
- No need to solve any PDE
- Only working with the scalar stress function

Complex numbers

- Complex numbers

$$z = x_1 + \boldsymbol{i}x_2 = \mathrm{Re}(z) + \boldsymbol{i}\mathrm{Im}(z)$$
$$\mathrm{Re}(z) = x_1$$
$$\mathrm{Im}(z) = x_2$$
$$z = re^{i\theta}$$
$$\bar{z} = x_1 - \boldsymbol{i}x_2 = re^{-i\theta} \text{ conjugate}$$

- Complex functions

$$f(z) = \mathrm{Re}f(z) + \boldsymbol{i}\mathrm{Im}f(z) = U(x_1, x_2) + \boldsymbol{i}V(x_1, x_2)$$

$U\&V$: conjugate harmonic functions: $\nabla^2 U = \nabla^2 V = 0$

- Derivative relations

$$\frac{\partial f(z)}{\partial x_1} = \frac{\partial f(z)}{\partial z}\frac{\partial z}{\partial x_1} = f'(z)$$
$$\frac{\partial f(z)}{\partial x_2} = \frac{\partial f(z)}{\partial z}\frac{\partial z}{\partial x_2} = \boldsymbol{i}f'(z)$$
$$\frac{\partial \mathrm{Re}f(z)}{\partial x_1} = \mathrm{Re}f'(z)$$
$$\frac{\partial \mathrm{Im}f(z)}{\partial x_1} = \mathrm{Im}f'(z)$$
$$\frac{\partial \mathrm{Re}f(z)}{\partial x_2} = -\mathrm{Im}f'(z)$$
$$\frac{\partial \mathrm{Im}f(z)}{\partial x_2} = \mathrm{Re}f'(z)$$

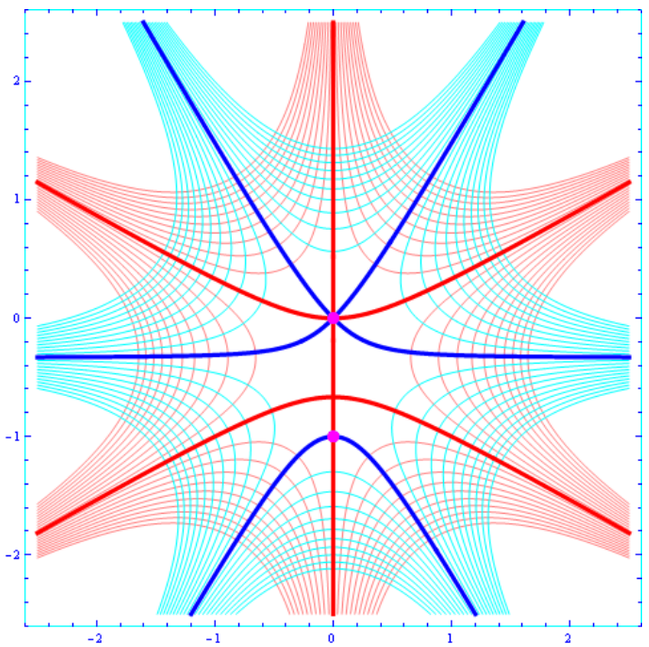

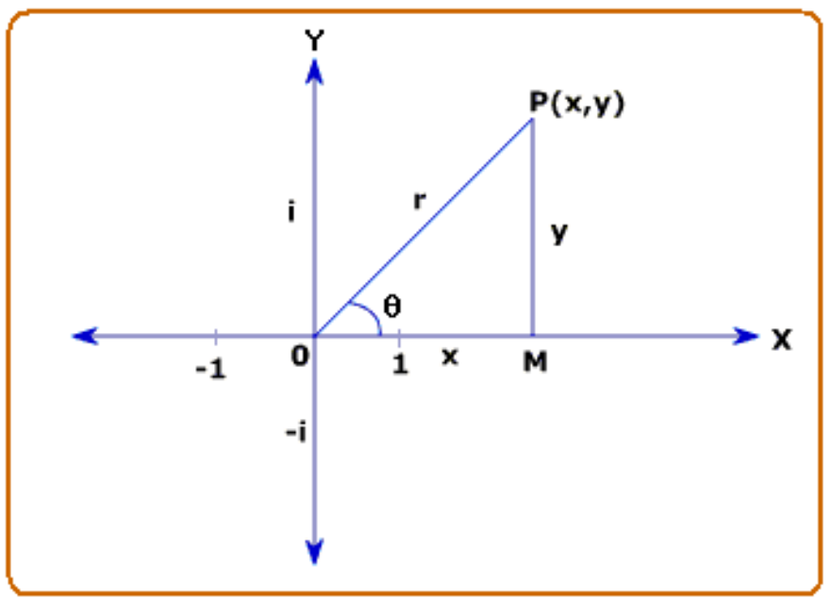

Stress function approach

- Any biharmonic solution can be expressed by Kolonov-Muskhelishvili complex potentials, ϕ, χ:

$$\boldsymbol{\Psi}(x_1, x_2) = \mathrm{Re}\left[\bar{z}\phi + \chi\right]$$

- Stresses are obtained differentiation,

$$\sigma_{11} = \boldsymbol{\Psi}_{,22} = \mathrm{Re}\left[\phi' - \frac{1}{2}\bar{z}\phi'' - \frac{1}{2}\chi''\right]$$

$$\sigma_{22} = \boldsymbol{\Psi}_{,11} = \mathrm{Re}\left[\phi' + \frac{1}{2}\bar{z}\phi'' + \frac{1}{2}\chi''\right]$$

$$\sigma_{12} = -\boldsymbol{\Psi}_{,12} = \frac{1}{2}\mathrm{Re}\left[\bar{z}\phi'' + \chi''\right]$$

- Displacements are obtained by integration of strains:

$$u_1 = \mathrm{Re}\left[\kappa\phi - \bar{z}\phi' - \chi'\right]$$

$$u_2 = \mathrm{Im}\left[\kappa\phi + \bar{z}\phi' + \chi'\right]$$

$$\kappa = \begin{cases} 3 - 4\nu & \text{plane strain} \\ \frac{3-\nu}{1+\nu} & \text{plane stress} \end{cases}$$

Crack modes

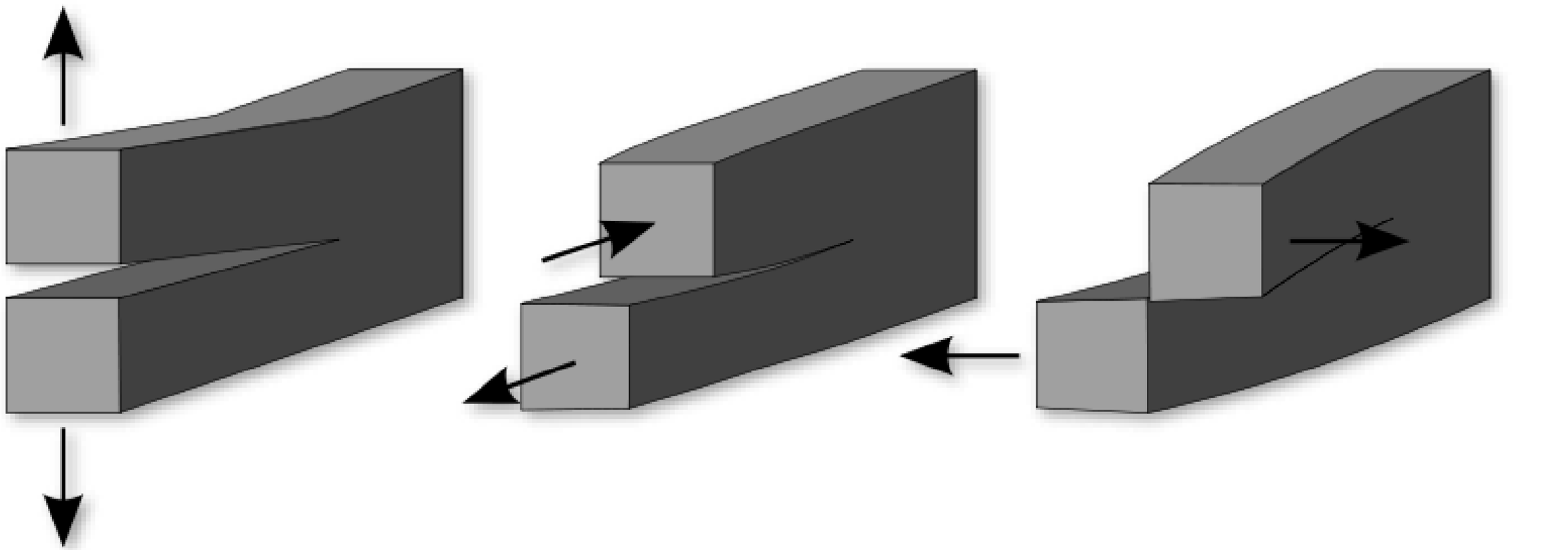

Mode I:
Opening

Mode II:
In-plane shear

Mode III:
Out-of-plane shear

Crack modes

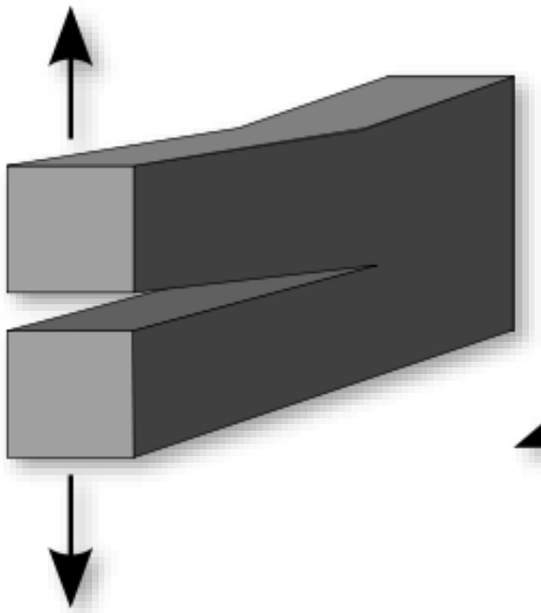

Mode I:
Opening

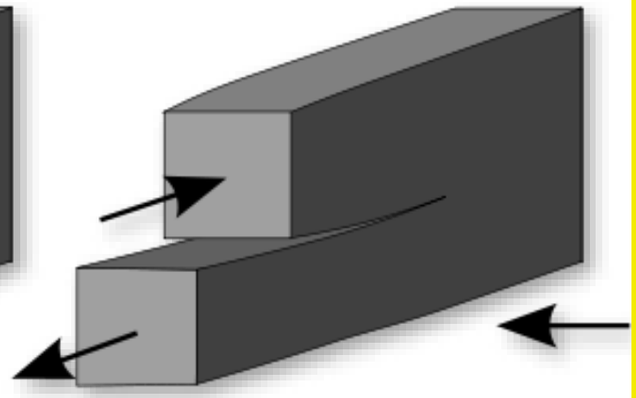

Mode II:
In-plane shear

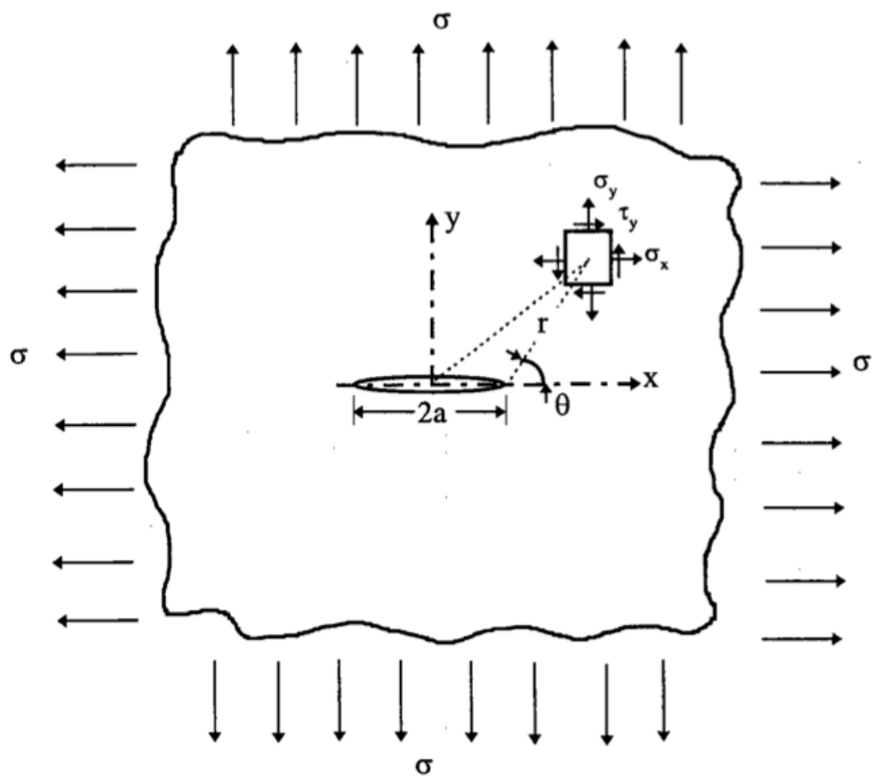

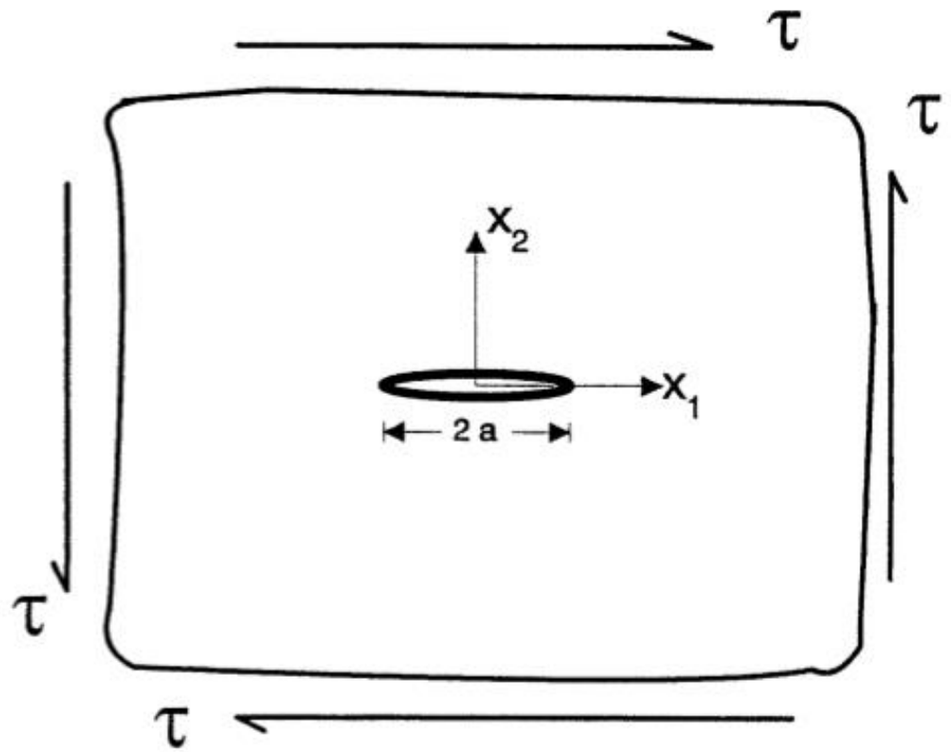

Westergaard's complex stress function for mode I

1937

- Constructing appropriate stress function (ignoring const. parts):

$$0 = \sigma_{12}(x_1, x_2 = 0) \quad \Rightarrow$$

$$\chi'' = -\bar{z}\phi'' = -z\phi'' \ (x_2 = 0) \quad \Rightarrow$$

$$\chi' = -z\phi' + \phi \quad \Rightarrow$$

$$\chi = -z\phi + 2\tilde{\phi} \ (\{\tilde{\phi}\}' = \phi) \quad \Rightarrow$$

$$\boldsymbol{\Psi} = \mathrm{Re}\left[\bar{z}\phi + \chi\right] = \mathrm{Re}\left[\bar{z}\phi - z\phi + 2\tilde{\phi}\right]$$

$$= 2\mathrm{Re}\left[-ix_2\phi + \tilde{\phi}\right] = 2\left[x_2 \mathrm{Im}\phi + \mathrm{Re}\tilde{\phi}\right]$$

$\tilde{Z} = \int f(z)\mathrm{d}z, \tilde{\tilde{Z}} = \int \tilde{Z}(z)\mathrm{d}z$

$\tilde{Z}$ and $\tilde{\tilde{Z}}$ are 1st, 2nd antiderivatives

- Using $\phi = \frac{1}{2}\tilde{Z}$

$$\boldsymbol{\Psi} = \mathrm{Re}\,\tilde{\tilde{Z}} + x_2 \mathrm{Im}\tilde{Z}$$

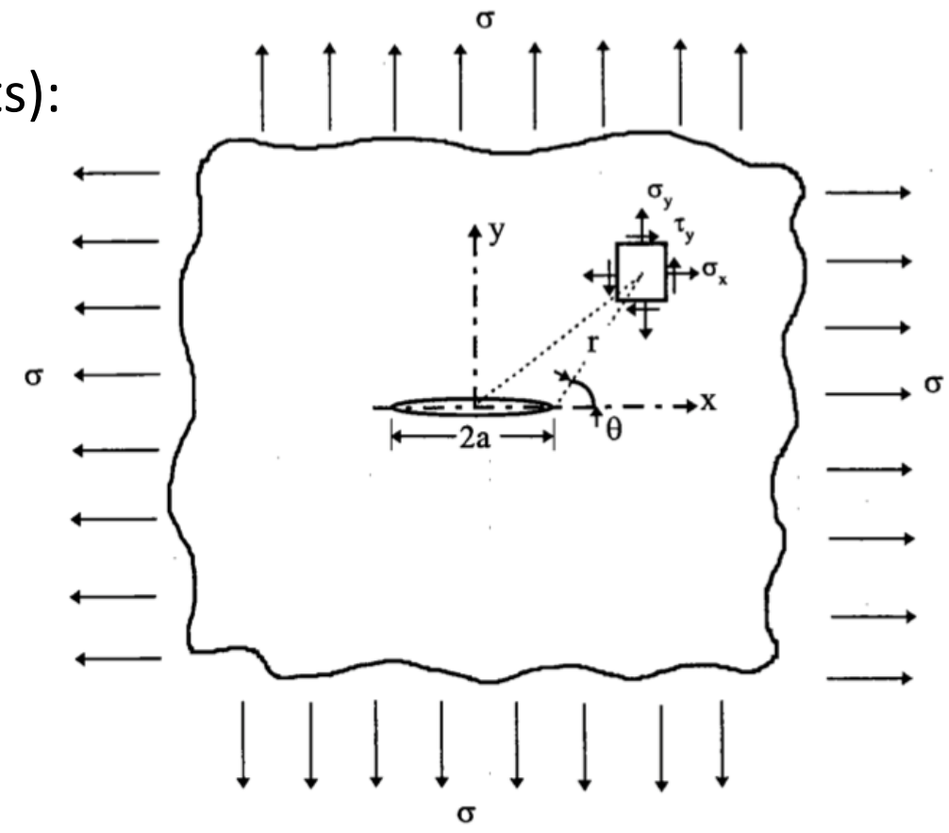

Westergaard's complex stress function for mode I

$$Z(z), z = x + iy, i^2 = -1$$

$$\boldsymbol{\Psi} = \mathrm{Re}\,\tilde{\tilde{Z}} + y\mathrm{Im}\tilde{Z}$$

$$\tilde{Z} = \int f(z)\mathrm{d}z, \tilde{\tilde{Z}} = \int \tilde{Z}(z)\mathrm{d}z$$

$$\sigma_{xx} = \mathrm{Re}Z - y\mathrm{Im}Z'$$

$$\sigma_{yy} = \mathrm{Re}Z + y\mathrm{Im}Z'$$

$$\tau_{xy} = -y\mathrm{Re}Z'$$

$$\epsilon_{ij} \rightarrow u_i$$

Kolosov coef. κ

$$\kappa = \begin{cases} 3 - 4\nu & \text{plane strain} \\ \dfrac{3-\nu}{1+\nu} & \text{plane stress} \end{cases}$$

$$\mu = \frac{E}{2(1+\nu)}$$ shear modulus

$$2\mu u = \frac{\kappa - 1}{2}\mathrm{Re}\tilde{Z} - y\mathrm{Im}Z$$

$$2\mu v = \frac{\kappa + 1}{2}\mathrm{Im}\tilde{Z} - y\mathrm{Re}Z$$

Griffith's crack (mode I)

$$(x,y)\to\infty : \sigma_{xx}=\sigma_{yy}=\sigma, \tau_{xy}=0$$

$$|x|<a, y=0 : \sigma_{yy}=\tau_{xy}=0$$

boundary conditions

$$Z(z)=\frac{\sigma z}{\sqrt{z^2-a^2}}$$

$$\sigma_{xx}=\mathrm{Re}Z-y\mathrm{Im}Z'$$
$$\sigma_{yy}=\mathrm{Re}Z+y\mathrm{Im}Z'$$
$$\tau_{xy}=-y\mathrm{Re}Z'$$

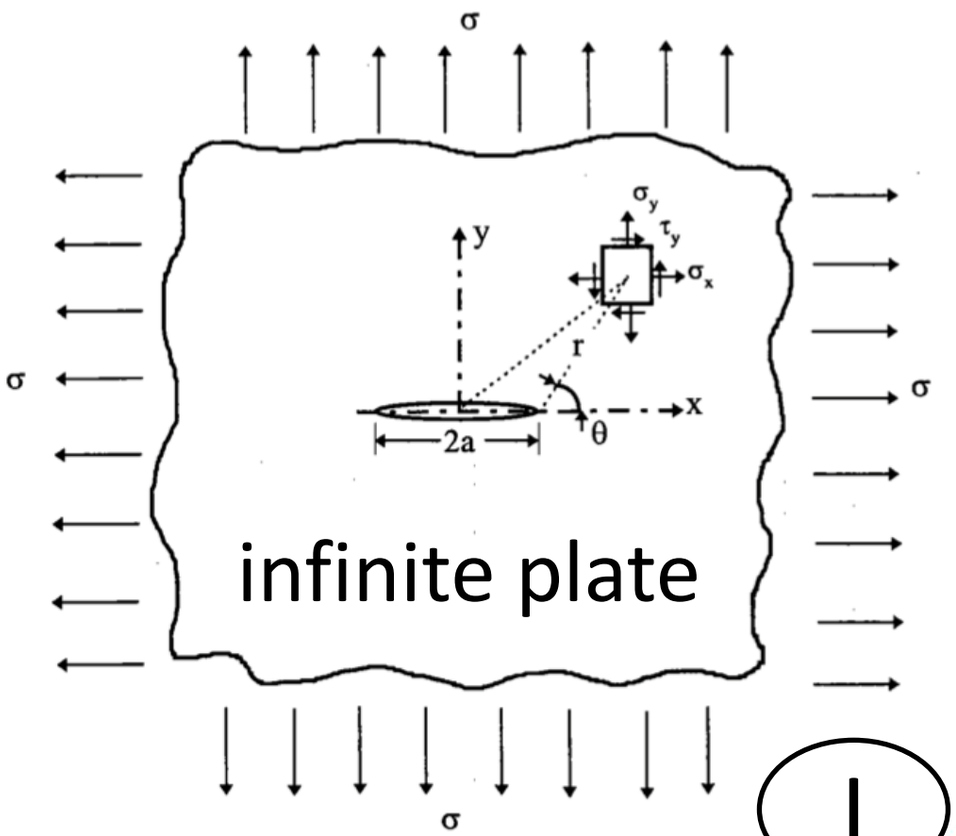

II

$$y=0,\ |x|<a$$

$$Z(z)=\frac{\sigma x}{\sqrt{x^2-a^2}}$$ is imaginary

I

$$Z(z)=\frac{\sigma}{\sqrt{1-(a/z)^2}}$$

$$Z'(z)=-\frac{\sigma a^2}{(z^2-a^2)^{3/2}}\to 0$$

$$(x,y)\to\infty : z\to\infty \quad Z\to\sigma$$

Griffith's crack (mode I)

$$(x,y) \to \infty : \sigma_{xx} = \sigma_{yy} = \sigma, \tau_{xy} = 0$$

$$|x| < a, y = 0 : \sigma_{yy} = \tau_{xy} = 0$$

$$Z(z) = \frac{\sigma z}{\sqrt{z^2 - a^2}}$$

boundary conditions

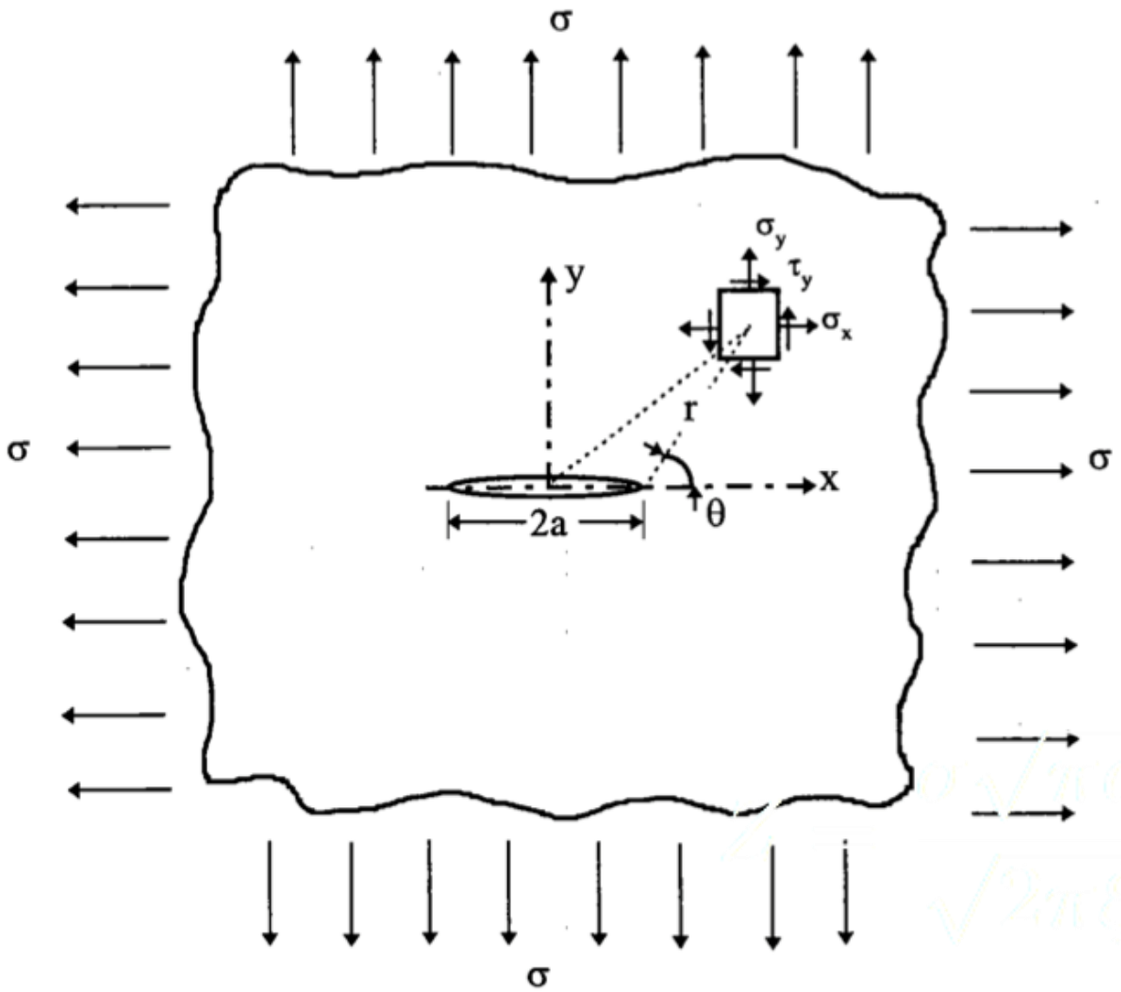

infinite plate

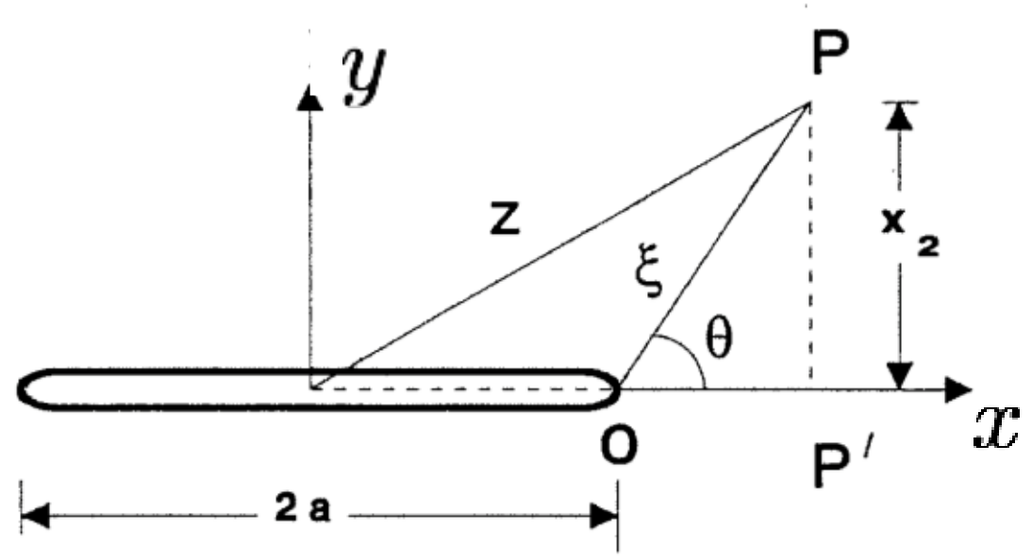

$$\xi = z - a, \xi = re^{i\theta}$$

$$Z(z) = \frac{\sigma(\xi + a)}{\sqrt{\xi(\xi + 2a)}}$$

Griffith's crack (mode I)

$$Z(z) = \frac{\sigma(\xi + a)}{\sqrt{\xi(\xi + 2a)}} = \frac{\sigma(\xi + a)}{\sqrt{2a\xi(1 + \xi/(2a))}}$$

$$\sqrt{1 + \xi/(2a)} = (1 + \xi/(2a))^{-1/2}$$

$$= 1 - \frac{1}{2}\frac{\xi}{2a} + \text{H.O.T}$$

$$= 1 \quad \xi \quad \text{small}$$

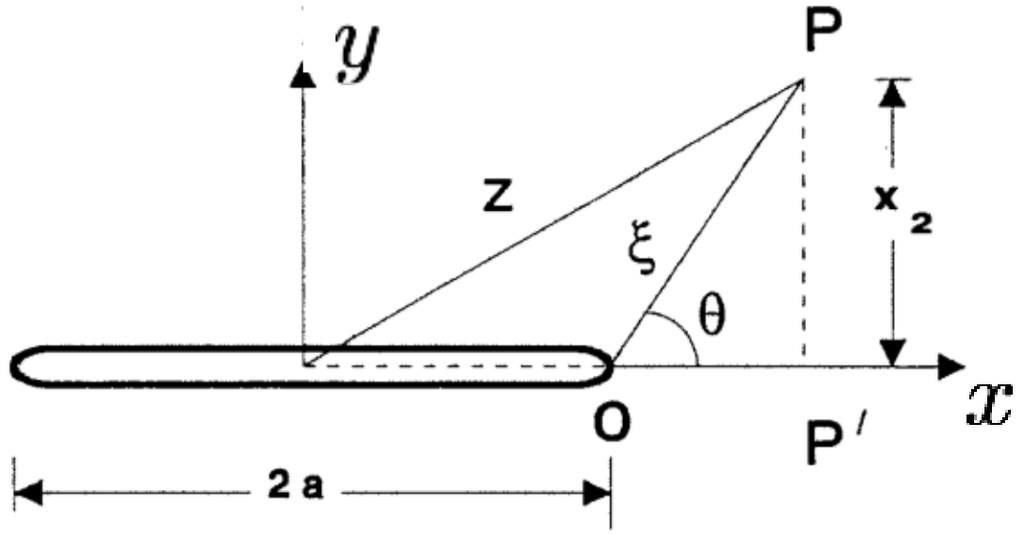

ξ small $\qquad \xi + a = a$

$$\longrightarrow \quad Z = \frac{\sigma\sqrt{\pi a}}{\sqrt{2\pi\xi}}$$

$$Z(z) = \frac{K_I}{\sqrt{2\pi\xi}}, K_I = \sigma\sqrt{\pi a}$$

$$Z(z) = \frac{K_I}{\sqrt{2\pi r}} e^{-i\theta/2}$$

$$\xi = re^{i\theta}$$

$$Z'(z) = -\frac{1}{2}\frac{K_I}{\sqrt{2\pi}}\xi^{-3/2} = -\frac{K_I}{2r\sqrt{2\pi r}}e^{-i3\theta/2}$$

Recall

$$\sigma_{xx} = \mathrm{Re}Z - y\mathrm{Im}Z'$$

$$\sigma_{yy} = \mathrm{Re}Z + y\mathrm{Im}Z'$$

$$\tau_{xy} = -y\mathrm{Re}Z'$$

$$e^{-ix} = \cos x - i\sin x$$

$$y = r\sin\theta$$

$$\sin\theta = 2\sin\frac{\theta}{2}\cos\frac{\theta}{2}$$

Crack tip stress field

$$\sigma_{xx} = \frac{K_I}{\sqrt{2\pi r}}\cos\left(\frac{\theta}{2}\right)\left[1 - \sin\left(\frac{\theta}{2}\right)\sin\left(\frac{3\theta}{2}\right)\right]$$

$$\sigma_{yy} = \frac{K_I}{\sqrt{2\pi r}}\cos\left(\frac{\theta}{2}\right)\left[1 + \sin\left(\frac{\theta}{2}\right)\sin\left(\frac{3\theta}{2}\right)\right]$$

$$\tau_{xy} = \frac{K_I}{\sqrt{2\pi r}}\cos\left(\frac{\theta}{2}\right)\sin\left(\frac{\theta}{2}\right)$$

inverse square root

$\frac{1}{\sqrt{r}}$ singularity

$$r \to 0 : \sigma_{ij} \to \infty$$

Plane strain problems

Hooke's law

$$\epsilon_{zz} = \frac{1}{E}\left(-\nu\sigma_{xx} - \nu\sigma_{yy} + \sigma_{zz}\right)$$

Plane strain $\epsilon_{zz} = 0$

$$\sigma_{xx} = \frac{K_I}{\sqrt{2\pi r}} \cos\frac{\theta}{2}\left(1 - \sin\frac{\theta}{2}\cos\frac{3\theta}{2}\right)$$
$$\sigma_{yy} = \frac{K_I}{\sqrt{2\pi r}} \cos\frac{\theta}{2}\left(1 + \sin\frac{\theta}{2}\cos\frac{3\theta}{2}\right)$$
$$\tau_{xy} = \frac{K_I}{\sqrt{2\pi r}} \sin\frac{\theta}{2}\cos\frac{\theta}{2}\sin\frac{3\theta}{2}$$

$$\longrightarrow \sigma_z = \nu(\sigma_x + \sigma_y) \longrightarrow$$

$$\sigma_z = 2\nu\frac{K_I}{\sqrt{2\pi r}}\cos\frac{\theta}{2}$$

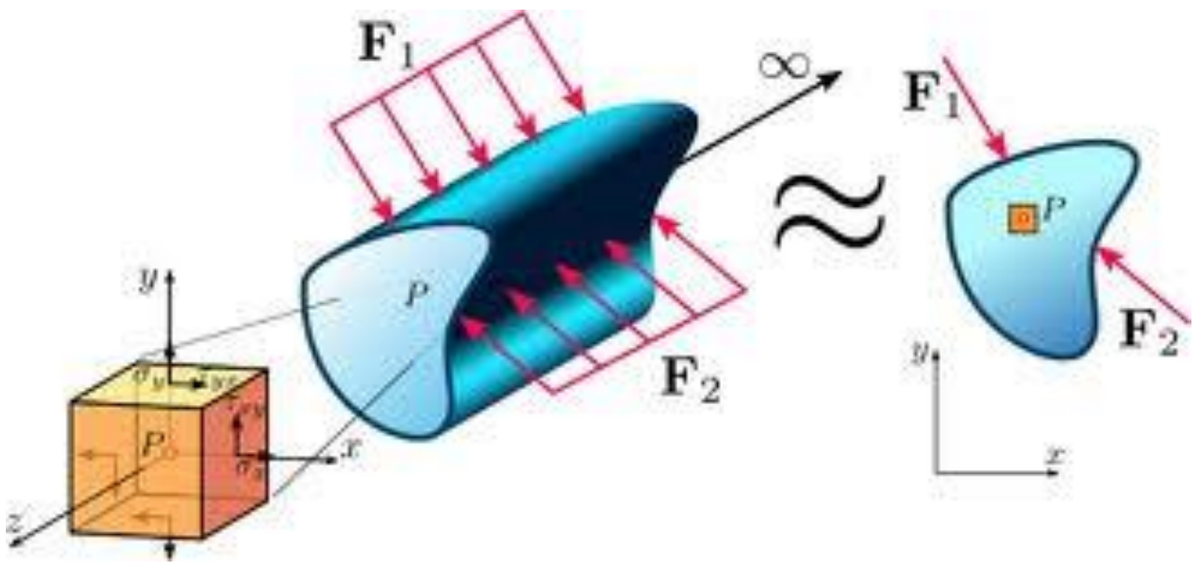

Stresses on the crack plane

$$\sigma_{xx} = \frac{K_I}{\sqrt{2\pi r}} \cos\frac{\theta}{2}\left(1 - \sin\frac{\theta}{2}\cos\frac{3\theta}{2}\right)$$

$$\sigma_{yy} = \frac{K_I}{\sqrt{2\pi r}} \cos\frac{\theta}{2}\left(1 + \sin\frac{\theta}{2}\cos\frac{3\theta}{2}\right)$$

$$\tau_{xy} = \frac{K_I}{\sqrt{2\pi r}} \sin\frac{\theta}{2}\cos\frac{\theta}{2}\sin\frac{3\theta}{2}$$

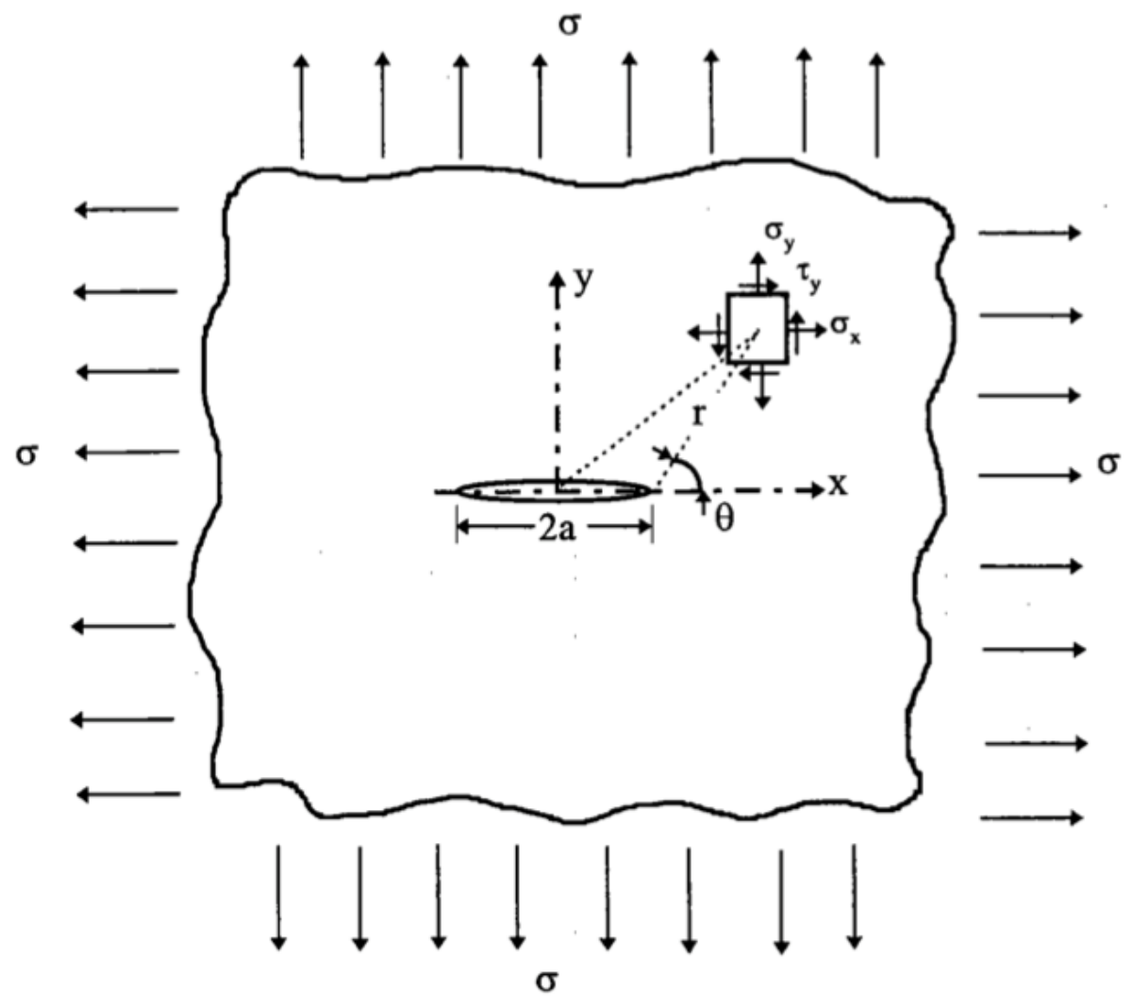

On the crack plane

$$\theta = 0, r = x$$

$$\sigma_{xx} = \sigma_{yy} = \frac{K_I}{\sqrt{2\pi x}}$$

crack plane is a principal plane with the following principal stresses

$$\tau_{xy} = 0$$

$$\sigma_1 = \sigma_2 = \sigma_{xx} = \sigma_{yy}$$

Stress Intensity Factor (SIF)

$$\sigma_{xx} = \frac{K_I}{\sqrt{2\pi r}}\cos\left(\frac{\theta}{2}\right)\left[1-\sin\left(\frac{\theta}{2}\right)\sin\left(\frac{3\theta}{2}\right)\right]$$

$$\sigma_{yy} = \frac{K_I}{\sqrt{2\pi r}}\cos\left(\frac{\theta}{2}\right)\left[1+\sin\left(\frac{\theta}{2}\right)\sin\left(\frac{3\theta}{2}\right)\right]$$

$$\tau_{xy} = \frac{K_I}{\sqrt{2\pi r}}\cos\left(\frac{\theta}{2}\right)\sin\left(\frac{\theta}{2}\right)$$

$$K_I = \sigma\sqrt{\pi a}$$

K_I

$[\mathrm{MPa}\sqrt{\mathrm{m}}]$

- Stresses-K: linearly proportional
- K uniquely defines the crack tip stress field
- modes I, II and III:
- LEFM: single-parameter K_I, K_{II}, K_{III}

SIMILITUDE

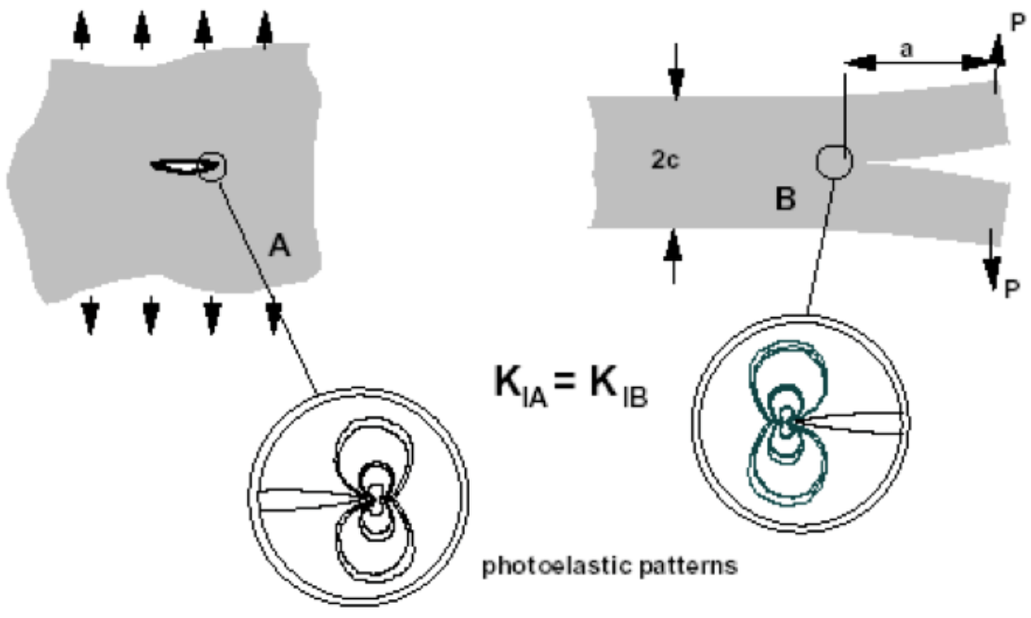

Mode II problem

Boundary conditions

$$(x,y)\to\infty:\sigma_{xx}=\sigma_{yy}=0,\tau_{xy}=\tau$$
$$|x|<a,y=0:\sigma_{yy}=\tau_{xy}=0$$

Stress function

$$Z=-\frac{i\tau z}{\sqrt{z^2-a^2}}$$

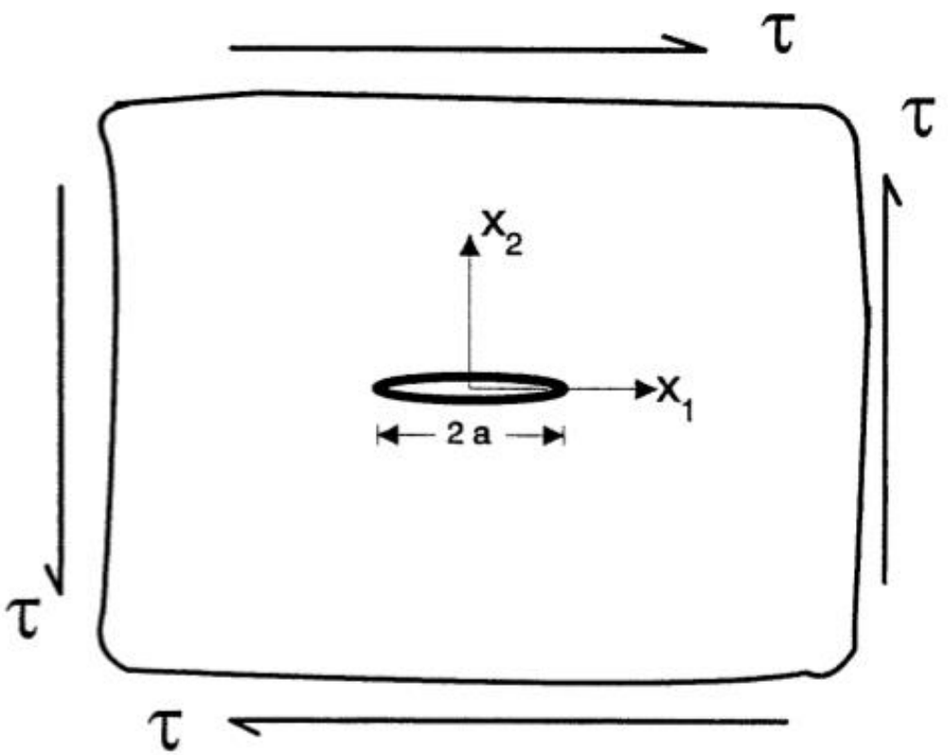

Check BCs

$$\sigma_{xx}=\mathrm{Re}Z-y\mathrm{Im}Z'$$
$$\sigma_{yy}=\mathrm{Re}Z+y\mathrm{Im}Z'$$
$$\tau_{xy}=-y\mathrm{Re}Z'$$

Mode II problem

Boundary conditions

$$(x,y) \to \infty : \sigma_{xx} = \sigma_{yy} = 0, \tau_{xy} = \tau$$
$$|x| < a, y = 0 : \sigma_{yy} = \tau_{xy} = 0$$

Stress function

$$Z = -\frac{i\tau z}{\sqrt{z^2 - a^2}}$$

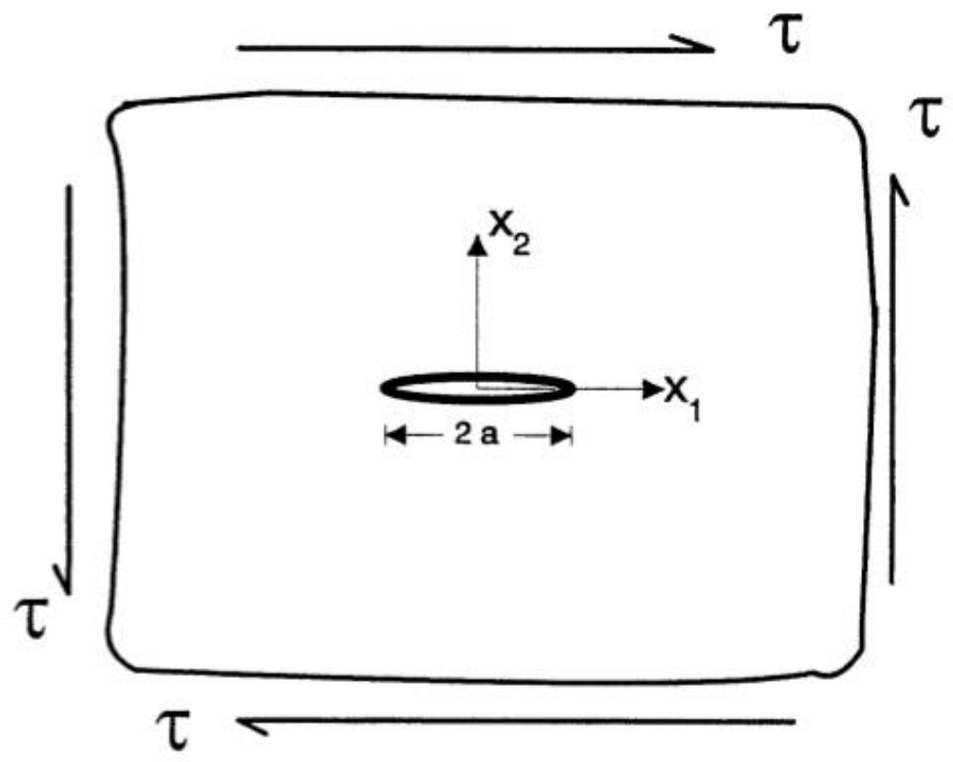

$$\sigma_{xx} = -\frac{K_{II}}{\sqrt{2\pi r}} \sin\frac{\theta}{2}\left(2 + \cos\frac{\theta}{2}\cos\frac{3\theta}{2}\right)$$
$$\sigma_{yy} = \frac{K_{II}}{\sqrt{2\pi r}} \sin\frac{\theta}{2}\cos\frac{\theta}{2}\cos\frac{3\theta}{2}$$
$$\tau_{xy} = \frac{K_{II}}{\sqrt{2\pi r}} \cos\frac{\theta}{2}\left(1 - \sin\frac{\theta}{2}\sin\frac{3\theta}{2}\right)$$

mode II SIF

$$K_{II} = \tau\sqrt{\pi a}$$

Mode II problem (cont.)

Stress function

$$(x,y)\to\infty:\sigma_{xx}=\sigma_{yy}=0,\tau_{xy}=\tau$$
$$|x|<a,y=0:\sigma_{yy}=\tau_{xy}=0$$

$$Z=-\frac{i\tau z}{\sqrt{z^2-a^2}}$$

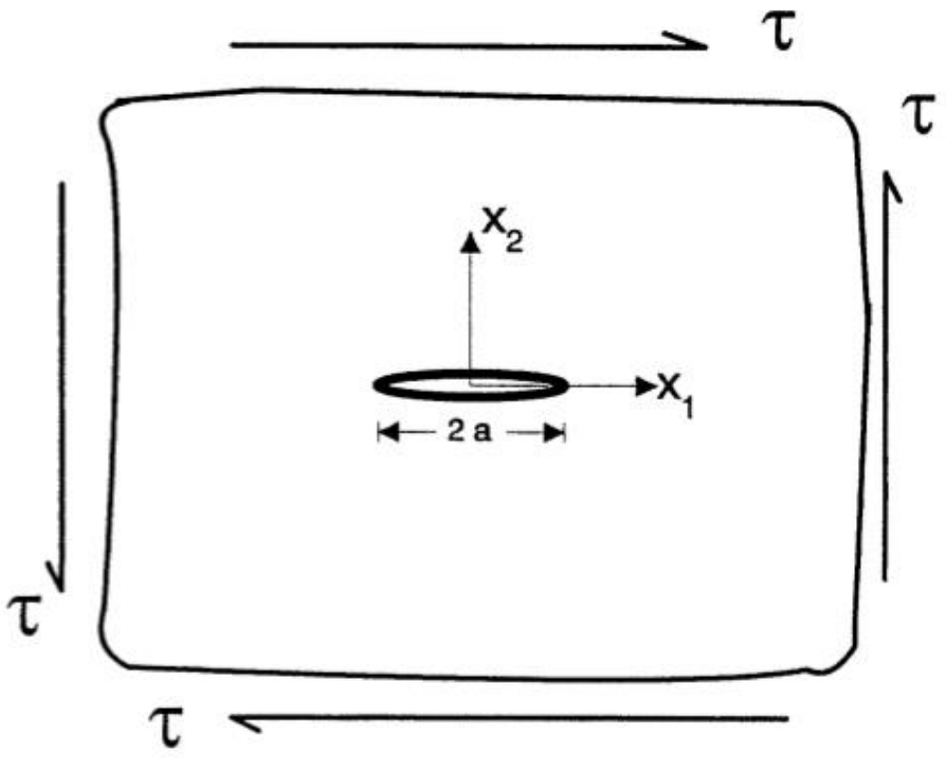

$$u=\frac{K_{II}}{2\mu}\sqrt{\frac{r}{2\pi}}\sin\frac{\theta}{2}\left(\kappa+1+2\cos^2\frac{\theta}{2}\right)$$
$$v=\frac{K_{II}}{2\mu}\sqrt{\frac{r}{2\pi}}\cos\frac{\theta}{2}\left(\kappa-1-2\sin^2\frac{\theta}{2}\right)$$

mode II SIF

$$K_{II}=\tau\sqrt{\pi a}$$

Universal nature of the asymptotic stress field

Westergaards, Sneddon etc.

$$\sigma_{xx} = \frac{K_I}{\sqrt{2\pi r}}\cos\left(\frac{\theta}{2}\right)\left[1-\sin\left(\frac{\theta}{2}\right)\sin\left(\frac{3\theta}{2}\right)\right]$$

$$\sigma_{yy} = \frac{K_I}{\sqrt{2\pi r}}\cos\left(\frac{\theta}{2}\right)\left[1+\sin\left(\frac{\theta}{2}\right)\sin\left(\frac{3\theta}{2}\right)\right]$$

$$\tau_{xy} = \frac{K_I}{\sqrt{2\pi r}}\cos\left(\frac{\theta}{2}\right)\sin\left(\frac{\theta}{2}\right)$$

(mode I)

$$\sigma_{xx} = -\frac{K_{II}}{\sqrt{2\pi r}}\sin\frac{\theta}{2}\left(2+\cos\frac{\theta}{2}\cos\frac{3\theta}{2}\right)$$

$$\sigma_{yy} = \frac{K_{II}}{\sqrt{2\pi r}}\sin\frac{\theta}{2}\cos\frac{\theta}{2}\cos\frac{3\theta}{2}$$

$$\tau_{xy} = \frac{K_{II}}{\sqrt{2\pi r}}\cos\frac{\theta}{2}\left(1-\sin\frac{\theta}{2}\sin\frac{3\theta}{2}\right)$$

(mode II)

Irwin $$\sigma_{ij} = \frac{K}{\sqrt{2\pi r}} f_{ij}(\theta) + \text{H.O.T}$$

Mode I: displacement field

$$Z(z) = \frac{K_I}{\sqrt{2\pi r}}\left(\cos\frac{\theta}{2} - i\sin\frac{\theta}{2}\right)$$

$$Z(z) = \frac{K_I}{\sqrt{2\pi\xi}} \qquad \bar{Z} = \int Z(z)dz$$

$$\tilde{Z}(z) = 2\frac{K_I}{\sqrt{2\pi}}\xi^{1/2} = 2K_I\sqrt{\frac{r}{2\pi}}\left(\cos\frac{\theta}{2} + i\sin\frac{\theta}{2}\right)$$

Recall

$$2\mu u = \frac{\kappa-1}{2}\mathrm{Re}\,\tilde{Z} - y\mathrm{Im}Z$$

$$2\mu v = \frac{\kappa+1}{2}\mathrm{Im}\,\tilde{Z} - y\mathrm{Re}Z$$

$$z = \xi + a$$

$$\xi = re^{i\theta}$$

$$e^{-ix} = \cos x - i\sin x$$

Displacement field

$$u = \frac{K_I}{2\mu}\sqrt{\frac{r}{2\pi}}\cos\frac{\theta}{2}\left(\kappa - 1 + 2\sin^2\frac{\theta}{2}\right)$$

$$v = \frac{K_I}{2\mu}\sqrt{\frac{r}{2\pi}}\sin\frac{\theta}{2}\left(\kappa + 1 - 2\cos^2\frac{\theta}{2}\right)$$

Kolosov coef. κ

$$\kappa = \begin{cases} 3-4\nu & \text{plane strain} \\ \dfrac{3-\nu}{1+\nu} & \text{plane stress} \end{cases}$$

Crack face displacement

$$y = 0, -a \leq x \leq a$$

$$2\mu v = \frac{\kappa+1}{2}\mathrm{Im}\tilde{Z} - y\mathrm{Re}Z \longrightarrow v = \frac{\kappa+1}{4\mu}\mathrm{Im}\tilde{Z}$$

$$Z(z) = \frac{\sigma x}{\sqrt{x^2 - a^2}} \longrightarrow \tilde{Z}(z) = \sigma\sqrt{x^2 - a^2}$$

$$-a \leq x \leq a \quad i = \sqrt{-1} \longrightarrow \tilde{Z}(z) = i(\sigma\sqrt{a^2 - x^2})$$

$$\boxed{v = \frac{\kappa+1}{4\mu}\sigma\sqrt{a^2 - x^2}}$$

ellipse

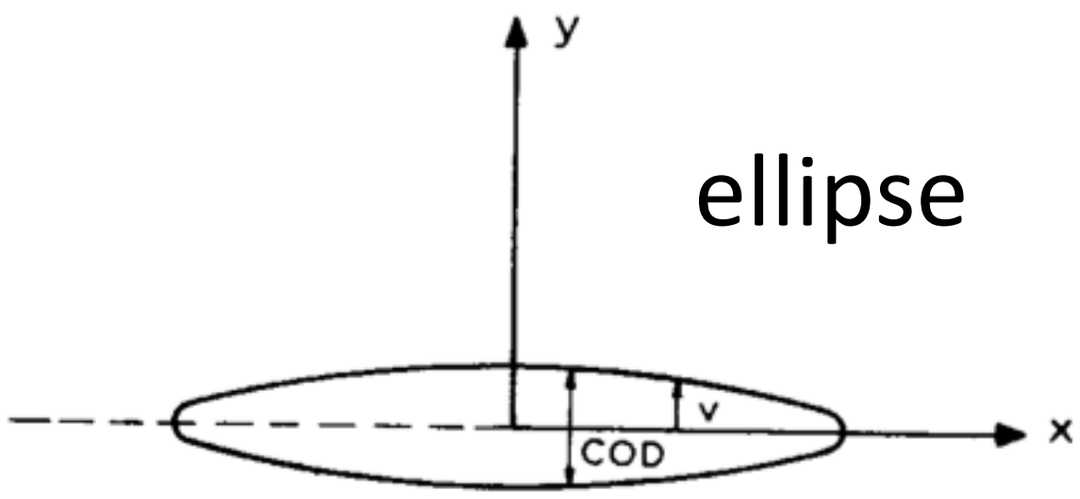

Crack Opening Displacement

$$\mathrm{COD} = 2v = \frac{\kappa+1}{2\mu}\sigma\sqrt{a^2 - x^2}$$

Crack tip stress field in polar coordinates-mode I

$$\sigma_{ij} = \frac{K_I}{\sqrt{\pi a}} f_{ij}(\theta)$$

$$\sigma_{rr} = \frac{K_I}{\sqrt{2\pi r}} \left(\frac{5}{4} \cos\frac{\theta}{2} - \frac{1}{4} \cos\frac{3\theta}{2} \right)$$

$$\sigma_{\theta\theta} = \frac{K_I}{\sqrt{2\pi r}} \left(\frac{3}{4} \cos\frac{\theta}{2} + \frac{1}{4} \cos\frac{3\theta}{2} \right)$$

$$\tau_{r\theta} = \frac{K_I}{\sqrt{2\pi r}} \left(\frac{1}{4} \sin\frac{\theta}{2} + \frac{1}{4} \sin\frac{3\theta}{2} \right)$$

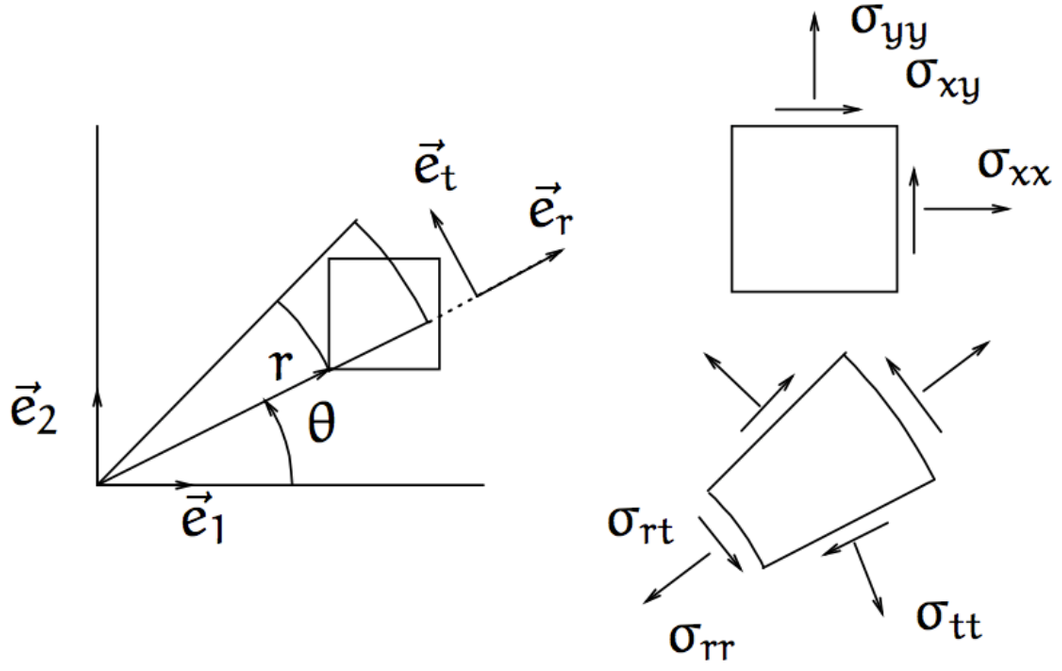

stress transformation

$$\begin{bmatrix} \sigma_{rr} & \sigma_{rt} \\ \sigma_{tr} & \sigma_{tt} \end{bmatrix} = \begin{bmatrix} c & s \\ -s & c \end{bmatrix} \begin{bmatrix} \sigma_{xx} & \sigma_{xy} \\ \sigma_{xy} & \sigma_{yy} \end{bmatrix} \begin{bmatrix} c & -s \\ s & c \end{bmatrix}$$

$$= \begin{bmatrix} c^2\sigma_{xx} + 2cs\sigma_{xy} + s^2\sigma_{yy} & \\ \quad - cs\sigma_{xx} + (c^2 - s^2)\sigma_{xy} + cs\sigma_{yy} & \\ -cs\sigma_{xx} + (c^2 - s^2)\sigma_{xy} + cs\sigma_{yy} & \\ \quad s^2\sigma_{xx} - 2cs\sigma_{xy} + c^2\sigma_{yy} & \end{bmatrix}$$

Principal crack tip stresses

$$\sigma_1, \sigma_2 = \frac{\sigma_{xx} + \sigma_{yy}}{2} \pm \sqrt{\left(\frac{\sigma_{xx} - \sigma_{yy}}{2}\right)^2 + \tau_{xy}^2}$$

$$\sigma_{xx} = \frac{K_I}{\sqrt{2\pi r}} \cos\frac{\theta}{2}\left(1 - \sin\frac{\theta}{2}\cos\frac{3\theta}{2}\right)$$

$$\sigma_{yy} = \frac{K_I}{\sqrt{2\pi r}} \cos\frac{\theta}{2}\left(1 + \sin\frac{\theta}{2}\cos\frac{3\theta}{2}\right)$$

$$\tau_{xy} = \frac{K_I}{\sqrt{2\pi r}} \sin\frac{\theta}{2}\cos\frac{\theta}{2}\sin\frac{3\theta}{2}$$

$$\sigma_1 = \frac{K_I}{\sqrt{2\pi r}} \cos\frac{\theta}{2}\left(1 + \sin\frac{\theta}{2}\right)$$

$$\sigma_2 = \frac{K_I}{\sqrt{2\pi r}} \cos\frac{\theta}{2}\left(1 - \sin\frac{\theta}{2}\right)$$

$$\sigma_3 = \begin{cases} 0 & \text{plane stress} \\ \dfrac{2\nu K_I}{\sqrt{2\pi r}} \cos\dfrac{\theta}{2} & \text{plane strain} \end{cases}$$

$\longleftarrow \quad \sigma_3 = \nu(\sigma_1 + \sigma_2)$

Crack solution using V-Notch

- Airy stress function assumed to be

$$\Phi(r,\theta) \equiv r^{\lambda+1} F(\theta,\lambda)$$

- Compatibility condition

$$\nabla^2\left(\nabla^2\Phi\right) = \left(\frac{\partial^2}{\partial r^2} + \frac{1}{r}\frac{\partial}{\partial r} + \frac{1}{r^2}\frac{\partial^2}{\partial\theta^2}\right)\left(\frac{\partial^2\Phi}{\partial r^2} + \frac{1}{r}\frac{\partial\Phi}{\partial r} + \frac{1}{r^2}\frac{\partial^2\Phi}{\partial\theta^2}\right) = 0 \quad \Rightarrow$$

$$\frac{\partial^4 F(\theta,\lambda)}{\partial\theta^4} + 2(\lambda^2+1)\frac{\partial^2 F(\theta,\lambda)}{\partial\theta^2} + (\lambda^2-1)^2 F(\theta,\lambda) = 0 \quad \Rightarrow$$

$$F(\theta) = e^{m\theta} \quad \Rightarrow$$

$$\left[(1-\lambda)^2 + m^2\right]\left[(1+\lambda)^2 + m^2\right] = 0 \quad \Rightarrow$$

$$m = \pm i(1 \pm \lambda) \quad \Rightarrow$$

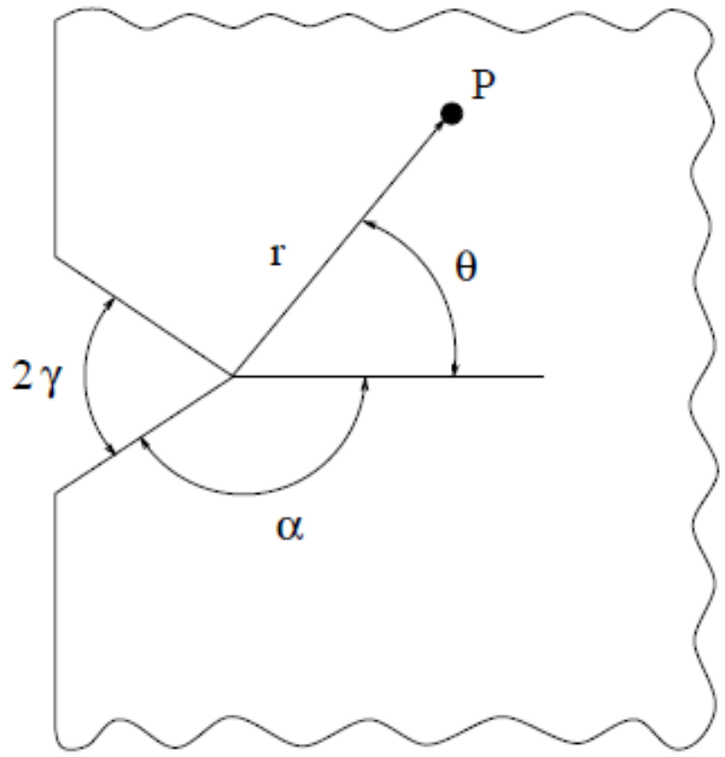

Source: Saouma:2010 Boulder Fracture Mechanics
Williams, 1952

- Final form of stress function

$$\Phi(r,\theta) = r^{\lambda+1}\underbrace{\left[A\cos(\lambda-1)\theta + B\cos(\lambda+1)\theta + C\sin(\lambda-1)\theta + D\sin(\lambda+1)\theta\right]}_{F(\theta,\lambda)}$$

Crack solution using V-Notch

- Stress values

$$\sigma_{\theta\theta} = \frac{\partial^2 \Phi}{\partial r^2} = r^{\lambda-1}\lambda(\lambda+1)F(\theta)$$

$$\sigma_{r\theta} = -\frac{\partial}{\partial r}\left(\frac{1}{r}\frac{\partial \Phi}{\partial \theta}\right) = r^{\lambda-1}[-\lambda F'(\theta)]$$

- Boundary conditions

$$\sigma_{\theta\theta}\,|_{\theta=\pm\alpha} = 0$$
$$\sigma_{r\theta}\,|_{\theta=\pm\alpha} = 0 \quad \Rightarrow$$

$$F(\alpha) = F(-\alpha) = F'(\alpha) = F'(-\alpha) = 0 \quad \Rightarrow$$

$$\begin{bmatrix} \cos(\lambda-1)\alpha & \cos(\lambda+1)\alpha & 0 & 0 \\ \omega\sin(\lambda-1)\alpha & \sin(\lambda+1)\alpha & 0 & 0 \\ 0 & 0 & \sin(\lambda-1)\alpha & \sin(\lambda+1)\alpha \\ 0 & 0 & \omega\cos(\lambda-1)\alpha & \cos(\lambda+1)\alpha \end{bmatrix} \begin{Bmatrix} A \\ B \\ C \\ D \end{Bmatrix} = 0$$

$\omega = \frac{\lambda-1}{\lambda+1}$.

$\Rightarrow$

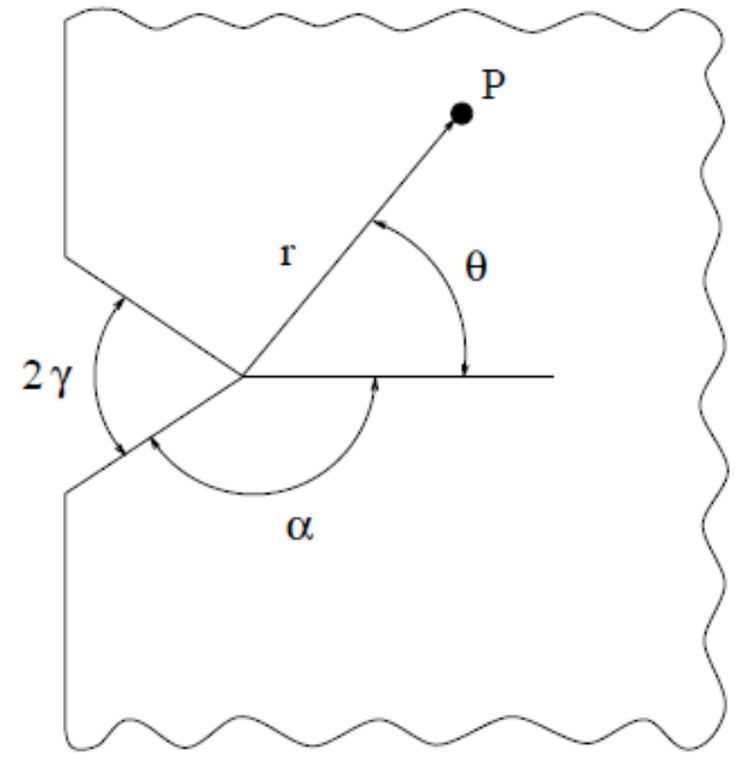

- Eigenvalues and eigenvectors for nontrivial solutions

$$\sin 2\lambda_n\alpha + \lambda_n \sin 2\alpha = 0 \quad \longleftarrow \text{Mode I}$$
$$\sin 2\xi_n\alpha - \xi_n \sin 2\alpha = 0 \quad \longleftarrow \text{Mode II}$$

Crack solution using V-Notch

- Sharp crack

$$\alpha = \pi \Longrightarrow \begin{aligned} \sin(2\pi\lambda_n) &= 0 \\ \sin(2\pi\xi_n) &= 0 \end{aligned} \Longrightarrow$$

$$\lambda_n = \tfrac{n}{2} \text{ with } n = 1, 3, 4, \cdots$$ (n = 2 constant stress)

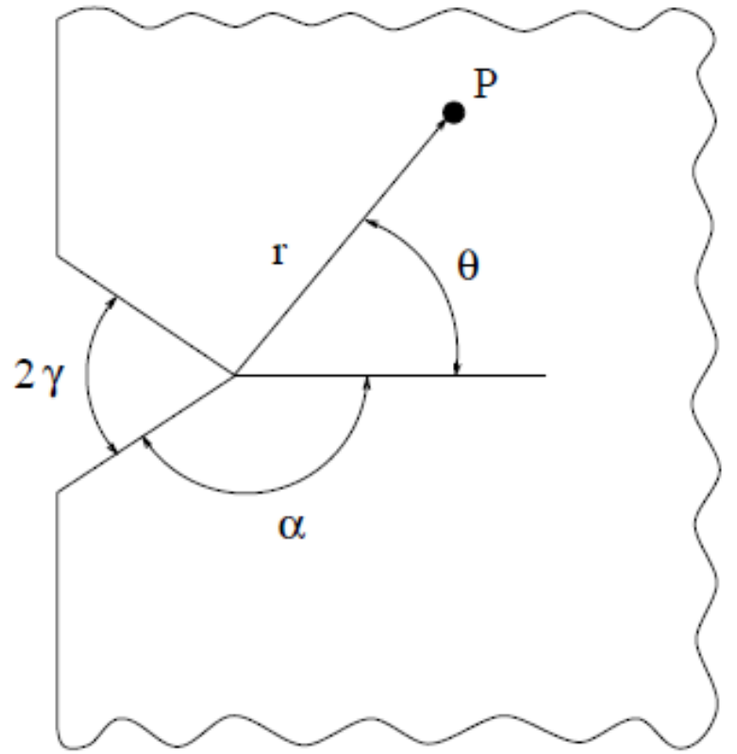

- After having eigenvalues, eigenvectors are obtained from

Mode I

$$\begin{aligned} A_n \cos(\lambda_n - 1)\alpha + B_n \cos(\lambda_n + 1)\alpha &= 0 \\ A_n \omega \sin(\lambda_n - 1)\alpha + B_n \sin(\lambda_n + 1)\alpha &= 0 \end{aligned}$$

Mode II

$$\begin{aligned} C_n \sin(\xi_n - 1)\alpha + D_n \sin(\xi_n + 1)\alpha &= 0 \\ C_n \omega \cos(\xi_n - 1)\alpha + D_n \cos(\xi_n + 1)\alpha &= 0 \end{aligned}$$

- **First term** of stress expansion

$$\begin{aligned} \sigma_{rr} &= \frac{K_I}{\sqrt{2\pi r}}\left(\frac{5}{4}\cos\frac{\theta}{2} - \frac{1}{4}\cos\frac{3\theta}{2}\right) + \frac{K_{II}}{\sqrt{2\pi r}}\left(-\frac{5}{4}\sin\frac{\theta}{2} + \frac{3}{4}\sin\frac{3\theta}{2}\right)\Big] \\ \sigma_{\theta\theta} &= \frac{K_I}{\sqrt{2\pi r}}\left(\frac{3}{4}\cos\frac{\theta}{2} + \frac{1}{4}\cos\frac{3\theta}{2}\right) + \frac{K_{II}}{\sqrt{2\pi r}}\left(-\frac{3}{4}\sin\frac{\theta}{2} - \frac{3}{4}\sin\frac{3\theta}{2}\right)\Big] \\ \sigma_{r\theta} &= \frac{K_I}{\sqrt{2\pi r}}\left(\frac{1}{4}\sin\frac{\theta}{2} + \frac{1}{4}\sin\frac{3\theta}{2}\right) + \frac{K_{II}}{\sqrt{2\pi r}}\left(\frac{1}{4}\cos\frac{\theta}{2} + \frac{3}{4}\cos\frac{3\theta}{2}\right)\Big] \end{aligned}$$

Inclined crack in tension

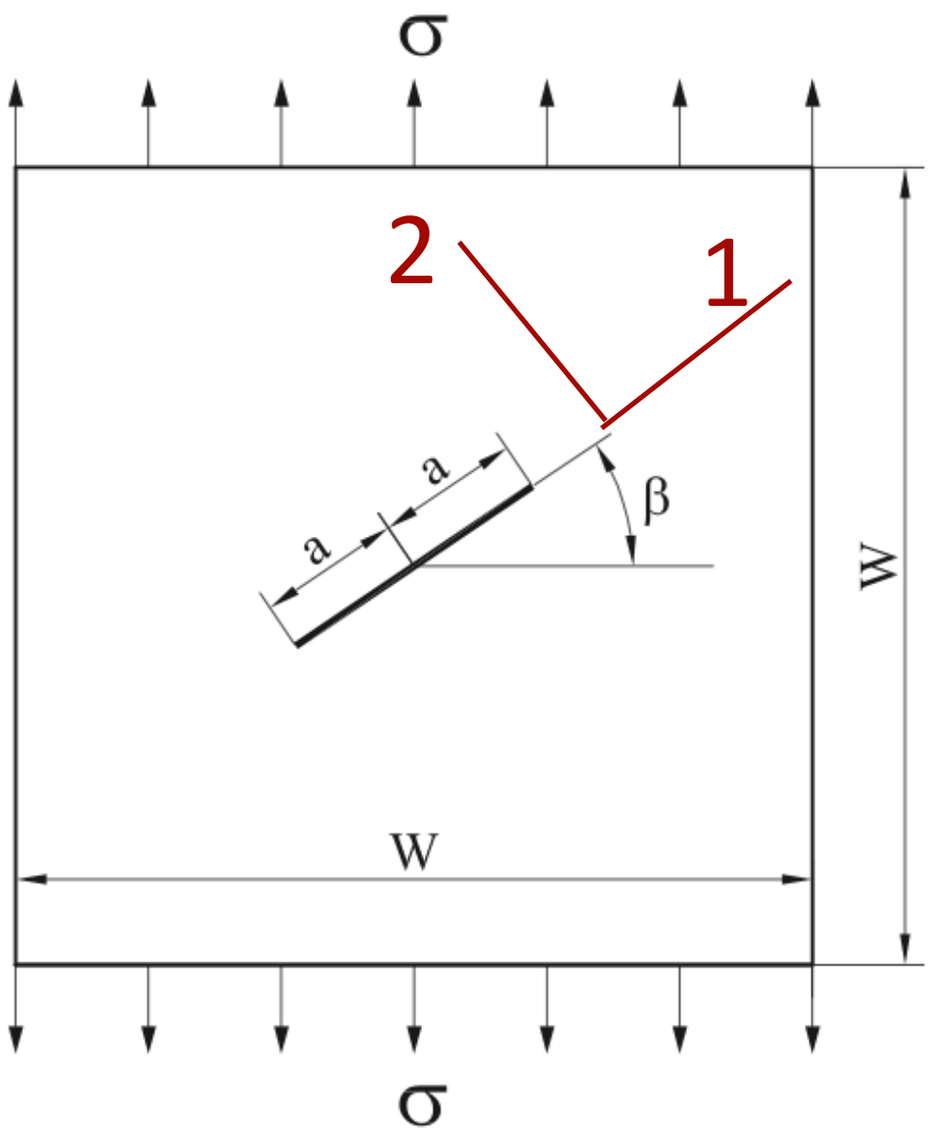

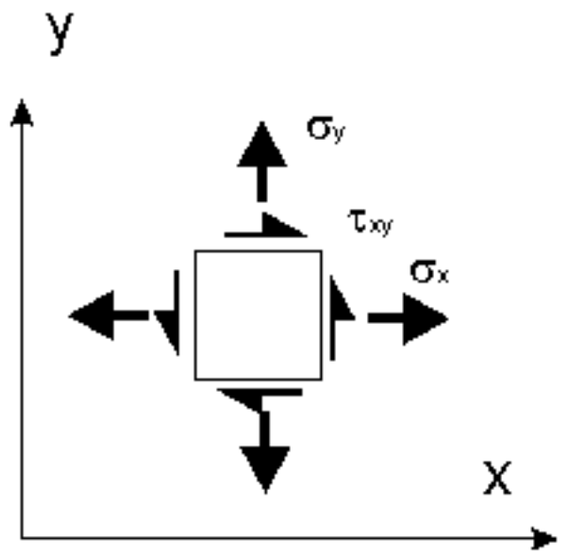

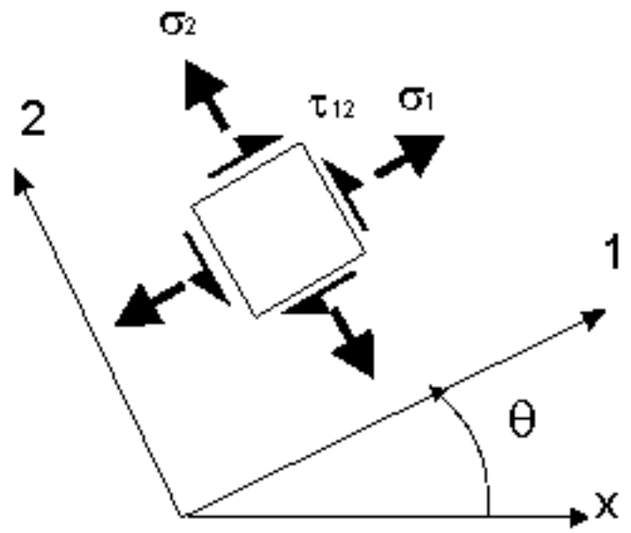

$$\sigma_1 = \sigma_x \cos^2\theta + 2\sin\theta\cos\theta\tau_{xy} + \sin^2\theta\sigma_y$$
$$\sigma_2 = \sigma_y \cos^2\theta - 2\sin\theta\cos\theta\tau_{xy} + \sin^2\theta\sigma_x$$
$$\tau_{12} = -\sigma_x \cos\theta\sin\theta + \cos 2\theta\tau_{xy} + 0.5\sin 2\theta\sigma_y$$

$$\sigma_1 = (\sin^2\beta)\sigma$$
$$\sigma_2 = (\cos^2\beta)\sigma$$
$$\tau_{12} = (\sin\beta\cos\beta)\sigma$$

Recall

+

$$K_I = \sigma_y\sqrt{\pi a}$$
$$K_{II} = \tau_{xy}\sqrt{\pi a}$$

Final result

$$K_I = \sigma\sqrt{\pi a}\cos^2\beta$$
$$K_{II} = \sigma\sqrt{\pi a}\sin\beta\cos\beta$$

Cylindrical pressure vessel with an inclined through-thickness crack

closed-ends

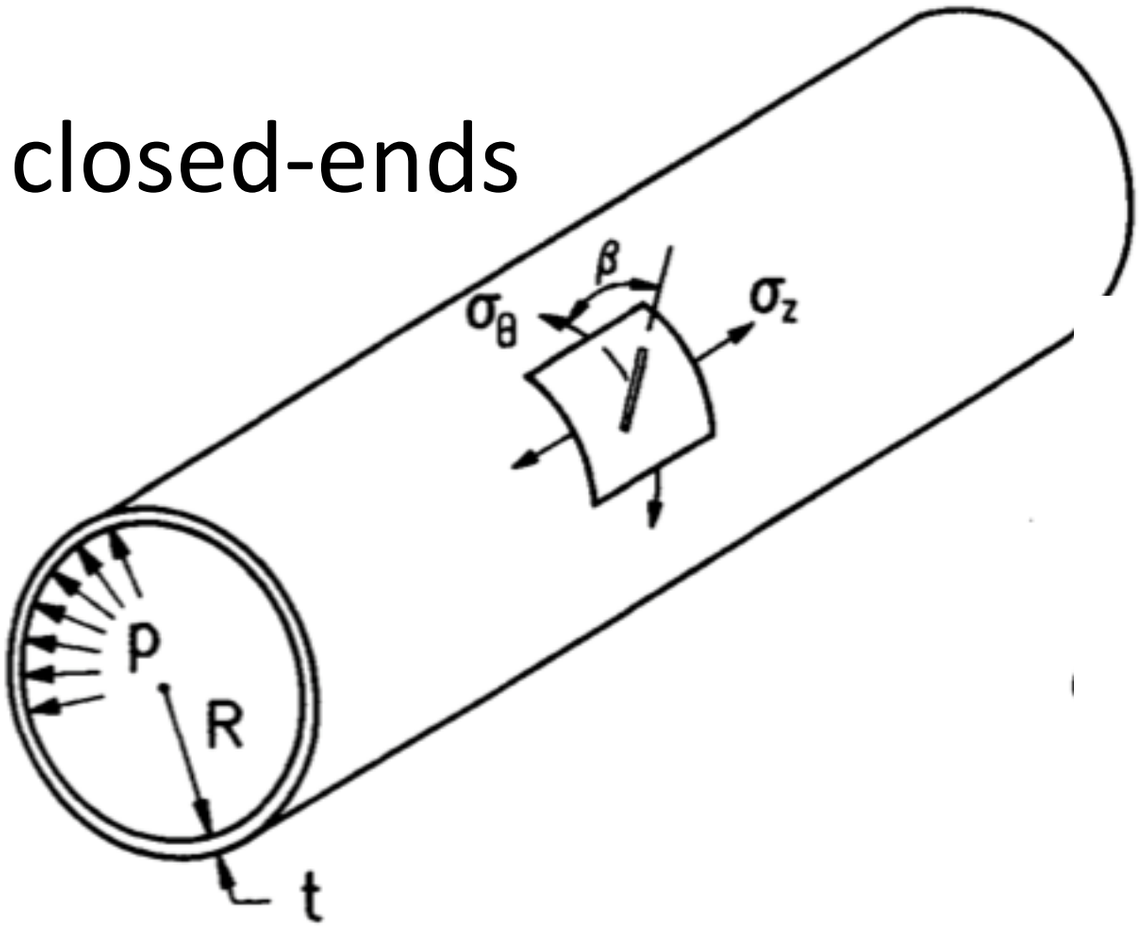

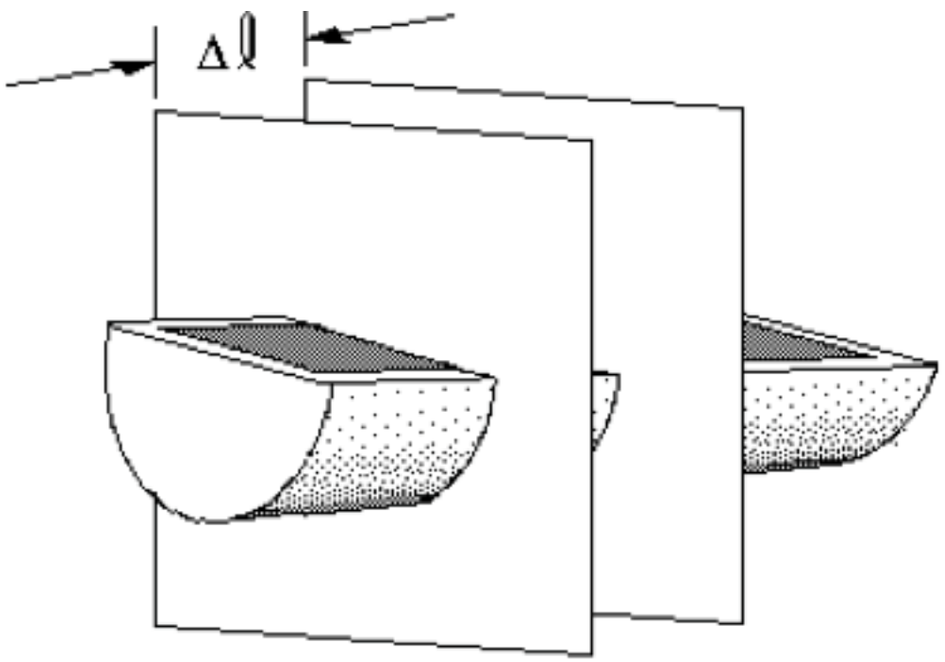

$\frac{R}{t} \geq 10$ thin-walled pressure

$$(\pi R^2)p = (2\pi Rt)\sigma_z$$

$$(\Delta l 2R)p = (2\Delta lt)\sigma_\theta$$

Cylindrical pressure vessel with an inclined through-thickness crack

$$\sigma_\theta = 2\sigma_z$$

This is why an overcooked hotdog usually cracks along the longitudinal direction first (i.e. its skin fails from hoop stress, generated by internal steam pressure).

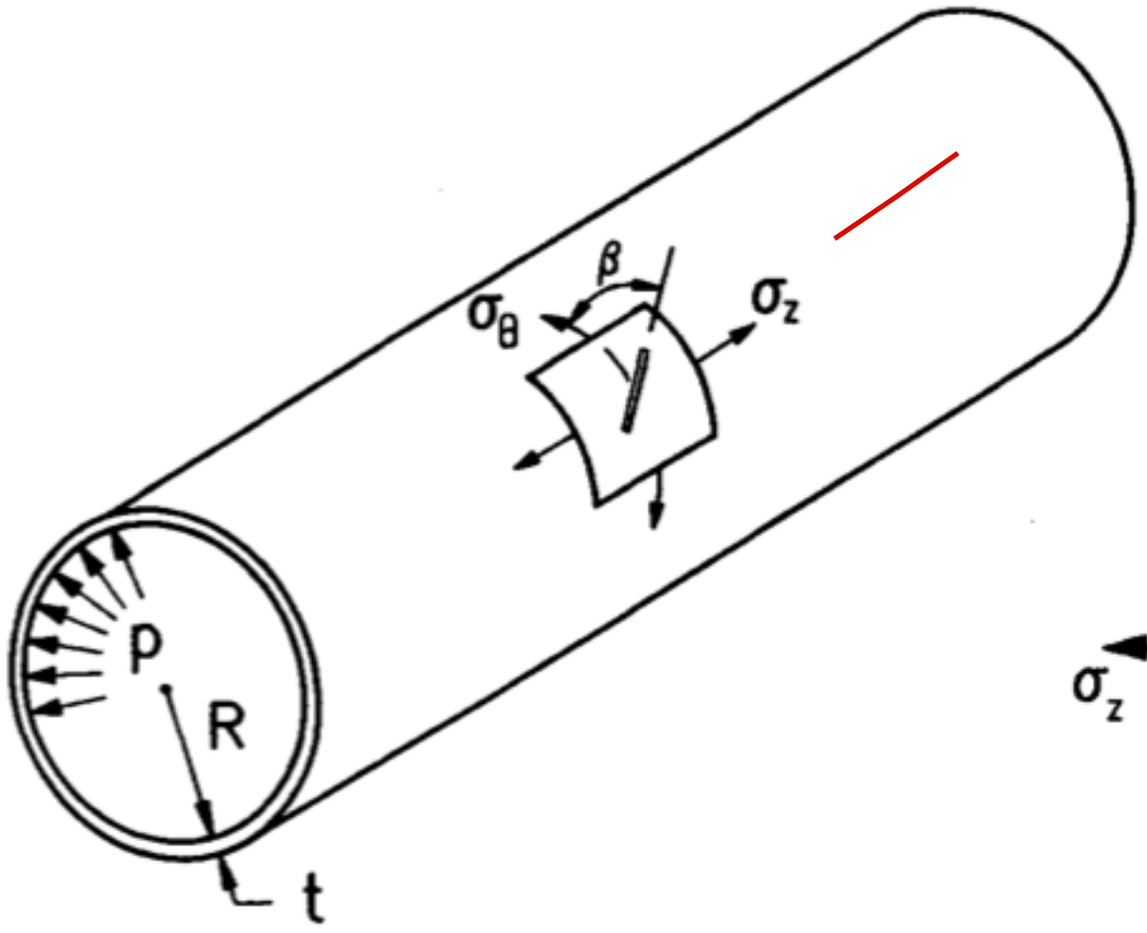

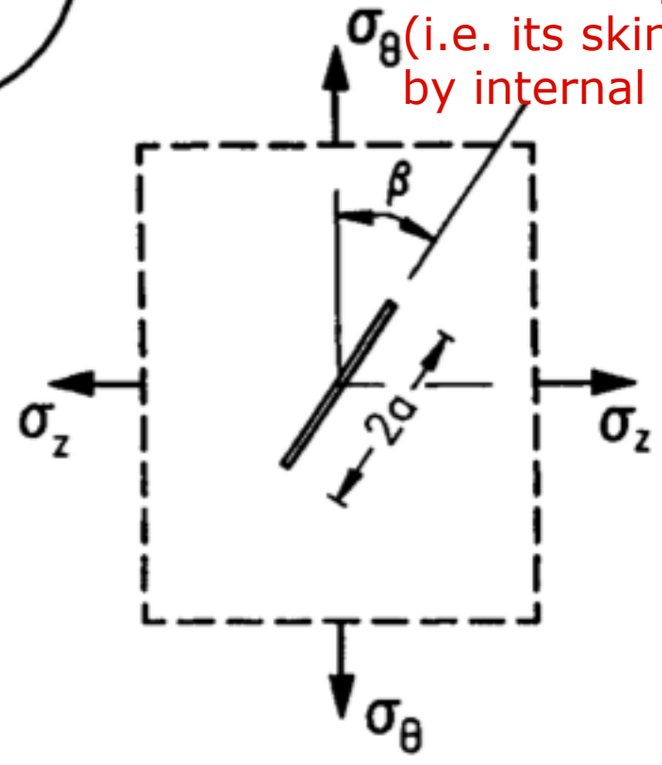

Equilibrium

$$\sigma_z = \frac{pR}{2t}$$

$$\sigma_\theta = \frac{pR}{t}$$

$$K_I = \frac{pR}{2t}\sqrt{\pi a}(1+\sin^2\beta)$$

$$K_{II} = \frac{pR}{2t}\sqrt{\pi a}\sin\beta\cos\beta$$

?

Computation of SIFs

- Analytical methods (limitation: simple geometry)

  - superposition methods
  - weight/Green functions

- Numerical methods (FEM, BEM, XFEM)

  numerical solutions -> data fit -> **SIF handbooks**

- Experimental methods
  - photoelasticity

SIF for finite size samples

Exact (closed-form) solution for SIFs: simple crack geometries in an **infinite** plate.

Cracks in finite plate: influence of external boundaries cannot be neglected -> generally, no exact solution

SIF for finite size samples

K_I < K_I

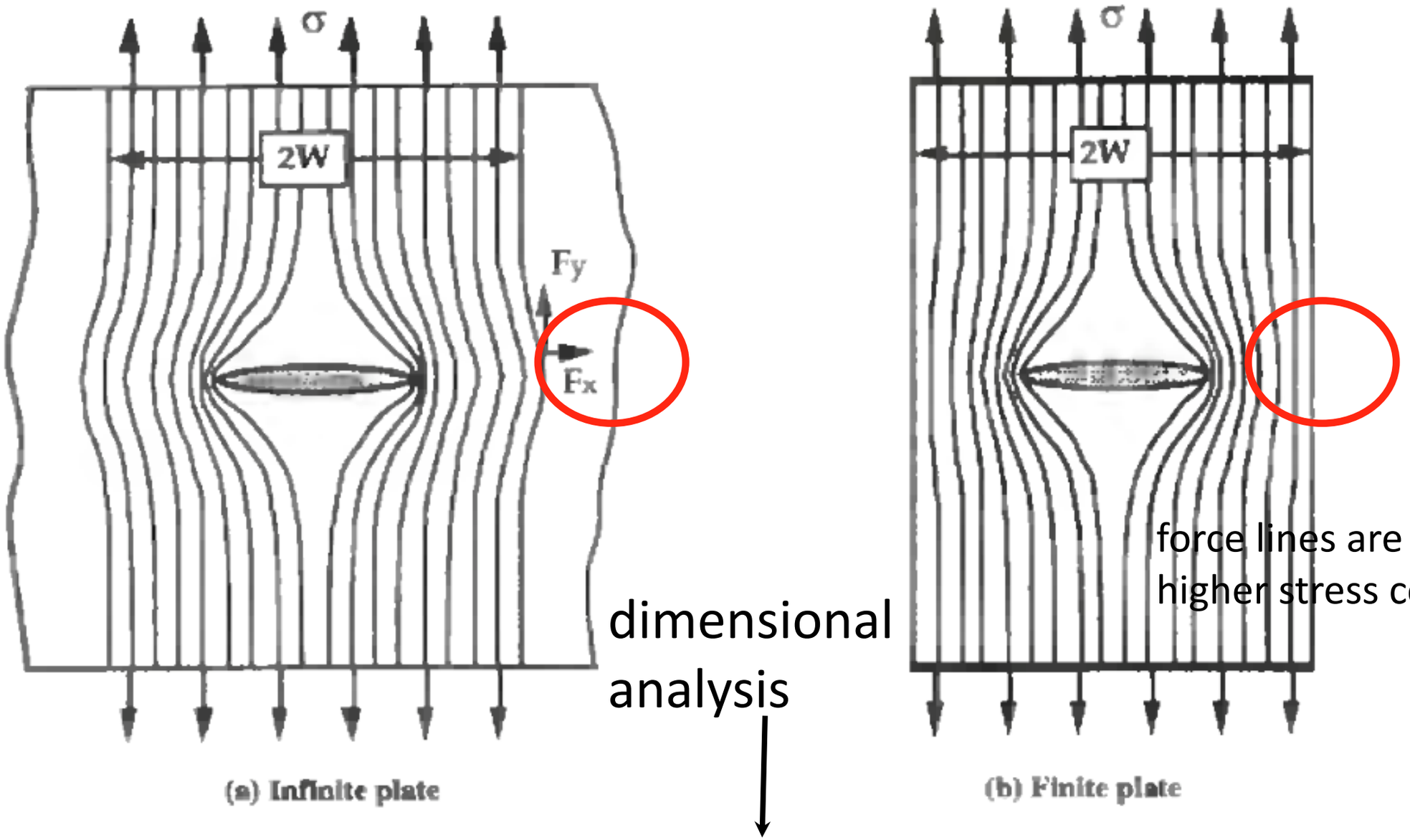

(a) Infinite plate

(b) Finite plate

force lines are compressed->> higher stress concentration

dimensional analysis

$$K_I = f(a/W)\sigma\sqrt{\pi a} \qquad a \ll W : f(a/W) \approx 1$$

geometry/correction factor [-]

SIFs handbook

Geometry	Stress Intensity Factor
1. Crack in an infinite body 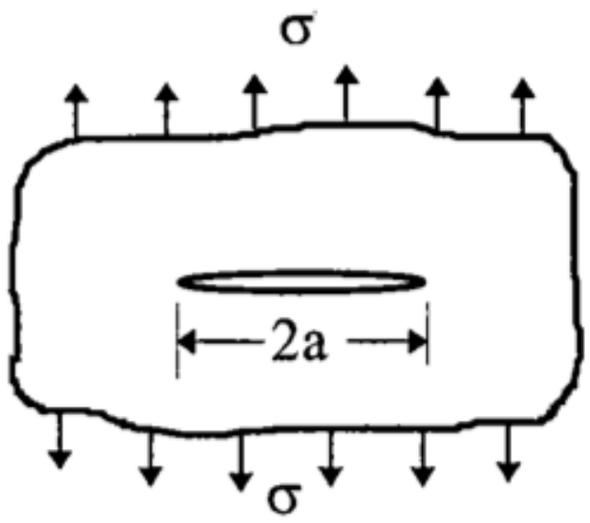	$K_I = \sigma\sqrt{\pi a}$
2. Centre crack in a strip of finite width 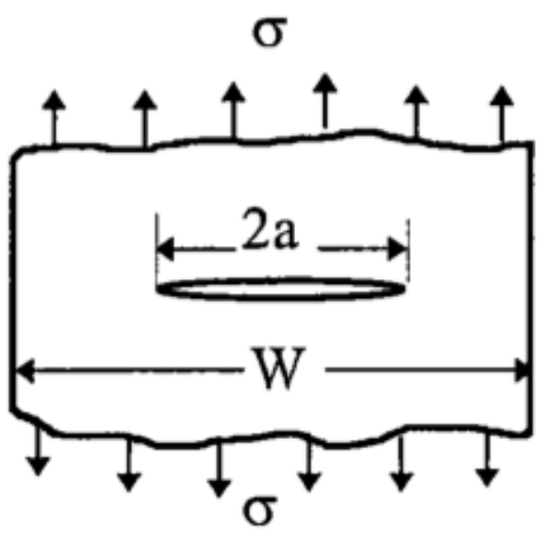	$K_I = \sqrt{\sec\frac{\pi a}{W}}\sigma\sqrt{\pi a}$

secant function

$$\sec\theta = \frac{1}{\cos\theta}$$

SIFs handbook

5. Edge crack in a beam of width B subjected to bending

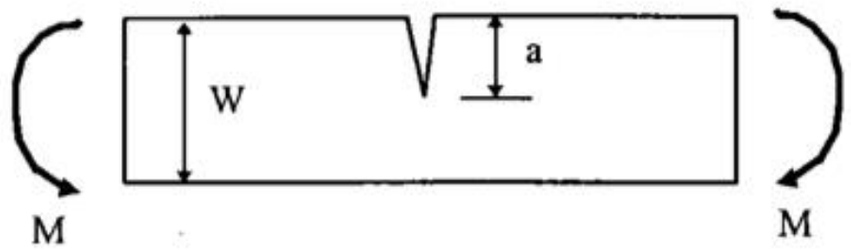

$$K_I = f\left(\frac{a}{W}\right)\sigma\sqrt{\pi a} \text{ where } \sigma = \frac{6M}{BW^2}$$

a/W	$f(a/W)$
0.1	1.044
0.2	1.055
0.3	1.125
0.4	1.257
0.5	1.500
0.6	1.915

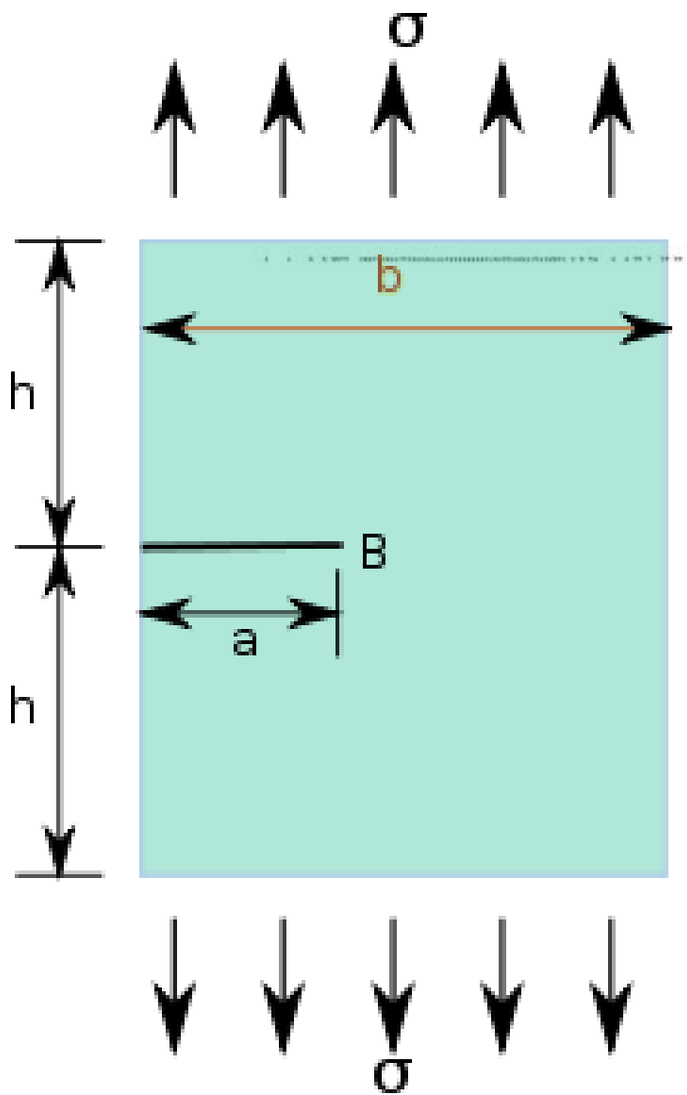

$h/b \geq 1$ and $a/b \leq 0.6$

$$K_I = \sigma\sqrt{\pi a}\left[1.12 - 0.23\left(\frac{a}{b}\right) + 10.6\left(\frac{a}{b}\right)^2 - 21.7\left(\frac{a}{b}\right)^3 + 30.4\left(\frac{a}{b}\right)^4\right]$$

SIFs handbook

9. Single-edge notch bend (SENB), thickness B

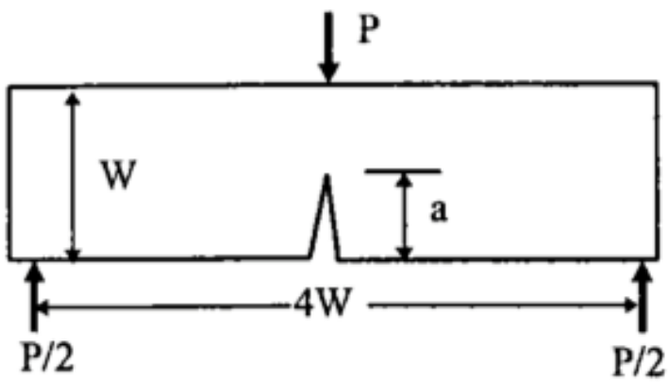

$$B = W / 2$$

$$K_I = Y \frac{4P\sqrt{\pi}}{B\sqrt{W}}$$

$$Y = 1.63\left(\frac{a}{W}\right)^{1/2} - 2.6\left(\frac{a}{W}\right)^{3/2} + 12.3\left(\frac{a}{W}\right)^{5/2} - 21.3\left(\frac{a}{W}\right)^{7/2} + 21.9\left(\frac{a}{W}\right)^{9/2}$$

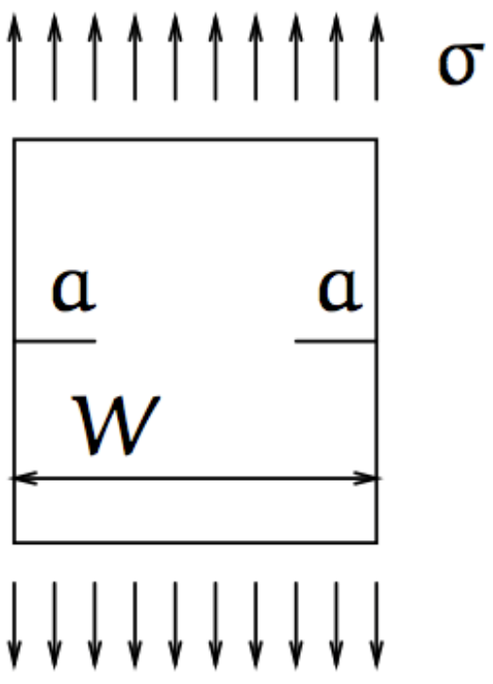

$$K_I = \sigma\sqrt{a}\left[1.12\sqrt{\pi} + 0.76\frac{a}{W} - 8.48\left(\frac{a}{W}\right)^2 + 27.36\left(\frac{a}{W}\right)^3\right]$$

$$\approx 1.12\sigma\sqrt{\pi a}$$

Superposition method

A sample in mode I subjected to tension and bending:

$$\sigma_{ij} = \frac{K_I^{\text{tension}}}{\sqrt{2\pi r}} f_{ij}(\theta) + \frac{K_I^{\text{bending}}}{\sqrt{2\pi r}} f_{ij}(\theta)$$

$$\sigma_{ij} = \frac{K_I^{\text{tension}} + K_I^{\text{bending}}}{\sqrt{2\pi r}} f_{ij}(\theta)$$

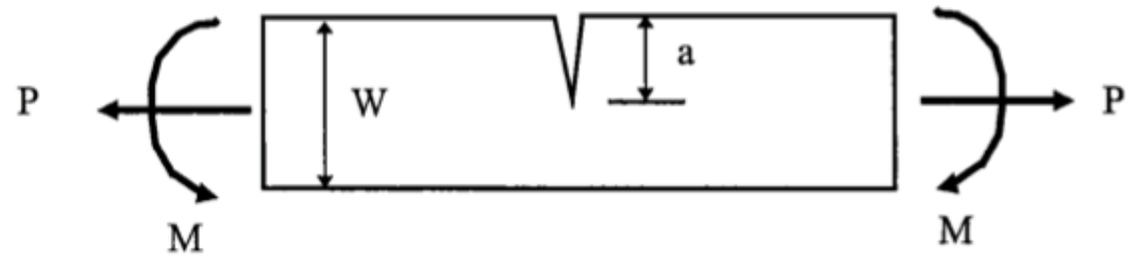

$$K_I = K_I^{\text{tension}} + K_I^{\text{bending}}$$

Is superposition of SIFs of different crack modes possible?

Determine the stress intensity factor for an edge cracked plate subjected to a combined tension and bending.

$a/W = 0.2$

B thickness

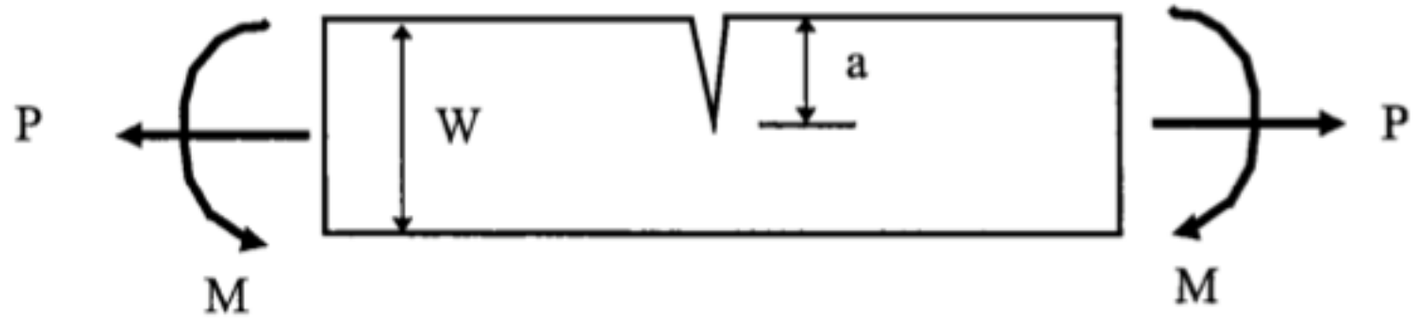

Solution

$$K_I^{\text{bend}} = f_M(a/W)\frac{6M}{BW^2}\sqrt{\pi a} \qquad K_I^{\text{ten}} = f_P(a/W)\frac{P}{BW}\sqrt{\pi a}$$

1.055 1.12

$$K_I = \left(1.055\frac{6M}{BW^2} + 1.12\frac{P}{BW}\right)\sqrt{\pi a}$$

Superposition method (cont.)

Centered crack under internal pressure

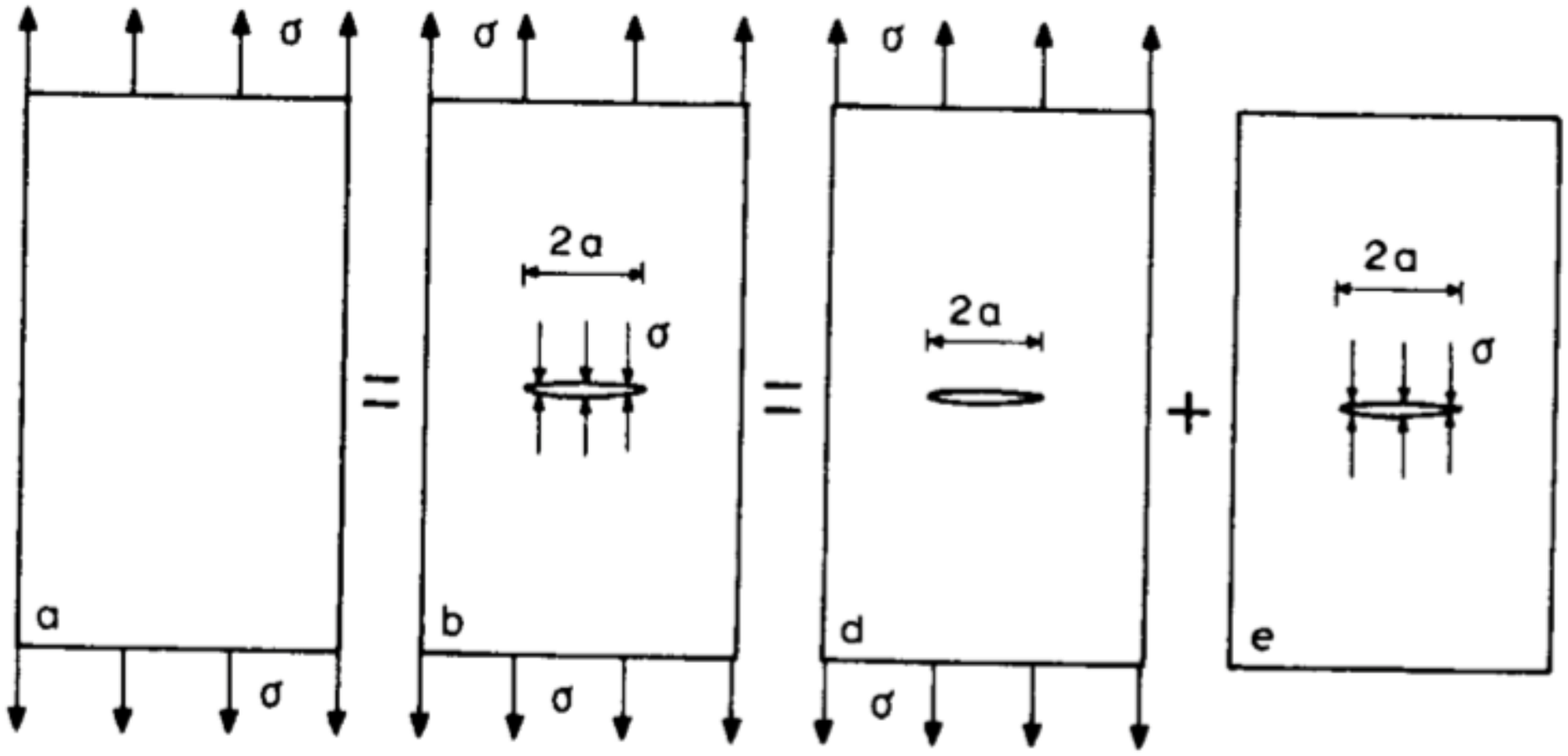

$$K_{Id} + K_{Ie} = K_{Ib} = 0 \rightarrow K_{Ie} = -K_{Id} = -\sigma\sqrt{\pi a}$$

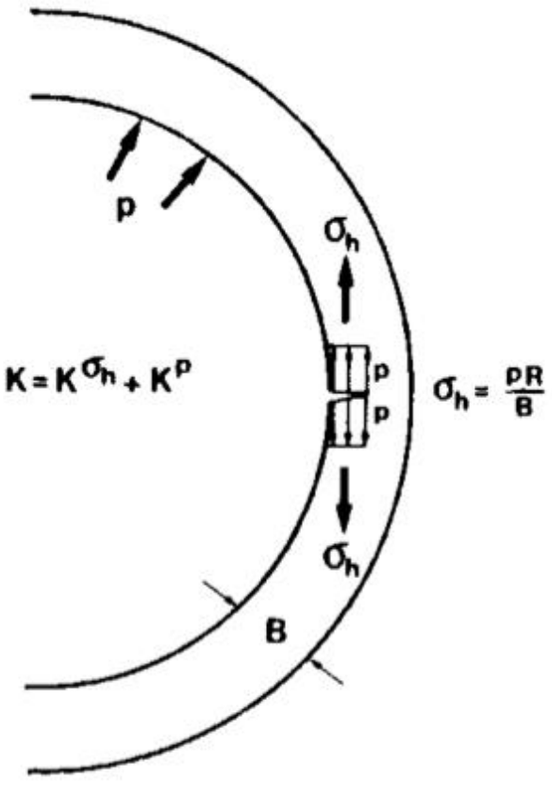

This result is useful for surface flaws along the internal wall of pressure vessels.

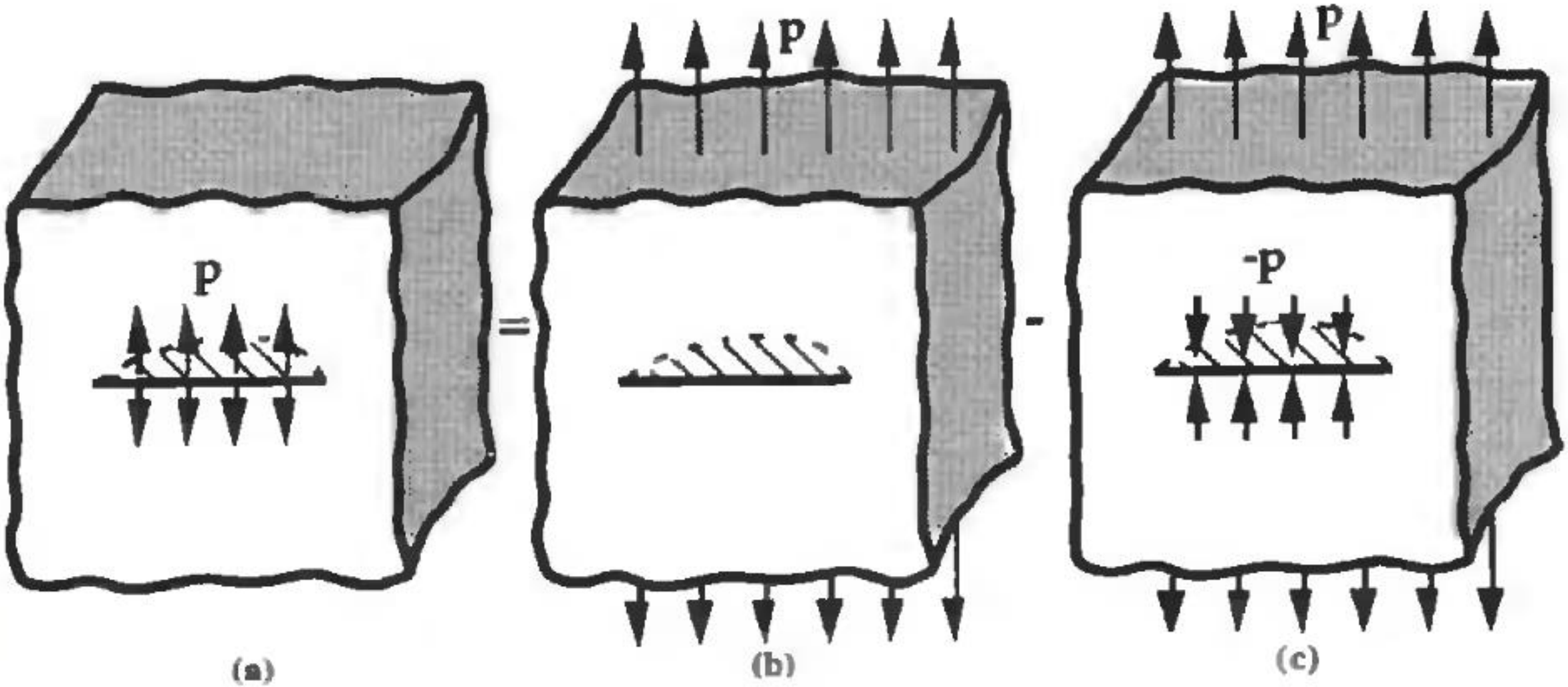

$$K_I = \sigma\sqrt{\pi a}$$

SIFs: asymmetric loadings

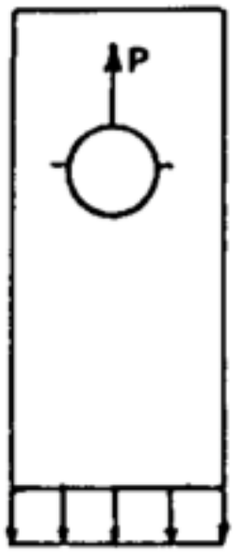

Procedure: build up the case from symmetric cases and then to subtract the superfluous loadings.

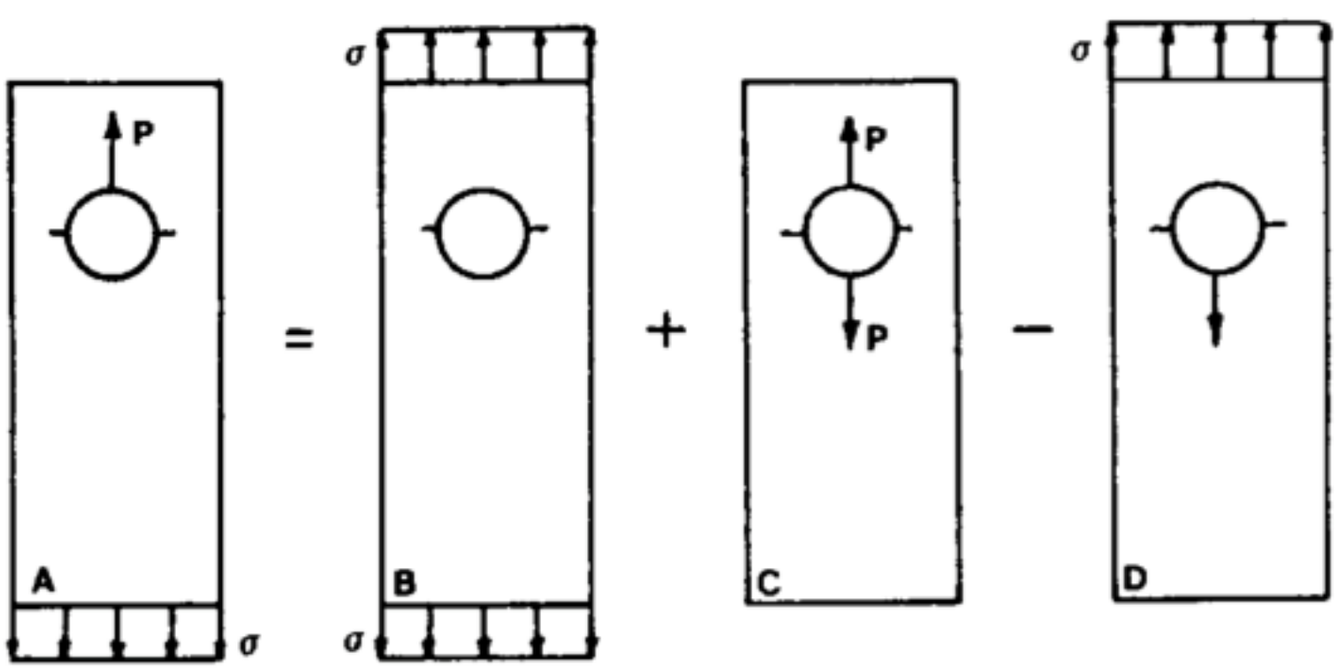

$$K_A = K_B + K_C - K_D$$

$$K_A = (K_B + K_C)/2$$

Note: The circle should be in the middle of the plate

Circle must be in the middle of domain (both vertically and horizontally)

Two small cracks at a hole

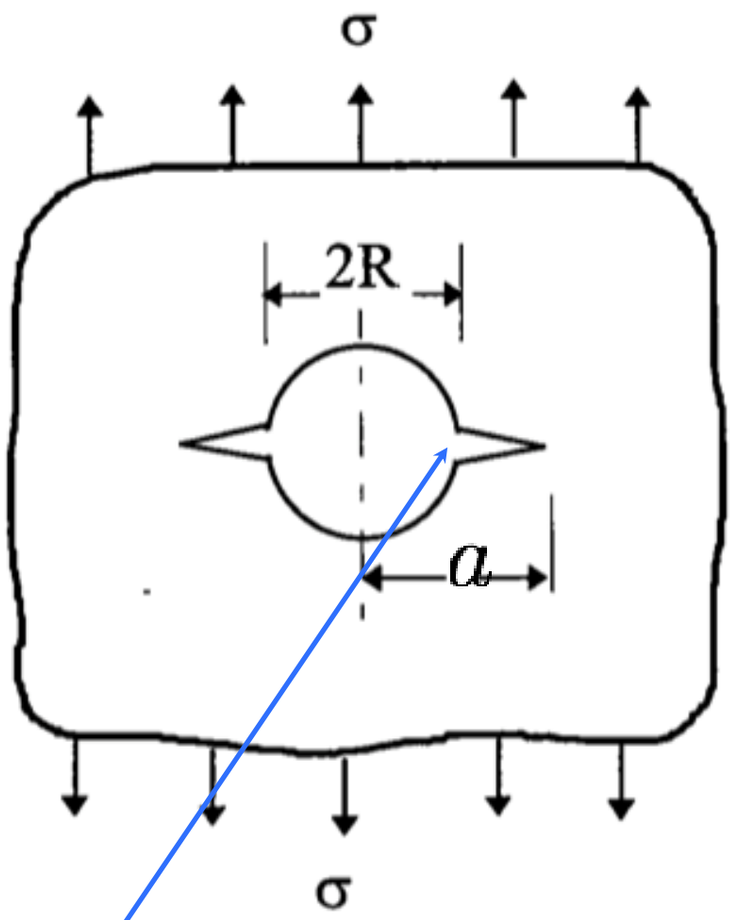

F_I

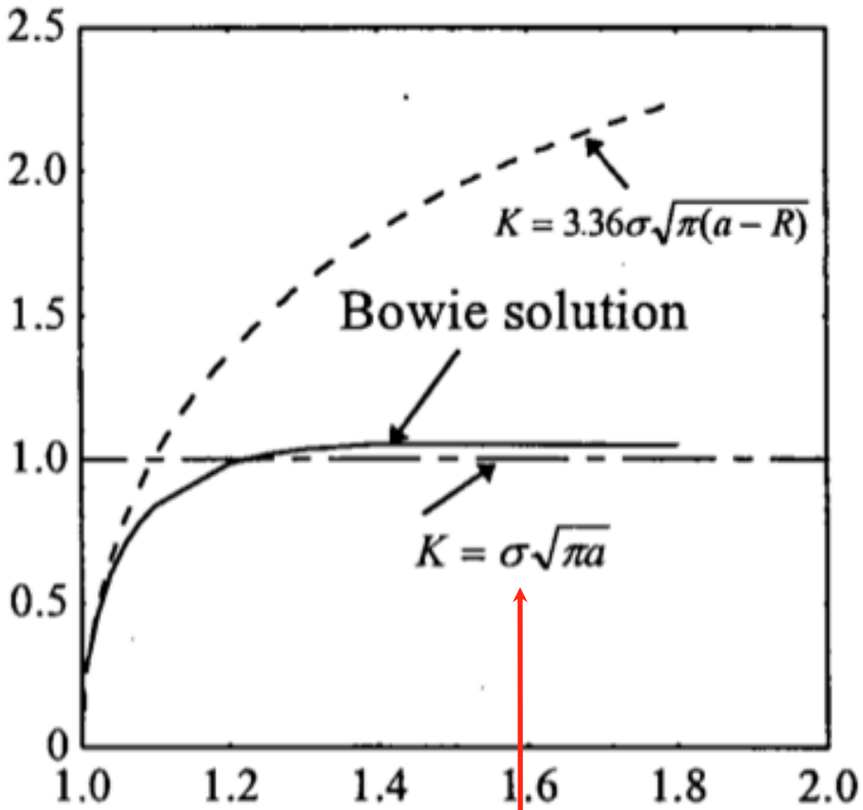

3σ edge crack

hole as a part of the crack

$$K_I = 1.12(3\sigma)\sqrt{\pi(a-R)} = 3.36\sigma\sqrt{\pi a}\sqrt{1-\frac{R}{a}} = 3.36\sqrt{1-\frac{1}{a/R}}\sigma\sqrt{\pi a}$$

Photoelasticity

Wikipedia

Photoelasticity is an experimental method to determine the stress distribution in a material. The method is mostly used in cases where mathematical methods become quite cumbersome. Unlike the analytical methods of stress determination, photoelasticity gives a fairly accurate picture of stress distribution, even around abrupt discontinuities in a material. The method is an important tool for determining critical stress points in a material, and is used for determining stress concentration in irregular geometries.

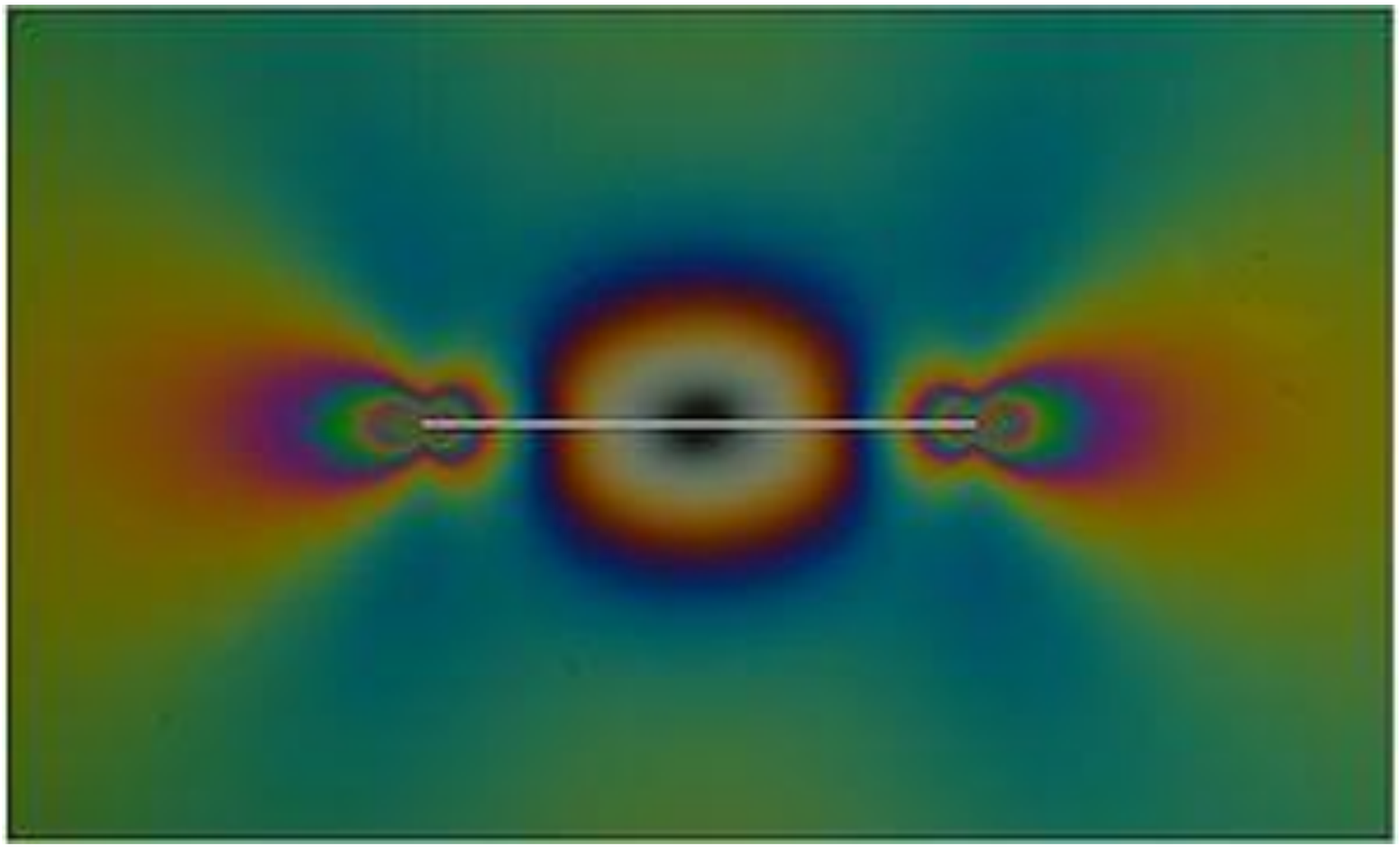

K-G relationship

So far, two parameters that describe the behavior of cracks: K and G.

K: local behavior (tip stresses)
G: global behavior (energy)

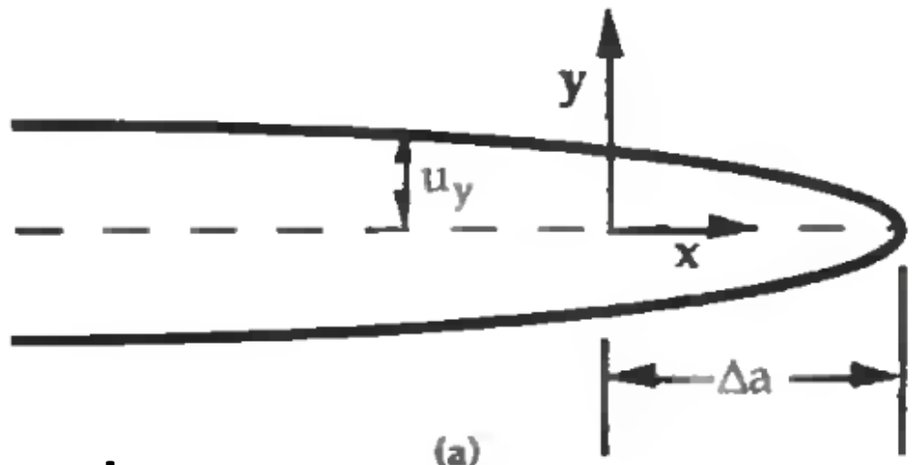

Irwin: for linear elastic materials, these two params are uniquely related

Crack closure analysis: work to open the crack = work to close the crack

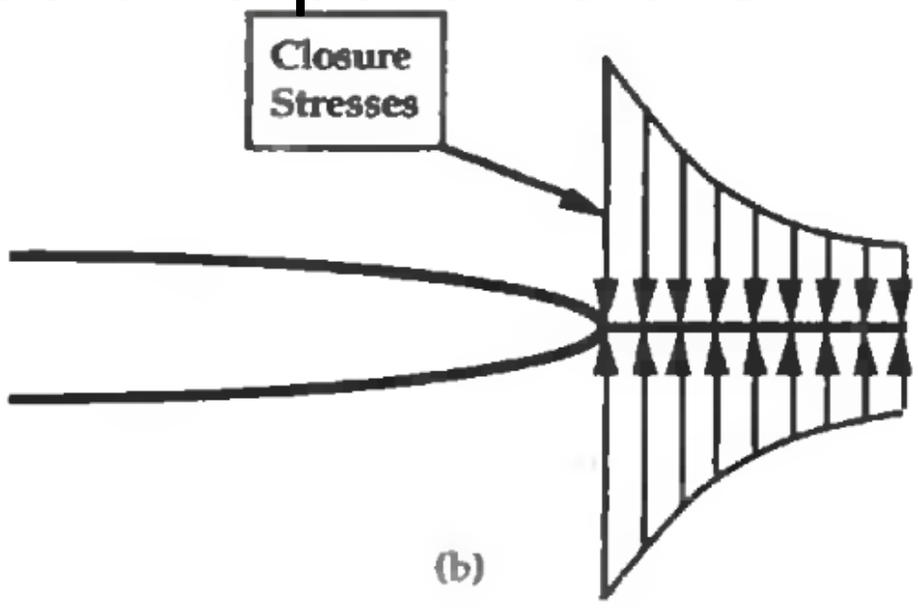

K-G relationship

Irwin

B=1 (unit thickness)

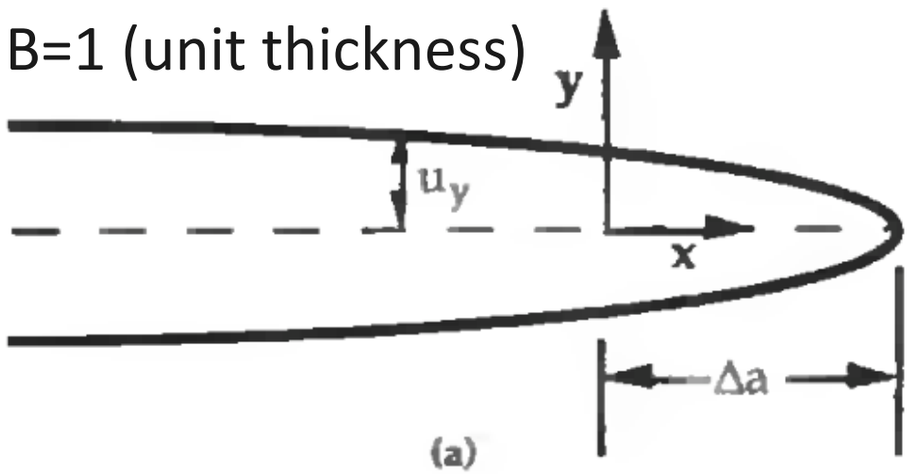

$$G = \lim_{\Delta a \to 0} \left(\frac{\Delta U}{\Delta a} \right)_{\text{fixed load}}$$

work of crack closure

$$\Delta U = \int_0^{\Delta a} dU(x)$$

$$dU(x) = 2\frac{1}{2}\sigma_{yy}(x)u_y(x)dx$$

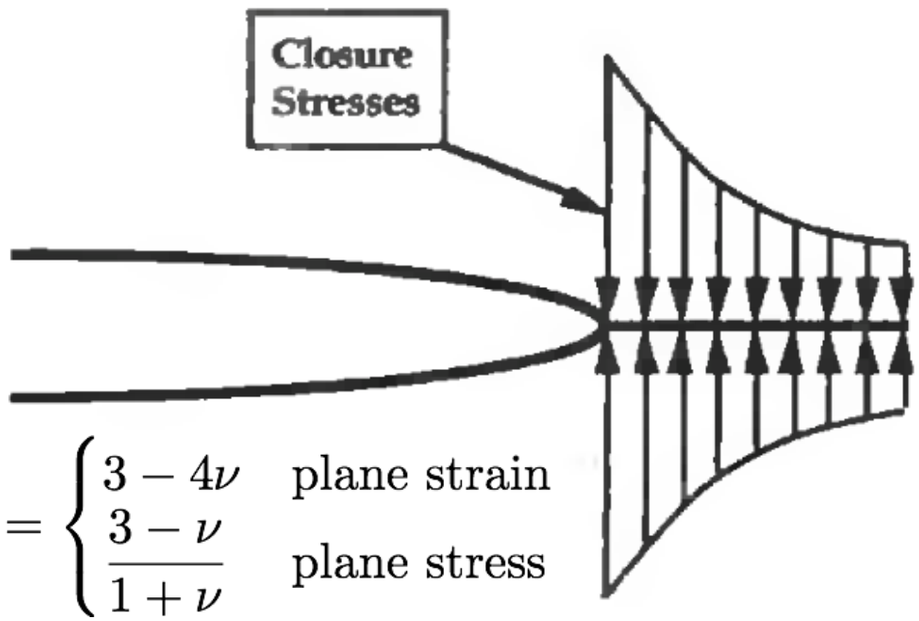

$$u_y = \frac{K_I}{2\mu}\sqrt{\frac{r}{2\pi}}\sin\frac{\theta}{2}\left(\kappa + 1 - 2\cos^2\frac{\theta}{2}\right),\ \theta = \pi \Rightarrow$$

$$\kappa = \begin{cases} 3 - 4\nu & \text{plane strain} \\ \dfrac{3-\nu}{1+\nu} & \text{plane stress} \end{cases}$$

$$u_y = \frac{(\kappa+1)K_I(a+\Delta a)}{2\mu}\sqrt{\frac{\Delta a - x}{2\pi}}$$

$$\sigma_{yy} = \frac{K_I(a)}{\sqrt{2\pi x}}$$

$$G = \lim_{\Delta a \to 0} \frac{(\kappa+1)K_I^2}{4\pi\mu\Delta a}\int_0^{\Delta a}\sqrt{\frac{\Delta a - x}{x}}dx \Rightarrow \boxed{G = \frac{(\kappa+1)K_I^2}{8\mu}}$$

K-G relationship (cont.)

Mode I

$$G_I = \begin{cases} \dfrac{K_I^2}{E} & \text{plane stress} \\ (1-v^2)\dfrac{K_I^2}{E} & \text{plane strain} \end{cases}$$

Mixed mode

$$G = \frac{K_I^2}{E'} + \frac{K_{II}^2}{E'} + \frac{K_{III}^2}{2\mu}$$

$$E' = \begin{cases} \dfrac{E}{1-\nu^2} & \text{for plane strain} \\ E & \text{for plane stress} \end{cases}$$

- Equivalence of the strain energy release rate and SIF approach
- Mixed mode: G is scalar => mode contributions are additive
- Assumption: self-similar crack growth!!!

Self-similar crack growth: planar crack remains planar (da same direction as a)

SIF in terms of compliance

$$G = \frac{1}{2B} P^2 \frac{dC}{da}$$

B: thickness

$$G_I = \frac{K_I^2}{E'}$$

$$K_I^2 = \frac{E' P^2}{2B} \frac{dC}{da}$$

A series of specimens with different crack lengths: measure the compliance C for each specimen -> dC/da -> K and G

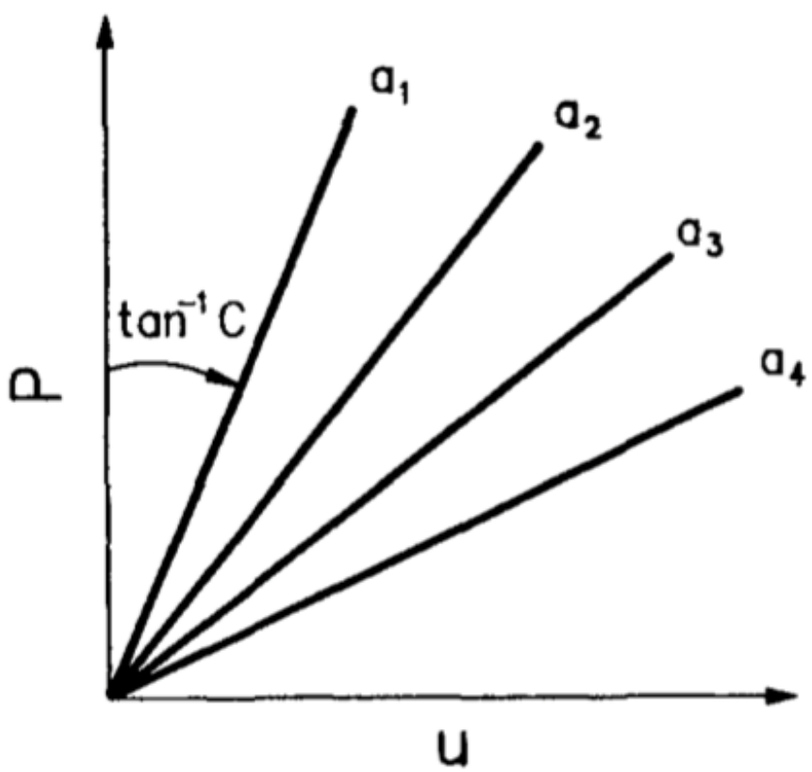

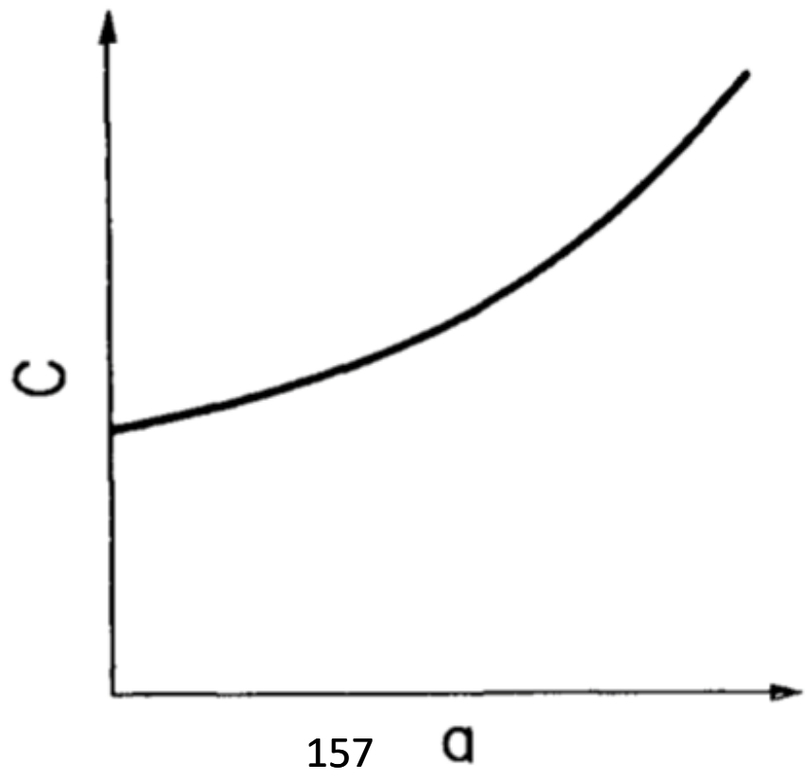

Compliance-SIF

$$K = \sqrt{\sec \frac{\pi a}{W}} \sigma \sqrt{\pi a}$$

$$G = \frac{P^2}{2} \frac{dC}{dA} = \frac{P^2}{4B} \frac{dC}{da}$$

$$G = \frac{K^2}{E}$$

$$\frac{P^2}{4B} \frac{dC}{da} = \frac{\sec \frac{\pi a}{W} \sigma^2 \pi a}{E}$$

$$\frac{dC}{da} = \frac{\sec \frac{\pi a}{W} \sigma^2 \pi a 4B}{P^2 E}$$

$$\frac{dC}{da} = \frac{4}{EBW^2} \pi a \sec \frac{\pi a}{W}$$

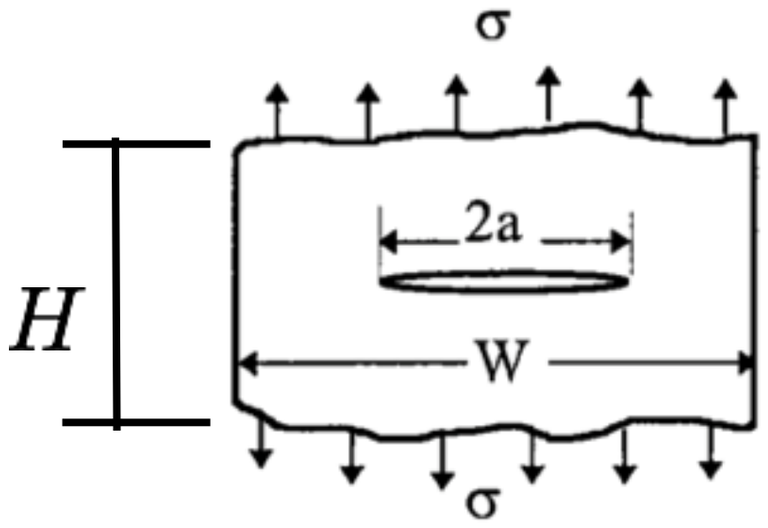

$$C = \int_0^a \frac{4}{EBW^2} \pi a \sec \frac{\pi a}{W} da + C_0$$

$$C_0 = \frac{\delta}{P} = \frac{H}{EBW}$$

$$\frac{\pi a}{W} \sec\left(\frac{\pi a}{W}\right) = \tan\left(\frac{\pi a}{W}\right) \frac{\frac{\pi}{W} a}{\sin\left(\frac{\pi a}{W}\right)} \approx \tan\left(\frac{\pi a}{W}\right)$$

$$C = -\frac{4}{EB\pi} \ln\left(\cos \frac{\pi a}{W}\right) + \frac{H}{EBW}$$

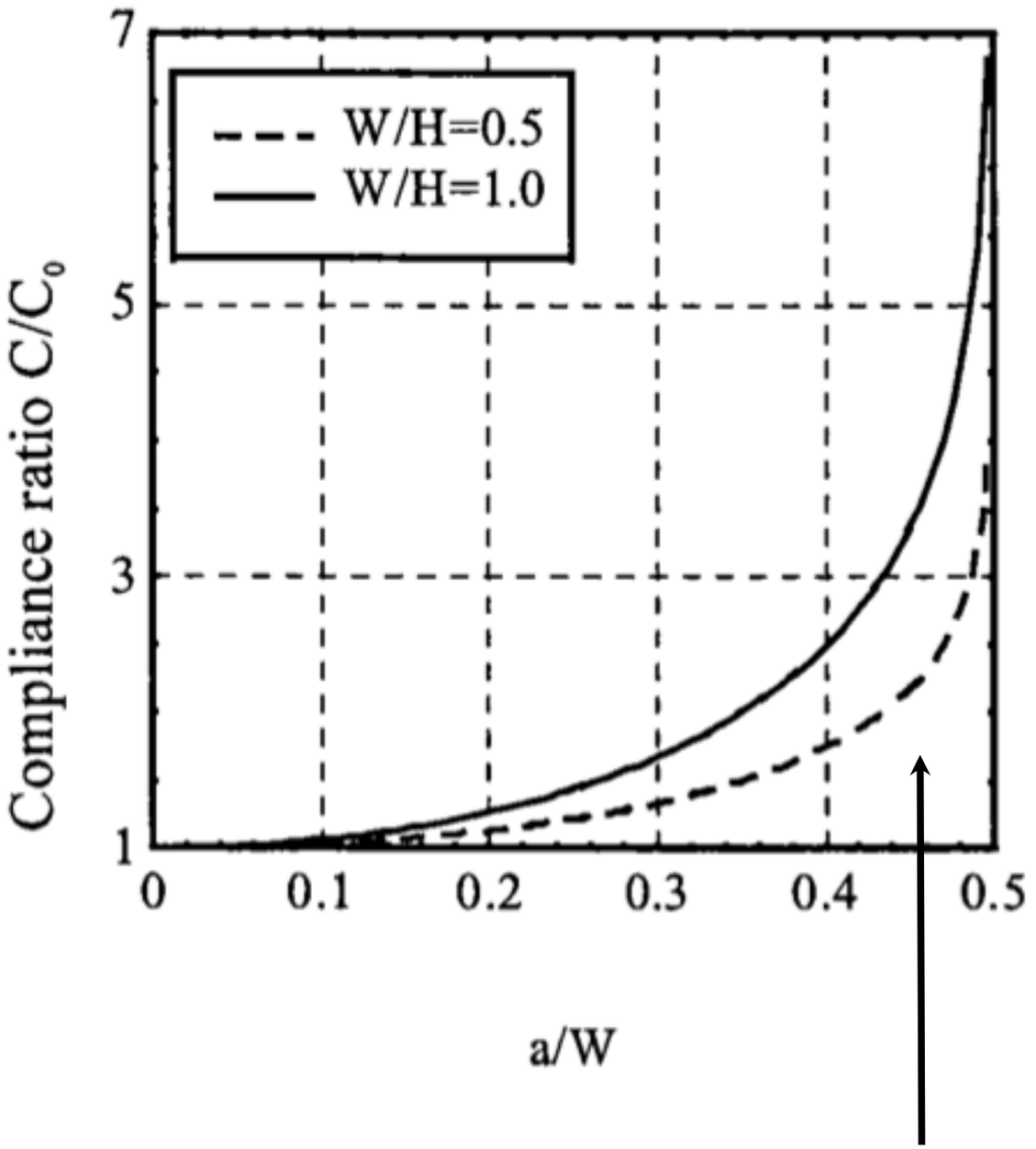

$$C/C_0 = -\frac{4}{\pi}\frac{W}{H}\ln\left(\cos\frac{\pi a}{W}\right) + 1$$

compliance rapidly increases

K as a failure criterion

Failure criterion $\boxed{K = K_c}$ $f(a/W)\sigma\sqrt{\pi a} = K_c$

fracture toughness

- Problem 1: given crack length a, compute the maximum allowable applied stress

$$\sigma_{\max} = \frac{K_c}{f(a/W)\sqrt{\pi a}}$$

- Problem 2: for a specific applied stress, compute the maximum permissible crack length (critical crack length)

$$f(a_c/W)\sigma\sqrt{\pi a_c} = K_c \longrightarrow a_c$$

- Problem 3: compute K_c provided crack length and stress at fracture

$$K_c = f(a_c/W)\sigma\sqrt{\pi a_c}$$

Example

A cylindrical pressure vessel with closed ends has a radius $R = 1$ m and thickness $t = 40$ mm and is subjected to internal pressure p. The vessel must be designed safely against failure by yielding (according to the von Mises yield criterion) and fracture. Three steels with the following values of yield stress σ_Y and fracture toughness K_{Ic} are available for constructing the vessel.

Steel	σ_Y(MPa)	K_{Ic}(MPa $\sqrt{\text{m}}$)
A: 4340	860	100
B: 4335	1300	70
C: 350 Maraging	1550	55

Fracture of the vessel is caused by a long axial surface crack of depth a. The vessel should be designed with a factor of safety $S = 2$ against yielding and fracture. For each steel:

(a) Plot the maximum permissible pressure p_c versus crack depth a_c;

(b) Calculate the maximum permissible crack depth a_c for an operating pressure $p = 12$ MPa;

(c) Calculate the failure pressure p_c for a minimum detectable crack depth $a = 1$ mm.

5. Elastoplastic fracture mechanics

5.1 Introduction to plasticity

5.2. Plastic zone models

5.3. J Integral

5.4. Crack tip opening displacement (CTOD)

5.2. Plastic zone models

- 1D Models: Irwin, Dugdale, and Barenbolt models
- 2D models:
    - Plastic zone shape
    - Plane strain vs. plane stress

Singular dominated zone

$$\sigma_{yy} = \frac{K_I}{\sqrt{2\pi r}} \cos\frac{\theta}{2}\left(1 + \sin\frac{\theta}{2}\cos\frac{3\theta}{2}\right)$$

$\theta = 0$ (crack plane)

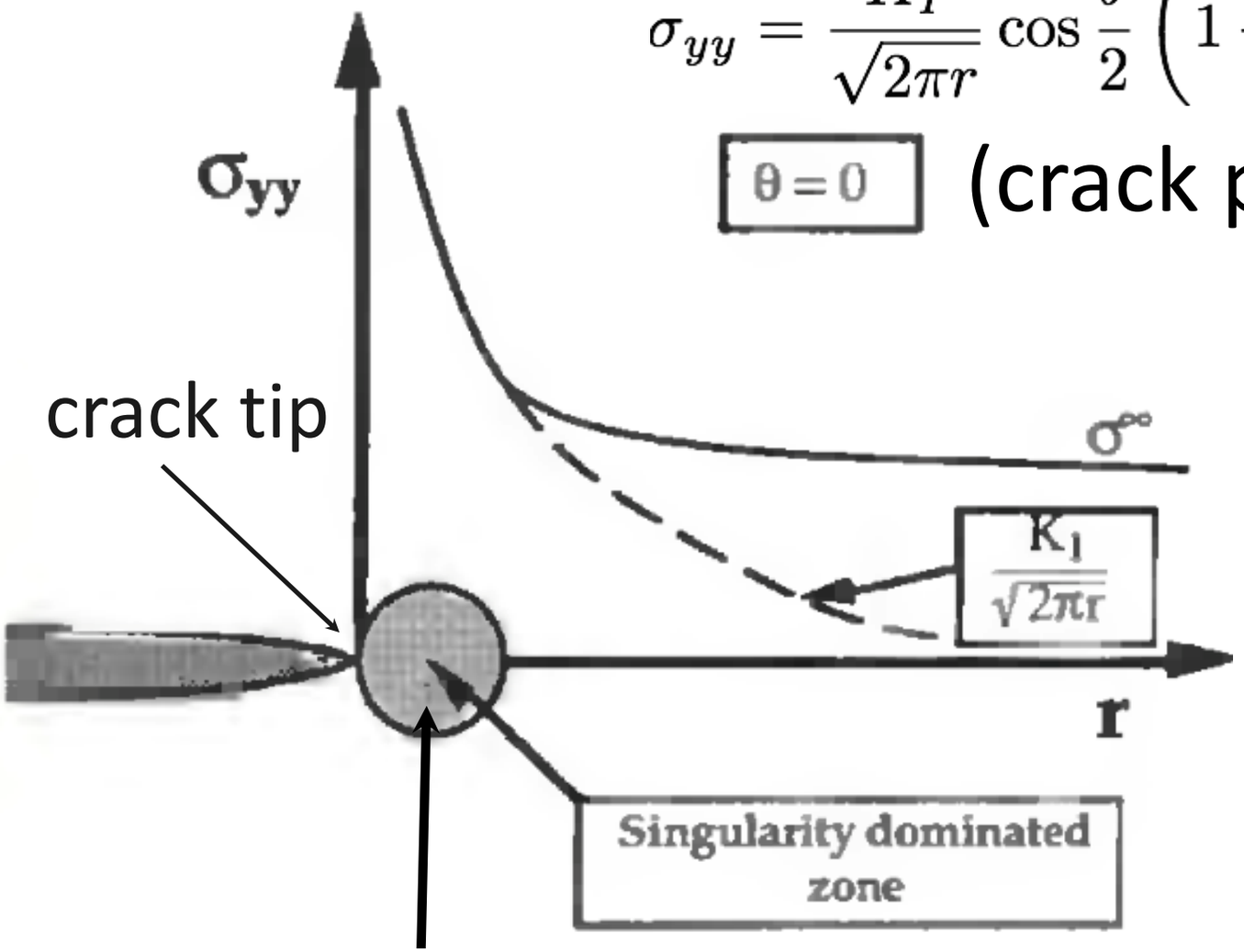

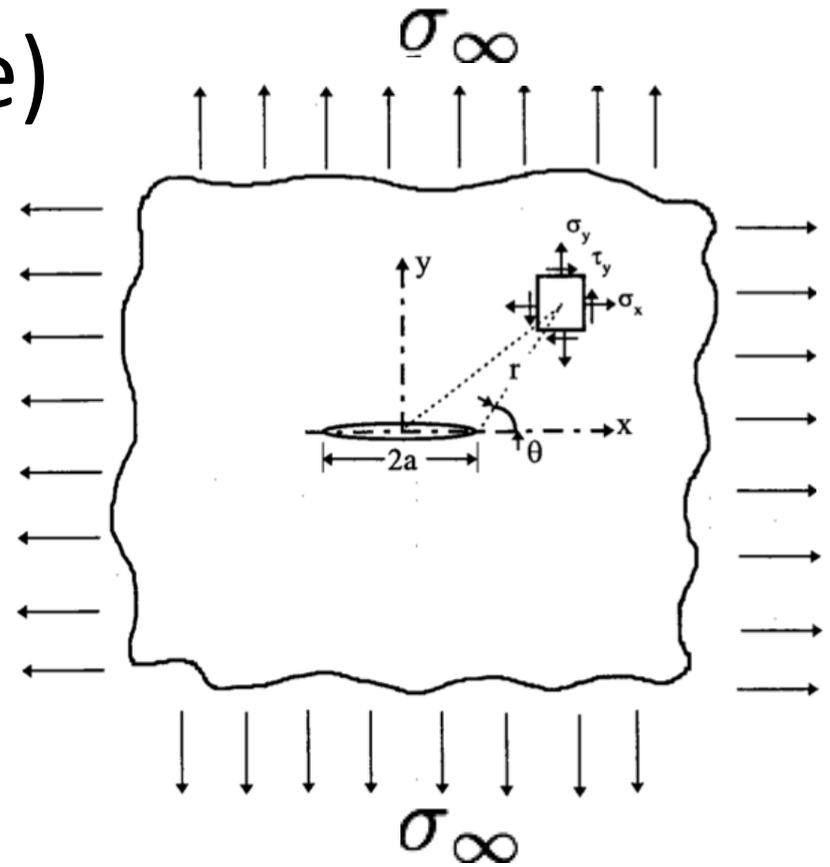

$$\sigma_{xx} = \frac{K_I}{\sqrt{2\pi r}} \cos\left(\frac{\theta}{2}\right)\left[1 - \sin\left(\frac{\theta}{2}\right)\sin\left(\frac{3\theta}{2}\right)\right]$$

$$\sigma_{yy} = \frac{K_I}{\sqrt{2\pi r}} \cos\left(\frac{\theta}{2}\right)\left[1 + \sin\left(\frac{\theta}{2}\right)\sin\left(\frac{3\theta}{2}\right)\right]$$

$$\tau_{xy} = \frac{K_I}{\sqrt{2\pi r}} \cos\left(\frac{\theta}{2}\right)\sin\left(\frac{\theta}{2}\right)$$

K-dominated zone

Introduction

- Griffith's theory provides excellent agreement with experimental data for brittle materials such as glass. For ductile materials such as steel, the surface energy (γ) predicted by Griffith's theory is usually unrealistically high. A group working under G. R. Irwin at the U.S. Naval Research Laboratory (NRL) during World War II realized that plasticity must play a significant role in the fracture of ductile materials.

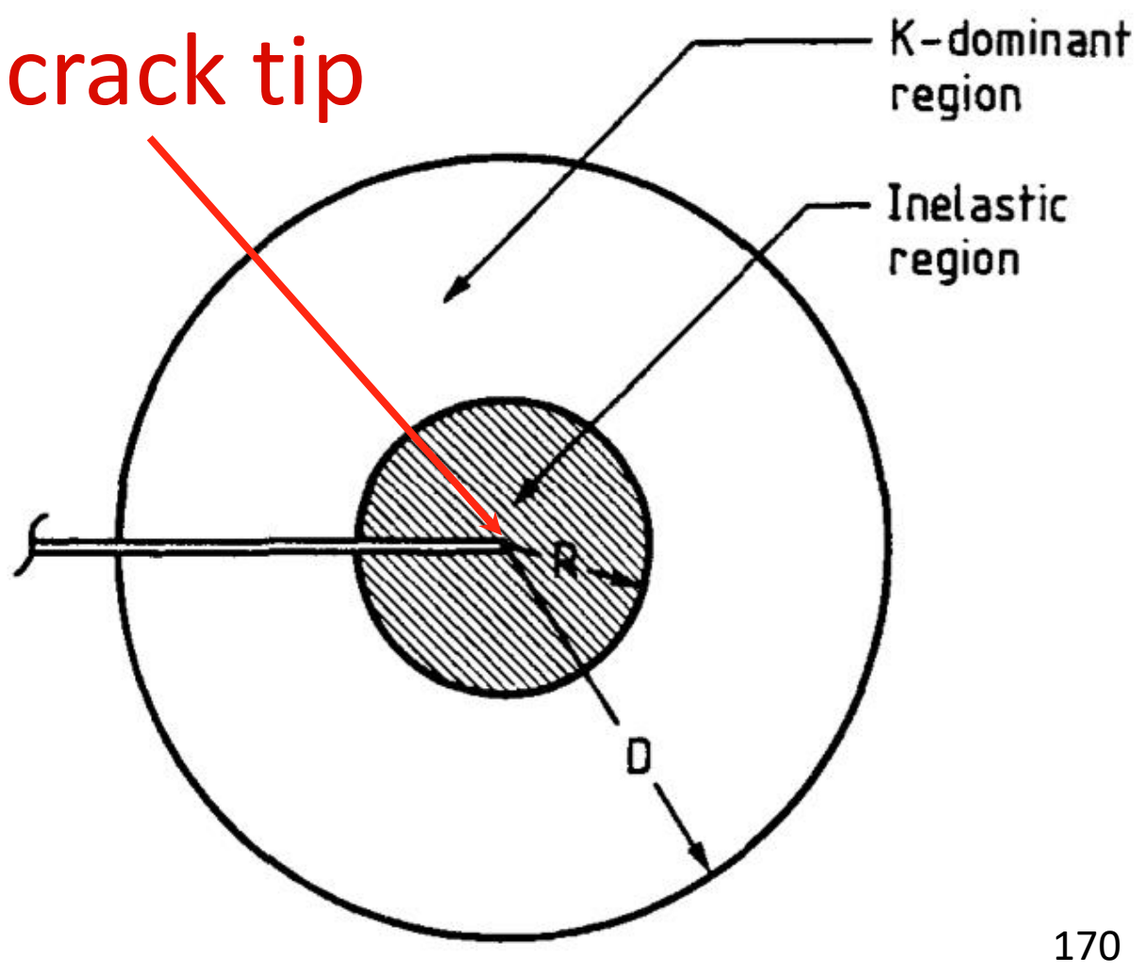

(SSY)

Small-scale yielding: LEFM still applies with minor modifications done by G. R. Irwin

$$R \ll D$$

Validity of K in presence of a plastic zone

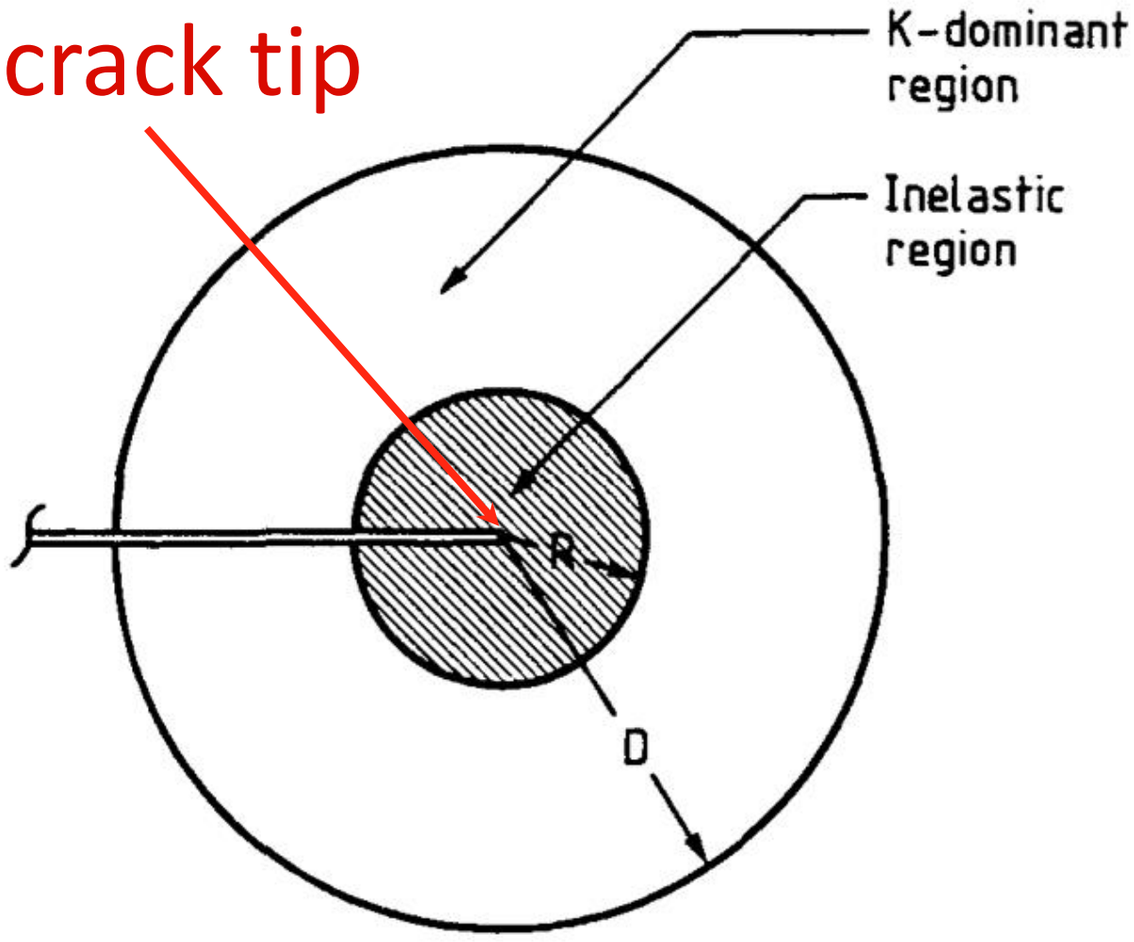

Fracture process usually occurs in the inelastic region not the K-dominant zone.

→ is SIF a valid failure criterion for materials that exhibit inelastic deformation at the tip ?

Validity of K in presence of a plastic zone

[Anderson]

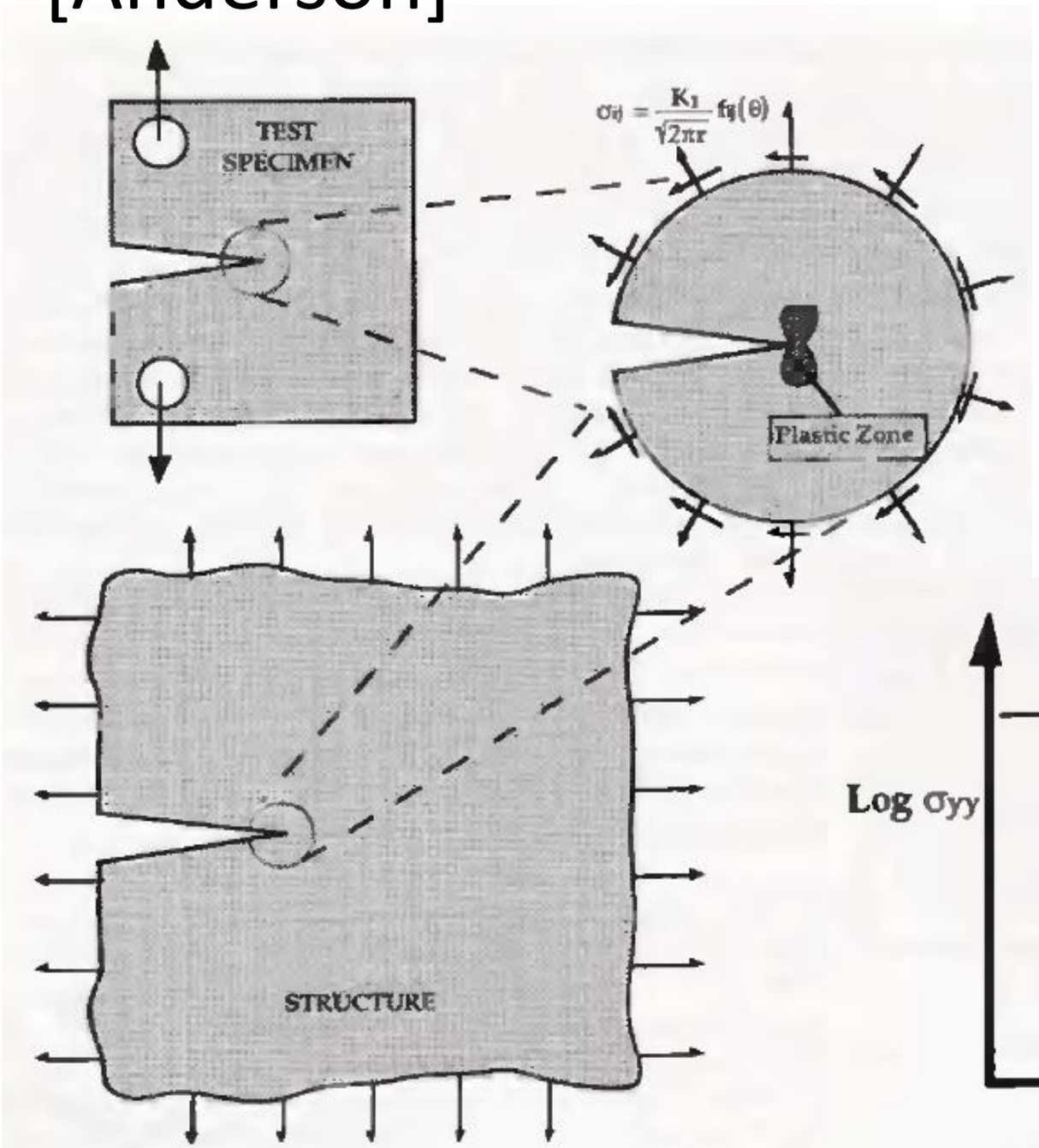

same K->same stresses applied on the disk

stress fields in the plastic zone: the same

K still uniquely characterizes the crack tip conditions in the presence of a small plastic zone.

LEFM solution

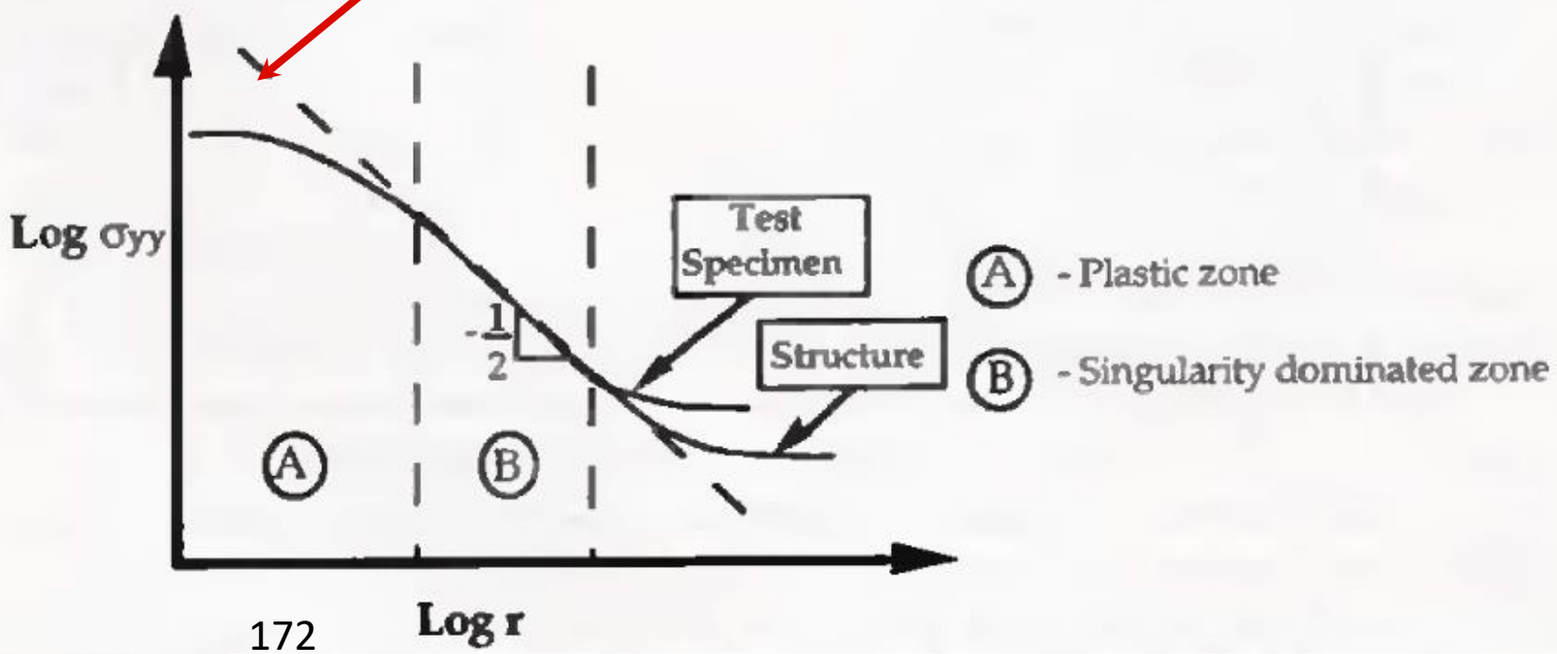

Paradox of a sharp crack

At crack tip:

$$r = 0 \rightarrow \sigma_{ij} = \infty$$

An infinitely sharp crack is merely a mathematical abstraction.

Crack tip stresses are **finite** because (i) crack tip radius is finite (materials are made of atoms) and (ii) plastic deformation makes the crack blunt.

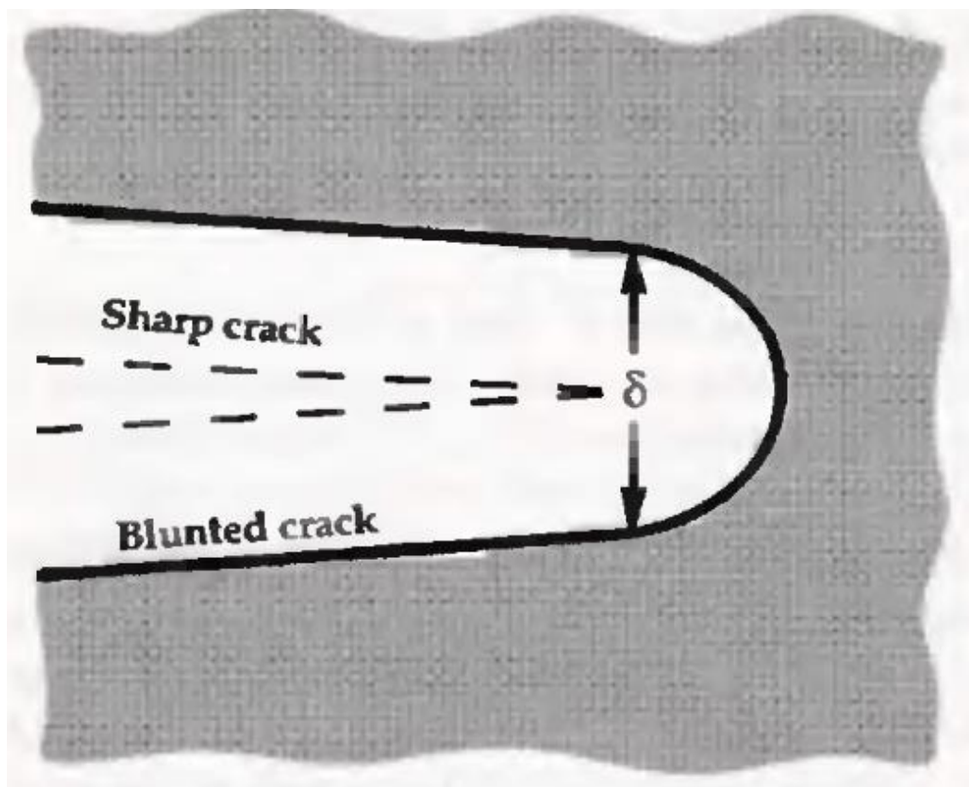

5.2.1 Plastic zone shape: 1D models

- 1st order approximation
- 2nd order Irwin model
- Strip yield models (Dugdale, and Barenbolt models)

- Effective crack length

Plastic correction:
1st order approximation

- A cracked body in a **plane stress** condition
- Material: **elastic perfectly plastic** with yield stress σ_{ys}

On the crack plane $\theta = 0$

$$\sigma_{yy} = \frac{K_I}{\sqrt{2\pi r}}$$

$\sigma_{yy} = \sigma_{ys}$ (yield occurs)

$$r_y = \frac{1}{2\pi}\left(\frac{K_I}{\sigma_{YS}}\right)^2$$

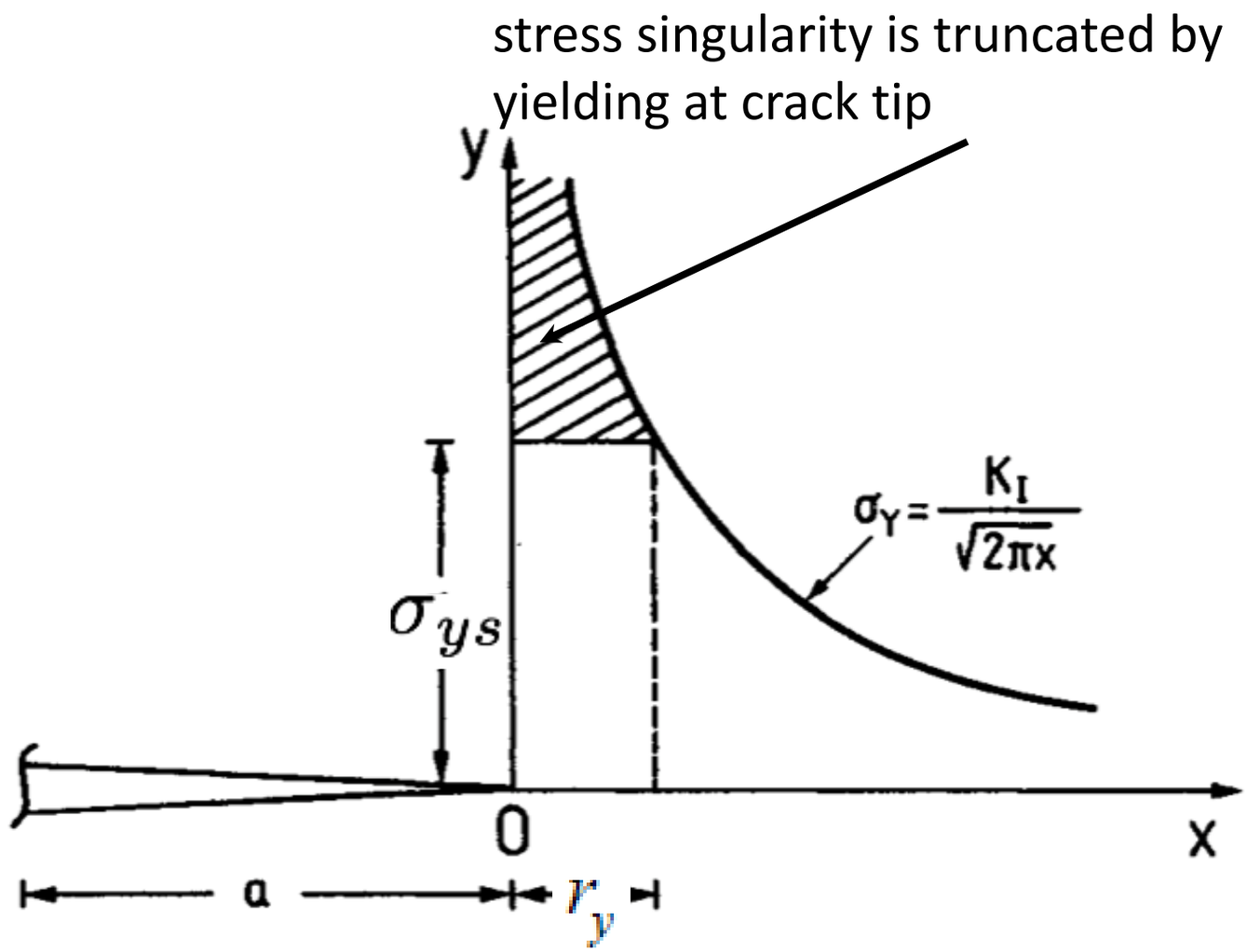

first order **approximation** of plastic zone size: equilibrium is not satisfied

2.Irwin’s plastic correction

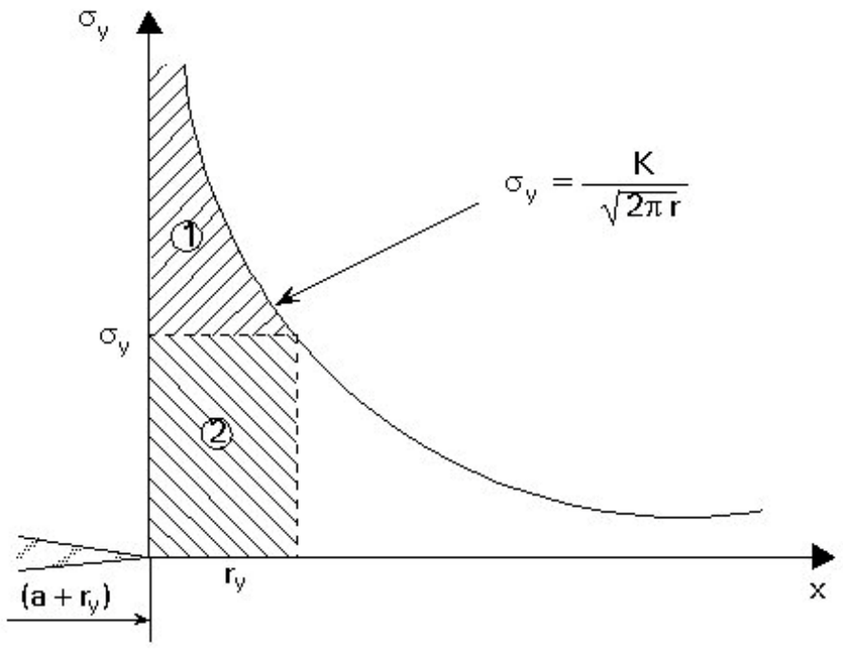

(a) Elastic crack

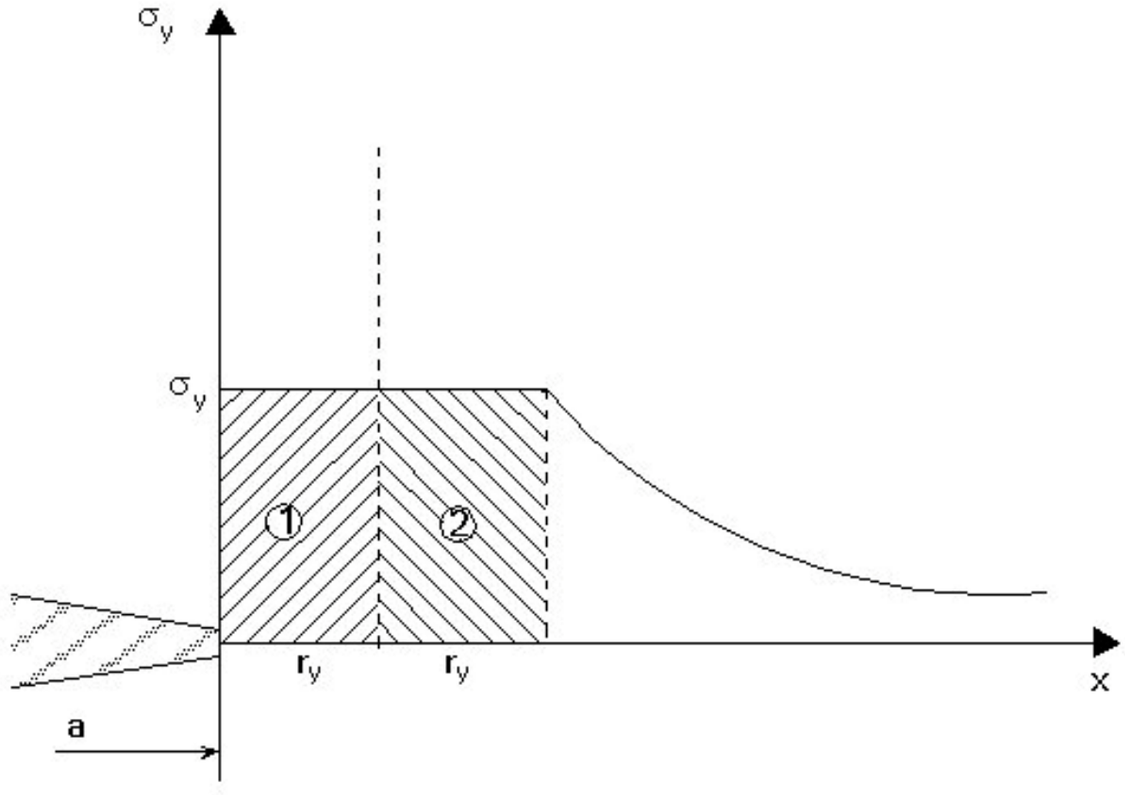

(b) Real crack with plastic zone

2.Irwin's plastic correction

stress redistribution:

$$\sigma_{ys} r_p = \int_0^{r_y} \sigma_{yy} dr$$

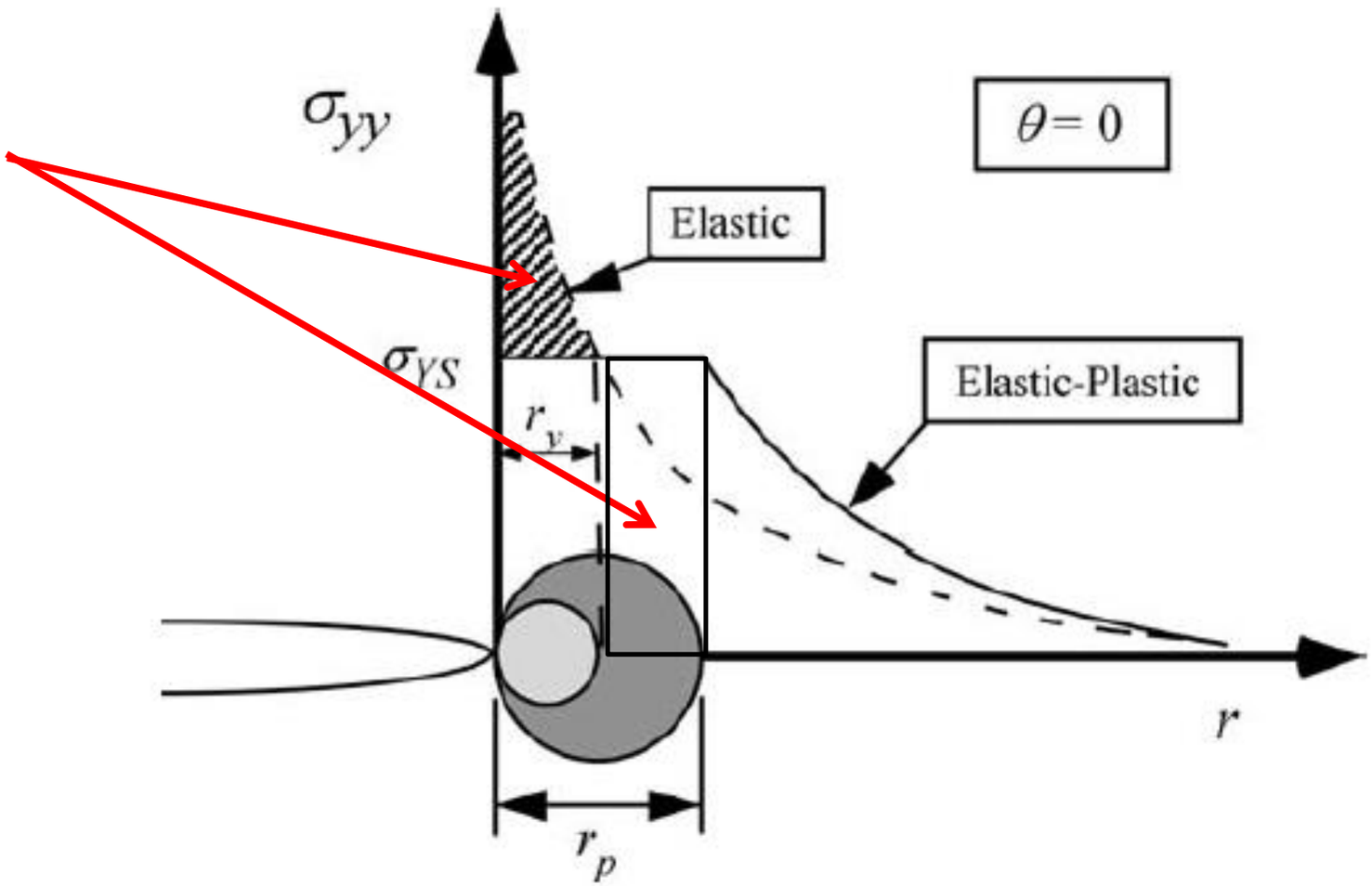

$$r_p = 2 r_y = \frac{K_I^2}{\pi \sigma_{ys}^2}$$

plastic zone: a CIRCLE !!!

$$r_p = \frac{1}{3\pi} \frac{K_I^2}{\sigma_y^2}$$

Plane strain

Von Mises Yield Criterion

$$\sigma_e = \frac{1}{\sqrt{2}}\left[(\sigma_1-\sigma_2)^2+(\sigma_1-\sigma_3)^2+(\sigma_2-\sigma_3)^2\right]^{1/2} = \sigma_y$$

Plane stress

$$\sigma_1 = \sigma_2 = \sigma_{yy}, \quad \sigma_3 = 0$$

$$\sigma_e = \sigma_1 = \sigma_y \quad \Rightarrow$$

$$\sigma_{ys} = \sigma_y \quad \Rightarrow$$

$$r_p = \frac{K_I^2}{\pi\sigma_y^2}$$

$$r_y = \frac{1}{2\pi}\left(\frac{K_I}{\sigma_{YS}}\right)^2$$

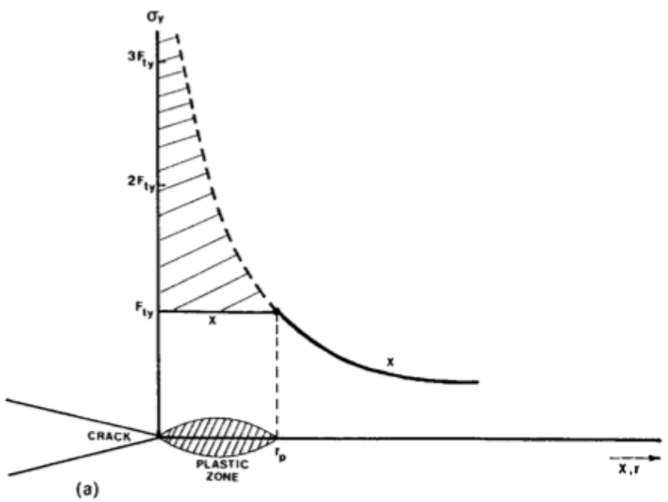

Plane strain

$$\sigma_1 = \sigma_2 = \sigma_{yy}$$

$$\sigma_3 = \nu(\sigma_{xx}+\sigma_{yy}) = 2\nu\sigma_{yy}$$

$$\sigma_e = (1-2\nu)\sigma_1 = \sigma_y \quad \Rightarrow$$

$$\sigma_{ys} = \frac{\sigma_y}{1-2\nu} \quad \Rightarrow$$

$$r_p = \frac{K_I^2}{\pi\sigma_{ys}^2} = (1-2\nu)^2\frac{K_I^2}{\pi\sigma_y^2} \quad \Rightarrow$$

$$r_p \approx \frac{K_I^2}{3\pi\sigma_y^2}$$

$(1 – 2 \times 0.2)^2 = 0.36$

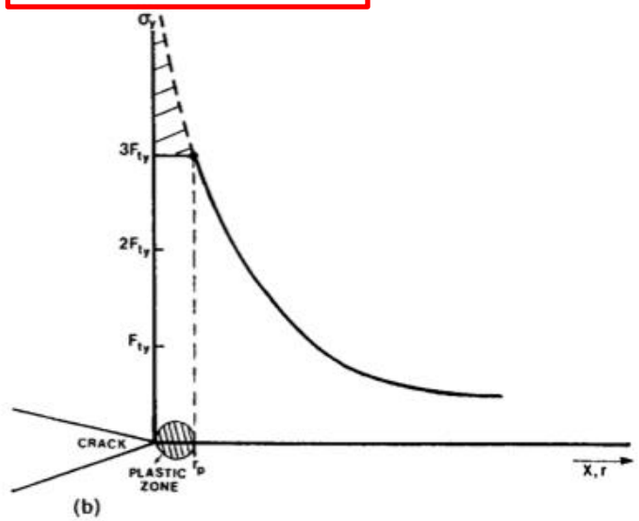

3. Strip Yield Model

proposed by Dugdale and Barrenblatt

- Infinite plate with though thickness crack 2a
- Plane stress condition
- Elastic perfectly plastic material

Hypotheses:

- All plastic deformation concentrates in a line in front of the crack.
- The crack has an effective length which exceeds that of the physical crack by the length of the plastic zone.
- ρ: **chosen such that stress singularity at the tip disappears**.

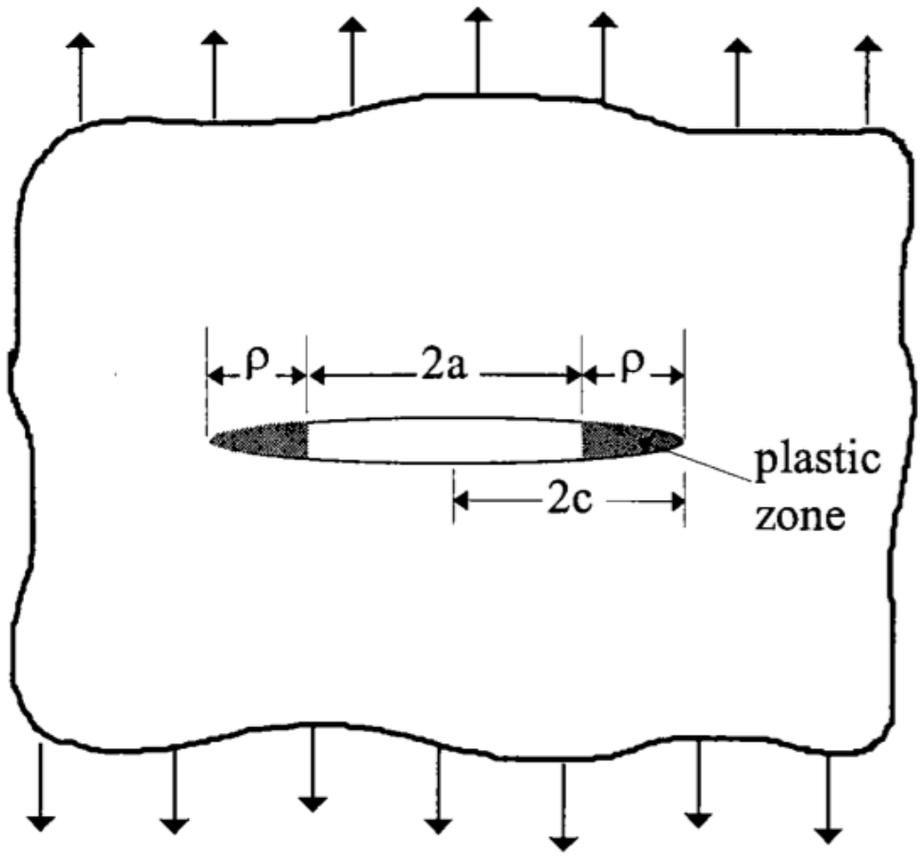

SIF for plate with normal force at crack

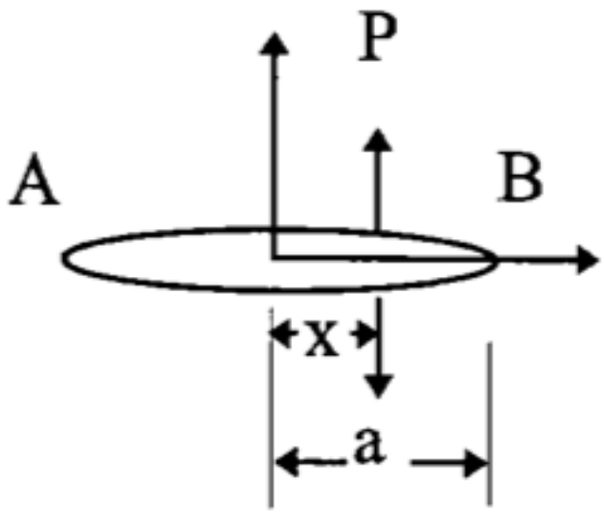

$$P = -\sigma_{ys} dx$$

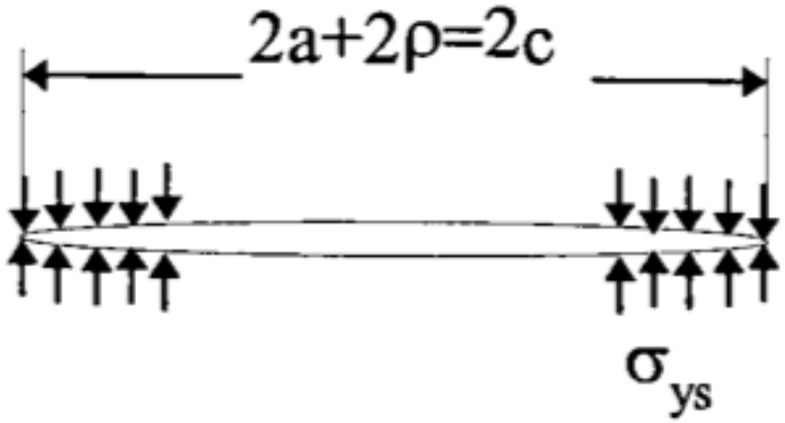

$$K_A = \frac{P}{\sqrt{\pi a}} \sqrt{\frac{a+x}{a-x}}$$

$$K_B = \frac{P}{\sqrt{\pi a}} \sqrt{\frac{a-x}{a+x}}$$

Anderson, p64

$$K_I^{\sigma_{ys}} = -\frac{\sigma_{ys}}{\sqrt{\pi c}} \int_a^c \left(\sqrt{\frac{c-x}{c+x}} + \sqrt{\frac{c+x}{c-x}} \right) dx$$

$$K_I^{\sigma_{ys}} = -2\sigma_{ys} \sqrt{\frac{a+\rho}{\pi}} \cos^{-1}\left(\frac{a}{a+\rho}\right)$$

3. Strip Yield Model (cont.)

Superposition principle

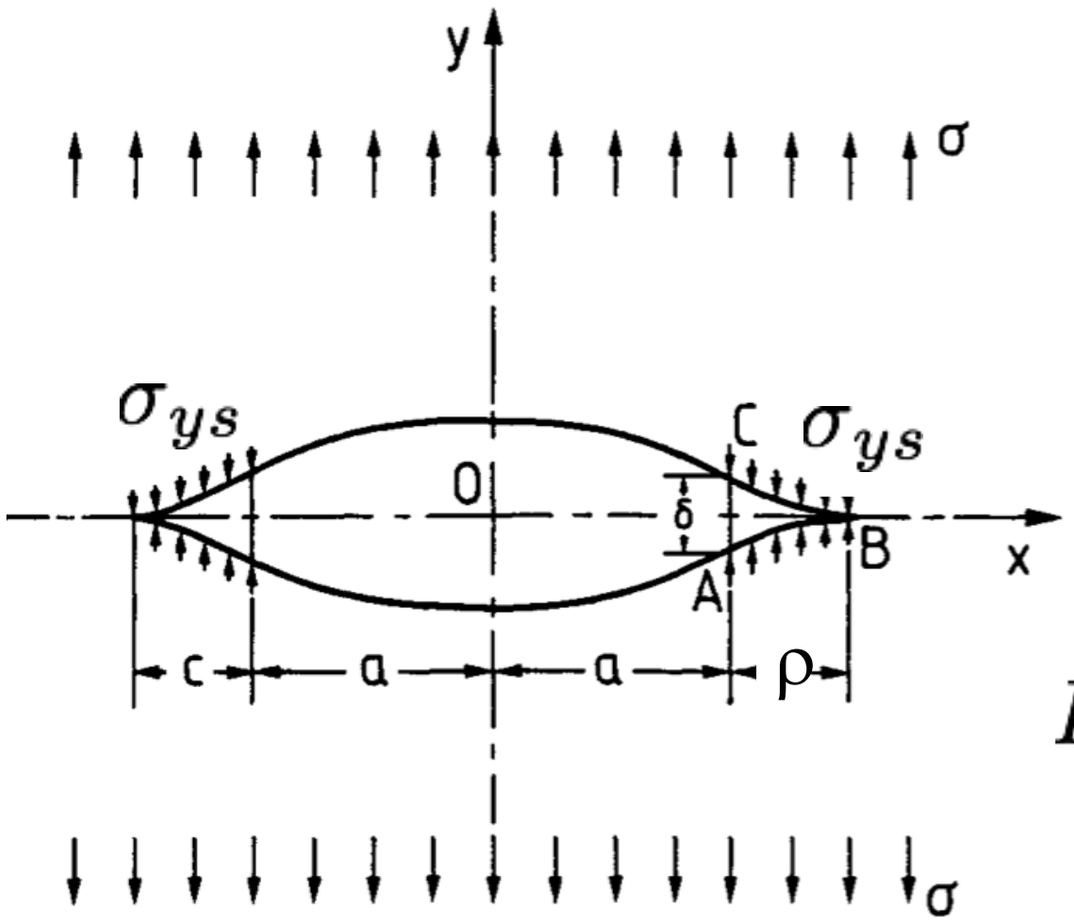

$$K_I = K_I^{\sigma} + K_I^{\sigma_{ys}}$$

$$K_I^{\sigma} = \sigma\sqrt{\pi(a+\rho)}$$

$$K_I^{\sigma_{ys}} = -2\sigma_{ys}\sqrt{\frac{a+\rho}{\pi}}\cos^{-1}\left(\frac{a}{a+\rho}\right)$$

(derivation follows) $\sigma \ll \sigma_{ys}$

$$\sigma_{ij} = \frac{K}{\sqrt{2\pi r}} f_{ij}(\theta) + \text{H.O.T}$$

$$\cos x = 1 - \frac{1}{2!}x^2 + \cdots$$

$$K_I = 0 \Rightarrow \frac{a}{a+\rho} = \cos\left(\frac{\pi\sigma}{2\sigma_{ys}}\right)$$

Irwin's result 0.318

$$\rho = \frac{\pi^2\sigma^2 a}{8\sigma_{ys}^2} = \frac{\pi}{8}\left(\frac{K_I}{\sigma_{ys}}\right)^2$$

close to 0.392

$$r_p = \frac{1}{\pi}\left(\frac{K_I}{\sigma_{ys}}\right)^2$$

3. Strip Yield Model: Dugdale vs Barenblatt model

Dugdale: Uniform stress

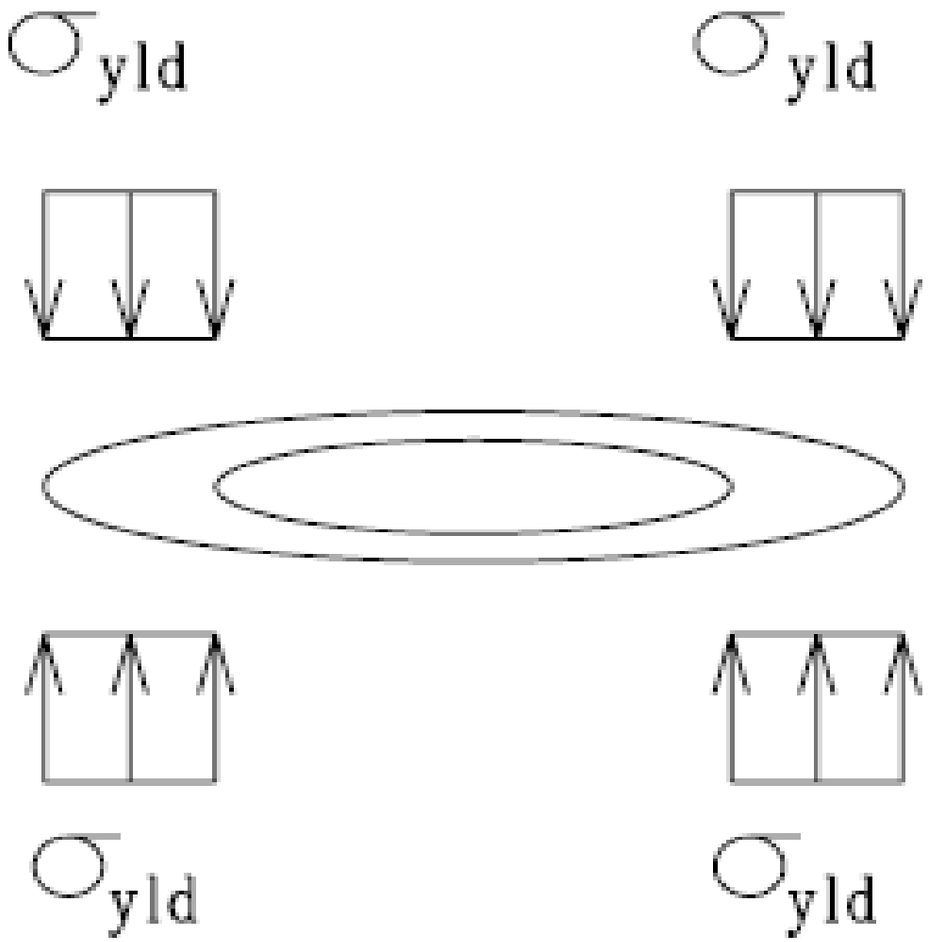

More appropriate for <u>polymers</u>

Barenblatt: Linear stress

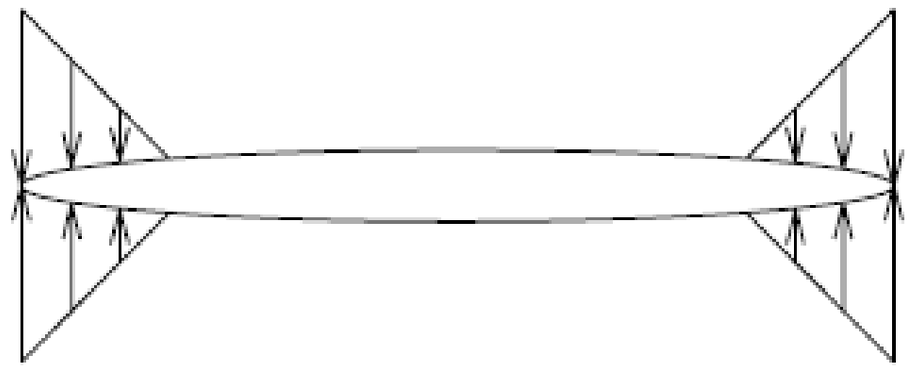

More appropriate for <u>metals</u>

5.2.1 Plastic zone shape: 1D models

- 1st order approximation
- 2nd order Irwin model
- Strip yield models (Dugdale, and Barenbolt models)

- Effective crack length

Effective crack length

Irwin

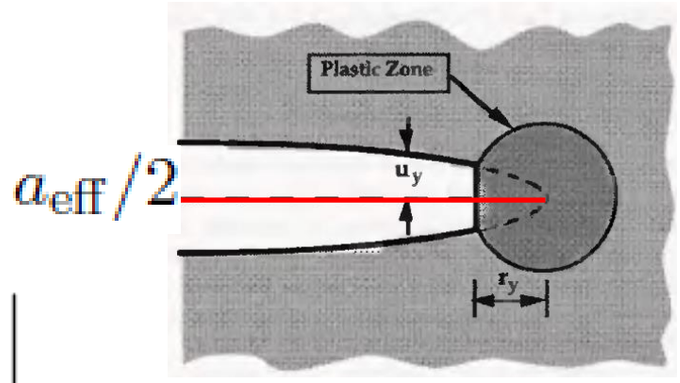

Crack tip blunting

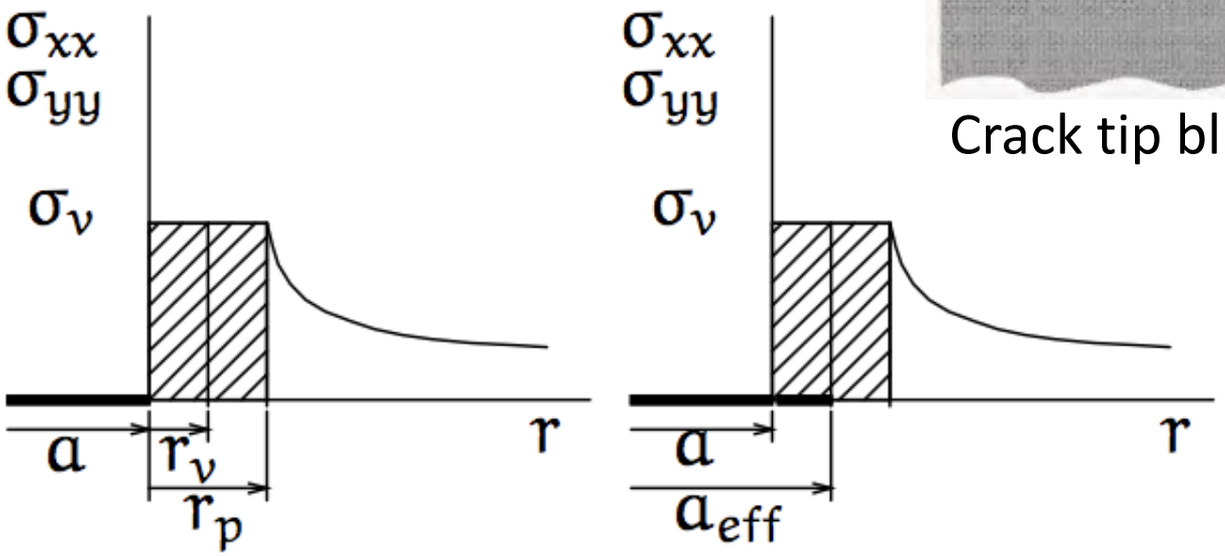

$$r_p = \frac{1}{\pi}\left(\frac{K_{I\,\text{eff}}}{\sigma_{ys}}\right)^2$$

$$a_{\text{eff}} = a + r_p$$

Dugdale

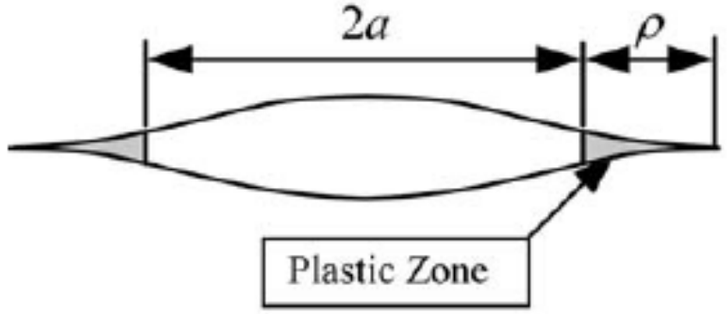

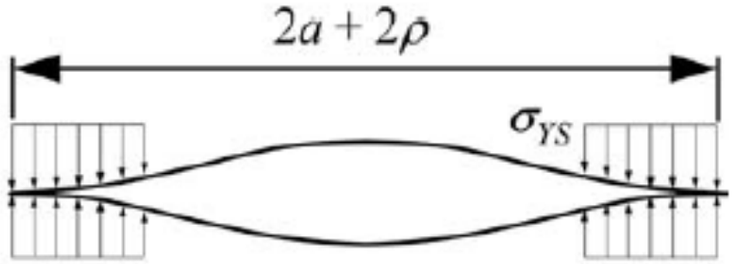

$$\rho = \frac{\pi}{8}\left(\frac{K_{I\,\text{eff}}}{\sigma_{ys}}\right)^2$$

$$a_{\text{eff}} = a + \rho$$

$K_{I\,\text{eff}} = f(a_{\text{eff}})$, (for example $K_{I\,\text{eff}} = \sigma_0\sqrt{\pi a_{\text{eff}}}$ infinite domain) $\Rightarrow$

Nonlinear equation to solve for $K_{I\,\text{eff}}$ and a_{eff}

Example

Consider an infinite plate with a central crack of length 2a subjected to a uniaxial stress perpendicular to the crack plane. Using the Irwin's model for a plane stress case, show that the effective SIF is given as follows

$$K_{\text{eff}} = \frac{\sigma\sqrt{\pi a}}{\left[1 - 0.5\left(\frac{\sigma}{\sigma_{ys}}\right)^2\right]^{1/2}}$$

Solution:

The effective crack length is $a + r_1$

The effective SIF is thus $K_{\text{eff}} = \sigma\sqrt{\pi\left(a + r_p\right)}$

with $r_p = \frac{1}{2\pi}\left(\frac{K_{I\,\text{eff}}}{\sigma_{ys}}\right)^2$

Consider a large central cracked plate subjected to a uniform stress of 130 MPa. The fracture toughness K_c=50MPa√m, the yield strength σ_{ys}=420MPa.

(a) What is the maximum allowable crack length?
(b) What is the maximum crack length if plastic correction is taken into account. Plane stress and Irwin's correction.

Solution:

(a) $$2a = 94.2 \text{ mm}$$

(b) $$K_{\text{eff}} = \frac{\sigma\sqrt{\pi a}}{\left[1 - 0.5\left(\frac{\sigma}{\sigma_{ys}}\right)^2\right]^{1/2}}$$ (previous slide)

$$K_{\text{eff}} = K_c \rightarrow 2a = 89.7 \text{ mm}$$

Effective crack length

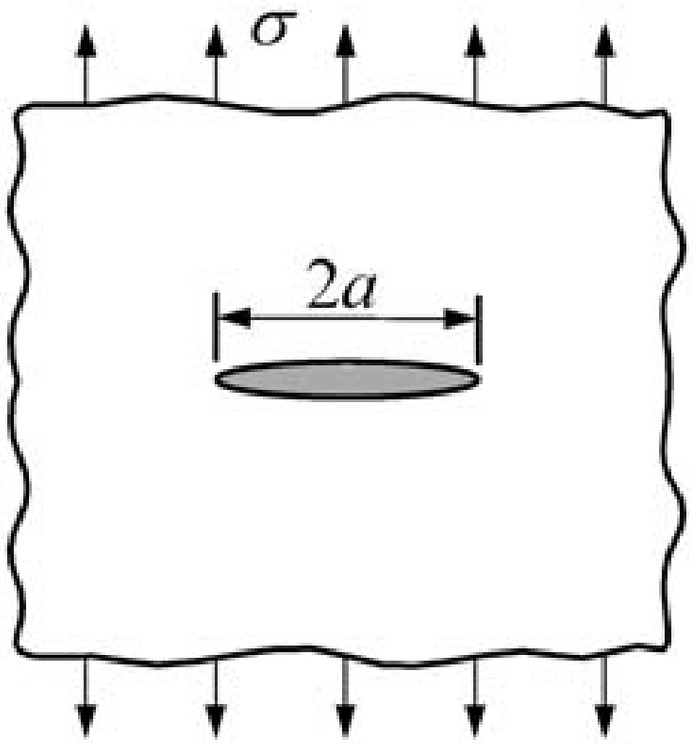

$$K_{eff} = \frac{\sigma\sqrt{\pi a}}{\sqrt{1-\frac{1}{2}\left(\frac{\sigma}{\sigma_{YS}}\right)^2}}$$

As $\frac{\sigma}{\sigma_{ys}}$ increases $\Rightarrow$

LEFM becomes less accurate

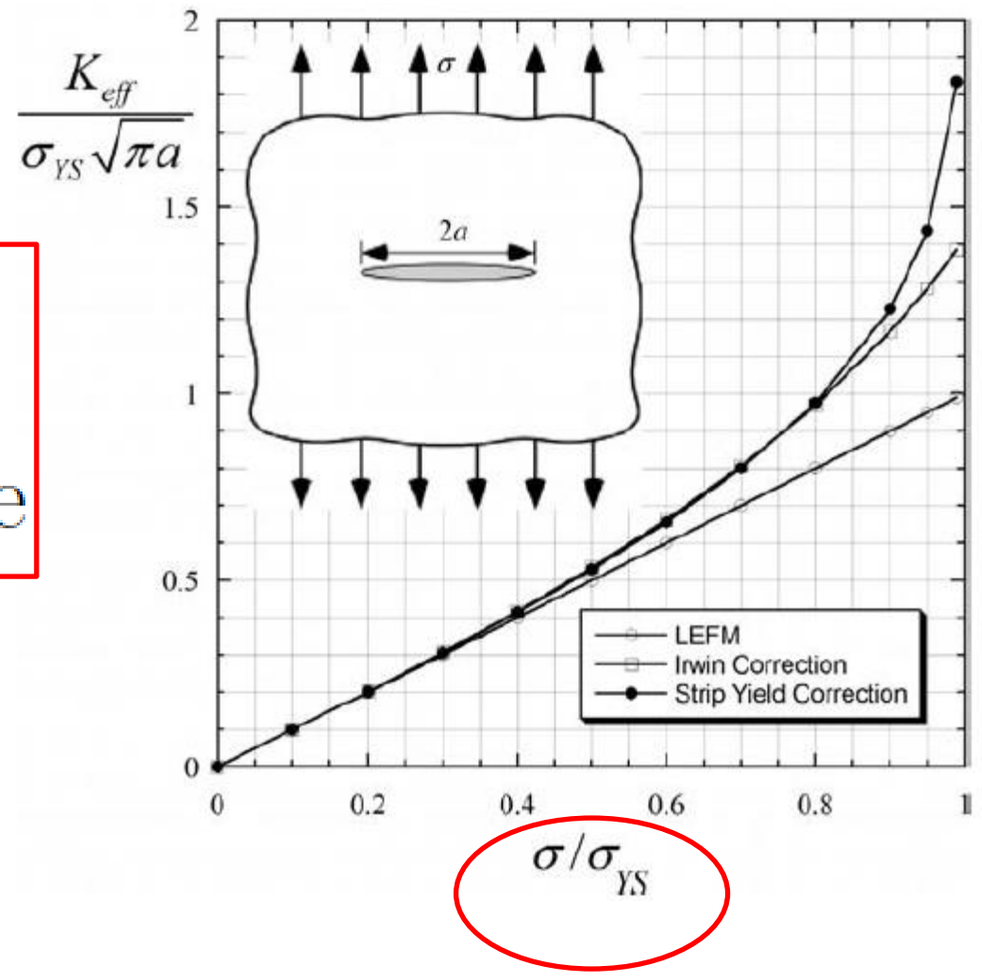

Validity of LEFM solution

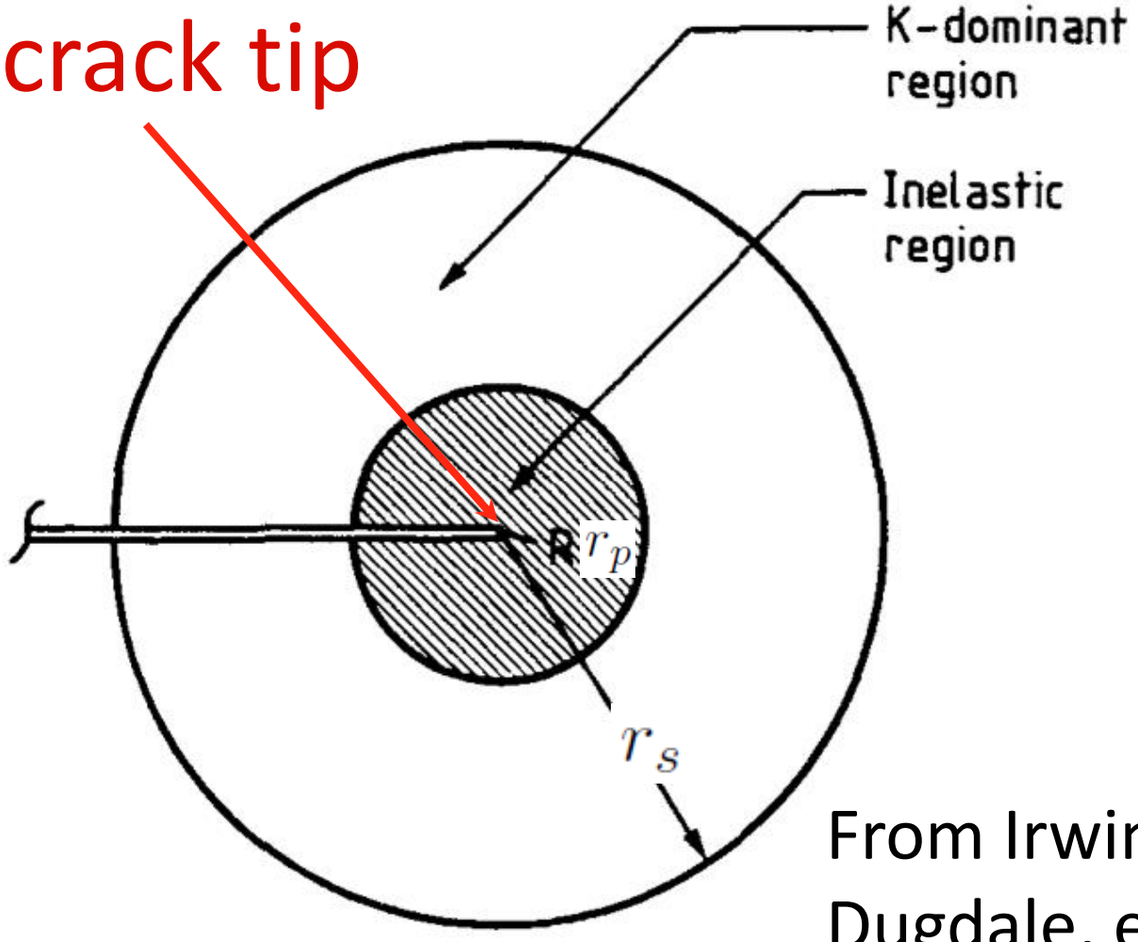

$$\text{LEFM: } \sigma = \frac{K}{\sqrt{2\pi r}} f(\theta) \Rightarrow$$

$$\text{for } r_s\text{: } \frac{K}{\sqrt{2\pi r_s}} \propto \sigma_0$$

$$(\sigma_0 = \text{applied stress}) \Rightarrow$$

$$r_s \propto \left(\frac{K}{\sigma_0}\right)^2$$

From Irwin, Dugdale, etc

$$r_p \propto \left(\frac{K}{\sigma_y}\right)^2$$

$$\frac{r_p}{r_s} \propto \left(\frac{\sigma_0}{\sigma_y}\right)^2$$

$$\text{LEFM is valid when } r_p \ll r_s \text{ (or } \sigma_0 \ll \sigma_y)$$

LEFM is better applicable to materials of high yield strength and low fracture toughness

5.2.2 Plastic zone shape: 2D models

- 2D models
- plane stress versus plane strain plastic zones

Plastic yield criteria

von-Mises criterion

$$\sigma_v = \sqrt{3J_2}$$
$$= \sqrt{\frac{(\sigma_{11}-\sigma_{22})^2 + (\sigma_{22}-\sigma_{33})^2 + (\sigma_{33}-\sigma_{11})^2 + 6(\sigma_{12}^2+\sigma_{23}^2+\sigma_{31}^2)}{2}}$$
$$= \sqrt{\frac{(\sigma_1-\sigma_2)^2 + (\sigma_2-\sigma_3)^2 + (\sigma_1-\sigma_3)^2}{2}}$$
$$= \sqrt{\tfrac{3}{2}\, s_{ij}s_{ij}}$$

s is stress deviator tensor

$$\boldsymbol{\sigma}^{dev} = \boldsymbol{\sigma} - \frac{1}{3}(\operatorname{tr}\boldsymbol{\sigma})\mathbf{I}$$

Tresca criterion

Maximum shear stress

$$\sigma_{tresca} = \sigma_1 - \sigma_3 > \sigma_{max}$$

3D

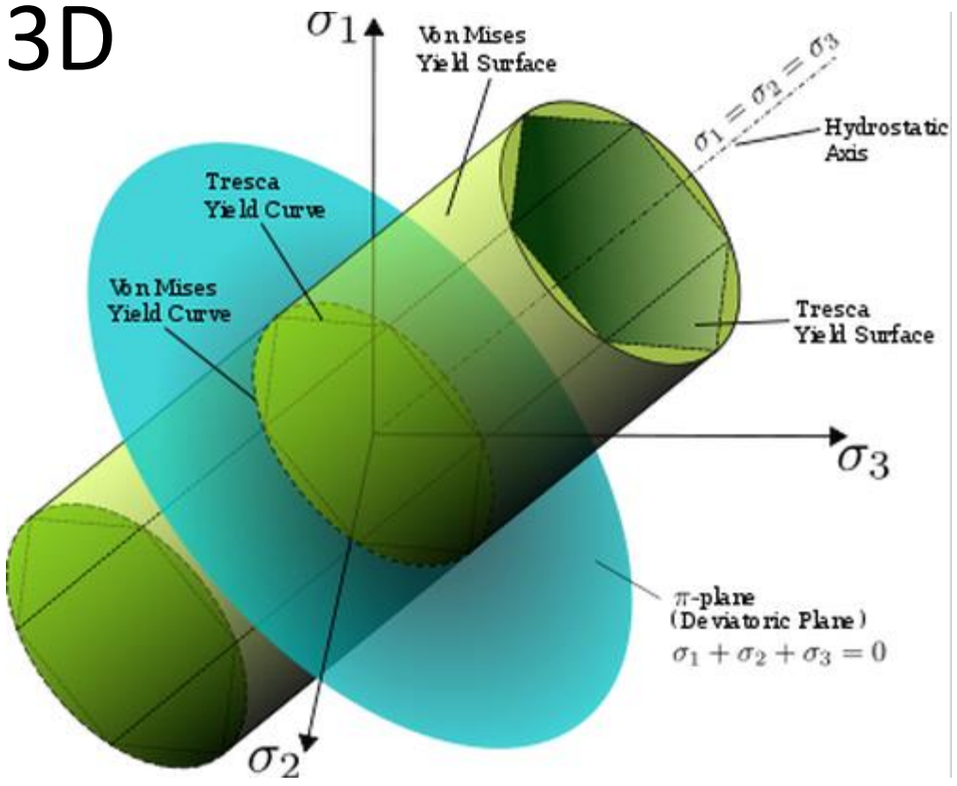

2D

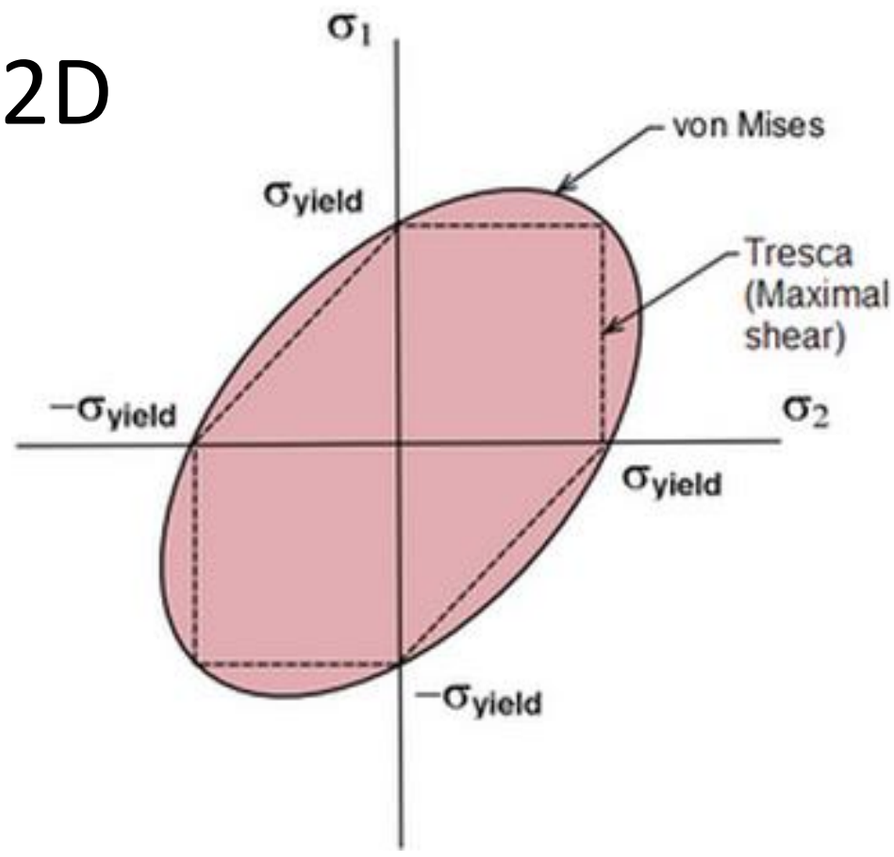

Plastic zone shape

von-Mises criterion

$$\sigma_e = \sigma_{ys}$$

$$\sigma_e = \frac{1}{\sqrt{2}}\left[(\sigma_1-\sigma_2)^2+(\sigma_1-\sigma_3)^2+(\sigma_2-\sigma_3)^2\right]^{1/2}$$

Principal stresses:

$$\sigma_1,\sigma_2 = \frac{\sigma_{xx}+\sigma_{yy}}{2} \pm \left[\left(\frac{\sigma_{xx}-\sigma_{yy}}{2}\right)^2 + \tau_{xy^2}\right]^{1/2}$$

Mode I, principal stresses

$$\sigma_1 = \frac{K_I}{\sqrt{2\pi r}}\cos\frac{\theta}{2}\left(1+\sin\frac{\theta}{2}\right)$$

$$\sigma_2 = \frac{K_I}{\sqrt{2\pi r}}\cos\frac{\theta}{2}\left(1-\sin\frac{\theta}{2}\right)$$

$$\sigma_3 = \begin{cases} 0 & \text{plane stress} \\ \dfrac{2\nu K_I}{\sqrt{2\pi r}}\cos\dfrac{\theta}{2} & \text{plane strain} \end{cases}$$

$$r_y(\theta) = \frac{1}{4\pi}\left(\frac{K_I}{\sigma_{ys}}\right)^2\left[1+\cos\theta+\frac{3}{2}\sin^2\theta\right]$$ plane stress

$$r_y(\theta) = \frac{1}{4\pi}\left(\frac{K_I}{\sigma_{ys}}\right)^2\left[(1-2\mu)^2(1+\cos\theta)+\frac{3}{2}\sin^2\theta\right]$$ plane strain

Plastic zone shape

von-Mises criterion

$$r_y(\theta) = \frac{1}{4\pi}\left(\frac{K_I}{\sigma_{ys}}\right)^2\left[1+\cos\theta+\frac{3}{2}\sin^2\theta\right]$$

plane stress

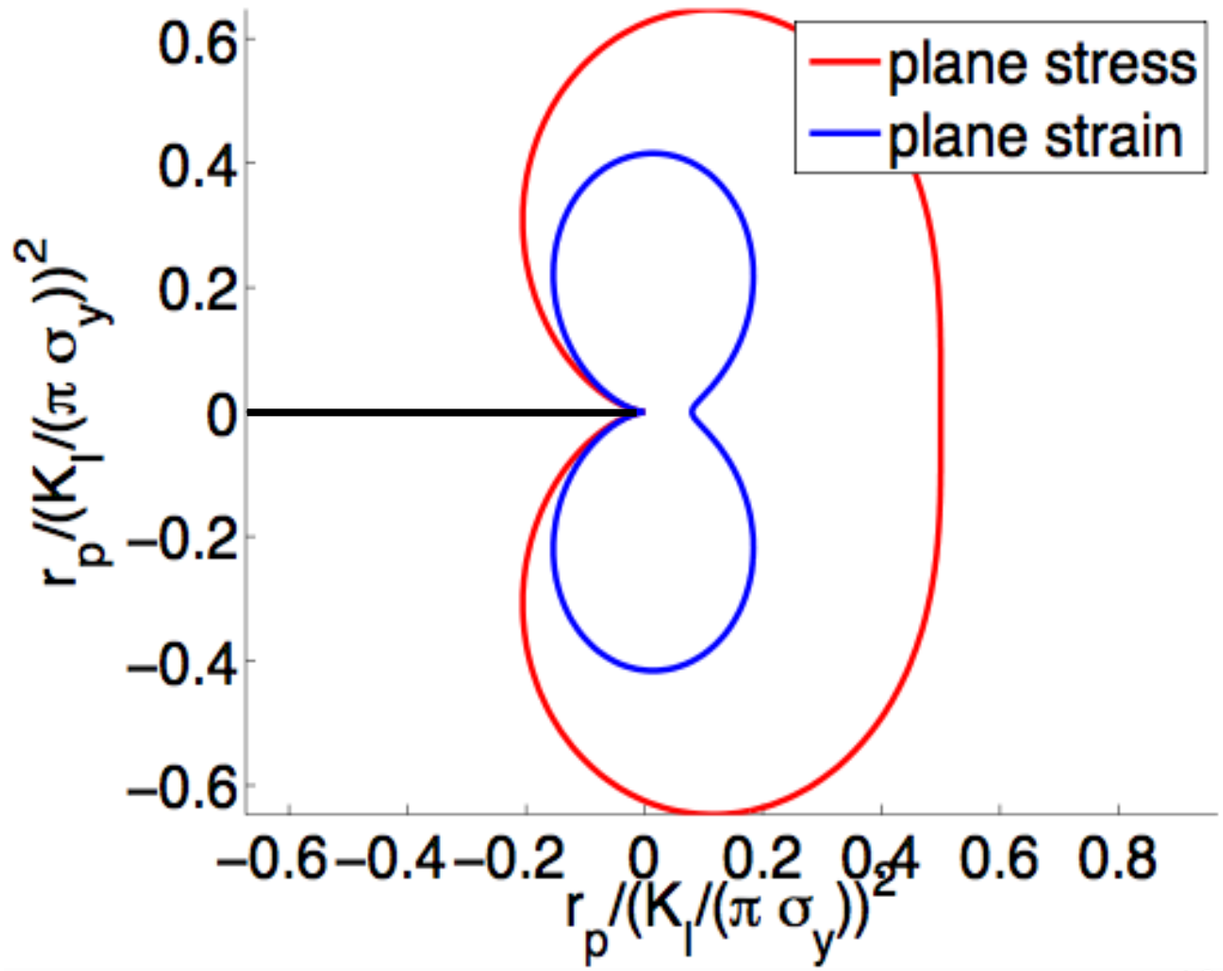

Tresca criterion

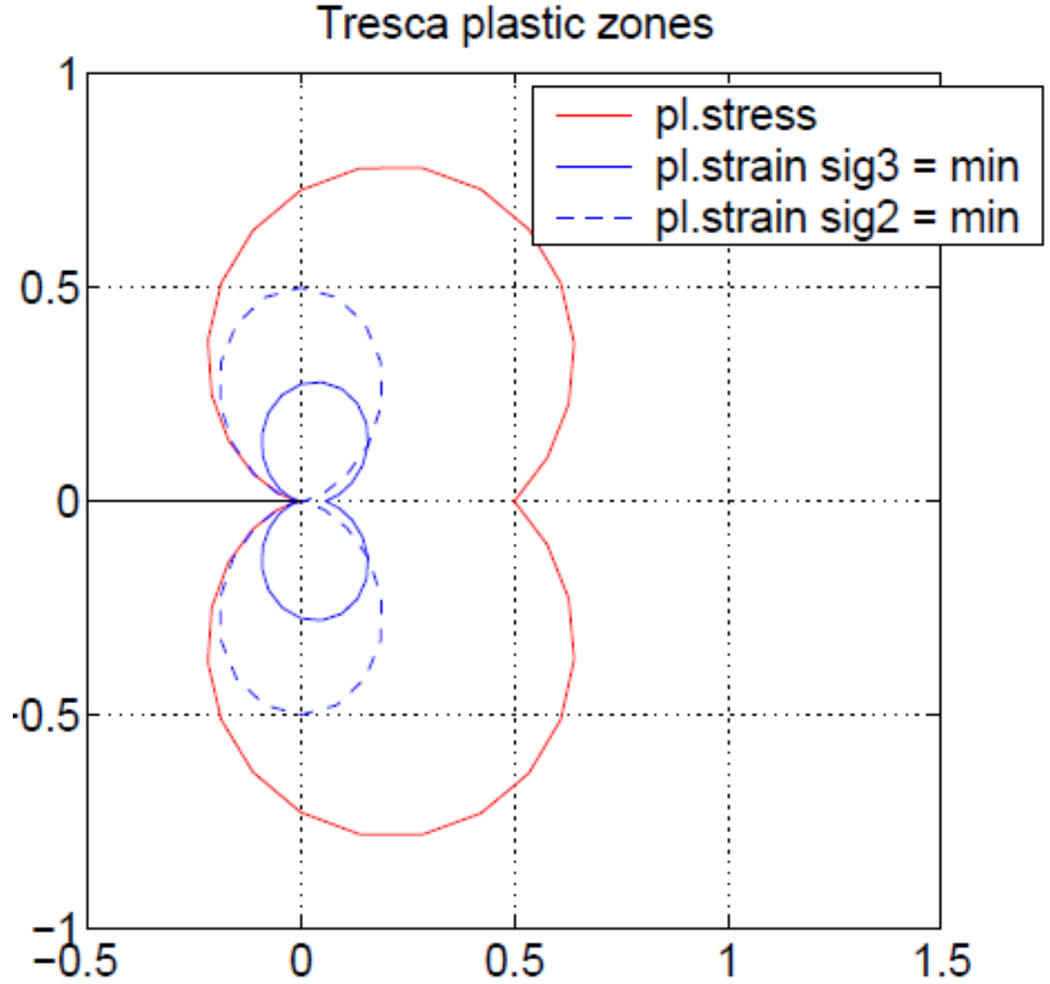

Plastic zone shape: Mode I-III

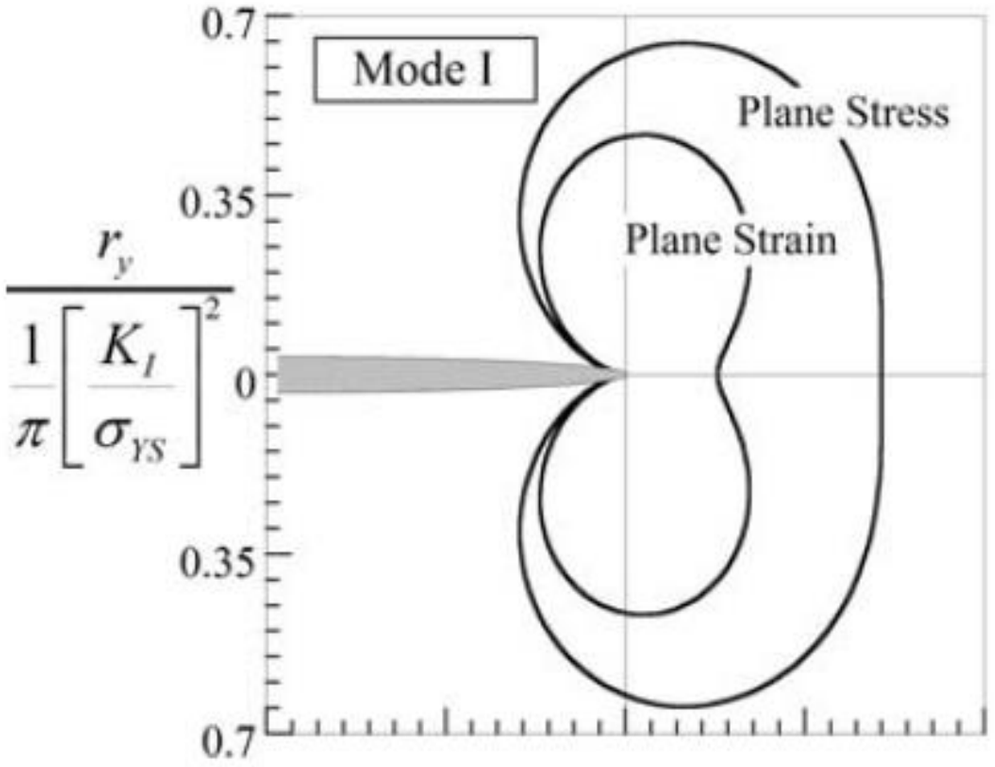

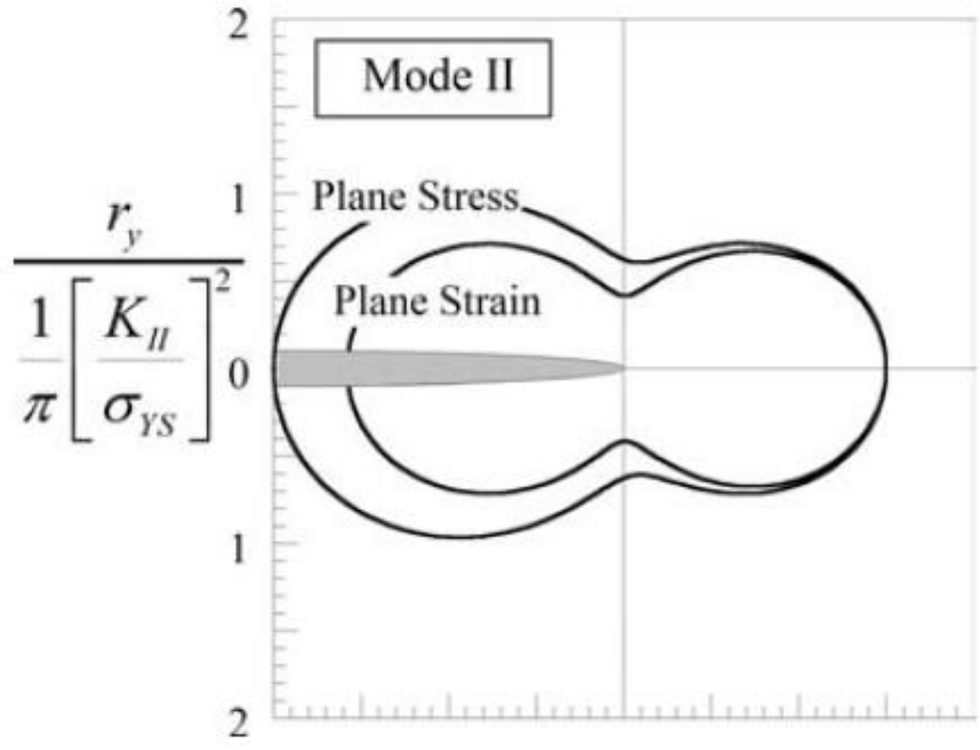

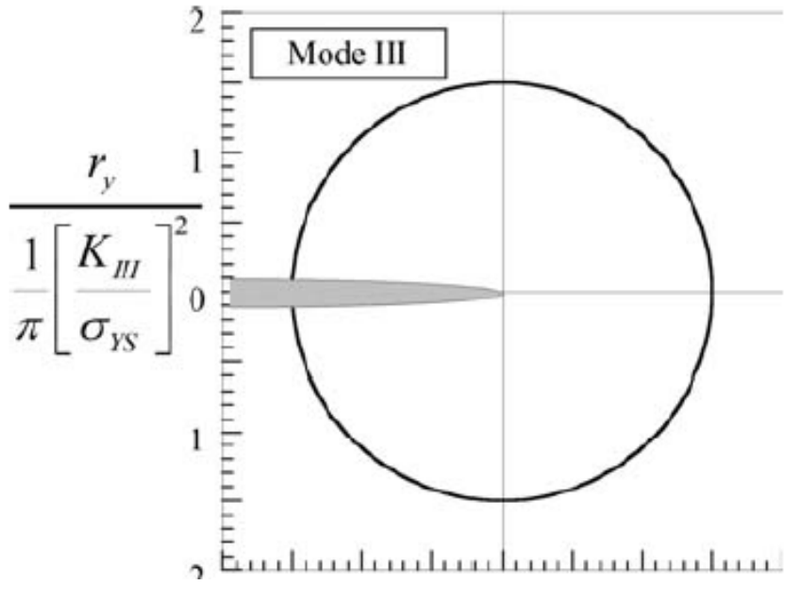

Plastic zone sizes:Summary

criterion	state	r_y or r_p	$\frac{r_y \vert r_p}{(K_I/\sigma_y)^2}$
Von Mises	plane stress	$\frac{1}{2\pi}\left(\frac{K_I}{\sigma_y}\right)^2$	0.1592
Von Mises	plane strain	$\frac{1}{18\pi}\left(\frac{K_I}{\sigma_y}\right)^2$	0.0177
Tresca	plane stress	$\frac{1}{2\pi}\left(\frac{K_I}{\sigma_y}\right)^2$	0.1592
Tresca	plane strain $\sigma_1 > \sigma_2 > \sigma_3$	$\frac{1}{18\pi}\left(\frac{K_I}{\sigma_y}\right)^2$	0.0177
Tresca	plane strain $\sigma_1 > \sigma_3 > \sigma_2$	0	0
Irwin	plane stress	$\frac{1}{\pi}\left(\frac{K_I}{\sigma_y}\right)^2$	0.3183
Irwin	plane strain (pcf $= 3$)	$\frac{1}{\pi}\left(\frac{K_I}{3\sigma_y}\right)^2$	0.0354
Dugdale	plane stress	$\frac{\pi}{8}\left(\frac{K_I}{\sigma_y}\right)^2$	0.3927
Dugdale	plane strain (pcf $= 3$)	$\frac{\pi}{8}\left(\frac{K_I}{3\sigma_y}\right)^2$	0.0436

Source: Schreurs (2012)

What is the problem with these 2D shape estimates?

Stress not redistributed

stress redistribution (approximately) in 1D

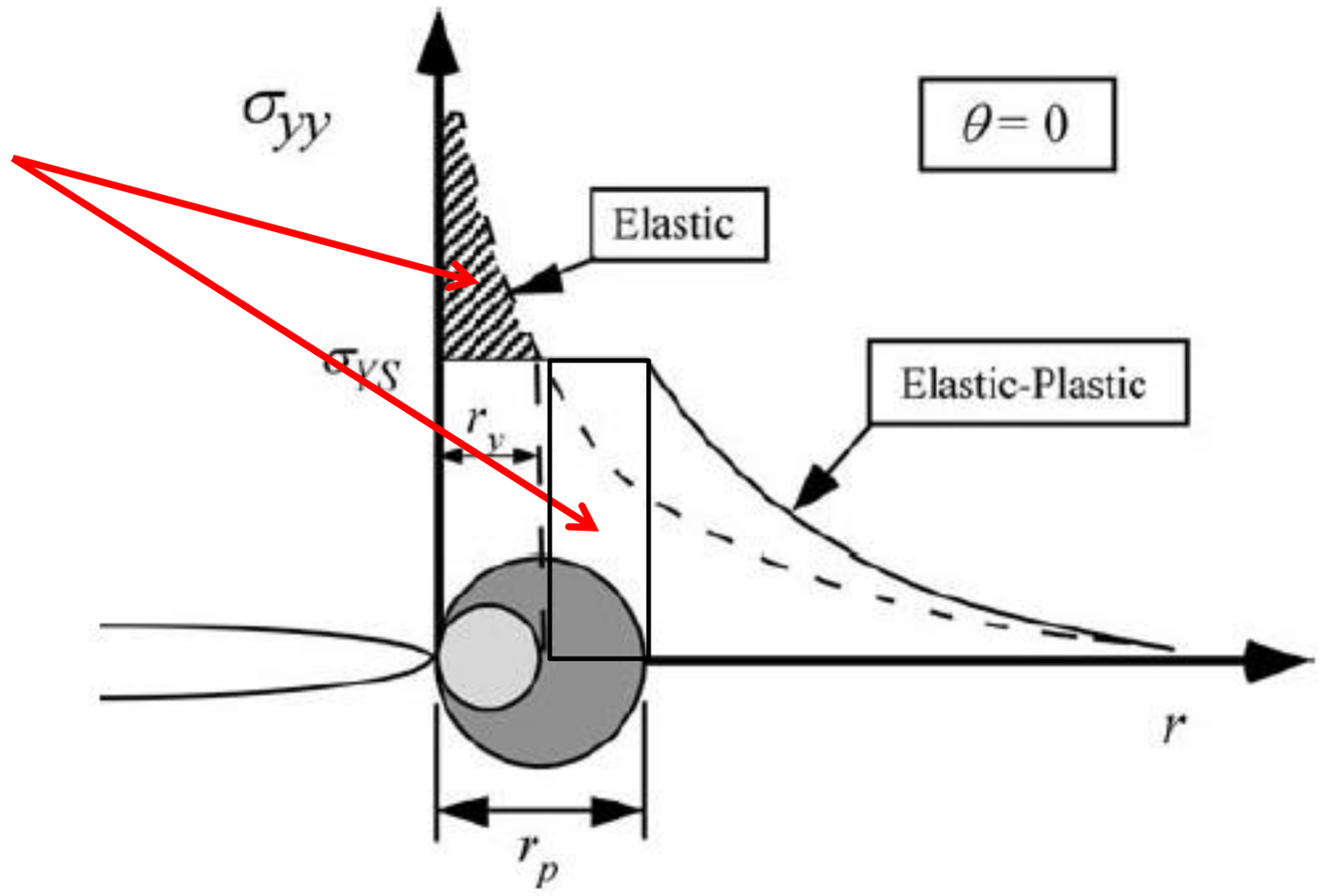

Stress redistributed for 2D

Dodds, 1991, FEM solutions

Ramberg-Osgood material model

$$\frac{\varepsilon}{\varepsilon_o} = \frac{\sigma}{\sigma_o} + \alpha\left(\frac{\sigma}{\sigma_o}\right)^n$$

- Low n: High strain-hardening.
- $n \to \infty$: Similar to elastic perfectly plastic.

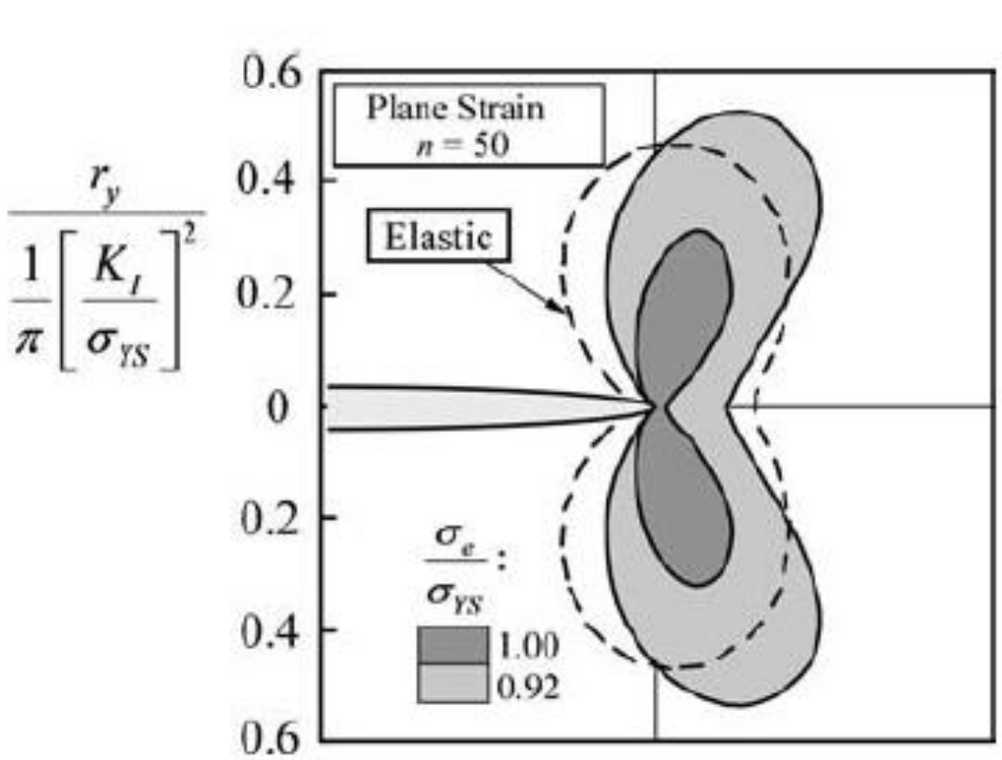

Effect of definition of yield (some level of ambiguity)

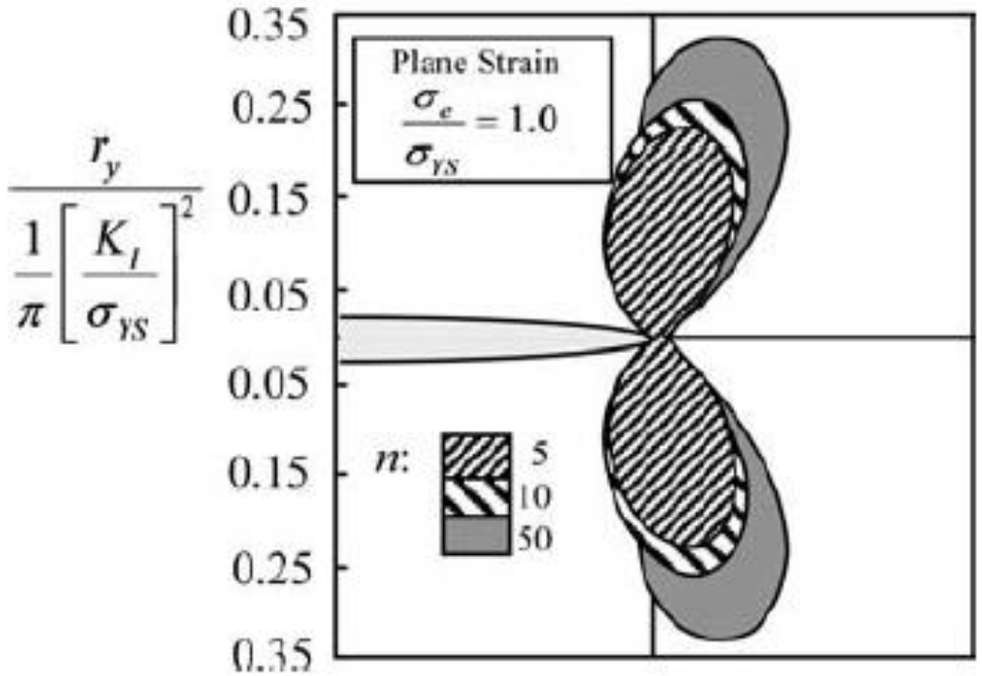

Effect of strain-hardening:

Higher hardening (lower n) => smaller zone

Plane stress/plane strain

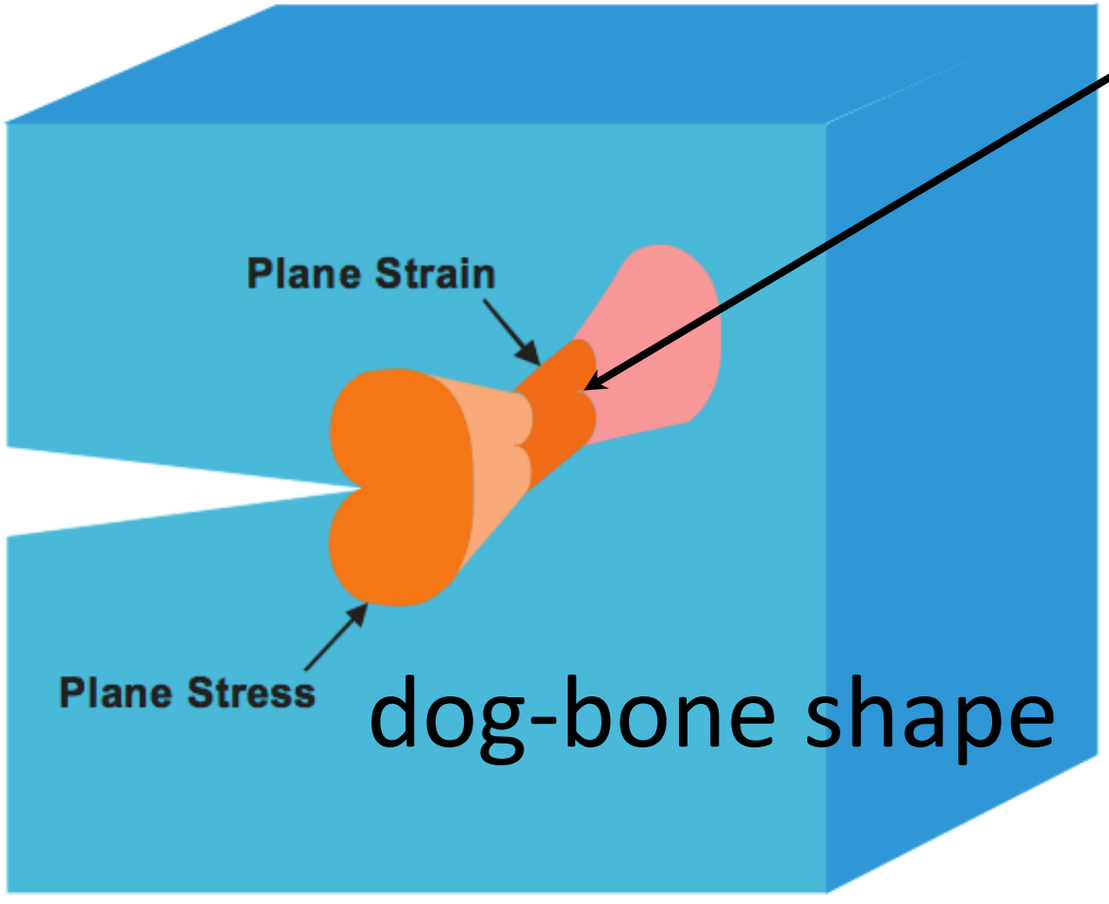

dog-bone shape

constrained by the surrounding material

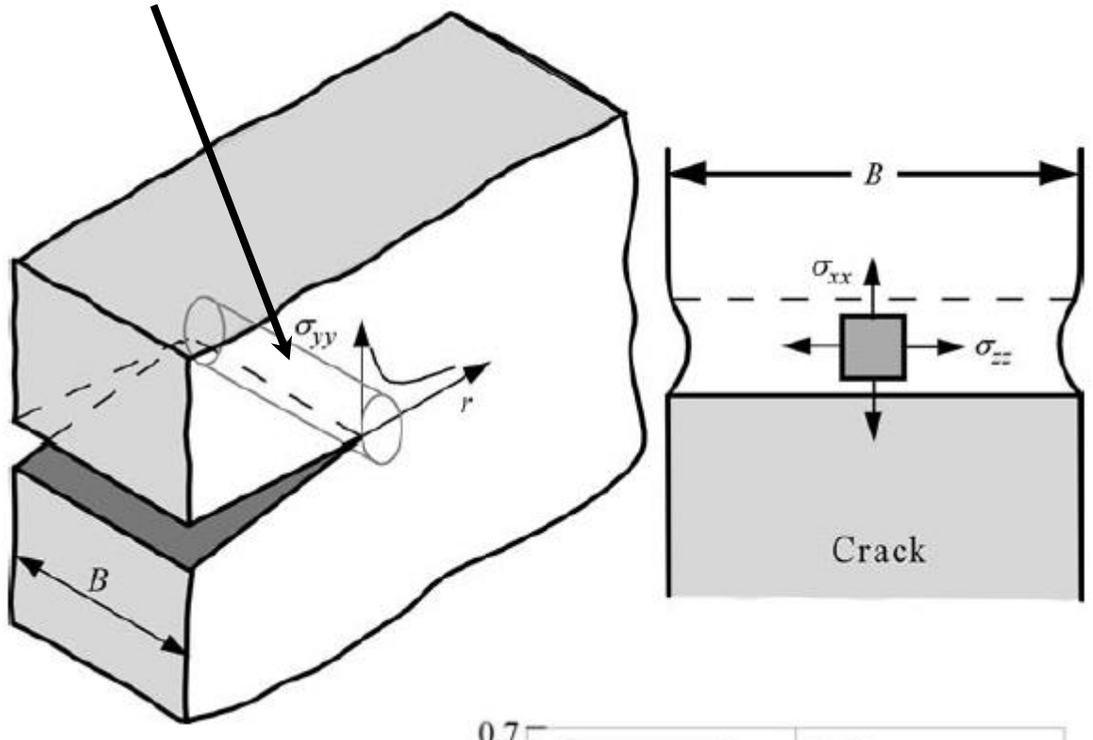

- Plane stress failure: more ductile
- Plane strain failure: mode brittle

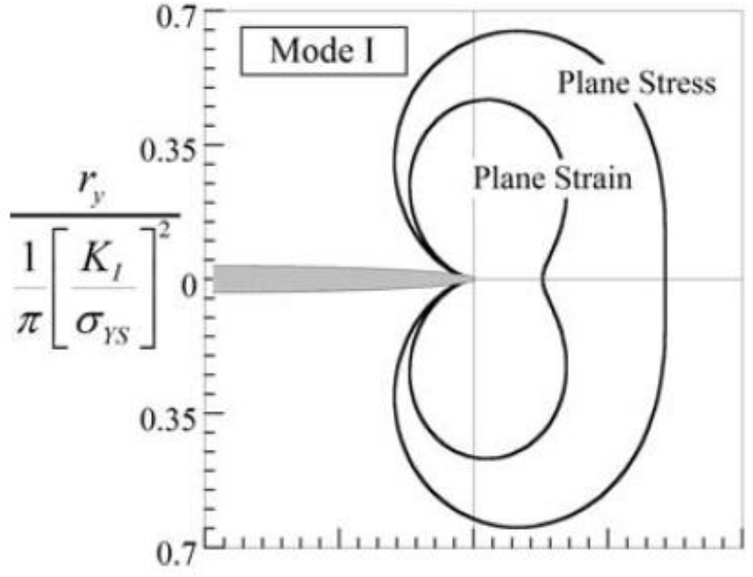

Plane stress/plane strain

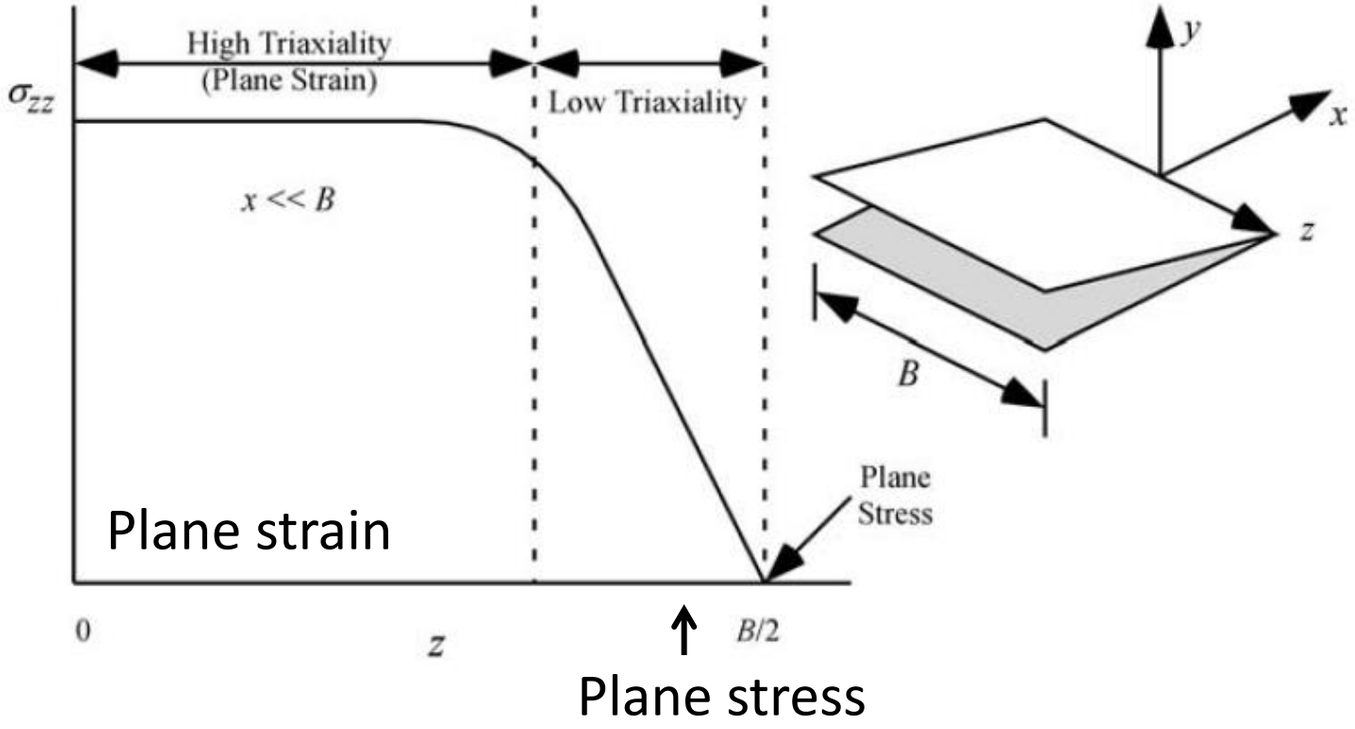

Plane strain

Plane stress

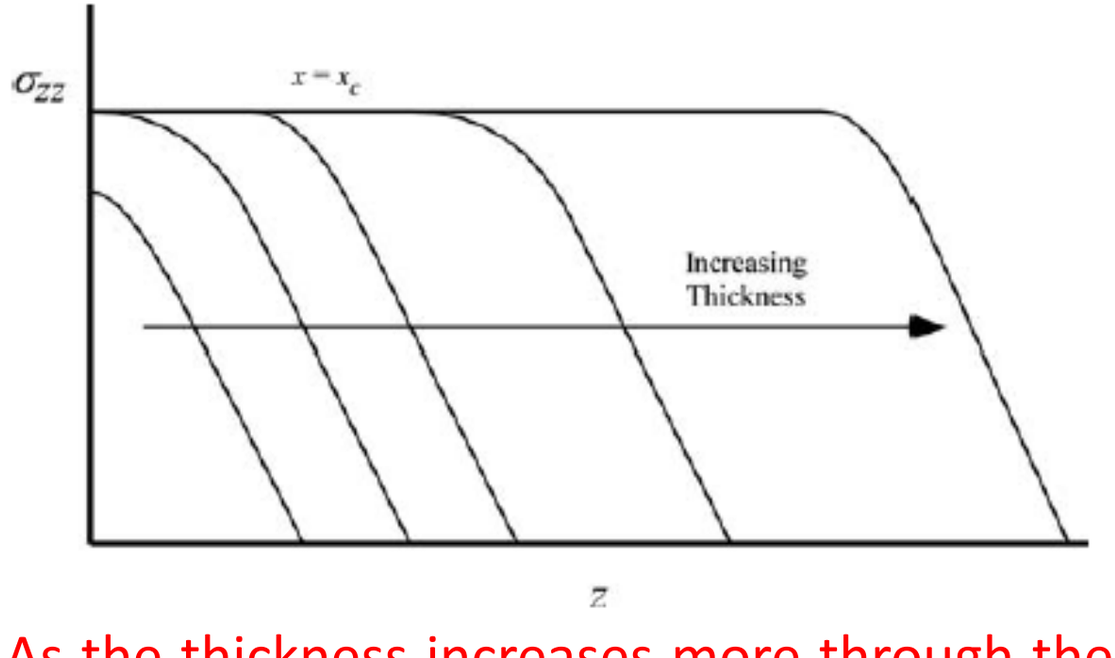

As the thickness increases more through the thickness bahaves as plane strain

Higher percentage of plate thickness is in plane strain mode for thicker plates

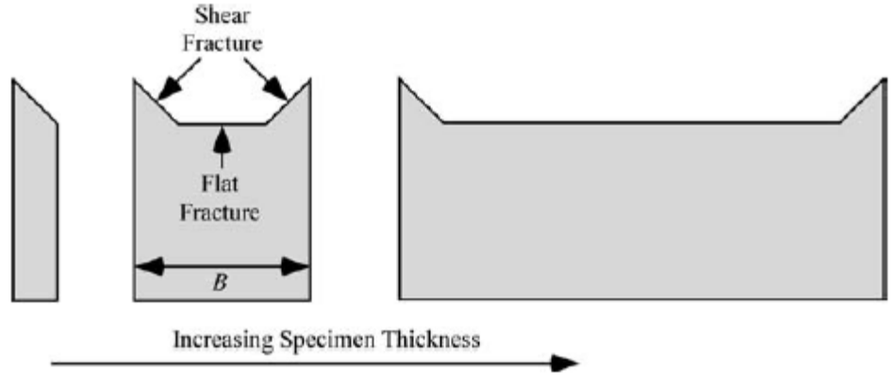

Plane stress/plane strain: Fracture loci

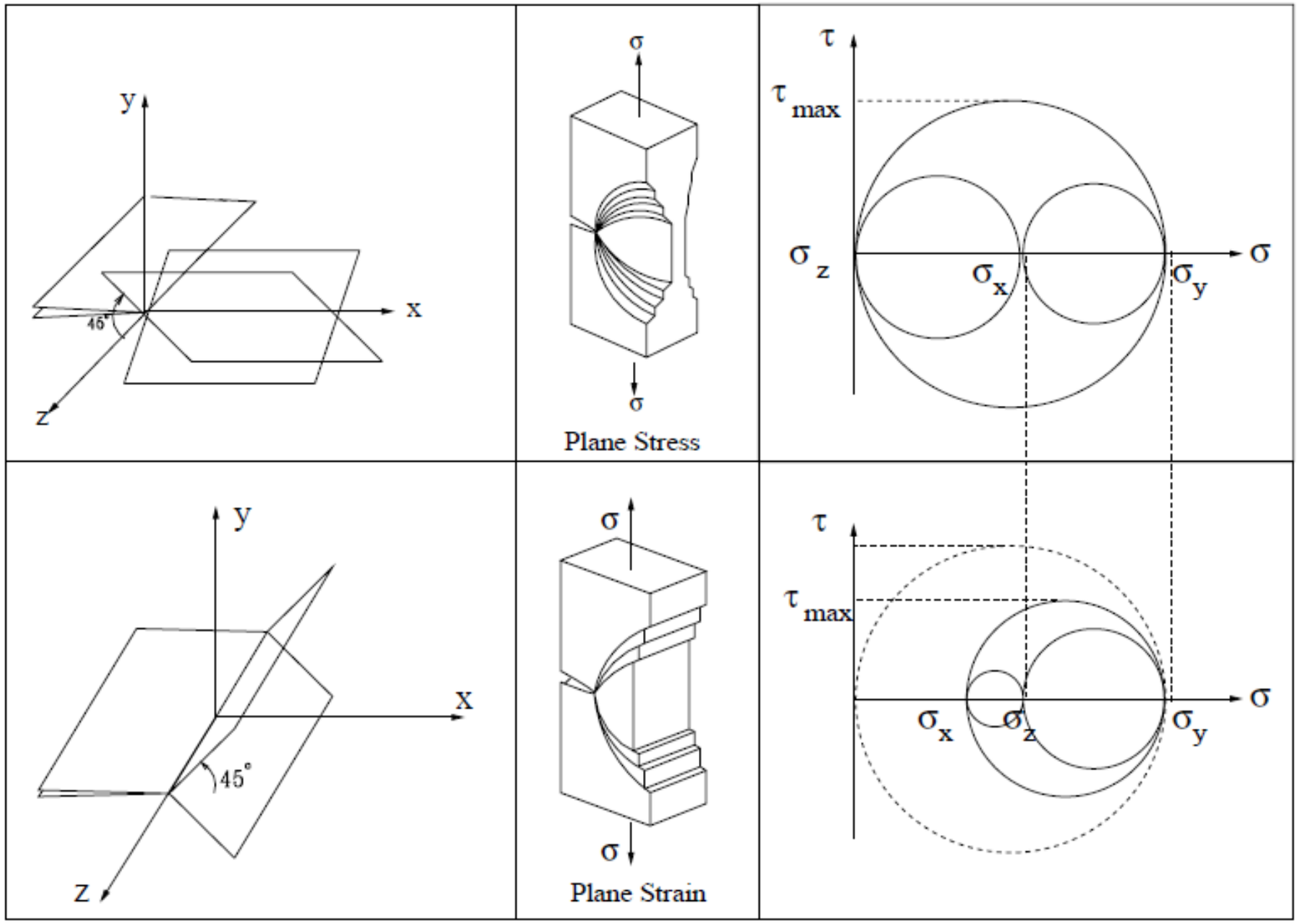

Loci of maximum shear stress for plane stress and strain

Plane stress/plane strain: What thicknesses are plane stress?

- As $\frac{\left(\frac{K}{\sigma_{ys}}\right)^2}{B}$ increases:
  1. The plastic zone expands (load is increasing)
  2. Plastic zone transitions from plane strain to plain stress
- Note that $r_p \propto \left(\frac{K}{\sigma_{ys}}\right)^2$

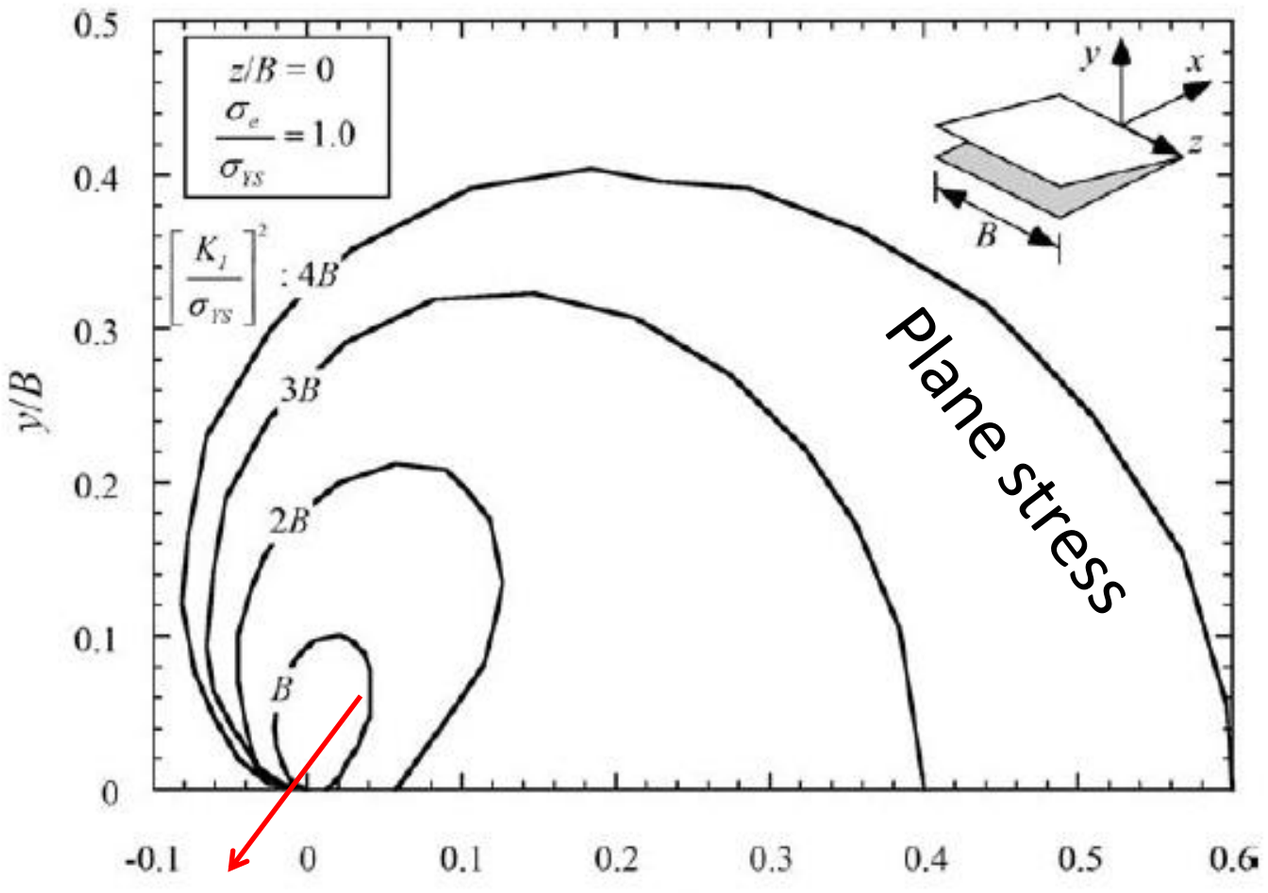

$$\frac{\left(\frac{K}{\sigma_{ys}}\right)^2}{B} \propto \frac{r_p}{B} : \begin{cases} \text{low (high } B) & \text{plane strain} \\ \text{high (low } B) & \text{plane stress} \end{cases}$$

Change of plastic loci to plane stress mode as "relative B decreases". Nakamura & Park, ASME 1988

Plane strain

For plane strain condition we must have $B > \left(\frac{K}{\sigma_{ys}}\right)^2 \propto r_p$

Plane stress/plane strain
Toughness vs. thickness

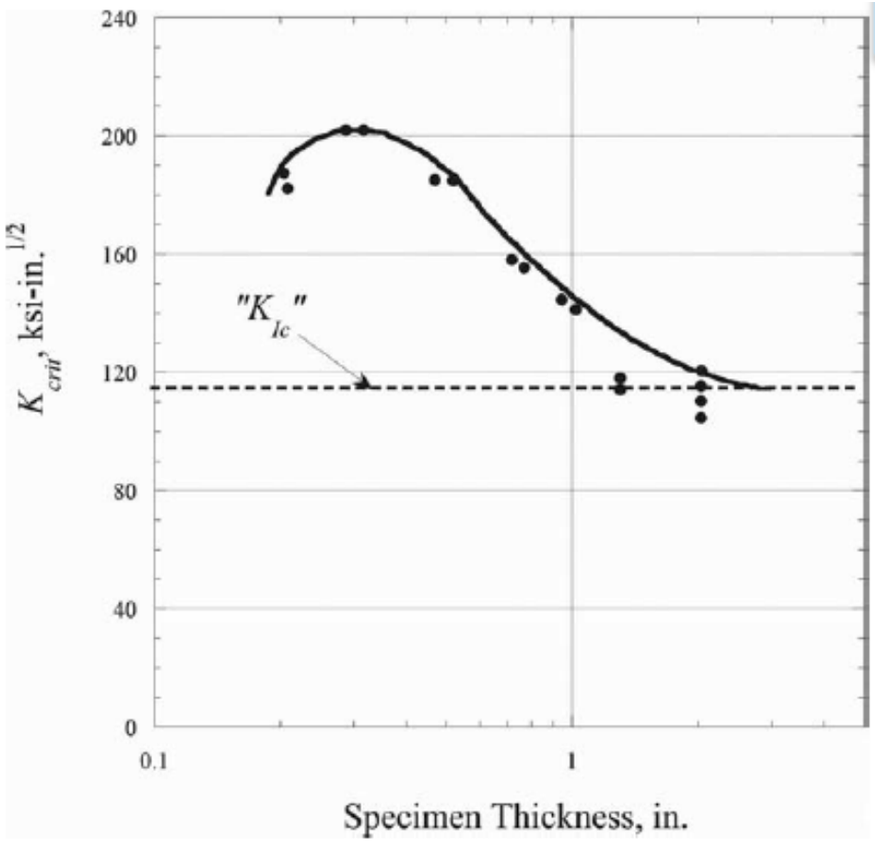

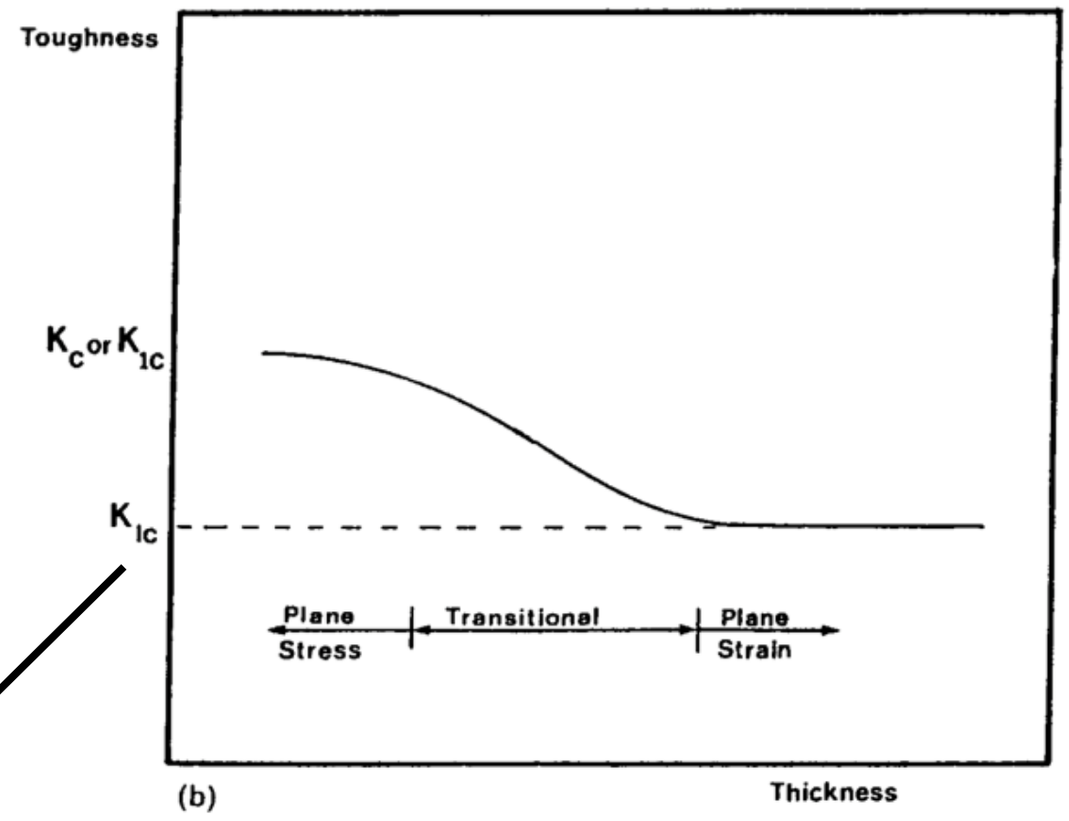

Plane strain fracture toughness **lowest K**

(safe)

(Irwin) $$K_c = K_{Ic}\left(1 + \frac{1.4}{B^2}\left[\frac{K_{Ic}}{\sigma_Y}\right]^4\right)^{1/2}$$ Note that $\frac{1}{B^2}\left[\frac{K}{\sigma_Y}\right]^4 \propto \left(\frac{r_p}{B}\right)^2$

σ_Y is the yield stress

Fracture toughness tests

- Prediction of failure in real-world applications: need the value of fracture toughness
- Tests on cracked samples: PLANE STRAIN condition!!!

Compact Tension Test

$$K_I = \frac{P}{B\sqrt{W}} \frac{\left(2+\frac{a}{W}\right)\left[0.886+4.64\frac{a}{W}-13.32\left(\frac{a}{W}\right)^2+14.72\left(\left(\frac{a}{W}\right)^3-5.6\left(\frac{a}{W}\right)^4\right]\right.}{\left(1-\frac{a}{W}\right)^{3/2}}$$

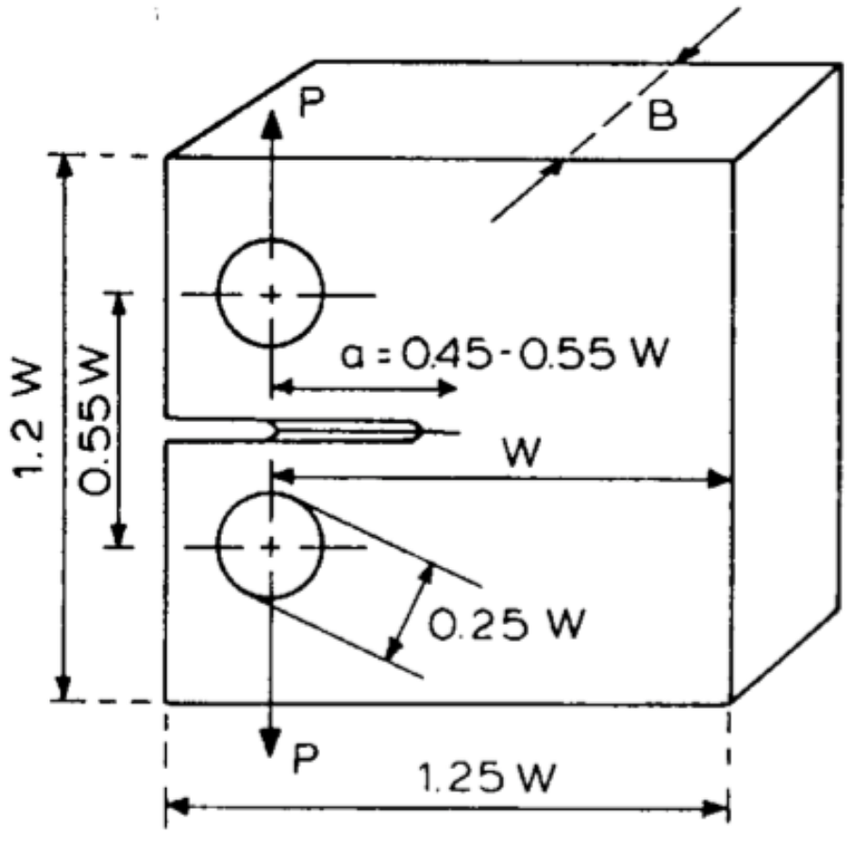

ASTM (based on Irwin's model) for plane strain condition (σ_Y is the yield stress NOT the adjusted $\sigma_{ys} \approx \sigma_Y/(1-2\nu)$):

$$a, B, (W-a) \geq 2.5\left(\frac{K_{Ic}}{\sigma_Y}\right)^2$$

Fracture toughness test

ASTM E399

$$B \geq 2.5 \left(\frac{K_{Ic}}{\sigma_Y} \right)^2$$

$$a \geq 2.5 \left(\frac{K_{Ic}}{\sigma_Y} \right)^2$$

$$W \geq 2.5 \left(\frac{K_{Ic}}{\sigma_Y} \right)^2$$

plane strain

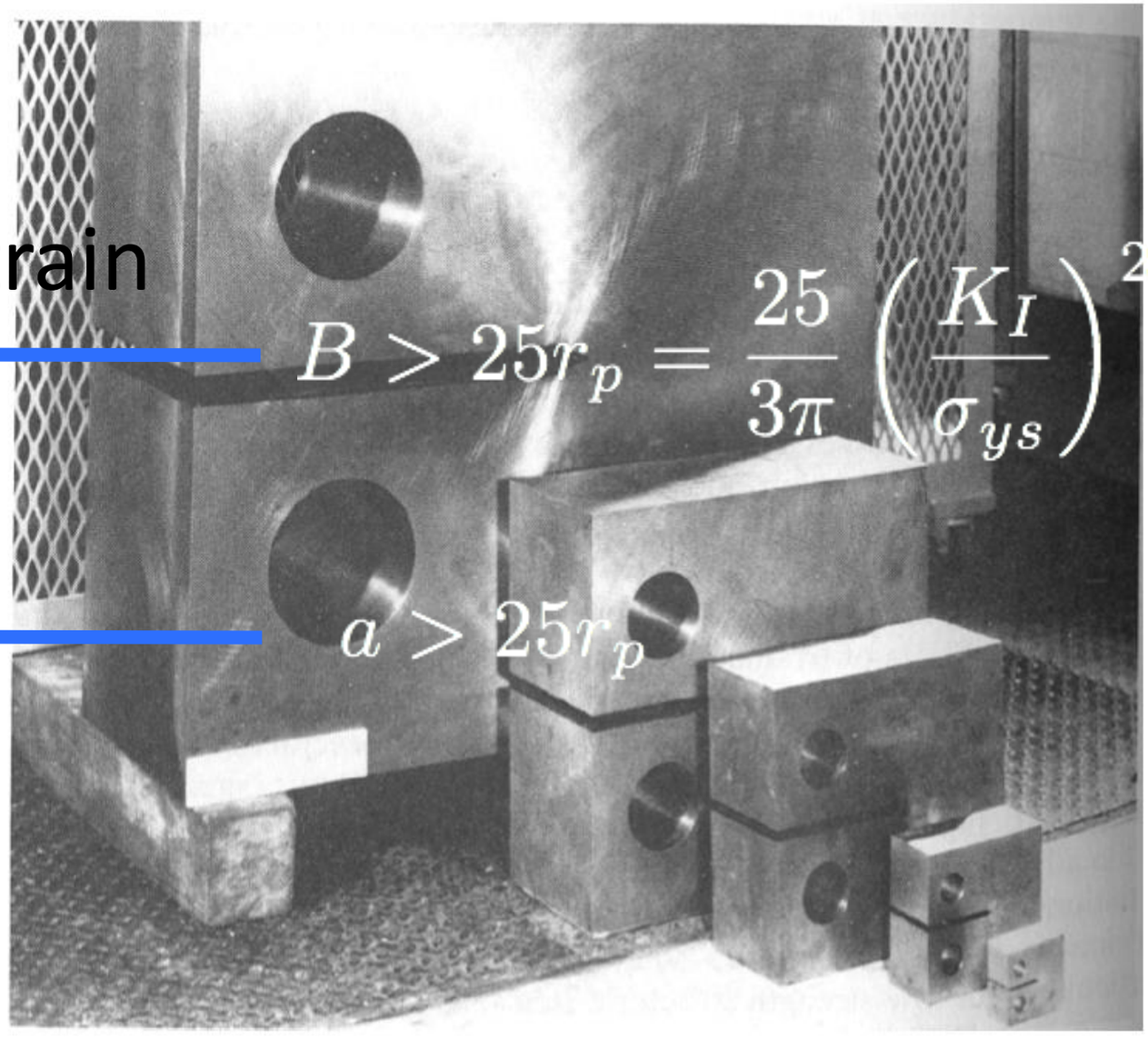

Linear fracture mechanics is only useful when the plastic zone size is much smaller than the crack size

5.3. J Integral (Rice 1958)

Introduction

Idea

Replace complicated plastic model with nonlinear elasticity (no unloading)

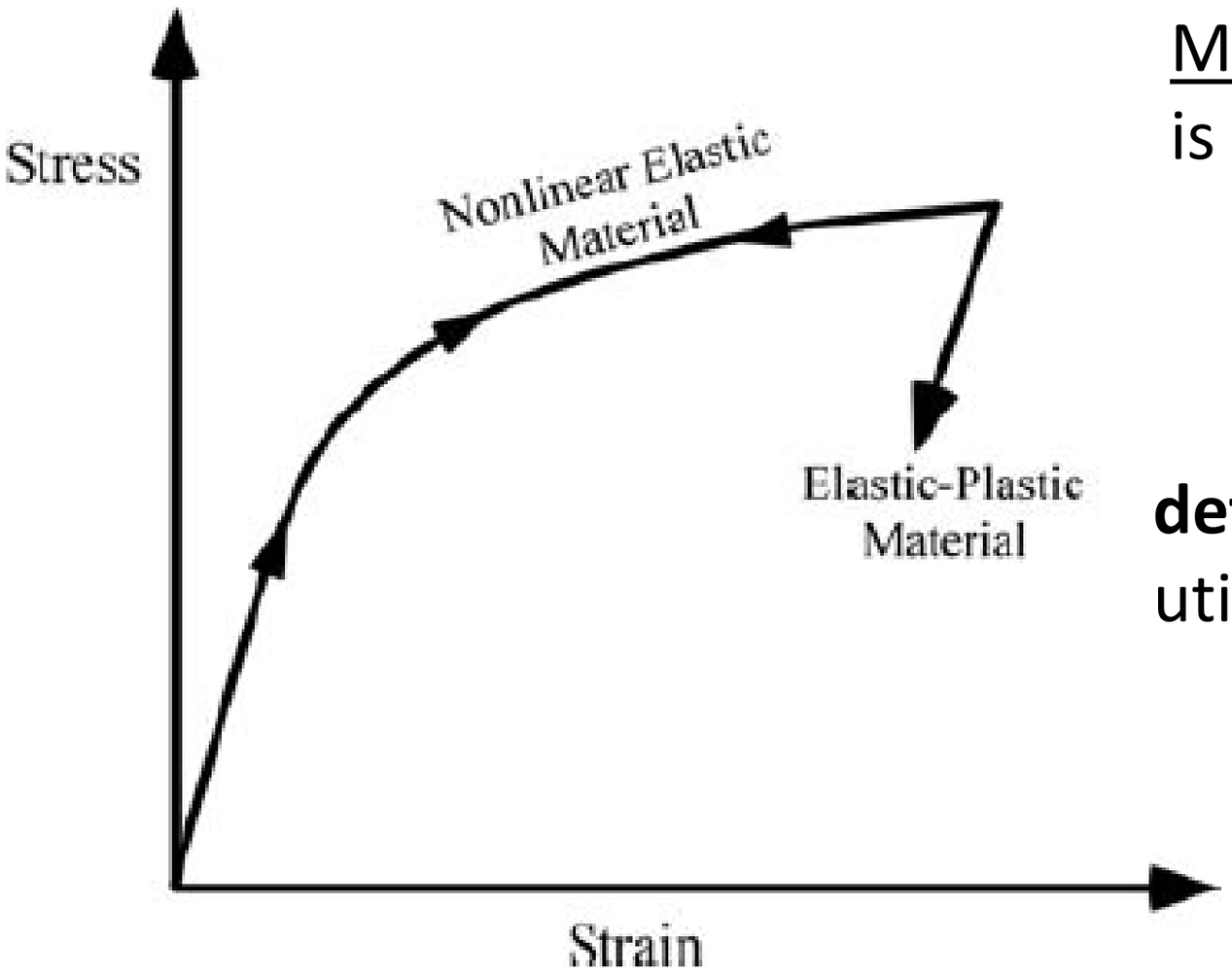

Monotonic loading: an elastic-plastic mate
is equivalent to a nonlinear elastic materia

deformation theory of plasticity can be utilized

J-integral

Eshelby, Cherepanov, 1967, Rice, 1968

- Components of J integral vector

$$J_k = \int_{\Gamma} \left(W n_k - t_i \frac{\partial u_i}{\partial x_k} \right) d\Gamma$$

- J integral in fracture

$$J = J_1 = \int_{\Gamma} \left(W n_1 - t_i \frac{\partial u_i}{\partial x_1} \right) d\Gamma \quad \left[\frac{\mathrm{N}}{\mathrm{m}} \right]$$

- strain energy density

$$W = \int_0^{\varepsilon_{pq}} \sigma_{ij} \, d\varepsilon_{ij}$$

- Surface traction

$$t_i = \sigma_{ij} n_j$$

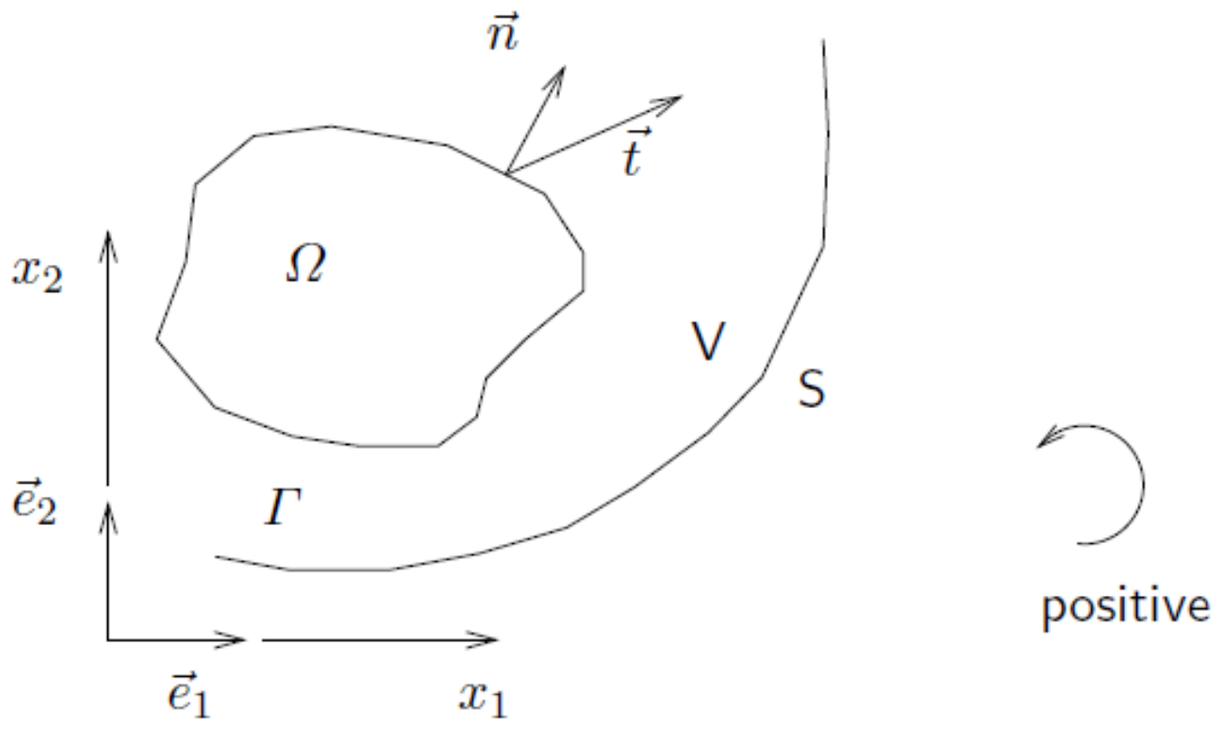

J-integral

Wikipedia

Rice used J1 for fracture characterization

$$J = \int_{\Gamma} \left(W n_1 - t_i \frac{\partial u_i}{\partial x_1} \right) d\Gamma$$

$$J = \int_{\Gamma} \left(W dx_2 - t_i \frac{\partial u_i}{\partial x_1} ds \right) \quad \left[\frac{N}{m} \right]$$

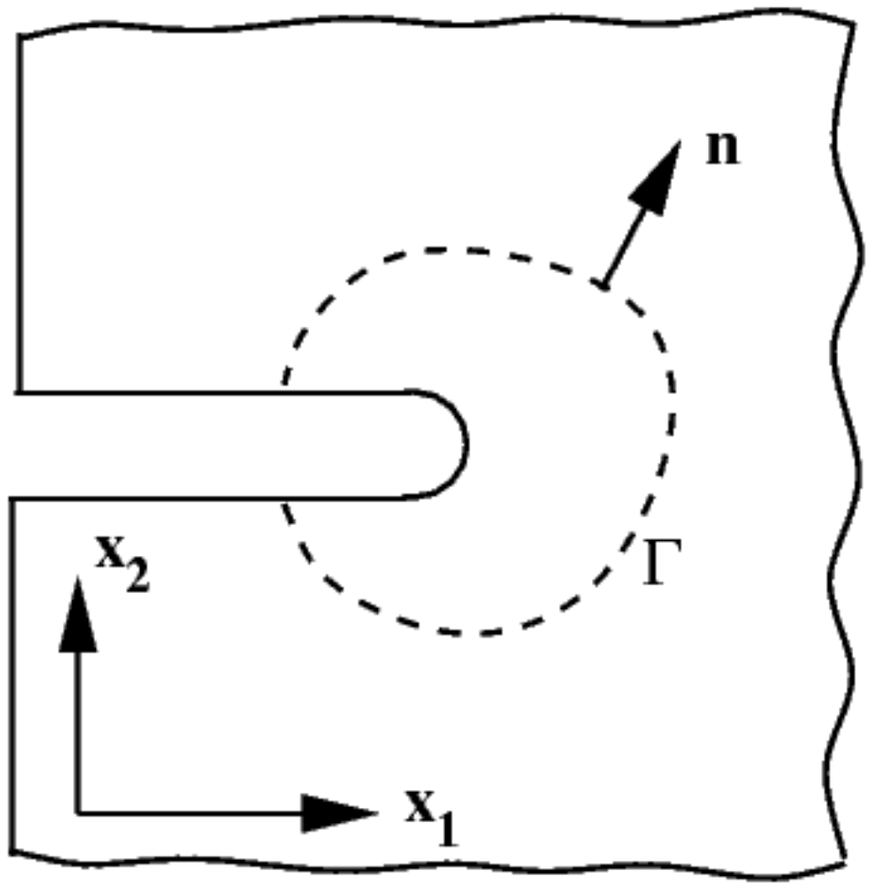

$J -$ integral

(1) J=0 for a closed path

(2) is path-independent

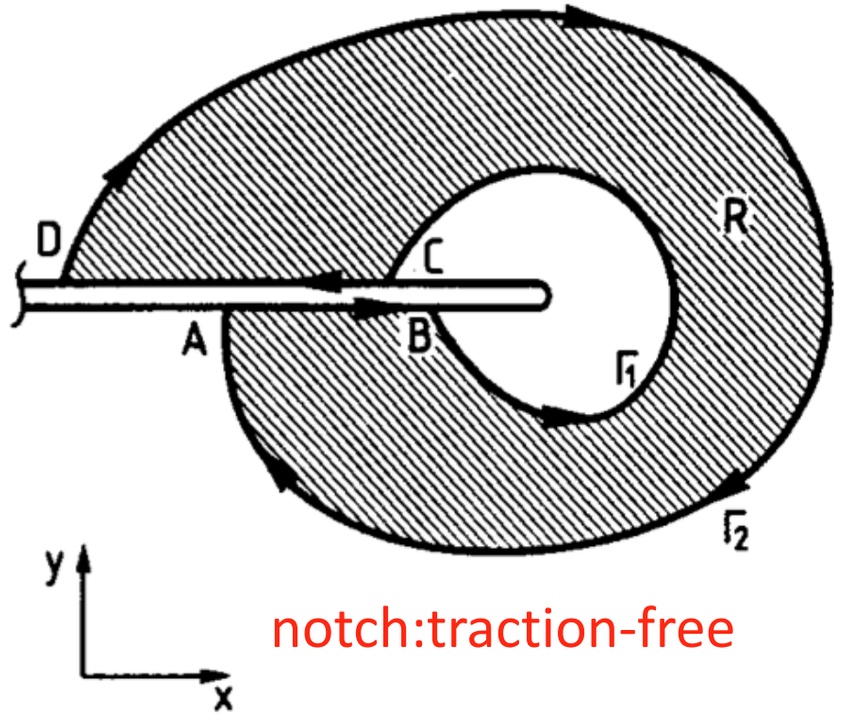

notch:traction-free

5.3. 1. Path independence of J

J Integral zero for a closed loop

$$J_k = \int_{\Gamma} \left(W n_k - t_i \frac{\partial u_i}{\partial x_k} \right) d\Gamma$$

$$J_k = \int_{\Gamma} \left(W \delta_{jk} - \sigma_{ij} u_{i,k} \right) n_j \, d\Gamma$$

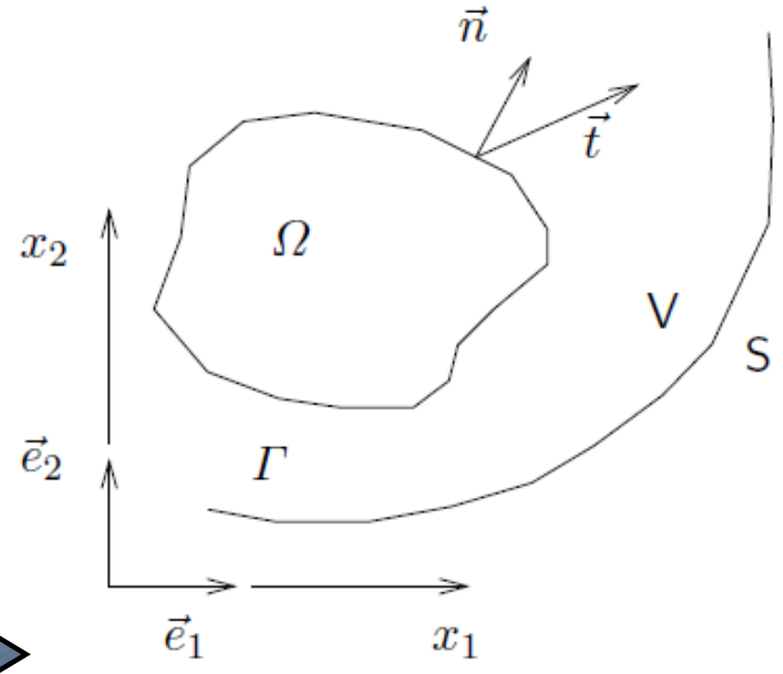

positive

inside Γ no singularities Gauss theorem

$$J_k = \int_{\Gamma} \left(\frac{\partial W}{\partial x_j} \delta_{jk} - \sigma_{ij,j} u_{i,k} - \sigma_{ij} u_{i,kj} \right) \mathrm{d}\Omega$$

and using chain rule: $$\frac{\partial W}{\partial x_j} = \frac{\partial W}{\partial \epsilon_{mn}} \frac{\partial \epsilon_{mn}}{\partial x_j}$$

$$J_k = \int_{\Omega} \left(\frac{dW}{d\varepsilon_{mn}} \frac{\partial \varepsilon_{mn}}{\partial x_j} \, \delta_{jk} - \sigma_{ij,j} u_{i,k} - \sigma_{ij} u_{i,kj} \right) d\Omega$$

J Integral zero for a closed loop

$$J_k = \int_\Omega \left(\frac{dW}{d\varepsilon_{mn}} \frac{\partial \varepsilon_{mn}}{\partial x_j} \delta_{jk} - \sigma_{ij,j} u_{i,k} - \sigma_{ij} u_{i,kj} \right) d\Omega$$

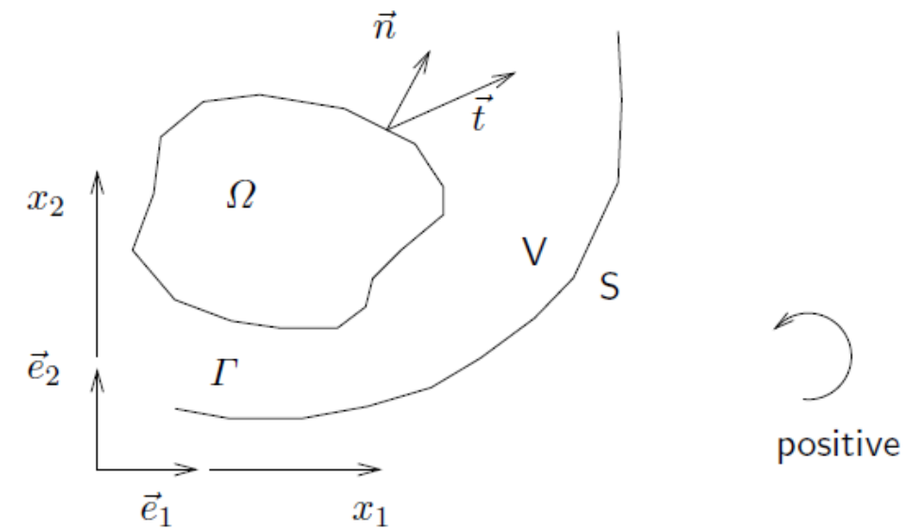

homogeneous hyper-elastic

$$\sigma_{mn} = \frac{\partial W}{\partial \varepsilon_{mn}}$$

linear strain

$$\varepsilon_{mn} = \tfrac{1}{2}(u_{m,n} + u_{n,m})$$

equilibrium equations

$$\sigma_{ij,j} = 0$$

$$J_k = \int_\Omega \left\{ \tfrac{1}{2}\sigma_{mn}(u_{m,nk} + u_{n,mk}) - \sigma_{ij} u_{i,kj} \right\} d\Omega =$$

$$\int_\Omega \left(\sigma_{mn} u_{m,nk} - \sigma_{ij} u_{i,kj} \right) d\Omega = 0$$

symmetry $\sigma_{mn} = \sigma_{nm}$

Path independence of J-integral

J is zero over a closed path

$$0 = J_{ABCDA} = J_{AB} + J_{BC} + J_{CD} + J_{DA}$$

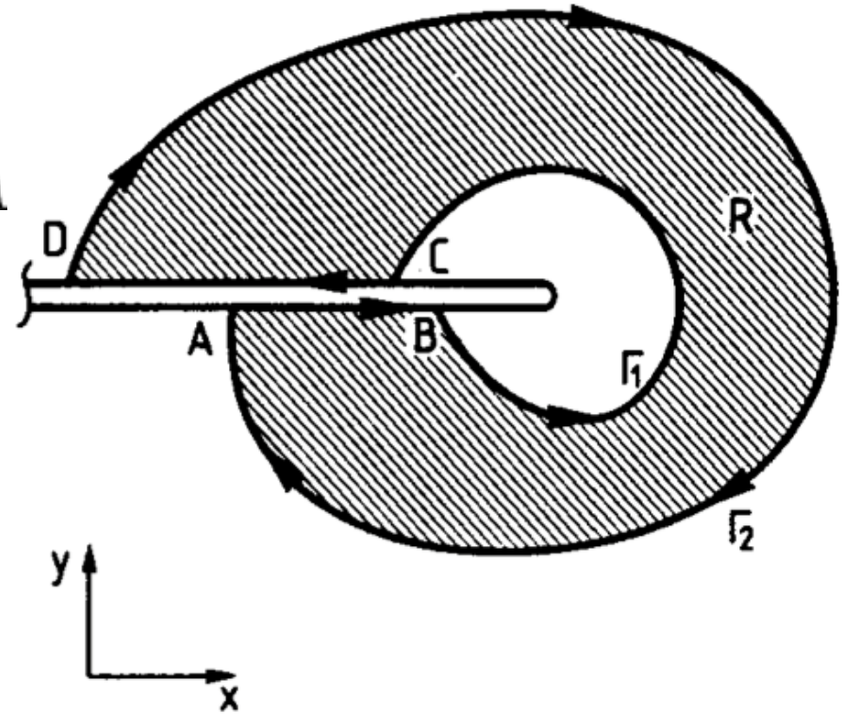

$$\boxed{J = \int_{\Gamma} \left(W dx_2 - t_i \frac{\partial u_i}{\partial x_1} ds \right)}$$

AB, CD: traction-free crack faces

$t_i = 0, dx_2 = 0$ (crack faces: parallel to x-axis)

$J_{AB} = J_{CD} = 0$

which path BC or AD should be used to compute J?

$J_{BC} + J_{DA} = 0$ → $\boxed{J_{BC} = J_{AD}}$

5.3. 2. Relation between J and G (energy release property of J)

Energy release rate of J integral: Assumptions

1. Homogeneous body
2. Linear or non-linear elastic solid
3. No inertia, or body forces; no initial stresses
4. No thermal loading
5. 2-D stress and deformation field
6. Plane stress or plane strain
7. Mode I loading
8. Stress free crack

Energy release rate of J-integral

$$\Pi = \int_{A'} W dA - \int_{\Gamma} t_i u_i ds$$

$$\frac{d\Pi}{da} = \int_{A'} \frac{dW}{da} dA - \int_{\Gamma} t_i \frac{du_i}{da} ds$$

Self-similar crack growth

crack grows, coord. axis move

$$\frac{d}{da} = \frac{\partial}{\partial a} + \frac{\partial}{\partial x}\frac{\partial x}{\partial a}, \quad \frac{\partial x}{\partial a} = -1$$

$$\frac{d}{da} = \frac{\partial}{\partial a} - \frac{\partial}{\partial x}$$

$$\frac{d\Pi}{da} = \int_{A'} \left(\frac{\partial W}{\partial a} - \frac{\partial W}{\partial x} \right) dA - \int_{\Gamma} t_i \left(\frac{\partial u_i}{\partial a} - \frac{\partial u_i}{\partial x} \right) ds$$

$$\frac{\partial W}{\partial a} = \frac{\partial W}{\partial \epsilon_{ij}} \frac{\partial \epsilon_{ij}}{\partial a}$$

$$\frac{\partial W}{\partial \epsilon_{ij}} = \sigma_{ij}$$

$$\frac{\partial \epsilon_{ij}}{\partial a} = \frac{1}{2} \frac{\partial}{\partial a} \left(\frac{\partial u_i}{\partial x_j} + \frac{\partial u_j}{\partial x_i} \right)$$

nonlinear elastic

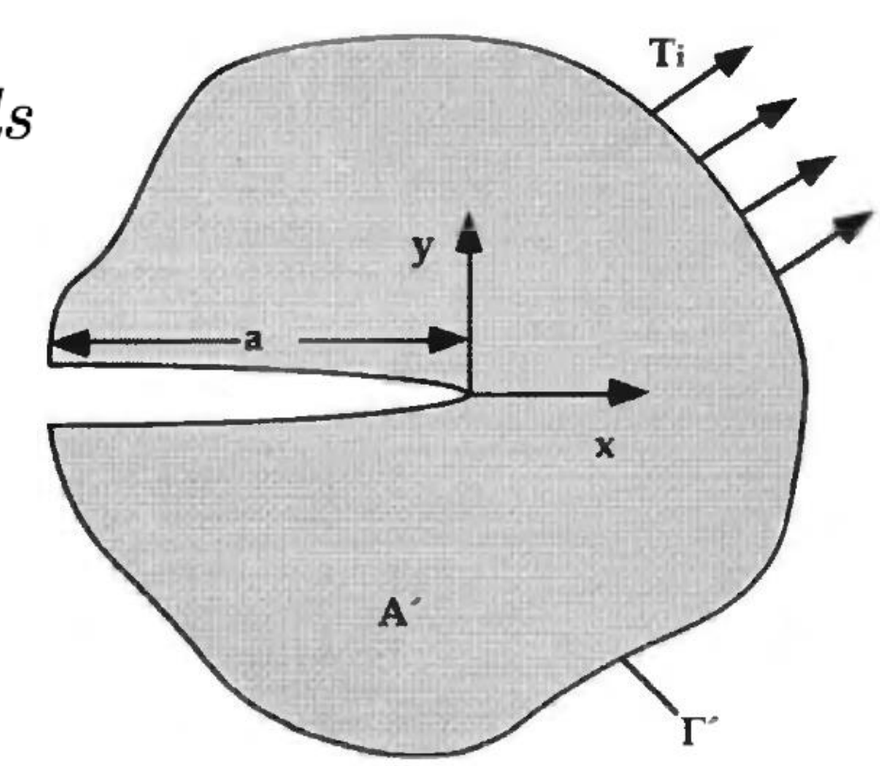

J-integral

$$\mathbf{A} : \mathbf{B} = 0$$

symmetric skew-symmetric

$$\frac{\partial W}{\partial a} = \sigma_{ij} \frac{1}{2} \frac{\partial}{\partial a} \left(\frac{\partial u_i}{\partial x_j} + \frac{\partial u_j}{\partial x_i} \right)$$

$$\frac{\partial W}{\partial a} = \sigma_{ij} \frac{\partial}{\partial a} \frac{\partial u_i}{\partial x_j} = \sigma_{ij} \frac{\partial}{\partial x_j} \frac{\partial u_i}{\partial a}$$

$$\int_{A'} \sigma_{ij} \frac{\partial}{\partial x_j} \frac{\partial u_i}{\partial a} dA = \int_{\Gamma} \sigma_{ij} n_j \frac{\partial u_i}{\partial a} ds$$

$$\boxed{\int_{A'} \frac{\partial W}{\partial a} dA = \int_{\Gamma} t_i \frac{\partial u_i}{\partial a} ds}$$

$$\sigma_{ij,j} = 0$$

Gauss theorem

$$\frac{d\Pi}{da} = -\int_{A'} \frac{\partial W}{\partial x} dA + \int_{\Gamma} t_i \frac{\partial u_i}{\partial x} ds$$

J

$$-\frac{d\Pi}{da} = \int_{\Gamma} \left(W dy - t_i \frac{\partial u_i}{\partial x} ds \right)$$

Gauss theorem, $n_x ds = dy$

J-integral is equivalent to the energy release rate for a nonlinear elastic material under quasi-static condition.

Generalization of J integral

- Dynamic loading
- Surface tractions on crack surfaces
- Body force
- Initial strains (e.g. thermal loading)
- Initial stress from pore pressures

cf. Saouma 13.11 & 13.12 for details

5.3. 3. Relation between J and K

J-K relationship

$$G = \frac{K_I^2}{E'} + \frac{K_{II}^2}{E'} + \frac{K_{III}^2}{2\mu}$$

By idealizing plastic deformation as nonlinear elastic, Rice was able to generalize the energy release rate to nonlinear materials.

$$-\frac{d\Pi}{da} = \int_\Gamma \left(W dy - t_i \frac{\partial u_i}{\partial x} ds \right)$$

(previous slide)

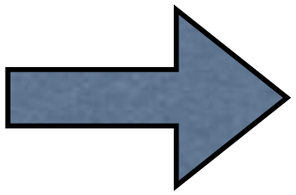

$$J = \frac{K_I^2}{E'} + \frac{K_{II}^2}{E'} + \frac{K_{III}^2}{2\mu}$$

J-integral: very useful in numerical computation of SIFs

J-K relationship

In fact both J1 (J) and J2 are related to SIFs:

$$J_1 = \int_\Gamma \left(w dy - \mathbf{t} \frac{\partial \mathbf{u}}{\partial x} d\Gamma \right)$$

$$J_2 = \int_\Gamma \left(-w dx - \mathbf{t} \frac{\partial \mathbf{u}}{\partial y} d\Gamma \right)$$

J1 & J2: crack advance for (θ = 0, 90) degrees

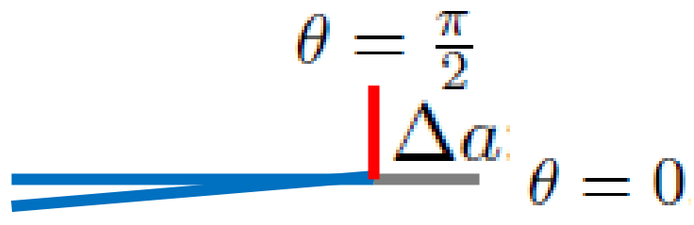

$$J = J_1 - iJ_2$$ Hellen and Blackburn (1975)

$$= \frac{(1+\nu)(1+\kappa)}{4E}(K_I^2 + K_{II}^2 + 2iK_I K_{II})$$

$$J_1 = \frac{K_I^2 + K_{II}^2}{E'}$$

$$J_2 = \frac{-2K_I K_{II}}{E'}$$

$$E' = \begin{cases} E & \text{plane strain} \\ \frac{E}{1-\nu^2} & \text{plane stress} \end{cases}$$

Note that if $K_I = a, K_{II} = b$ is a solution the general solution is:
$K_I = \pm a, K_{II} = \pm b$ and $K_I = \pm b, K_{II} = \pm a$

5.3. 4. Energy Release Rate, crack growth and R curves

Nonlinear energy release rate

Goal: Obtain J from P-Δ Curve

$$J = -\frac{\partial \Pi}{\partial A} = -\frac{1}{B}\frac{\partial \Pi}{\partial a}$$

- $\Pi = U_e - W$: Potential energy
- W: External work
- $U_e = \int_V e \, \mathrm{dv}$: Internal energy
- $e(\epsilon_0)$ (or $w(\epsilon_0)$) $= \int_0^{\epsilon_0} \sigma(\epsilon) \mathrm{d}\epsilon$

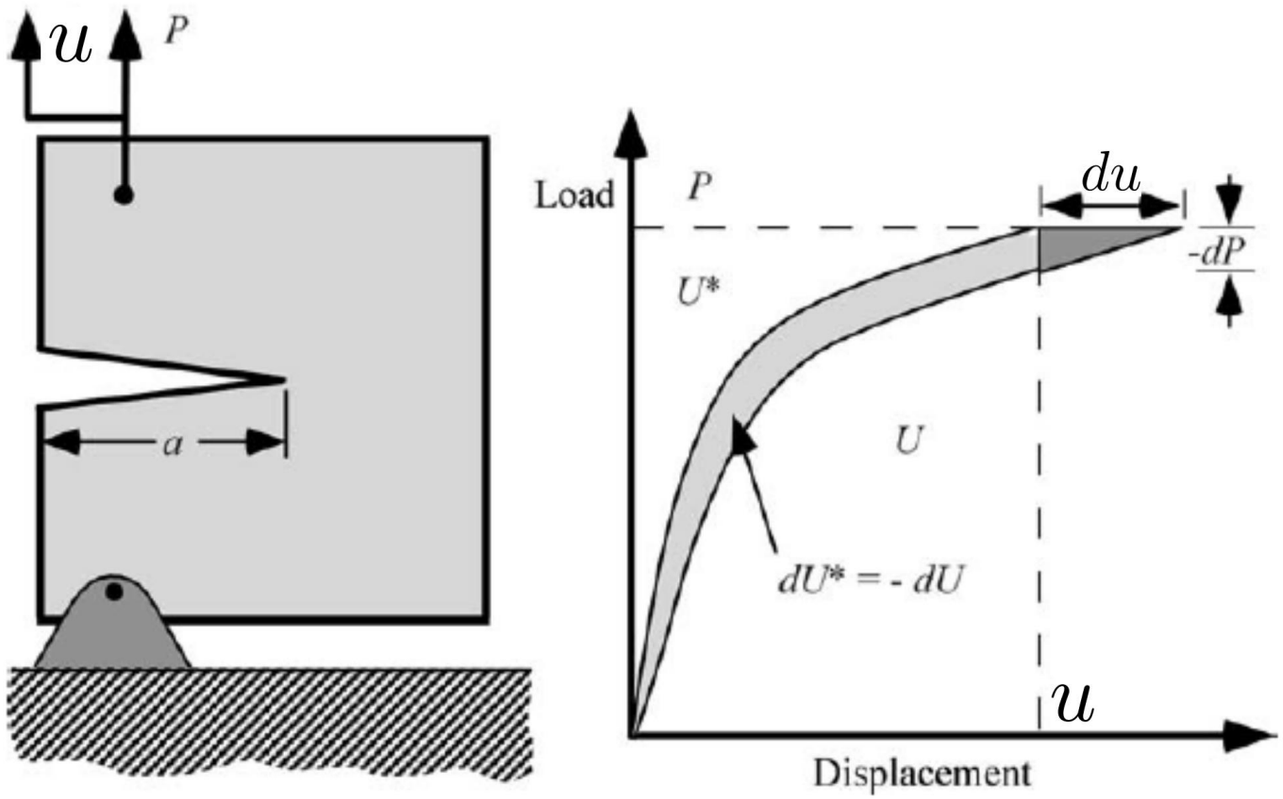

1. Load Control (P fixed, u increases):

$$W = Pu \quad \Rightarrow \quad \Pi = U_e - Pu$$

$$\Pi = -U_e^* \quad \text{load control}$$

$$U_e^* = \int_0^P u \mathrm{d}P \text{ (complimentary strain energy)}$$

$$J = \frac{1}{B}\left(\frac{\partial U_e^*}{\partial a}\right)_P \text{ (load control)}$$

Note $U_e = U_e^* = \frac{1}{2}Pu$ for linear solid

2. Displacement Control (u fixed, P decreases):

$$W = 0 \quad \Rightarrow \quad \Pi = U_e$$

$$\Pi = U_e \quad \text{displacement control}$$

$$J = -\frac{1}{B}\left(\frac{\partial U_e}{\partial a}\right)_u \text{ (displacement control)}$$

Nonlinear energy release rate

Goal: Obtain J from P-Δ Curve

$$\left.\begin{aligned} U_{e1} &= A_1 + A_2 \\ U_{e2} &= A_1 + A_3 \\ W_{12} &= A_3 + A_4 \end{aligned}\right\} \quad \Rightarrow$$

$$\Delta\Pi = \{U_{e2} - U_{e1}\} - W_{12} = \left(A_2 + A_4\right)$$

$$J \approx -\frac{1}{B}\frac{\Delta\Pi}{\Delta a} = \frac{1}{Ba} \text{ (shaded area)}$$

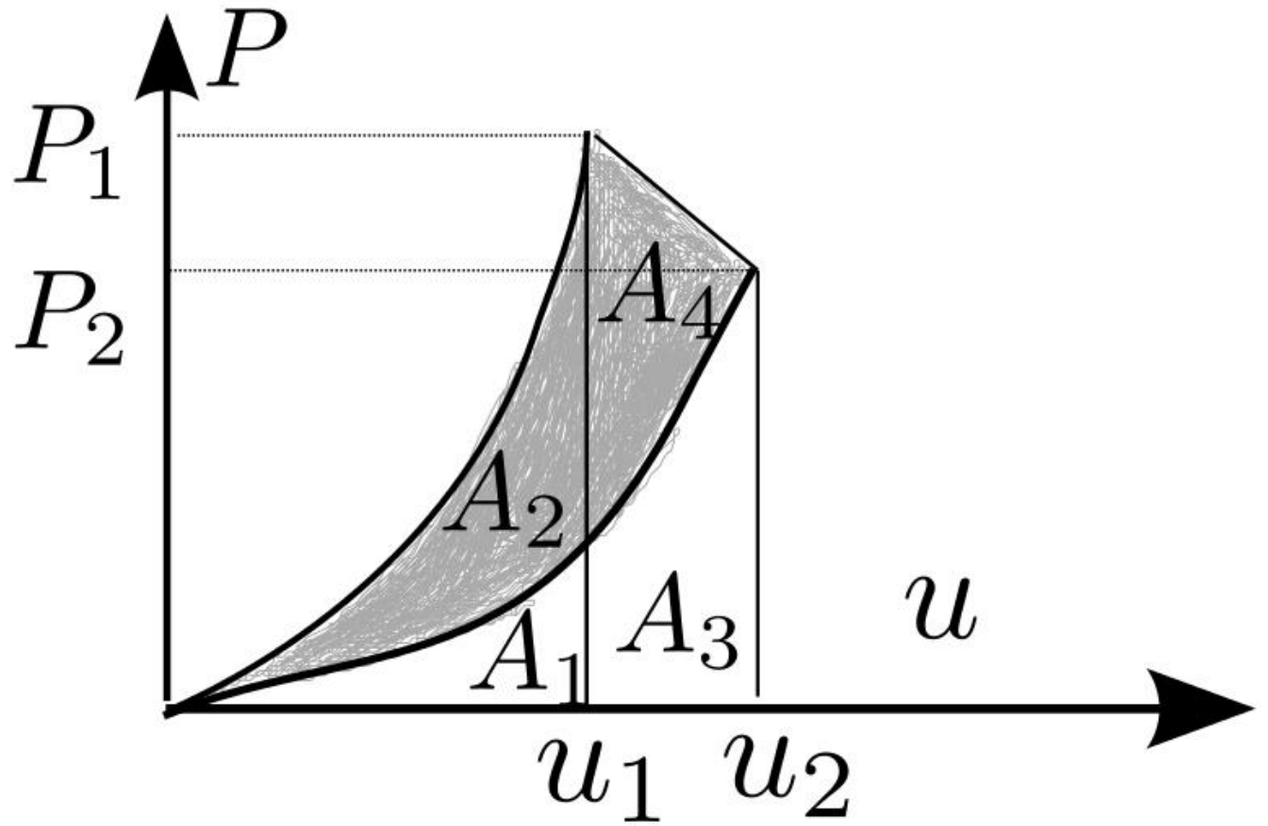

Similar to G!

Nonlinear energy release rate

Goal: Analytical equation for J

$$
\begin{aligned}
J &= -\lim_{a\to 0}\frac{\Delta\Pi}{B\Delta a} \\
&= -\lim_{a\to 0}\frac{U_{e2}-U_{e1}-W_{12}}{B\Delta a} \\
&= -\lim_{a\to 0}\frac{1}{B}\left\{\frac{U_{e2}-U_{e1}}{a_2-a_1}-\frac{P_1+P_2}{2}\frac{u_2-u_1}{a_2-a_1}\right\} \\
&= \frac{1}{B}\left\{-\frac{\mathrm{d}U_e}{\mathrm{d}a}+P\frac{\mathrm{d}u}{\mathrm{d}a}\right\}
\end{aligned}
$$

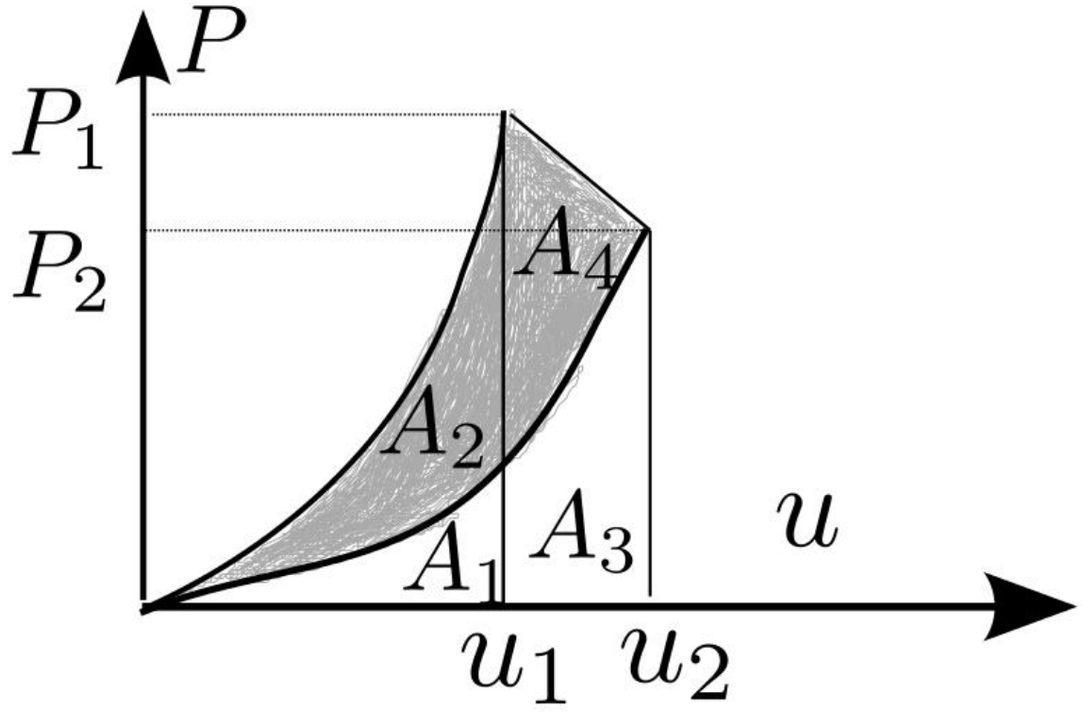

$$
J = \frac{1}{B}\left\{-\frac{\mathrm{d}U_e}{\mathrm{d}a}+P\frac{\mathrm{d}u}{\mathrm{d}a}\right\} = \frac{1}{B}\left\{-\frac{\mathrm{d}U_e}{\mathrm{d}u}+P\right\}\frac{\mathrm{d}u}{\mathrm{d}a}
$$

- Compare this equation with $G = -\frac{u^2}{2B}\frac{\mathrm{d}K}{\mathrm{d}a} = \frac{P^2}{2B}\frac{\mathrm{d}C}{\mathrm{d}a}$
- For linear case $U_e = \frac{1}{2}K u^2$ and $P = K u$. Show that equation for J agrees for the two for G

Nonlinear energy release rate

Goal: Experimental evaluation of J

- P-Δ curves for different crack lengths a ➡ J as a function of Δ
- Rice proposes a method to obtain J with <u>only one test</u> for certain geometries

cf. Anderson 3.2.5 for details

Landes and Begley, ASTM 1972

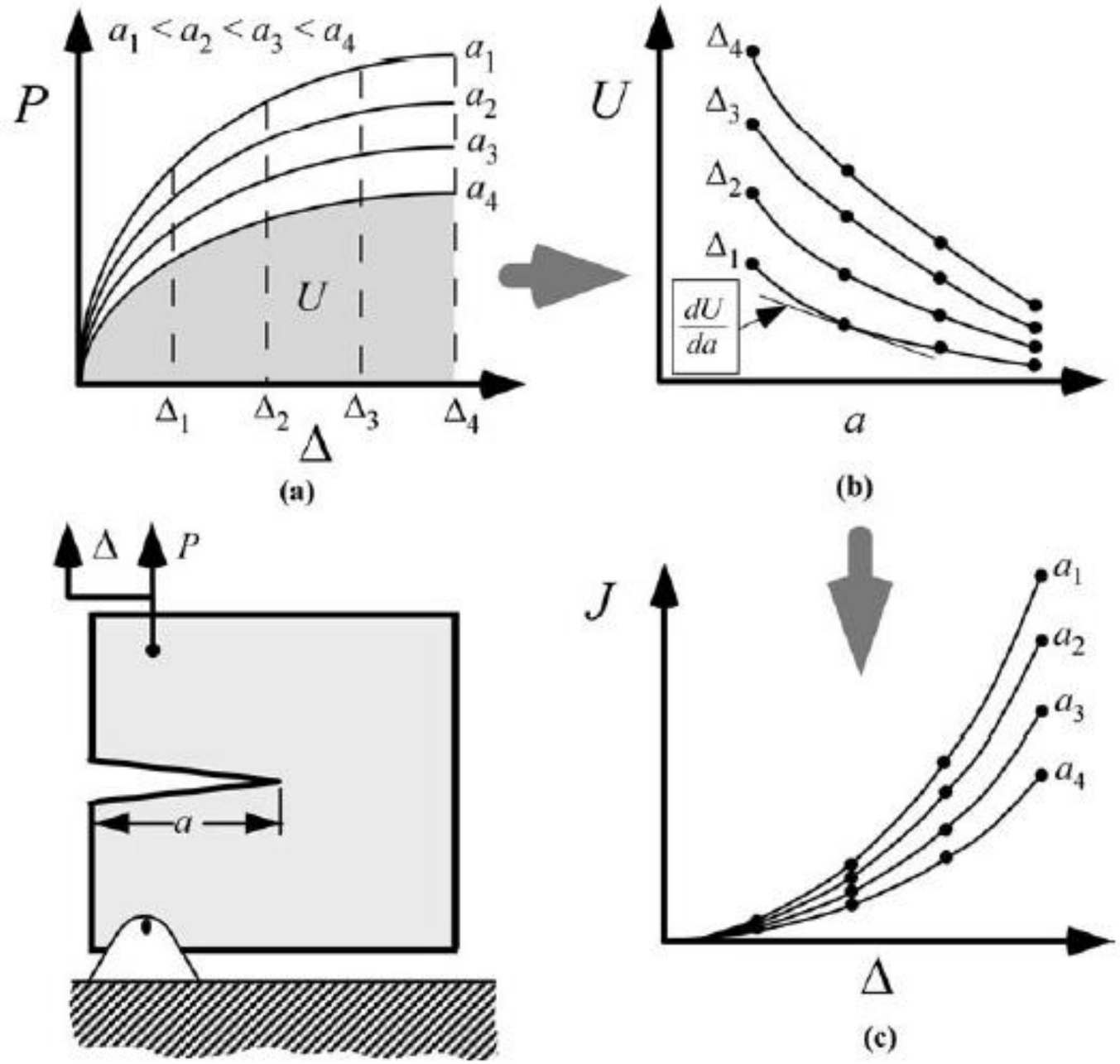

Crack growth resistance curve

- A: R curve is nearly vertical:
  - small amount of apparent crack growth from blunting
- J_{I_c} measure of ductile fracture toughness
- Tearing modulus $T_R = \frac{E}{\sigma_0^2}\frac{\mathrm{d}J_R}{\mathrm{d}a}$ is a measure of crack <u>stability</u>

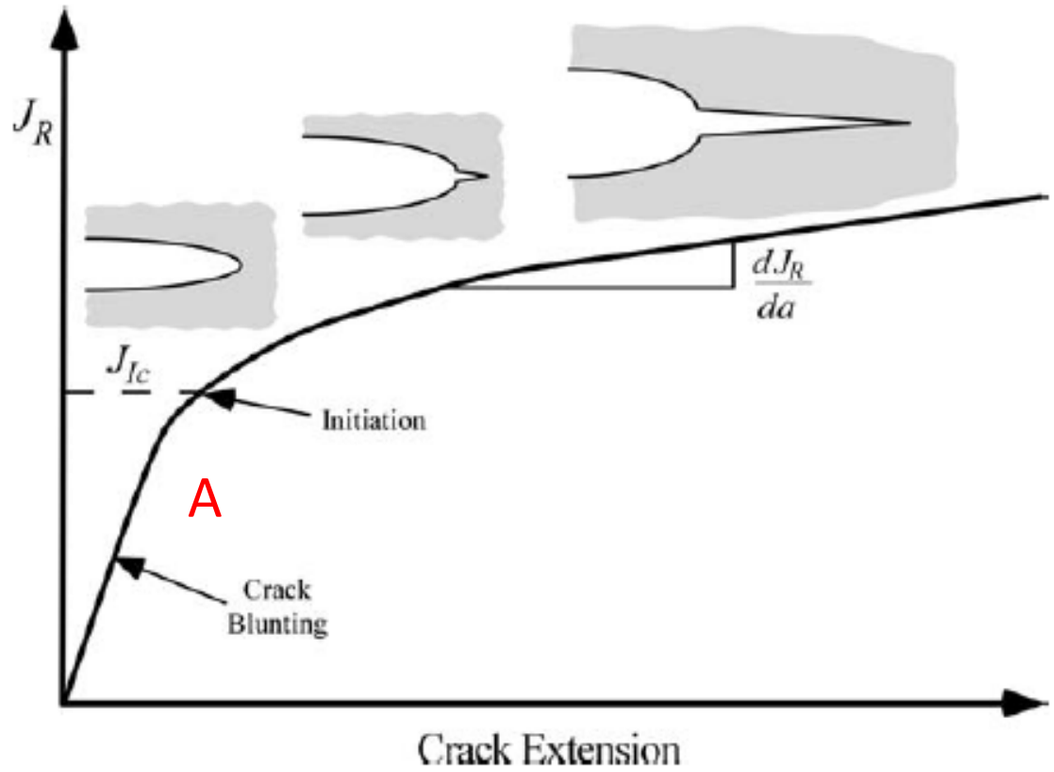

If the crack propagates longer we even observe a flag R value

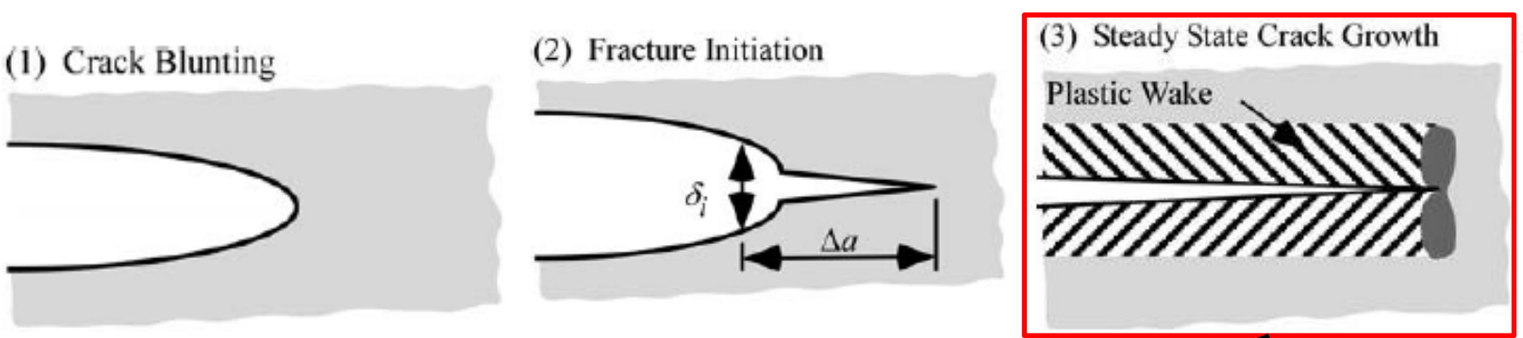

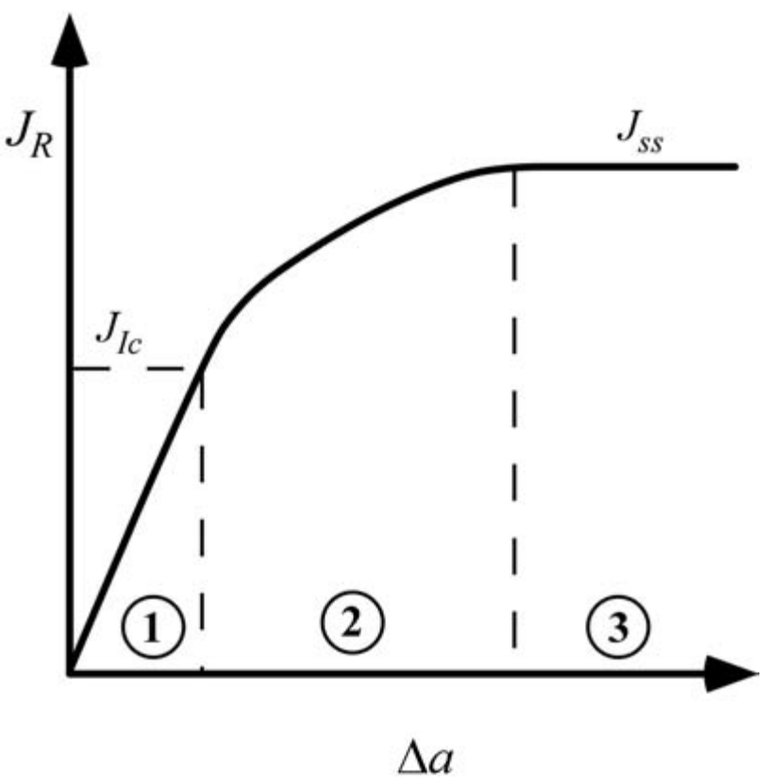

Rare in experiments because it requires large geometries!

Crack growth and stability

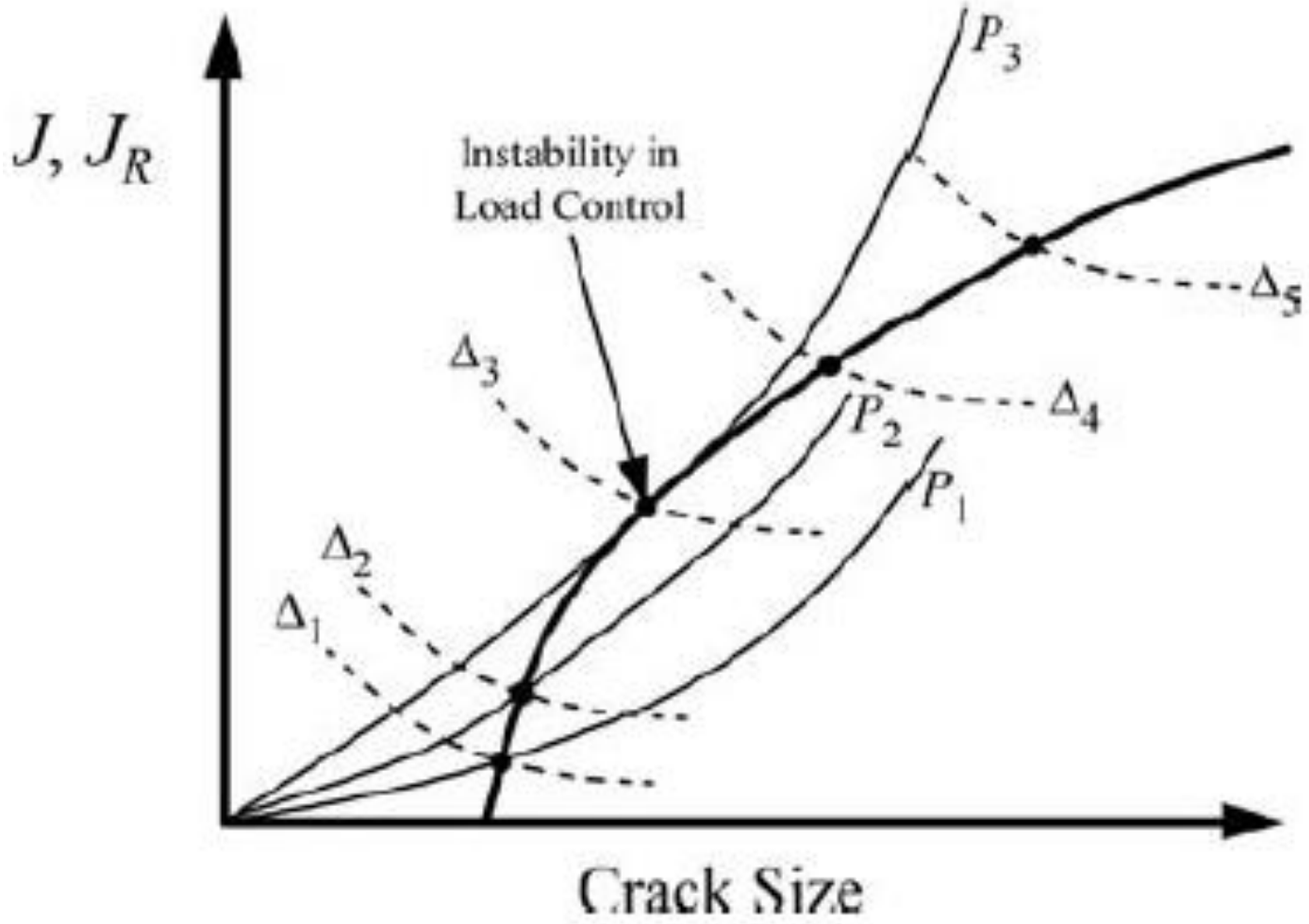

- The J_R and J are similar to R and G curves for LEFM:
  - Crack growth can happen when $J = J_R$
  - Crack growth is unstable when $\frac{dJ}{da} > \frac{dJ_R}{da}$

5.3. 7. Fracture mechanics versus material (plastic strength

Governing fracture mechanism and fracture toughness

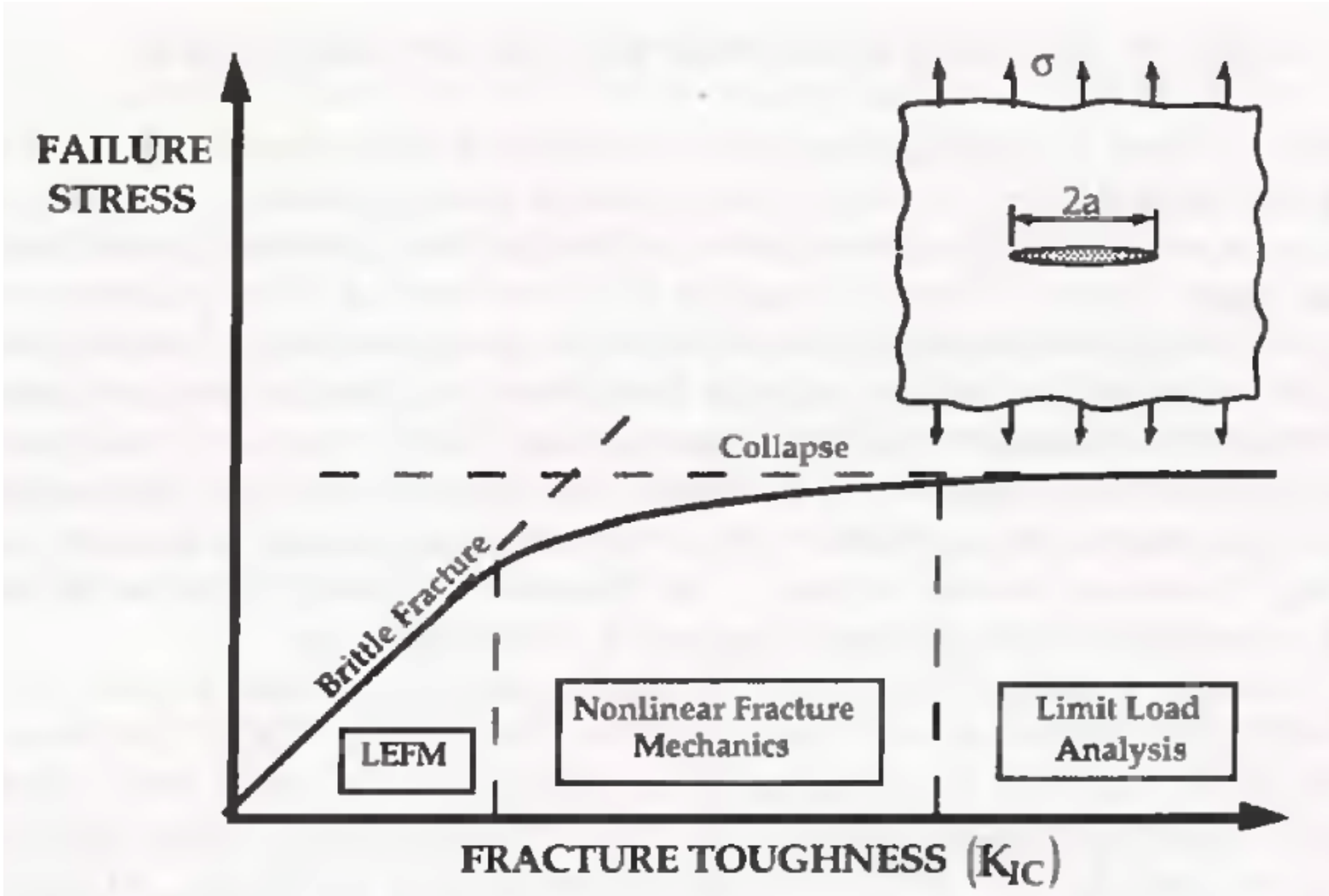

Fracture vs. Plastic collapse

$$\sigma_{\text{net}} = \frac{P}{W-a} = \sigma \frac{W}{W-a}$$

(cracked section)

$$\sigma = \frac{P}{W}$$

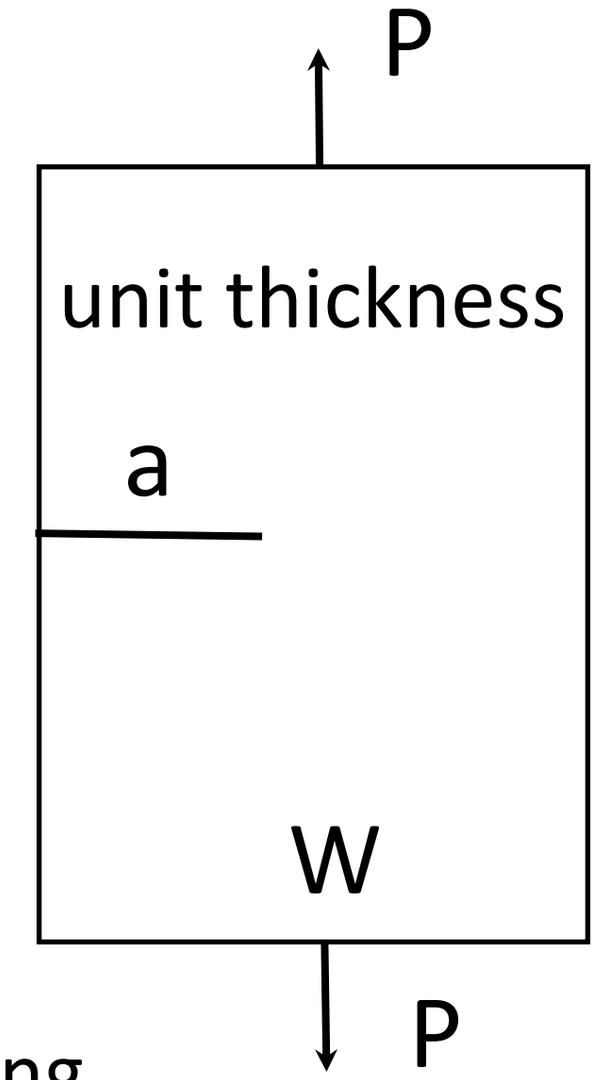

Yield: $\sigma \frac{W}{W-a} = \sigma_{ys} \longrightarrow \sigma = \sigma_{ys}\left(1 - \frac{a}{W}\right)$

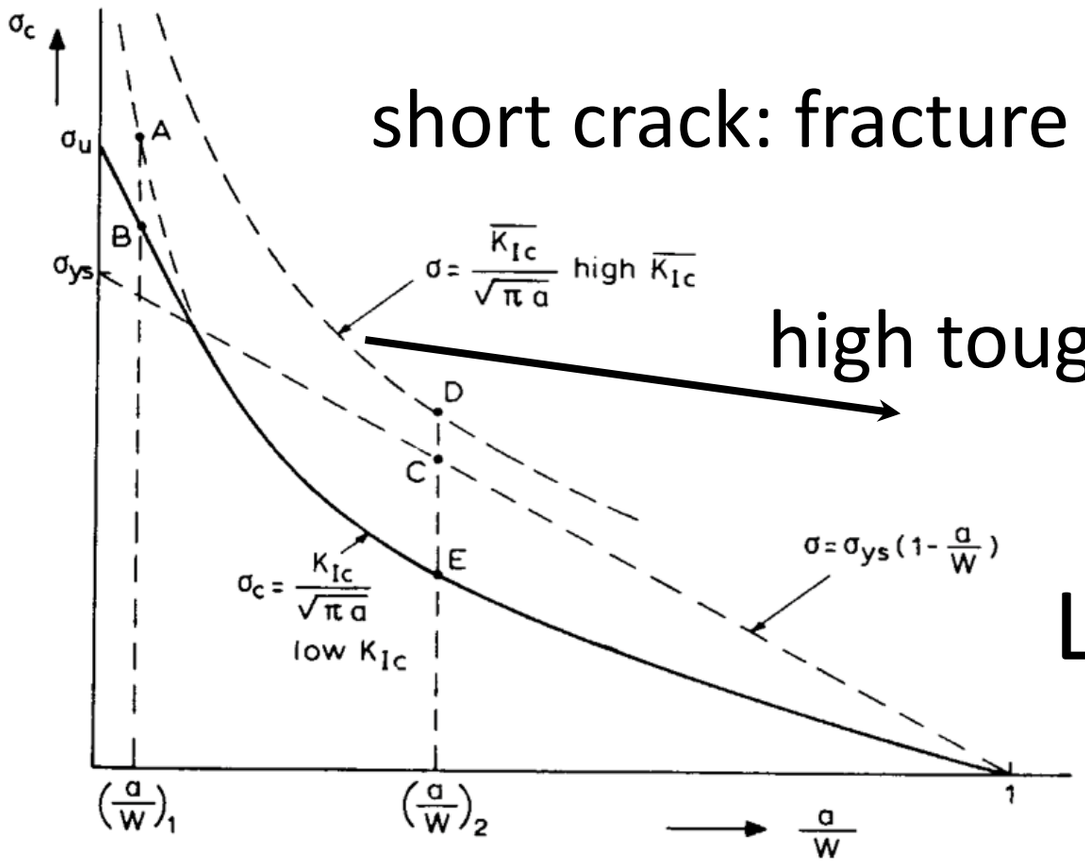

short crack: fracture by plastic collapse!!!

high toughness materials:yielding before fracture

LEFM applies when $\sigma_c \leq 0.66\sigma_{ys}$

Example

Example 4.11 Estimate the failure load under uniaxial tension for a centre-cracked panel of aluminium alloy of width W=500 mm, and thickness B=4 mm, for the following values of crack length $2a$ = 20 mm and $2a$ = 100 mm. Yield stress σ_y =350 MPa and fracture toughness K_{Ic}=70 MPa $\sqrt{m}$

Solution There are two possible failure modes: plastic collapse and brittle fracture. We will assess the load level required for each mode to prevail.

(i) $2a$ = 20 mm.

Plastic collapse load $F_{pc} = \sigma_{ys} \cdot (W - 2a) \cdot B = 672$ kN

Fracture load $F_c = \sigma_c \cdot W \cdot B$ where $\sigma_c = \dfrac{K_{IC}}{\sqrt{\pi a \sec(\pi a / W)}} = 394.6$ MPa

thus F_c = 790 kN.

The actual failure load is the smaller of the above results, 672 kN.

(ii) $2a$ = 100 mm.

Plastic collapse load $F_{pc} = \sigma_{ys} \cdot (W - 2a) \cdot B = 560$ kN

Fracture load $F_c = \sigma_c \cdot W \cdot B$ where $\sigma_c = \dfrac{K_{IC}}{\sqrt{\pi a \sec(\pi a / W)}} = 172.2$ MPa

thus F_c = 334.57 kN.

The actual failure load is the smaller of the above results, 334.6 kN.

5.3. 5. Plastic crack tip fields; Hutchinson, Rice and Rosengren (HRR) solution

Ramberg–Osgood model

$$\frac{\varepsilon}{\varepsilon_{y0}} = \frac{\sigma}{\sigma_{y0}} + \alpha \left(\frac{\sigma}{\sigma_{y0}} \right)^n$$

Compare with $\epsilon = \epsilon^e + \epsilon^p$

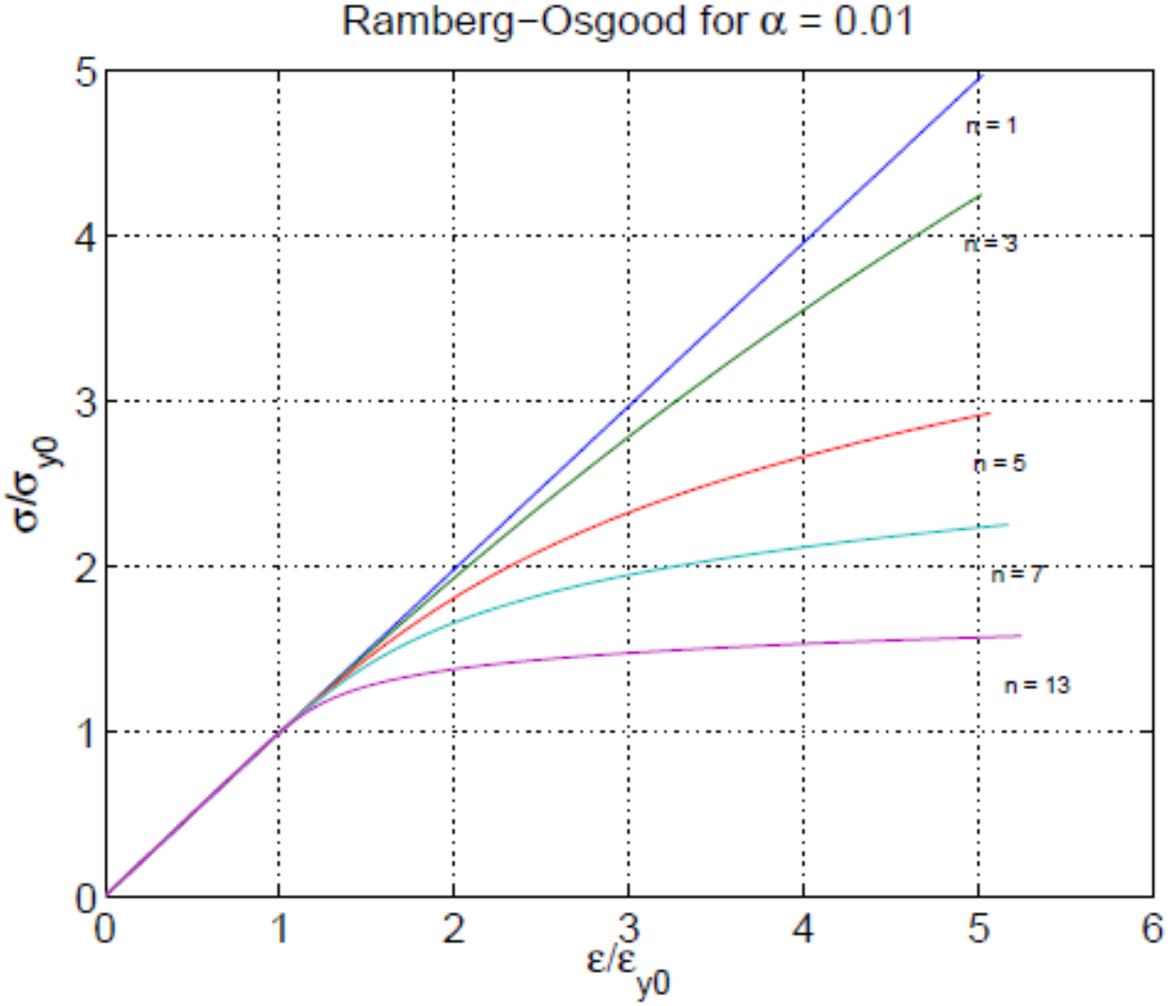

- Elastic model:

Unlike plasticity unloading in on the same line

- Higher n closer to elastic perfectly plastic

Hutchinson, Rice and Rosengren(HRR) solution

- Near crack tip “plastic” strains dominate:

$$\frac{\epsilon}{\epsilon_0} = \alpha \left(\frac{\sigma}{\sigma_0} \right)^n \qquad *$$

- Assume the following r dependence for σ and ε

$$\sigma = \frac{c_1}{r^x}$$

$$\varepsilon = \frac{c_2}{r^y}$$

1. Bounded energy:

$$\sigma\varepsilon \propto \frac{1}{r} \Rightarrow x + y = 1$$

2. ε - σ relation ∗

$$y = nx$$

$$\Rightarrow \quad x = \frac{1}{1+n}, \qquad y = \frac{n}{1+n}$$

HRR solution:
Local stress field based on J

- Final form of HRR solution:

$$\sigma_{ij} = \sigma_0 \left(\frac{EJ}{\alpha \sigma_0^2 I_n r} \right)^{\frac{1}{n+1}} \tilde{\sigma}_{ij}(n, \theta)$$

$$\epsilon_{ij} = \frac{\alpha \sigma_0}{E} \left(\frac{EJ}{\alpha \sigma_0^2 I_n r} \right)^{\frac{n}{n+1}} \tilde{\epsilon}_{ij}(n, \theta)$$

J plays the role of K for local σ, ε, u fields

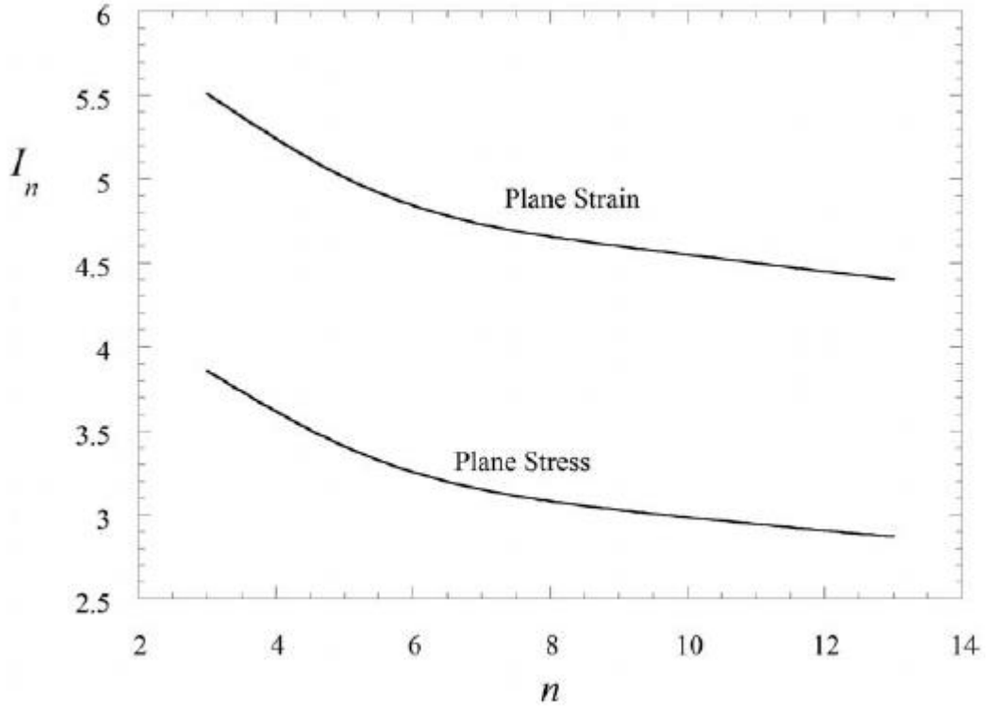

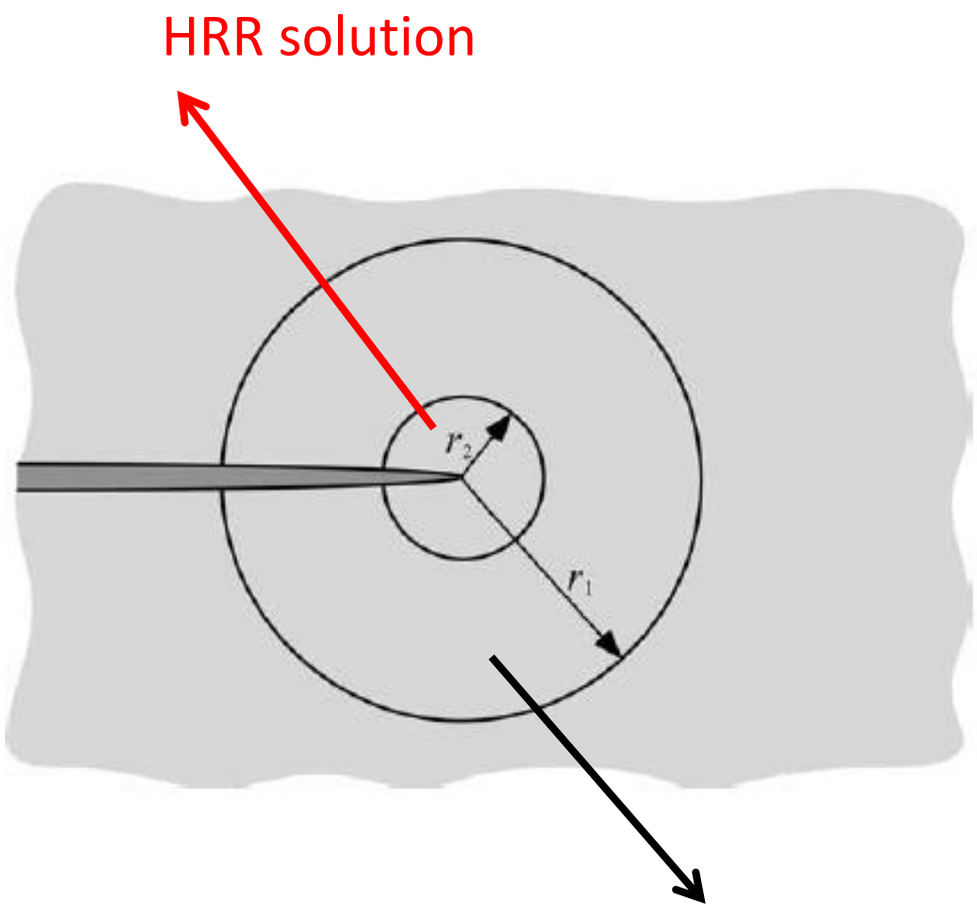

HRR solution:Angular functions

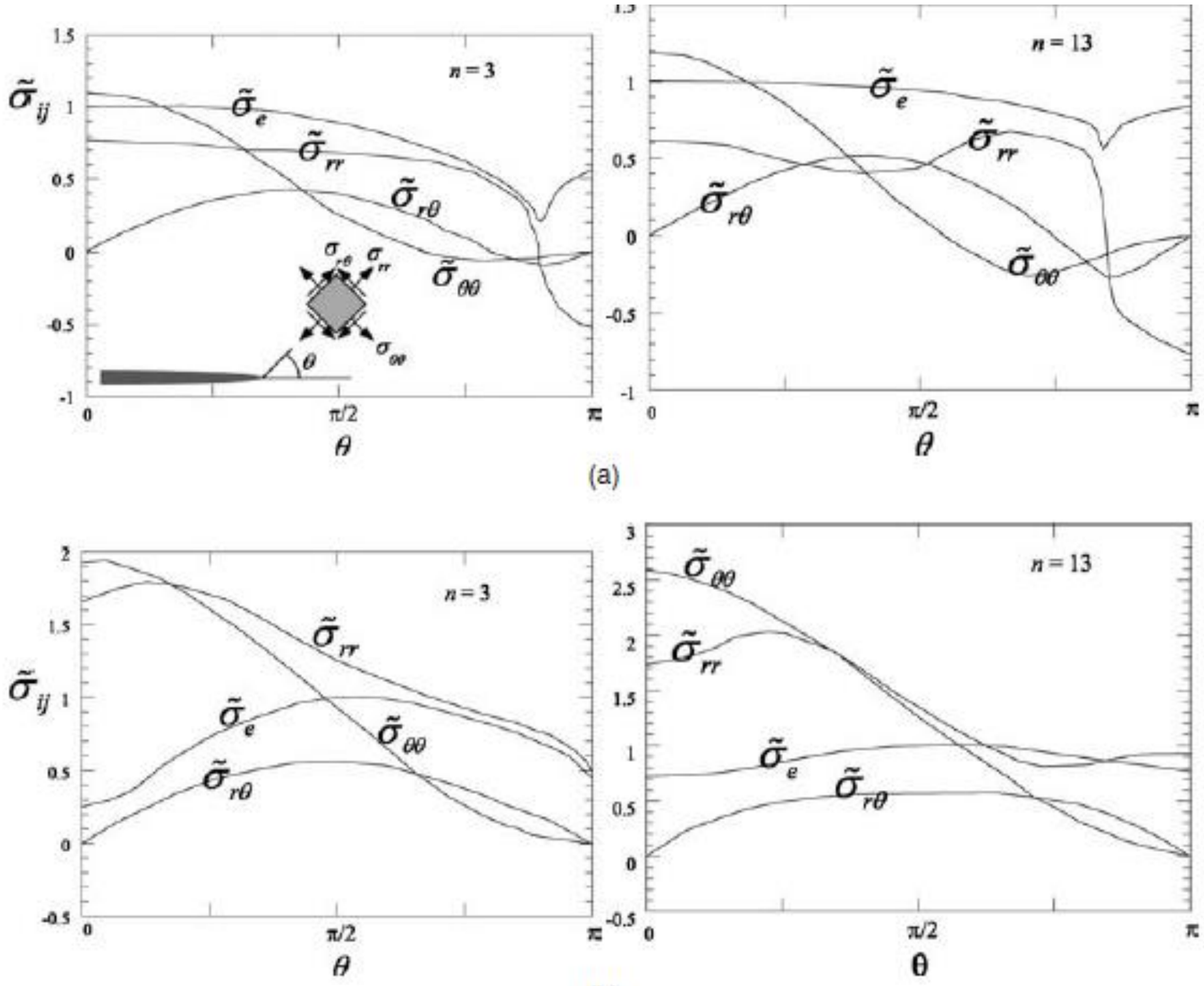

HRR solution:
Stress singularity

$$\sigma_{ij} = \sigma_0 \left(\frac{EJ}{\alpha \sigma_0^2 I_n r} \right)^{\frac{1}{n+1}} \tilde{\sigma}_{ij}(n, \theta)$$

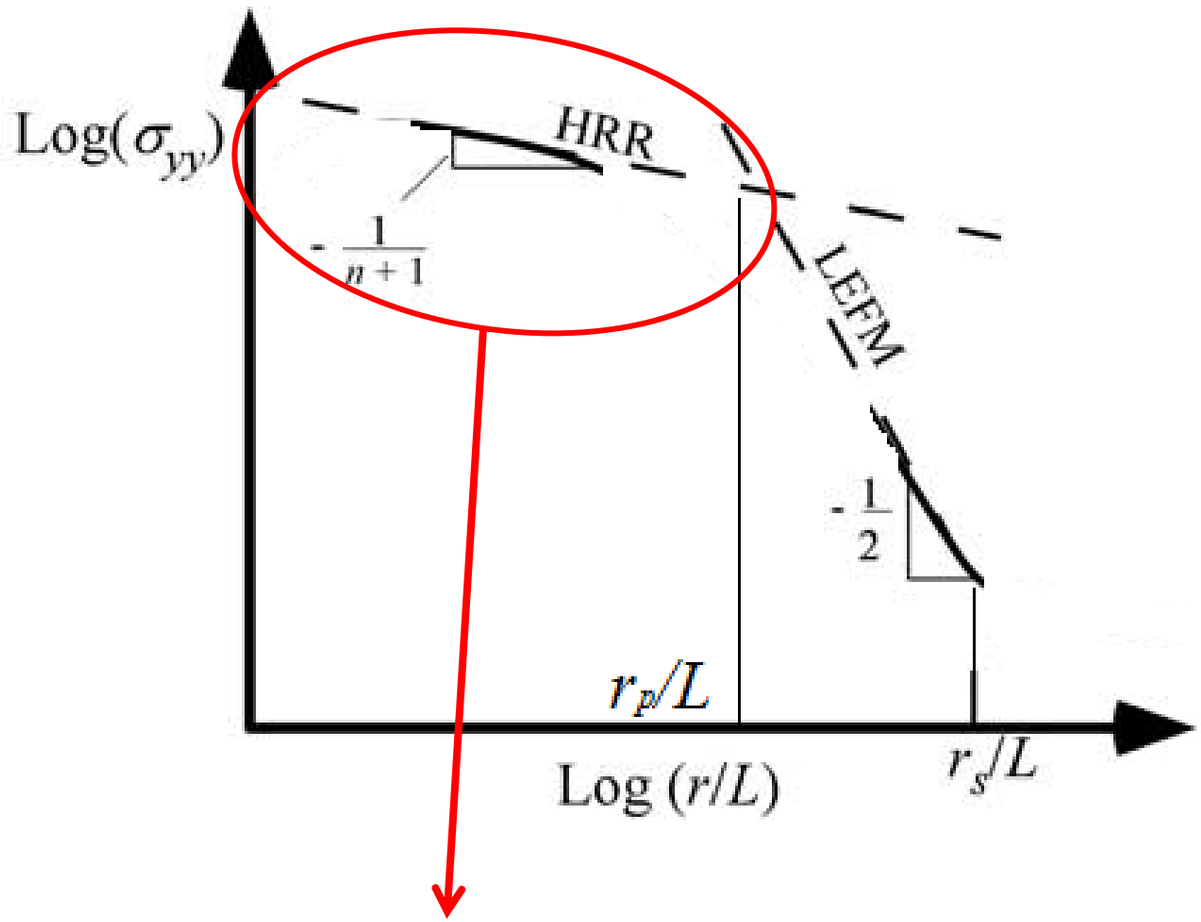

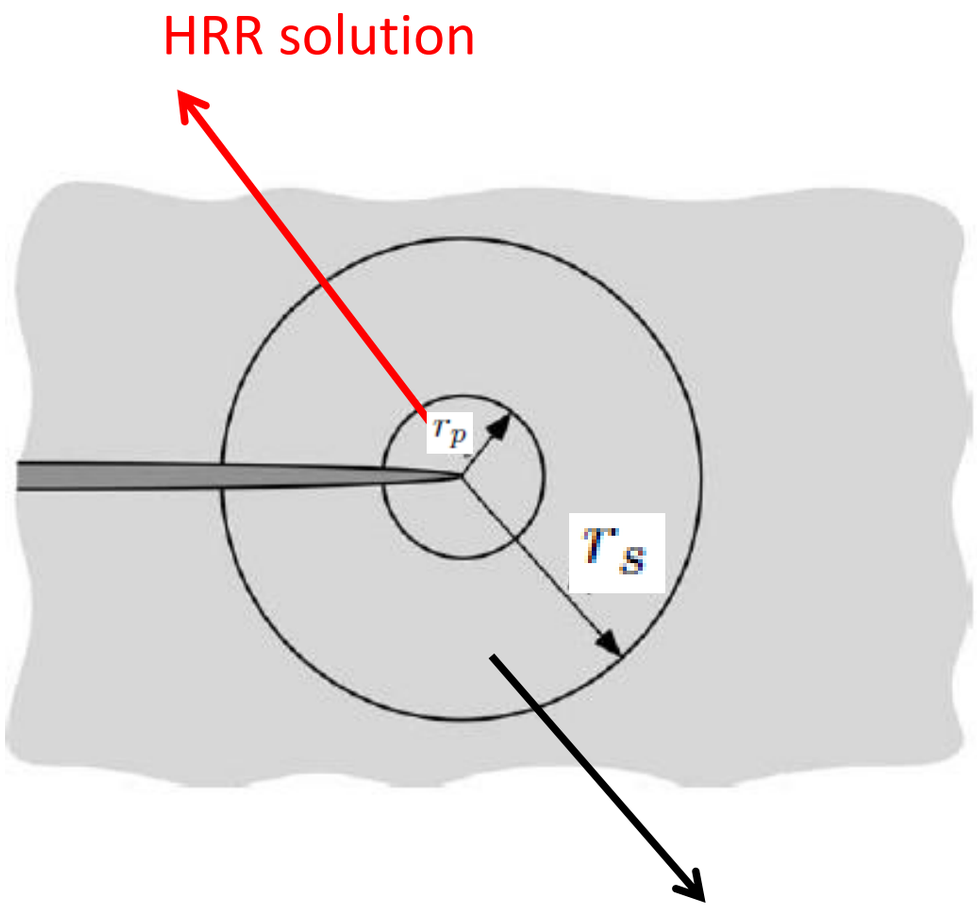

Stress is still singular but with a weaker power of singularity!

5.3. 6. Small scale yielding (SSY) versus large scale yielding (LSY)

Limitations of HRR solution

Limitations of HRR analysis

- Small strain: $\epsilon = \frac{1}{2}\left(\nabla \mathbf{u} + \nabla^{\mathrm{T}}\mathbf{u}\right)$ (accurate for $\epsilon \lesssim 0.1$)
- Small deformation theory (*e.g.*, not using PK stresses, etc)
- Elastic HRR model instead of plastic model
- Crack tip blunting: $\Rightarrow \sigma_{xx} = 0$

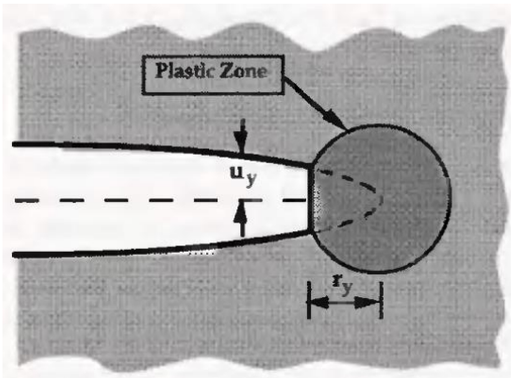

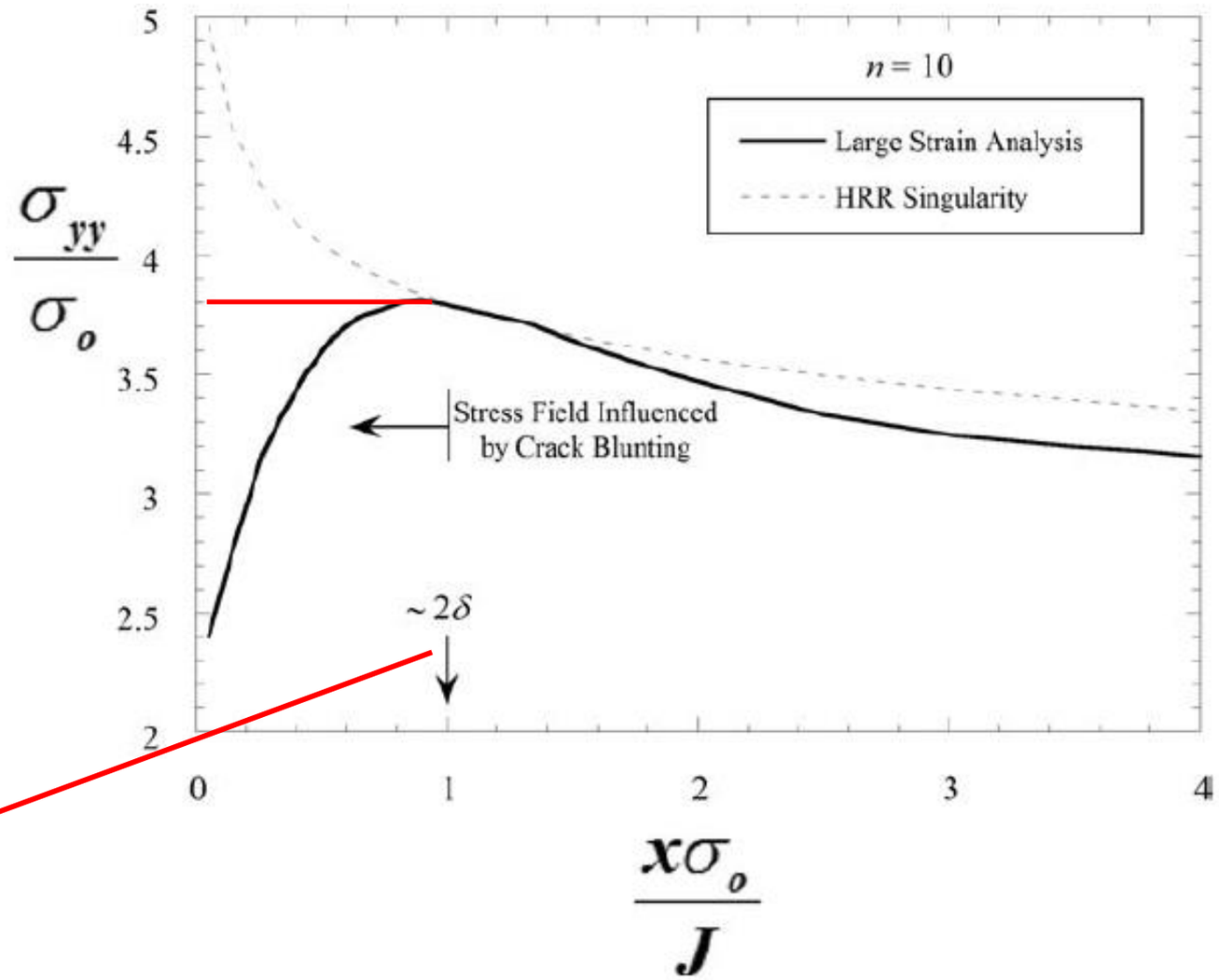

McMeeking and Parks, ASTM STP 668, ASTM 1979

δ: Crack tip opening

$\delta \propto \frac{K^2}{\sigma_y E}$

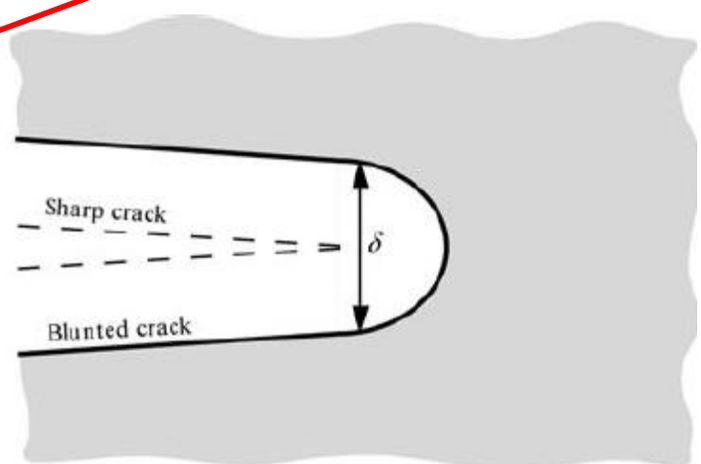

From SSY to LSY

Large strain radius $r_n \propto \delta$ (CTOD): $\delta = \mathcal{O}\left(\frac{K^2}{E\sigma_y}\right)$

plastic radius: $r_p = \mathcal{O}\left(\frac{K^2}{\sigma_y^2}\right)$

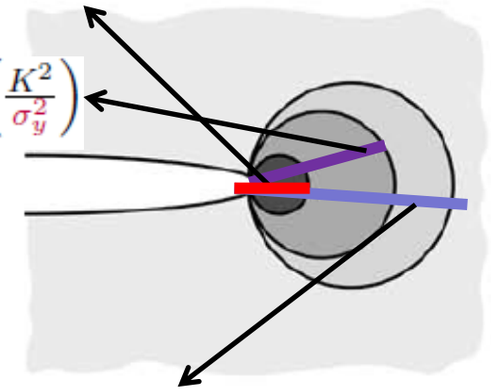

K-dominant radius: $r_s = \mathcal{O}\left(\frac{K^2}{\bar{\sigma}^2}\right)$

$\bar{\sigma}$: applied stress

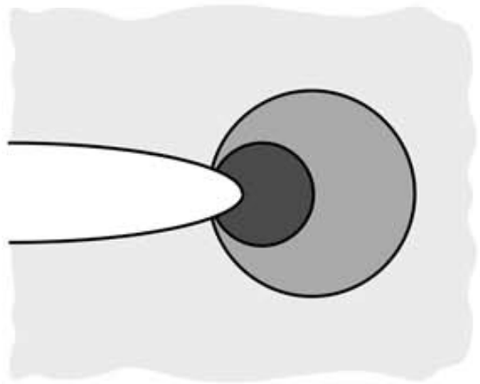

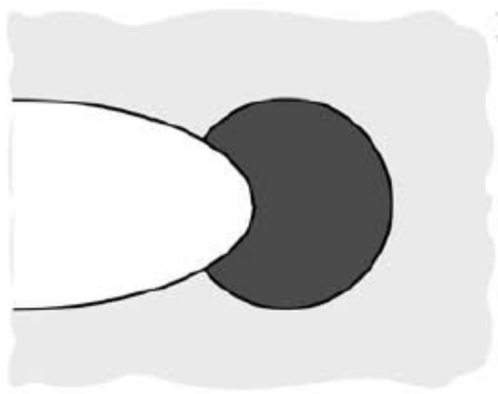

Large Strain Region

J-Dominated Zone

K-Dominated Zone

No Single-Parameter Characterization

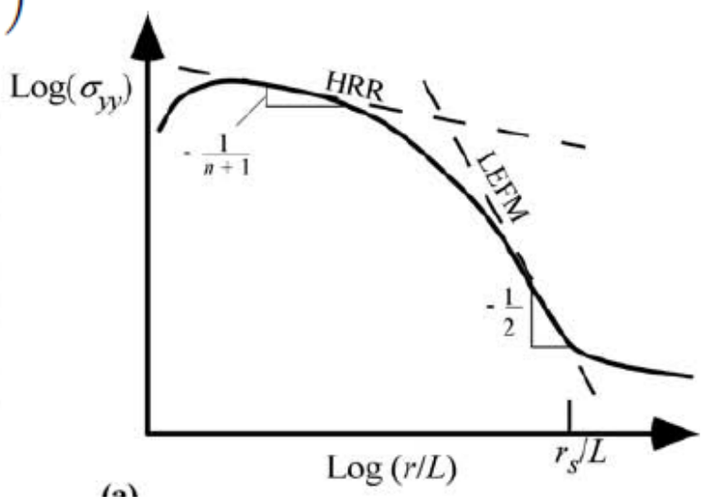

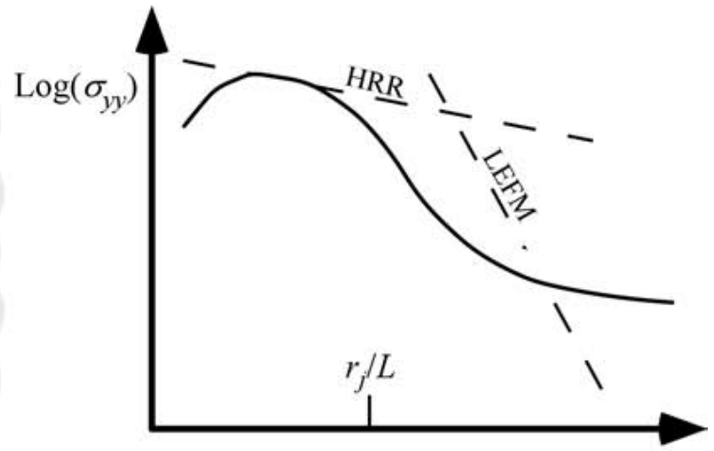

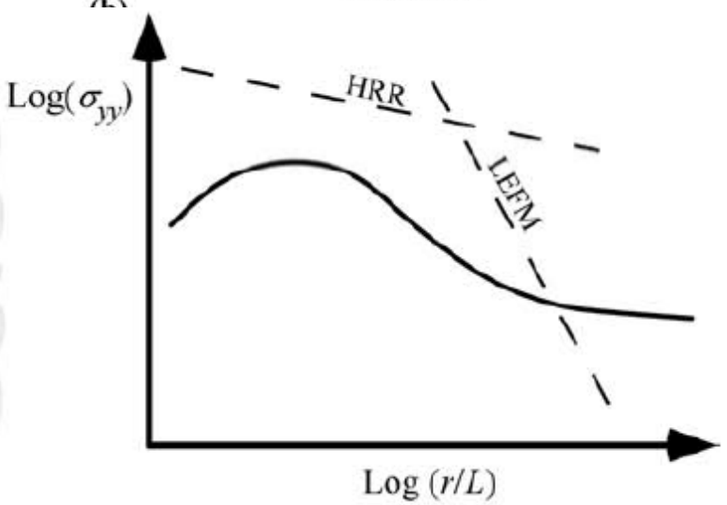

SSY (Small Scale Yielding)

$r_n \ll r_p \ll r_s \quad \Rightarrow$

$$\frac{r_p}{r_s} \propto \left(\frac{\bar{\sigma}}{\sigma_y}\right)^2 \ll 1$$

Elastic plastic condition

$r_n \ll r_p \approx r_s \quad \Rightarrow$

$$\frac{r_n}{r_p} \ll 1, \quad \frac{r_p}{r_s} \propto \left(\frac{\bar{\sigma}}{\sigma_y}\right)^2 \approx 1$$

LSY(Large Scale Yielding)

$r_n \approx r_p$

Note that $\frac{\delta}{r_p} \propto \left(\frac{\sigma_y}{E}\right)$

From SSY to LSY

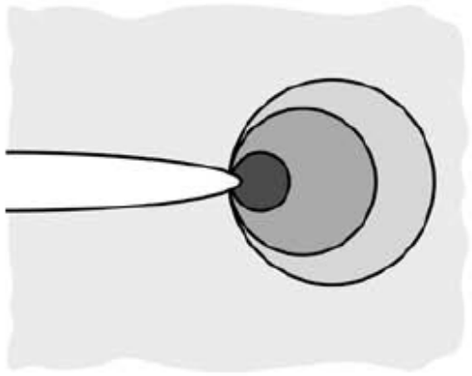

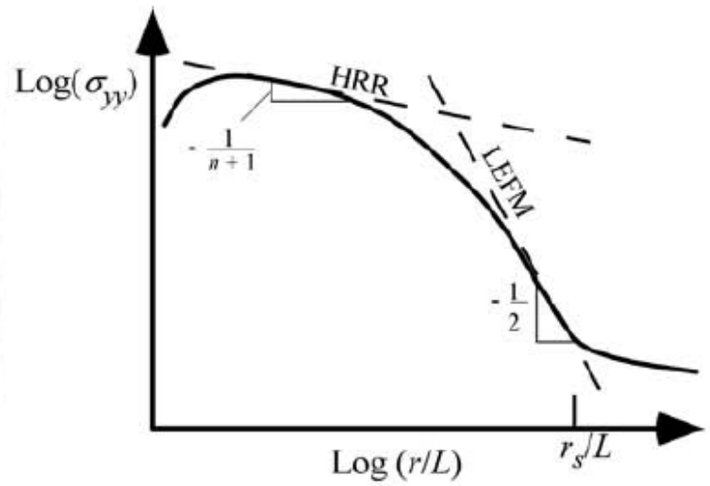

LEFM: SSY satisfied and genera
have Generally have

$$\bar{\sigma} \ll \sigma_y$$

Relevant parameters:
G (energy) K (stress)

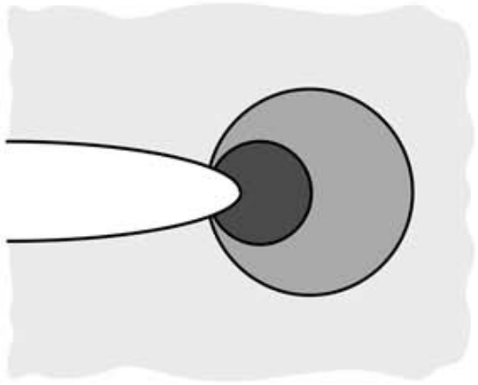

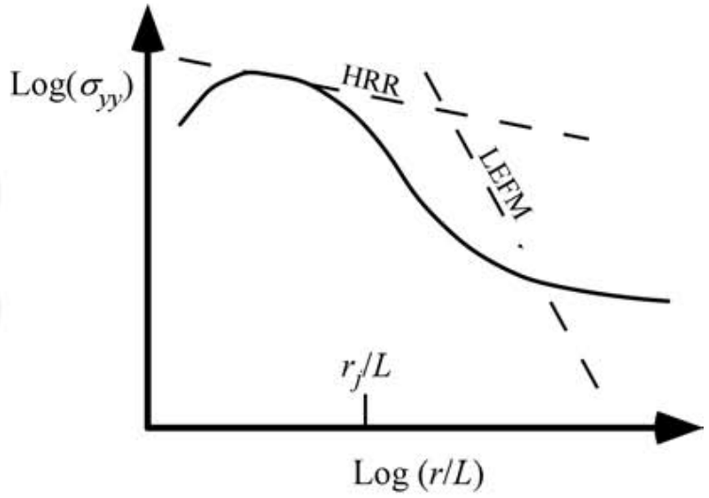

PFM (or NFM): SSY is
gradually violated and

$$\bar{\sigma} \approx \sigma_y$$

Relevant parameters:
J (energy & used for stress)

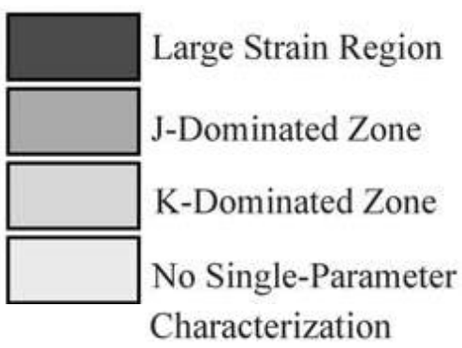

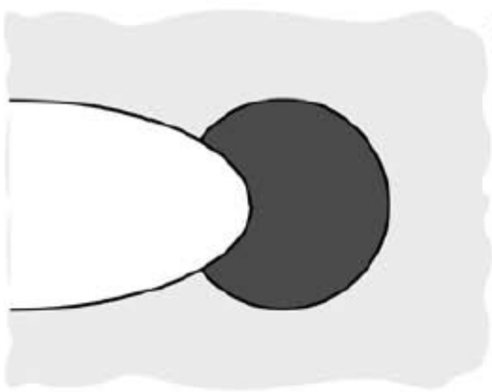

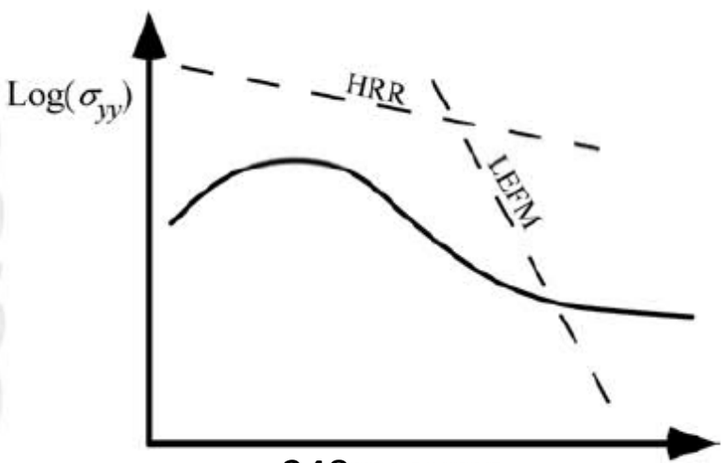

LSY condition:
No single parameter can
characterize fracutre!
J + other parameters (e.g. T
stress, Q-J, etc)

LSY: When a single parameter (G, K, J, CTOD) is not enough?

- Under considerable plastic deformation and crack propagation when unloading and non-proportional zones grow out of J dominant zone with crack propagation. Reasons are:
  - Unloading: In J integral analysis plastic model was replaced by a nonlinear solid
  - Single-parameter identification not valid since various stress components increase at different rates

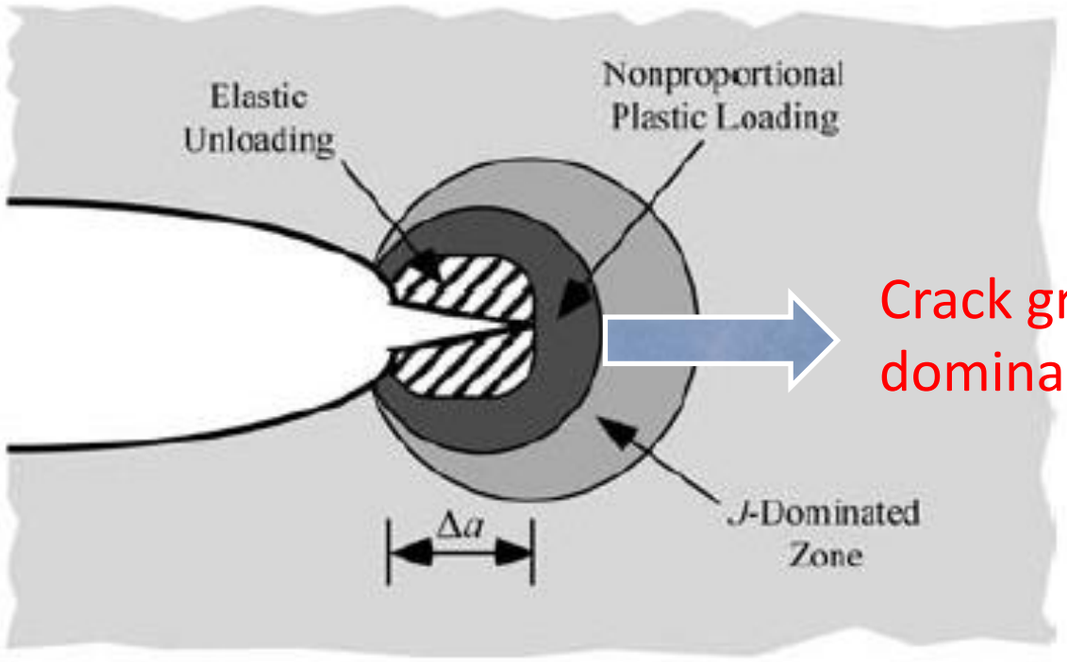

Crack growing out of J-dominant zone

Nonlinear vs plastic models

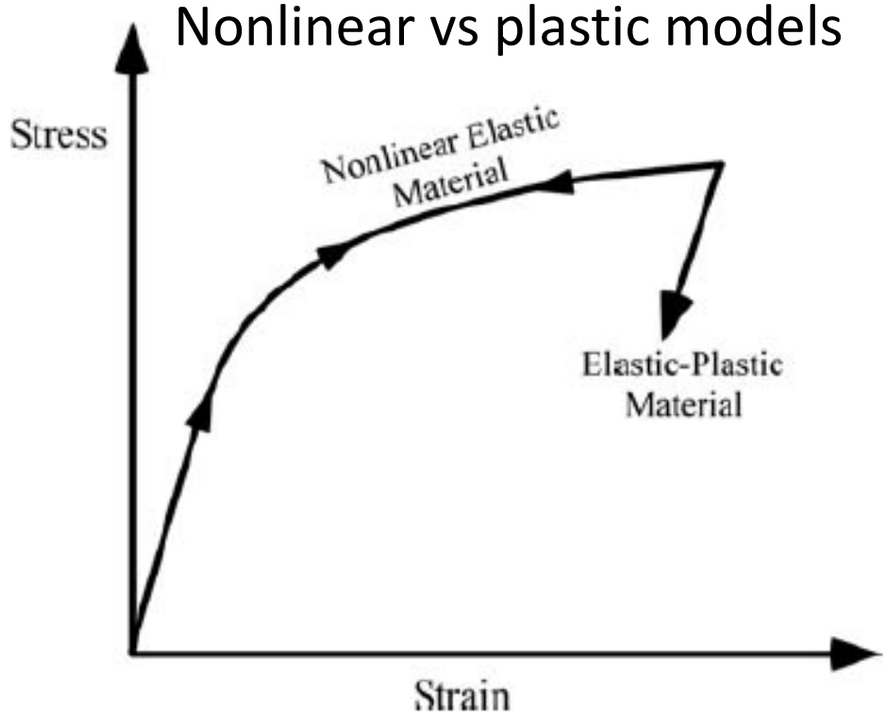

LSY: When a single parameter (G, K, J, CTOD) is not enough? T stress

- Higher order terms in stress expansion:
  - T stress (linear analysis)
    - Constant σ_{xx} in LEFM expansion
    - Nondimensional biaxiality ratio: $\beta = \frac{T\sqrt{\pi a}}{K_I}$
    - Example $\beta = -1$ for mode-I crack in infinite domain.
    - T stress redistributes plastic stress
    - $\beta(T)$ depend on particular geometry/loading configuration
    - Effect of $T(\beta)$ on toughness:

$$\sigma_{ij} = \frac{K_I}{\sqrt{2\pi r}} f_{ij}(\theta) + \begin{bmatrix} T & 0 & 0 \\ 0 & 0 & 0 \\ 0 & 0 & \nu T \end{bmatrix}$$

plane strain

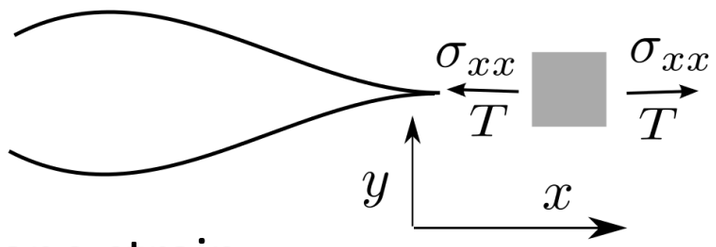

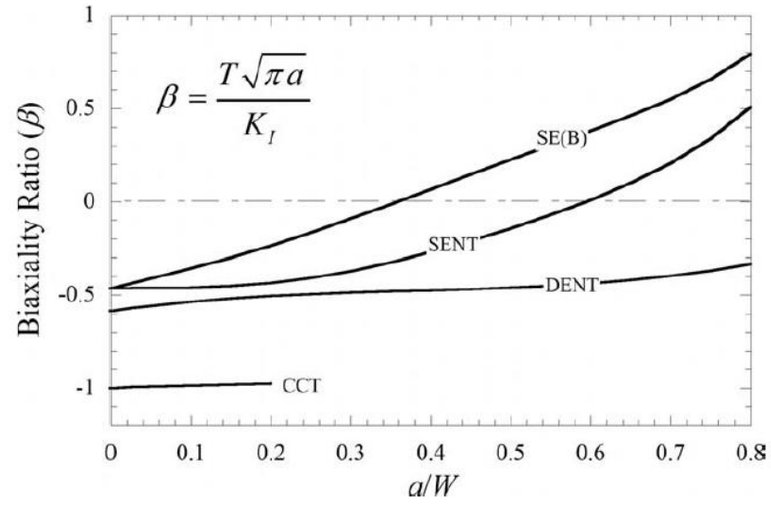

High $(+)$ $T \Rightarrow$ Constrained (triaxial) stress $\Rightarrow$ Toughness $\searrow$ Ductility $\searrow$

Low $(-)$ $T \Rightarrow$ Lose constraint $\Rightarrow$ Toughness $\nearrow$ Ductility $\nearrow$

- T stress also influnces crack path stability (particulary in dynamic fracture)

Plastic analysis: σ_{yy} is redistributed!

Kirk, Dodds, Anderson

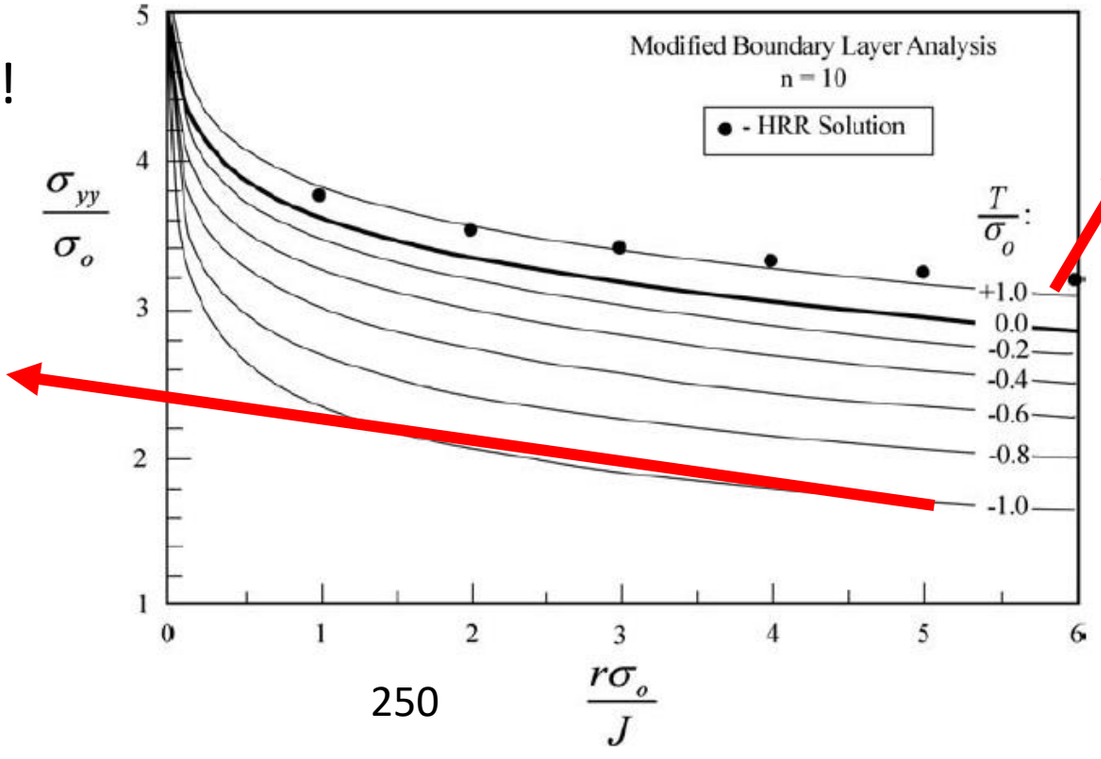

High negative T stress:
- Decreases σ_{yy}
- Decreases triaxiality

Positive T stress:
- Slightly Increases σ_{yy} and increase triaxiality

LSY: When a single parameter (G, K, J, CTOD) is not enough? J-Q theory

– Q parameter (J-Q theory) Valid for nonlinear analysis

* Added as a hydrostatic shift in front of crack to (HRR) stress fields

$$\sigma_{ij} \approx (\sigma_{ij})_{T=0} + Q\sigma_0\delta_{ij} \quad \left(|\theta| \le \frac{\pi}{2}\right)$$

* Similar to T positive Q increases triaxiality and reduces fracture resistance

$$J_c = J_c(Q)$$

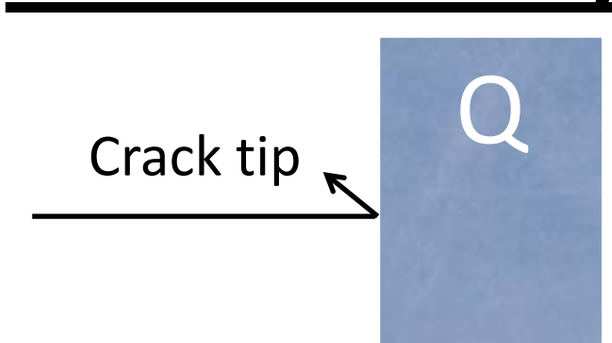

High (+) $Q \Rightarrow$ Constrained (triaxial) stress $\Rightarrow$ Toughness ↘ Ductility ↘

Low (-) $Q \Rightarrow$ Lose constraint $\Rightarrow$ Toughness ↗ Ductility ↗ Q

– More number of parameters: With extensive deformation two-parameter models such as K,T or J,Q evnetully break.

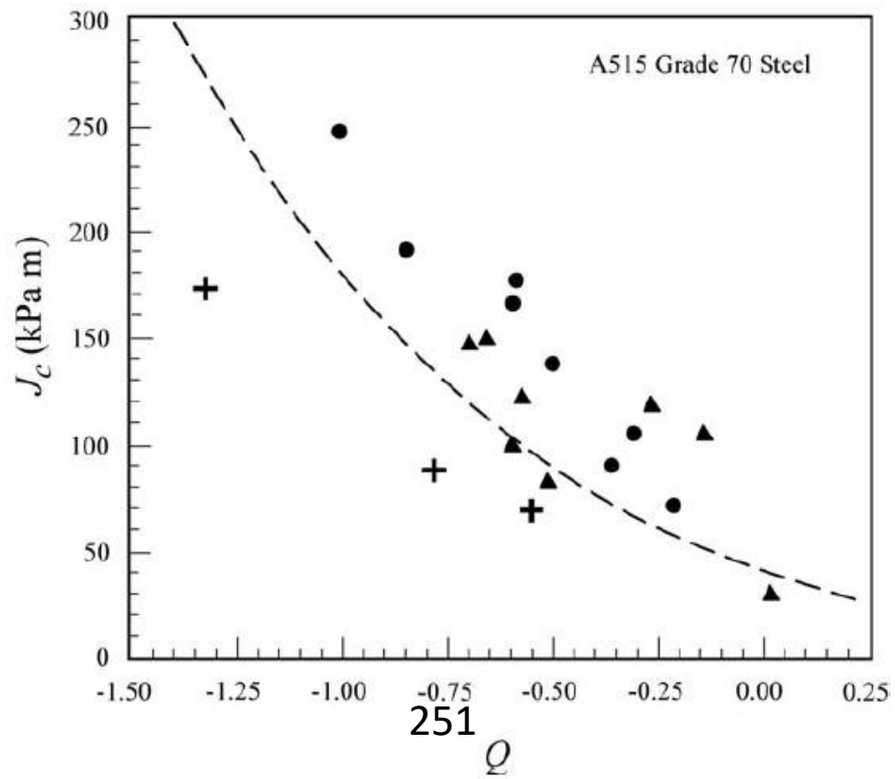

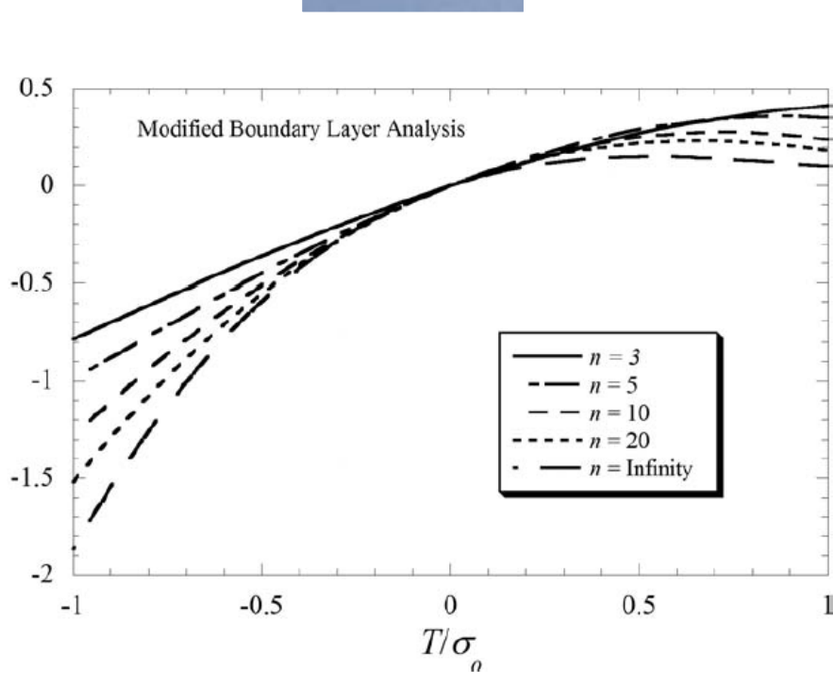

n: strain hardening in HRR analysis

5.4. Crack tip opening displacement (CTOD), relations with J and G

Crack Tip Opening Displacement

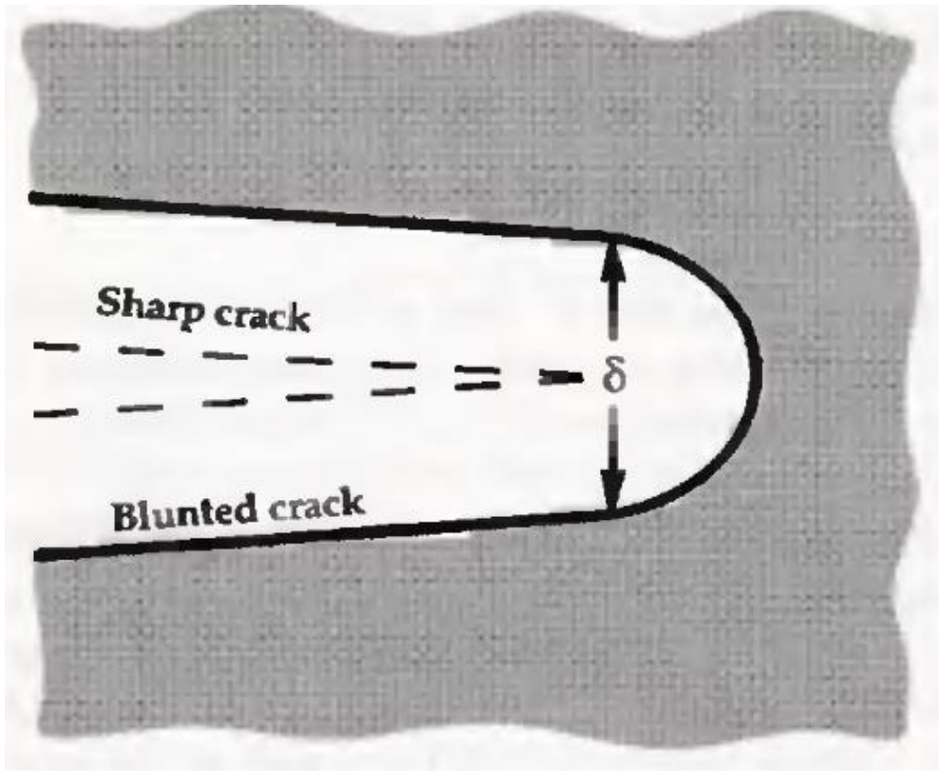

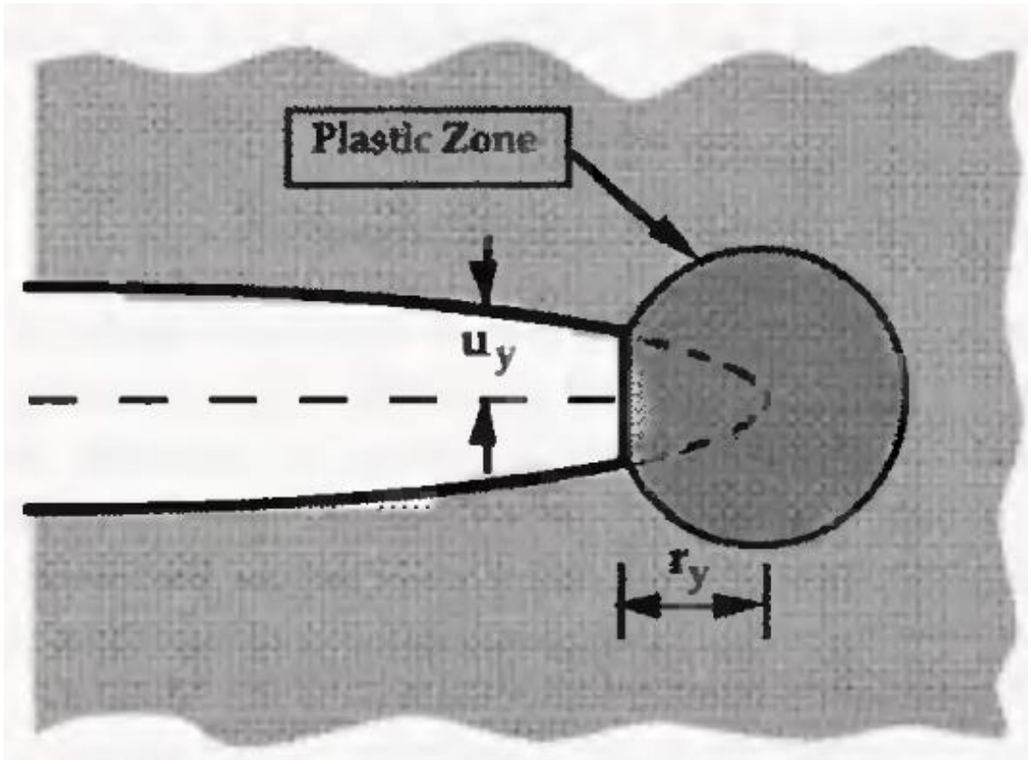

$$v = \frac{\kappa + 1}{4\mu}\sigma\sqrt{a^2 - x^2}$$

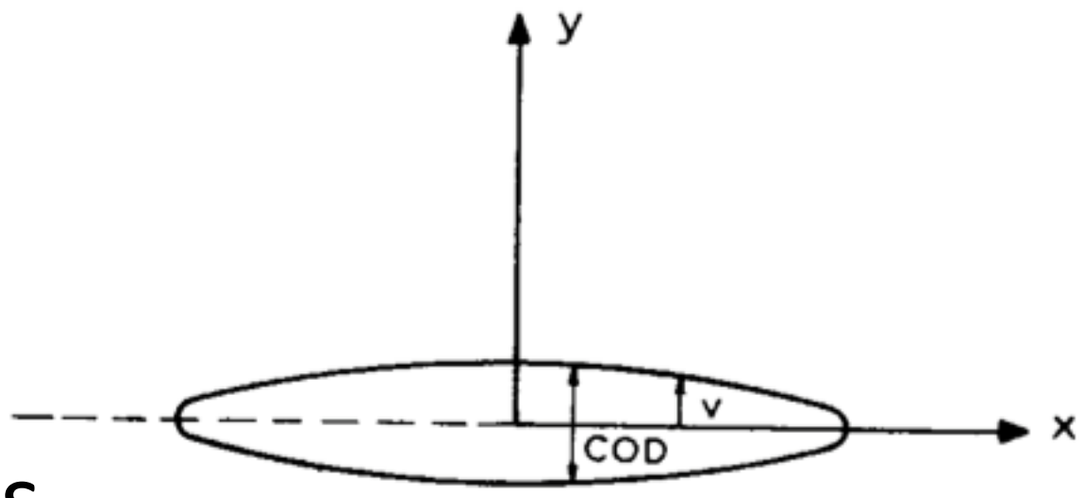

COD is zero at the crack tips.

Crack Tip Opening Displacement: First order aproximation

Wells 1961

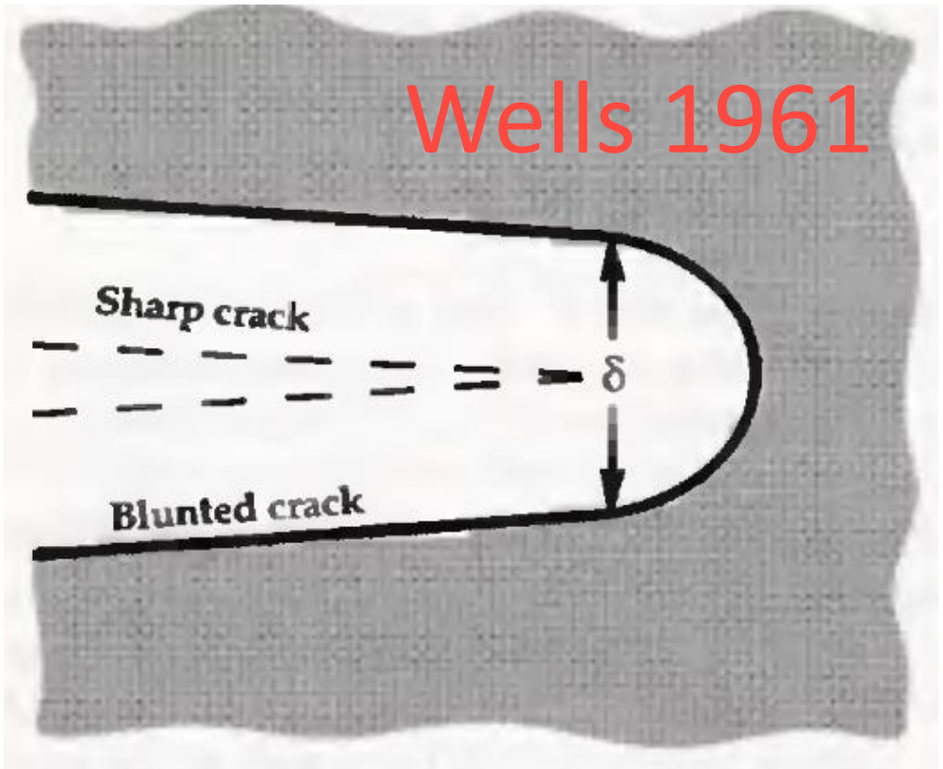

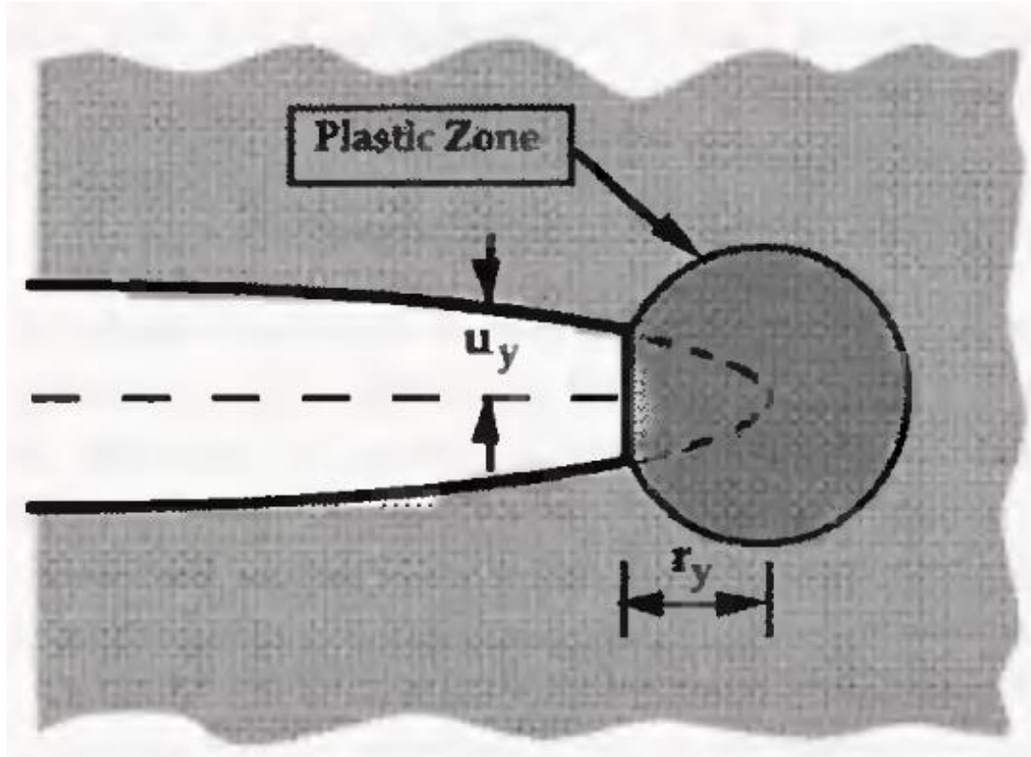

COD is taken as the separation of the faces of the effective crack at the tip of the physical crack

$$u_y = \frac{\kappa+1}{2\mu} K_I \sqrt{\frac{r_y}{2\pi}} \qquad \kappa = \frac{3-\nu}{1+\nu}$$

$$r_y = \frac{1}{2\pi}\left(\frac{K_I}{\sigma_{ys}}\right)^2 \qquad 2\mu = \frac{E}{1+\nu}$$

CTOD

$$\delta = 2u_y = \frac{4}{\pi}\frac{K_I^2}{\sigma_{ys}E}$$

(Irwin's plastic correction, **plane stress**)

Crack Tip Opening Displacement: Strip yield model

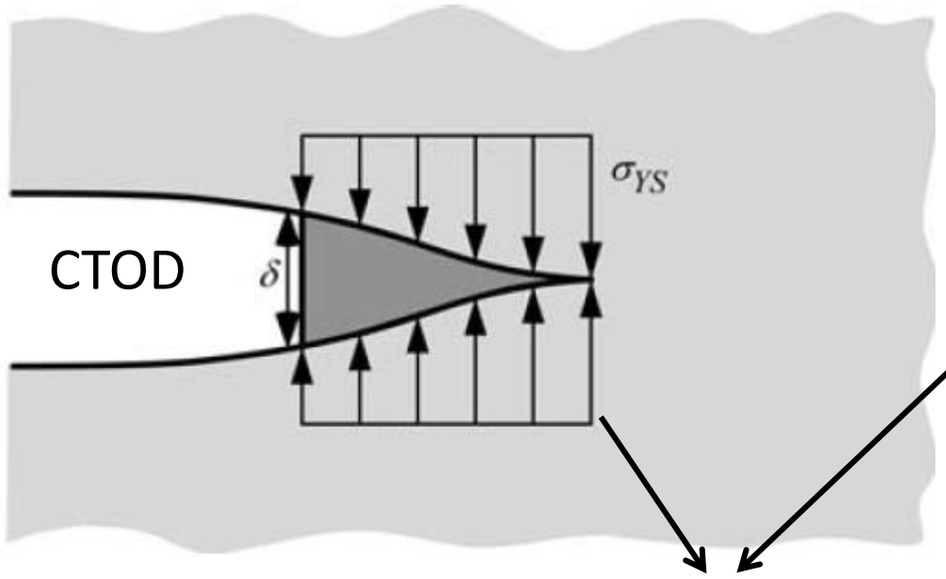

Stresses that yielded K = 0

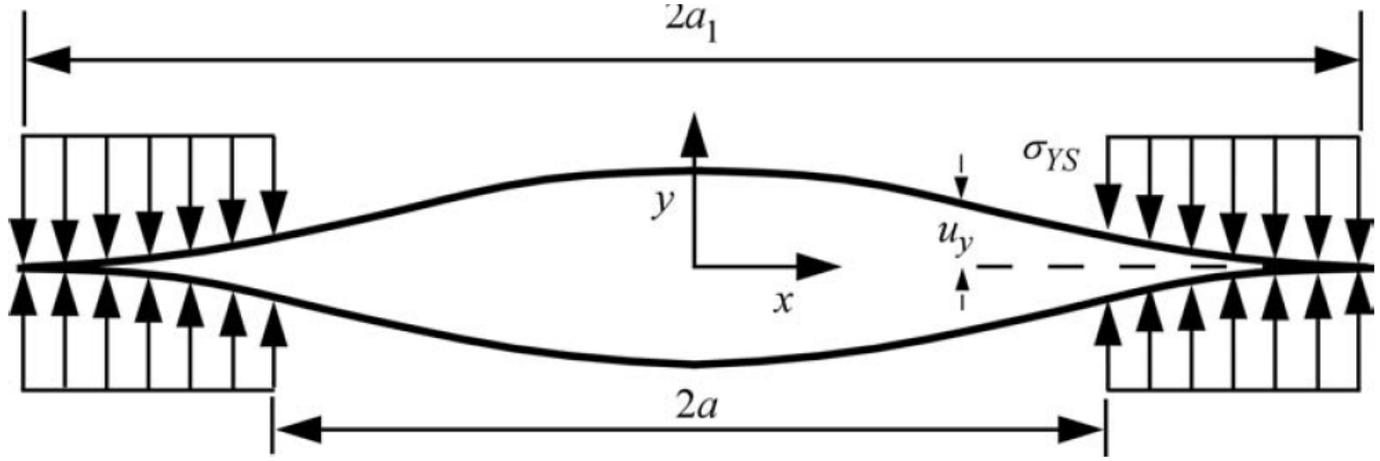

K = 0 ➡ $Z = \frac{2\sigma_{YS}}{\pi}\left[\frac{k}{z}\sqrt{\frac{z^2-a_1^2}{1-k^2}}\right]$ ➡ $\tilde{Z} = \frac{2\sigma_{YS}}{\pi}[z\omega_1 - a\omega_2]$

➡ $u_y = \frac{2}{E}\mathrm{Im}\tilde{Z} = \frac{4\sigma_{YS}}{\pi E}\left[a\coth^{-1}\left(\frac{1}{a_1}\sqrt{\frac{a_1^2-z^2}{1-k^2}}\right) - z\coth^{-1}\left(\frac{k}{z}\sqrt{\frac{a_1^2-z^2}{1-k^2}}\right)\right]$

$z = a$ ➡ $\delta = 2u_y = \frac{8\sigma_{YS}a}{\pi E}\ln\left(\frac{1}{k}\right) = \frac{8\sigma_{YS}a}{\pi E}\left[\frac{1}{2}\left(\frac{\pi}{2}\frac{\sigma}{\sigma_{YS}}\right)^2 + \frac{1}{12}\left(\frac{\pi}{2}\frac{\sigma}{\sigma_{YS}}\right)^4 + \cdots\right]$ ➡

For $\sigma/\sigma_{YS} \to 0$ $\quad \delta = \frac{K_I^2}{\sigma_{YS}E}$

CTOD-G-K relation

Wells observed:

The degree of crack blunting increases in proportion to the toughness of the material

→ Fracture occurs $\delta = \delta_c$

material property independent of specimen and crack length (confirmed by experiments)

$$\delta = \frac{4}{\pi}\frac{K_I^2}{\sigma_{ys}E}$$

$$G_I = \frac{K_I^2}{E}$$

→ $$G_I = \frac{\pi}{4}\sigma_{ys}\delta$$

→ Under conditions of SSY, the fracture criteria based on the stress intensity factor, the strain energy release rate and the crack tip opening displacement are equivalent.

CTOD-J relation

- When SSY is satisfied G = J so we expect:

$$G = m\sigma_y\delta \quad \Rightarrow \quad \boxed{J = m\sigma_y\delta}$$

- In fact this equation is valid well beyond validity of LEFM and SSY

- E.g. for HRR solution Shih showed that:

$$u_i = \frac{\alpha\sigma_o}{E}\left(\frac{EJ}{\alpha\sigma_o^2 I_n r}\right)^{\frac{n}{n+1}} r\tilde{u}_i(\theta, n)$$

$$d_n = \frac{2\tilde{u}_y(\pi,n)\left[\frac{\alpha\sigma_o}{E}\{\tilde{u}_x(\pi,n)+\tilde{u}_y(\pi,n)\}\right]^{1/n}}{I_n}$$

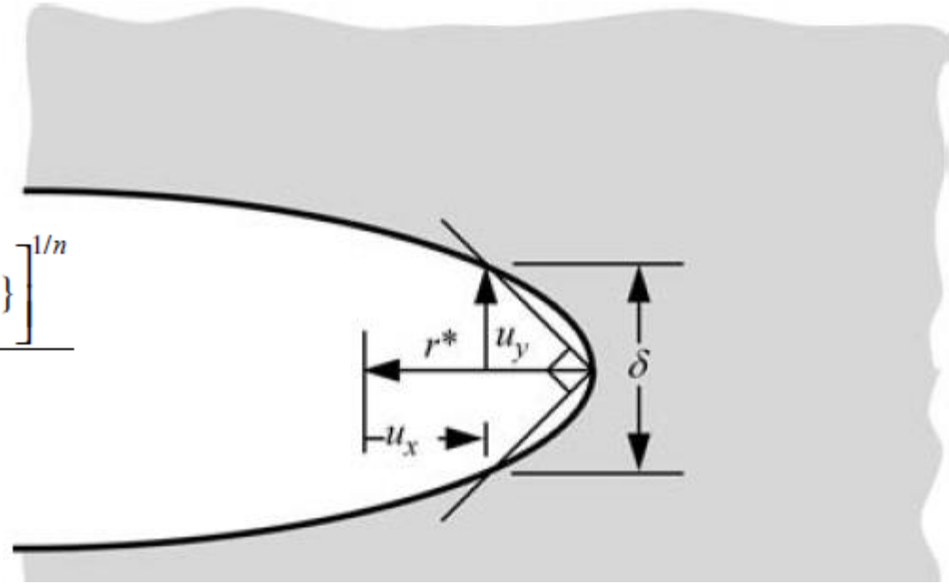

- δ is obtained by 90 degree method:
  Deformed position corresponding to $r^* = r$ and $\varphi = -\pi$ forms 45 degree w.r.t crack tip)

$$\frac{\delta}{2} = u_y(r^*, \pi) = r^* - u_x(r^*, \pi)$$

$$r^* = \left(\frac{\alpha\sigma_o}{E}\right)^{1/n}\{\tilde{u}_x(\pi,n)+\tilde{u}_y(\pi,n)\}^{\frac{n+1}{n}}\frac{J}{\sigma_o I_n} \quad \Rightarrow \quad J = m\sigma_0\delta$$

for $\boxed{m = \frac{1}{d_n},\ d_n = \frac{2\tilde{u}_y(\pi,n)\left[\frac{\alpha\sigma_o}{E}\{\tilde{u}_x(\pi,n)+\tilde{u}_y(\pi,n)\}\right]^{1/n}}{I_n}}$

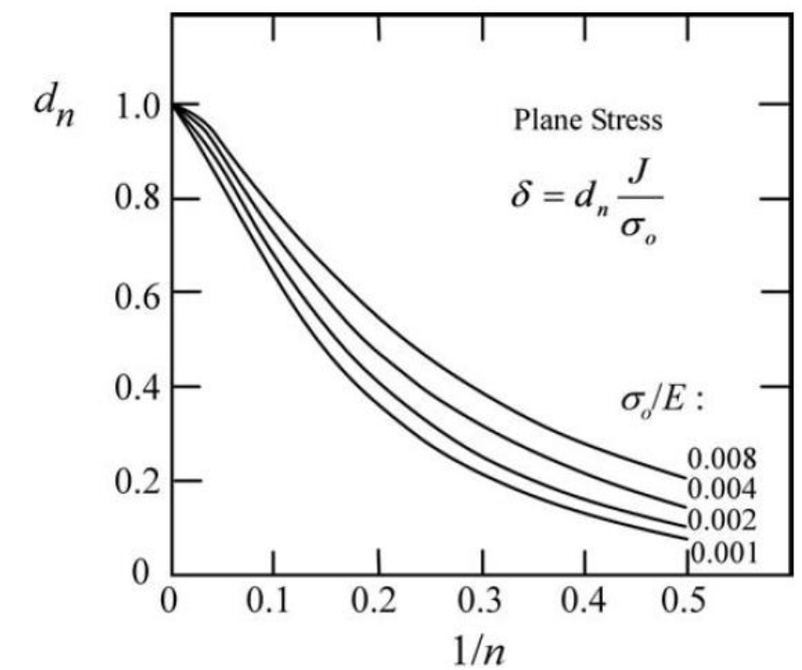

CTOD experimental determination

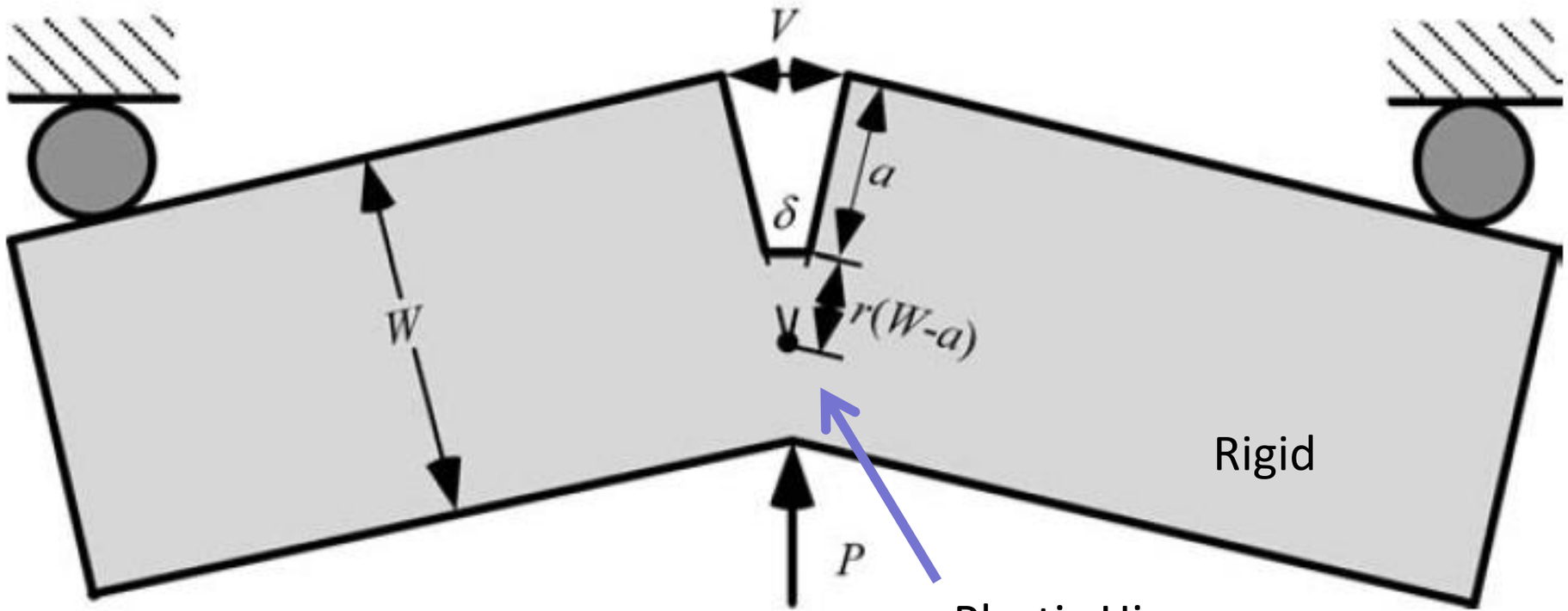

$$\frac{\delta_t}{CMOD} = \frac{r(W-a)}{r(W-a)+a}$$

similarity of triangles

r : rotational factor [-], between 0 and 1

For high elastic deformation contribution, elastic corrections should be added

6. Computational fracture mechanics

6.1. Fracture mechanics in Finite Element Methods

6.2. Traction Separation Relations (TSRs)

6.1Fracture mechanics in Finite Element Methods (FEM)

6.1.1. Introduction to Finite Element method

6.1.2. Singular stress finite elements

6.1.3. Extraction of K (SIF), G

6.1.4. J integral

6.1.5. Finite Element mesh design for fracture mechanics

6.1.6. Computational crack growth

6.1.7. Extended Finite Element Method (XFEM)

Numerical methods to solve PDEs

- Finite Difference (FD) & Finite Volume (FV) methods
- FEM (Finite Element Method)
- BEM (Boundary Element Method)
- MMs (Meshless/Meshfree methods)

FD

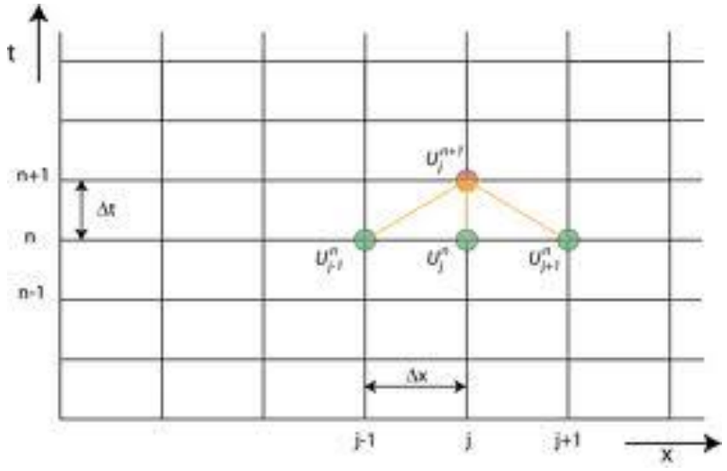

FEM

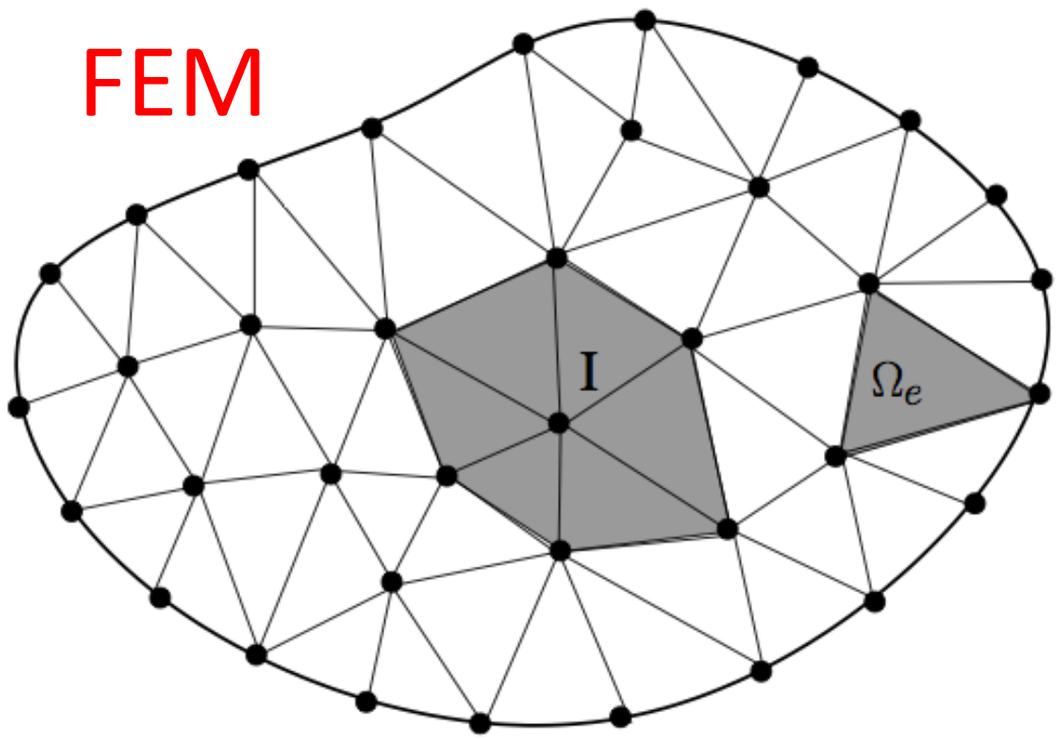

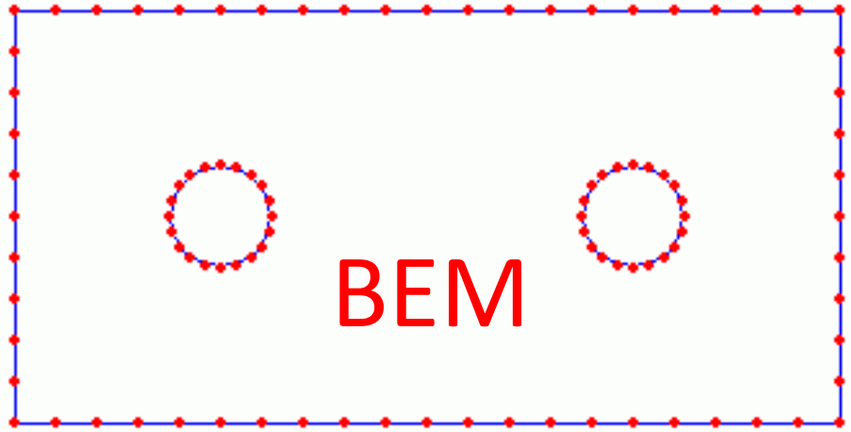

BEM

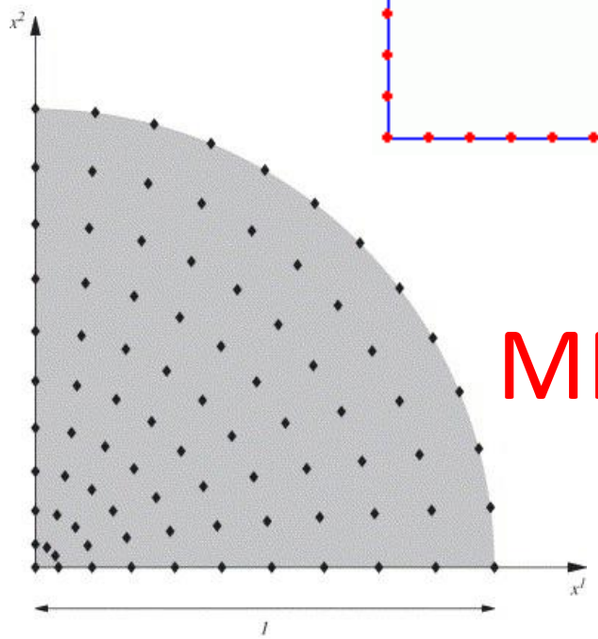

MMs

Fracture models

- Discrete crack models (discontinuous models):
  Cracks are explicitly modeled
  - LEFM
  - EPFM
  - Cohesive zone models

- Continuous models: Effect of (micro)cracks and voids are incorporated in bulk damage
  - Continuum damage models
  - Phase field models

- Peridynamic models: Material is modeled as a set of particles

Finite Element Method

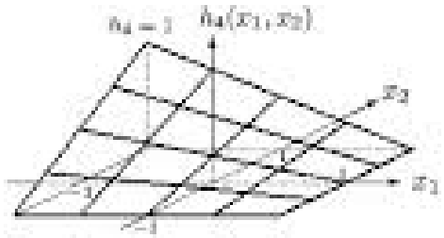

$$h_4 = \frac{1}{4}(1 - x_1)(1 + x_2)$$

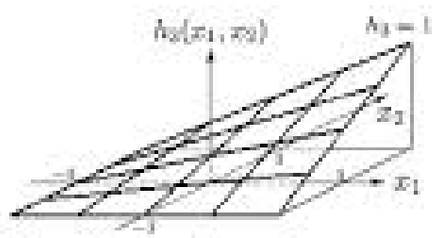

$$h_3 = \frac{1}{4}(1 + x_1)(1 + x_2)$$

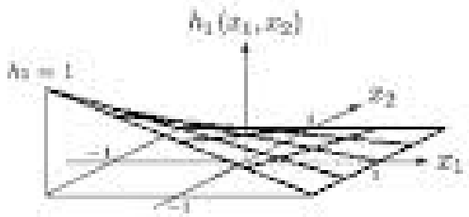

$$h_1 = \frac{1}{4}(1 - x_1)(1 - x_2)$$

$$h_2 = \frac{1}{4}(1 + x_1)(1 - x_2)$$

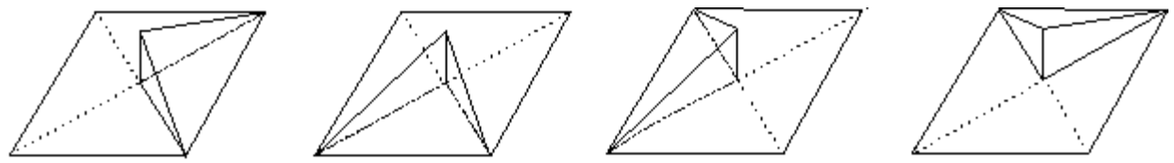

Global level: The nodal dof at the center node is shared by all four elements

Element level: 4 Shape functions for a linear quad element

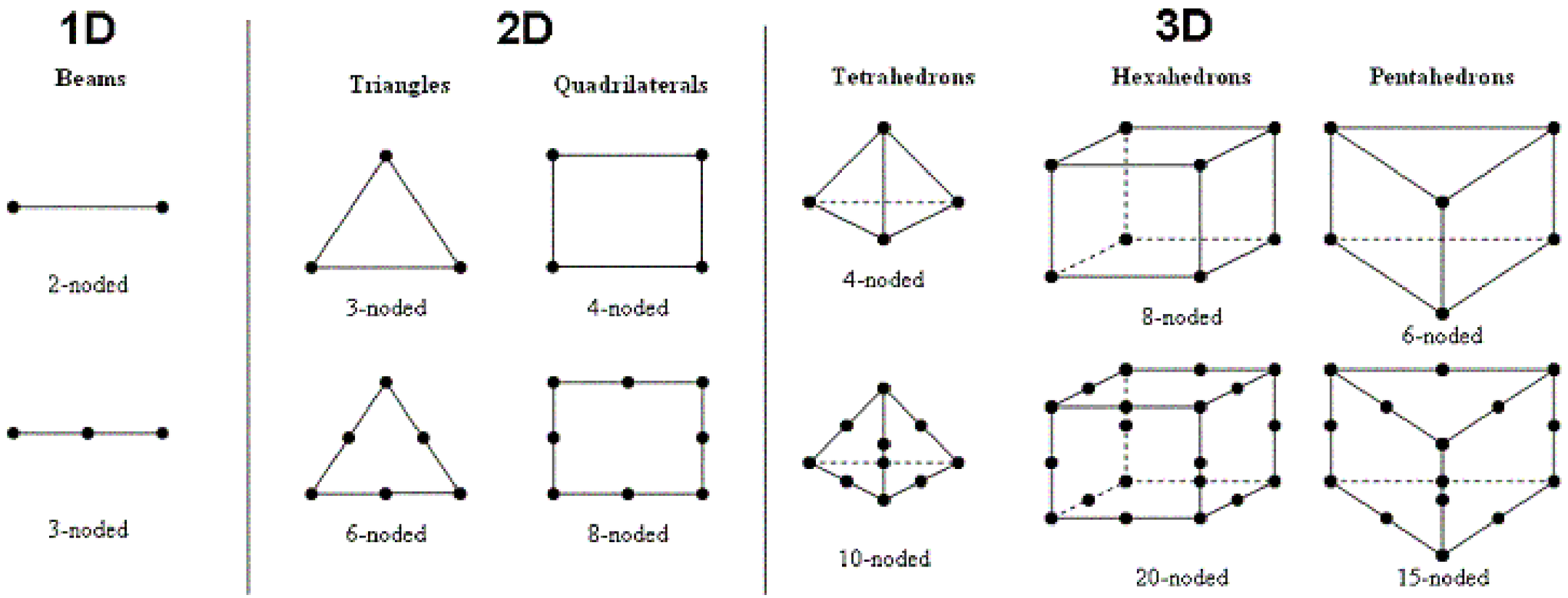

6.1Fracture mechanics in Finite Element Methods (FEM)

6.1.1. Introduction to Finite Element method

6.1.2. Singular stress finite elements

6.1.3. Extraction of K (SIF), G

6.1.4. J integral

6.1.5. Finite Element mesh design for fracture mechanics

6.1.6. Computational crack growth

6.1.7. Extended Finite Element Method (XFEM)

Isoparametric Elements

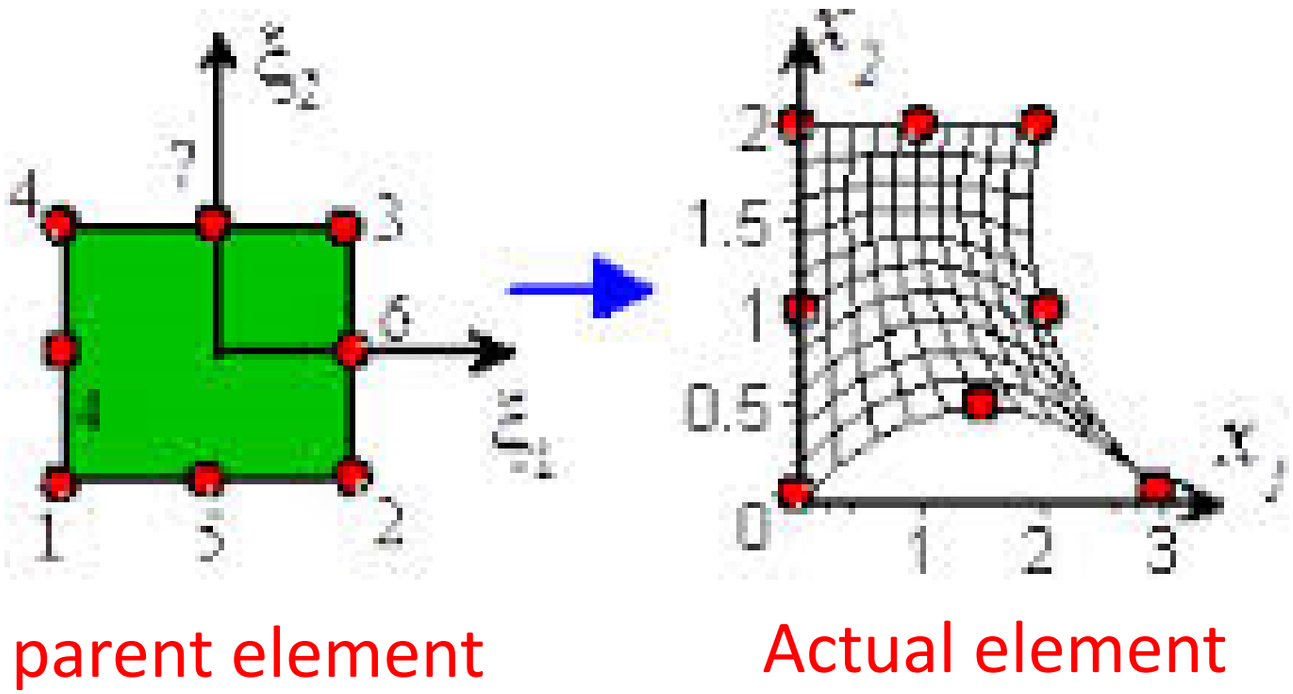

parent element

Actual element

- Geometry is mapped from a parent element to the actual element
- The same interpolation is used for geometry mapping and FEM solution (in the figure 2nd order shape functions are used for solution and geometry)
- Geometry map and solution are expressed in terms of ξ

Order of element

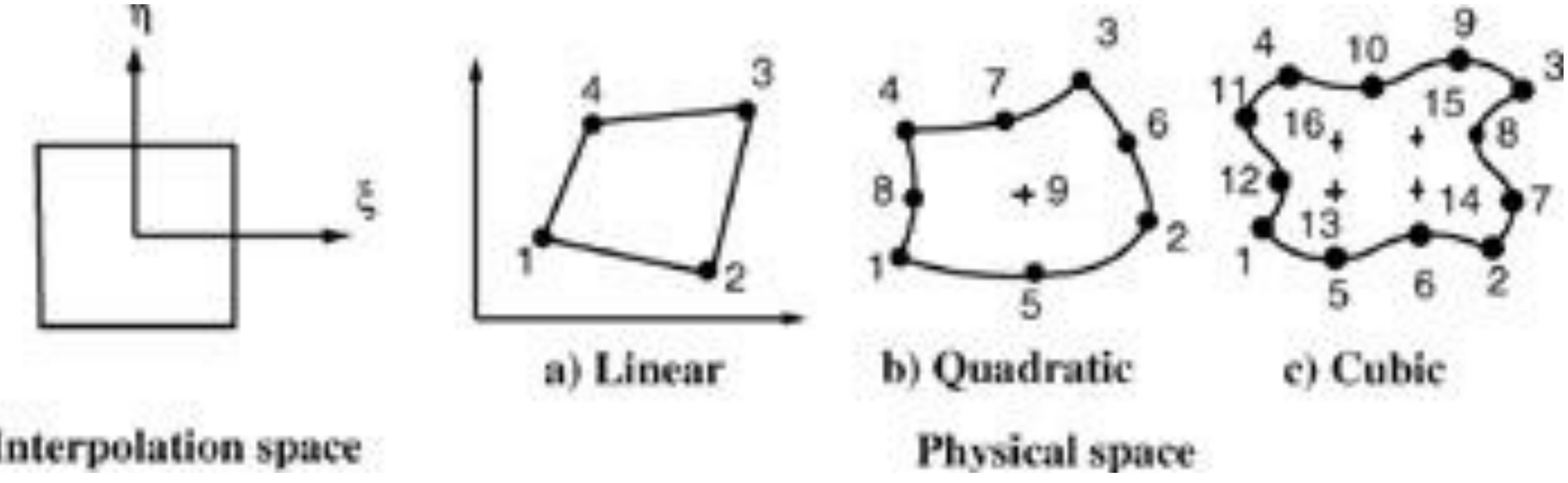

(Same number of nodes based on the order)

Singular crack tip solutions

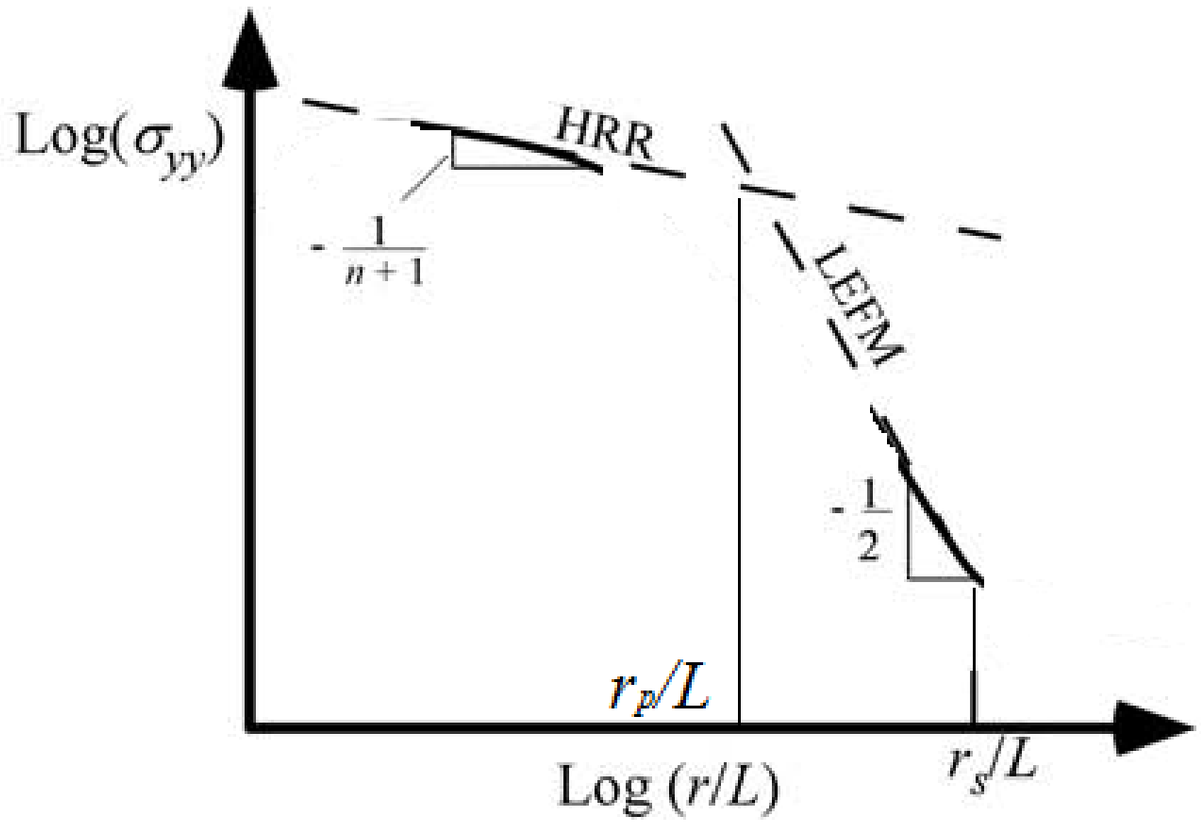

$$\sigma_{ij} = \sigma_0 \left(\frac{EJ}{\alpha \sigma_0^2 I_n r} \right)^{\frac{1}{n+1}} \tilde{\sigma}_{ij}(n, \theta)$$

$$\epsilon_{ij} = \frac{\alpha \sigma_0}{E} \left(\frac{EJ}{\alpha \sigma_0^2 I_n r} \right)^{\frac{n}{n+1}} \tilde{\epsilon}_{ij}(n, \theta)$$

- NLFM (PFM): For HRR solution stress $\frac{1}{r^{\frac{1}{n+1}}}$ and strain $\frac{1}{r^{\frac{n}{n+1}}}$ are still singular $\Rightarrow$
  - for elastic-perfectly plastic ($n \to \infty$) stress is bounded and strain is $\frac{1}{r}$ singular

Isoparametric singular elements

- **LEFM**

$\epsilon, \sigma : \frac{1}{\sqrt{r}}$

Quarter point
Quad element

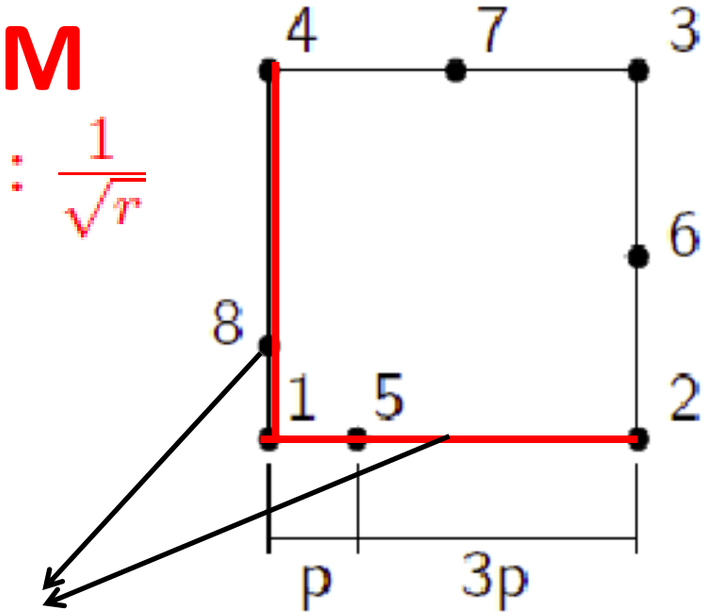

singular form $\frac{1}{\sqrt{r}}$ nly along these lines
NOT recommended

Quarter point **collapsed**
Quad element

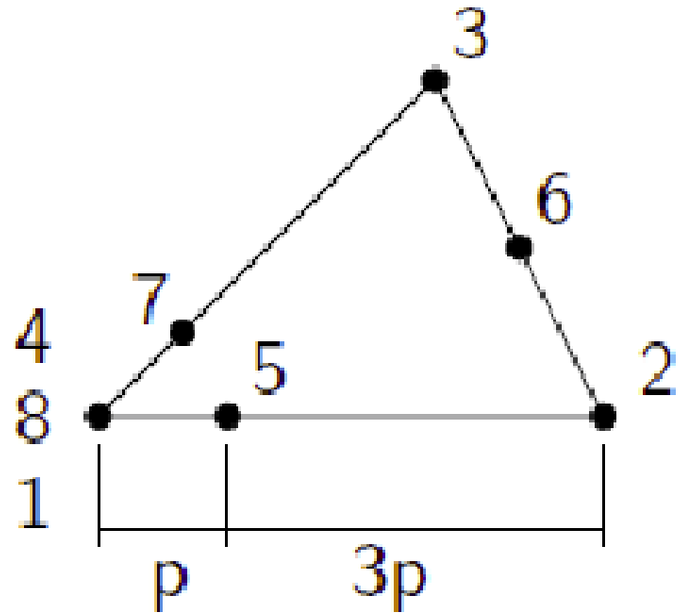

Improvement:
- $\frac{1}{\sqrt{r}}$ rom inside all element

Problem
- Solution inaccuracy and sensitivity when opposite edge 3-6-2 is curved

Quarter point
Tri element

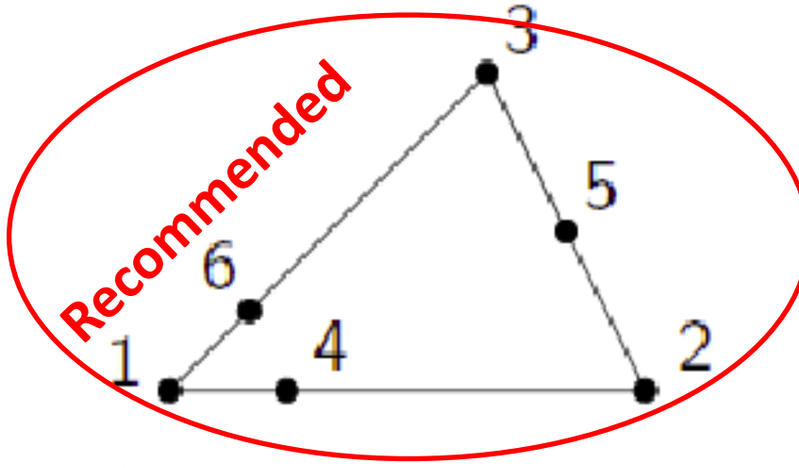

Improvement:
- Better accuracy and less mesh sensitivity

- **Elastic-perfectly plastic**

$\epsilon : \frac{1}{r}$

Collapsed Quad elements

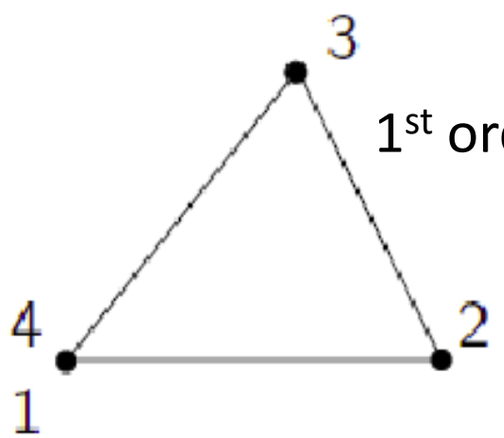

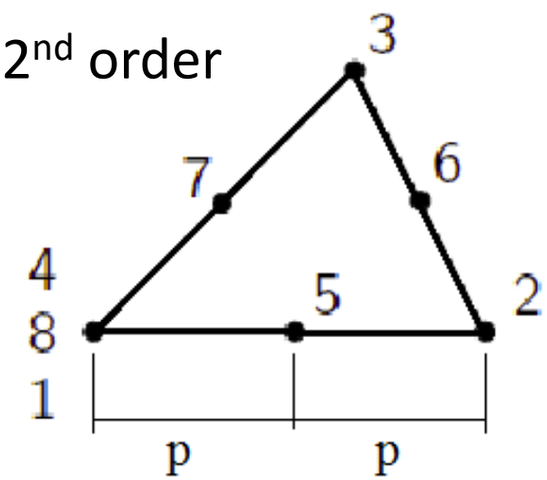

Motivation: 1D quadrature element

Find α that yields ε singularity at x_1

Isoparametric element:

1. Geometry:

$$x = \Sigma_{i=1}^{3} N_i(\xi) x_i \quad \Rightarrow \quad \boxed{x = L\left\{\xi^2(\frac{1}{2}-\alpha)+\frac{1}{2}\xi+\alpha\right\}}$$

$$\frac{\mathrm{d}x}{\mathrm{d}\xi} = L\left\{2\xi(\frac{1}{2}-\alpha)+\frac{1}{2}\right\}$$

$$N_1(\xi) = \frac{\xi(\xi-1)}{2} \qquad N_2(\xi) = 1-\xi^2 \qquad N_3(\xi) = \frac{\xi(\xi+1)}{2}$$

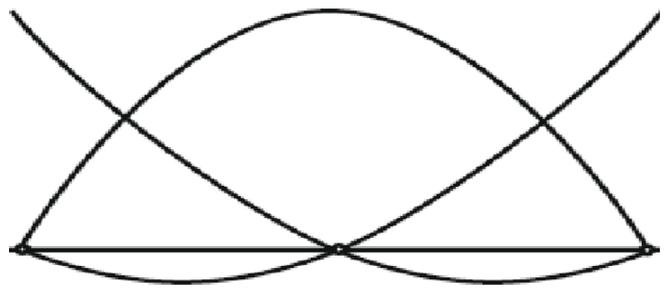

$\xi = -1$ $\xi = 0$ $\xi = 1$

Parent element

Singularity of $\epsilon(x) = \frac{\mathrm{d}u}{\mathrm{d}x} = \overbrace{\frac{\mathrm{d}u}{\mathrm{d}\xi}}^{\text{nonsingular}} / \frac{\mathrm{d}x}{\mathrm{d}\xi}$ at $x_1(\xi=-1) \Rightarrow$

$$\frac{\mathrm{d}x}{\mathrm{d}\xi}(\xi=-1) = 0 \quad \Rightarrow -2(\frac{1}{2}-\alpha)+\frac{1}{2} = 0 \Rightarrow \boxed{\alpha = \frac{1}{4}}$$

Hence,

$$x = \frac{L}{4}(\xi+1)^2 \quad \Rightarrow \quad \boxed{\xi = 2\sqrt{\frac{x}{L}}-1}$$

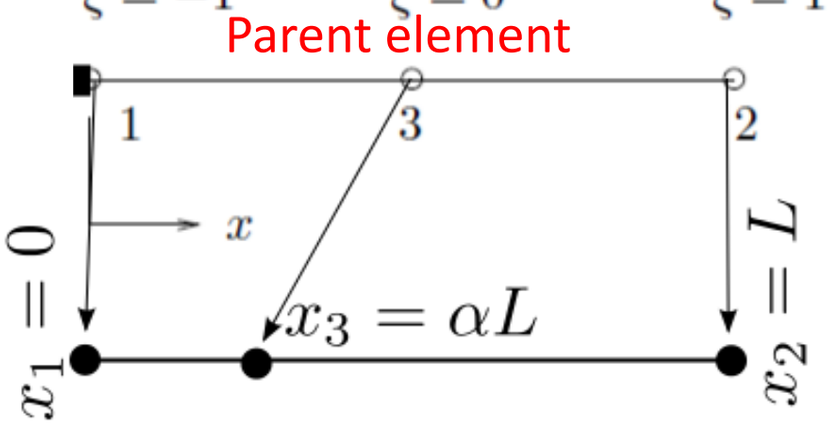

Motivation: 1D quadrature element

2. FEM solution

- Displacement

$$u = \Sigma_{i=1}^{3} N_i(\xi) u_i \quad \Rightarrow$$

$$u = u_1 \left[\frac{\xi(\xi-1)}{2}\right] + u_2 \left[\frac{\xi(\xi+1)}{2}\right] + u_3 \left[1-\xi^2\right] \Rightarrow$$

$$\boxed{u = u_1 + \frac{\sqrt{x}}{\sqrt{L}}(-3u_1 - u_2 + 4u_3) + \frac{2x}{L}(u_1 + u_2 - 2u_3)}$$

which matches $\sqrt{x}$ from asymptotic displacement solution.

- Strain

$$\left.\begin{aligned} \epsilon &= \frac{\mathrm{d}u}{\mathrm{d}x} = \frac{\mathrm{d}u}{\mathrm{d}\xi} / \frac{\mathrm{d}x}{\mathrm{d}\xi} \\ \frac{\mathrm{d}x}{\mathrm{d}\xi} &= L\frac{\xi+1}{2} = \sqrt{xL} \\ \frac{\mathrm{d}u}{\mathrm{d}\xi} &= u_1\left[\frac{2\xi-1}{2}\right] + u_2\left[\frac{2\xi+1}{2}\right] - 2u_3\xi \end{aligned}\right\} \Rightarrow$$

$$\boxed{\epsilon = \frac{1}{\sqrt{xL}}\left(-\frac{3}{2}u_1 - \frac{1}{2}u_2 + 2u_3\right) + \frac{1}{L}(2u_1 + 2u_2 - 4u_3)}$$

Strain field too matches asymptotic term $\frac{1}{\sqrt{r}}$

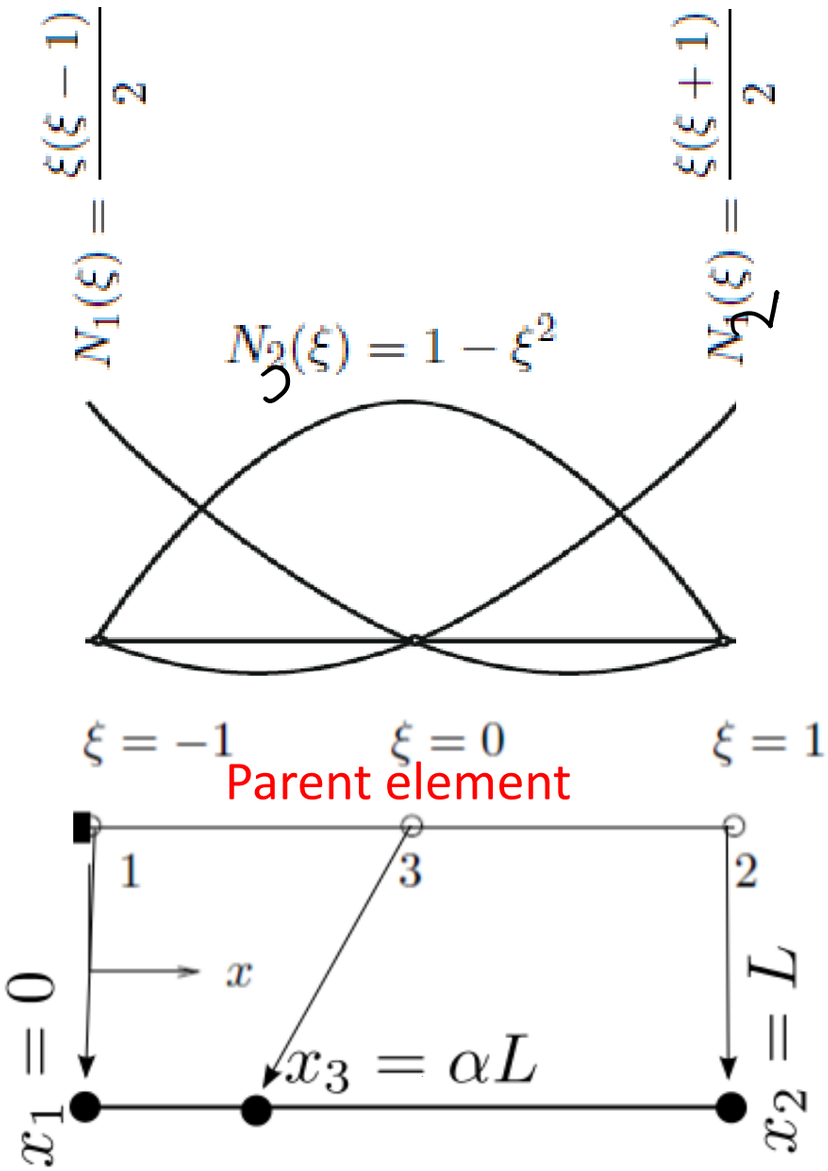

Moving singular ε position

Strain singularity at ξ means

$$\frac{\mathrm{d}x}{\mathrm{d}\xi} = L\left\{2\xi(\frac{1}{2}-\alpha)+\frac{1}{2}\right\}$$

must be zero. Accordingly,

Singularity at infinity($\xi \to -\infty$) $\quad \alpha -> (\frac{1}{2})^-$

Singularity at crack tip($\xi = -1$) $\quad \alpha = \frac{1}{4}$

Singularity inside element(not of interest)($-1 < \xi < 0$) $\quad 0 < \alpha < \frac{1}{4}$

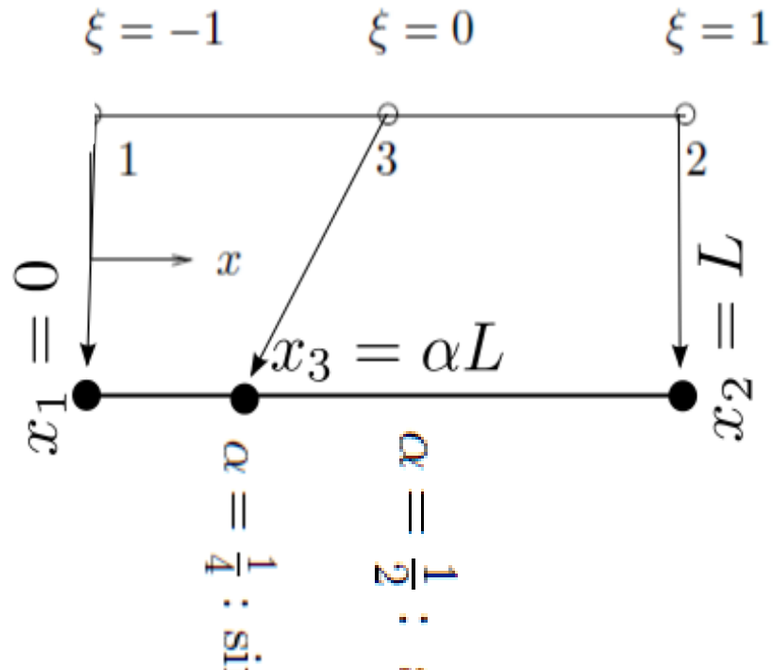

- Transition elements:
  According to this analysis
  mid nodes of next layers move
  to ½ point from ¼ point

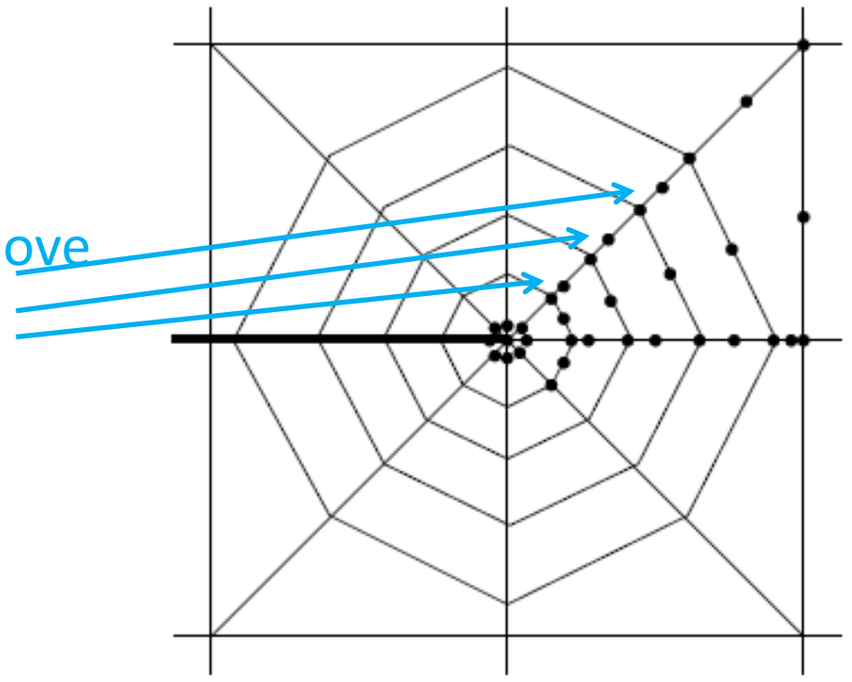

Lynn and Ingraffea 1977)

6.1Fracture mechanics in Finite Element Methods (FEM)

6.1.1. Introduction to Finite Element method
6.1.2. Singular stress finite elements
6.1.3. Extraction of K (SIF), G
6.1.4. J integral
6.1.5. Finite Element mesh design for fracture mechanics
6.1.6. Computational crack growth
6.1.7. Extended Finite Element Method (XFEM)

1. K from local fields

1. Displacement

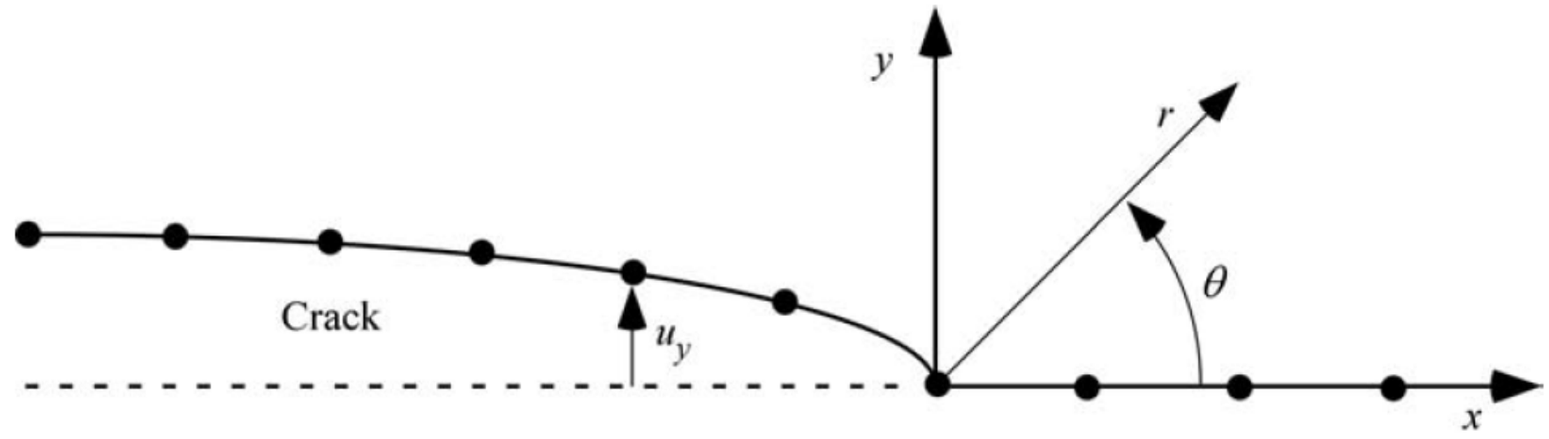

$$u_y(r,\theta=\pi)=\frac{4K_I\sqrt{r}}{\sqrt{2\pi}E'} \quad \Rightarrow \quad \boxed{K_I=\lim_{r\to 0}\left[\frac{E'u_y}{4}\sqrt{\frac{2\pi}{r}}\right] \qquad (\theta=\pi)}$$

$$E'=\begin{cases} E & \text{plane stress} \\ \frac{E}{1-\nu^2} & \text{plane strain} \end{cases}$$

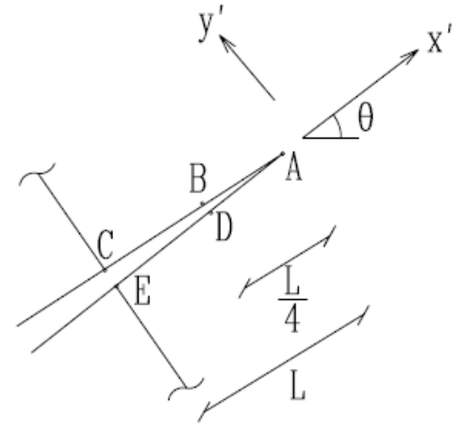

or alternatively from the first quarter point element:

$$\left.\begin{aligned} v &= K_{\mathrm{I}}\frac{\kappa+1}{2G}\sqrt{\frac{r}{2\pi}} \\ u' &= \overline{u}'_A+\left(-3\overline{u}'_A+4\overline{u}'_B-\overline{u}'_C\right)\sqrt{\tfrac{r}{L}}+\left(2\overline{u}'_A+2\overline{u}'_C-4\overline{u}'_B\right)\tfrac{r}{L} \\ v' &= \overline{v}'_A+\left(-3\overline{v}'_A+4\overline{v}'_B-\overline{v}'_C\right)\sqrt{\tfrac{r}{L}}+\left(2\overline{v}'_A+2\overline{v}'_C-4\overline{v}'_B\right)\tfrac{r}{L} \end{aligned}\right\} \Rightarrow$$

$$\boxed{K_{\mathrm{I}}=\frac{2G}{\kappa+1}\sqrt{\frac{2\pi}{L}}\left(-3\overline{v}'_A+4\overline{v}'_B-\overline{v}'_C\right)}$$

Recall for 1D

$$u=u_1+\frac{\sqrt{x}}{\sqrt{L}}\left(-3u_1-u_2+4u_3\right)+\frac{2x}{L}\left(u_1+u_2-2u_3\right)$$

$$\boxed{\left\{\begin{array}{c} K_{\mathrm{I}} \\ K_{\mathrm{II}} \end{array}\right\}=\frac{1}{2}\frac{2G}{\kappa+1}\sqrt{\frac{2\pi}{L}}\left[\begin{array}{cc} 0 & 1 \\ 1 & 0 \end{array}\right]\left[\begin{array}{c} -3\overline{u}'_A+4\left(\overline{u}'_B-\overline{u}'_D\right)-\left(\overline{u}'_C-\overline{u}'_E\right) \\ -3\overline{v}'_A+4\left(\overline{v}'_B-\overline{v}'_D\right)-\left(\overline{v}'_C-\overline{v}'_E\right) \end{array}\right]}$$

Mixed mode generalization:

1. K from local fields

2. Stress

$$K_I = \lim_{r \longrightarrow 0} \left(\sqrt{2\pi r}\ \sigma_{22}|_{\theta=0} \right) \quad ; \quad K_{II} = \lim_{r \longrightarrow 0} \left(\sqrt{2\pi r}\ \sigma_{12}|_{\theta=0} \right)$$

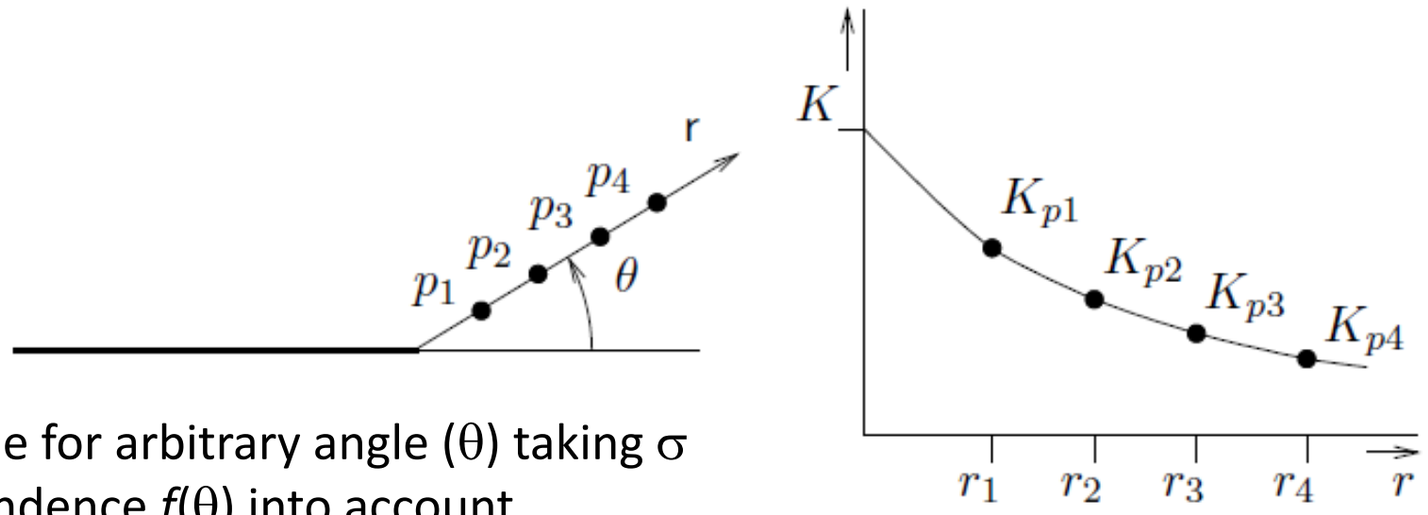

or can be done for arbitrary angle (θ) taking σ angular dependence $f(\theta)$ into account

Stress based method is less accurate because:

- Stress is a derivative field and generally is one order less accurate than displacement
- Stress is singular as opposed to displacement
- Stress method is much more sensitive to where loads are applied (crack surface or far field)

2. K from energy approaches

1. Elementary crack advance (two FEM solutions for a and $a + \Delta a$)
2. Virtual Crack Extension: Stiffness derivative approach
3. J-integral based approaches (next section)

After obtaining G (or $J=G$ for LEFM) K can be obtained from

$$K_I^2 = E'G \qquad E' = \begin{cases} E & \text{plane stress} \\ \frac{E}{1-\nu^2} & \text{plane strain} \end{cases}$$

2.1 Elementary crack advance

For fixed grip boundary condition perform two simulations (1, a) and (2, $a+\Delta a$):
All FEM packages can compute strain (internal) energy U_i

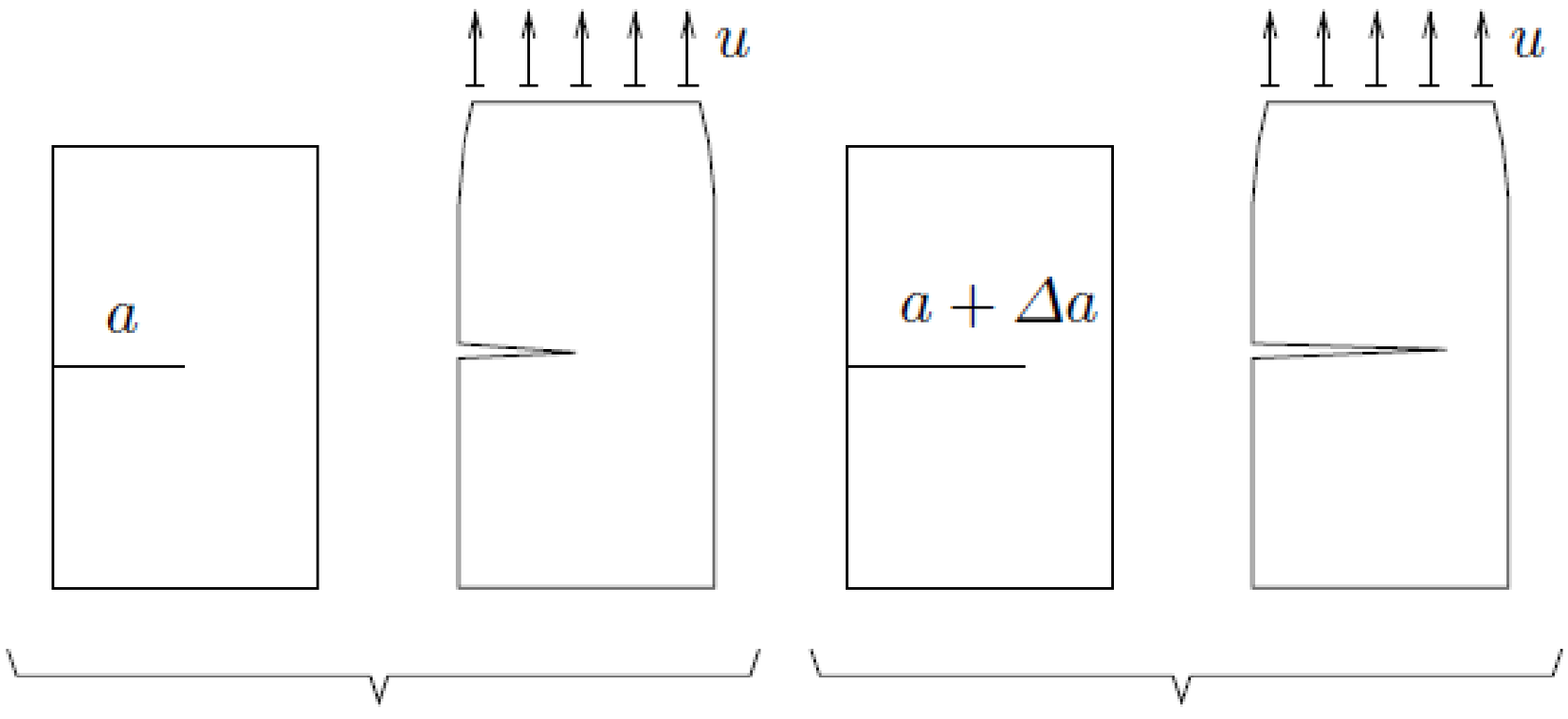

$$\text{fixed grips} \quad \rightarrow \quad \frac{dU_e}{da} = 0 \quad \Rightarrow \quad G = -\frac{1}{B}\frac{dU_i}{da} \approx -\frac{1}{B}\frac{U_i(a+\Delta a) - U_i(a)}{\Delta a}$$

Drawback:

1. Requires two solutions
2. Prone to Finite Difference (FD) errors

2.2 Virtual crack extension

- Potential energy is given by

$$\Pi = \frac{1}{2}\lfloor u \rfloor [K] \{u\} - \lfloor u \rfloor \{p\}$$

$$-G = \frac{\partial \Pi}{\partial a} = \frac{\partial \lfloor u \rfloor}{\partial a}[K]\{u\} + \frac{1}{2}\lfloor u \rfloor \frac{\partial [K]}{\partial a}\{u\} - \frac{\partial \lfloor u \rfloor}{\partial a}\{P\} - \lfloor u \rfloor \frac{\partial \{P\}}{\partial a}$$

$$= -\frac{\partial \lfloor u \rfloor}{\partial a} \underbrace{([K]\{u\} - \{P\})}_{0} + \frac{1}{2}\lfloor u \rfloor \frac{\partial [K]}{\partial a}\{u\} - \lfloor u \rfloor \frac{\partial \{P\}}{\partial a}$$

$$G = -\frac{1}{2}\lfloor u \rfloor \frac{\partial [K]}{\partial a}\{u\} + \lfloor u \rfloor \frac{\partial \{P\}}{\partial a}$$

Furthermore when the loads are constant: $\mathcal{G} = \frac{K_I^2}{E'} = -\frac{1}{2}[\mathbf{u}]^T \frac{\partial [\mathbf{K}]}{\partial a}[\mathbf{u}]$

- Only the few elements that are distrorted contribute to $\frac{\partial K}{\partial a}$
- We may not even need to form elements and assemble K for a and $a + \Delta a$ to obtain $\frac{\partial K}{\partial a}$. We can explicitly obtain $\frac{\partial k^e}{\partial a}$ for elements affected by crack growth by computing derivatives of actual geometry of the element to parent geometry.

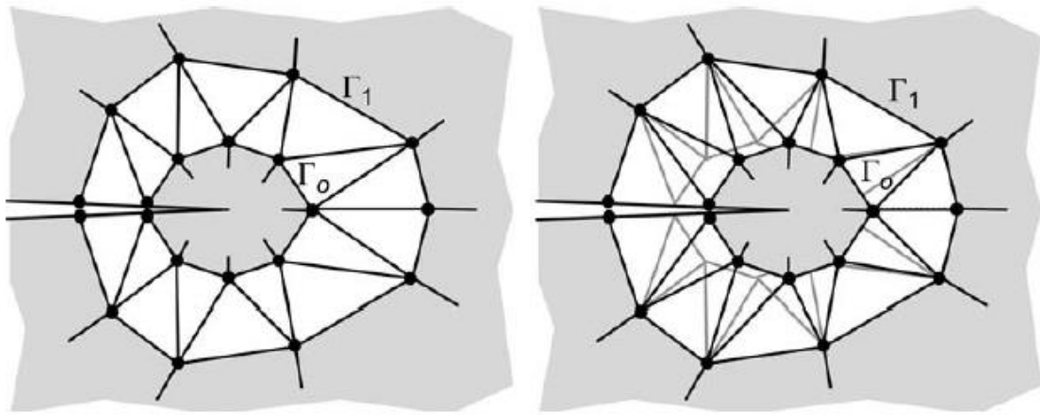

- This method is equivalent to J integral method (Park 1974)

2.2 Virtual crack extension: Mixed mode

- For LEFM energy release rates G_1 and G_2 are given by

$$J_1 = G_1 = \frac{K_I^2 + K_{II}^2}{E'} + \frac{K_{III}^2}{2\mu}$$
$$J_2 = G_2 = \frac{-2K_I K_{II}}{E'}$$

- Using Virtual crack extension (or elementary crack advance) compute G_1 and G_2 for crack lengths a, $a + \Delta a$

$$J_1 = G_1 = \frac{K_I^2 + K_{II}^2}{E'} + \frac{K_{III}^2}{2\mu}$$
$$J_2 = G_2 = \frac{-2K_I K_{II}}{E'}$$

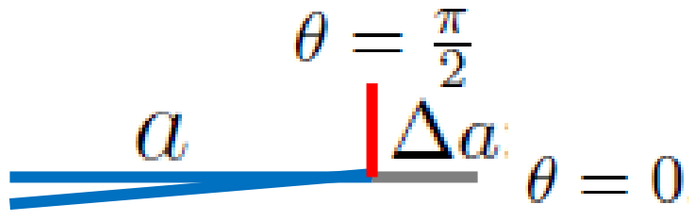

- Obtain K_I and K_{II} from:

$$K_I = \frac{s \pm \sqrt{s^2 + \frac{8G_2}{\alpha}}}{4}$$
$$K_{II} = \frac{s \mp \sqrt{s^2 + \frac{8G_2}{\alpha}}}{4}$$

Note that there are two sets of solutions!

$$s = 2\sqrt{\frac{G_1 - G_2}{\alpha}} \text{ and } \alpha = \frac{(1+\nu)(1+\kappa)}{E}$$

6.1Fracture mechanics in Finite Element Methods (FEM)

6.1.1. Introduction to Finite Element method
6.1.2. Singular stress finite elements
6.1.3. Extraction of K (SIF), G
6.1.4. J integral
6.1.5. Finite Element mesh design for fracture mechanics
6.1.6. Computational crack growth
6.1.7. Extended Finite Element Method (XFEM)

J integral

Uses of J integral:

1. LEFM: Can obtain K_I and K_{II} from J integrals (G = J for LEFM)

$$J_1 = G_1 = \frac{K_I^2 + K_{II}^2}{E'} + \frac{K_{III}^2}{2\mu}$$

$$J_2 = G_2 = \frac{-2K_I K_{II}}{E'}$$

2. Still valid for nonlinear (NLFM) and plastic (PFM) fracture mechanics

---

Methods to evaluate J integral:

1. Contour integral:

$$J_1 = \int_\Gamma \left(wdy - \mathbf{t}\frac{\partial \mathbf{u}}{\partial x} d\Gamma \right)$$

$$J_2 = \int_\Gamma \left(-wdx - \mathbf{t}\frac{\partial \mathbf{u}}{\partial y} d\Gamma \right)$$

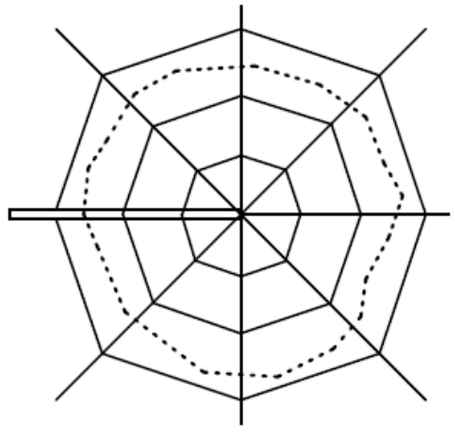

2. Equlvalent (Energy) **domain** integral (**EDI**):
   - Gauss theorem: line/surface (2D/3D) integral → surface/volume integral
   - Much simpler to evaluate computationally
   - Easy to incorporate plasticity, crack surface tractions, thermal strains, *etc.*
   - Prevalent method for computing J-integral

Line integral

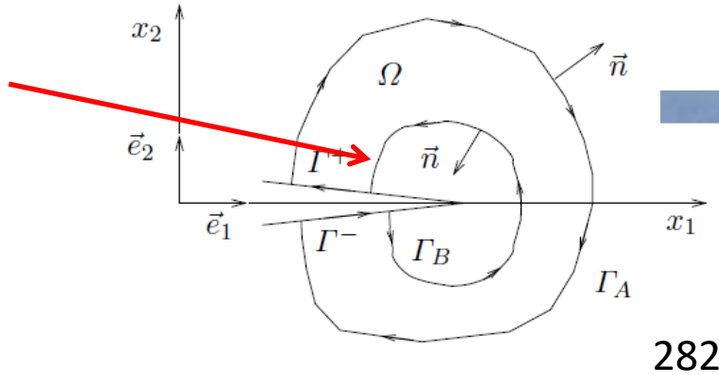

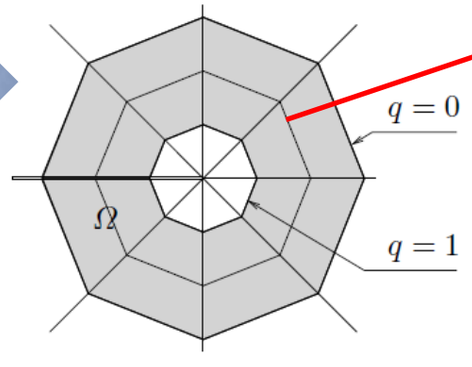

Volume integral

J integral: 1.Contour integral

- Stresses are available and also more accurate at Gauss points
- Integral path goes through Gauss points

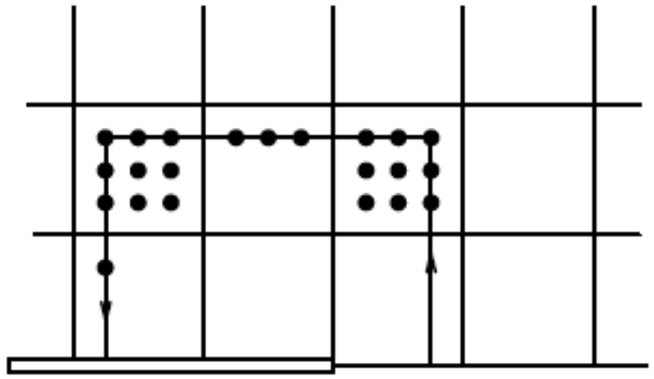

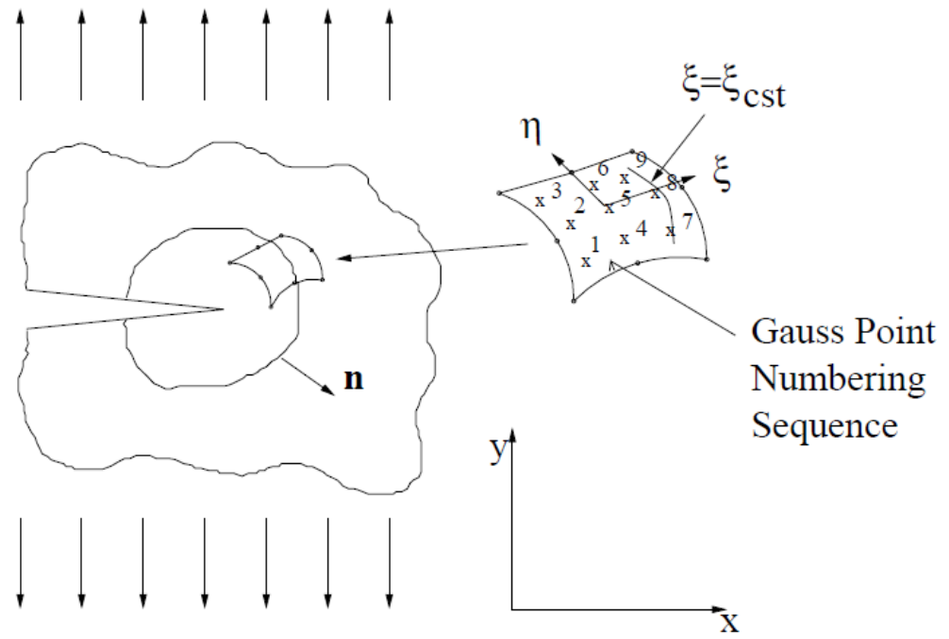

$$J = \int_\Gamma w dy - \mathbf{t} \cdot \frac{\partial \mathbf{d}}{\partial x} ds \quad \Rightarrow \quad J^e = \int_{-1}^{1} \left\{ \underbrace{\frac{1}{2}\left[\sigma_x \frac{\partial u}{\partial x} + \tau_{xy}\left(\frac{\partial u}{\partial y} + \frac{\partial v}{\partial x}\right) + \sigma_y \frac{\partial v}{\partial y}\right]}_{w} \underbrace{\frac{\partial y}{\partial \eta}}_{dy} \right.$$

$$\left. - \underbrace{\left[(\sigma_x n_1 + \tau_{xy} n_2)\frac{\partial u}{\partial x} + (\tau_{xy} n_1 + \sigma_y n_2)\frac{\partial v}{\partial x}\right]}_{\mathbf{t}\cdot\frac{\partial \mathbf{d}}{\partial x}} \underbrace{\sqrt{\left(\frac{\partial x}{\partial \eta}\right)^2 + \left(\frac{\partial y}{\partial \eta}\right)^2}}_{ds} \right\} d\eta$$

$$= \int_{-1}^{1} I \, d\eta$$

Cumbersome to formulate the integrand, evaluate normal vector, and integra over lines (2D) and surfaces (3D)

Not commonly used

J integral: 2.Equivalent Domain Integral (EDI)

General form of J integral

$$J = \lim_{\Gamma_o \to 0} \int_{\Gamma_o} \left[(w + T)\delta_{1i} - \sigma_{ij} \frac{\partial u_j}{\partial x_1} \right] n_i d\Gamma$$

$$w = \int_0^{\varepsilon_{kl}^m} \sigma_{ij} d\varepsilon_{ij}^m$$

Inelastic stress

Kinetic energy density

$$T = \frac{1}{2}\rho \frac{\partial u_i}{\partial t} \frac{\partial u_i}{\partial t}$$

Can include (visco-) plasticity, and thermal stresses

$$\varepsilon_{ij}^{total} = \varepsilon_{ij}^{e} + \varepsilon_{ij}^{p} + \alpha\Theta\delta_{ij} = \varepsilon_{ij}^{m} + \varepsilon_{kk}^{t}$$

Elastic

Plastic

Thermal (Θ temperature)

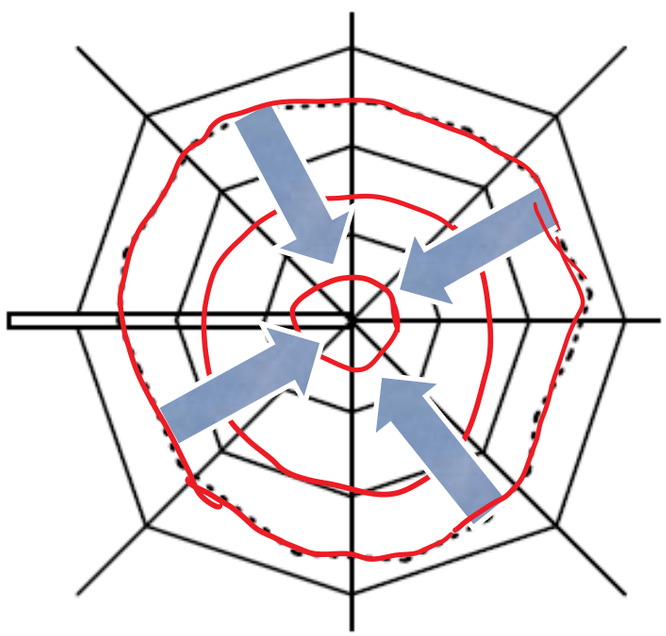

$\Gamma_o \to 0$: J contour approaches Crack tip (CT) ⇒

Accuracy of the solution deteriorates at CT ⇒

Inaccurate/Impractical evaluation of J using contour integral

J integral: 2. EDI: Derivation

Divergence theorem: Line/Surface (2D/3D) integral **~~Surface~~/Volume Integral**

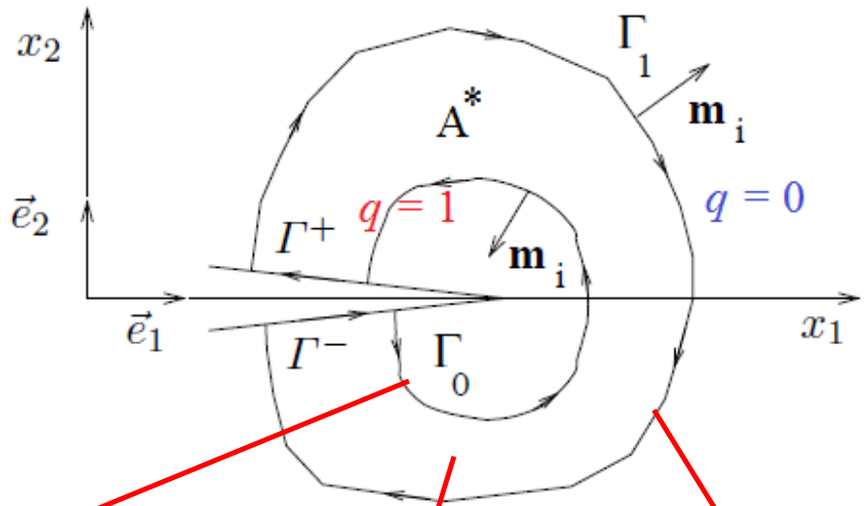

Original J integral contour

Surface integral after using divergence theorem

Application in FEM meshes

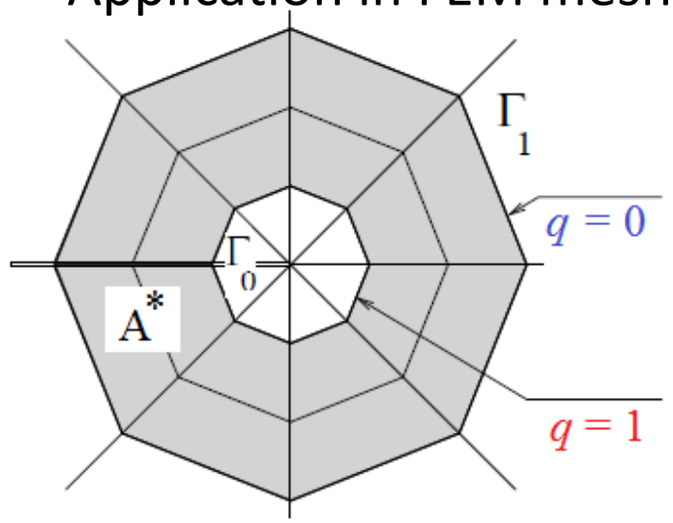

$\Gamma_o \to 0$ ⇒ 2D mesh covers crack tip

- Contour integral added to create closed surface
- By using $q = 0$ this integral in effect is zero

$$J = \int_{\Gamma_o} \left[(w+T)\delta_{1i} - \sigma_{ij} \frac{\partial u_j}{\partial x_1} \right] n_i d\Gamma = \int_{\Gamma^*} \left[\sigma_{ij} \frac{\partial u_j}{\partial x_1} - w\delta_{1i} \right] q m_i d\Gamma - \int_{\Gamma_+ + \Gamma_-} \sigma_{2j} \frac{\partial u_j}{\partial x_1} q d\Gamma$$

Zero integral on Γ_1 ($q = 0$)

⇓ Divergence theorem

$$J = \int_{A^*} \frac{\partial}{\partial x_i} \left\{ \left[\sigma_{ij} \frac{\partial u_j}{\partial x_1} - w\delta_{1i} \right] q \right\} dA - \int_{\Gamma_+ + \Gamma_-} \sigma_{2j} \frac{\partial u_j}{\partial x_1} q d\Gamma$$

J integral: 2. EDI

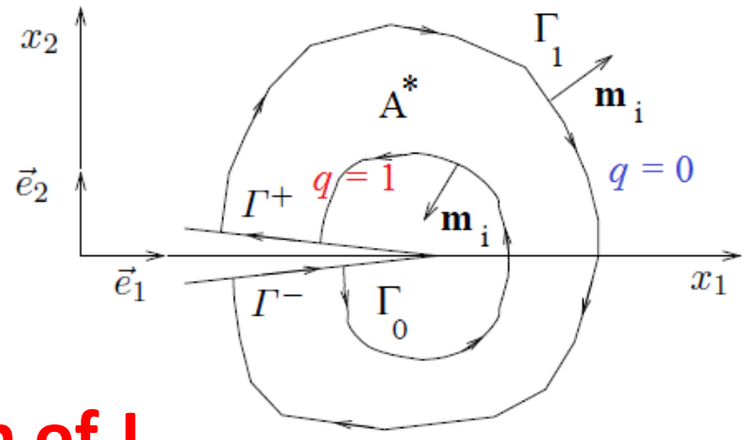

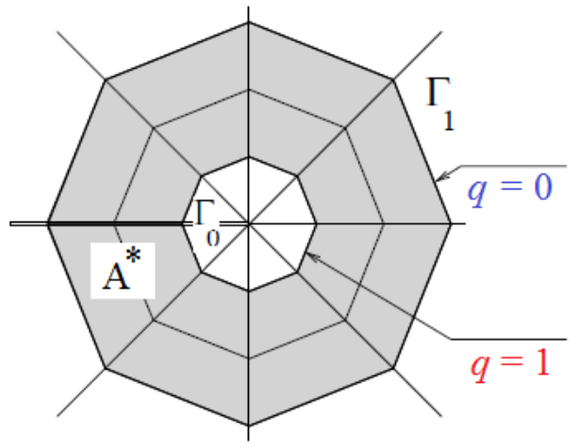

General form of J

$$J = \int_{A^*} \left\{ \left[\sigma_{ij} \frac{\partial u_j}{\partial x_1} - w\delta_{1i} \right] \frac{\partial q}{\partial x_i} + \left[\sigma_{ij} \frac{\partial \varepsilon_{ij}^p}{\partial x_1} - \frac{\partial w^p}{\partial x_1} + \alpha\sigma_{ii} \frac{\partial \Theta}{\partial x_1} - F_i \frac{\partial u_j}{\partial x_1} \right] q \right\} dA - \int_{\Gamma_+ + \Gamma_-} \sigma_{2j} \frac{\partial u_j}{\partial x_1} q \, d\Gamma$$

Plasticity effects

Thermal effects

Body force

Nonzero crack surface traction

Simplified Case:

(Nonlinear) elastic, no thermal strain, no body force, traction free crack surfaces

$$J = \int_{A^*} \left[\sigma_{ij} \frac{\partial u_j}{\partial x_1} - w\delta_{1i} \right] \frac{\partial q}{\partial x_i} dA$$

This is the same as deLorenzi's approach where finds a physical interpretation (virtual crack extension)

$$q = \frac{1}{\Delta a} \frac{\partial \Delta x_1}{\partial x_i}$$

$$\mathcal{G} = \frac{1}{\Delta a} \int_A \left(\sigma_{ij} \frac{\partial u_j}{\partial x_1} - w\delta_{i1} \right) \frac{\partial \Delta x_1}{\partial x_i} dA$$

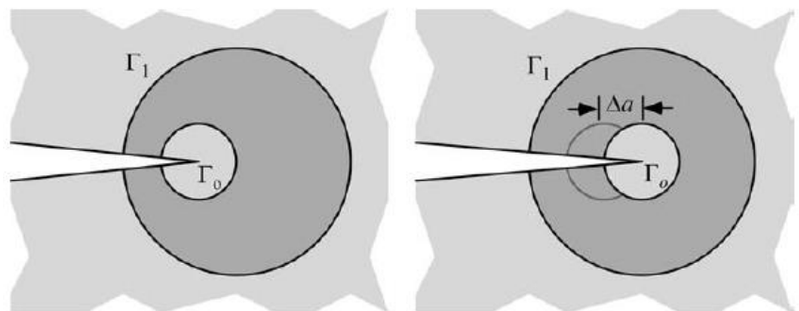

J integral: 2. EDI FEM Aspects

- Since J_0 ~~→ 0~~ the inner J_0 collapses to the crack tip (CT)
- J_1 will be formed by element edges
- By using spider web (rozet) meshes any reasonable number of layers can be used to compute J:

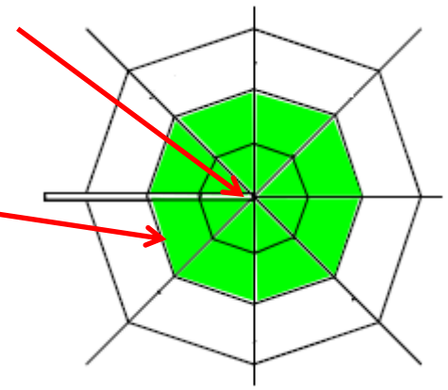

1 layer

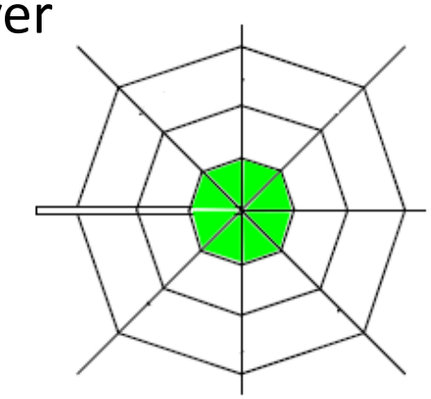

2 layer

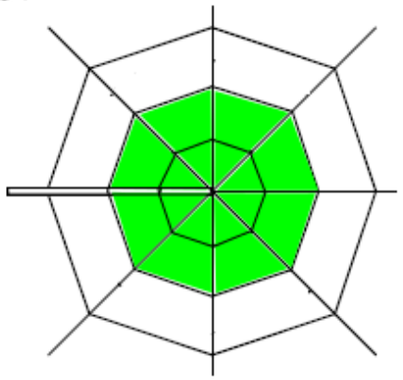

3 layer

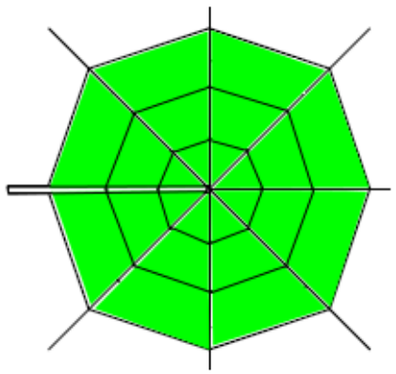

- Spider web (rozet) mesh:
  - One layer of triangular elements (preferably singular, quadrature point elements)
  - Surrounded by quad elements

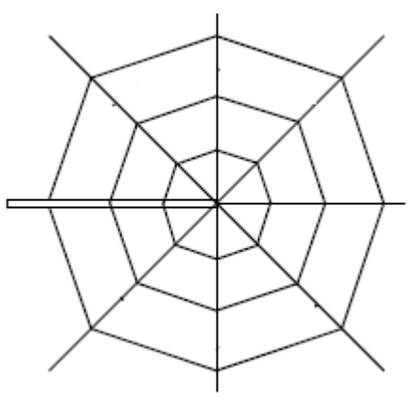

J integral: 2. EDI FEM Aspects

- Shape of decreasing function *q*:

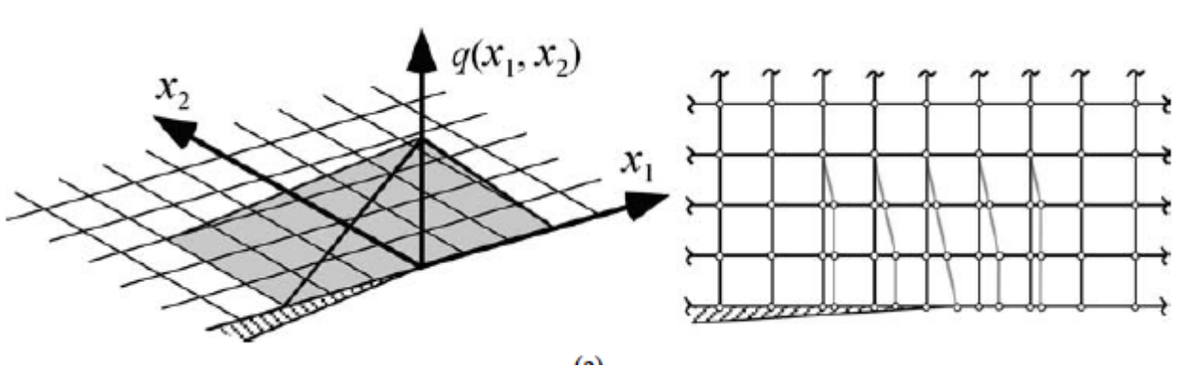

Pyramid *q* function

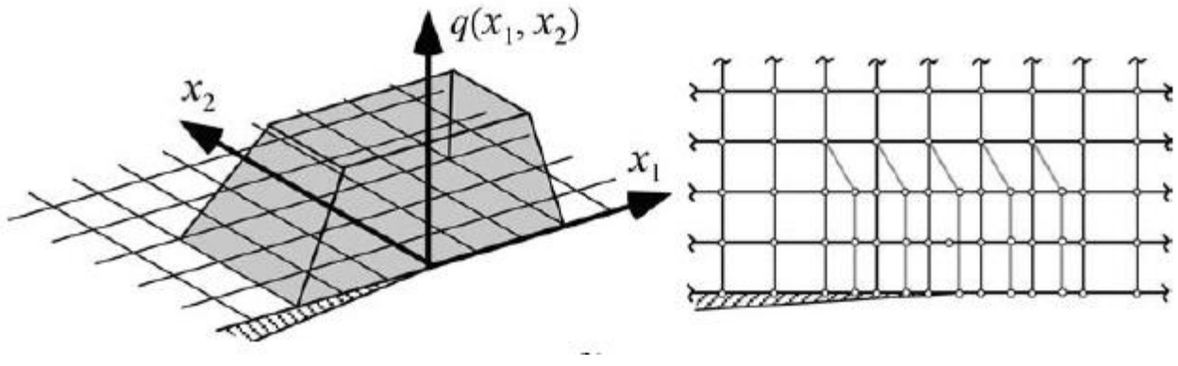

Plateau *q* function

- Plateau q function useful when inner elements are not very accurate:
  e.g. when singular/quarter point elements are not used

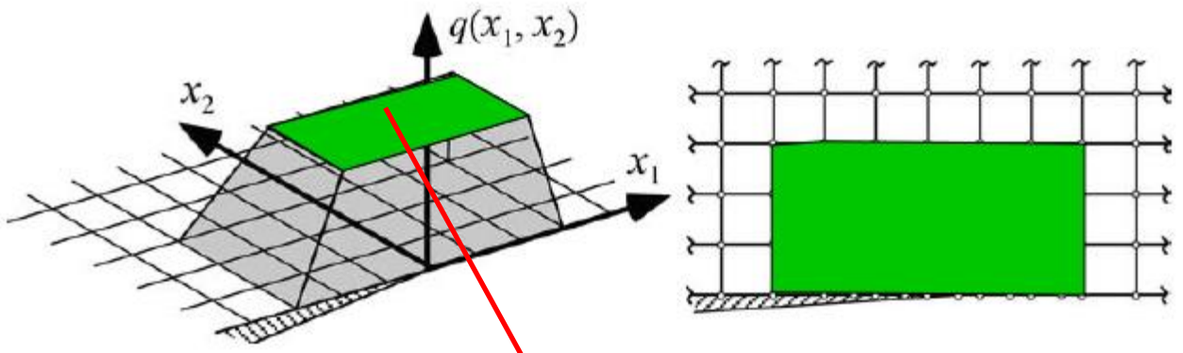

$$J = \int_{A^*} \left[\sigma_{ij} \frac{\partial u_j}{\partial x_1} - w\delta_{1i} \right] \frac{\partial q}{\partial x_i} dA$$

$$\frac{\partial q}{\partial x_i} = 0$$ These elements do not contribute to J

J integral: Mixed mode loading

- For LEFM we can obtain K_I, K_{II}, K_{III} from J_1, J_2, G_{III}:

$$\bar{J}_k \Delta L = \int_{V^*} \left(\sigma_{ij} \frac{\partial u_i}{\partial x_k} \frac{\partial q}{\partial x_j} - w \frac{\partial q}{\partial x_k} \right) dV$$

$$G_{III} = \int_{V^*} \left(\sigma_{3j} \frac{\partial u_3}{\partial x_1} \frac{\partial q}{\partial x_j} - w^{III} \frac{\partial q}{\partial x_1} \right) dV$$

$$\begin{aligned} K_I &= \frac{1}{2}\sqrt{E^*}\left(\sqrt{(J_1 - J_2 - G_3)} + \sqrt{(J_1 + J_2 - G_3)}\right) \\ K_{II} &= \frac{1}{2}\sqrt{E^*}\left(\sqrt{(J_1 - J_2 - G_3)} - \sqrt{(J_1 + J_2 - G_3)}\right) \\ K_{III} &= \sqrt{2\mu G_3} \end{aligned}$$

Nikishkov and Vainshtok 1980

$E^* = E\left[\frac{1}{1-\nu^2} + \left(\frac{\nu}{1+\nu}\right)\frac{\varepsilon_{33}}{\varepsilon_{11}+\varepsilon_{22}}\right]$ $E^* = \frac{E}{1-\nu^2}$ for plane strain and $E^* = E$ for plane stress

6.1Fracture mechanics in Finite Element Methods (FEM)

Different elements/methods to compute K

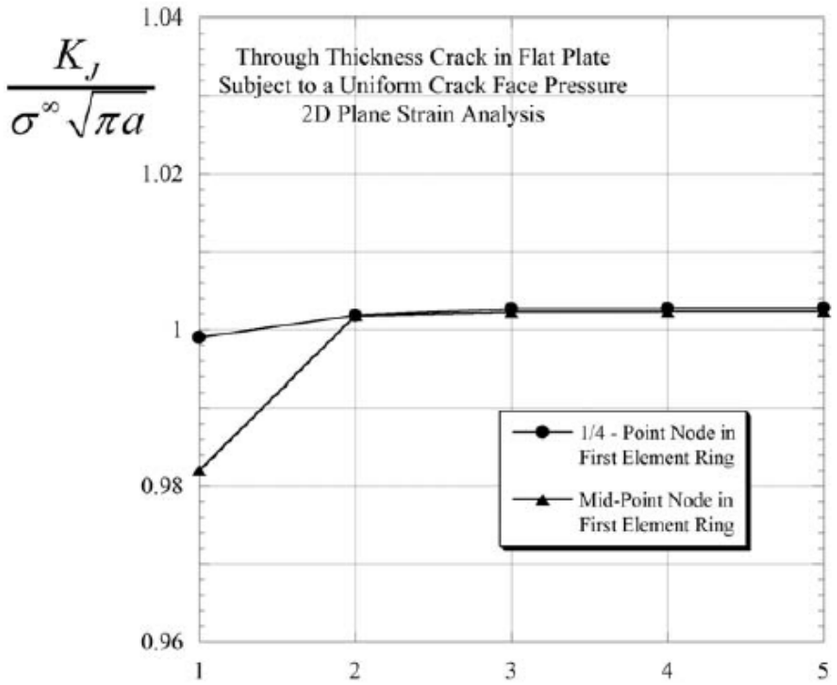

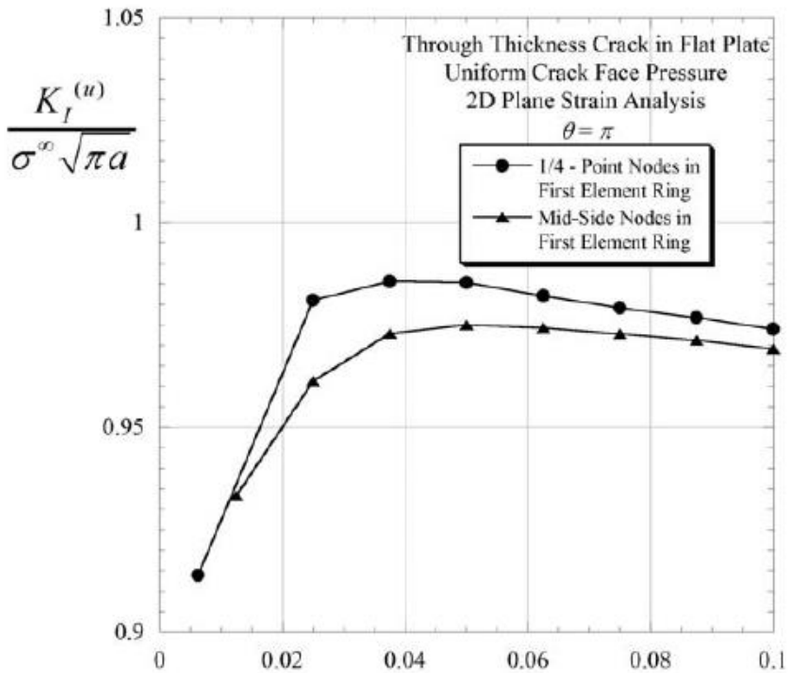

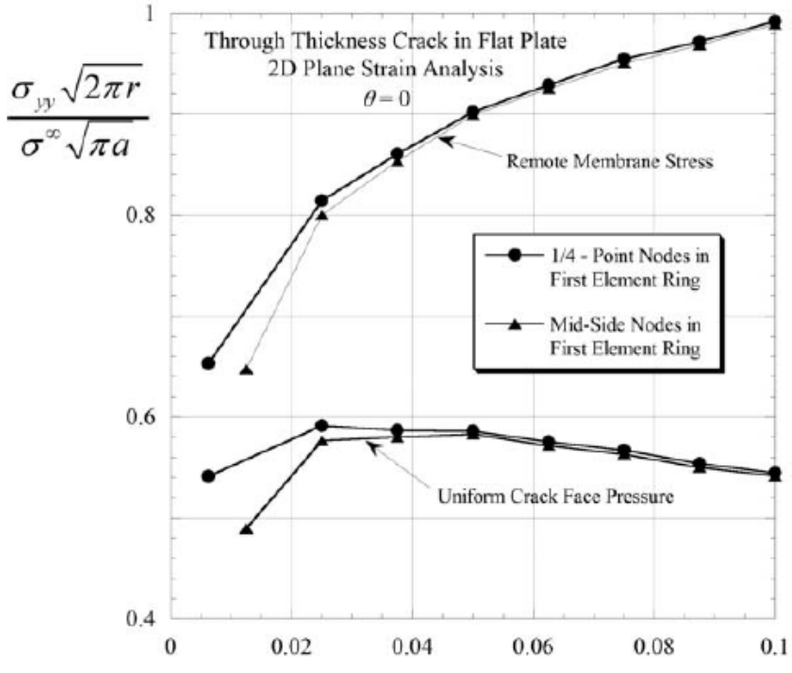

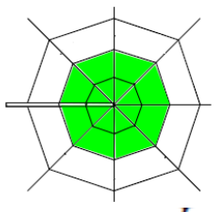

J integral EDI

$$J=\int_{A^*}\left[\sigma_{ij}\frac{\partial u_j}{\partial x_1}-w\delta_{1i}\right]\frac{\partial q}{\partial x_i}dA$$

K from displacement ***u***

$$K_I=\lim_{r\to 0}\left[\frac{E'u_y}{4}\sqrt{\frac{2\pi}{r}}\right]\quad(\theta=\pi)$$

K from stress σ

$$K_I=\lim_{r\to 0}\left(\sqrt{2\pi r}\;\sigma_{22}|_{\theta=0}\right)$$

- J integral EDI method is by far the most accurate method
- Interpolation of K from ***u*** is more accurate from σ: 1) higher convergence rate, 2) nonsingular field. Unlike σ it is almost insensitive to surface crack or far field loading
- Except the first contour (J integral) or very small *r* the choice of element has little effect

Different elements/methods to compute K: Effect of adaptivity on local field methods

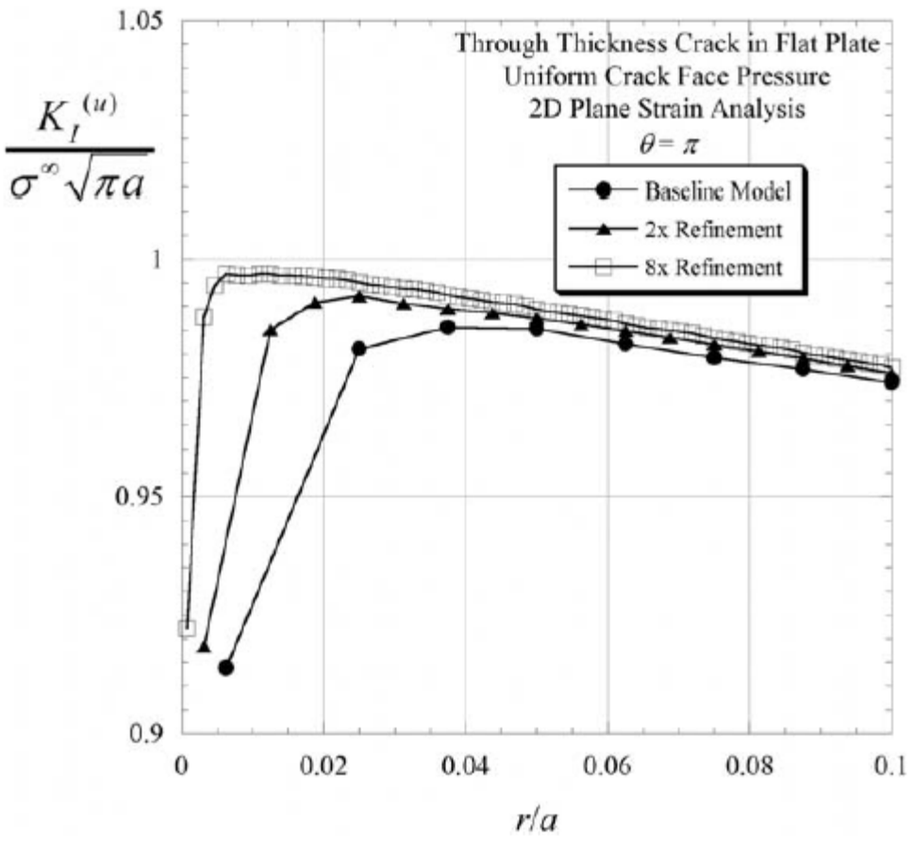

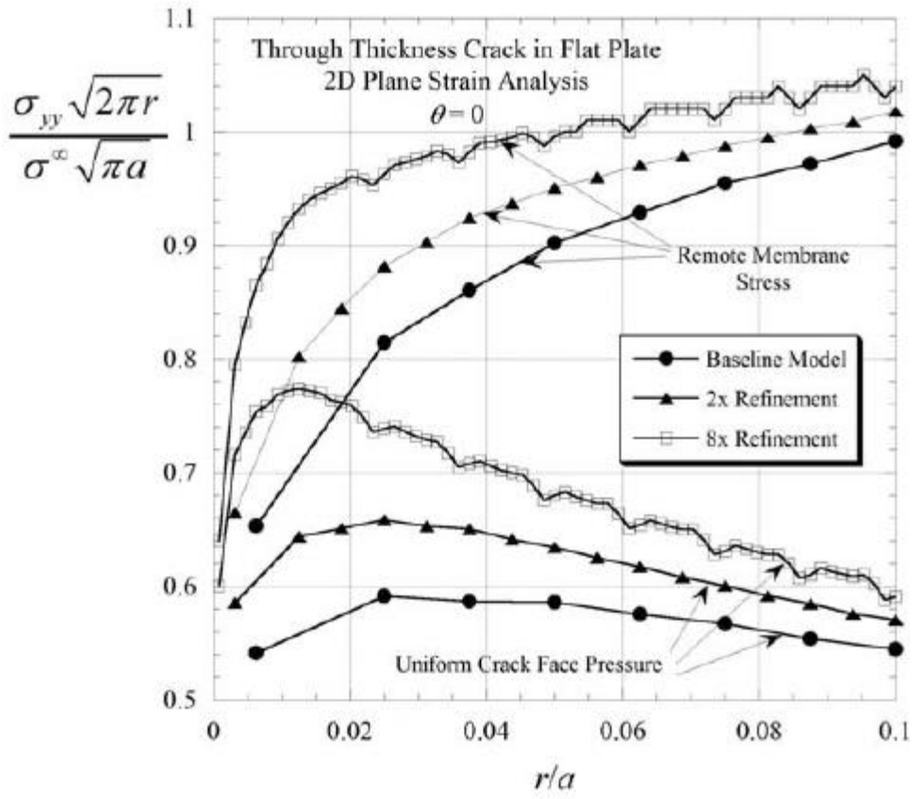

K from displacement ***u***

$$K_I = \lim_{r \to 0} \left[\frac{E' u_y}{4} \sqrt{\frac{2\pi}{r}} \right] \quad (\theta = \pi)$$

K from stress σ

$$K_I = \lim_{r \to 0} \left(\sqrt{2\pi r}\ \sigma_{22}|_{\theta=0} \right)$$

Even element h-refinement cannot improve K values by much particularly for stress based method

General Recommendations

1. Crack surface meshing:
   - Nodes in general should be duplicated:
     - Modern FEM can easily handle duplicate nodes

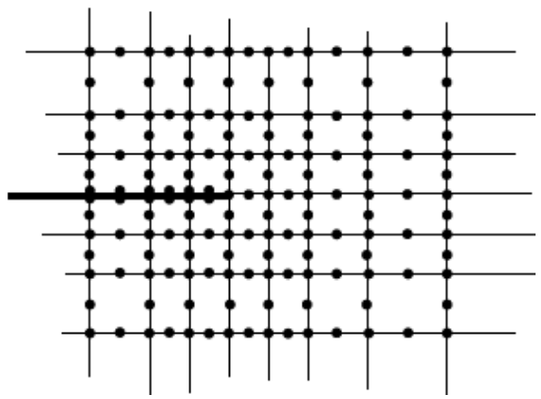

   - If not, small initial separation is initially introduced

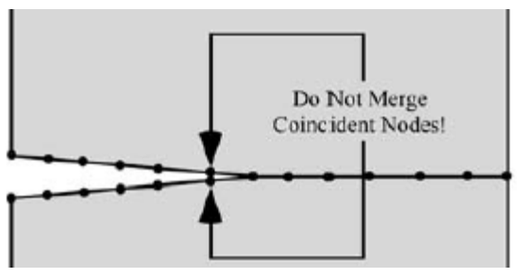

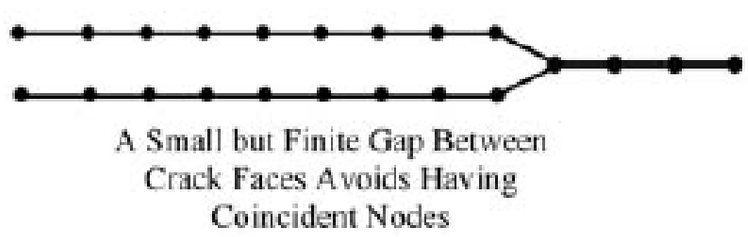

   - When large strain analysis is required, initial mesh has finite crack tip radius. The opening should be smaller than 5-10 times smaller than CTOD. Why?

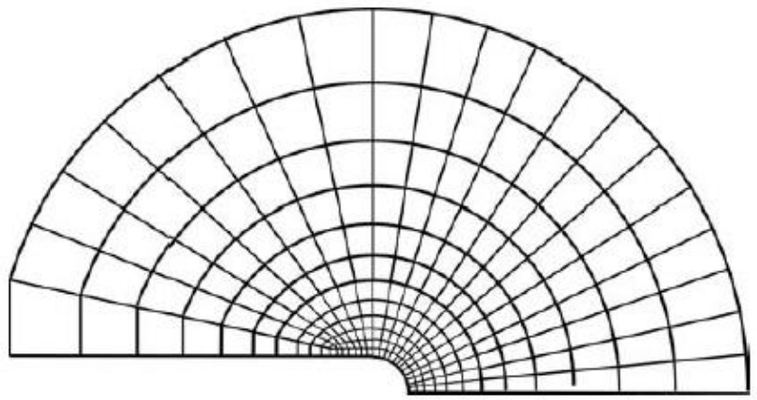

General Recommendations

2. Quarter point vs mid point elements / Collapsed elements around the crack tip

- For LEFM singular elements triangle quarter elements are better than normal tri/quad, and quarter point quad elements (collapsed or not)

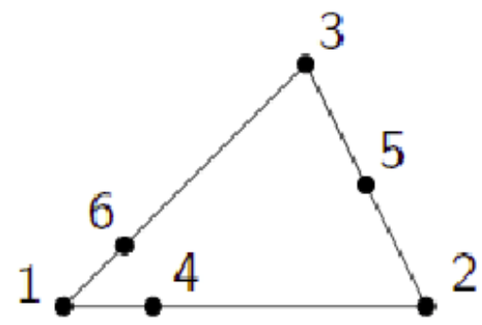

- Perturbation of quarter point by *e* results in $O(ge^2)$ error in *K* ($g = h/a$)
- For elastic perfectly plastic material collapsed quad elements (1st / 2nd order) are recommended

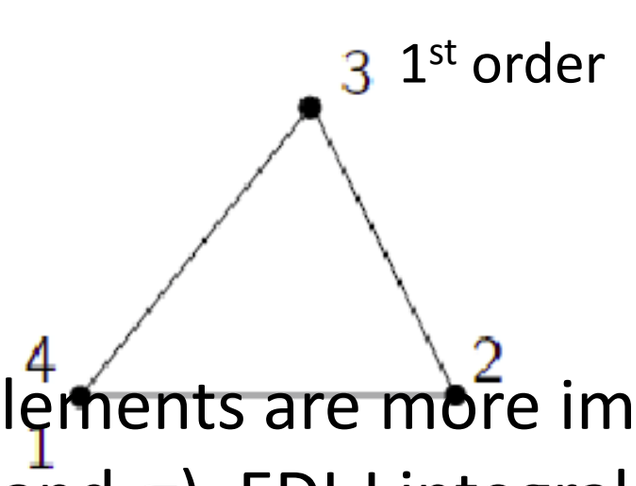

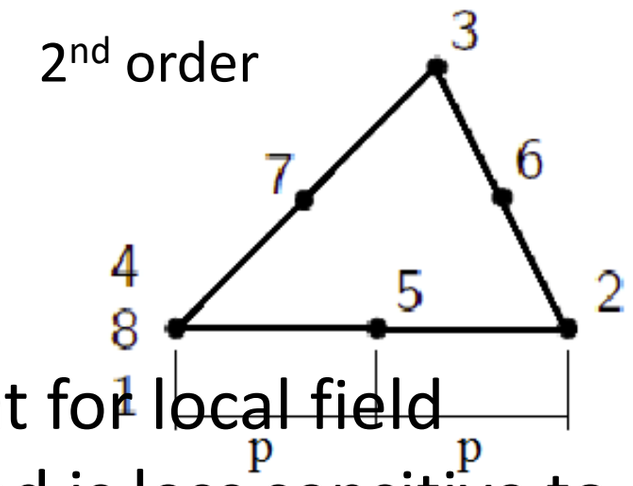

- Use of crack tip singular elements are more important for local field interpolation methods (***u*** and σ). EDI J integral method is less sensitive to accuracy of the solution except the 1st contour is used.

General Recommendations

3. Shape of the mesh around a crack tip

a) Around the crack tip triangular singular elements are recommended (little effect for EDI J integral method)
b) Use quad elements (2nd order or higher) around the first contour
c) Element size: Enough number of elements should be used in region of interest: r_s, r_p, large strain zone, etc.
d) Use of transition elements away from the crack tip although increases the accuracy has little effect

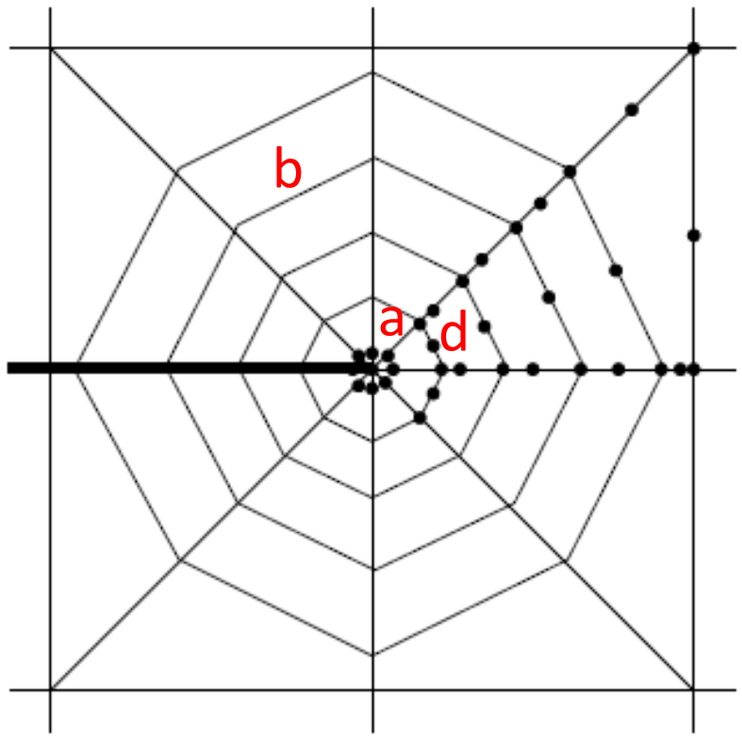

Spider-web mesh (rozet)

General Recommendations

4. Method for computing *K*

- Energy methods such as J integral and G virtual crack extension (virtual stiffness derivative) are more reliable
  - J integral EDI is the most accurate and versatile method
    - Least sensitive method to accuracy of FEM solution at CT particularly if plateau q is used

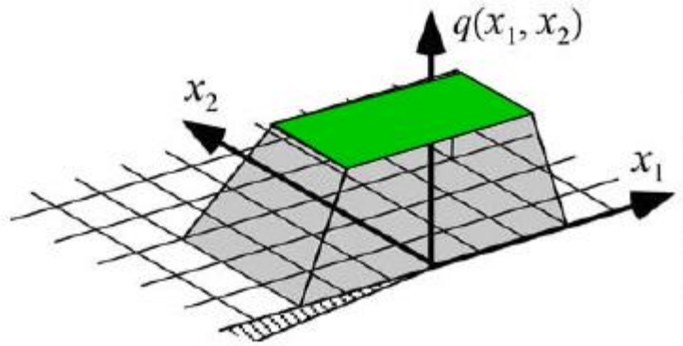

- K based on local fields is the least accurate and most sensitive to CT solution accuracy.
  - Particularly stress based method is not recommended.
  - Singular/ quarter point elements are recommended for these methods especially when *K* is obtained at very small *r*

6.1Fracture mechanics in Finite Element Methods (FEM)

6.1.1. Introduction to Finite Element method
6.1.2. Singular stress finite elements
6.1.3. Extraction of K (SIF), G
6.1.4. J integral
6.1.5. Finite Element mesh design for fracture mechanics
6.1.6. Computational crack growth
6.1.7. Extended Finite Element Method (XFEM)

What's wrong with FEM for crack problems

- Element edges must conform to the crack geometry: make such a mesh is time-consuming, especially for 3D problems.
- Remeshing as crack advances: difficult. Example:

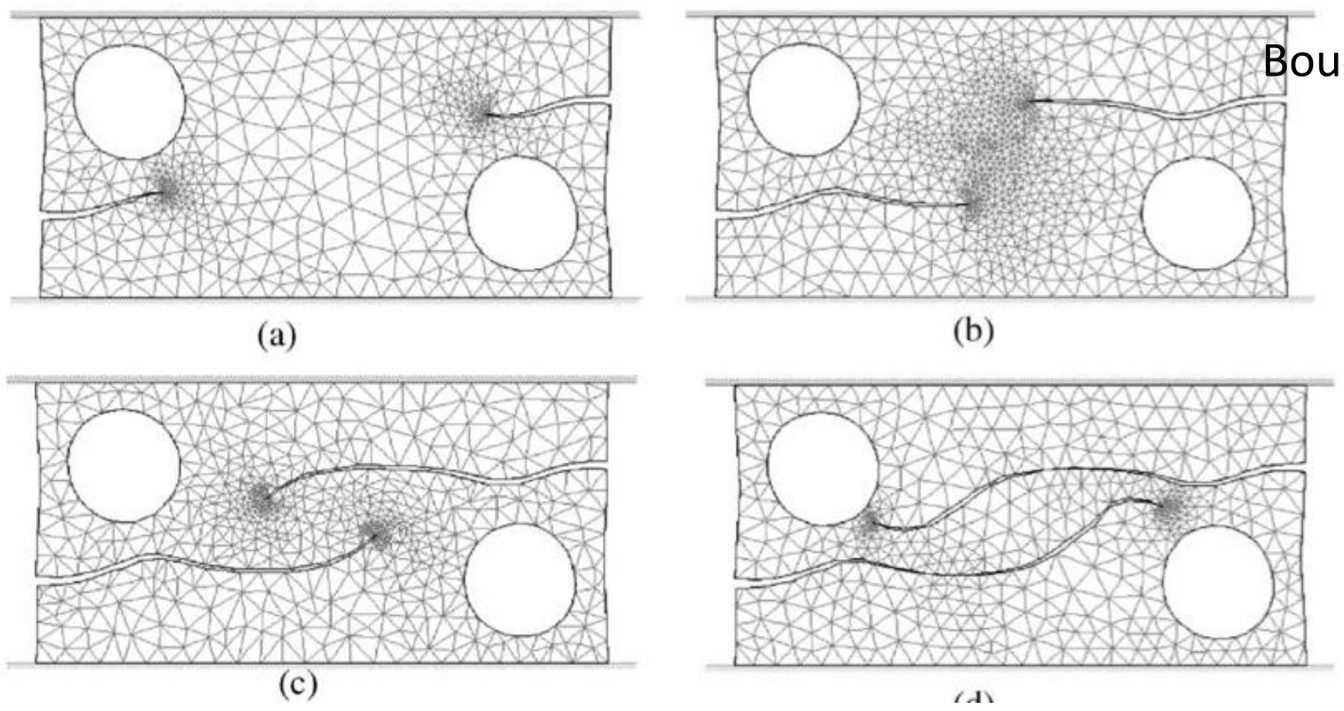

Bouchard et al. CMAME 2003

Capturing/tracking cracks

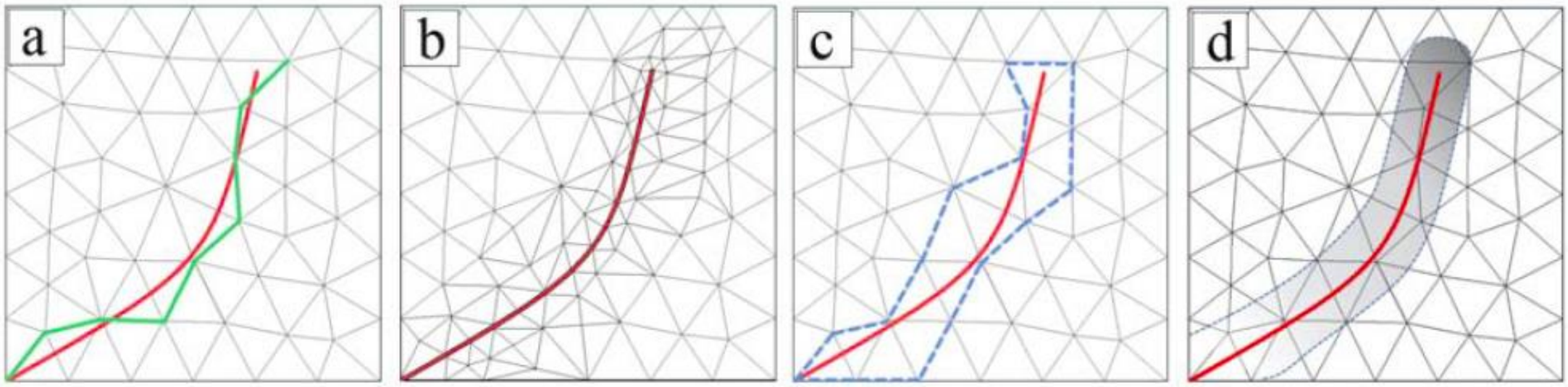

Fixed mesh

Crack tracking

XFEM enriched elements

Brief overview in the next section

Crack/void capturing by bulk damage models

Brief overview in continuum damage models

Fixed meshes

- Nodal release method (typically done on fixed meshes)
  - Crack advances one element edge at a time by releasing FEM nodes
  - Crack path is restricted by discrete geometry

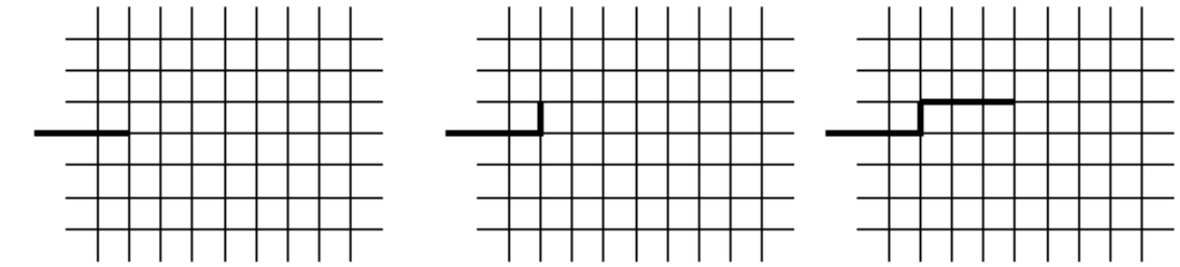

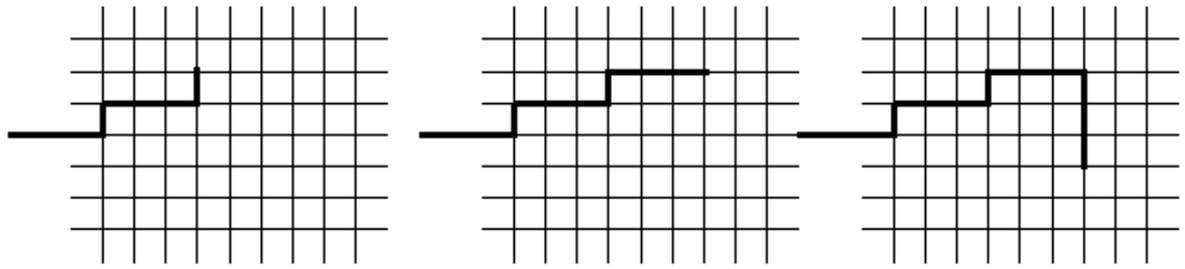

- Also for cohesive elements they can be used for both extrinsic and intrinsic schemes. For intrinsic ones, cohesive surfaces between all elements induces an artificial compliance (will be explained later)

Adaptive meshes

- Adaptive operations align element boundaries with crack direction

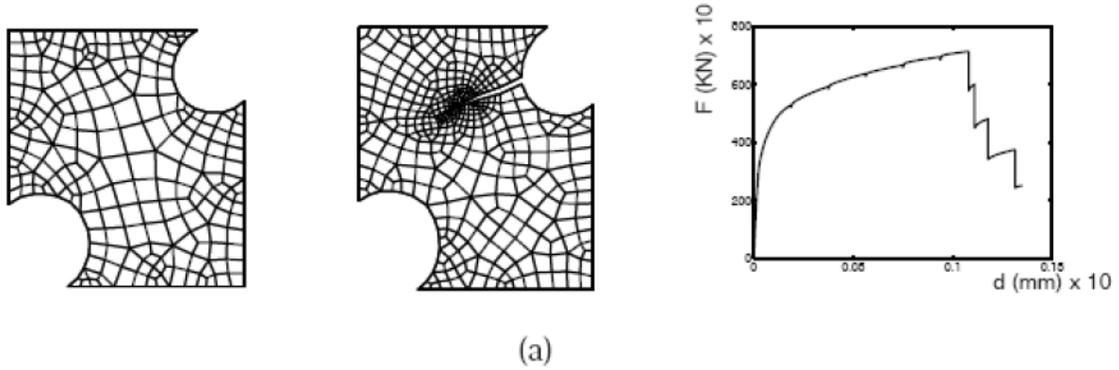

(a)

Element splitting:

Smoother crack path by element splitting: cracks split through and propagate between newly generated elements

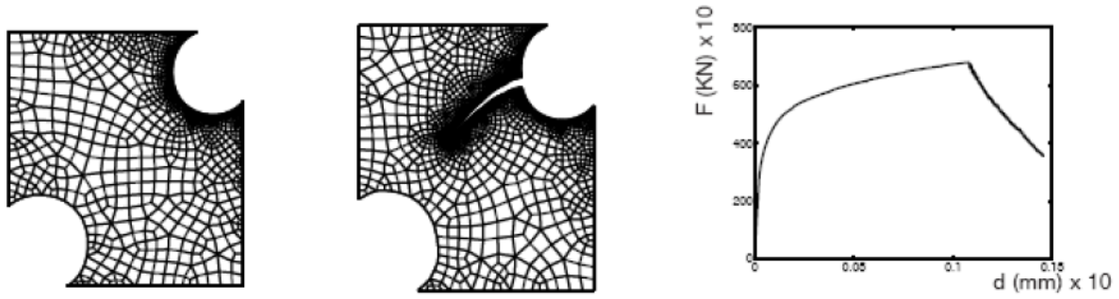

Abedi:2010

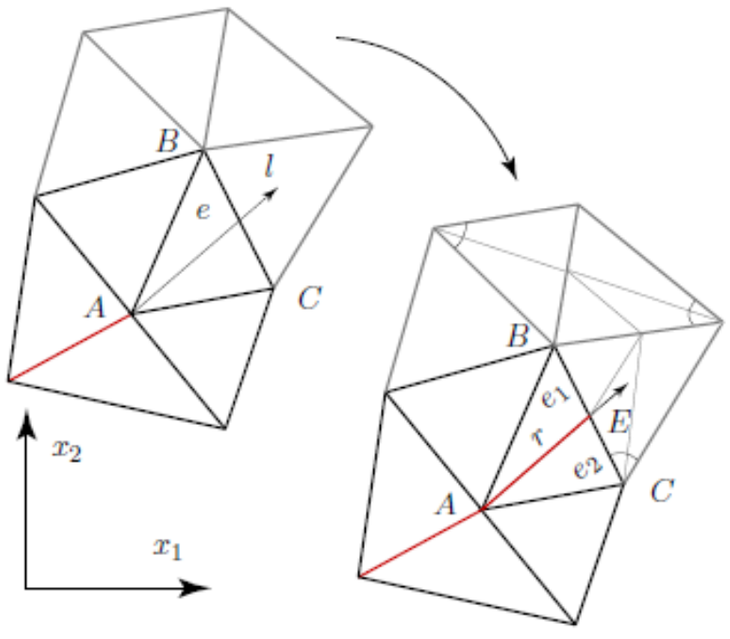

Cracks generated by refinement options

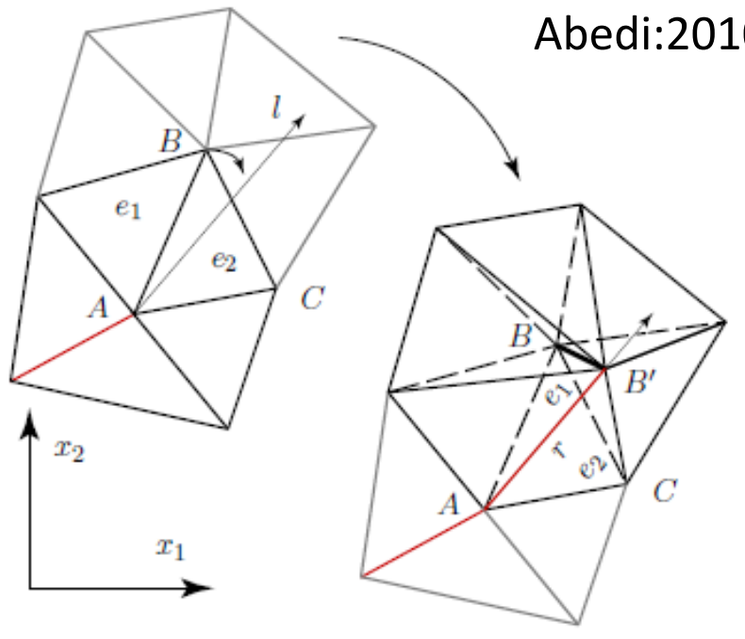

Element edges move to desired direction

6.1Fracture mechanics in Finite Element Methods (FEM)

6.1.1. Introduction to Finite Element method
6.1.2. Singular stress finite elements
6.1.3. Extraction of K (SIF), G
6.1.4. J integral
6.1.5. Finite Element mesh design for fracture mechanics
6.1.6. Computational crack growth
6.1.7. Extended Finite Element Method (XFEM)

Finite Elements for singular crack tip solutions

$$u = \frac{K_I}{2\mu}\sqrt{\frac{r}{2\pi}}\cos\frac{\theta}{2}\left(\kappa - 1 + 2\sin^2\frac{\theta}{2}\right)$$
$$v = \frac{K_I}{2\mu}\sqrt{\frac{r}{2\pi}}\sin\frac{\theta}{2}\left(\kappa + 1 - 2\cos^2\frac{\theta}{2}\right)$$

- Direct incorporation of singular terms: e.g. enriched elements by Benzley (1974), shape functions are enriched by K_I, K_{II} singular terms
  - XFEM method falls into this group (discussed later)

$$u_i = \sum_{k=1}^{4} f_k \bar{u}_{ik} + K_{\mathrm{I}}\left(Q_{1i}\sum_{k=1}^{4} f_k \bar{Q}_{1ik}\right) + K_{\mathrm{II}}\left(Q_{2i}\sum_{k=1}^{4} f_k \bar{Q}_{2ik}\right)$$

$$Q_{ij} = \frac{u_{ij}}{k_i}$$

$$u' = \left(1 + \frac{2x}{L} - 3\sqrt{\frac{x}{L}}\right)u_1' + \left(4\sqrt{\frac{x}{L}} - 4\frac{x}{L}\right)u_2' + \left(\frac{2x}{L} - \sqrt{\frac{x}{L}}\right)u_3'$$

More accurate

- Quarter point (LEFM) and Collapsed half point (Elastic-perfectly plastic) elements: By appropriate positioning of isoparametric element nodes create strain singularities

Can be easily used in FEM software

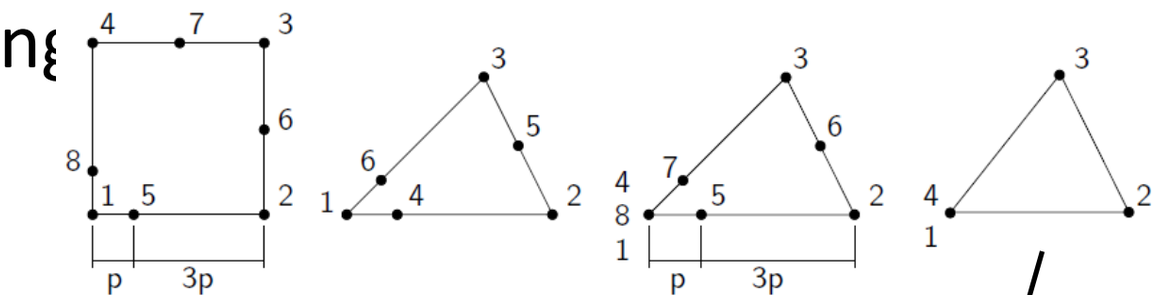

LEFM: $\epsilon, \sigma : \frac{1}{\sqrt{r}}$ singular

Elastic-perfectly plastic: $\epsilon : \frac{1}{r}$ singular

Extended Finite Element Method (XFEM)

Belytschko et al 1999

set of enriched nodes

$$\mathbf{u}^h(\mathbf{x}) = \sum_{I \in \mathcal{S}} N_I(\mathbf{x})\mathbf{u}_I + \sum_{J \in \mathcal{S}^c} N_J(\mathbf{x})\Phi(\mathbf{x})\mathbf{a}_J$$

standard part enrichment part

Partition of Unity (PUM)

enrichment function

$$\sum_J N_J(\mathbf{x}) = 1 \longrightarrow \sum_J N_J(\mathbf{x})\Phi(\mathbf{x}) = \Phi(\mathbf{x})$$

$\Phi(\mathbf{x})$ known characteristics of the problem (crack tip singularity, displaceme jump etc.) into the approximate space.

XFEM: enriched nodes

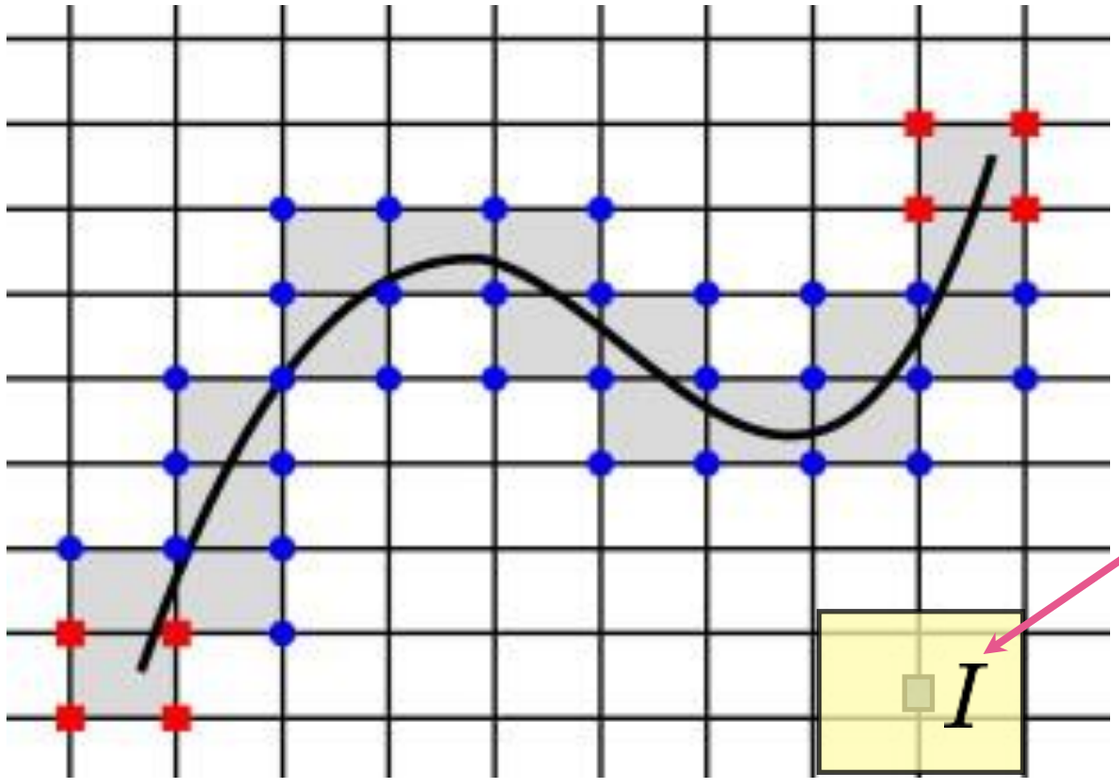

nodal support

$$N_I(\mathbf{x}) \neq 0$$

$$\sum_J N_J(\mathbf{x})\Phi(\mathbf{x}) = \Phi(\mathbf{x})$$

enriched nodes = nodes whose support is cut by the item to be enriched

enriched node I: standard degrees of freedoms (dofs) and additional dofs

XFEM for LEFM

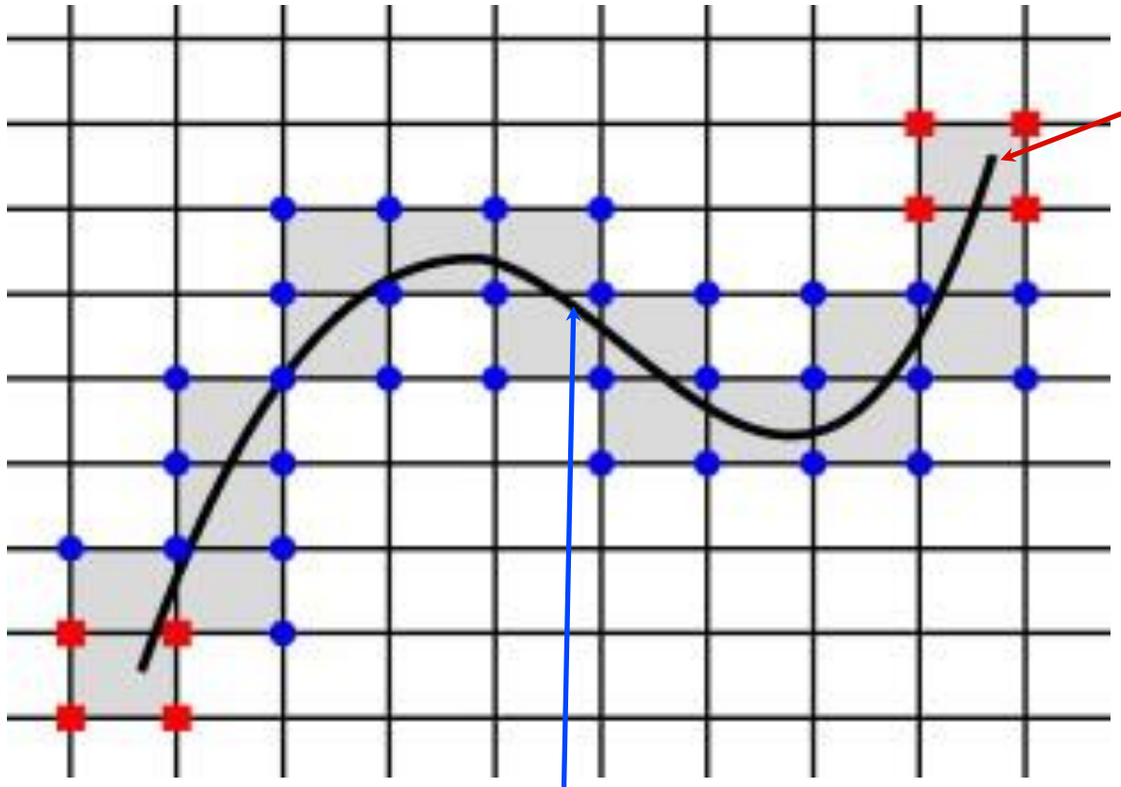

crack tip with known displacement

$$u = \frac{K_I}{2\mu}\sqrt{\frac{r}{2\pi}}\cos\frac{\theta}{2}\left(\kappa - 1 + 2\sin^2\frac{\theta}{2}\right)$$
$$v = \frac{K_I}{2\mu}\sqrt{\frac{r}{2\pi}}\sin\frac{\theta}{2}\left(\kappa + 1 - 2\cos^2\frac{\theta}{2}\right)$$

$$\Phi_1 = f(\sqrt{r}, \theta)$$

crack edge

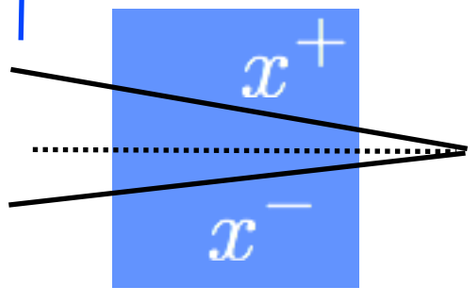

displacement: discontinuous across crack edge

$$\Phi_2 : \Phi_2(x^+) \neq \Phi_2(x^-)$$

XFEM for LEFM (cont.)

Crack tip enrichment functions:

$$u = \frac{K_I}{2\mu}\sqrt{\frac{r}{2\pi}}\cos\frac{\theta}{2}\left(\kappa - 1 + 2\sin^2\frac{\theta}{2}\right)$$
$$v = \frac{K_I}{2\mu}\sqrt{\frac{r}{2\pi}}\sin\frac{\theta}{2}\left(\kappa + 1 - 2\cos^2\frac{\theta}{2}\right)$$

$$[B_\alpha] = \left[\sqrt{r}\sin\frac{\theta}{2}, \sqrt{r}\cos\frac{\theta}{2}, \sqrt{r}\sin\frac{\theta}{2}\sin\theta, \sqrt{r}\cos\frac{\theta}{2}\sin\theta\right]$$

Crack edge enrichment functions:

$$H(\mathbf{x}) = \begin{cases} +1 & \text{if } (\mathbf{x} - \mathbf{x}^*)\cdot\mathbf{n} \geq 0 \\ -1 & \text{otherwise} \end{cases}$$

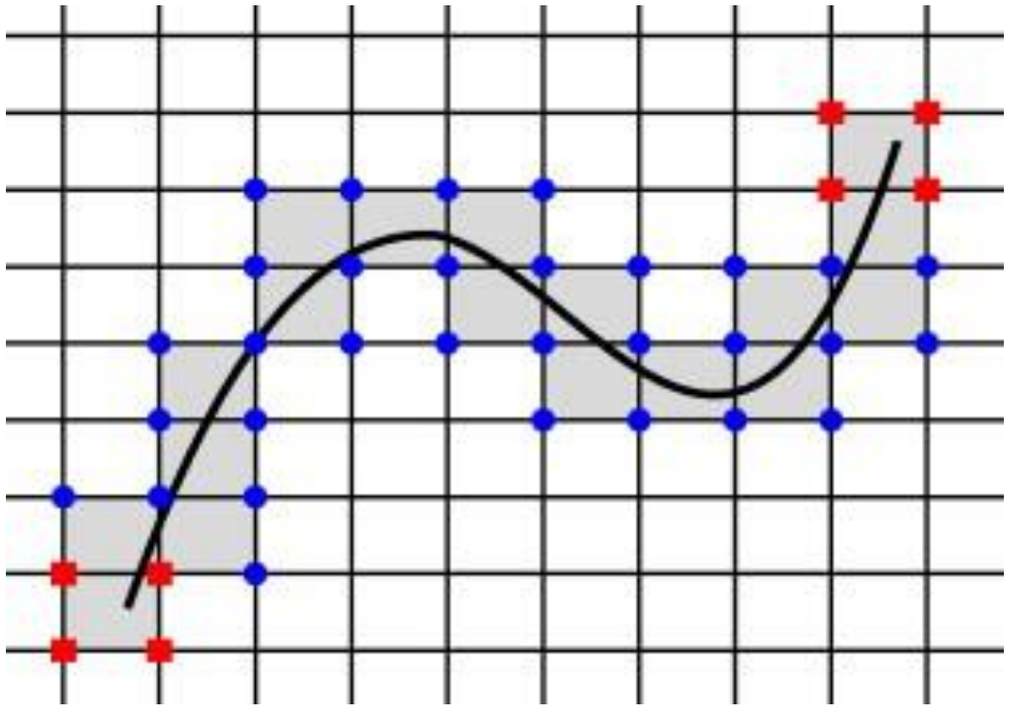

S^c	blue nodes
S^t	red nodes

$$\mathbf{u}^h(\mathbf{x}) = \sum_{I\in\mathcal{S}} N_I(\mathbf{x})\mathbf{u}_I + \sum_{J\in\mathcal{S}^c} N_J(\mathbf{x})H(\mathbf{x})\mathbf{a}_J + \sum_{K\in\mathcal{S}^t} N_K(\mathbf{x})\left(\sum_{\alpha=1}^{4} B_\alpha \mathbf{b}_K^\alpha\right)$$

XFEM for cohesive cracks

Wells, Sluys, 2001

$$\mathbf{u}^h(\mathbf{x}) = \sum_{I \in \mathcal{S}} N_I(\mathbf{x}) \mathbf{u}_I + \sum_{J \in \mathcal{S}^c} N_J(\mathbf{x}) H(\mathbf{x}) \mathbf{a}_J$$

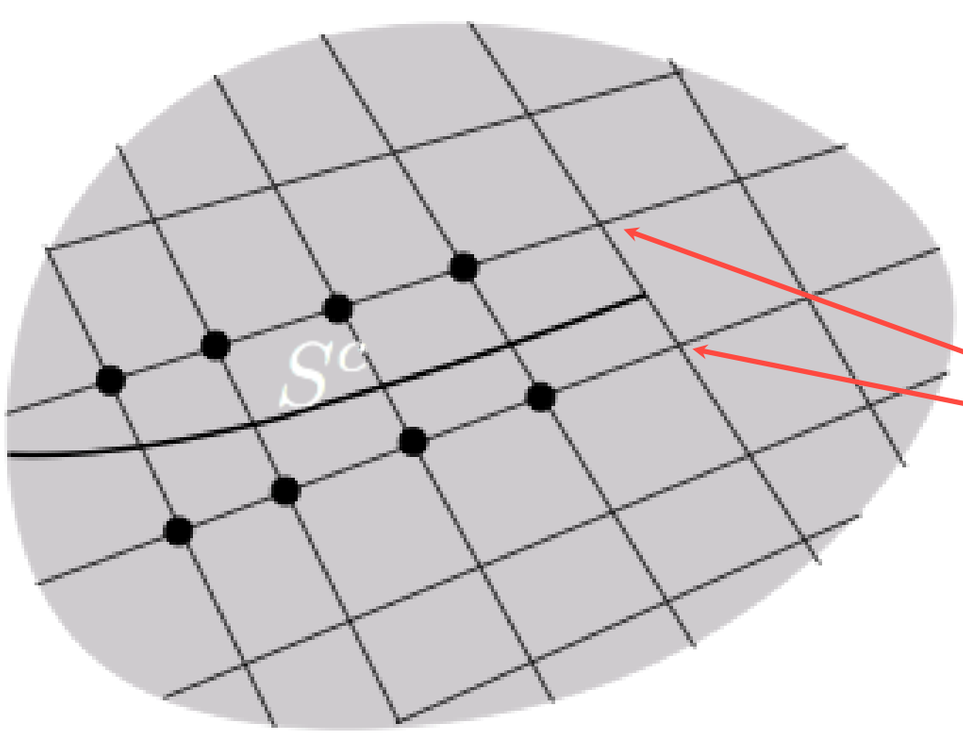

No crack tip solution is known, no tip enrichment!!!

not enriched to ensure zero crack tip opening!!!

$$H(\mathbf{x}) = \begin{cases} +1 & \text{if } (\mathbf{x} - \mathbf{x}^*) \cdot \mathbf{n} \geq 0 \\ -1 & \text{otherwise} \end{cases}$$

XFEM: examples

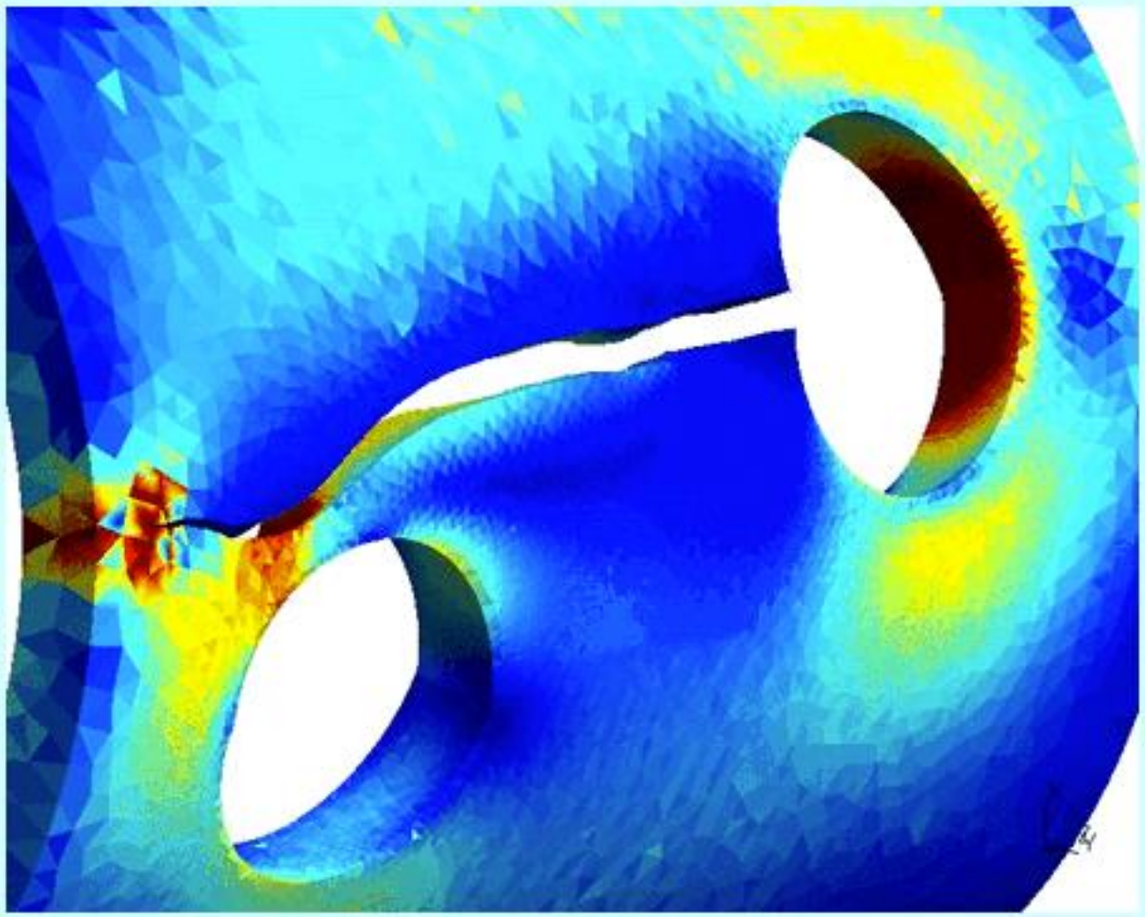

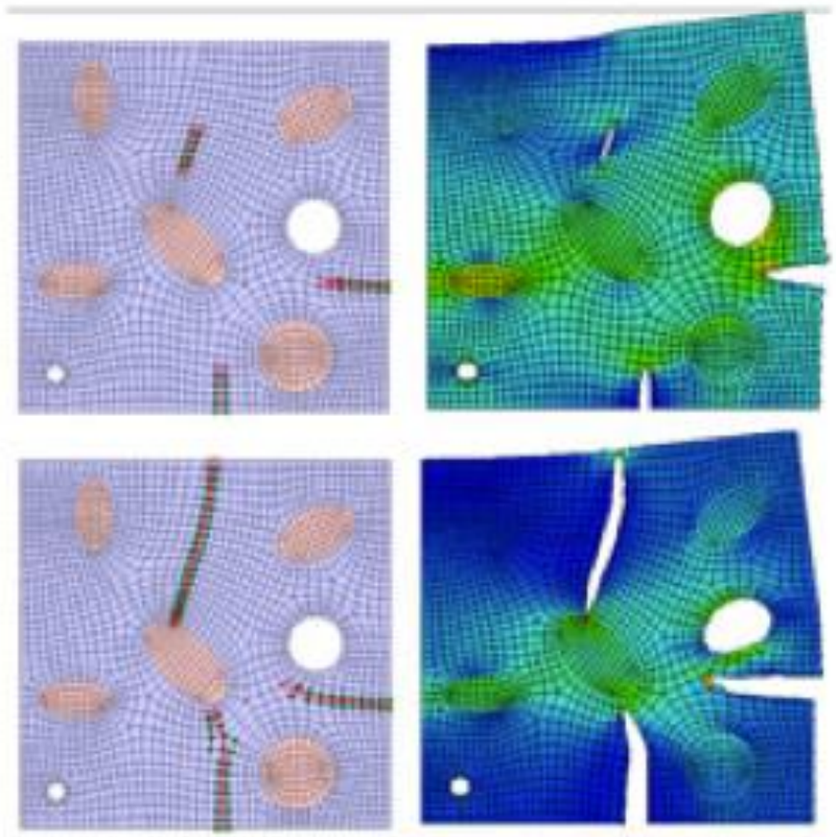

CENAERO, M. Duflot

Northwestern Univ.

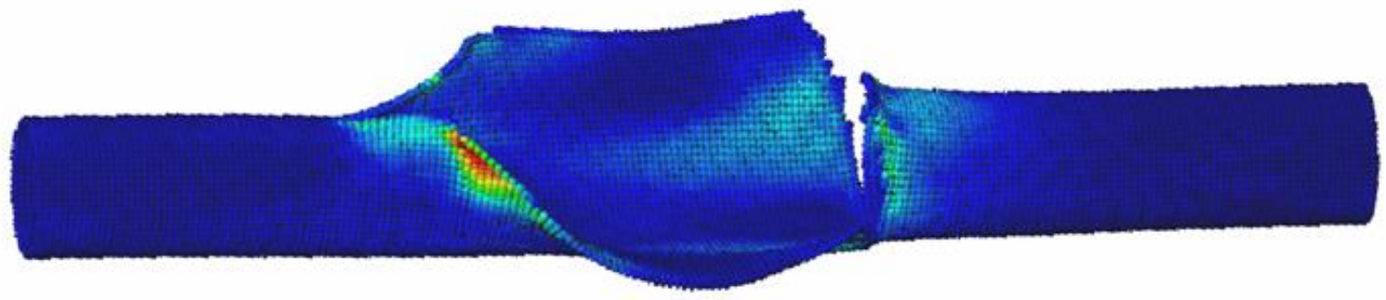

Meshfree methods

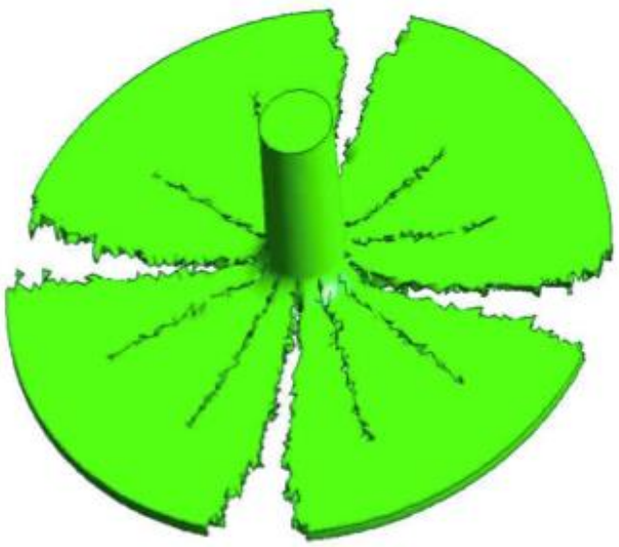

Bordas et al.

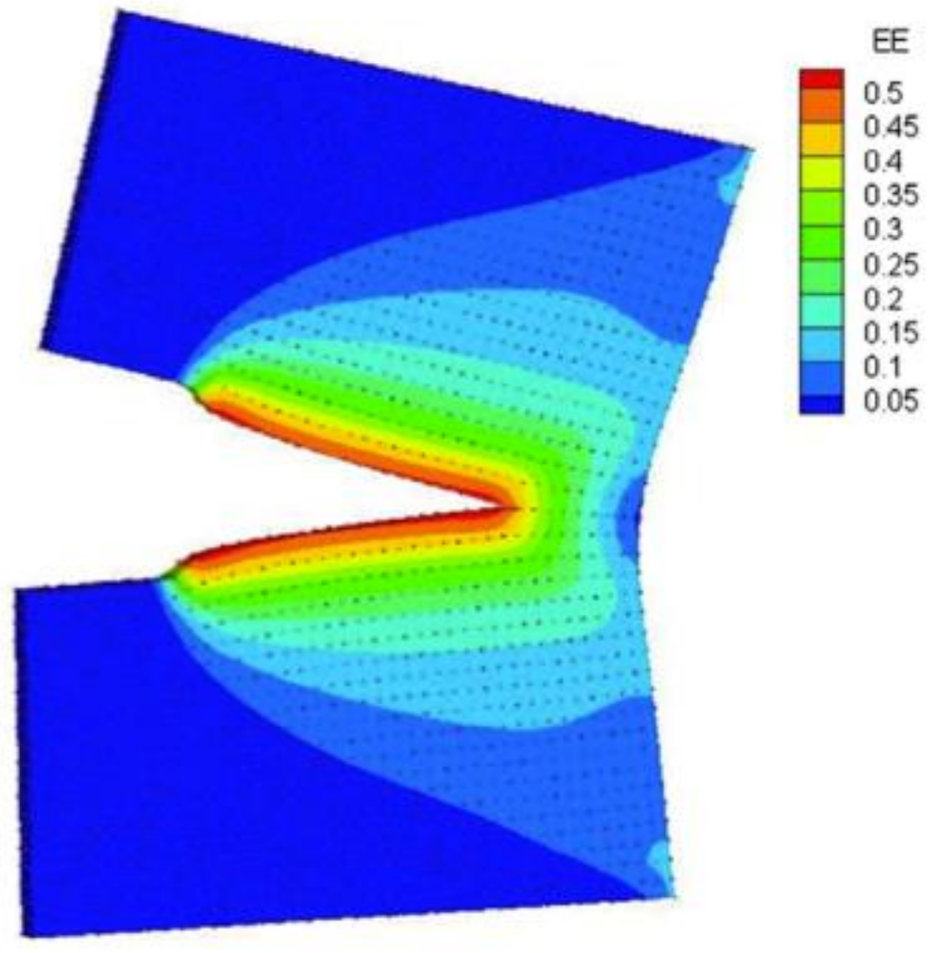

Elastic-plastic fracture

Shaofan Li 2012

6.2. Traction Separation Relations (TSRs)

Cohesive models

- Cohesive models remove stress singularity predicted by Linear Elastic Fracture Mechanics (LEFM)

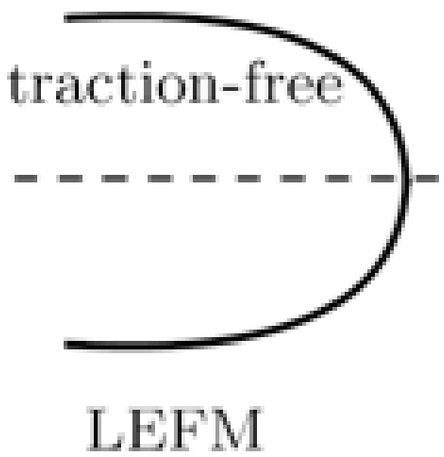

LEFM

$$s \propto \frac{1}{\sqrt{r}}$$

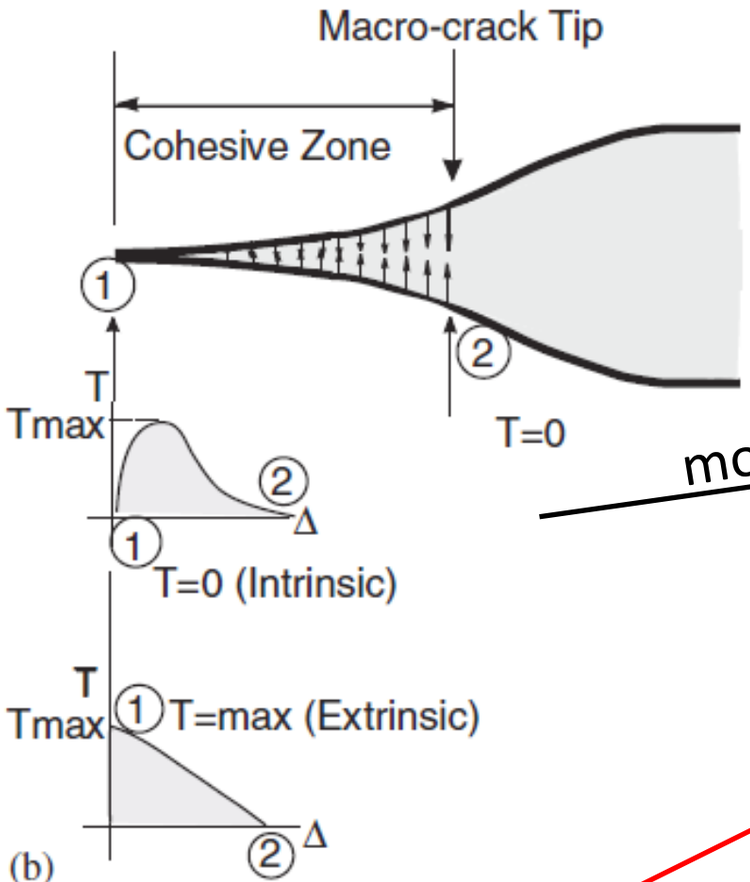

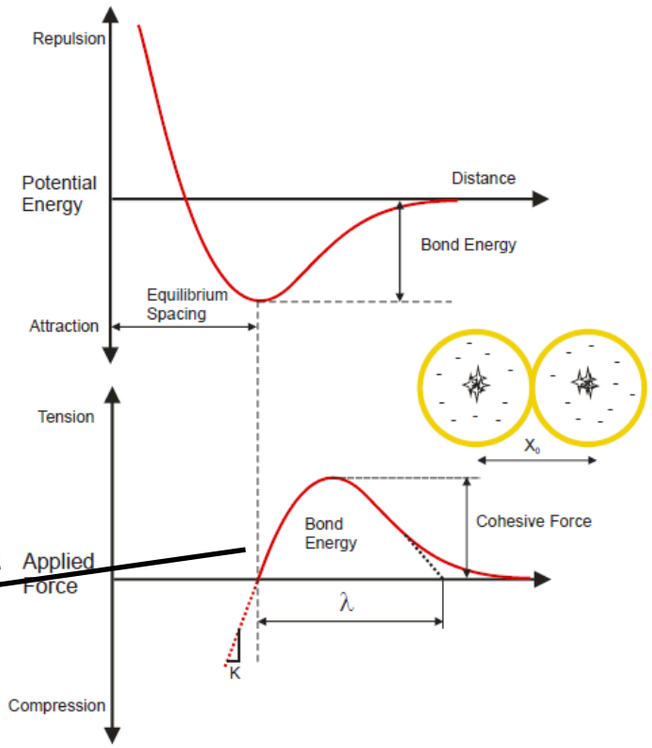

motivation

$\tilde{\sigma}$: Stress scale

$\tilde{\delta}$: Displacement scale

Λ : Length scale

$$\mathbf{s} = \tilde{\sigma}\mathbf{f}(\Delta\mathbf{u}/\tilde{\delta})$$

Traction is related to displacement jump across fracture surface

Sample applications of cohesive models

fracture of polycrystalline material

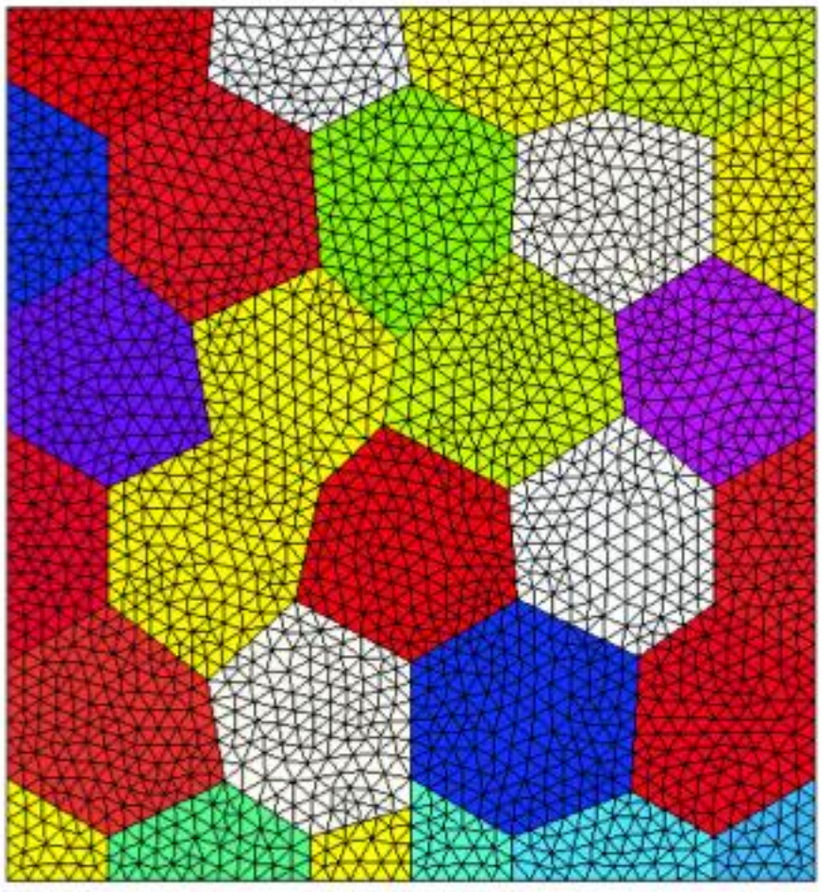

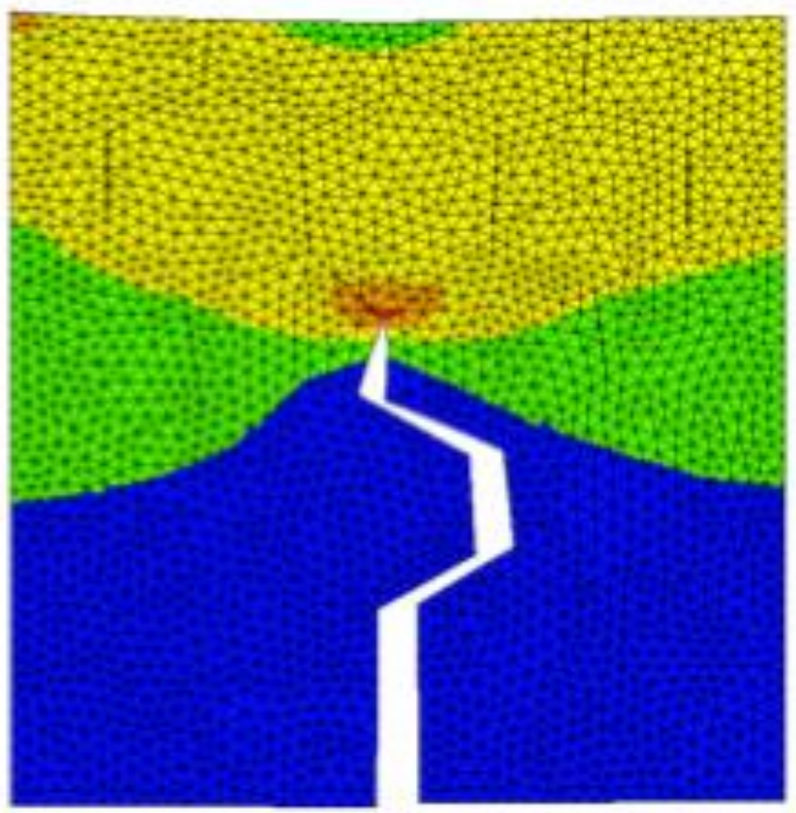

delamination of composites

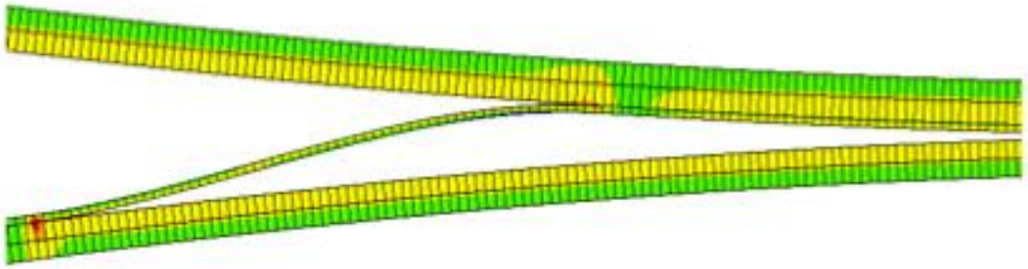

fragmentation

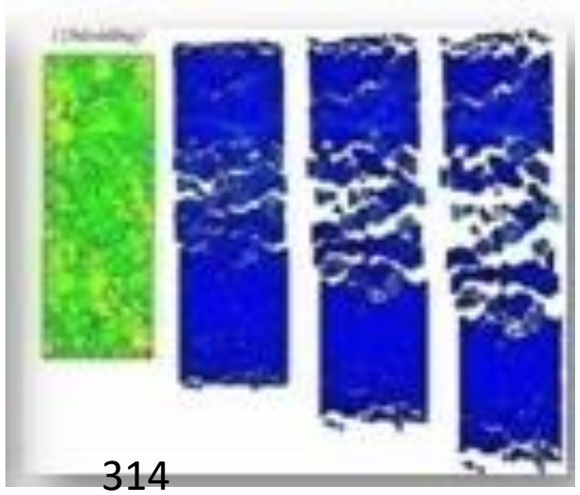

Microcracking and branching

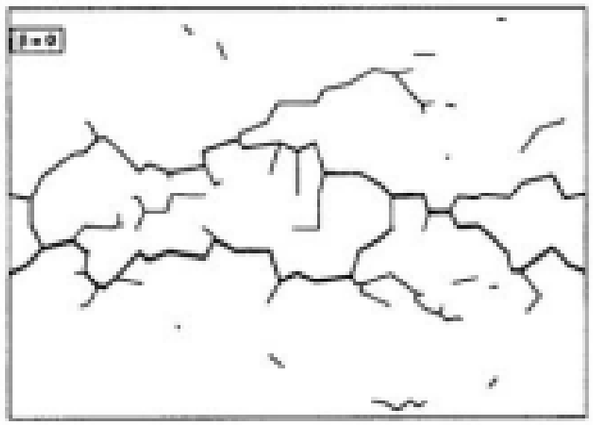

Cohesive models

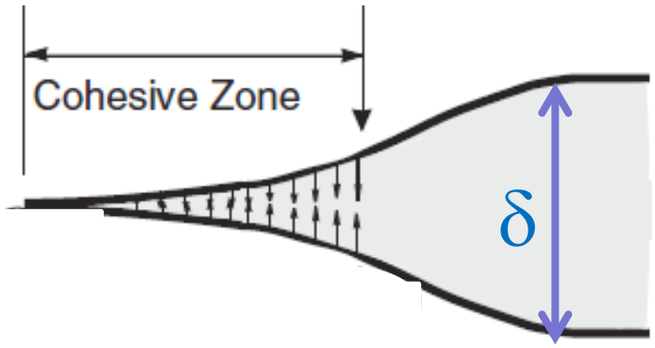

- Traction Separation Relation (TSR): Relation between traction (stress) and displacement jump

$$\sigma = \tilde{\sigma} f(\delta/\tilde{\delta})$$

- Parameters of a cohesive model(Only 2 out of 3 are needed)
  - Stress (traction) scale $\tilde{\sigma}$: Maximum traction in TSR
  - Displacement scale $\tilde{\delta}$: Separation corresponding to maximum traction (extrinsic models) or maximum nonzero traction
  - Work of Separation $\tilde{\phi}$: Area under $\sigma - \delta$ curve is the work needed to complete debond a unit surface area. This can be associated with G_c in LEFM theory.

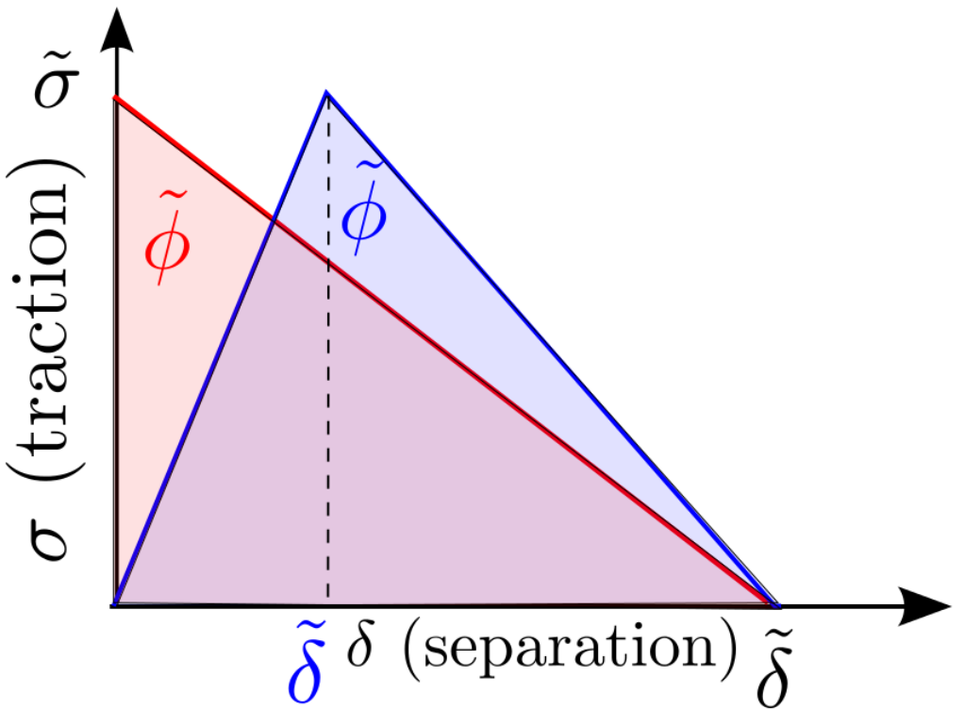

- Types of Cohesive models
  - Intrinsic cohesive models:
    - It has and initial hardening $\sigma - \delta$ part
    - σ starts from 0
    - Can be inserted in FEM mesh from the start of the simulation (along certain lines or between all elements)
  - Extrinsic cohesive models:
    - Generally has only softening $\sigma - \delta$ behavior.
    - σ starts from maximum stress ($\tilde{\sigma}$)
    - Should be adaptively inserted between elements when traction between elements approach $\tilde{\sigma}$

Process zone (Cohesive zone)

- Process zone Important Points and lengths
  - Nominal crack tip x_{CT} Generally corresponds to the point with maximum traction ($\tilde{\sigma}$)
  - Nominal trailing edge of the process zone x_{T}: The point where traction goes to zero (or if asymptotically goes to zero taken when stress is arbirary small *e.g.*, 0.01 or 0.001 *sigma*.
  - Nominal leading edge of the process zone x_{L}: When general crack-like (*e.g.*, highly nonlinear response) starts. Often, x_{L} is set to x_{CT}.
  - Process zone size $\Lambda = |x_{\mathrm{L}} - x_{\mathrm{T}}|$: Characteristic length scale corresponding to cohesive models ($\tilde{L}$)

- Cohesive model shape
  - Can have important influence on the response of cohesive model
  - The shape can be based on ductile/brittle response of TSR and can make it intrinsic or extrinsic

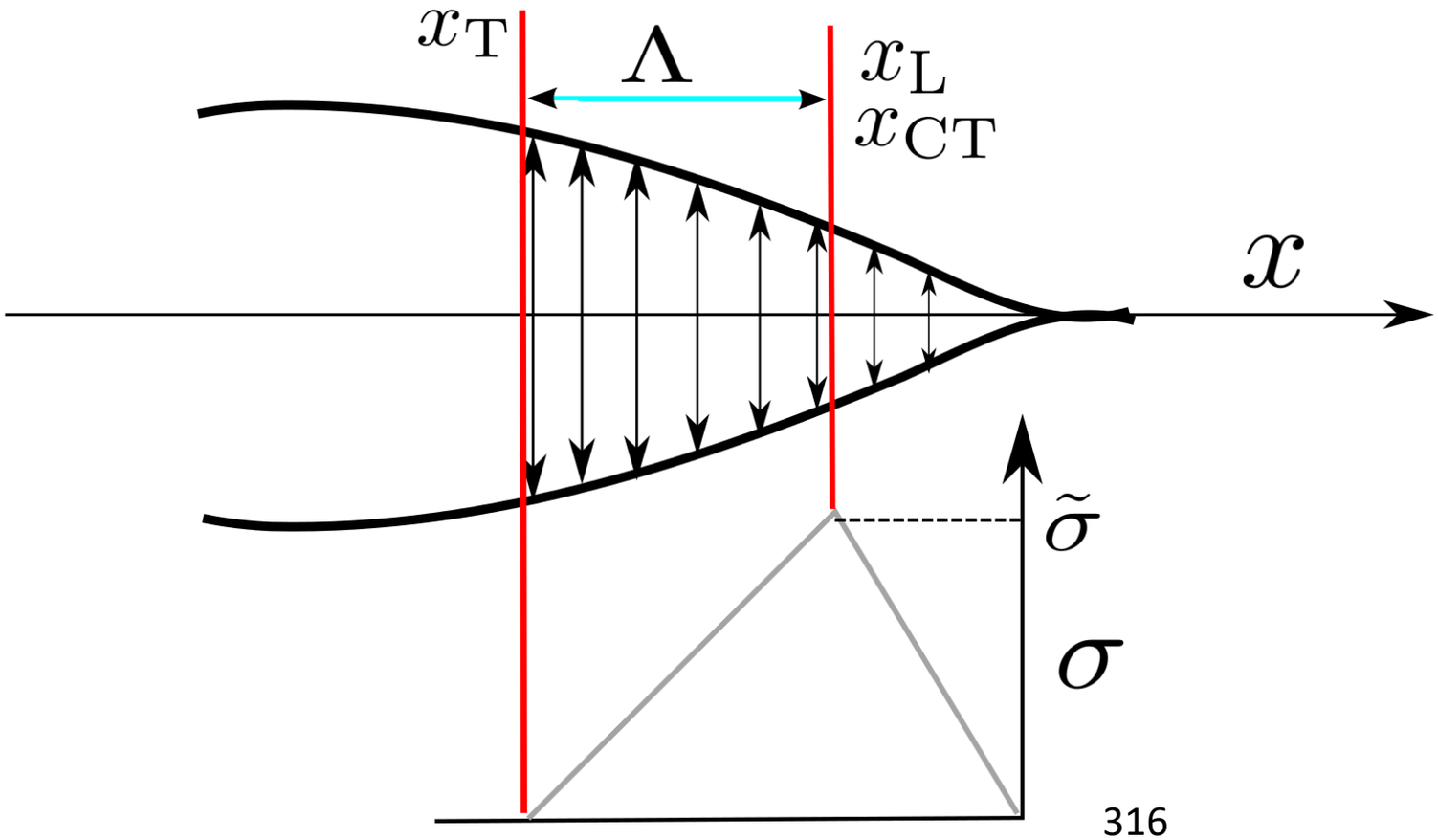

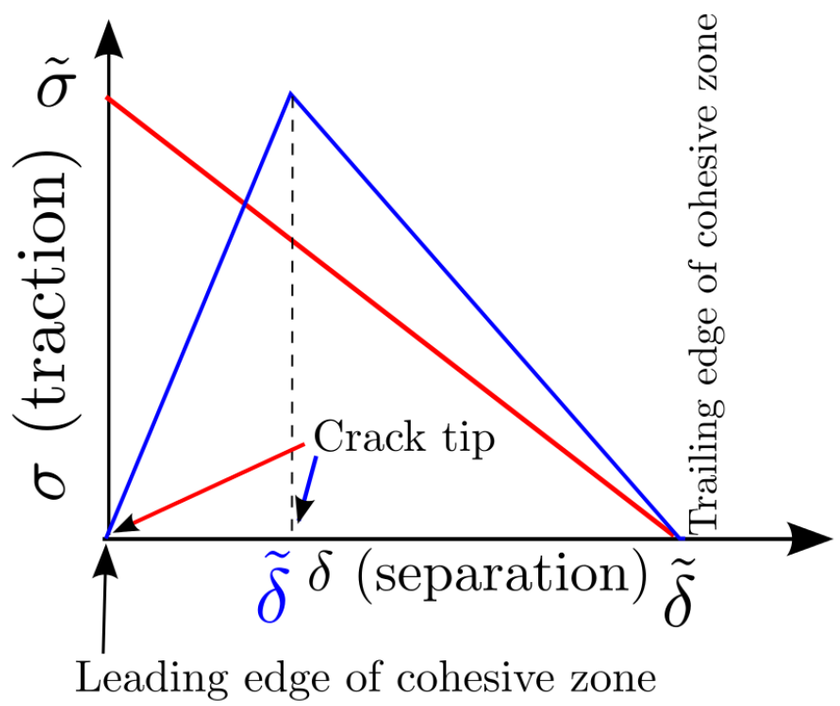

Shape of TSR

- Cohesive model shape
  - Can have important influence on the response of cohesive model
  - The shape can be based on ductile/brittle response of TSR and can make it intrinsic or extrinsic

cubic polynomial

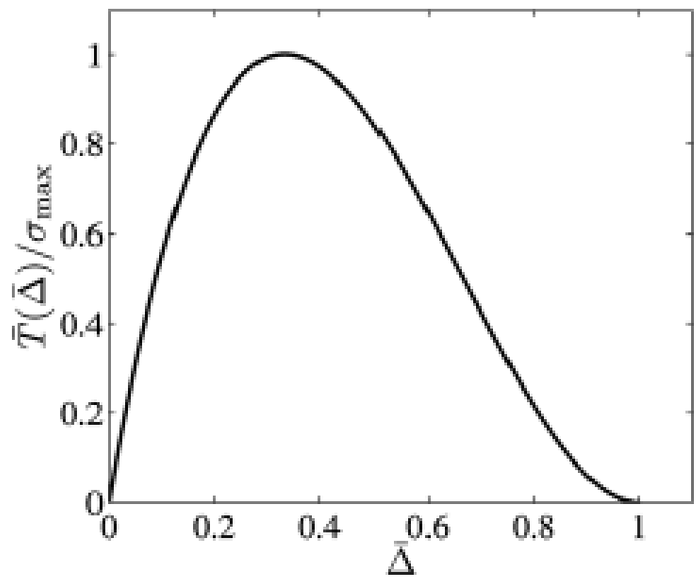

trapezoidal

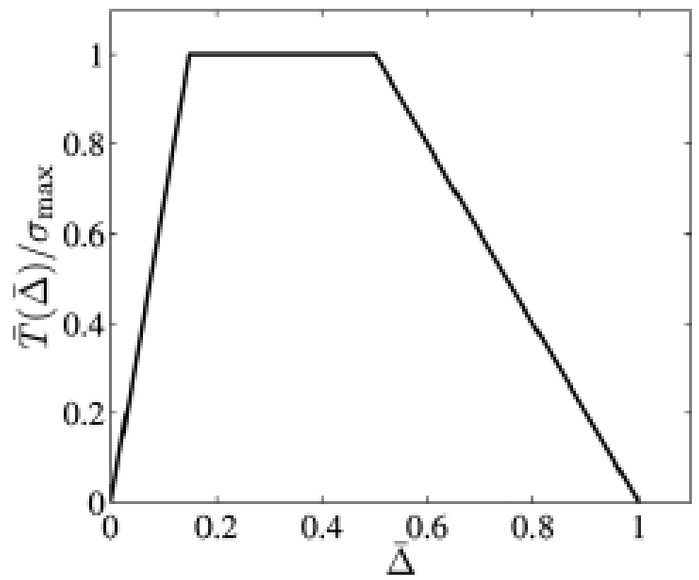

smoothed trapezoidal

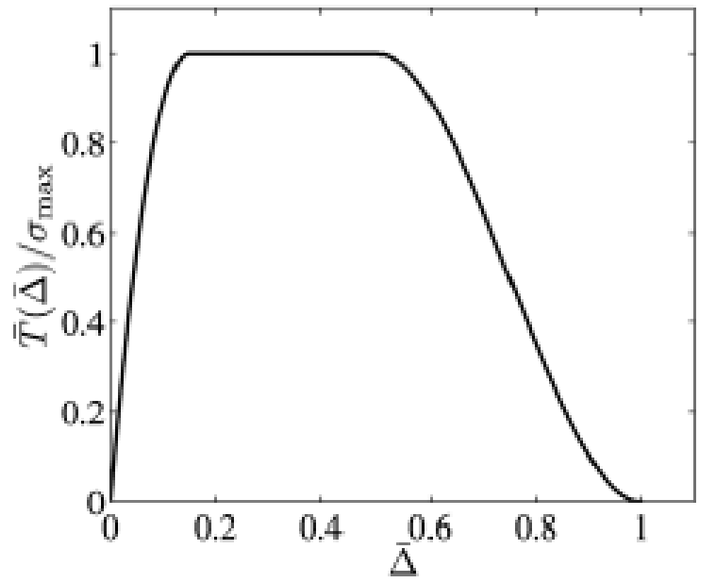

exponential

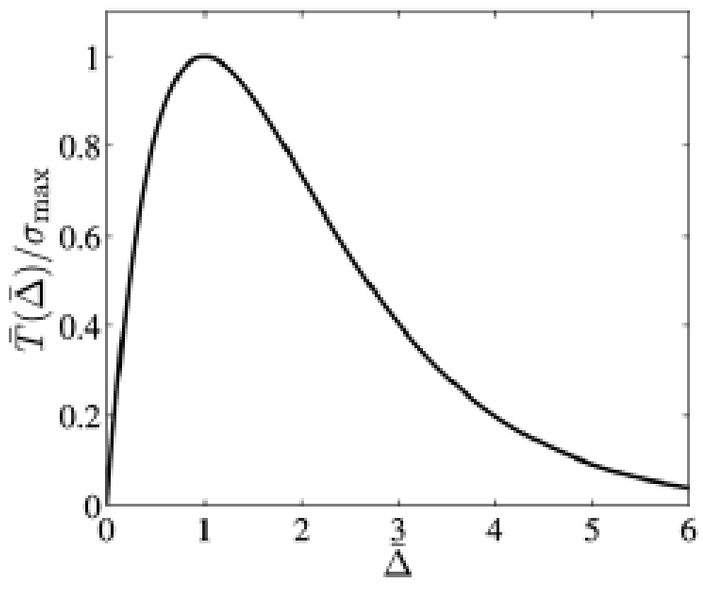

linear softening

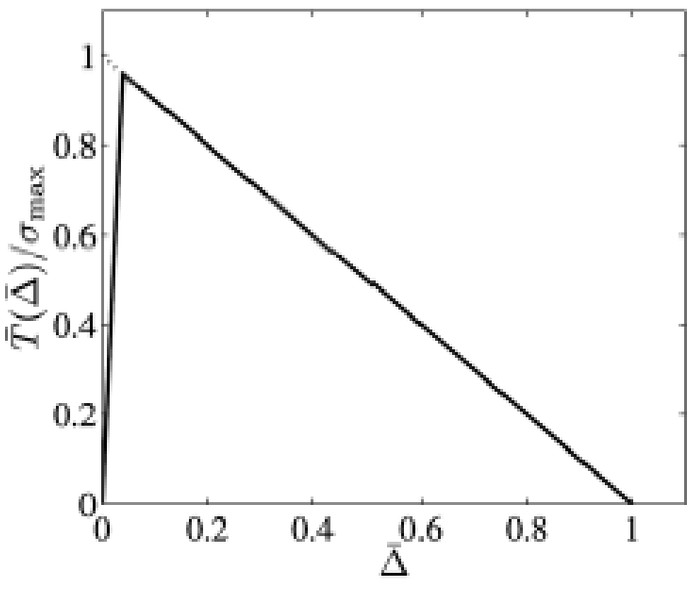

bilinear softening

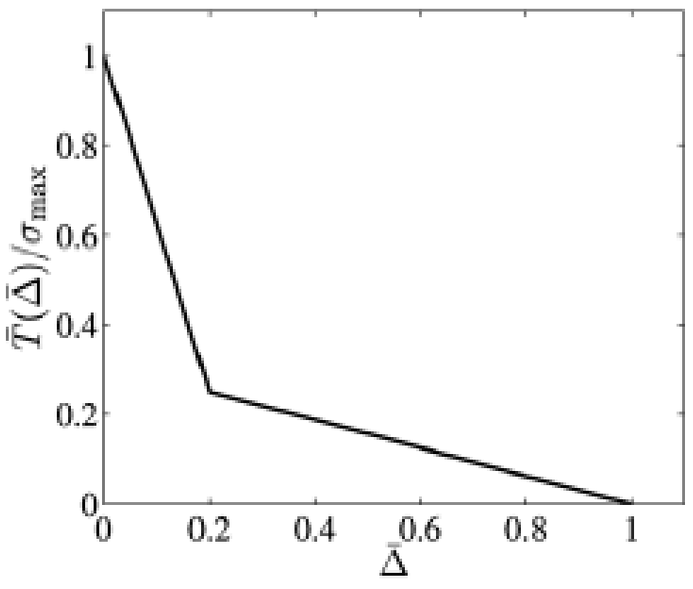

Cohesive model Table

Source: Namas Chandra, Theoretical and Computational Aspects of Cohesive Zone Modeling, Department of Mechanical Engineering, FAMU-FSU College of Engineering, Florida State University

Year and author	Proposed Model	Model parameters	Problem solved	Model constants	Comments
1959, 1962 Barenblatt, G.I.	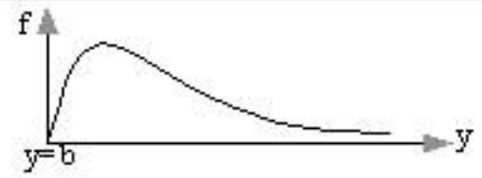	$K=\int_0^{d+d} \frac{G_1(t)dt}{\sqrt{t}} = \sqrt{\frac{\pi E T_0}{1-\nu^2}}$ (ductile) $= \sqrt{\frac{\pi E T_1}{1-\nu^2}}$ (brittle) $T = T_0 + T_1$ T_0 = work of separation for brit. mat T_1 = work of plastic deformation	Brittle materials		First to propose the concept
1960 Dugdale	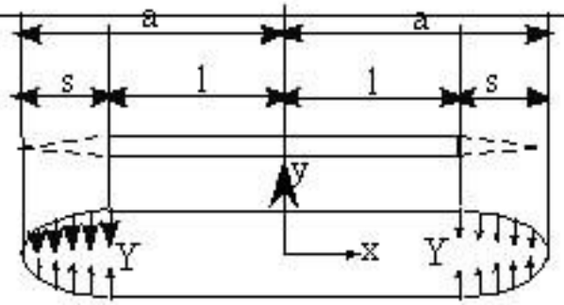	$\frac{a}{a} = 2 \sin^2\left(\frac{\pi}{4}\frac{T}{Y}\right)$ For small value of T/Y $\frac{s}{1} = 1.23\left(\frac{T}{Y}\right)^2$	Steel sheets	Plastic zone ranges from 0.042 to 0.448 (in)	Cohesive stress equated to yield stress of material
1987 Needleman	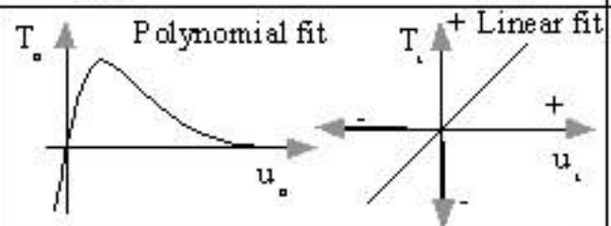	ϕ_{sep} = wk. of Sep. δ = normalizing Par. σ_{max} = Max. Stress	Particle-matrix decohesion	$\delta = 10^{0}$ to 10^{-3} m Cohesive Energy 1 to 10 J/m^2 σ_{max} = 1000 MPa	Phenomenological model. predict normal separation
1989 Rice & Wang	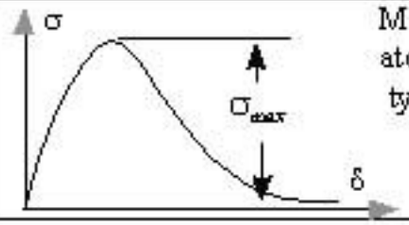	Model based on atomic fit of the type $(1+x)e^{-x}$ E_0 = Init. Young's mod h = normalizing Par. σ_{max} = Max. Stress α = constant$(\frac{\varepsilon_0 h}{\sigma_0} = 2\gamma)$	Solute segregation		Ascending part is equated to E_0 Normal separation. Ignores shear separation
1990 Needleman	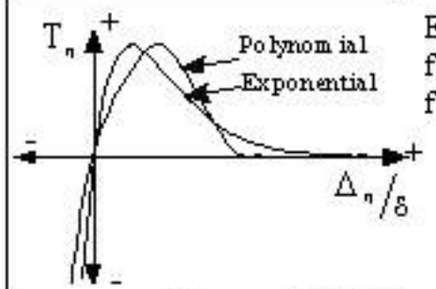	Exponential fit for Tn. Lineat fit for Ts ϕ_{sep} = wk. of Sep. δ = normalizing Par. σ_{max} = Max. Stress	Particle-matrix decohesion	$\delta = 10^{0}$ to 10^{-3} m	predict normal separation
1990 Needleman	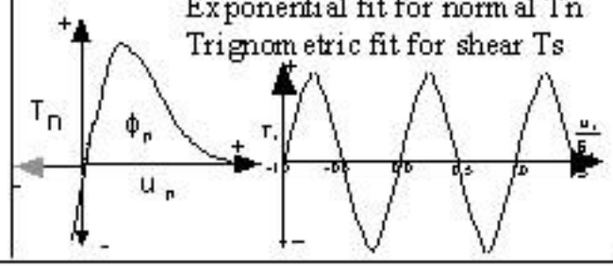	ϕ_n = wk. of Nor. Sep. ϕ_t = wk. of Shr. Sep. δ_n, δ_t = critical displacements. σ_{max} = Max. Stress	Decohesion of interface under hydrostatic tension	$\delta_n = \delta_t =$ 2x10^{10} to 2x10^{-9} m $J/\phi_n = 0.57 - 2.59$ $\sigma_{max}/\sigma_0 = 2,3$	Periodic shear traction to model Pieriels shear stress due to slip

Cohesive model Table

Source: Namas Chandra, Theoretical and Computational Aspects of Cohesive Zone Modeling, Department of Mechanical Engineering, FAMU-FSU College of Engineering, Florida State University

Year and author	Proposed Model	Model parameters	Problem solved	model constants	Comments
1992 Tvergaard & Hutchinson	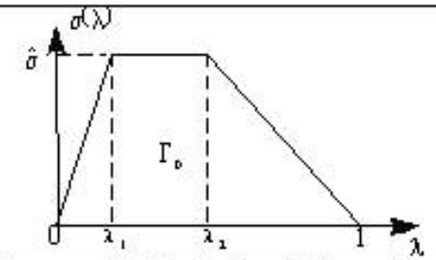	Γ_0 = wk. of Separation. δ_n^c, δ_t^c = critical displ. $\hat{\sigma}$ = Peak nor. trn./int. face str. λ_1, λ_2 = factors governing shape of sep	Crack growth in elasto-plastic material, peeling of adhesive joints	$\Gamma_{\infty}/\Gamma_0 = 0-10.$ (Γ_{∞} = Pl wk.), $\delta_n^c/\delta_t^c = 1$ $\hat{\sigma}/\sigma_y = 0-14$ $\lambda_1, \lambda_2 = 0.15, 0.5$ $\sigma_y/E = 1/300$	Claims shape of separation law are relatively unimportant
1993 Xu & Needleman	Exponential fit for both Tn and Tt 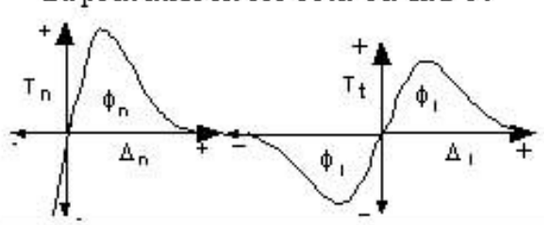	ϕ_n = wk. of Nor. Sep. ϕ_t = wk. of Shr. Sep. δ_n, δ_t = critical displacements. σ_{max} = Max. Stress	Particle-matrix decohesion	δ_n, δ_t = 2×10^{-10} to 2×10^{-9} m	Predicts shear and normal separation
1990 Tvergaard	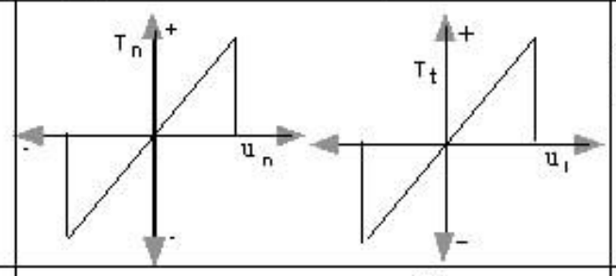	δ_n, δ_t = critical displacements. σ_{max} = Max. Stress	Interfaces of whisker-reinforced metal matrix composites	$\delta_n = \delta_t = 1X10^{-9}$m. E=60GPa(Young's mod) $\sigma_y/E = 0.005$ $\sigma_{max}/\sigma_y = 5-9$	Linear Model
1996 Camacho and Ortiz	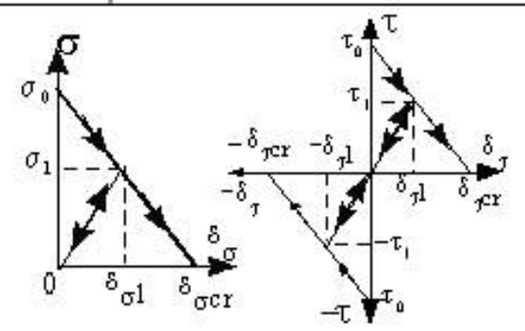	σ_0 , τ_0 = Nor. and Shr stress at fracture initiation $\delta_{\sigma cr}, \delta_{\tau cr}$ = crit. nor. opening and shr. opening displ. G_c = Fracture energy	Impact	Alumina: σ_0= 400 MPa $\delta_{\sigma cr} = 1.7\times10^{-7}m$ Steel: $\sigma_0 = 1500MPa$ $\delta_{\sigma cr} = 2.7\times10^{-4}m$	Predicts failure by both shear and normal separation in tension and by shear separation in compression
1997 Gaubelle & Bayler	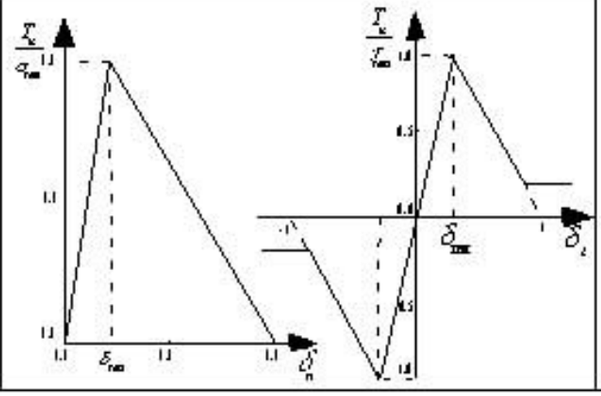	Φ_n, Φ_t: Work of normal and tangential separation Δ_n, Δ_t: Normal and Tangential displacement jump δ_n, δ_t: Normal and tangential interface characteristic-length	delamination by low-velocity impact	σ_{max}= E/10 Critical normal displacement jump $\Delta_{nc} = 10^{-5}\sim10^{-4}$ m	Bilinear model Ascending curve can be matched to initial stiffness of the material

Scales of cohesive model

$$\tilde{\phi} = \tilde{\sigma}\tilde{\delta} \qquad \text{Energy}$$

2 out of the three are independent

$$\tilde{p} = \rho\tilde{v} = \frac{\tilde{\sigma}}{c_\mathrm{d}} \qquad \text{Linear momentum}$$

$$\tilde{E} = \frac{\tilde{v}}{c_\mathrm{d}} = \frac{\tilde{\sigma}}{\rho c_\mathrm{d}^2} \propto \frac{\tilde{\sigma}}{\|\mathbf{C}\|} \qquad \text{Strain}$$

$$\tilde{v} = \frac{\tilde{\delta}}{\tilde{\tau}} = \frac{\tilde{\sigma}}{\rho c_\mathrm{d}} \qquad \text{Velocity}$$

$$\tilde{L} = c_\mathrm{d}\tilde{\tau} = \frac{\rho c_\mathrm{d}^2 \tilde{\delta}}{\tilde{\sigma}} \propto \Lambda^0 \qquad \text{Length}$$

Process zone size Λ

$$\tilde{\tau} = \frac{\rho c_\mathrm{d} \tilde{\delta}}{\tilde{\sigma}} \qquad \text{Time}$$

Influences time step for time marching methods

Why process zone size is important?

- Importance of process zone size Λ
  - Static estimate:

$$\Lambda = \varsigma\pi \frac{\mu}{1-\nu} \frac{\tilde{\phi}}{\tilde{\sigma}^2} \propto \tilde{L}$$

$$\varsigma = \begin{cases} \frac{1}{4} & \text{Dugdale model} \\ \frac{9}{16} & \text{Potential-based TSRs} \end{cases}$$

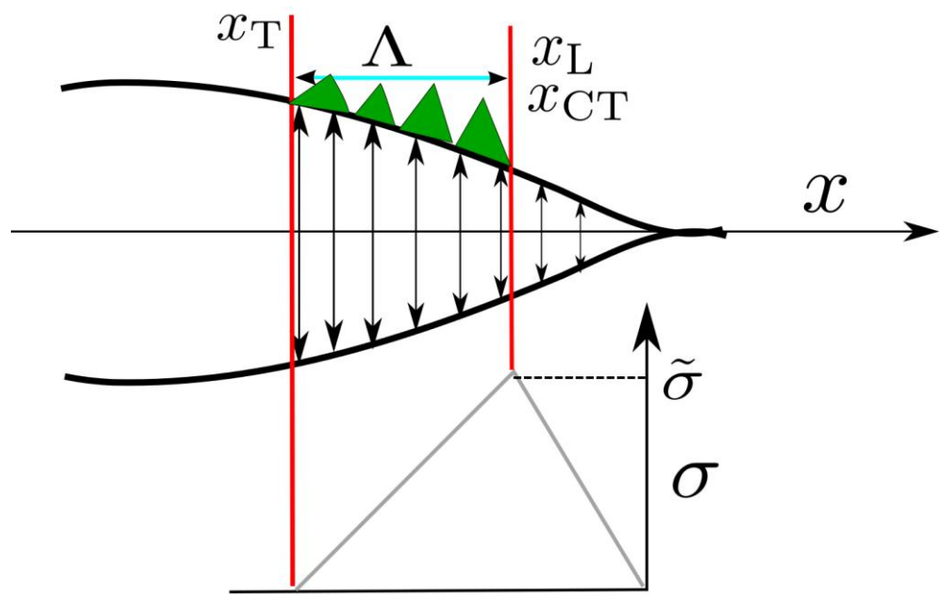

  - Minimum number of elements in process zone size: There should be at least 4-10 elements along the PZ
  - Dynamic estimate: PZS decreases as crack speed $\hat{v}$ approaches Rayleigh wave speed c_{R}

$$\Lambda(\hat{v}) = \frac{\Lambda}{A(\hat{v})}, \quad A(\hat{v}) \to 0 \text{ as } \hat{v} \to c_{\mathrm{R}} \quad \Rightarrow$$

Smaller elements are needed in PZT as crack accelerates!

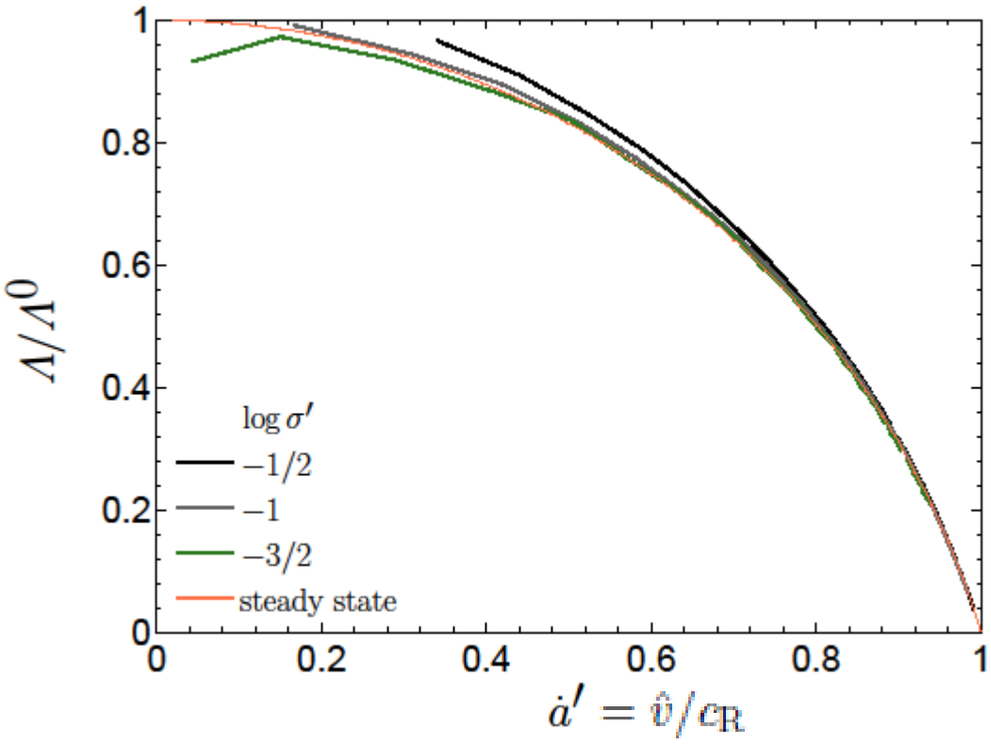

When LEFM results match cohesive solutions?

- When SSY condition is satisfied LEFM and Cohesive Fracture Mechanics (CFM) solutions are expected to be close ⇒

- When $\sigma' = \frac{\bar{\sigma}}{\sigma} \to 0$ LEFM & CFM are expected give similar results

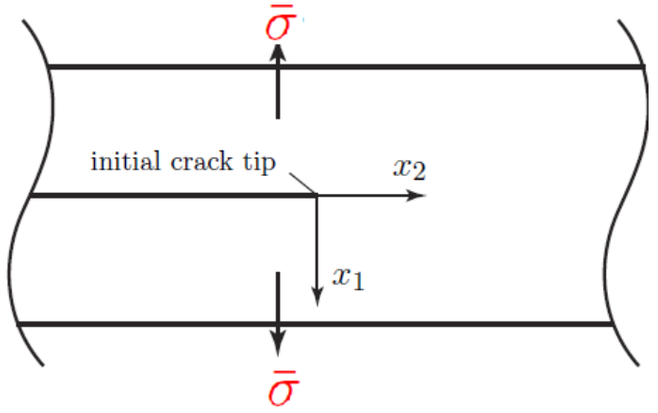

crack speed

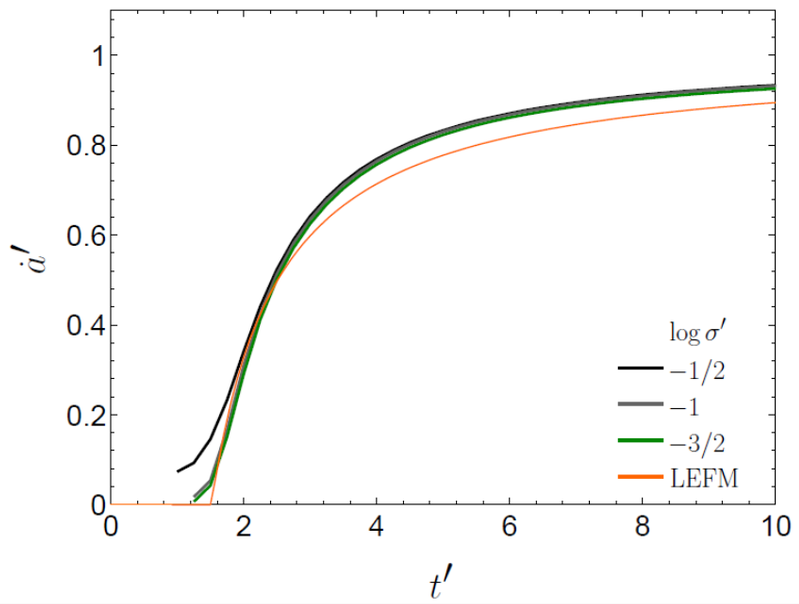

Low $\sigma' = \frac{\bar{\sigma}}{\sigma}$
SSY
LEFM ≈ CFM

process zone size

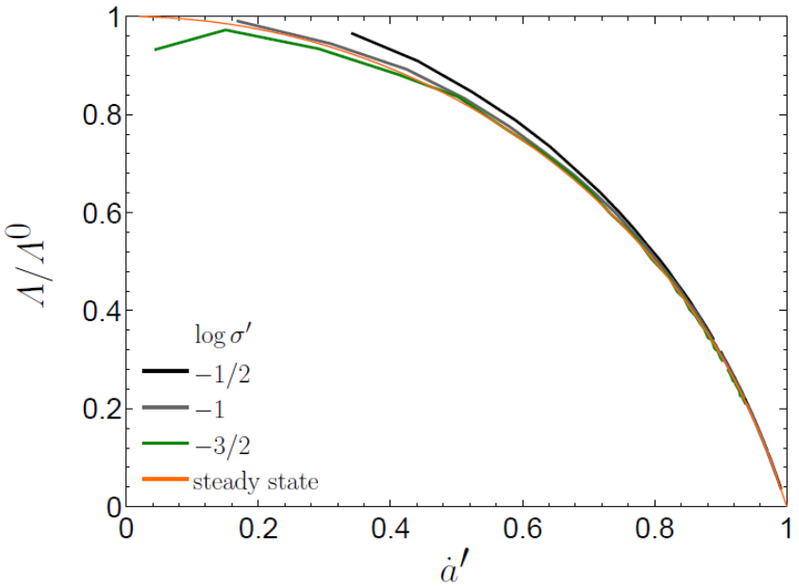

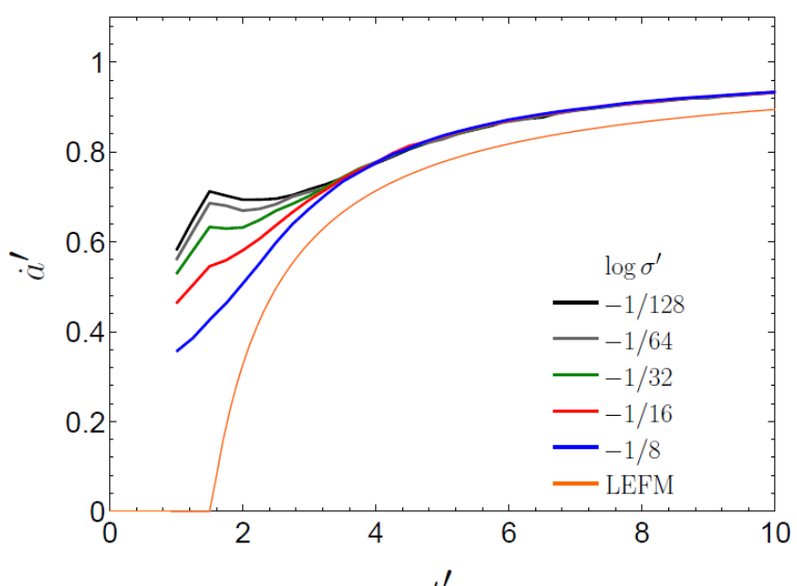

High $\sigma' = \frac{\bar{\sigma}}{\sigma}$
LSY
LEFM ≠ CFM

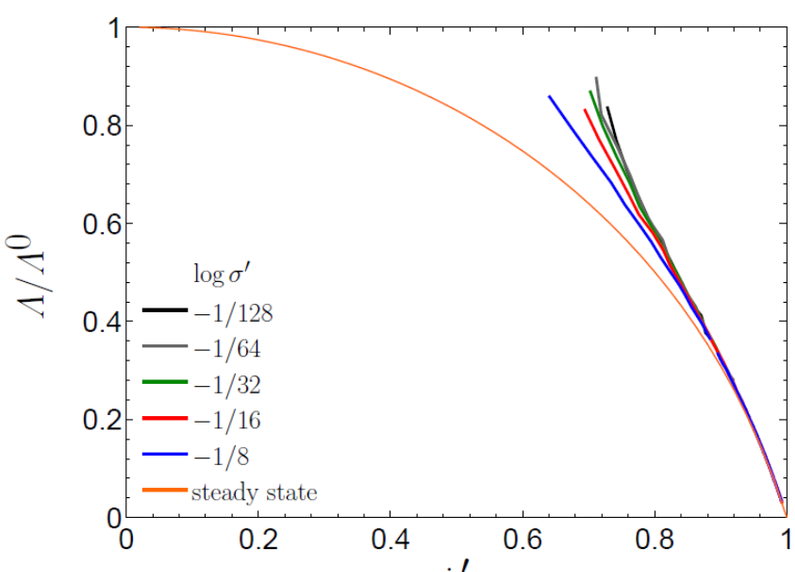

Resistance (fracture toughness) versus work of separation

- Fracture toughness (Γ): LEFM: Energy needed to create one unit surface of crack
- Work of separation (ϕ): CFM: Energy needed to entirely debond a point in time per area (following a traction-separation-relation)
  - Relation between ϕ and G:

$$G = \frac{1}{\hat{v}} \int_{-\Lambda_{(k)}}^{0} \tilde{s}(\delta_k) \frac{\partial \delta_k}{\partial t} \, \mathrm{d}x + \int_{0}^{\delta_T} \tilde{s}(\delta_k) \, \mathrm{d}\delta_k = I_t + \tilde{\phi}_{(k)}$$

  - Dynamic part () goes to zero when:
    - Steady state crack propagation (crack speed does not change).
    - When the crack speed tends to Rayleigh wave speed (c_R)

$$\left| \frac{I_t}{\tilde{\phi}_{(k)}} \right| \leq \frac{\tilde{\sigma}_{(k)} \Lambda_{(k)}}{\hat{v} \tilde{\phi}_{(k)}} \left| \frac{\partial \delta_k}{\partial t} \right|_\infty \approx \frac{\zeta_{(k)} \pi \mu}{(1-\nu) \hat{v} A_{(k)}(\hat{v}) \tilde{\sigma}_{(k)}} \left| \frac{\partial \delta_k}{\partial t} \right|_\infty$$

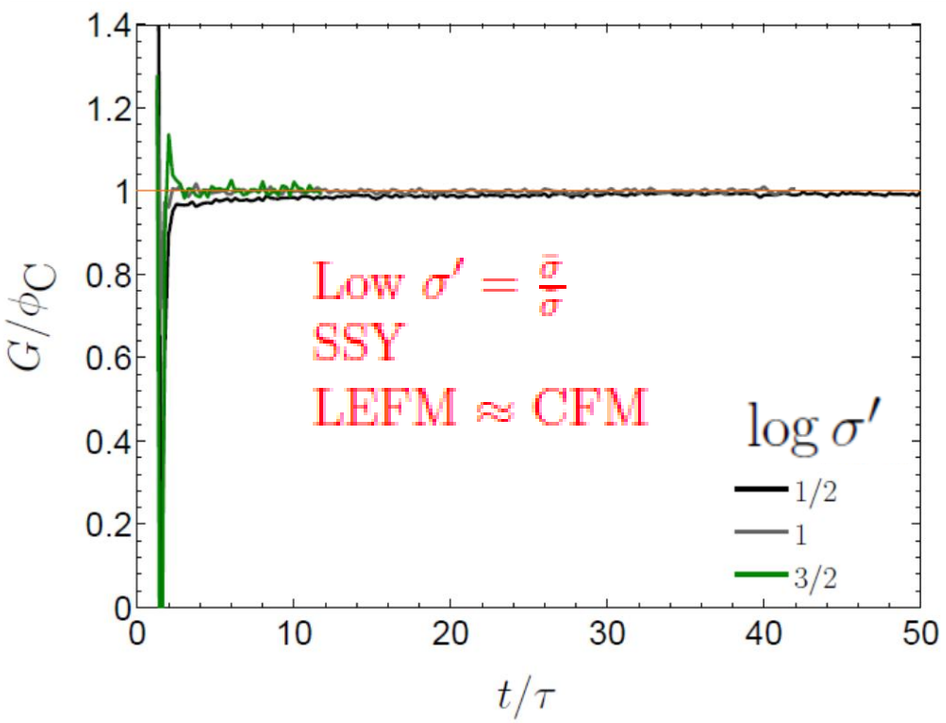

LEFM CFM comparison:
set $\Gamma = \phi$
accurate except unsteady / low crack speed OR if SSY is not satisfied

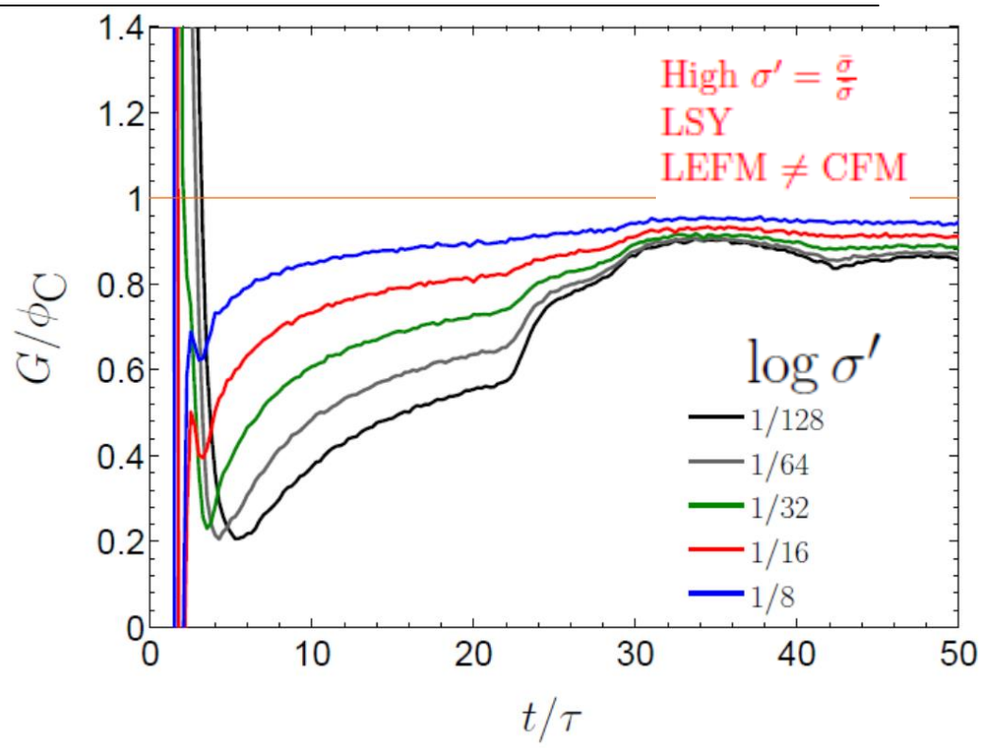

Artificial compliance for intrinsic cohesive models

- Artificial compliance becomes important if cohesive surfaces are added between all elements for intrinsic models to find crack propagation path.
- The artifical compliance is computed as,

$$\begin{aligned} \Delta &= \Delta_e + \Delta_c, \quad \Delta_e = \text{ elastic displacement}, \Delta_c = \text{ cohesive separation} \quad \Rightarrow \\ \frac{\sigma}{E_{\text{eff}}}h &= \frac{\sigma}{E}h + \frac{\sigma}{K} \quad \Rightarrow \\ \frac{1}{E_{\text{eff}}} &= \frac{1}{E} + \frac{1}{Kh} \quad \Rightarrow \end{aligned}$$

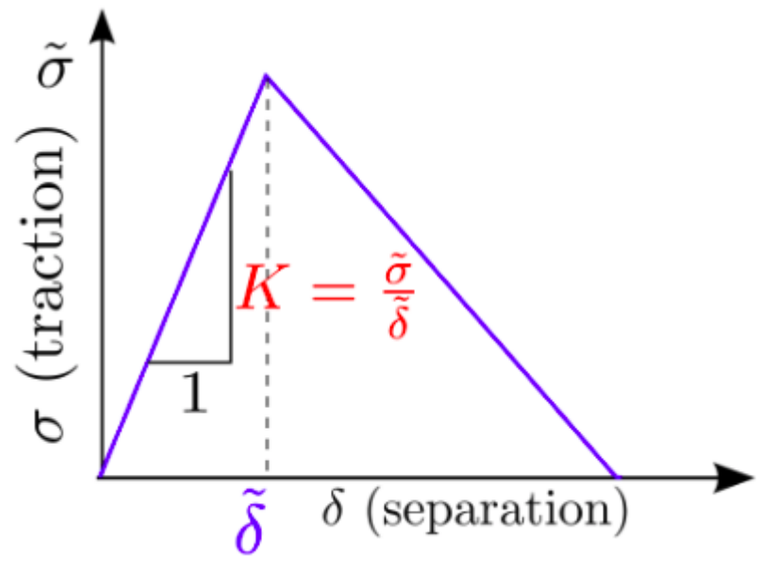

Artificial compliance is,

$$C_c = \frac{1}{Kh} = \frac{\tilde{\delta}}{\tilde{\sigma}h} = \frac{1}{E_c}, \text{ where}$$

$$E_c = Kh = \frac{\tilde{\sigma}h}{\tilde{\delta}}, \text{ and effective elastic modulus is}$$

$$\frac{1}{E_{\text{eff}}} = \frac{1}{E} + \frac{1}{E_c}, \quad \Rightarrow E_{\text{eff}} = \frac{EE_c}{E + E_c}$$

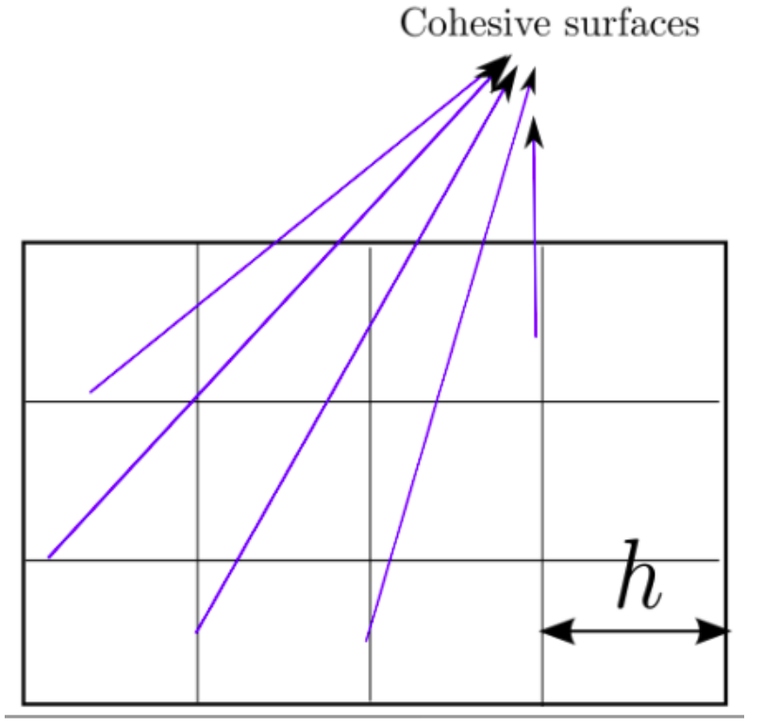

- That is the smaller element spacing h or softer the initial slope K of TSR the higher artificial compliance (higher errors)
- While extrinsic cohesive models do not have the same problem, adaptive insertion of cohesive surfaces is more challenging for them.

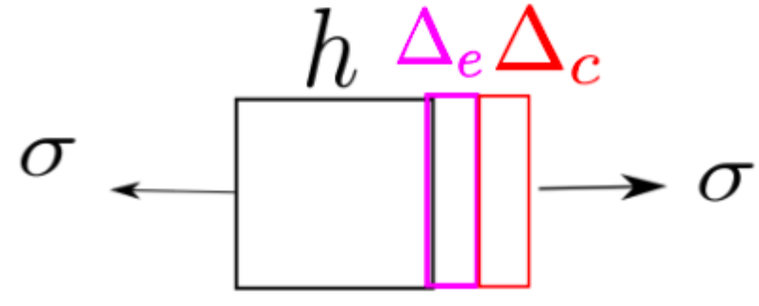

4.3 Mixed mode fracture

4.3.1 Crack propagation criteria

a) Maximum Circumferential Tensile Stress

b) Maximum Energy Release Rate

c) Minimum Strain Energy Density

4.3.2 Crack Nucleation criteria

Motivation: Mixed mode crack propagation criteria

- Pure Mode I fracture:

$$K_{\mathrm{I}} \geq K_{\mathrm{Ic}}$$

- Mixed mode fracture (in-plane)

$$F\left(K_{\mathrm{I}}, K_{\mathrm{II}}, K_{\mathrm{Ic}}\right) = 0$$

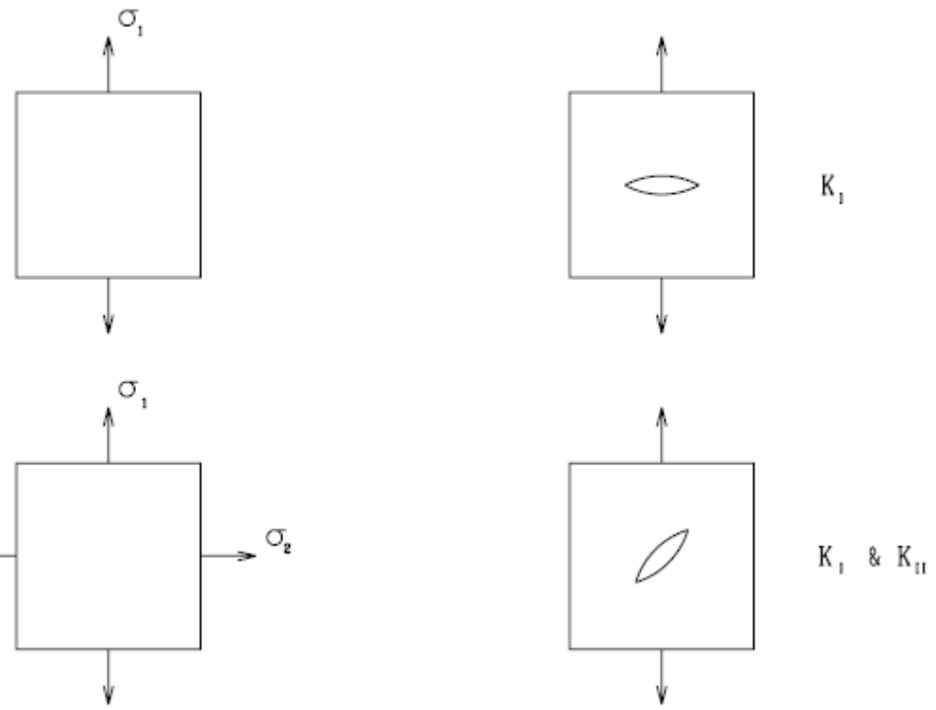

- Note the similarity with yield surface plasticity model:

$$F_{yld}(\sigma_1, \sigma_2, \sigma_y) = 0$$

$$\sigma_v = \sigma_y \quad \text{for} \quad \sigma_v = \sqrt{\frac{(\sigma_1 - \sigma_2)^2 + (\sigma_2 - \sigma_3)^2 + (\sigma_3 - \sigma_1)^2}{2}}$$

Example: von Mises yield criterion

Motivation: Experiment verification of the mixed-mode failure criterion

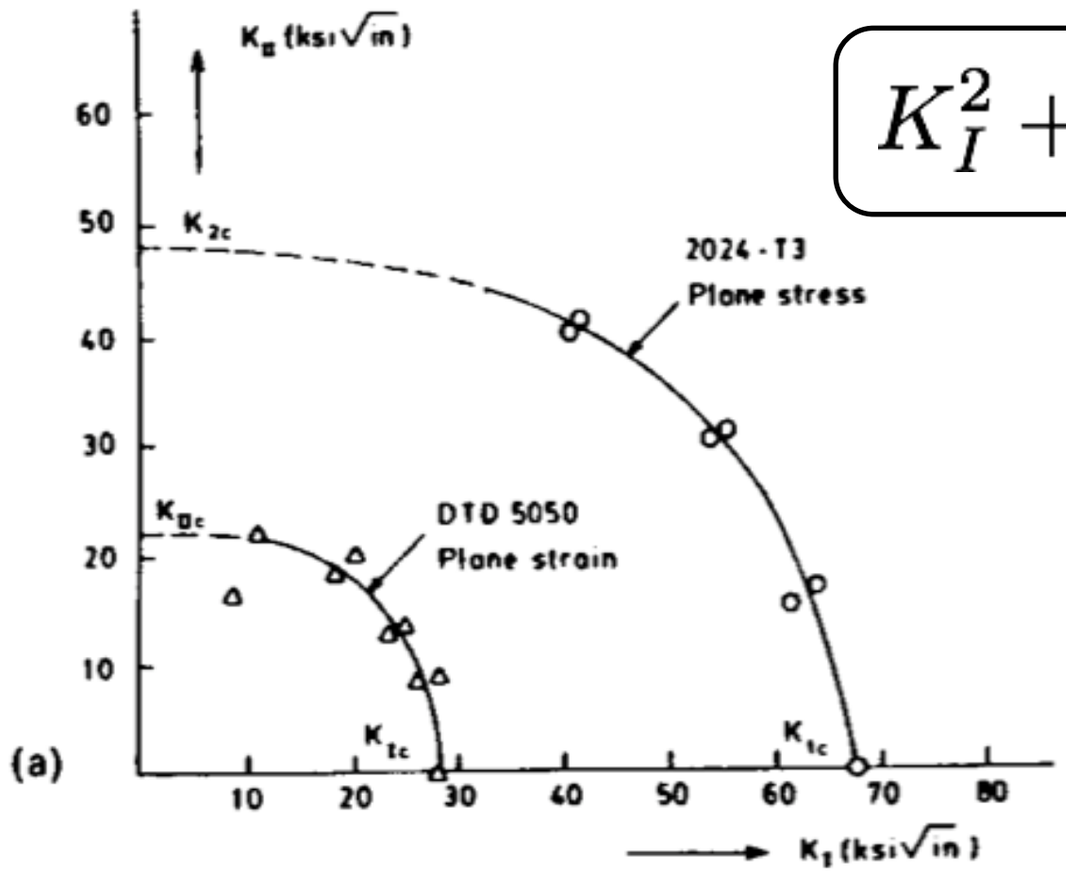

$$K_I^2 + K_{II}^2 = K_{Ic}^2$$

a circle in KI, KII plane

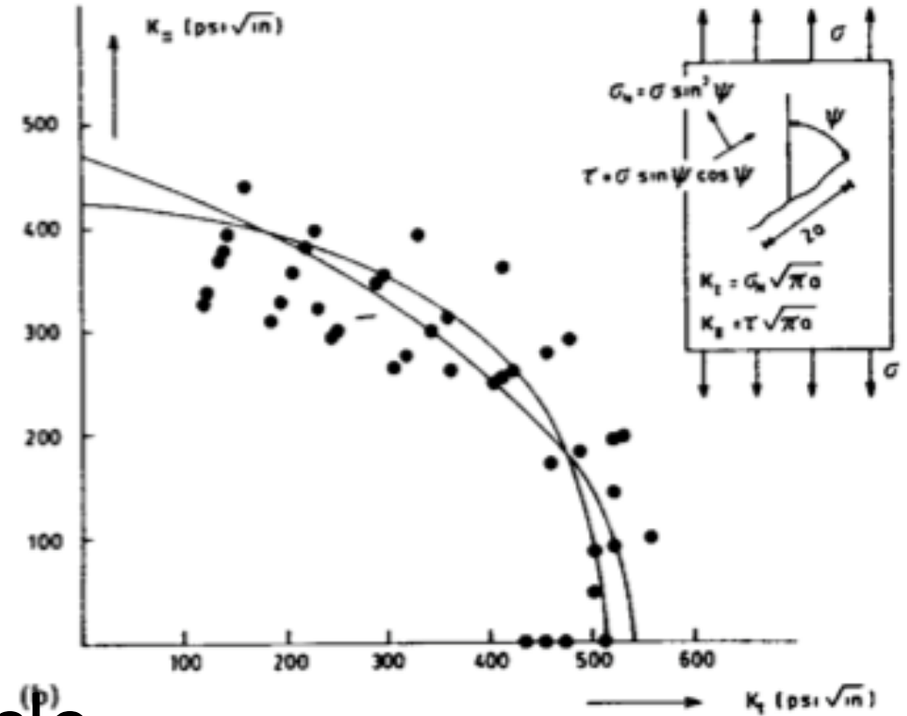

Data points do not fall exactly on the circle.

$$\left(\frac{K_I}{K_{Ic}}\right)^2 + \left(\frac{K_{II}}{K_{IIc}}\right)^2 = 1$$

self-similar growth

$$G = \frac{(\kappa+1)K_I^2}{8\mu}$$

Mixed-mode crack growth

Combination of mode-I, mode-II and mode-III loadings: mixed-mode loading.

Cracks will generally propagate along a curved surface as the crack seeks out its path of **least resistance**.

Only a 2D mixed-mode loading (mode-I and mode-II) is discussed.

4.3 Mixed mode fracture

4.3.1 Crack propagation criteria

a) Maximum Circumferential Tensile Stress

b) Maximum Energy Release Rate

c) Minimum Strain Energy Density

4.3.2 Crack Nucleation criteria

Maximum circumferential stress criterion

Erdogan and Sih

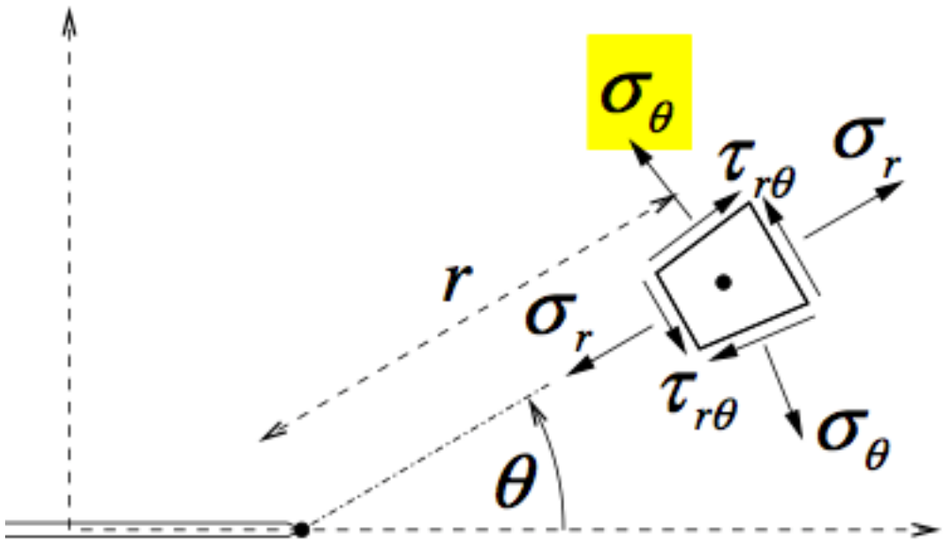

maximum circumferential stress criterion (maximum hoop stress criterion):

crack propagates in the direction perpendicular to the maximum circumferential stress

(evaluated on a circle of a small diameter centered at the tip)

the direction of propagation is given by the angle θ_c for which

$$\sigma_\theta(r,\theta_c) = \max_{-\pi<\theta<\pi} \sigma_\theta(r,\theta)$$

(from M. Jirasek)

principal stress → $\tau_{r\theta} = 0$

Maximum circumferential stress criterion

$$\sigma_r = \frac{K_{\mathrm{I}}}{\sqrt{2\pi r}} \left(\frac{5}{4} \cos \frac{\theta}{2} - \frac{1}{4} \cos \frac{3\theta}{2} \right) + \frac{K_{\mathrm{II}}}{\sqrt{2\pi r}} \left(-\frac{5}{4} \sin \frac{\theta}{2} + \frac{3}{4} \sin \frac{3\theta}{2} \right)$$

(7.35a)

$$\sigma_\theta = \frac{K_{\mathrm{I}}}{\sqrt{2\pi r}} \left(\frac{3}{4} \cos \frac{\theta}{2} + \frac{1}{4} \cos \frac{3\theta}{2} \right) + \frac{K_{\mathrm{II}}}{\sqrt{2\pi r}} \left(-\frac{3}{4} \sin \frac{\theta}{2} - \frac{3}{4} \sin \frac{3\theta}{2} \right)$$

(7.35b)

$$\tau_{r\theta} = \frac{K_{\mathrm{I}}}{\sqrt{2\pi r}} \left(\frac{1}{4} \sin \frac{\theta}{2} + \frac{1}{4} \sin \frac{3\theta}{2} \right) + \frac{K_{\mathrm{II}}}{\sqrt{2\pi r}} \left(\frac{1}{4} \cos \frac{\theta}{2} + \frac{3}{4} \cos \frac{3\theta}{2} \right) .$$

(7.35c)

$$\tau_{r\theta} = 0 \longrightarrow K_I \left(\sin \frac{\theta}{2} + \sin \frac{3\theta}{2} \right) + K_{II} \left(\cos \frac{\theta}{2} + 3 \cos \frac{3\theta}{2} \right) = 0$$

$$\longrightarrow \theta_c = 2 \arctan \frac{1}{4} \left(K_I / K_{II} \pm \sqrt{(K_I / K_I I)^2 + 8} \right)$$

Maximum circumferential stress criterion

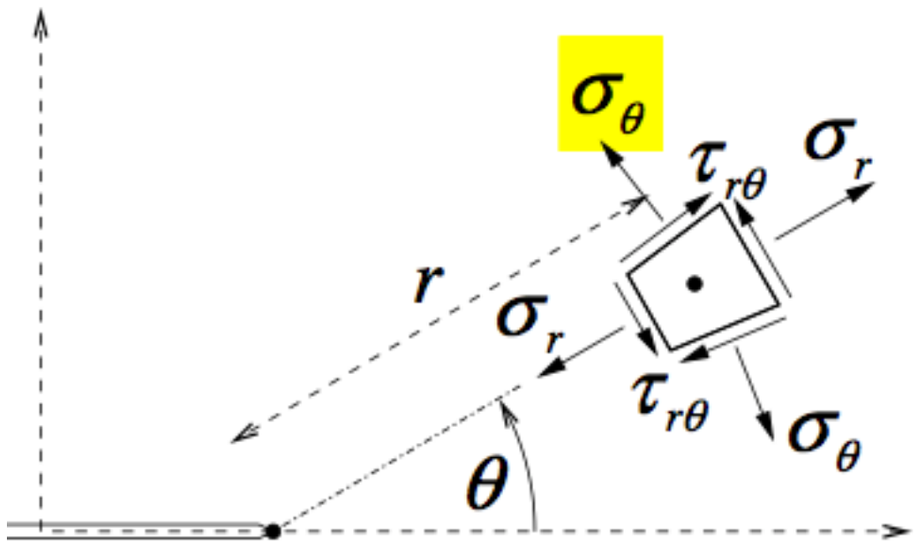

$$\sigma_\theta(r,\theta_c) = \max_{-\pi<\theta<\pi} \sigma_\theta(r,\theta)$$

$$\tau_{r\theta} = 0$$

$$\tan\frac{\theta_0}{2} = \frac{1}{4}\frac{K_I}{K_{II}} \pm \frac{1}{4}\sqrt{\left(\frac{K_I}{K_{II}}\right)^2 + 8}$$

Maximum allowable traction $\sigma_{\theta max}$ is reached at angle $\theta = \theta max$ and distance from crack tip r_0:

$$\sigma_{\theta max}\sqrt{2\pi r_0} = K_{Ic} = \cos\frac{\theta_0}{2}\left[K_I\cos^2\frac{\theta_0}{2} - \frac{3}{2}K_{II}\sin\theta_0\right]$$

Maximum circumferential stress criterion

Fracture criterion $$K_{eq} \geq K_{Ic}$$

$$\sigma_\theta = \frac{K_\mathrm{I}}{\sqrt{2\pi r}} \cos\frac{\theta_0}{2}\left(1-\sin^2\frac{\theta_0}{2}\right) + \frac{K_\mathrm{II}}{\sqrt{2\pi r}}\left(-\frac{3}{4}\sin\frac{\theta_0}{2} - \frac{3}{4}\sin\frac{3\theta_0}{2}\right) \tag{7.9}$$

must reach a critical value which is obtained by rearranging the previous equation

$$\sigma_{\theta max}\sqrt{2\pi r} = K_\mathrm{Ic} = \cos\frac{\theta_0}{2}\left[K_\mathrm{I}\cos^2\frac{\theta_0}{2} - \frac{3}{2}K_\mathrm{II}\sin\theta_0\right] \tag{7.10}$$

which can be normalized as

$$\boxed{\frac{K_\mathrm{I}}{K_\mathrm{Ic}}\cos^3\frac{\theta_0}{2} - \frac{3}{2}\frac{K_\mathrm{II}}{K_\mathrm{Ic}}\cos\frac{\theta_0}{2}\sin\theta_0 = 1} \tag{7.11}$$

11 This equation can be used to define an equivalent stress intensity factor K_{eq} for mixed mode problems

$$\boxed{K_{eq} = K_\mathrm{I}\cos^3\frac{\theta_0}{2} - \frac{3}{2}K_\mathrm{II}\cos\frac{\theta_0}{2}\sin\theta_0} \tag{7.12}$$

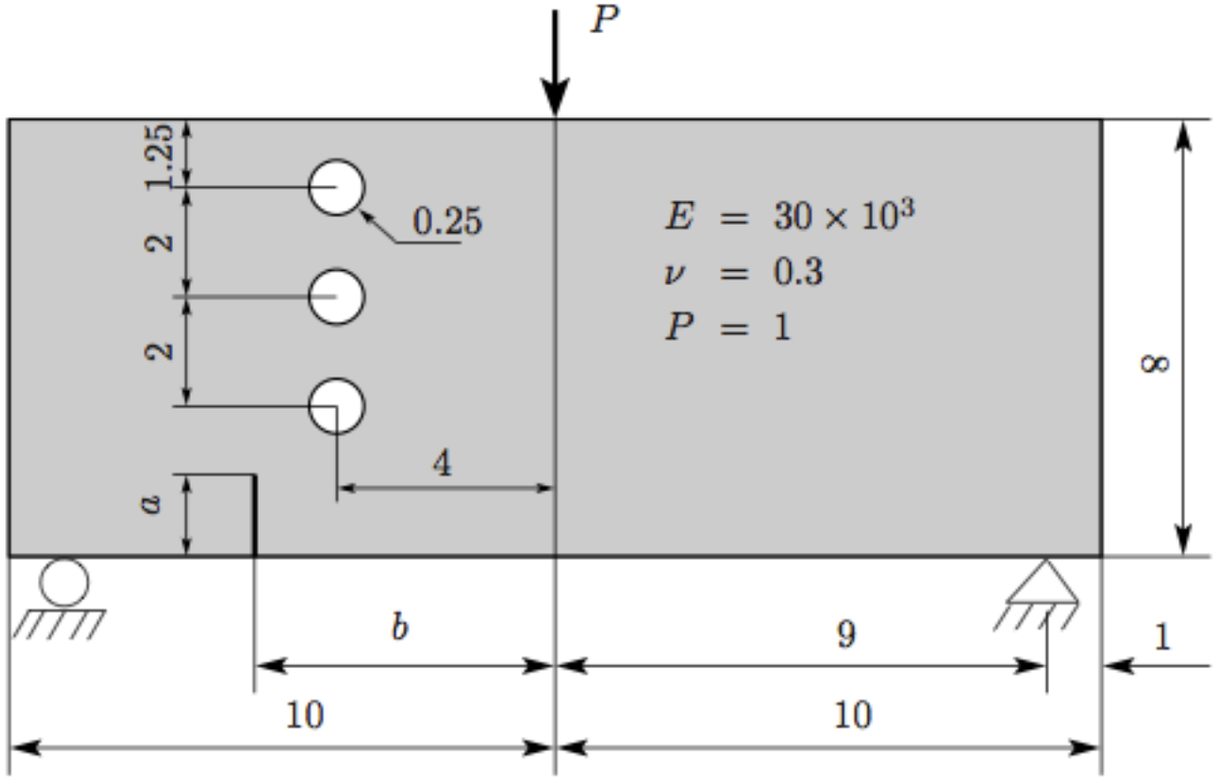

Experiment

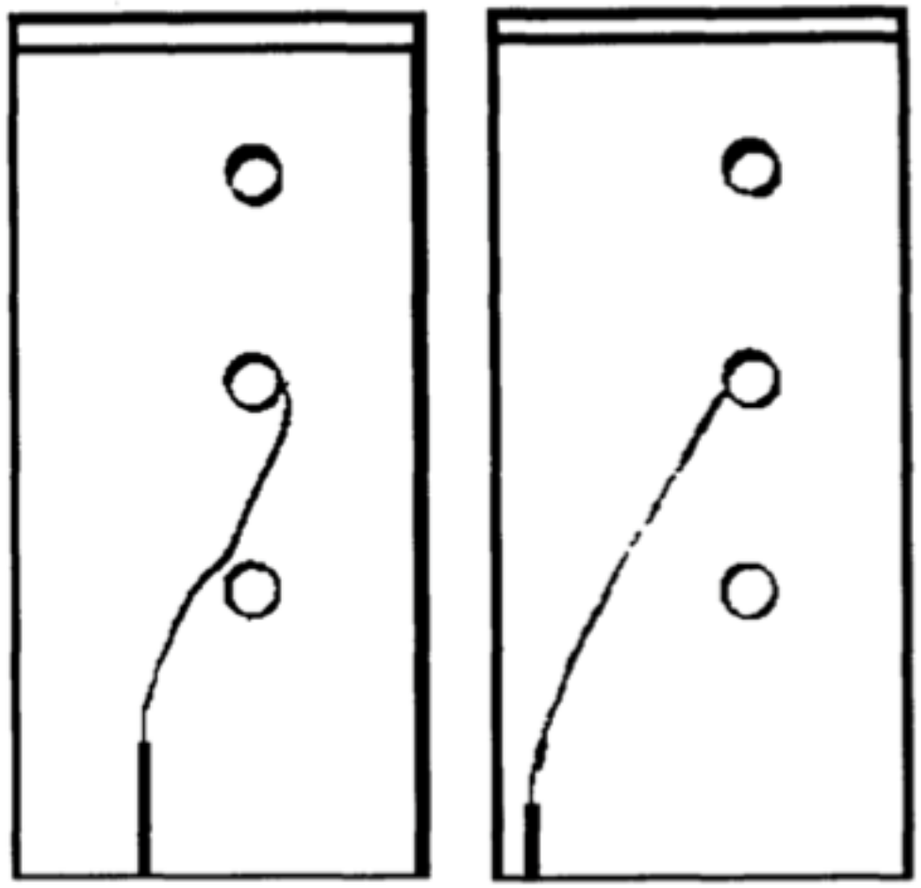

XFEM

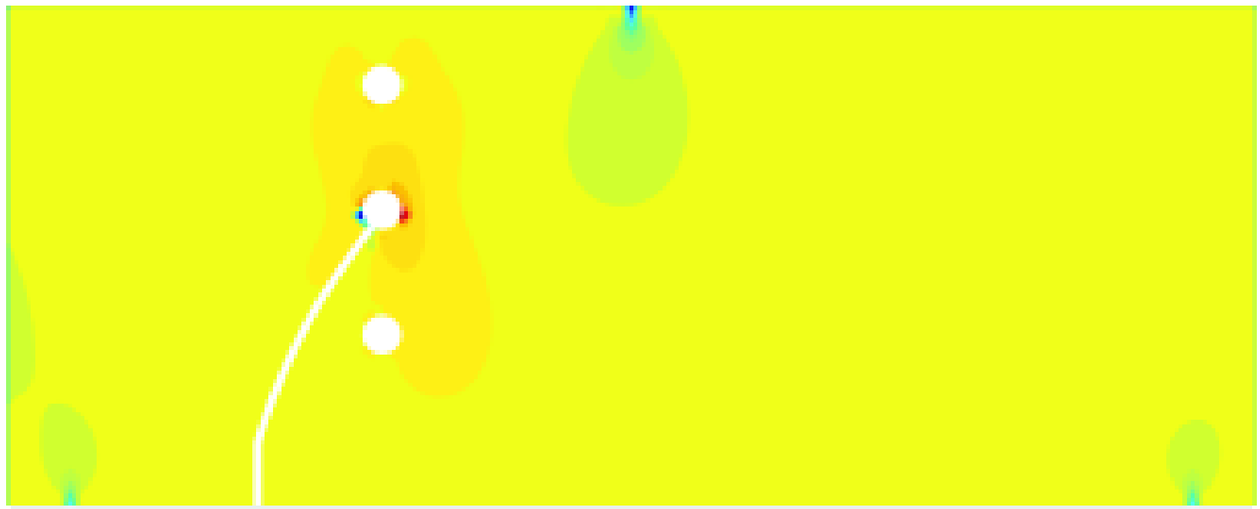

$$\theta_c = 2 \arctan \frac{1}{4} \left(K_I / K_{II} \pm \sqrt{(K_I / K_I I)^2 + 8} \right)$$

Modifications to maximum circumferential stress criterion

- **Effective traction** can be defined as a function of both normal σ_θ and tangential $\tau r\theta$ components of traction. For example:

$$\sigma_{\text{eff}} = \sqrt{\sigma_\theta^2 + (\alpha\tau_{r\theta})^2}$$

combines normal and tangential components through **mode mixity parameter** α.

- Crack propagation direction θ_c can be based on maximizing effective traction:

$$\sigma_{\text{eff}}(r, \theta_c) = \max_{-\pi<\theta<\pi}\sigma_{\text{eff}}(r, \theta)$$

- For example, in soil and rock applications normal tractions can be compressive for cracks that propagate under high shear tractions.

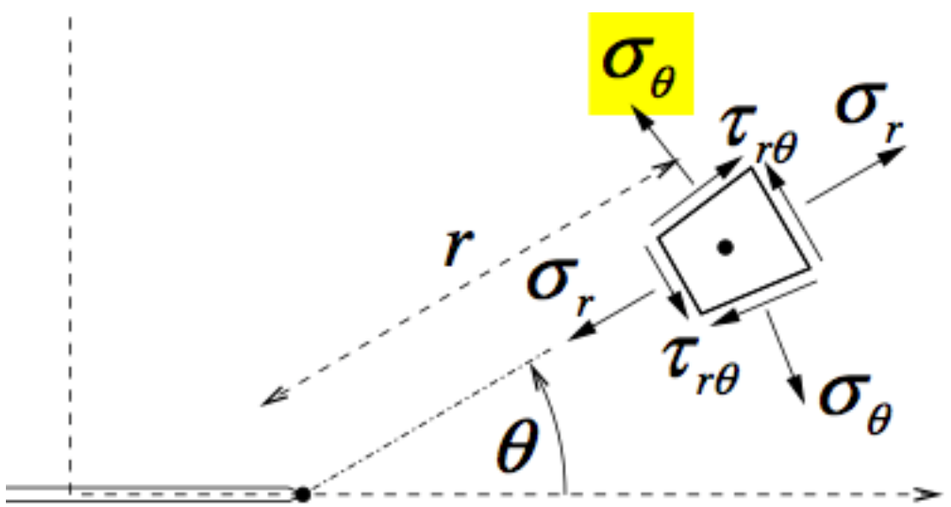

4.3 Mixed mode fracture

4.3.1 Crack propagation criteria

a) Maximum Circumferential Tensile Stress

b) Maximum Energy Release Rate

c) Minimum Strain Energy Density

4.3.2 Crack Nucleation criteria

Maximum Energy Release Rate

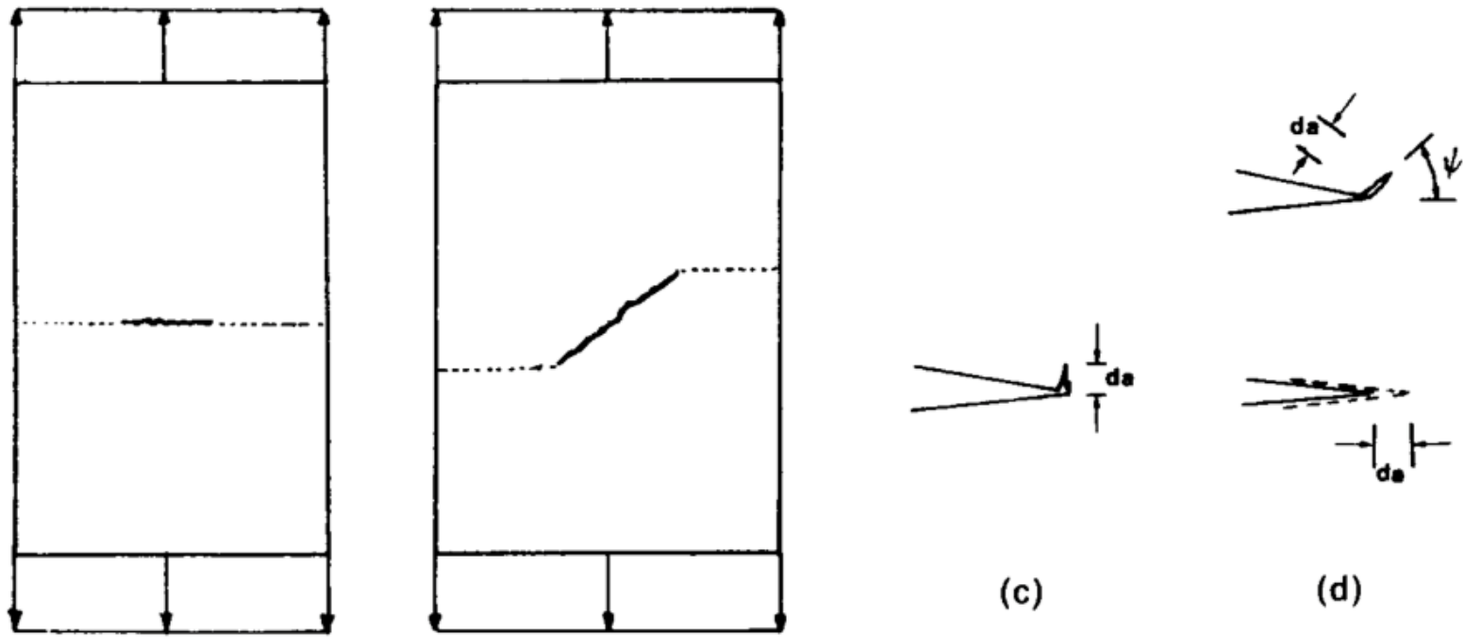

G: crack driving force -> crack will grow in the direction that G is maximum

Erdogan, F. and Sih, G.C. 1963

"If we accept Griffith (energy) theory as the valid criteria which explains crack growth, then the crack will grow in the direction along which the elastic energy release per unit crack extension will be maximum and the crack will start to grow when this energy reaches a critical value (or $G = G(\delta, \theta)$). Evaluation of $G(\delta, \theta)$ poses insurmountable mathematical difficulties."

Maximum Energy Release Rate

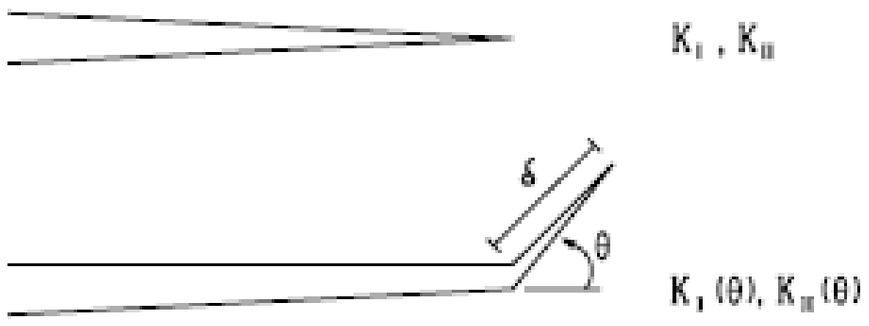

Stress intensity factors for **kinked crack extension**:
Hussain, Pu and Underwood (Hussain et al. 1974)

$$\begin{Bmatrix} K_I(\theta) \\ K_{II}(\theta) \end{Bmatrix} = \left(\frac{4}{3+\cos^2\theta}\right)\left(\frac{1-\frac{\theta}{\pi}}{1+\frac{\theta}{\pi}}\right)^{\frac{\theta}{2\pi}} \begin{Bmatrix} K_I\cos\theta + \frac{3}{2}K_{II}\sin\theta \\ K_{II}\cos\theta - \frac{1}{2}K_I\sin\theta \end{Bmatrix}$$

$$G(\theta) = \frac{1}{E'}\left(K_I^2(\theta) + K_{II}^2(\theta)\right)$$

$$G(\theta) = \frac{4}{E'}\left(\frac{1}{3+\cos^2\theta}\right)^2\left(\frac{1-\frac{\theta}{\pi}}{1+\frac{\theta}{\pi}}\right)^{\frac{\theta}{\pi}}$$
$$[(1+3\cos^2\theta)K_I^2 + 8\sin\theta\cos\theta K_I K_{II} + (9-5\cos^2\theta)K_{II}^2]$$

Maximum Energy Release Rate

Maximization condition

$$\frac{\partial G(\theta)}{\partial \theta} = 0$$

$$\frac{\partial^2 G(\theta)}{\partial \theta^2} < 0$$

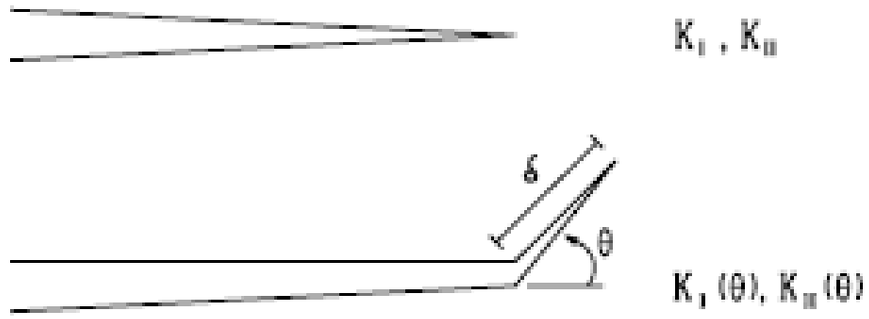

$$G(\theta) = \frac{4}{E'}\left(\frac{1}{3+\cos^2\theta}\right)^2\left(\frac{1-\frac{\theta}{\pi}}{1+\frac{\theta}{\pi}}\right)^{\frac{\theta}{\pi}}$$

$$[(1+3\cos^2\theta)K_I^2 + 8\sin\theta\cos\theta K_I K_{II} + (9-5\cos^2\theta)K_{II}^2]$$

$$\boxed{4\left(\frac{1}{3+\cos^2\theta_0}\right)^2\left(\frac{1-\frac{\theta_0}{\pi}}{1+\frac{\theta_0}{\pi}}\right)^{\frac{\theta_0}{\pi}} \left[\left(1+3\cos^2\theta_0\right)\left(\frac{K_{\mathrm{I}}}{K_{\mathrm{Ic}}}\right)^2 + 8\sin\theta_0\cos\theta_0\left(\frac{K_{\mathrm{I}}K_{\mathrm{II}}}{K_{\mathrm{Ic}}^2}\right) + \left(9-5\cos^2\theta_0\right)\left(\frac{K_{\mathrm{II}}}{K_{\mathrm{Ic}}}\right)^2\right] = 1}$$

4.3 Mixed mode fracture

4.3.1 Crack propagation criteria

a) Maximum Circumferential Tensile Stress

b) Maximum Energy Release Rate

c) Minimum Strain Energy Density

4.3.2 Crack Nucleation criteria

Strain Energy Density (SED) criterion

Sih 1973

$$U_i = \int_0^{\epsilon_{ij}} \sigma_{ij} d\epsilon_{ij} \qquad U_i = \frac{1}{4\mu}\left[\frac{\kappa+1}{4}(\sigma_x^2+\sigma_y^2) - 2(\sigma_x\sigma_y - \tau_{xy}^2)\right]$$

$$\sigma_x = \frac{K_{\mathrm{I}}}{\sqrt{2\pi r}} \cos\frac{\theta}{2}\left(1 - \sin\frac{\theta}{2}\sin\frac{3\theta}{2}\right) - \frac{K_{\mathrm{II}}}{\sqrt{2\pi r}} \sin\frac{\theta}{2}\left(2 + \cos\frac{\theta}{2}\cos\frac{3\theta}{2}\right)$$

$$\sigma_y = \frac{K_{\mathrm{I}}}{\sqrt{2\pi r}} \cos\frac{\theta}{2}\left(1 + \sin\frac{\theta}{2}\sin\frac{3\theta}{2}\right) + \frac{K_{\mathrm{II}}}{\sqrt{2\pi r}} \sin\frac{\theta}{2}\cos\frac{\theta}{2}\cos\frac{3\theta}{2} \quad (7.13)$$

$$\tau_{xy} = \frac{K_{\mathrm{I}}}{\sqrt{2\pi r}} \cos\frac{\theta}{2}\sin\frac{\theta}{2}\cos\frac{3\theta}{2} + \frac{K_{\mathrm{II}}}{\sqrt{2\pi r}} \cos\frac{\theta}{2}\left(1 - \sin\frac{\theta}{2}\sin\frac{3\theta}{2}\right) .$$

$$S = rU_i$$

Strain Energy Density (SED) criterion

- Crack direction θ_0 which **minimizes** the strain energy density S
- Crack Extends when S reaches a critical value at a distance r_0

Minimization condition

$$\frac{\partial S}{\partial \theta} = 0$$

$$\frac{\partial^2 S}{\partial \theta^2} > 0$$

Pure mode I (0 degree has smallest S)

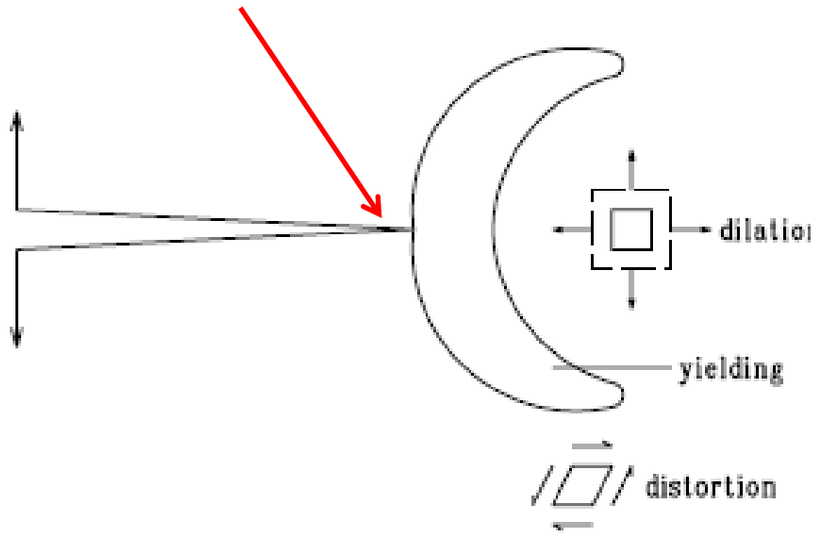

Strain Energy Density (SED) criterion

$$\boxed{\frac{8\mu}{(\kappa-1)}\left[a_{11}\left(\frac{K_{\mathrm{I}}}{K_{\mathrm{Ic}}}\right)^2+2a_{12}\left(\frac{K_{\mathrm{I}}K_{\mathrm{II}}}{K_{\mathrm{Ic}}^2}\right)+a_{22}\left(\frac{K_{\mathrm{II}}}{K_{\mathrm{Ic}}}\right)^2\right]=1}$$

$$a_{11} = \frac{1}{16\mu}\left[(1+\cos\theta)\left(\kappa-\cos\theta\right)\right]$$

$$a_{12} = \frac{\sin\theta}{16\mu}\left[2\cos\theta-(\kappa-1)\right]$$

$$a_{22} = \frac{1}{16\mu}\left[(\kappa+1)\left(1-\cos\theta\right)+(1+\cos\theta)\left(3\cos\theta-1\right)\right]$$

$$\kappa = \frac{3-\nu}{1+\nu} \quad \text{(plane stress)}$$

$$\kappa = 3-4\nu \quad \text{(plane strain)}$$

Comparison:
a) Crack Extension angle

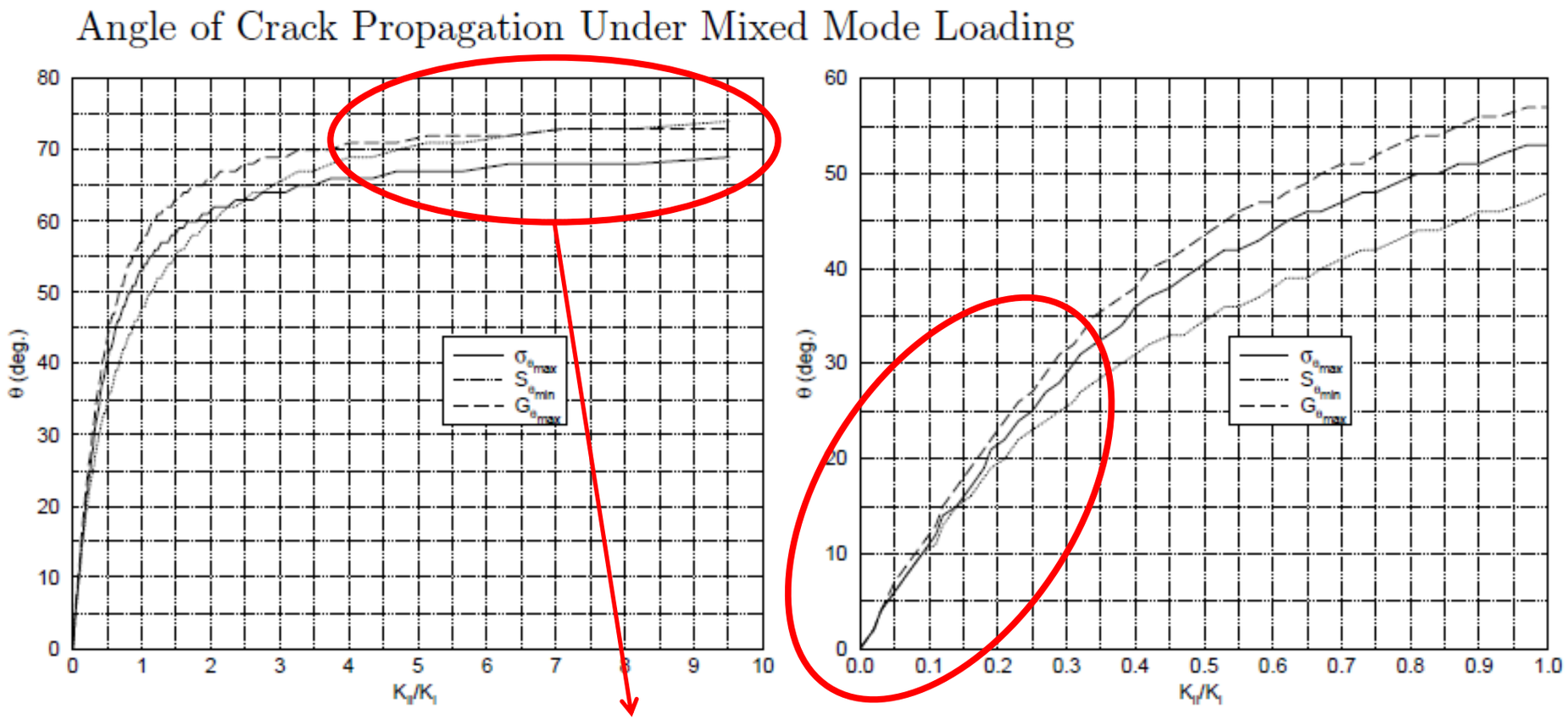

~ 70 degree angle for mode II !

Zoom view (low K_{II} component)

Good agreement for low K_{II}

Comparison:
b) Locus of crack propagation

Most conservative

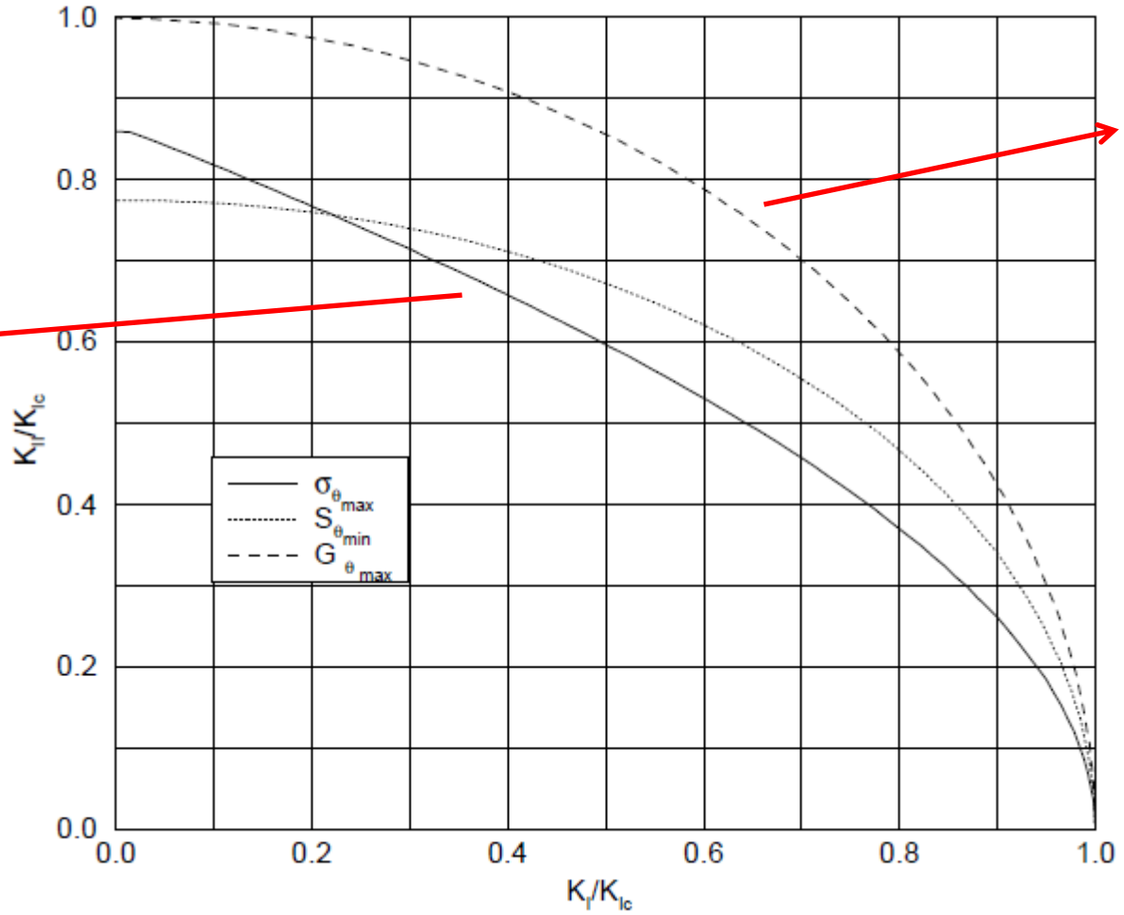

Least conservative

Mixed mode criteria: Observations

1. First crack extension θ_0 is obtained followed by on whether crack extends in θ_0 direction or not.
2. Strain Energy Density (SED) and Maximum Circumferential Tensile Stress require an r_0 but the final crack propagation locus is independent of r_0.
3. SED theory depends on Poisson ratio ν.
4. All three theories give identical results for **small ratios of K_{II}/K_I** and diverge slightly as this ratio increases
5. Crack will always extend in the direction which attempts to minimize K_{II}/K_I.
6. For practical purposes during crack propagation all three theories yield very similar paths as from 4 and 5 cracks extend mostly in mode I where the there is a better agreement between different criteria

Implication on close to mode I crack propagation

Criterion of local symmetry

When cracks grow in non-uniform stress fields, the path of the fracture is generally curved. The path taken by a crack in brittle homogeneous isotropic material can be assumed to be one for which the local stress field at the tip is of a Mode I type*:

$$K_{II} = 0 \qquad \text{at the tip}$$

*Cotterell, Brian, and JRf Rice. "Slightly curved or kinked cracks." International journal of fracture 16.2 (1980): 155-169

[1] N.V. Banichuk, "Determination of the Form of a Curvilinear Crack by Small Parameter Technique" Izv. An SSR, MTT 7, 2 (1970) 130-7 (in Russian).
[2] R.V. Goldstein and R.L. Salganik, "Plane Problem of Curvilinear Cracks in an Elastic Solid", Izv. An SSR, MIT 7, 3 (1970) 69-82 (in Russian).
[3] R.V. Goldstein and R.L. Salganik, International Journal of Fracture 10 (1974) 507-23.

If $K_{II} \neq 0$ at the crack tip, the crack would abruptly change its direction; the crack path would exhibit a kink at this position, and hence it would not be smooth [21]. By driving a curved crack straightly in the tangent direction at the crack tip the local symmetry (2) will be broken ($K_{II} \neq 0$). The change of $K_{II}(s)$ along a straight extension s in the tangent direction determines the curvature C of the crack path according to Amestoy and Leblond [see Eq. (104) in Ref. [25]]

$$C = -\frac{2}{K_I}\left[\frac{dK_{II}(s)}{ds}\right]_{\text{straight}}. \qquad (3)$$

Van-Bac Pham,Hans-Achim Bahr,Ute Bahr,Herbert Balke, Hans-Jürgen Weiss, Global bifurcation criterion for oscillatory crack path instability, PHYSICAL REVIEW E 77, 066114 (2008)

[21] B. Cotterell and J. R. Rice, Int. J. Fract. 16, 155 (1980)
[25] M. Amestoy and J. B. Leblond, Int. J. Solids Struct. 29, 465 (1992)

Example of critical local symmetry

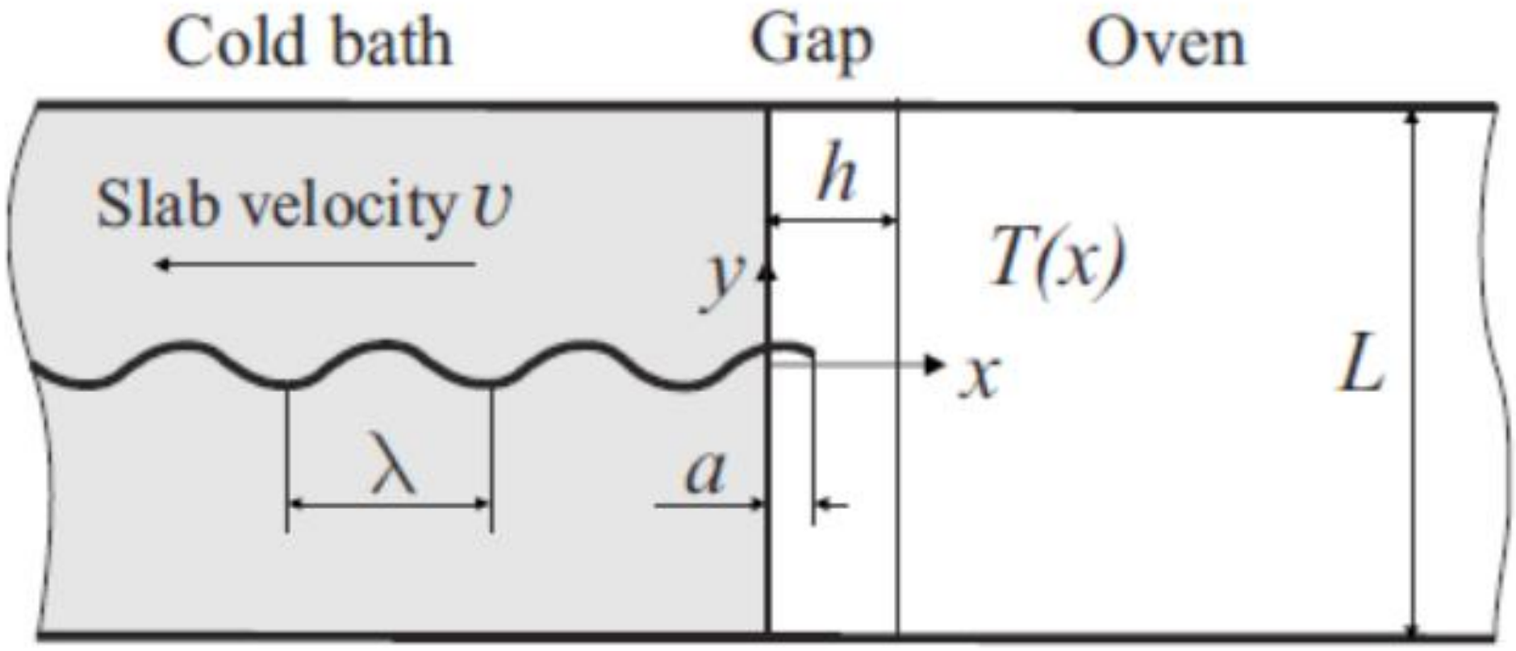

FIG. 1. Experiment by Yuse and Sano [1].

6.2 (1980): 155-169

Van-Bac Pham,Hans-Achim Bahr,Ute Bahr,Herbert Balke, Hans-Jürgen Weiss, Global bifurcation criterion for oscillatory crack path instability, PHYSICAL REVIEW E 77, 066114 (2008)

4.3 Mixed mode fracture

4.3.1 Crack propagation criteria

a) Maximum Circumferential Tensile Stress

b) Maximum Energy Release Rate

c) Minimum Strain Energy Density

4.3.2 Crack Nucleation criteria

Crack nucleation criterion

- Cracks nucleate from microscopic material defects under high stress/ strain loads.
- For each crack propagation criterion there can be a corresponding nucleation criterion.
- For example for maximum circumferential tensile stress, a crack nucleates when the maximum principle stress σ_1 at a point reaches material strength σ_0:

$$\max_{-\pi<\theta<\pi}\sigma_\theta(r\to 0^+,\theta)=\sigma_1=\sigma_0,\quad \text{crack nucleates}$$

Although we assume that there is no initial crack tip, we can measure r relative to the potential nucleation point.

- Same concept applies to modified maximum circumferential tensile stress criteria:

$$\max_{-\pi<\theta<\pi}\sigma_{\text{eff}}(r\to 0^+,\theta)=\sigma_0,\quad \text{crack nucleates}$$

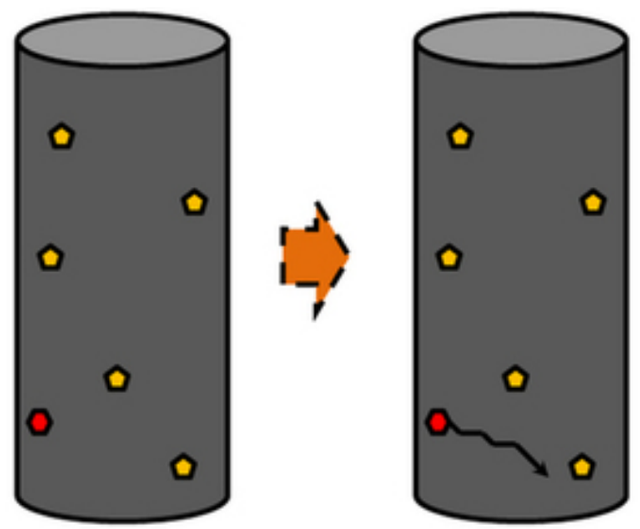

Crack nucleation criterion

- For Maximum Energy Release Rate Criterion if we assume there are no defects, there will be no crack nucleation. However, assuming that local stress field generates a tensile maximum principal stress of σ_1 a "microscopic" initial crack (defect) of length a_{ini} perpendicular to σ_1 direction generates,

$$G = \frac{K_I^2 + K_{II}^2}{E'} = \pi a_{\text{ini}} \sigma_1^2$$

so the microcrack propagates (*i.e.*, a "macroscopic" crack nucleates) when,

$$G = G_c \quad \Leftrightarrow \quad \sigma_1 = \sqrt{\frac{G_c}{\pi a_{\text{ini}}}}$$

  - Initial crack direction perpendicular to σ_1 is chosen to maximize G.
  - We have assumed the initial crack to be small enough to use the infinite domain SIF formula of $K_I = \sqrt{\pi a}\bar{\sigma}$.

8. Fatigue

8.1. Fatigue regimes

8.2. S-N, P-S-N curves

8.3. Fatigue crack growth models (Paris law)

- Fatigue life prediction

8.4. Variable and random load

- Crack retardation due to overload

Fatigue examples

Key Idea: Fluctuating loads are more dangerous than monotonic loads.

Example: *Comet Airliner* (case study). The actual cabin pressure differential when the plane was in flight was $\approx$ **8.5** pounds per square inch (psi). The design pressure was $\approx$ **20** psi (a factor of safety greater than 2). Thought to be safe! However, crack growth due to *cyclic* loading caused catastrophic failure of the aircraft.

(source Course presentation S. Suresh MIT)

Fatigue fracture is prevalent!

- Deliberately applied load reversals (e.g. rotating systems)
- Vibrations (machine parts)
- Repeated pressurization and depressurization (airplanes)
- Thermal cycling (switching off electronic devices)
- Random forces (ships, vehicles, planes)

(source: Schreurs fracture notes 2012)

Fatigue occurs always and everywhere and is a major source of mechanical failure

Fatigue

- Fatigue occurs when a material is subjected to repeated loading and unloading (cyclic loading).
- Under cyclic loadings, materials can fail (due to fatigue) at stress levels well below their yield strength or crack propagation limit-> fatigue failure.
- ASTM defines *fatigue life*, N_f, as the number of stress cycles of a specified character that a specimen sustains before failure of a specified nature occurs.

blunting

resharpening

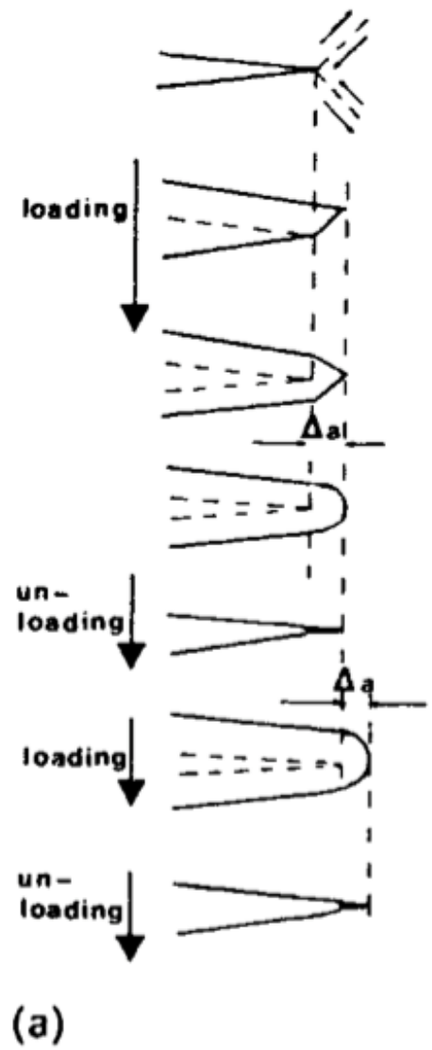

(a)

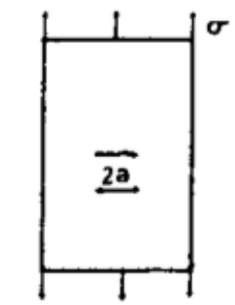

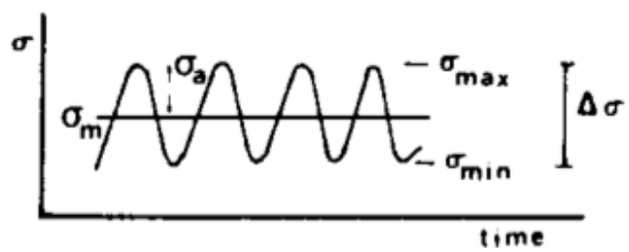

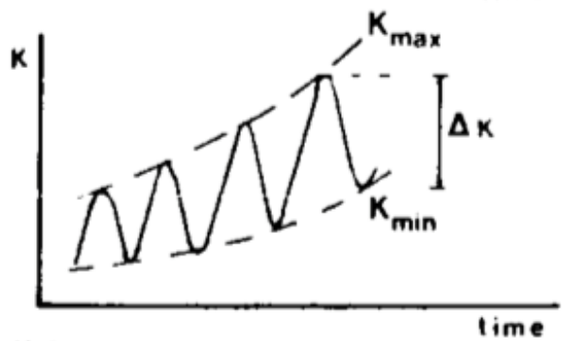

(b)

Fatigue striations

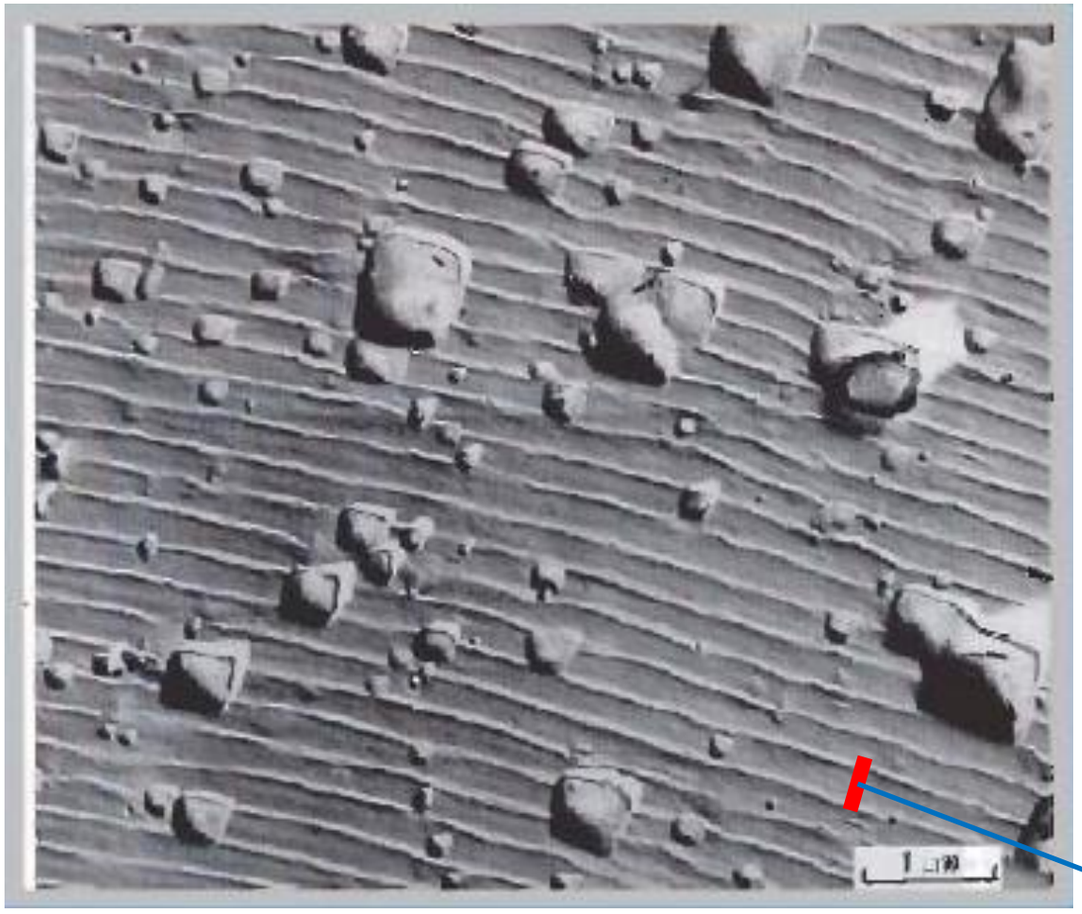

Fracture surface of a 2024-T3 aluminum alloy (source S. Suresh MIT)

Fatigue crack growth:
Microcrack formation in accumulated slip bands due to repeated loading

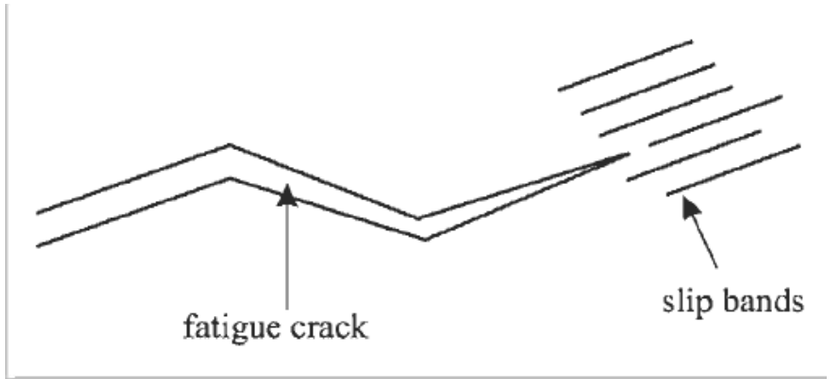

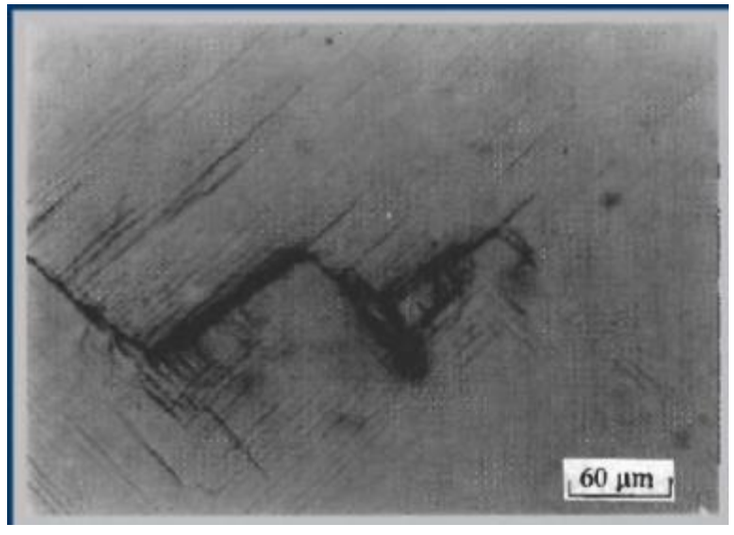

Striation caused by individual microscale crack advance incidents

Fatigue Regimes

Table 7.1 Classification of fatigue damage

Fatigue	Failure cycles N_R	Pertinent stress	Strain ratio $\Delta\varepsilon^p/\Delta\varepsilon^e$	Energy ratio $\Delta W^p/\Delta W^e$
Very high cycle fatigue	$> 10^7$	$< \sigma_F$	≈ 0	≈ 0
High cycle fatigue	10^5 to 10^6	$< \sigma_Y$	≈ 0	≈ 0
Low cycle fatigue	10^2 to 10^4	σ_Y to σ_U	1 to 10	1 to 10
Very low cycle fatigue	1 to 20	$\approx \sigma_U$	10 to 100	10 to 100

Source: Dufailly and Lemaitre (1995)

- Very high cycle and high cycle fatigue:
  - Stresses are well below yield/ultimate strength.
  - There is almost no plastic deformation (in terms of strain and energy ratios)
  - Fatigue models based on LEFM theory (e.g. SIF K) are applicable.
  - Stress-life approaches are used (stress-centered criteria)
- Low cycle and very low cycle fatigue:
  - Stresses are in the order of yield/ultimate strength.
  - There is considerable plastic deformation.
  - Fatigue models based on PFM theory (e.g. J integral) are applicable.
  - Strain-life approaches are used (strain-centered criteria)

Cyclic loadings

$$\sigma_{\max} = -\sigma_{\min}$$

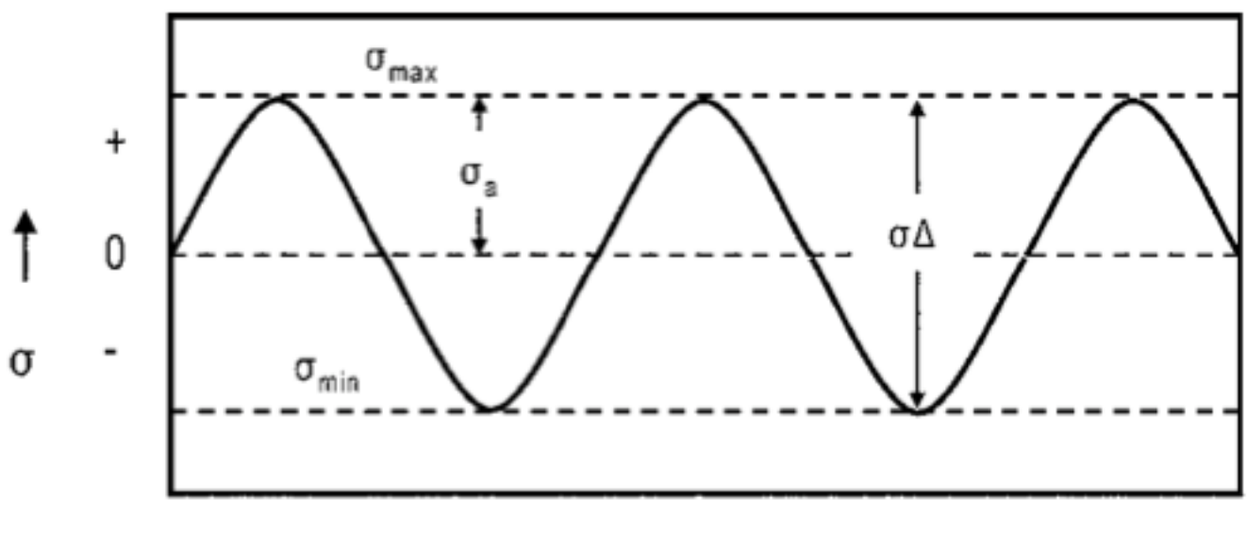

Fully Reversed Loading

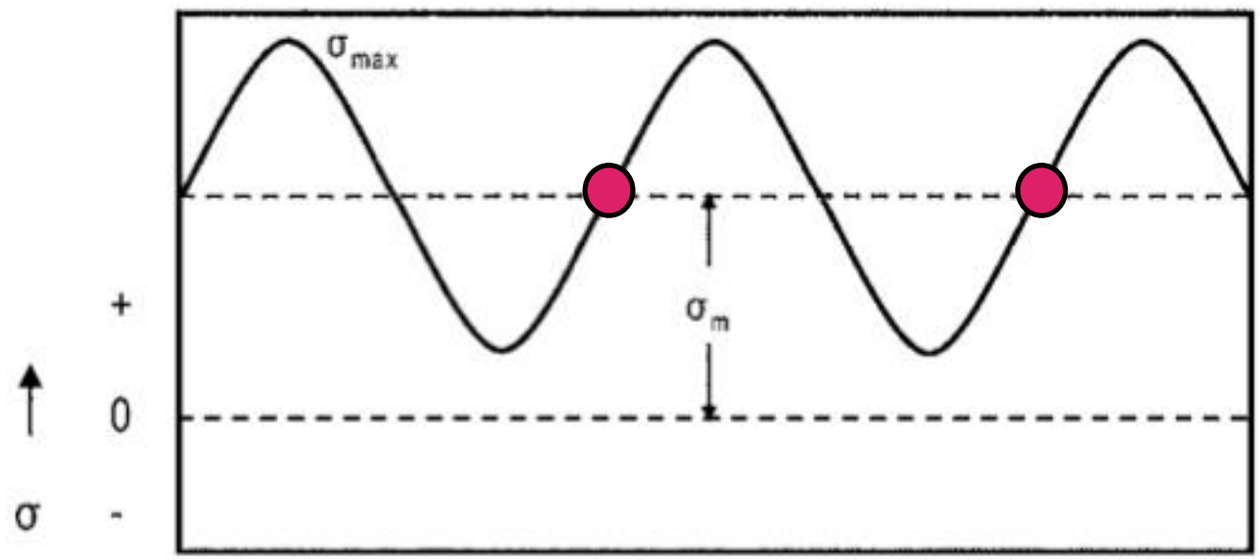

Tension-Tension with Applied Stress

$$\Delta\sigma = \sigma_{\max} - \sigma_{\min}$$

$$\sigma_a = 0.5(\sigma_{\max} - \sigma_{\min})$$

$$\sigma_m = 0.5(\sigma_{\max} + \sigma_{\min})$$

$$R = \frac{\sigma_{\min}}{\sigma_{\max}}$$ load ratio

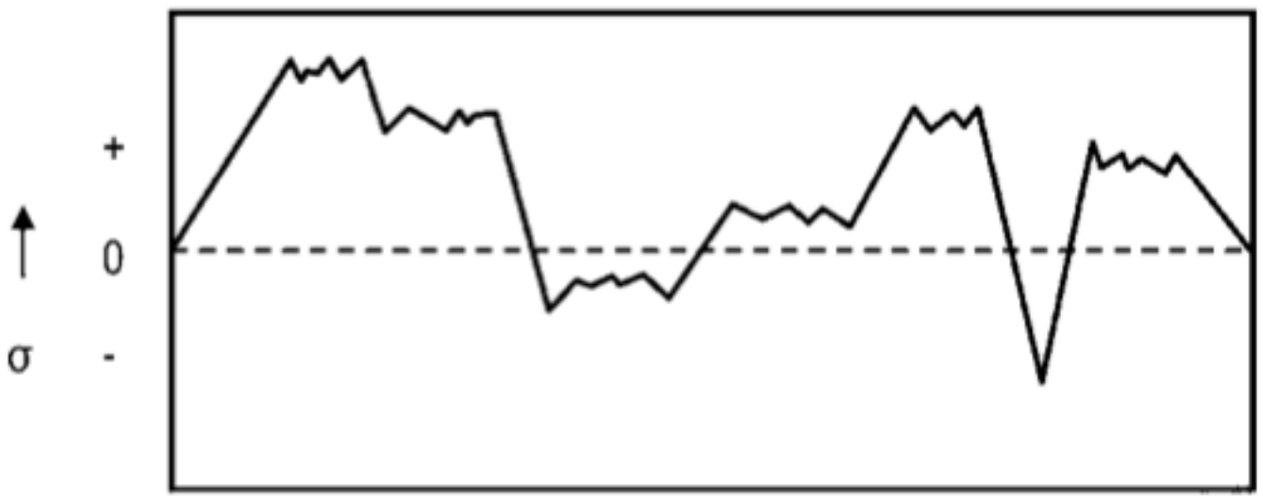

Random or Spectrum Loading

Cyclic vs. static loadings

- Static: Until K reaches K_c, crack will not grow
- Cyclic: K applied can be well below K_c, crack still grows!!!
- 1961, Paris Erdogan used the theory of LEFM to explain fatigue cracking successfully.
- Methodology: experiments first, then empirical equations are proposed.

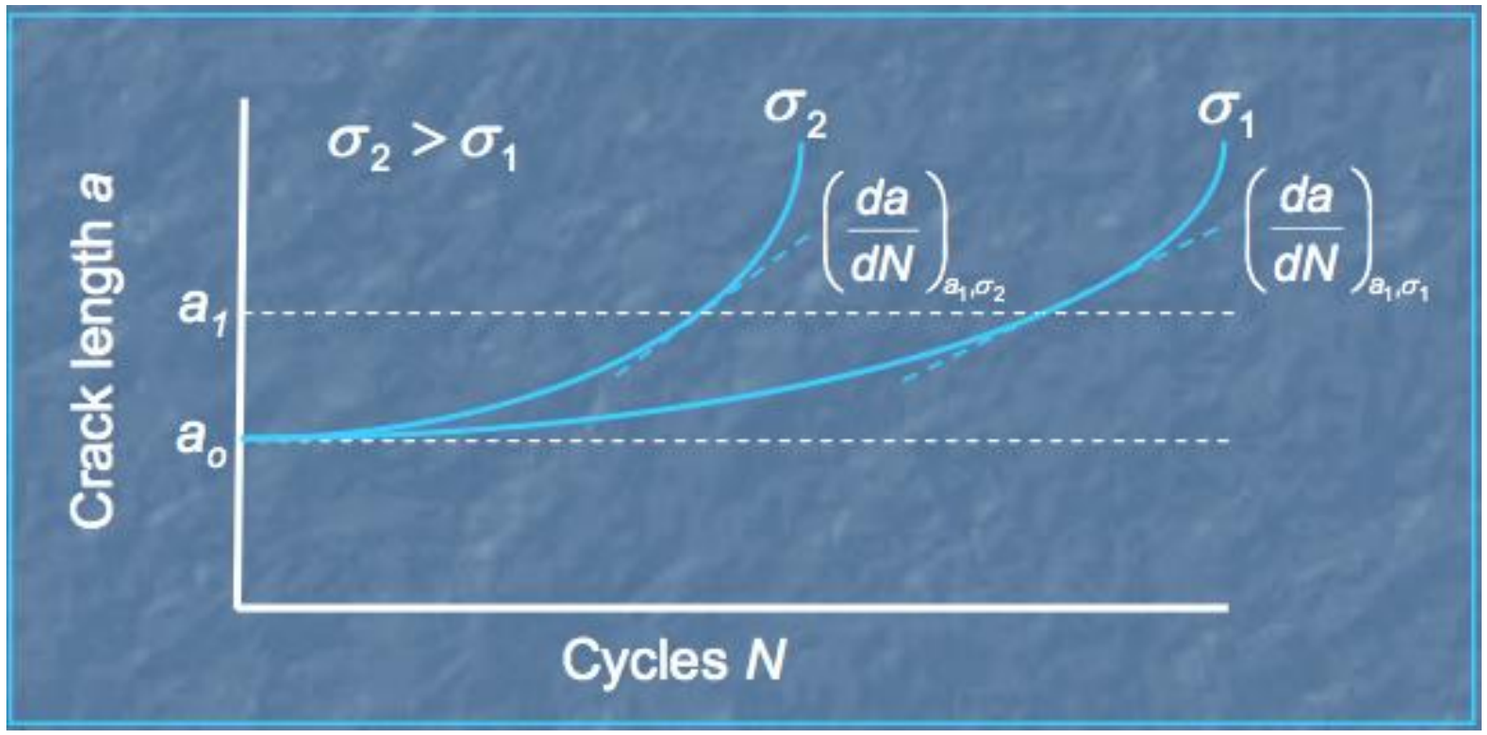

1. Initially, crack growth rate is small
2. Crack growth rate increases rapidly when a is large
3. Crack growth rate increases as the applied stress increases

S-N curve

Reminder: ASTM defines *fatigue life*, N_f, as the number of stress cycles of a specified character that a specimen sustains before failure of a specified nature occurs.

- Stress->Nf
- Nf->allowable S

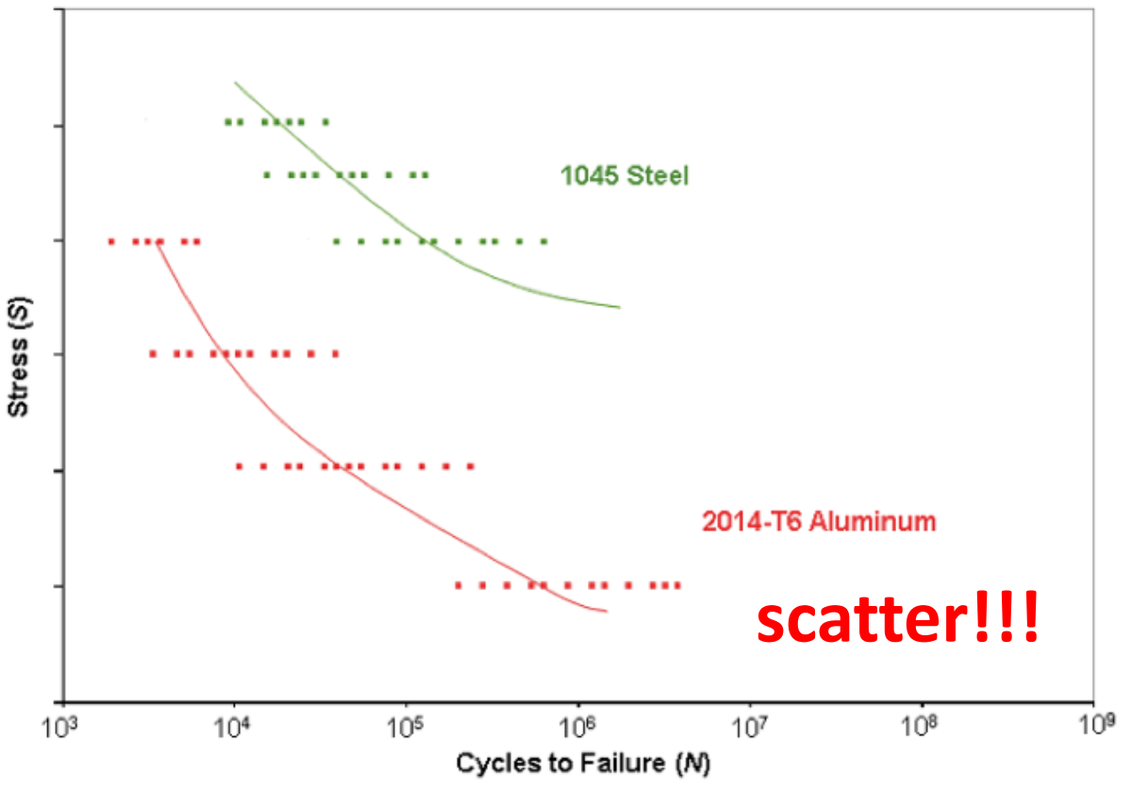

scatter!!!

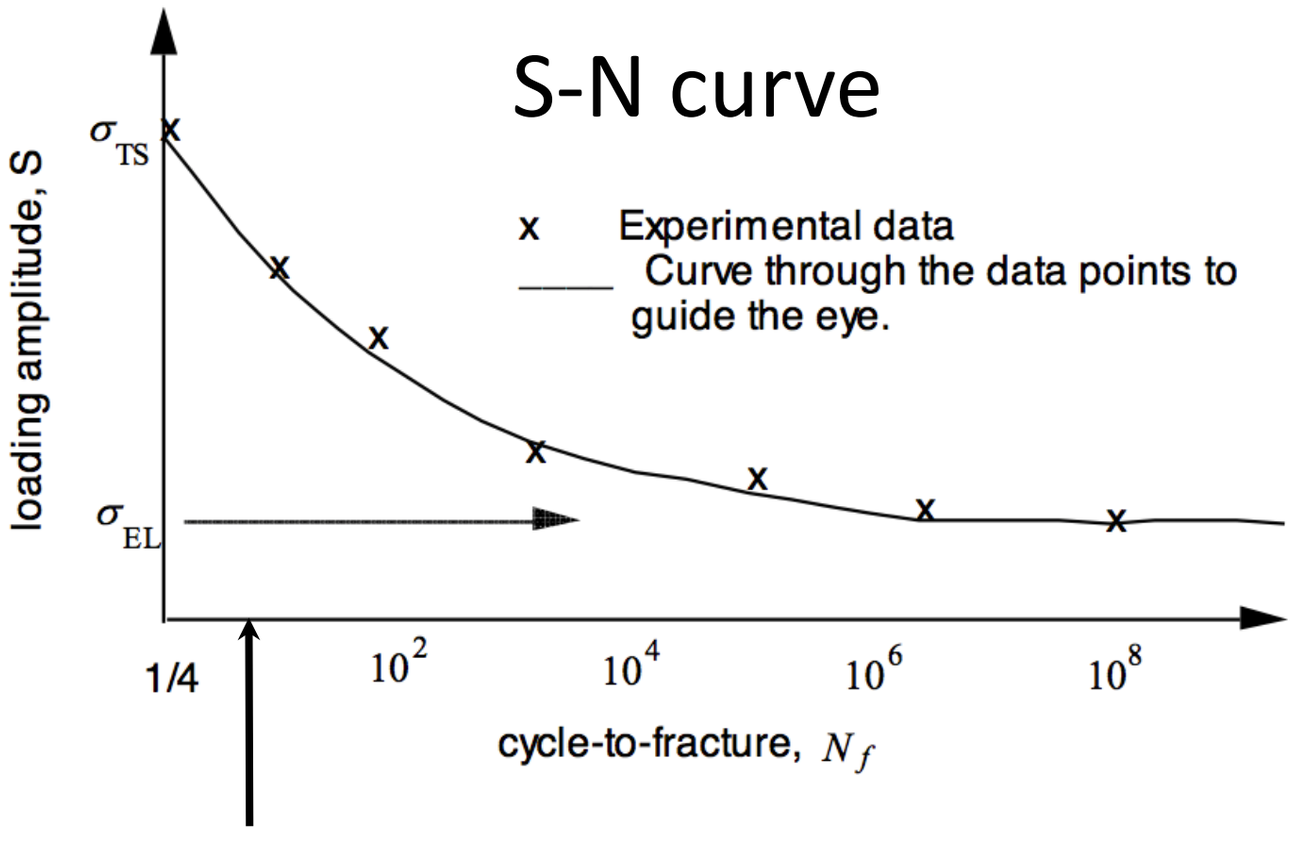

endurance limit (g.han keo dai)

S-N-P curve: scatter effects

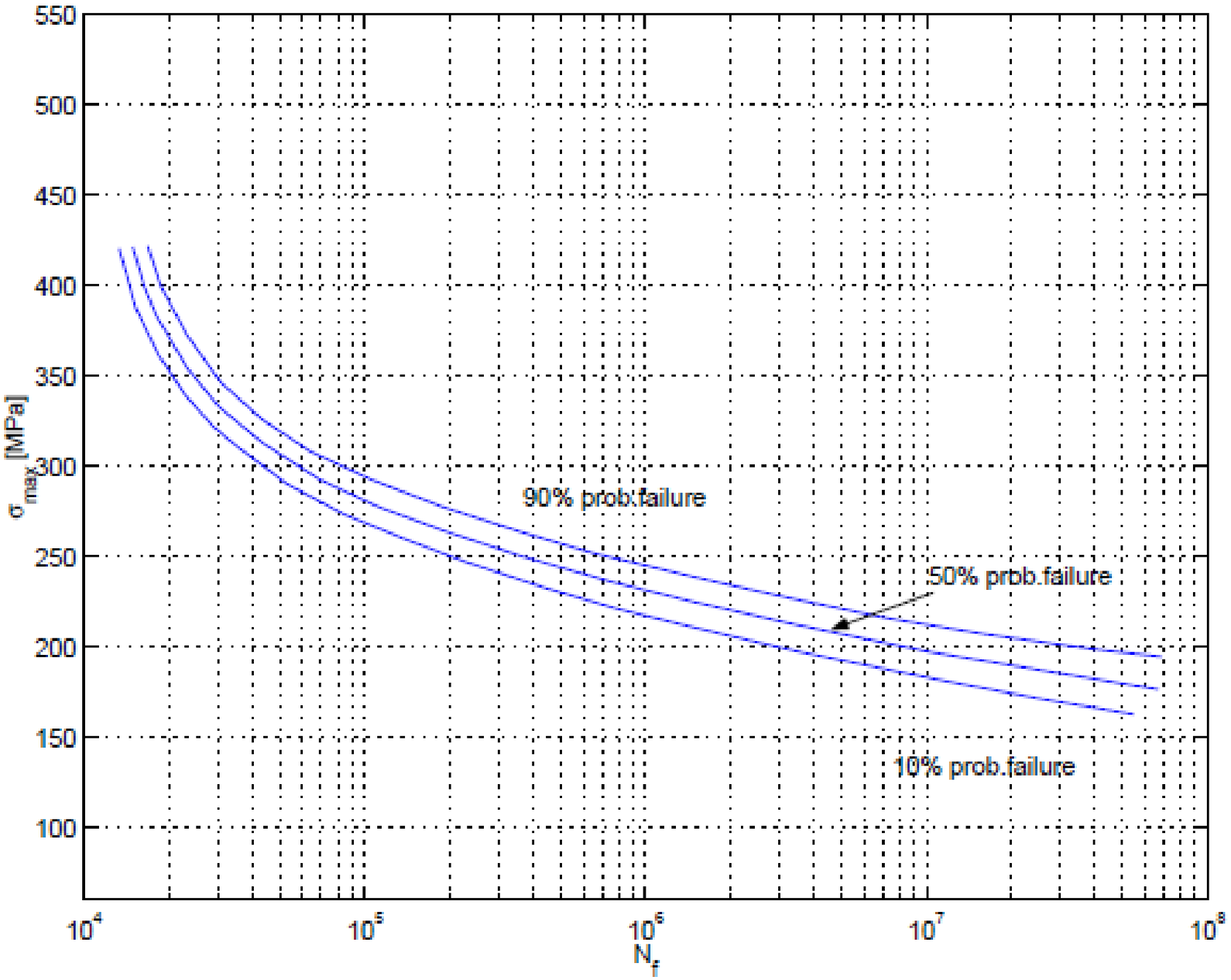

P-S-N-curves

Effect of mean stress

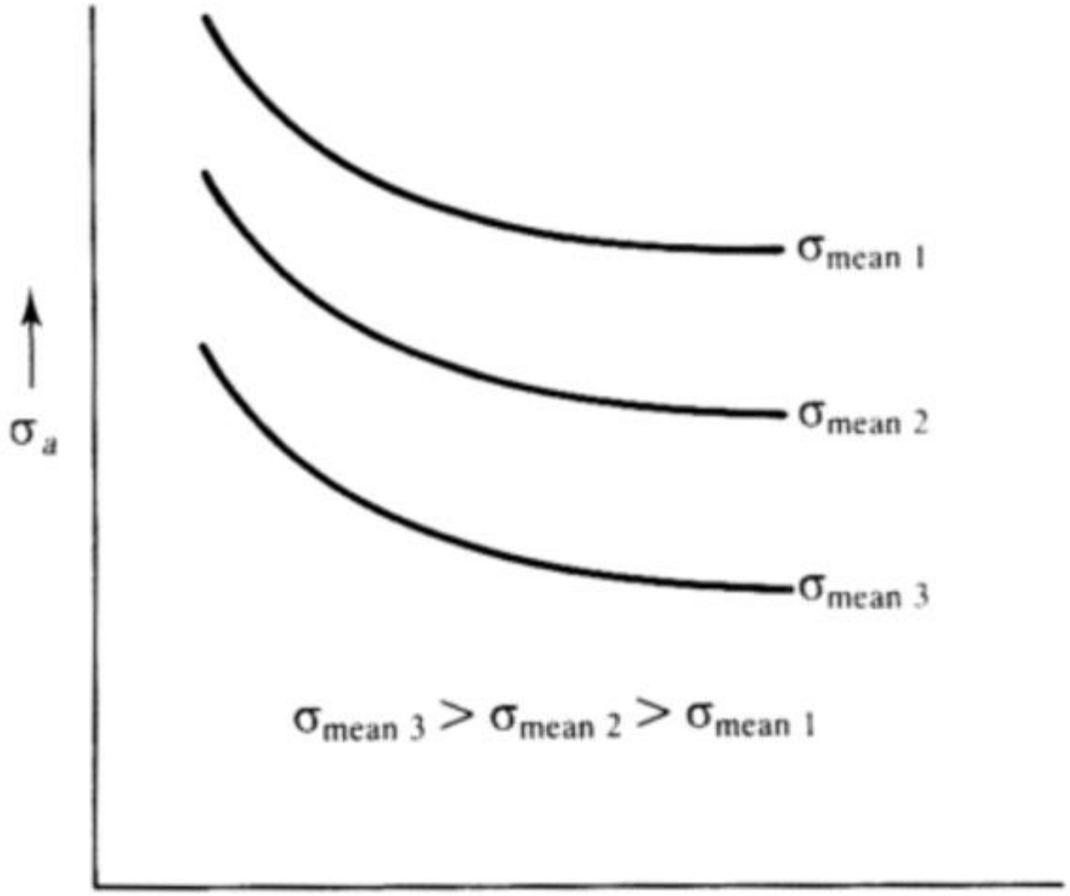

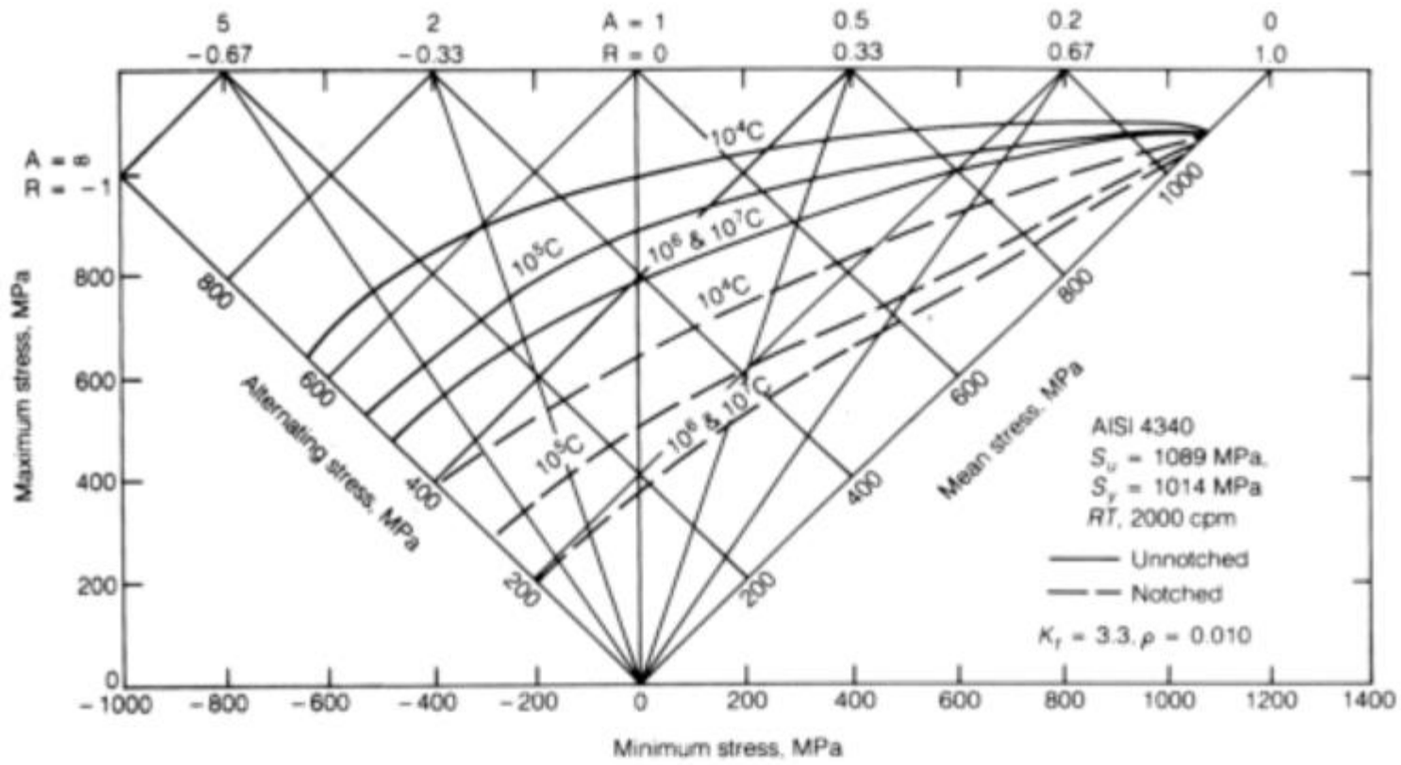

Approach 2:
Correction-factor formulas

$$\sigma_a = \sigma_{f0}\left[1-\left(\frac{\sigma_m}{\sigma_u}\right)^r\right]$$

Approach 1:
Master diagram

$$R = \frac{\sigma_{min}}{\sigma_{max}}$$

$$A = \frac{\sigma_a}{\sigma_m} = \frac{1-R}{1+R}$$

where σ_a is the amplitude of allowable stress (alternating stress).

σ_{f0} is the stress at fatigue fracture when the material under zero mean stress cycled loading

σ_m is the mean stress of the actual loading.

σ_u is the tensile strength of the material.

r = 1 is called Goodman line which is close to the results of notched specimens.

r = 2 is the Gerber parabola which better represents ductile metals.

Other correction factor

Gerber (1874) $\quad \frac{\sigma_a^*}{\sigma_a} = 1 - \left(\frac{\sigma_m}{\sigma_u}\right)^2$

Goodman (1899) $\quad \frac{\sigma_a^*}{\sigma_a} = 1 - \frac{\sigma_m}{\sigma_u}$

Soderberg (1939) $\quad \frac{\sigma_a^*}{\sigma_a} = 1 - \frac{\sigma_m}{\sigma_{y0}}$

Constant variable cyclic load

SSY

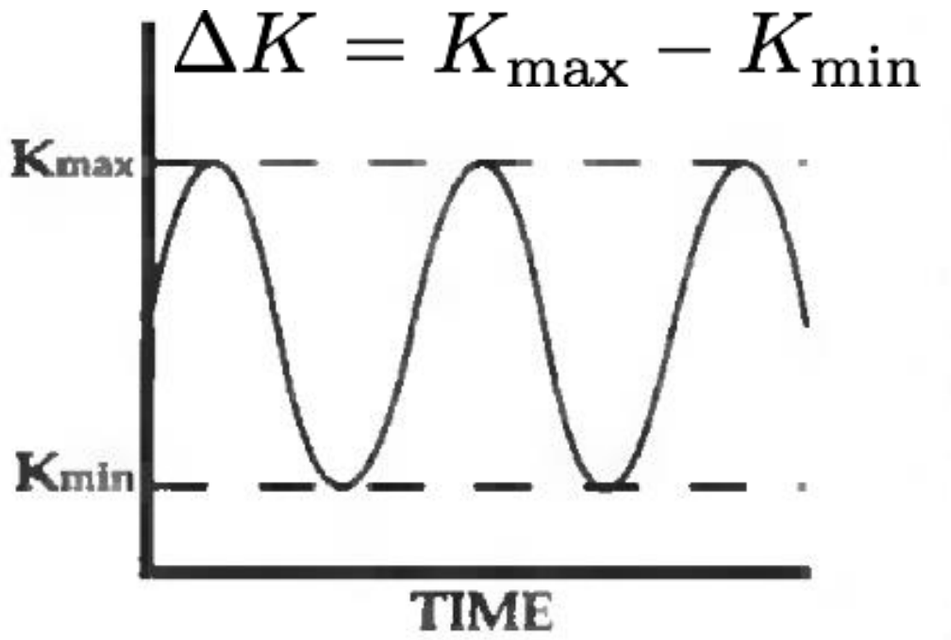

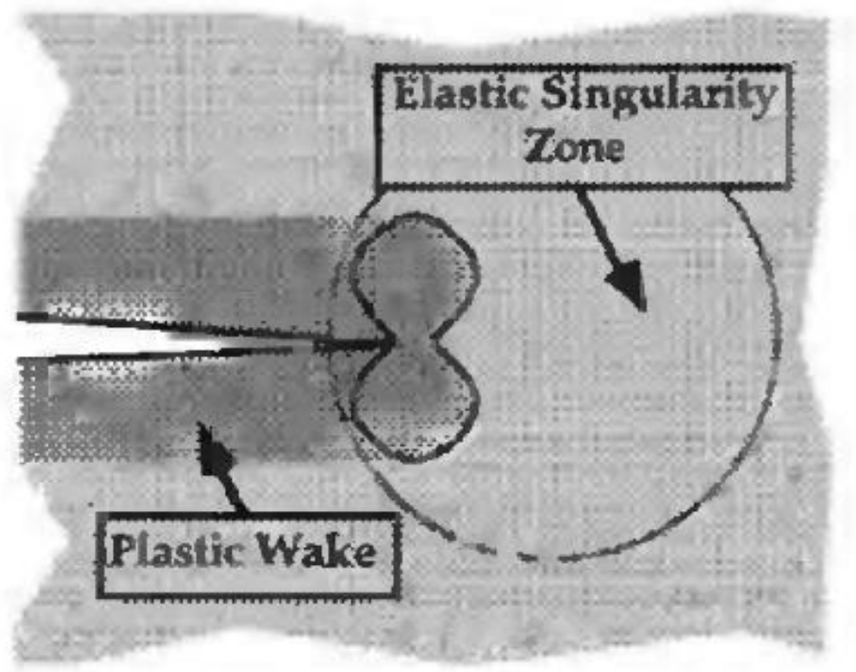

$$R = K_{\min}/K_{\max}$$

$$\Delta K = K_{\max} - K_{\min}$$

$$\Delta K = K_{\max} - K_{\min} = K_{\max}(1 - R)$$

crack growth rate

$$\frac{da}{dN} = f_1(\Delta K, R)$$

crack growth models

Crack growth data

$$K = \sigma\sqrt{\pi a}$$

1

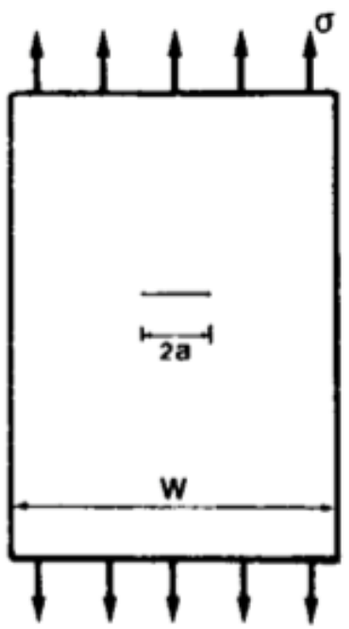

2

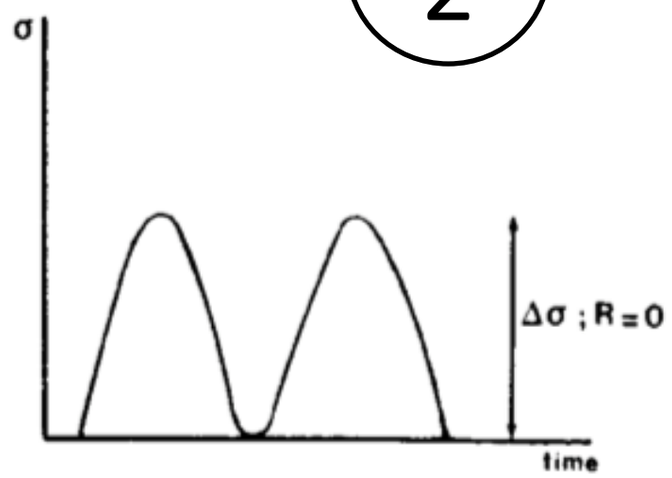

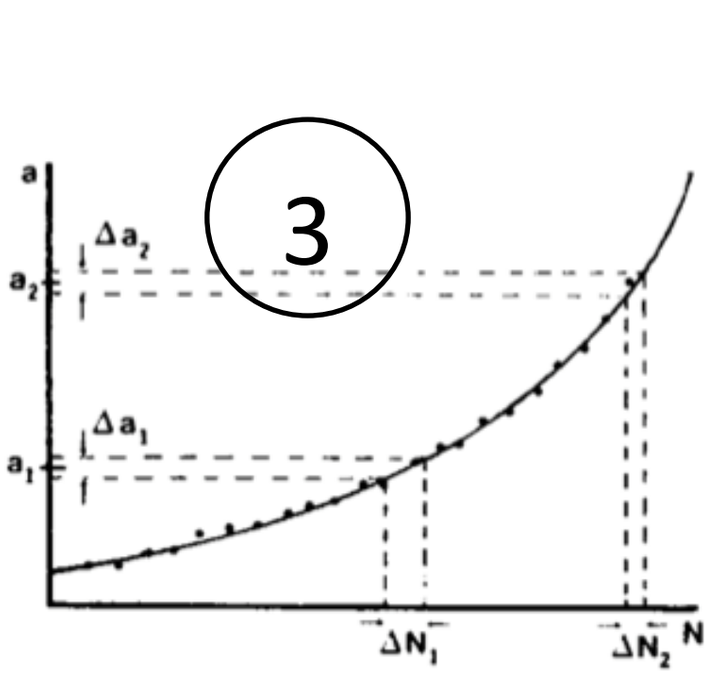

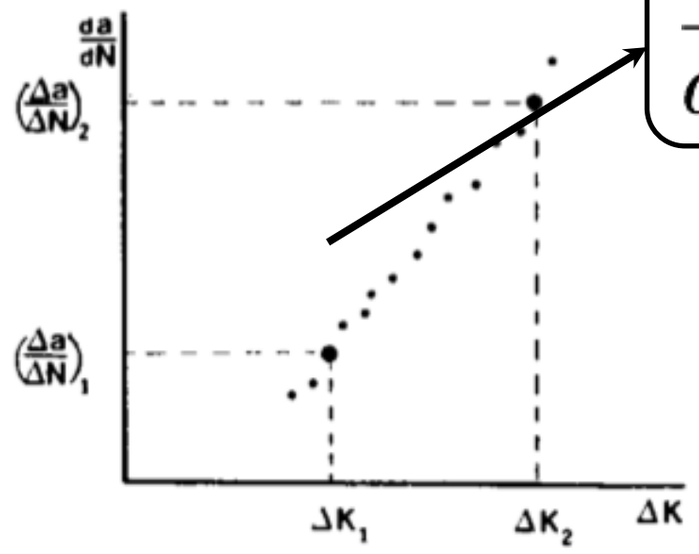

$$\frac{da}{dN} = f_1(\Delta K, R)$$

Paris' law (fatigue)

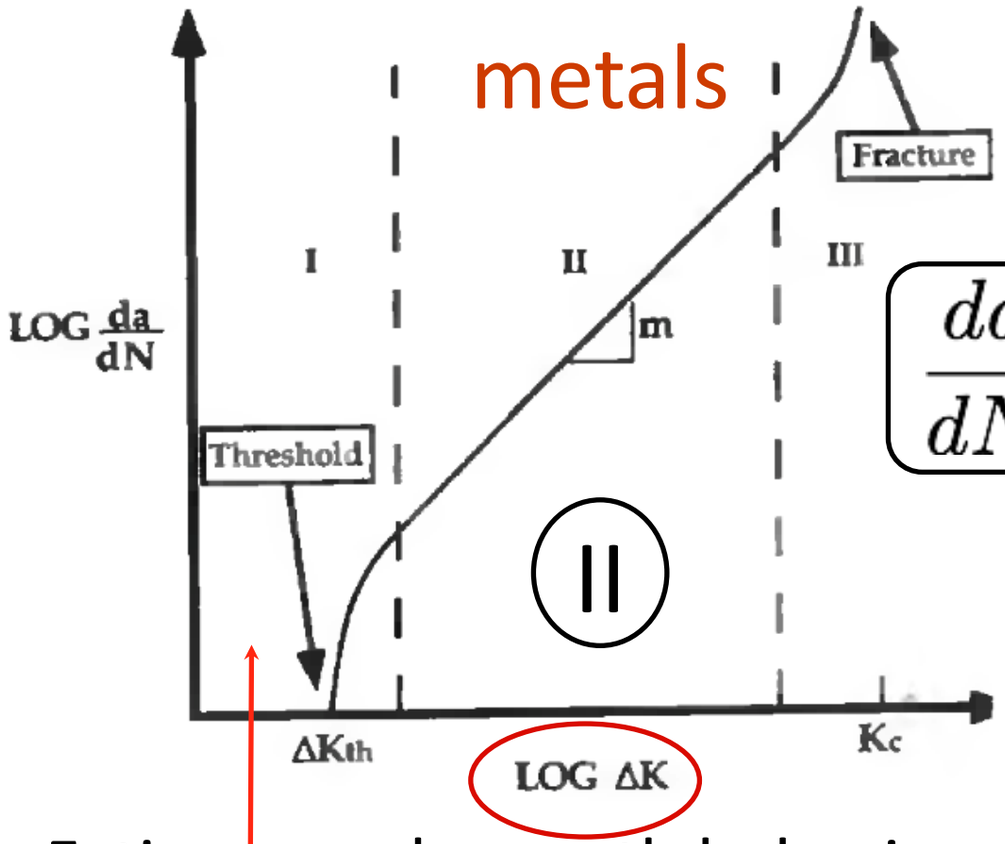

Fatigue crack growth behavior in metals

Paris' law $2 \leq m \leq 7$

$$\frac{da}{dN} = C(\Delta K)^m, \quad \Delta K = K_{\max} - K_{\min}$$

(Power law relationship for fatigue crack growth in region II)

N: number of load cycles

base 10 logarithm

Paris' law is the most popular fatigue crack growth model

Paris' law can be used to quantify the residual life (in terms of load cycles) of a specimen given a particular crack size.

$\Delta K \leq \Delta K_{\text{th}}$: no crack growth (dormant period)

10^{-8} mm/cycle

Fatigue crack growth stages

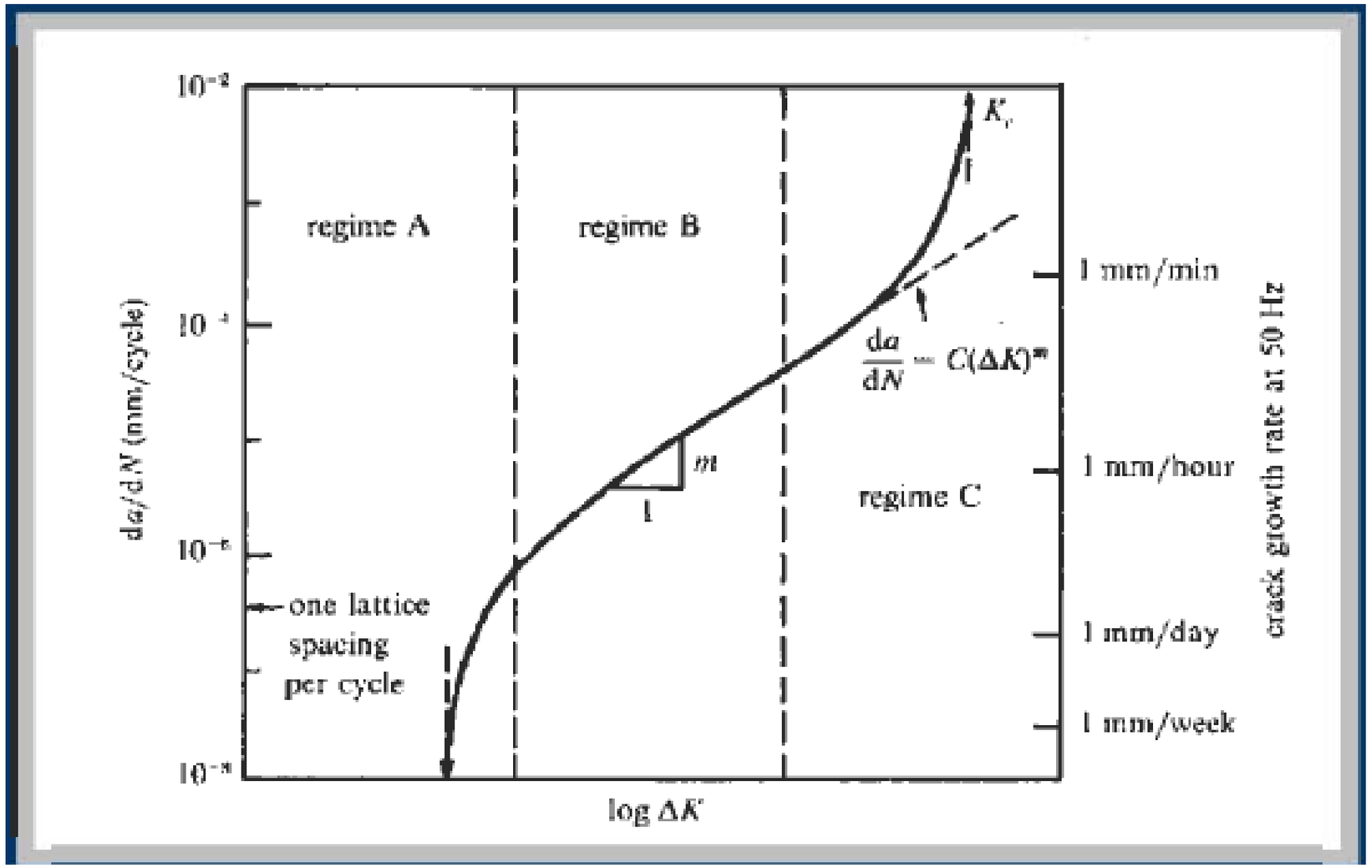

(source Course presentation S. Suresh MIT)

Fatigue crack growth stages

Regime	A	B	C
Terminology	Slow-growth rate (near-threshold)	Mid-growth rate (Paris regime)	High-growth rate
Microscopic failure mode	Stage I, single shear	Stage II, (striations) duplex slip	Additional static modes
Fracture surface features	Faceted or serrated	Planar with ripples	Additional cleavage or microvoid coalescence
Crack closure levels	High	Low	—
Microstructural effects	Large	Small	Large
Load ratio effects	Large	Small	Large
Environmental effects	Large	*	Small
Stress state effects	—	Large	Large
Near-tip plasticity†	$r_c \leq d_g$	$r_c \geq d_g$	$r_c \gg d_g$

*large influence on crack growth for certain combinations of environment, load ratio and frequency.

† r_c and d_g refer to the cyclic plastic zone size and the grain size, respectively.

(source Course presentation S. Suresh MIT)

Paris' law

not depends on load ratio R

$$\frac{da}{dN} = C(\Delta K)^m, \quad \Delta K = K_{\max} - K_{\min}$$

Table 1: Numerical parameters in the Paris equation.

alloy	m	A
Steel	3	10^{-11}
Aluminum	3	10^{-12}
Nickel	3.3	4×10^{-12}
Titanium	5	10^{-11}

C, m

are material properties that must be determined experimentally from a log(delta K)-log(da/dN) plot.

m

2-4 metals

4-100 ceramics/ polymers

Other fatigue models

Forman's model (stage II-III)

$$\frac{\mathrm{d}a}{\mathrm{d}N} = \frac{C(\Delta K)^n}{(1-R)K_c - \Delta K}$$

Paris' model

$$\frac{da}{dN} = C(\Delta K)^m$$

$$R = K_{\min}/K_{\max}$$

$$\frac{K_{\max} - K_{\min}}{K_{\max}} K_c - (K_{\max} - K_{\min}) \longrightarrow K_{\max} = K_c : \frac{da}{dN} = \infty$$

Crack closure

- At low loads, the compliance of cracked specimens are close to that of un-cracked specimens.

- Contact of crack faces:
<u>crack closure</u>

- Fatigue crack growth occurs only when crack is fully open.

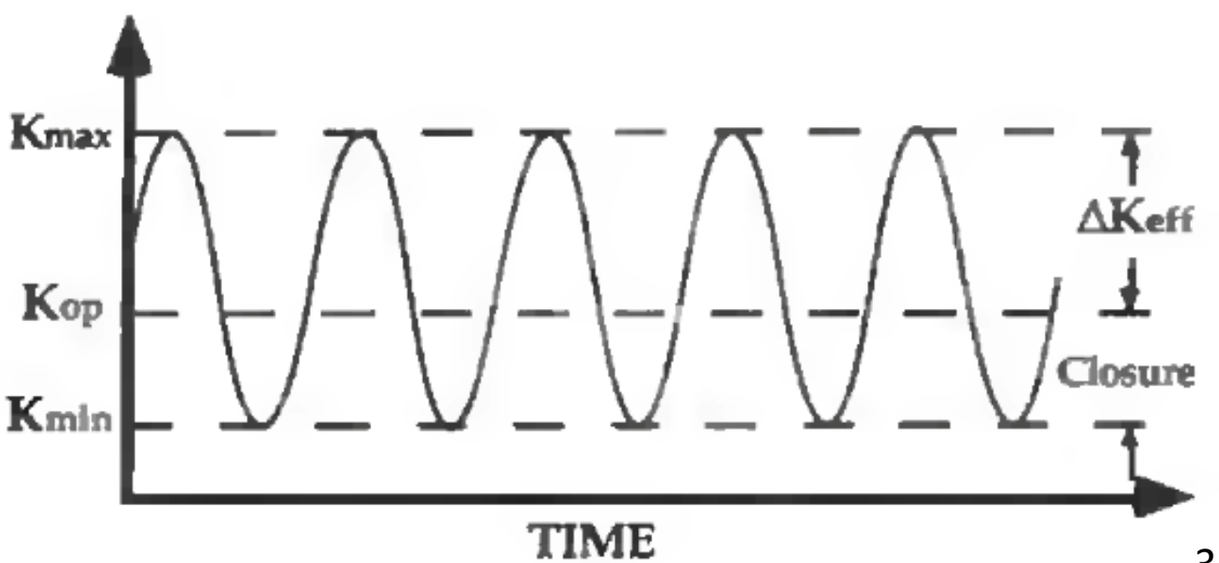

$$\Delta K_{\text{eff}} = K_{\max} - K_{\text{op}}$$

K_{op}: opening SIF

$$\frac{da}{dN} = C\Delta K_{\text{eff}}^{m}$$

371

Tension/compression cyclic loads

$$R = \frac{\sigma_{\min}}{\sigma_{\max}} < 0$$

$$\frac{da}{dN} = C(\Delta K)^m, \quad \Delta K = K_{\max} - K_{\min}$$

$$\boxed{\frac{da}{dN} = C(K_{\max})^m}$$

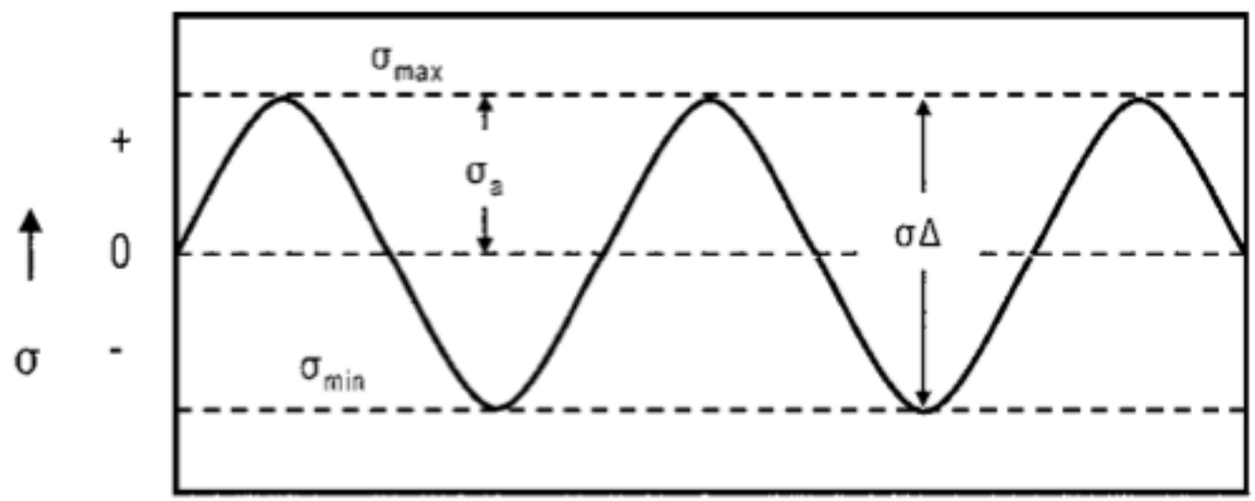

Fully Reversed Loading

Fatigue life calculation

When we are in regime B (*Paris* regime) the following calculation can be carried out to determine the number of cycles to failure. From the Paris Law:

$$\frac{da}{dN} = C\,(\Delta K)^m$$

ΔK can be expressed in terms of $\Delta\sigma$

$$\Delta K = Y\,\Delta\sigma\sqrt{\pi a}$$

Where Y depends the specific specimen geometry.

(source Course presentation S. Suresh MIT)

Fatigue life calculation

Thus the Paris Law becomes:

$$\frac{da}{dN} = C\left(Y\Delta\sigma\sqrt{\pi a}\right)^m$$

Assume that Y is a constant. Solve for da and integrate both sides:

$$\int_{a_0}^{a_f} \frac{da}{a^{m/2}} = CY^m(\Delta\sigma)^m\pi^{m/2}\int_0^{N_f} dN$$

(source Course presentation S. Suresh MIT)

Fatigue life calculation

For $m > 2$:

$$N_f = \frac{2}{(m-2)\,CY^m\,(\Delta\sigma)^m\,\pi^{m/2}}\left[\frac{1}{(a_0)^{(m-2)/2}} - \frac{1}{(a_f)^{(m-2)/2}}\right]$$

For $m = 2$:

$$N_f = \frac{1}{CY^2\,(\Delta\sigma)^2\,\pi}\ln\frac{a_f}{a_0}$$

(source Course presentation S. Suresh MIT)

Fatigue life calculation: Initial crack length a_0

In these expressions, we need to determine the initial crack length a_0 and the final crack length a_f (sometimes called the critical crack length).

How do we determine the initial crack length a_0?

Cracks can be detected using a variety of techniques, ranging from simple visual inspection to more sophisticated techniques based on ultrasonics or x-rays. If no cracks are detectable by our inspection, we must assume that a crack just at the resolution of our detection system exists.

(source Course presentation S. Suresh MIT)

Nondestructive testing (NDT)

Nondestructive Evaluation (NDE), nondestructive Inspection (NDI)

NDT is a wide group of analysis techniques used in science and industry to evaluate the properties of a material, component or system without causing damage

NDT: provides input (e.g. crack size) to fracture analysis

safety factor s

$$K(a,\sigma) = K_c \rightarrow a_c -> a_t * s$$

$$\text{NDT} \rightarrow a_o$$

$$t: \quad a_o \rightarrow a_t \quad \text{(Paris)}$$

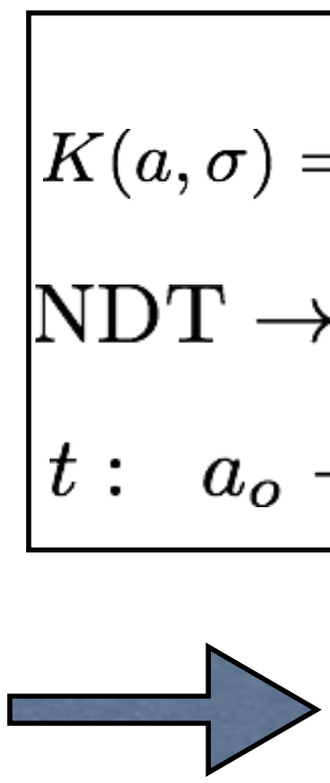

inspection time

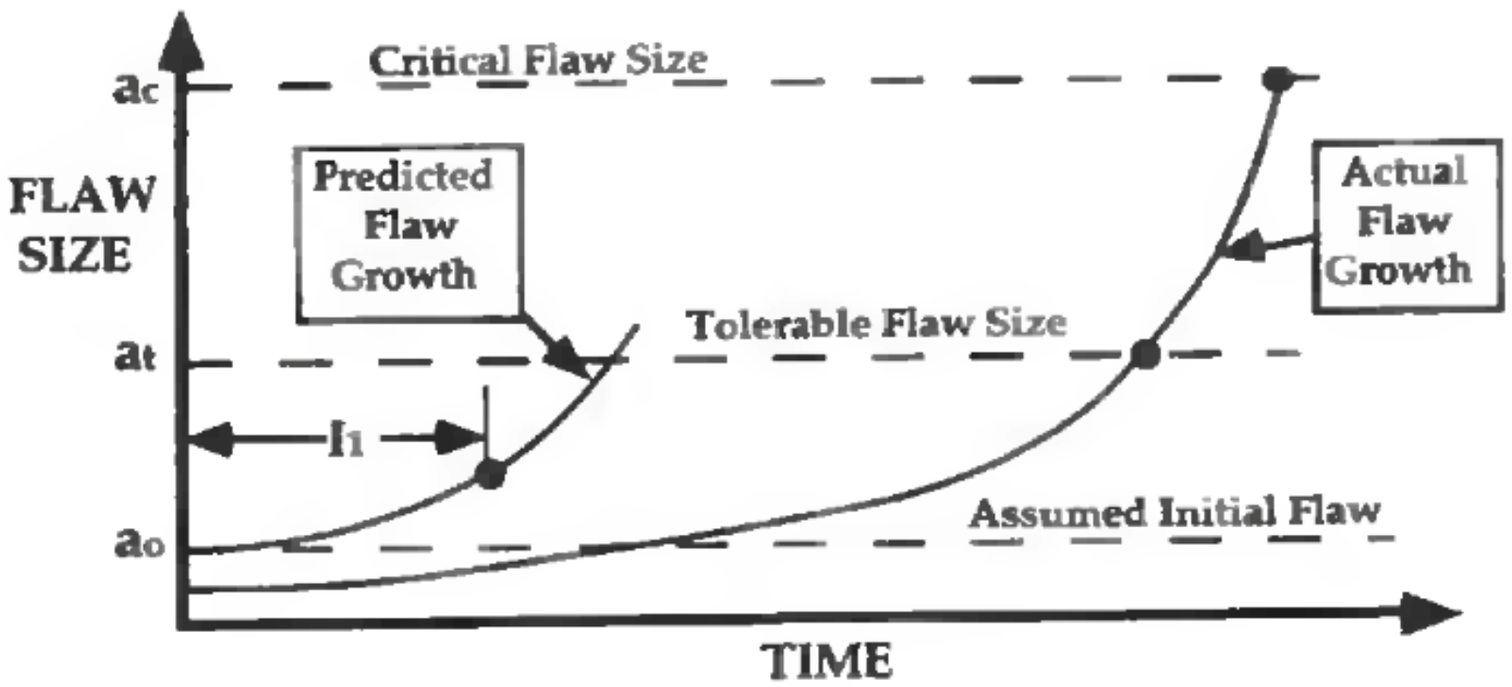

377 (a) Determination of first inspection interval, I_1.

Fatigue life calculation: Final crack length a_f

How do we determine the final crack length a_f ? We know that eventually the crack can grow to a length at which the material fails immediately, i.e.

$$K_{\max} \rightarrow K_c$$

or

$$Y\sigma_{\max}\sqrt{\pi a_f} \rightarrow K_c$$

(source Course presentation S. Suresh MIT)

Fatigue life calculation:

Crack-tolerant design

Thus we may solve for a_f as follows:

$$a_f = \frac{1}{\pi} \frac{K_c^2}{Y^2 \sigma_{\max}^2}$$

A very important idea that comes from this analysis is the following: even if a component has a detectable crack, it need not be removed from service! Using this framework, the remaining life can be assessed. The component can remain in service provided it is inspected periodically. This is the **crack-tolerant** or **damage tolerant** design approach.

(source Course presentation S. Suresh MIT)

Fatigue life calculation: Example

- Given: Griffith crack, $2a_0, \Delta\sigma, C, m, K_{Ic}, N_0$
- Question: compute N_f

$$\boxed{K = \sigma\sqrt{\pi a}}$$

analytical integration

$$dN = \frac{da}{C(\Delta K)^m} = \frac{da}{C(\Delta\sigma\sqrt{\pi a})^m}$$

$$N = N_0 + \int_{a_0}^{a_f} \frac{da}{C(\Delta\sigma\sqrt{\pi a})^m}$$

$$\boxed{m = 4}$$

$$N = N_0 + \frac{1}{C(\Delta\sigma)^4\pi^2}\int_{a_0}^{a_f}\frac{da}{a^2} = N_0 + \frac{1}{C(\Delta\sigma)^4\pi^2}\left(\frac{1}{a_0} - \frac{1}{a_f}\right)$$

measurement $K_{\max} = \sigma_{\max}\sqrt{\pi a_f} = K_{Ic}$

Numerical integration of fatigue law

$$N = N_0 + \int_{a_0}^{a_f} \frac{da}{C(\Delta\sigma f(a/W)\sqrt{\pi a})^m}$$ tedious to compute

set $\Delta\sigma$, ΔN, a_c

initialize $N = 0$, $a = a_0$

while $a < a_c$

$$\Delta K = \beta\, \Delta\sigma \sqrt{\pi * a}$$

$$\frac{da}{dN} = C * (\Delta K)^m \quad \rightarrow \quad \Delta a = \frac{da}{dN} * \Delta N$$

$$a = a + \Delta a$$

$$N = N + \Delta N$$

end

Importance of initial crack length

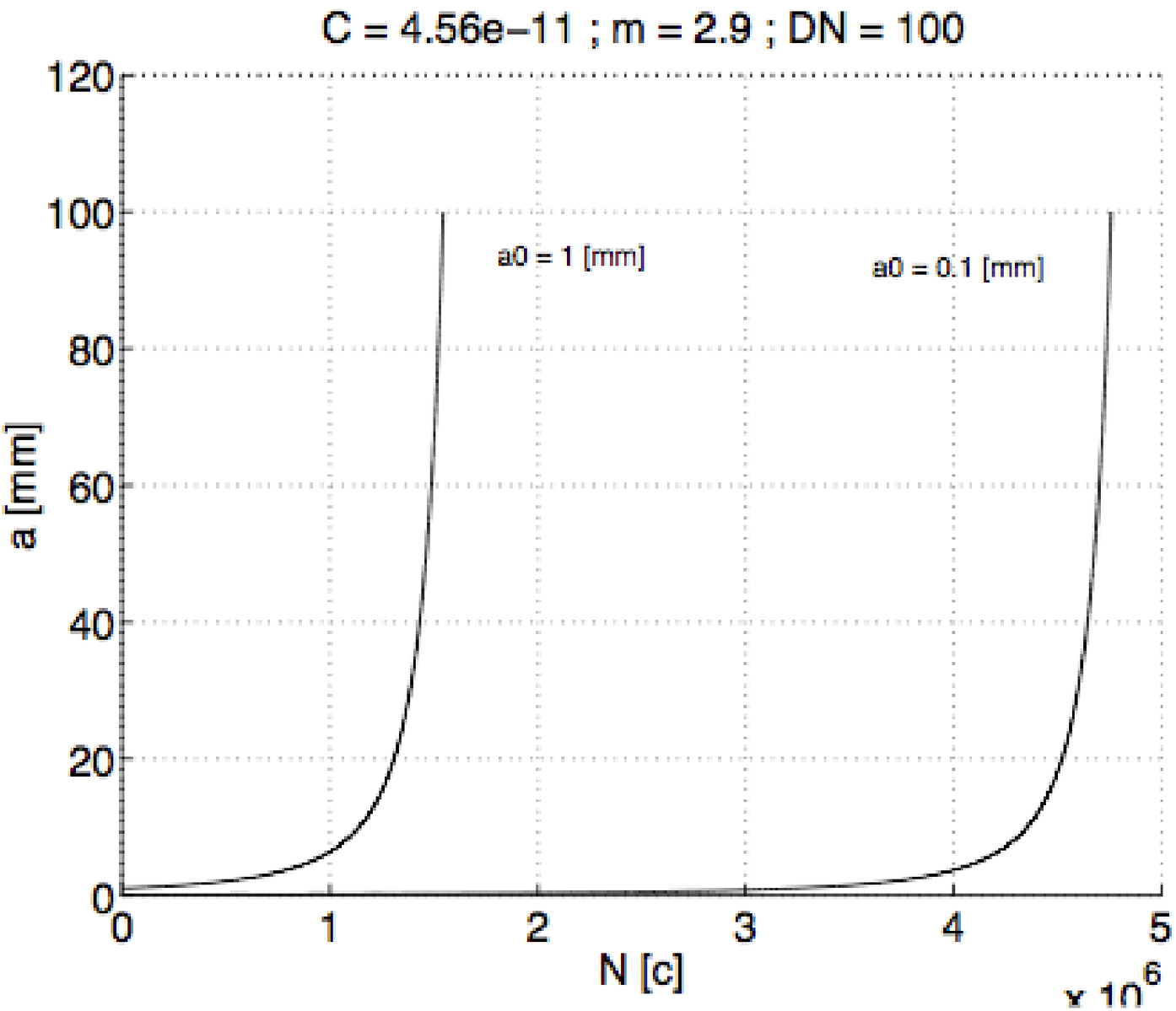

aluminum ; $\Delta\sigma = 50$ [MPa]

Fatigue design philosophies:

Safe-life approach

- Determine typical service spectra.
- Estimate useful fatigue life based on laboratory tests or analyses.
- Add factor of safety.
- At the end of the **expected** life, the component is retired from service, **even if** no failure has occurred and the component has considerable residual life.
- Emphasis on prevention of **crack initiation**.
- Approach is theoretical in nature.

(source Course presentation S. Suresh MIT)

Fatigue design philosophies:

Fail-safe approach

- Even if an individual member of a component fails, there should be sufficient **structural integrity** to operate safely.
- Multiple load paths and **crack arresters**.
- Mandates periodic inspection.
- Accent on **crack growth** rather than **crack initiation**.

(source Course presentation S. Suresh MIT)

Fatigue design philosophies:

Case study

F-100 gas turbine engines in F-15 and F-16 fighter aircraft for U.S. Airforce.

Old Approach:

- 1000 disks could be retired from service when, statistically, only one disk had a fatigue crack ($a \leq 0.75$ mm).

New, RFC Approach (since 1986):

- Retirement of a component occurs when the unique fatigue life of that particular component is expended.
- Retirement only when there is reason for removal (e.g. crack).

(source Course presentation S. Suresh MIT)

Fatigue design philosophies:

Case study

- Twin engine F-15 and single engine F-16.
- 3200 engines in the operational inventory of U.S. Air Force.
- 23 components of the engine are managed under RFC.
- 1986-2005 life cycle cost savings: $1,000,000,000
- Additional labor and fuel costs: $655,000,000

(source Course presentation S. Suresh MIT)

Miner's rule for variable load amplitudes

1945

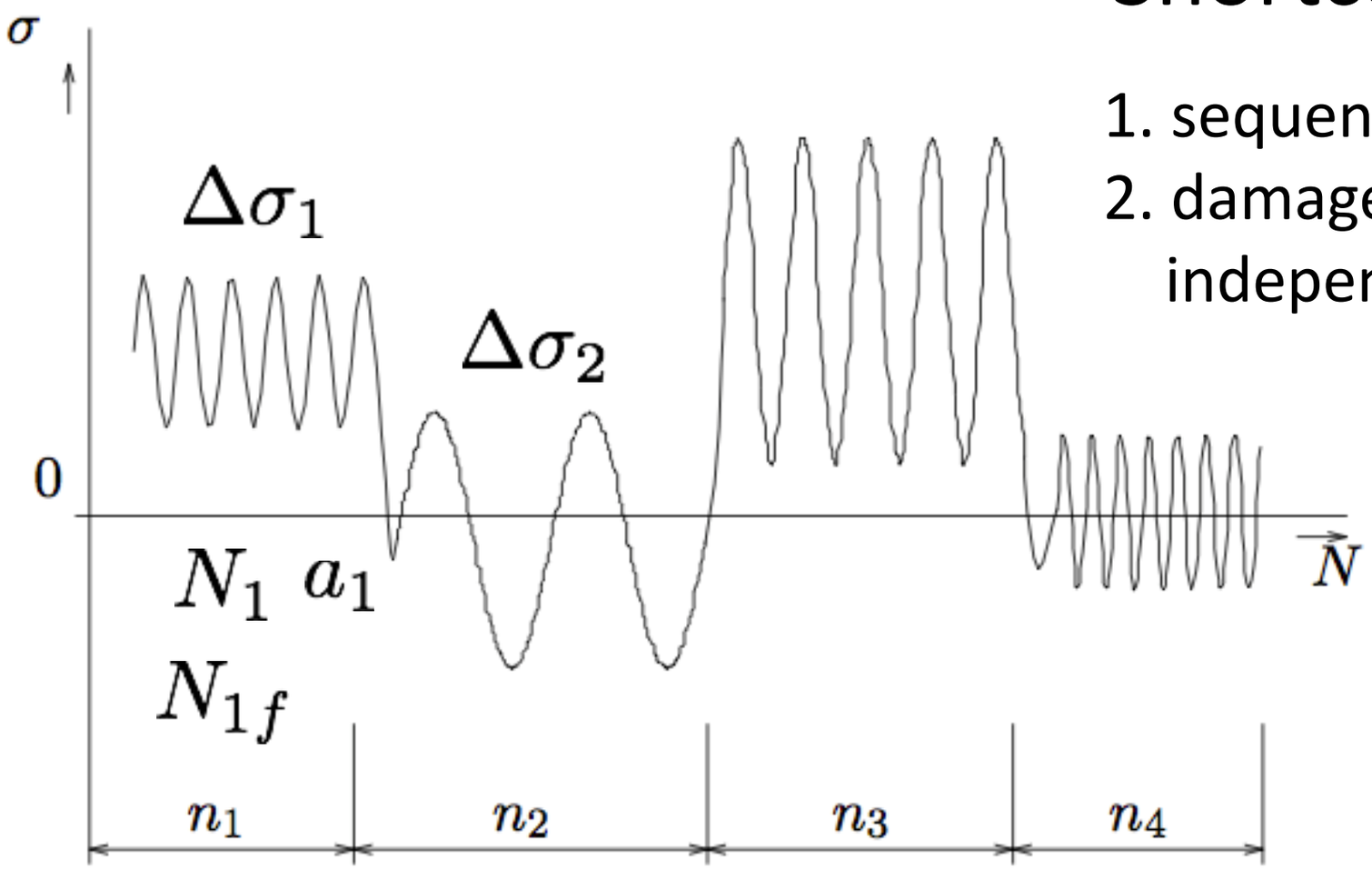

Shortcomings:

1. sequence effect not considered
2. damage accumulation is independent of stress level

N_i/N_{if} : damage

$$\sum_{i=1}^{n} \frac{N_i}{N_{if}} = 1$$

$\Delta\sigma_i$

N_i number of cycles a_0 to a_i

N_{if} number of cycles a_0 to a_c

Influence of sequence of loading

The component is assumed to fail when the total damage becomes equal to 1, or

$$\sum_i \frac{n_i}{N_{fi}} = 1$$

It is assumed that the **sequence** in which the loads are applied has no influence on the lifetime of the component. In fact, the sequence of loads *can* have a large influence on the lifetime of the component.

(source Course presentation Hanlon, S. Suresh MIT)

Influence of sequence of loading

Consider a sequence of two different cyclic loads, σ_{a1} and σ_{a2}. Let $\sigma_{a1} > \sigma_{a2}$.

Case 1: Apply σ_{a1} then σ_{a2}.

In this case, $\sum_i \frac{n_i}{N_{fi}}$ can be less than 1. During the first loading (σ_{a1}) numerous microcracks can be initiated, which can be further propagated by the second loading (σ_{a2}).

(source Course presentation Hanlon, S. Suresh MIT)

Influence of sequence of loading

Case 2: Apply σ_{a2} then σ_{a1}.

In this case $\sum_i \frac{n_i}{N_{fi}}$ can be greater than 1. The first loading (σ_{a2}) is not high enough to cause any microcracks, but it is high enough to *strain harden* the material. Then in the second loading (σ_{a1}), since the material has been hardened it is more difficult to initiate any damage in the material.

(source Course presentation Hanlon, S. Suresh MIT)

Variable amplitude cyclic loadings

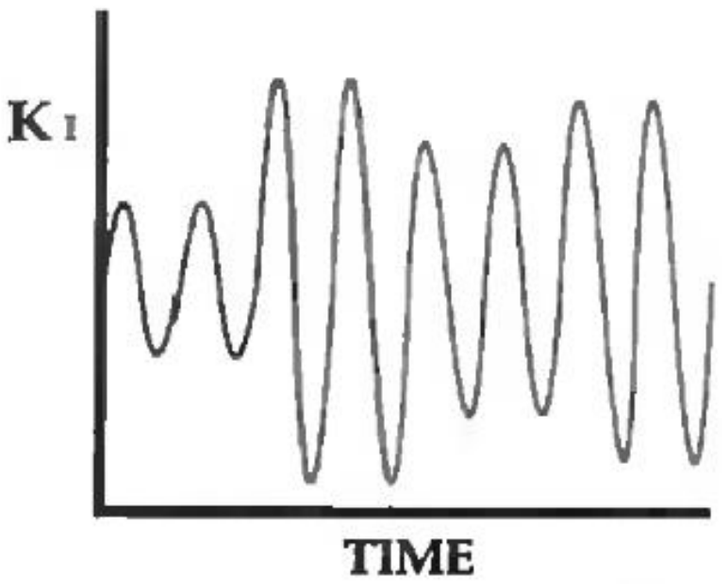

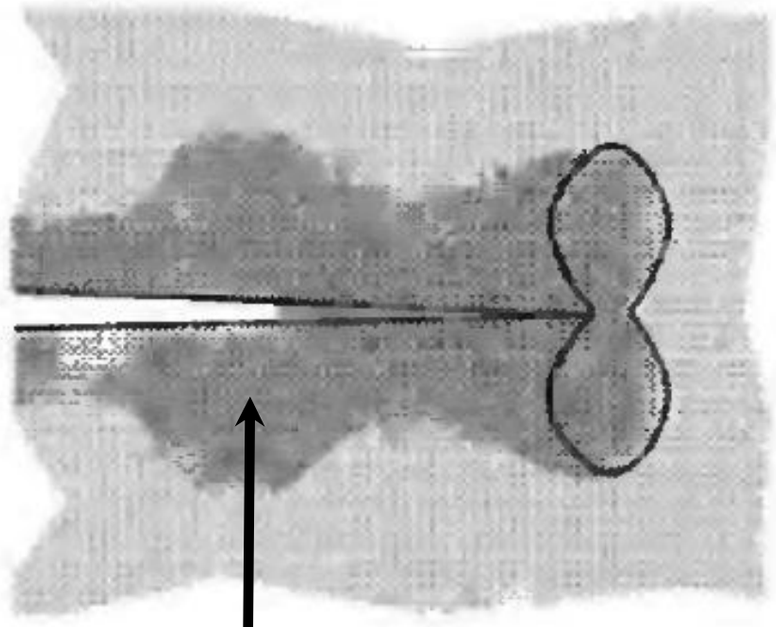

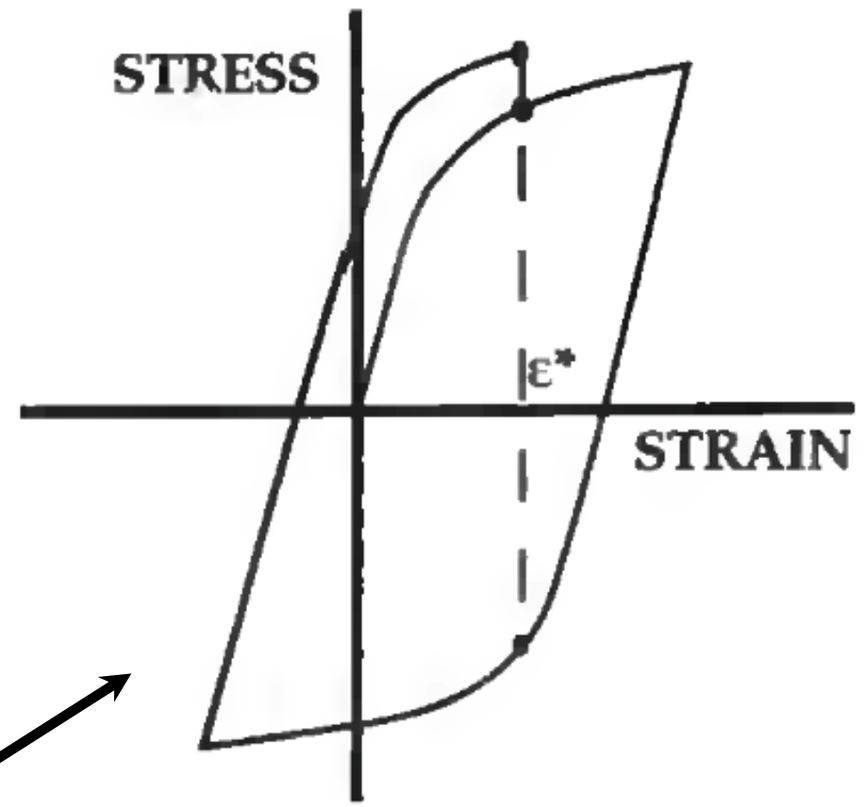

$$\frac{da}{dN} = f_2(\Delta K, R, H)$$

history variables

plasticity: history dependent

plastic wake

Overload and crack retardation

It was recognized empirically that the application of a tensile overload in a constant amplitude cyclic loa
leads to crack retardation following the overload; that is, the crack growth rate is smaller than it would
have been under constant amplitude loading.

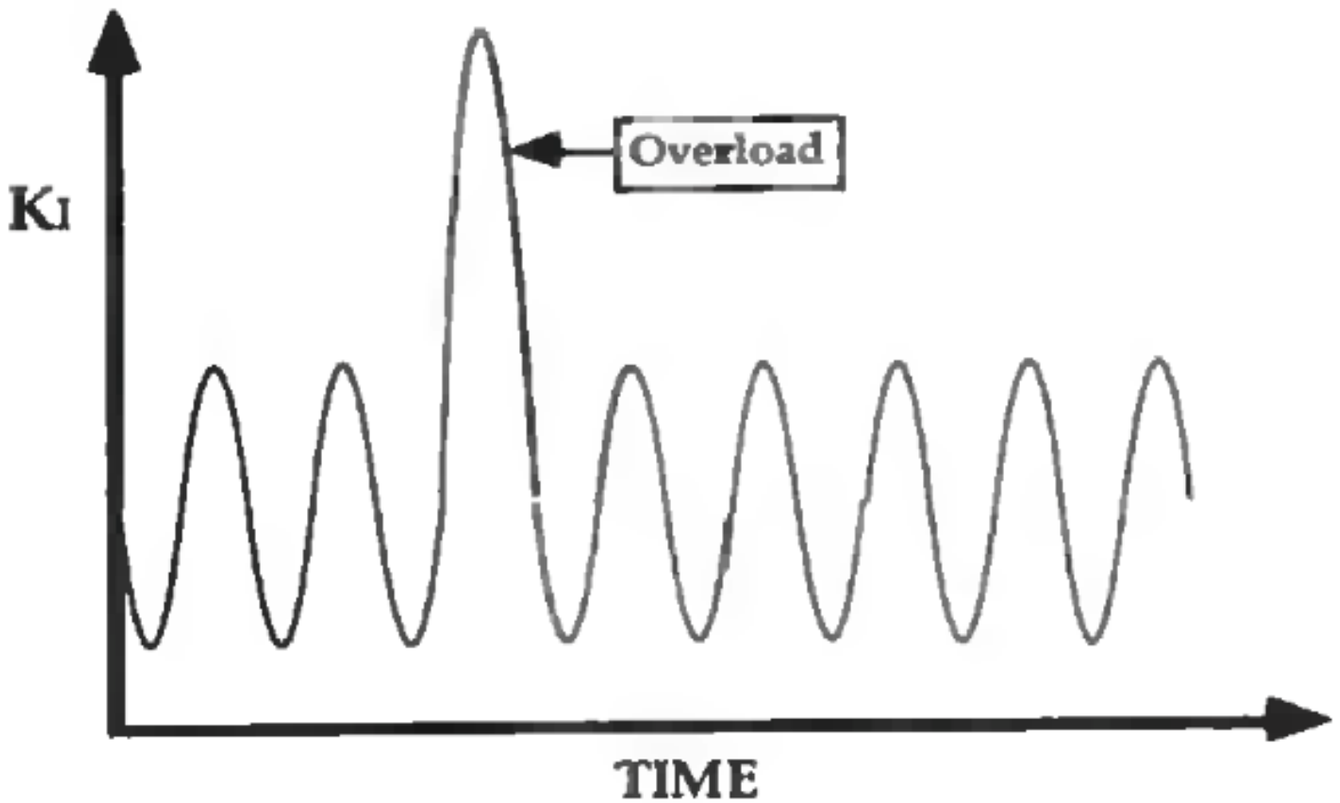

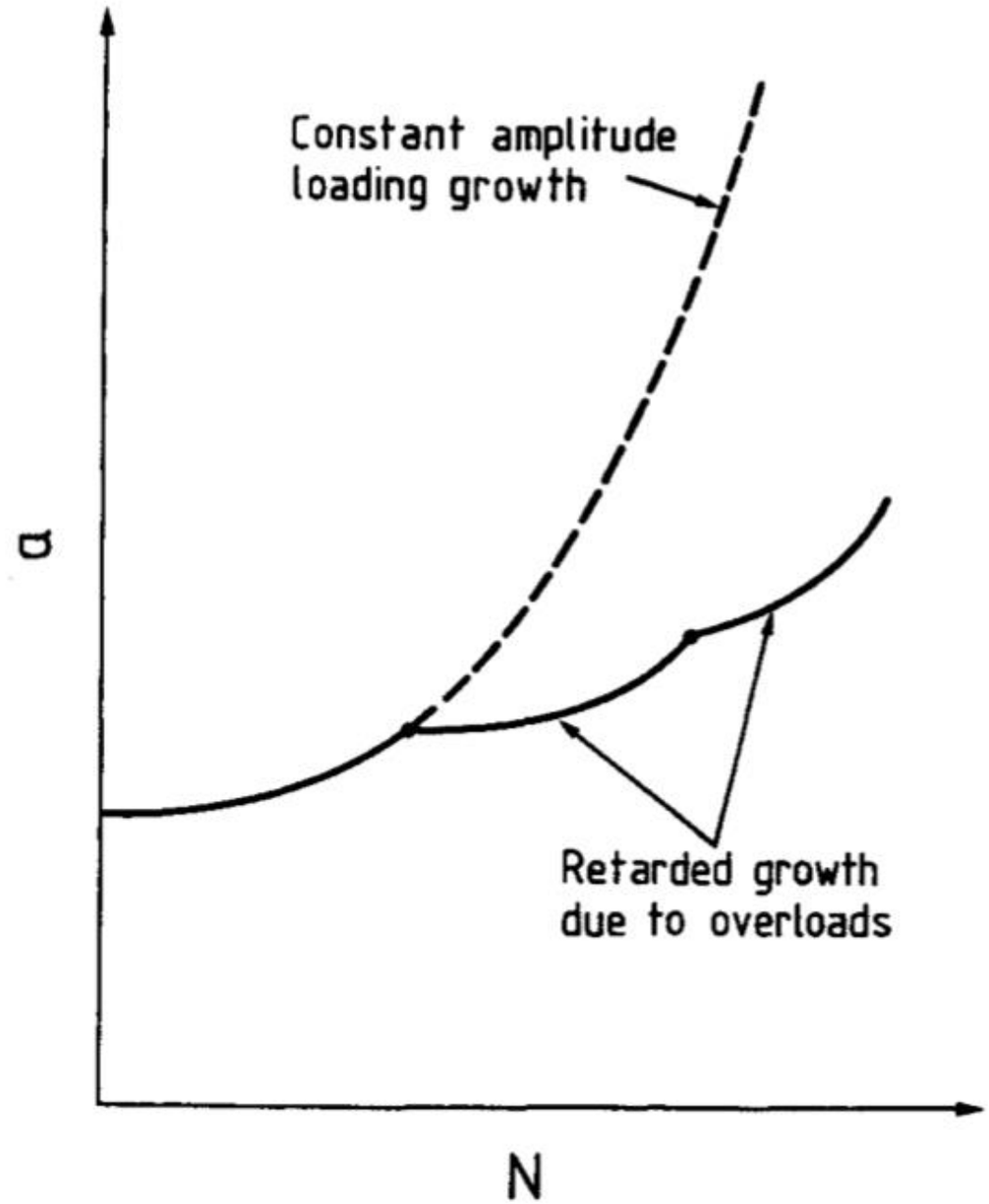

Crack retardation

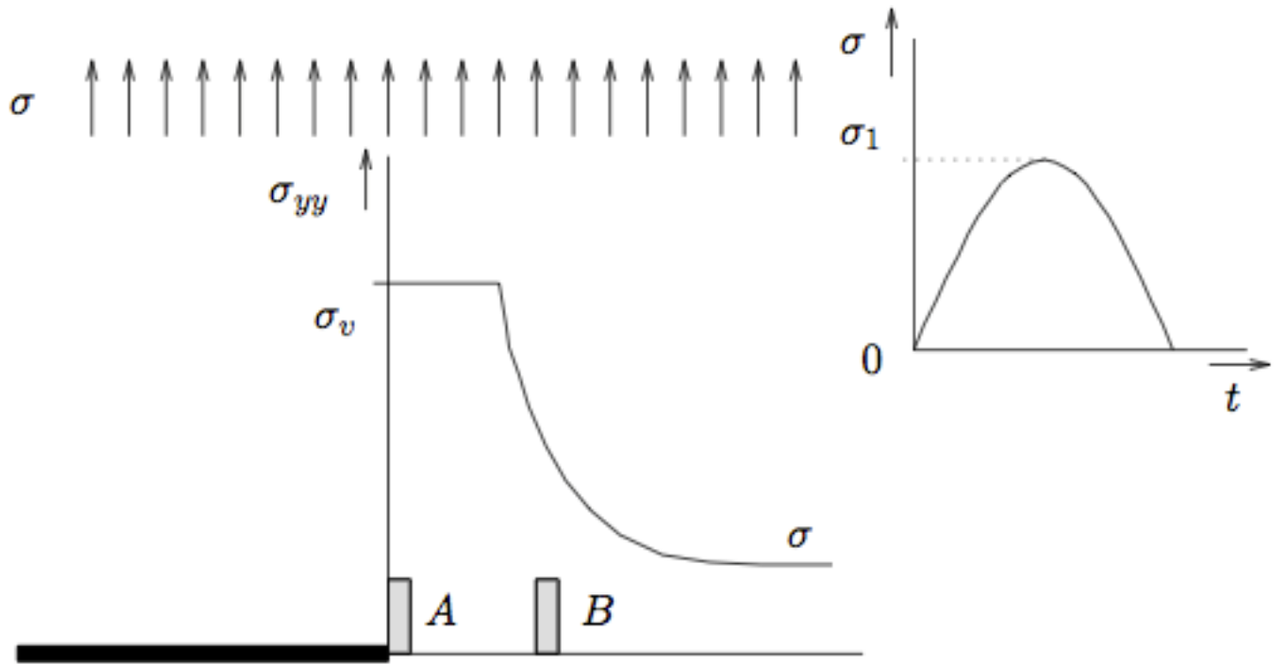

Point A: plastic
point B: elastic

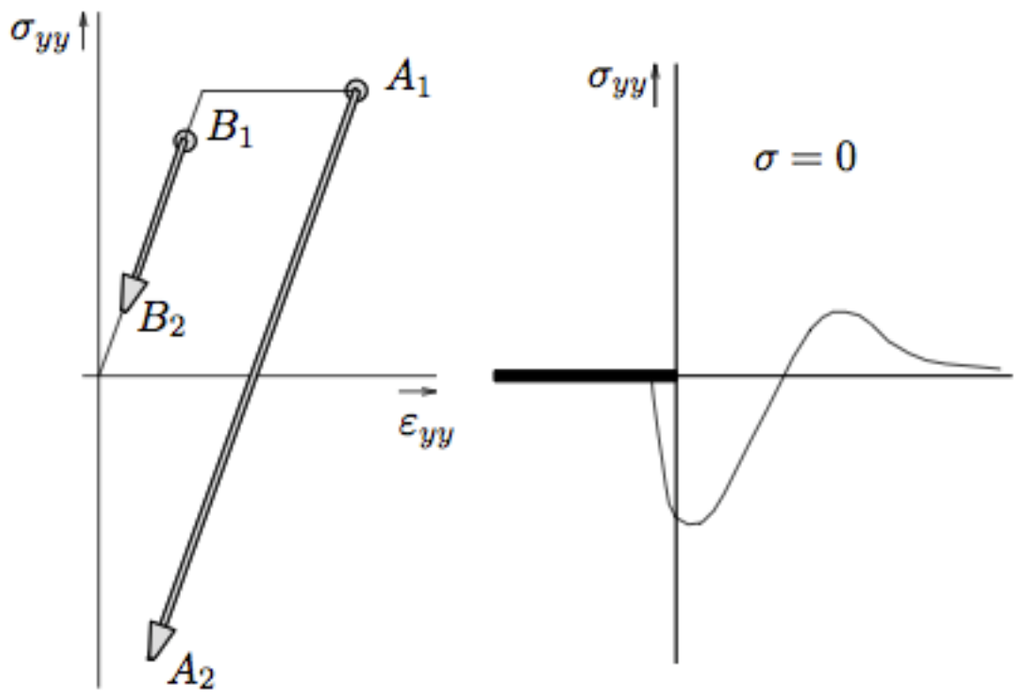

After unloading: point A and B has more or less the same strain ->
point A : compressive stress.

Crack retardation

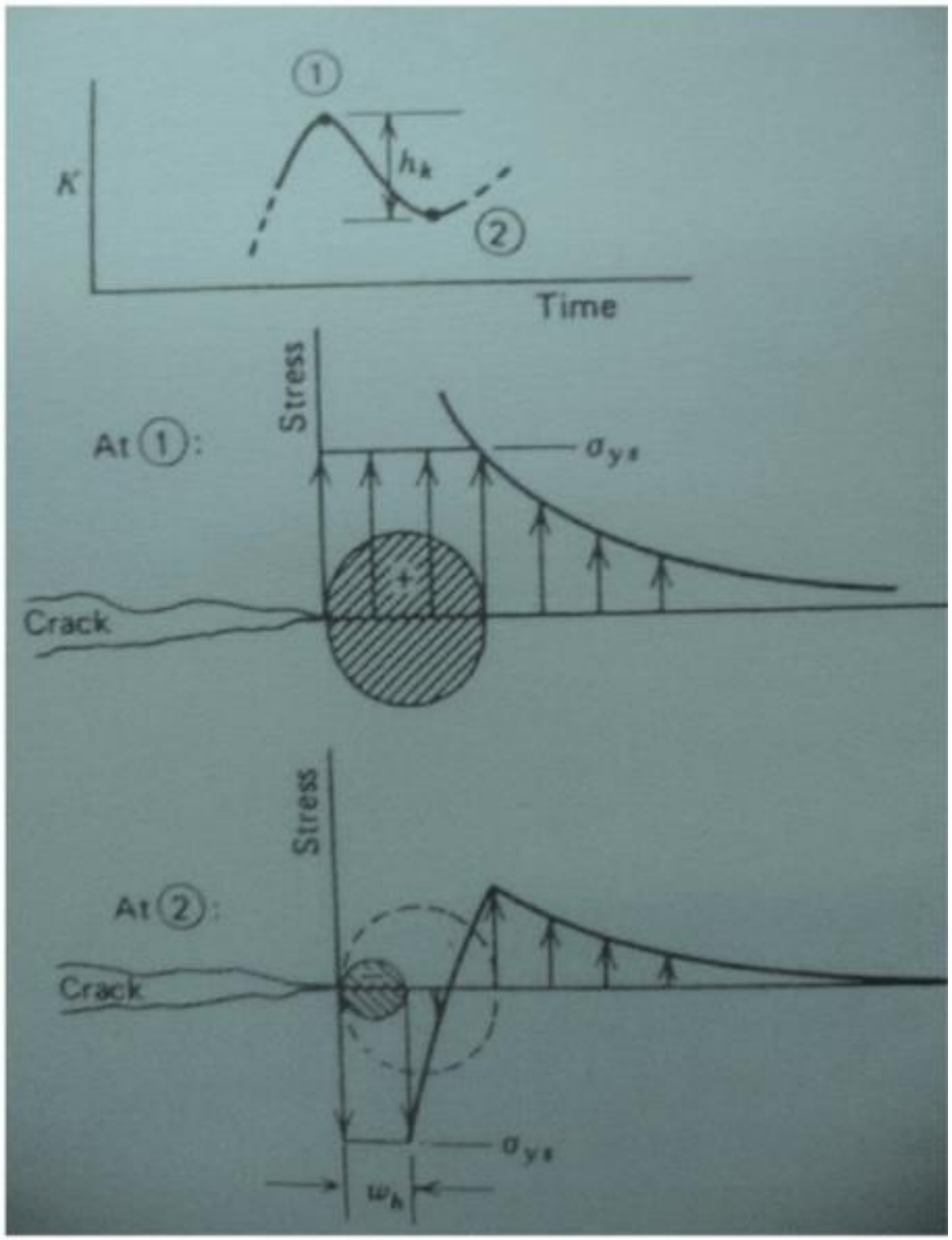

a large plastic zone at overload has left behind

residual compressive plastic zone

close the crack->crack retards

Overload and crack retardation

It was recognized empirically that the application of a tensile overload in a constant amplitude cyclic load leads to crack retardation following the overload; that is, the crack growth rate is smaller than it would have been under constant amplitude loading.

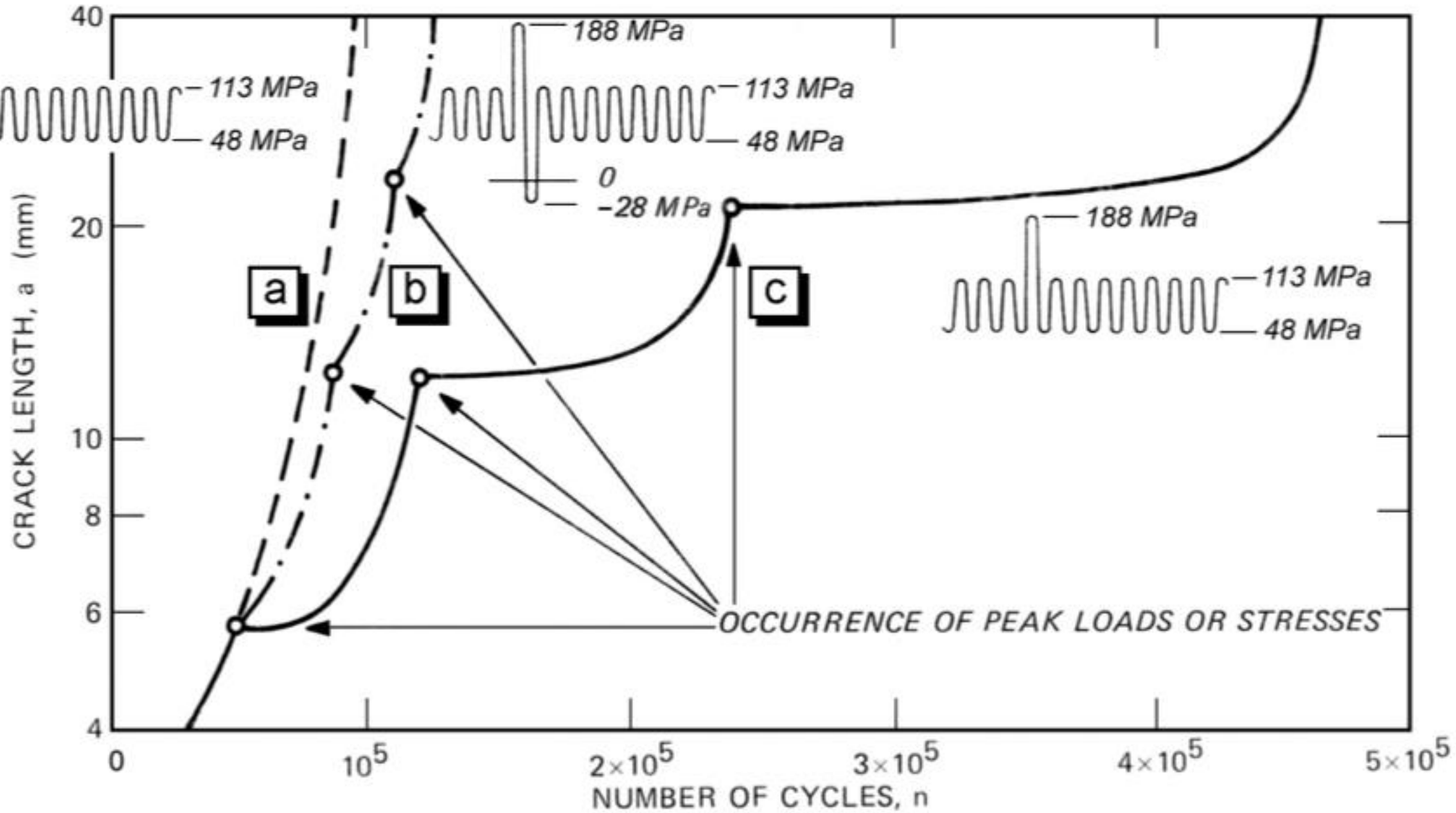

Fatigue crack inhibition: Shot-peening

Shot peening is a cold working process in which the surface of a part is bombarded with small spherical media called *shot*. Each piece of shot striking the surface acts as a tiny peening hammer, imparting to the surface a small indentation or dimple. The net result is a layer of material in a state of residual compression. It is well established that cracks will not initiate or propagate in a compressively stressed zone.

(source Course presentation Hanlon, S. Suresh MIT)

Fatigue crack inhibition: Shot-peening

A typical residual stress profile created by shot peening is shown below:

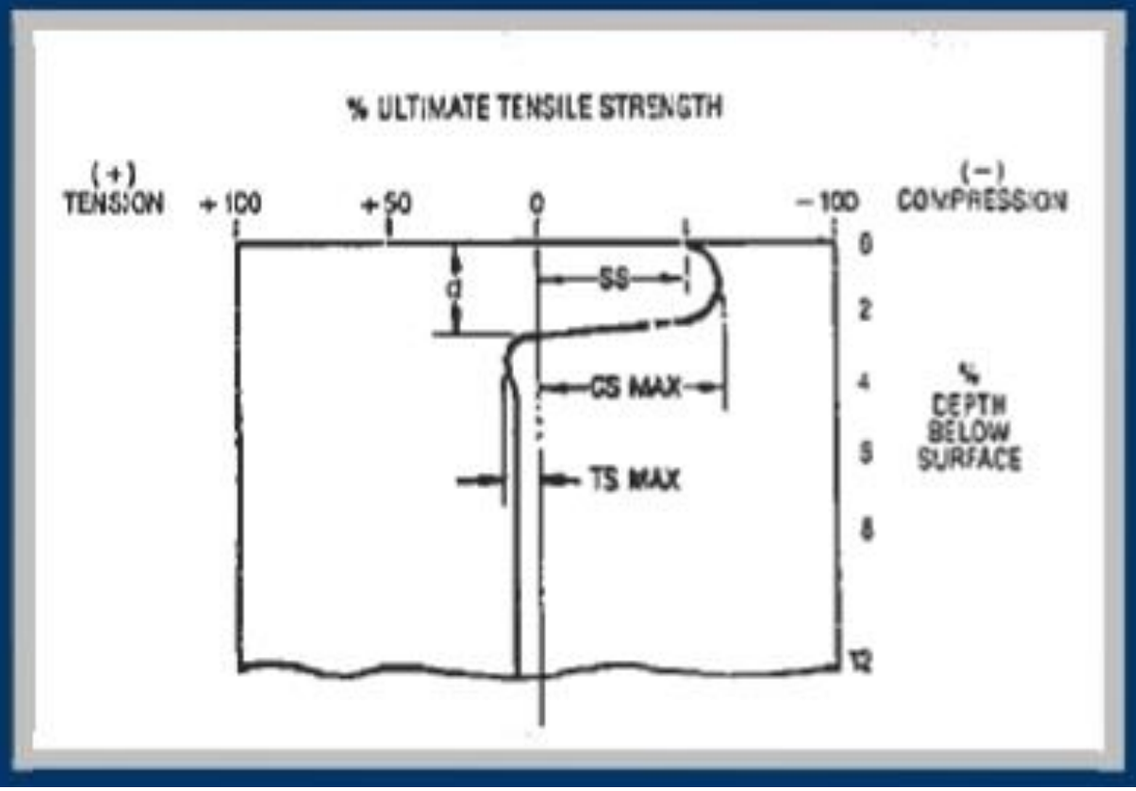

(source Course presentation Hanlon, S. Suresh MIT)

Fatigue crack inhibition: Shot-peening

Since nearly all fatigue and stress corrosion failures originate at the surface of a part, compressive stresses induced by shot peening provide *considerable* increases in part life. Typically the residual stress produced is at least half the yield strength of the material being peened.

The benefits of shot peening are a result of the *residual compressive stress* and the *cold working* of the surface.

(source Course presentation Hanlon, S. Suresh MIT)

Fatigue crack inhibition: Shot-peening

Residual stress: Increases resistance to fatigue crack growth, corrosion fatigue, stress corrosion cracking, hydrogen assisted cracking, fretting, galling and erosion caused by cavitation.

Cold Working: Benefits include work hardening (strengthening), intergranular corrosion resistance, surface texturing, closing of porosity and testing the bond of coatings.

(source Course presentation Hanlon, S. Suresh MIT)

Fatigue crack inhibition: Shot-peening

Residual stresses are those stresses remaining in a part after all manufacturing operations are completed, and with no external load applied. In most applications for shot peening, the benefit obtained is the direct result of the residual compressive stress produced.

(source Course presentation Hanlon, S. Suresh MIT)

Damage tolerance design 1970s

(stress concentration: possible crack sites)

1. Determine the size of initial defects , a_0 NDI
2. Calculate the critical crack size at a_c which failure would occur $\sigma\sqrt{\pi a_c} = K_{Ic}$
3. Integrate the fatigue crack growth equations to compute the number of load cycles for the crack to grow from initial size to the critical size

$$N = N_0 + \int_{a_0}^{a_c} \frac{da}{C(\Delta\sigma\sqrt{\pi a})^m}$$

4. Set inspection intervals

Examples for Fatigue

A large plate contains a crack of length $2a_0$ and is subjected to a constant-amplitude tensile cyclic stress normal to the crack which varies between 100 MPa and 200 MPa. The following data were obtained: for $2a_0 = 2$ mm it was found that $N = 20,000$ cycles were required to grow the crack to $2a_f = 2.2$ mm, while for $2a = 20$ mm it was found that $N = 1000$ cycles were required to grow the crack to $2a_f = 22$ mm. The critical stress intensity factor is $K_c = 60$ MPa $\sqrt{m}$. Determine the constants in the Paris (Equation (9.3)) and Formam (Equation (9.4)) equations.

$$\log \frac{da}{dN} = \log C + m \log \Delta K$$

$$\boxed{\begin{aligned} &\log(xy) = \log(x) + \log(y) \\ &\log(x^p) = p \log(x) \end{aligned}}$$

$$\Delta K = \Delta\sigma\sqrt{\pi a} \begin{cases} 5.6 \text{ MPa}\sqrt{m} & a_0 = 1 \text{ mm} \\ 17.72 \text{ MPa}\sqrt{m} & a_0 = 10 \text{ mm} \end{cases}$$

$\log_{10}(x)$

$$\frac{da}{dN} = \frac{a_f - a_0}{N} \begin{cases} 5 \times 10^{-9} \text{ m/cycle} & -8.30 = \log C + 0.748\, m \\ 1 \times 10^{-6} \text{ m/cycle} & -6.00 = \log C + 1.248\, m \end{cases}$$

$$\boxed{m = 4.6 \quad C = 1.82 \times 10^{-12} \frac{\text{m}}{(\text{MPa}\sqrt{m})^{4.6} \text{ cycle}}}$$

$MN^{-4.6}\, m^{7.9}$/cycle

Forman's model

$$R = \frac{\sigma_{\min}}{\sigma_{\max}} = 0.5$$

$$[(1-R)K_c - \Delta K]\,\frac{da}{dN} = C(\Delta K)^m$$

$$K_c = 60\ \mathrm{MPa}\sqrt{\mathrm{m}}$$

$$\log\left\{[(1-R)K_c - \Delta K]\,\frac{da}{dN}\right\} = \log C + m\log(\Delta K)$$

$$\log[(0.5\times 60 - 5,6)\times 5\times 10^{-9}] = \log C + m\log 5.6$$

$$\log[(0.5\times 60 - 17.72)\times 10^{-6}] = \log C + m\log 17.72$$

$$\boxed{\begin{aligned} -6.914 &= \log C + 0.748m \\ -4.911 &= \log C + 1.248m \end{aligned}}$$

$$C = 1.229\ MN^{-3.3}\,m^{5.95}/\text{cycle}\ ,\ m = 4.006$$

C and m in Forman's model are different from those in Paris's model.

9. Dynamic fracture mechanics and rate effects

9.1. LEFM solution fields

9.2. Dynamics of moving crack tip, process zone size, crack speed

9.3. Crack path instabilities

Dynamic stress intensity factor

$$s^{ij}(r,\theta,t) = \frac{K_I(t)}{\sqrt{2\pi r}}\Sigma_I^{ij}(\theta,\hat{v}) + \frac{K_{II}(t)}{\sqrt{2\pi r}}\Sigma_{II}^{ij}(\theta,\hat{v}) \quad \text{as} \quad r \to 0,$$

Crack speed

$$K_I(t) = \lim_{x_2\to 0}\sqrt{2\pi x_2}s^{11}(x_2,0,t), \qquad K_{II}(t) = \lim_{x_2\to 0}\sqrt{2\pi x_2}s^{12}(x_2,0,t)$$

$$\Sigma_I^{11} = -\frac{1}{D}\left\{(1+\alpha_{II}^2)^2\frac{\cos\frac{1}{2}\theta_I}{\sqrt{\gamma_I}} - 4\alpha_I\alpha_{II}\frac{\cos\frac{1}{2}\theta_{II}}{\sqrt{\gamma_{II}}}\right\},$$

$$\Sigma_I^{12} = \frac{2\alpha_I(1+\alpha_{II}^2)}{D}\left\{\frac{\sin\frac{1}{2}\theta_I}{\sqrt{\gamma_I}} - \frac{\sin\frac{1}{2}\theta_{II}}{\sqrt{\gamma_{II}}}\right\},$$

$$\Sigma_I^{22} = \frac{1}{D}\left\{(1+\alpha_{II}^2)(1+2\alpha_I^2-\alpha_{II}^2)\frac{\cos\frac{1}{2}\theta_I}{\sqrt{\gamma_I}} - 4\alpha_I\alpha_{II}\frac{\cos\frac{1}{2}\theta_{II}}{\sqrt{\gamma_{II}}}\right\}$$

Mode I

$$\Sigma_{II}^{11} = \frac{2\alpha_{II}(1+\alpha_{II}^2)}{D}\left\{\frac{\sin\frac{1}{2}\theta_I}{\sqrt{\gamma_I}} - \frac{\sin\frac{1}{2}\theta_{II}}{\sqrt{\gamma_{II}}}\right\},$$

$$\Sigma_{II}^{12} = \frac{1}{D}\left\{4\alpha_I\alpha_{II}\frac{\cos\frac{1}{2}\theta_I}{\sqrt{\gamma_I}} - (1+\alpha_{II}^2)^2\frac{\cos\frac{1}{2}\theta_{II}}{\sqrt{\gamma_{II}}}\right\},$$

Mode II

$$\Sigma_{II}^{22} = -\frac{2\alpha_{II}}{D}\left\{(1+2\alpha_I^2-\alpha_{II}^2)\frac{\sin\frac{1}{2}\theta_I}{\sqrt{\gamma_I}} - (1+\alpha_{II}^2)\frac{\sin\frac{1}{2}\theta_{II}}{\sqrt{\gamma_{II}}}\right\}$$

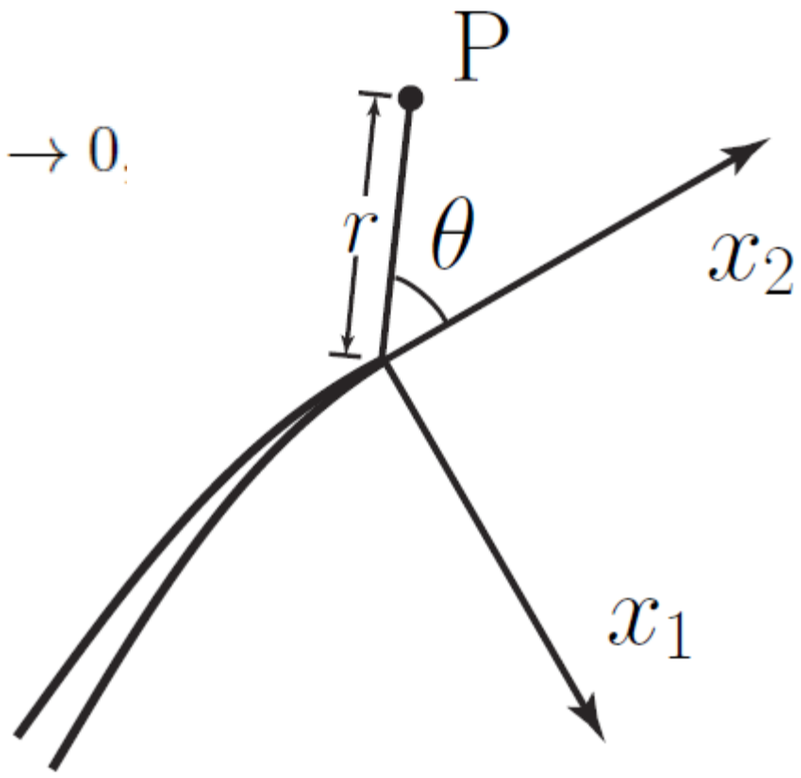

Dynamic angular dependence function

$$\Sigma_I^{11} = -\frac{1}{D}\left\{(1+\alpha_{II}^2)^2 \frac{\cos\frac{1}{2}\theta_I}{\sqrt{\gamma_I}} - 4\alpha_I\alpha_{II}\frac{\cos\frac{1}{2}\theta_{II}}{\sqrt{\gamma_{II}}}\right\}$$

$$\alpha_{(k)} = \sqrt{1-\hat{v}^2/c_{(k)}^2}$$

$$\gamma_{(k)} = \sqrt{1-(\hat{v}\sin\theta/c_{(k)})^2}$$

$$\tan\theta_{(k)} = \alpha_{(k)}\tan\theta, \quad k=1,2,$$

$$D = 4\alpha_I\alpha_{II} - (1+\alpha_{II}^2)^2.$$

Longitudinal and shear wave speeds are $c_I := c_\mathrm{d}$ and $c_{II} := c_\mathrm{s}$

$$c_\mathrm{d} = \sqrt{\frac{\lambda+2\mu}{\rho}}, \quad c_\mathrm{s} = \sqrt{\frac{\mu}{\rho}}.$$

3D and 2D plane strain $c_d = \sqrt{\frac{E(1-v)}{\rho(1+v)(1-2v)}}$, $c_s = \sqrt{\frac{E}{2\rho(1+v)}}$, $c_R \approx c_s \frac{0.862+1.14v}{1+v}$

Longitudinal (pressure) and shear waves

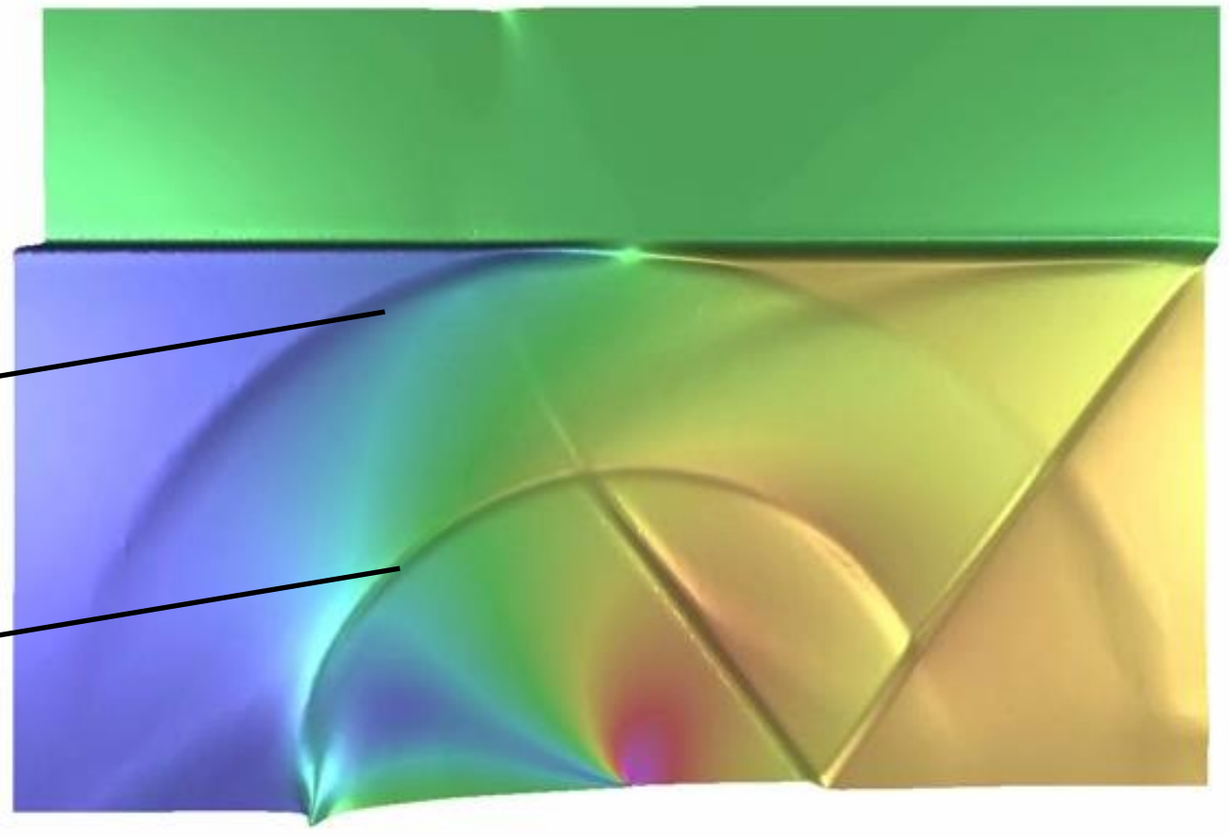

Pressure wave front

Shear wave front

link

9. Dynamic fracture mechanics and rate effects

9.1. LEFM solution fields

9.2. Dynamics of moving crack tip, process zone size, crack speed

9.3. Crack path instabilities

Rayleigh wave speed limit

$$\Sigma_I^{11} = -\frac{1}{D}\left\{(1+\alpha_{II}^2)^2 \frac{\cos\frac{1}{2}\theta_I}{\sqrt{\gamma_I}} - 4\alpha_I\alpha_{II}\frac{\cos\frac{1}{2}\theta_{II}}{\sqrt{\gamma_{II}}}\right\}$$

For one material under mode I maximum possible crack speed is Rayleigh wave speed where angular functions tend to infinity:

It can be shown that the *Rayleigh wave speed*, denoted by c_{R}, equals the non-zero value of $\hat{v}$ at which D vanishes (Rayleigh, 1885).

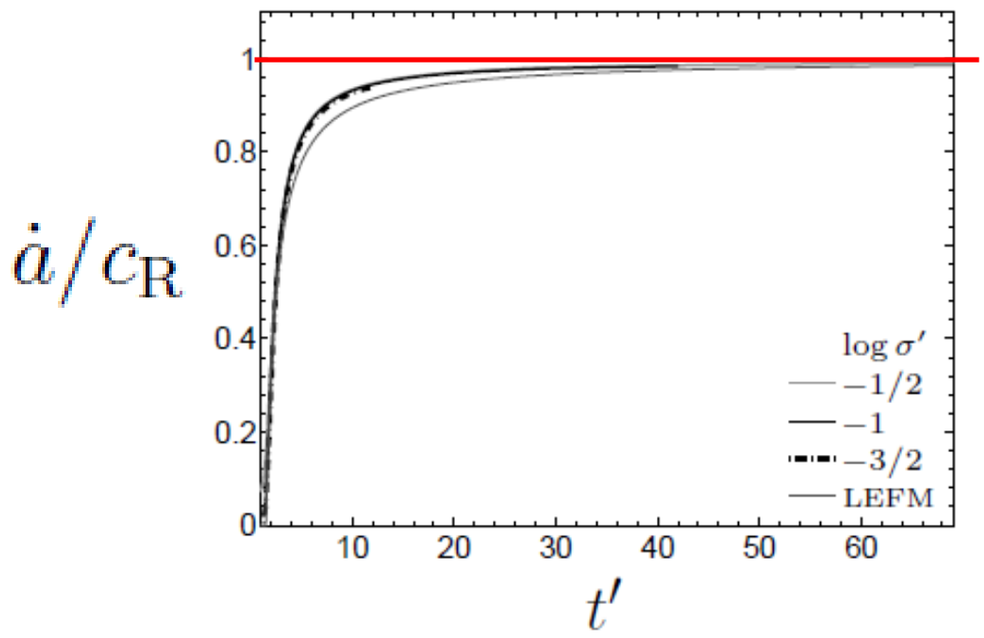

Dynamic stress intensity factor

$$K_{(k)}(t, a, \hat{v}) = k_{(k)}(\hat{v}) K_{(k)}(t, a, 0)$$

stationary stress intensity factor, $K_{(k)}(t, a, 0)$, is the stress intensity factor that would result from the same applied loading if the crack tip were stationary at the instantaneous position corresponding to the crack length a

$k_{(k)}(\hat{v})$ is a universal function of crack-tip speed for mode-(k) crack growth that is independent of the loading and the geometry of the body and that can be approximated as

$$k_{(k)}(\hat{v}) \approx (1 - \hat{v}/c_{\mathrm{R}})/\sqrt{1 - \hat{v}/c_{(k)}}$$

Note that k(v) approaches 0 as the crack speed tends to Rayleigh wave speed.

Dynamic energy release rate

- K, G relation:

$$G = \frac{1-\nu}{2\mu}\left[A_I(\hat{v})K_I^2 + A_{II}(\hat{v})K_{II}^2\right]$$

- Remember that for static case: $G = \frac{1-\nu}{2\mu}\left[K_I^2 + K_{II}^2\right]$

The functions $A_{(k)}$ are universal functions that do not depend on the details of the loading or on the domain geometry. These functions have the properties,

- Static limit: $A_{(k)} \to 1 \text{ as } \hat{v} \to 0^+$

- Rayleigh speed limit (G tends to infinity)

$$A_{(k)} = O[(c_R - \hat{v})^{-1}]$$

Dynamic crack propagation criterion

- Dynamic Griffith criterion:
  Crack propagates when energy release rate reaches fracture toughness Λ_0 (resistance):

$$G = \Gamma_0$$

- Noting that:

$$K_{(k)}(t, a, \hat{v}) = k_{(k)}(\hat{v}) K_{(k)}(t, a, 0)$$

$$G = \frac{1-\nu}{2\mu} \left[A_I(\hat{v}) K_I^2 + A_{II}(\hat{v}) K_{II}^2 \right]$$

- For mode I we obtain:

$$\frac{1-\nu}{2\mu} A(\hat{v}) k(\hat{v})^2 \left[K(t, a, 0) \right]^2 = \Gamma_0$$

Dynamic crack propagation criterion

$$\frac{1-\nu}{2\mu} A(\hat{v}) k(\hat{v})^2 \left[K(t,a,0)\right]^2 = \Gamma_0$$

$$\Leftrightarrow \quad \boxed{g(\hat{v}) = \frac{2\mu\Gamma_0}{(1-\nu)\left[K(t,a,0)\right]^2}}$$

$\boxed{g(\hat{v}) := A(\hat{v})k(\hat{v})^2}$ is a universal function of the crack-tip speed that is very accurately approximated by

$$\boxed{g(\hat{v}) \approx 1 - \hat{v}/c_{\mathrm{R}} \text{ for } 0 \leq \hat{v} \leq c_{\mathrm{R}}}$$

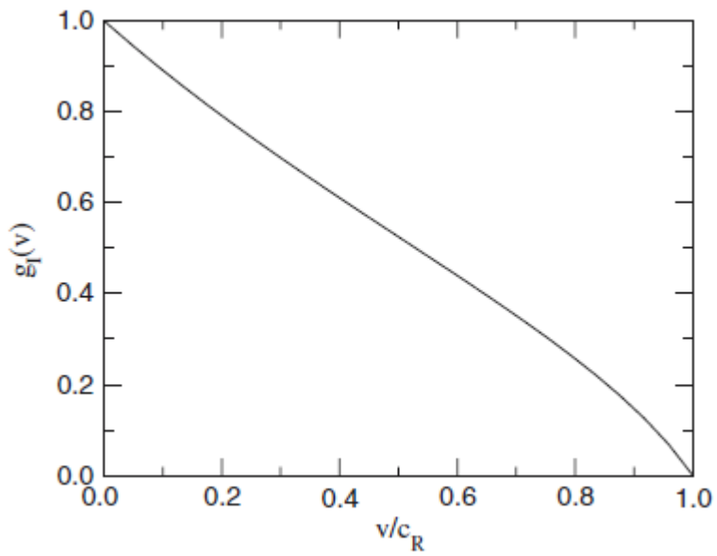

Final note:
fracture toughness Λ_0 itself depends on crack speed *v!*

Example of dynamic fracture

- Infinite domain under dynamic mode I load

$$\bar{\sigma} = 2\bar{t}_\infty$$

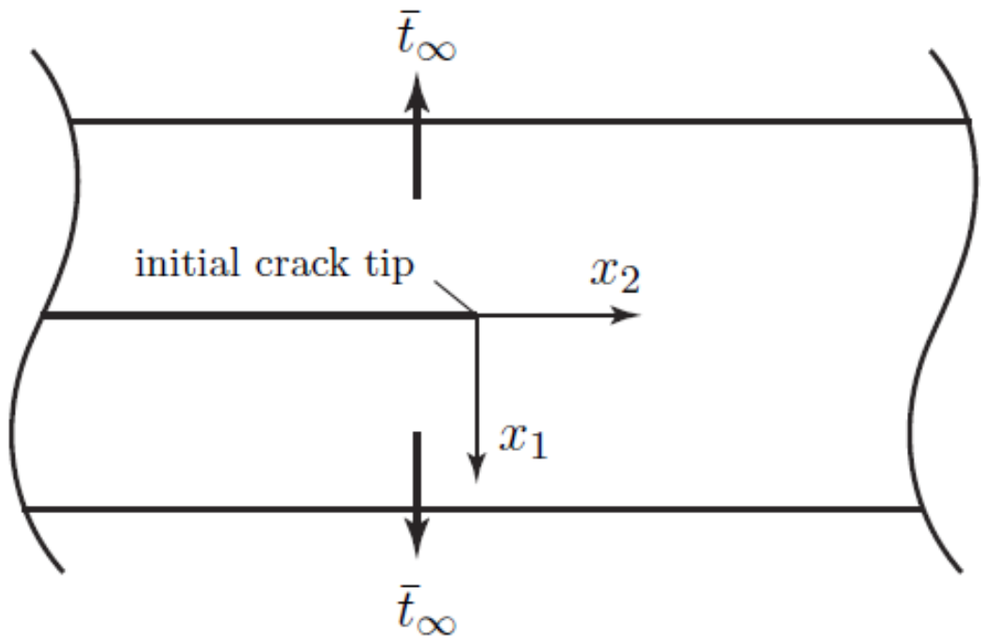

- Static intensity factor is evaluated as,

$$K(t, a, 0) = C\sqrt{2\pi c_\mathrm{d} t}\,\bar{\sigma}$$

- Crack propagates when $g(\hat{v}) = \dfrac{2\mu\Gamma_0}{(1-\nu)\left[K(t,a,0)\right]^2}$,

$$g(\hat{v}) = \frac{\mu\Gamma_0}{(1-\nu)\pi c_\mathrm{d}\left(C\bar{\sigma}\right)^2 t}.$$

- Crack initiation time then is,

$$\tau_0 = \frac{\pi\mu\tilde{\phi}c_\mathrm{d}}{4\left(c_\mathrm{s}\bar{\sigma}\right)^2}$$

Rayleigh wave speed limit

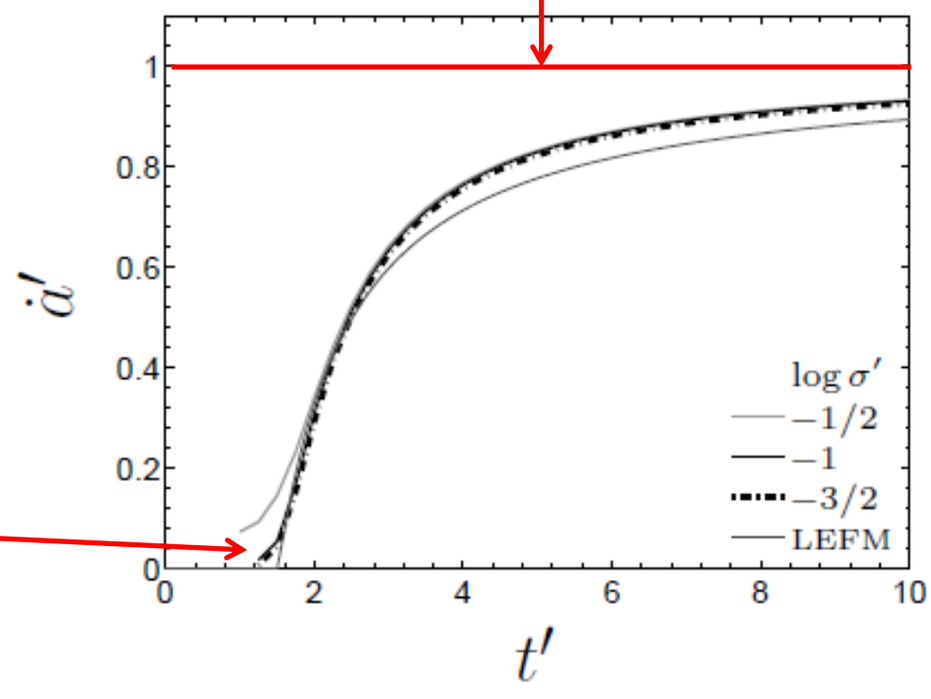

Reminder:
Fracture process zone in dynamic fracture

- Importance of process zone size Λ
  - Static estimate:

$$\Lambda = \varsigma\pi \frac{\mu}{1-\nu}\frac{\tilde{\phi}}{\tilde{\sigma}^2} \propto \tilde{L}$$

$$\varsigma = \begin{cases} \frac{1}{4} & \text{Dugdale model} \\ \frac{9}{16} & \text{Potential-based TSRs} \end{cases}$$

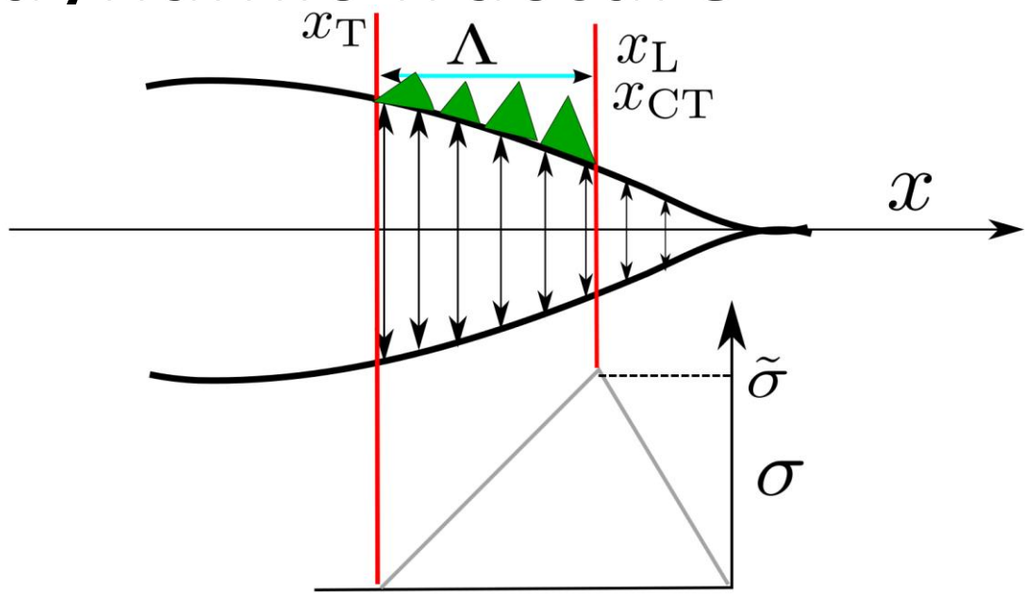

  - Minimum number of elements in process zone size:
    There should be at least 4-10 elements along the PZ
  - Dynamic estimate: PZS decreases as crack speed $\hat{v}$ approaches Rayleigh wave speed c_{R}

$$\Lambda(\hat{v}) = \frac{\Lambda}{A(\hat{v})}, \quad A(\hat{v}) \to 0 \text{ as } \hat{v} \to c_{\mathrm{R}} \quad \Rightarrow$$

Smaller elements are needed in PZT as crack accelerates!

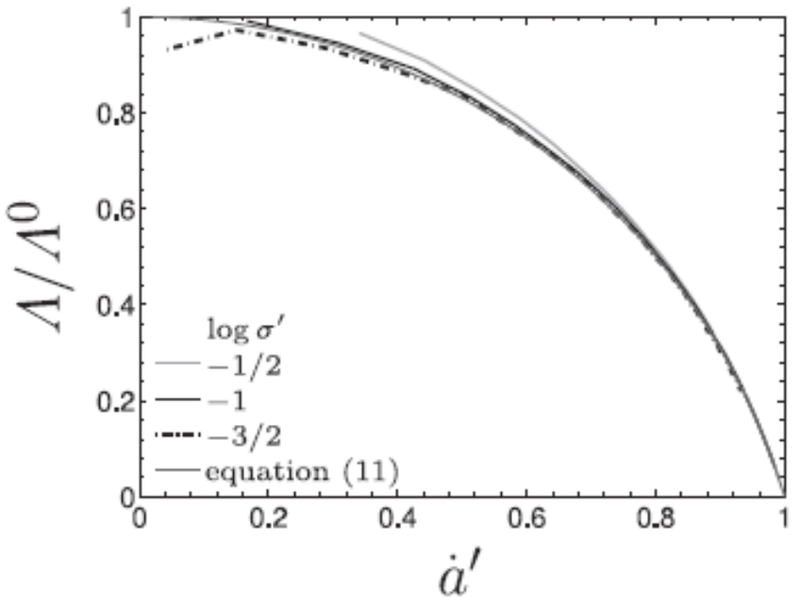

(a) Low-amplitude loading, $\bar{t}_\infty \ll \tilde{\sigma}$.

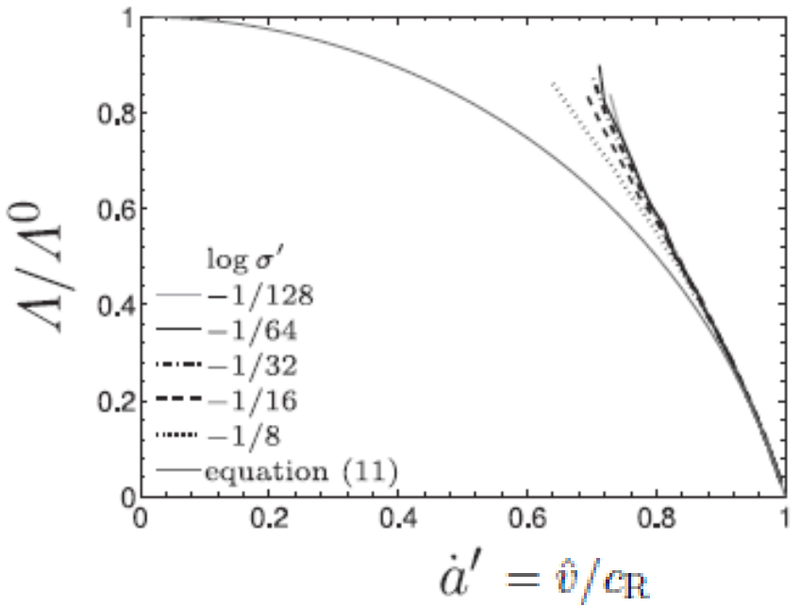

(b) High-amplitude loading, $\bar{t}_\infty \to \tilde{\sigma}^-$.

Small scale yielding in dynamic fracture

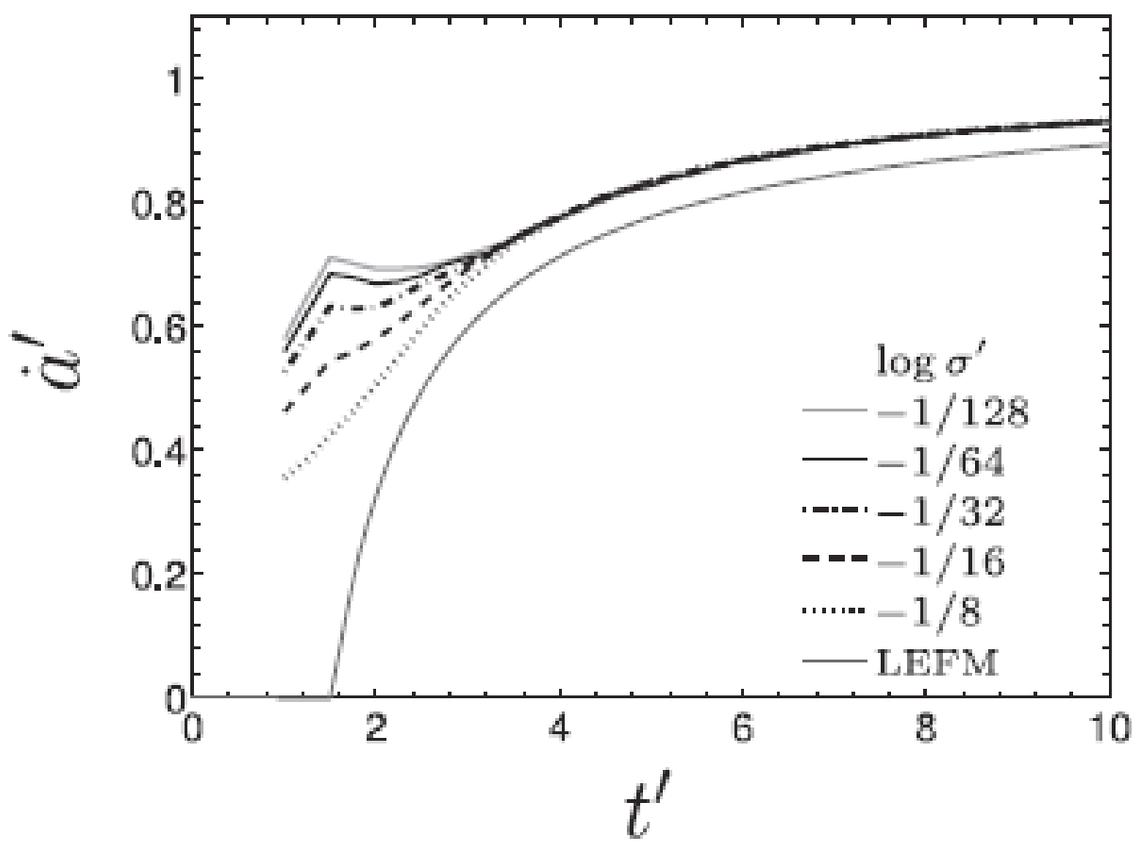

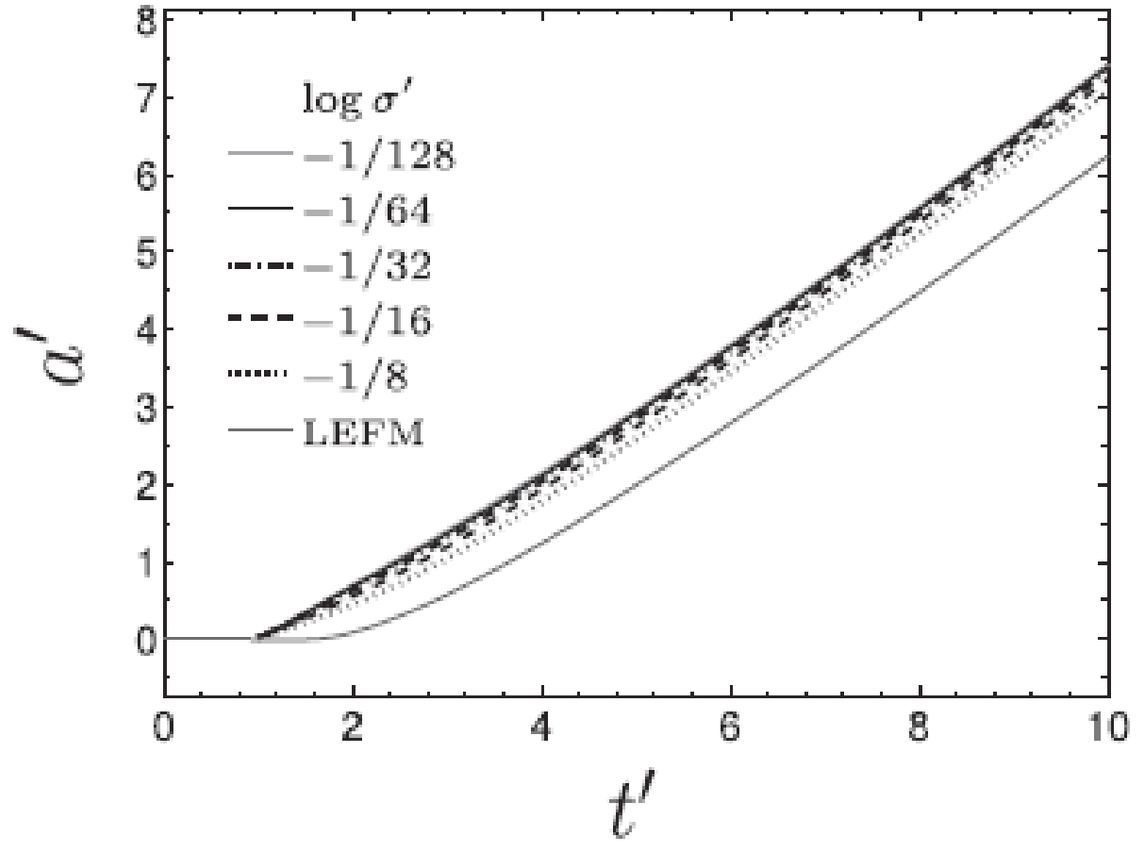

Super-shear crack propagation

Crack propagation speed background

- For a homogeneous solid, crack speed cannot exceed Rayleigh wave speed (c_R).
  - In practice, speed often does not exceed 50% of c_R.
  - Experiment with two weakly joined identical solids, where the weak interface confines the crack to the plane, an interfacial crack indeed approaches c_R.

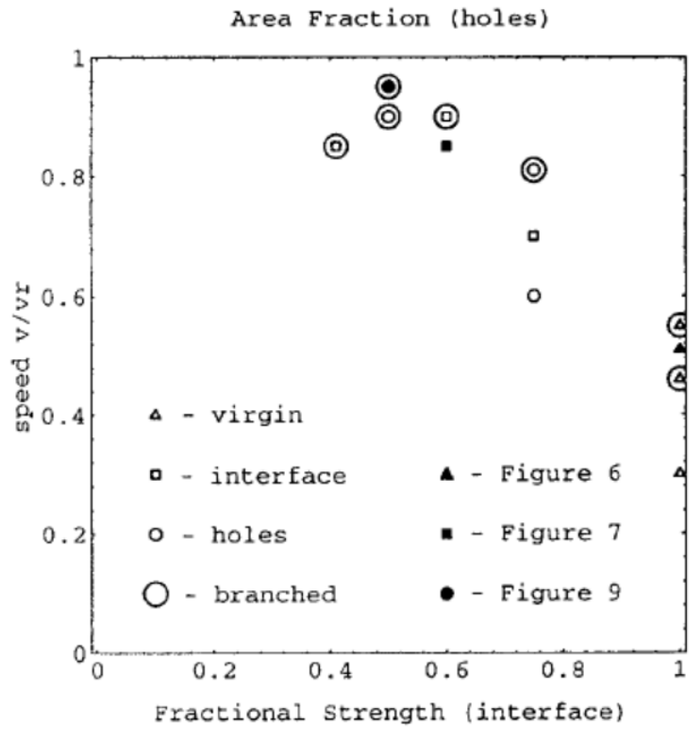

Washabaugh, P. D. & Knauss, W. G. 1994 A reconciliation of dynamic crack velocity and Rayleigh wave speed in isotropic brittle solids. Int. J. Fracture 65, 97{114

Fig. 8. Dependence of the crack velocity on the property of the material (i.e. fractional strength or area fraction) preceding the crack front.

Do cracks do really reach Rayleigh speed?

Sharon Fineberg:
mirror, mist, hackle patterns as the crack accelerates

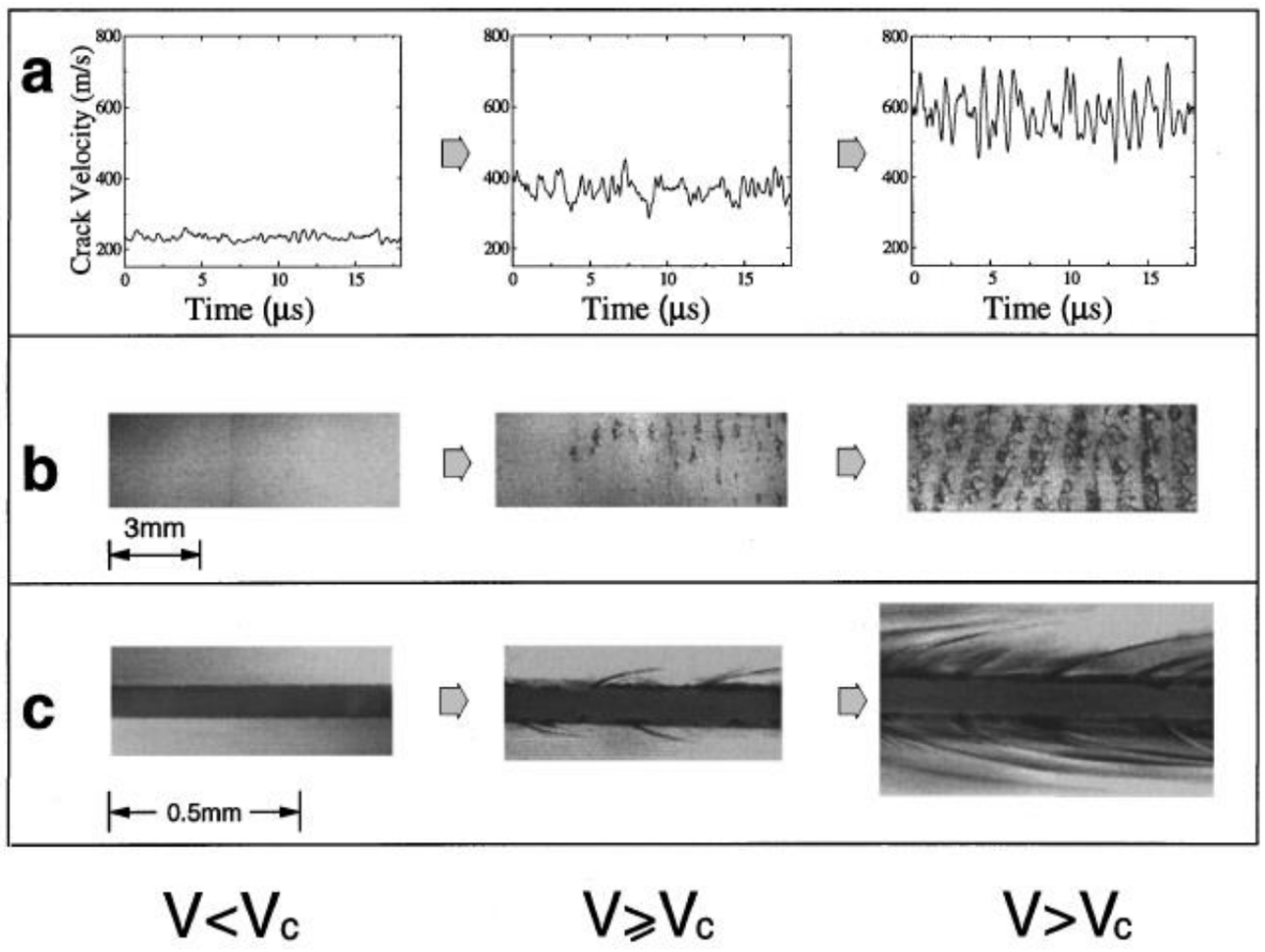

$v_c = 340\text{m/s}$

$(\text{or } 0.36 V_R)$

- Crack starts oscillating well before reaching Rayleigh wave speed V_R (c_R)
- Crack speed does not reach V_R (c_R)!
- For this material critical speed $v_c = 0.36\ V_R$

Do cracks do really reach Rayleigh speed?

Confirming the continuum theory of dynamic brittle fracture for fast cracks

Eran Sharon & Jay Fineberg

$$\Gamma = G(l)A(v) \approx G(l)\left(1 - \frac{v}{v_R}\right) \quad (1)$$

$$v(l) = v_R\left(1 - \frac{\Gamma}{G(l)}\right) \quad (2)$$

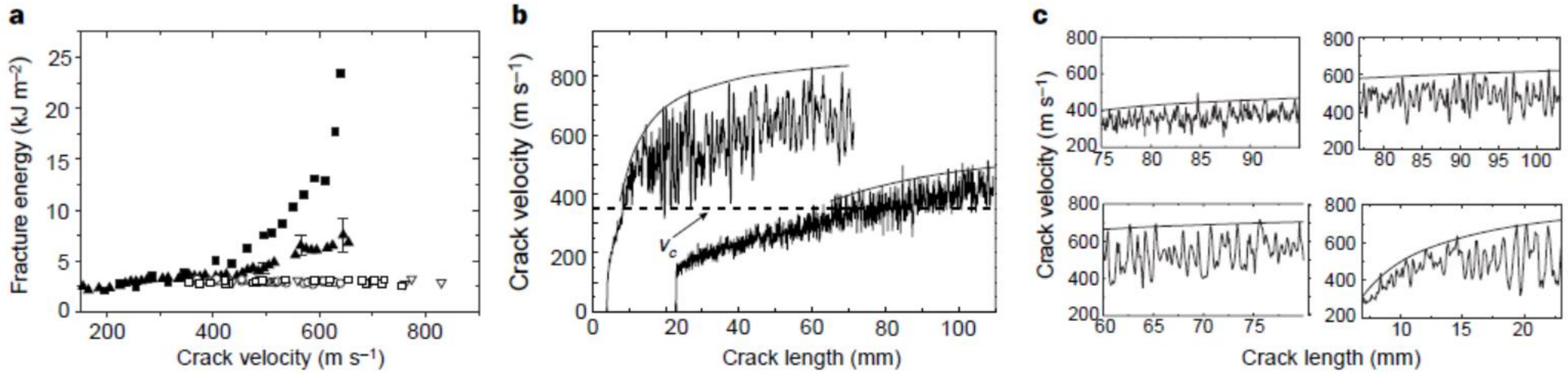

Figure 3 A comparison of theory with measurements in PMMA, for $v > v_c$. **a**, The total measured[14] fracture energy, $\Gamma(v)$, (filled squares) compared with derived values, obtained using equation (1) with the velocity measurements shown in Fig. 2a as input. The derived values, $\Gamma_d(v)$, (filled triangles) coincide with $\Gamma(v)$ for $v < 400\,\mathrm{m\,s^{-1}}$ ($1.17v_c$), and diverge for $v > 400\,\mathrm{m\,s^{-1}}$. This divergence occurs simultaneously with increased 'scatter' in $\Gamma_d(v)$, indicating that Γ_d is no longer a well-defined function of v. Thus, due to micro-branch formation, the single-crack assumption necessary for equation (1) is invalid when the average velocity is used. As a crack possesses no inertia, instantaneous single-crack states that correspond to the highest velocity peaks beyond v_c, are still described by equation (1). The derived fracture energy (open symbols), using the peak velocities presented in **b** and **c**, indeed collapses to the well-defined value of $3{,}000\,\mathrm{J\,m^{-2}}$. This value equals $0.9\Gamma(v_c)$, the same as the value of Γ (per unit fracture surface) obtained in ref. 14 for $v > v_c$. **b**, **c**, Full (**b**) and close-up (**c**) measurements of the instantaneous velocities (thin lines) corresponding to Fig. 2a, compared to the single-crack predictions of equation (2) (heavy lines) using $\Gamma = 3{,}000\,\mathrm{J\,m^{-2}}$. With no adjustable parameters, the velocity peaks agree well with the theoretical curve at v of up to 90% of the asymptotic crack speed, v_R.

Beyond v_c, agreement breaks down owing to the appearance of the multiple-crack ensemble. But in this regime, the **micro-branching process can momentarily produce a single-crack state which instantaneously attains its predicted single-crack velocity, for velocities up to $0.9c_R$.**

- Crack dynamics does not have interia →
- Crack reaches Rayleigh wave speed at instances

Cases that the crack speed exceed Rayleigh wave speed: Dissimilar material interfaces

Intersonic crack growth on an interface

By H. H. Yu† and Z. Suo

Department of Mechanical and Aerospace Engineering and Princeton Materials Institute, Princeton University, Princeton, NJ 08544, USA

- Crack can propagate on an interface between dissimilar solids at speeds between the smallest and the largest sonic speeds of the constituent solids.
  - Assuming the existence of a sharp crack tip:
    - The stress field is singular not only at the crack tip, but also along the shock front.
    - The singularity exponents differ from one half. →
    - the energy release rate is either zero or infinite.

Crack propagation in homogeneous medium

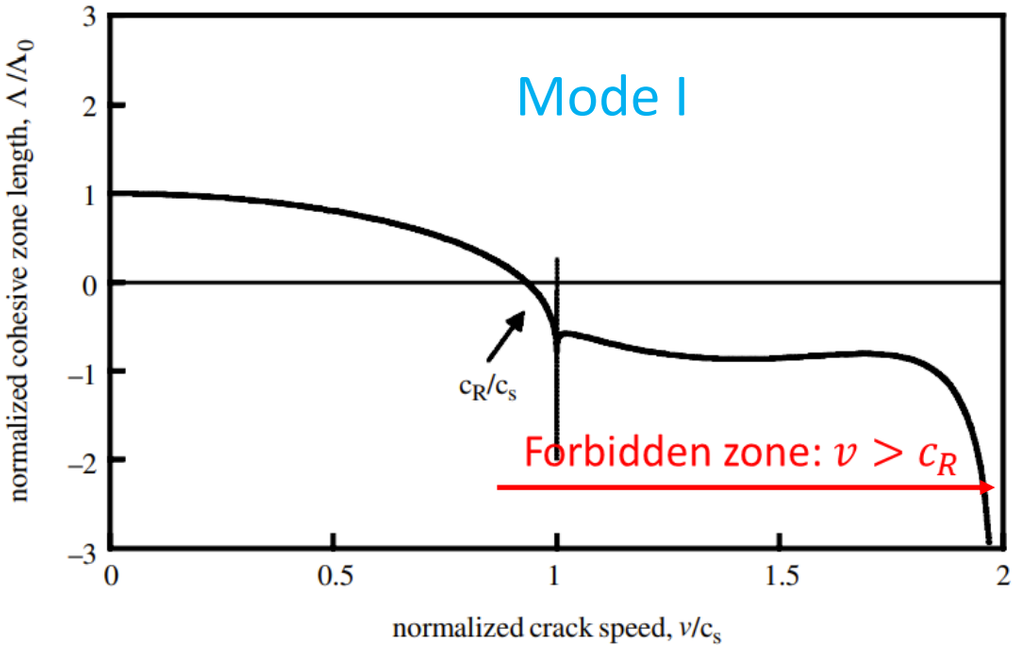

Figure 5. Cohesive zone length as a function of the crack speed for weakly joined identical solids (opening mode).

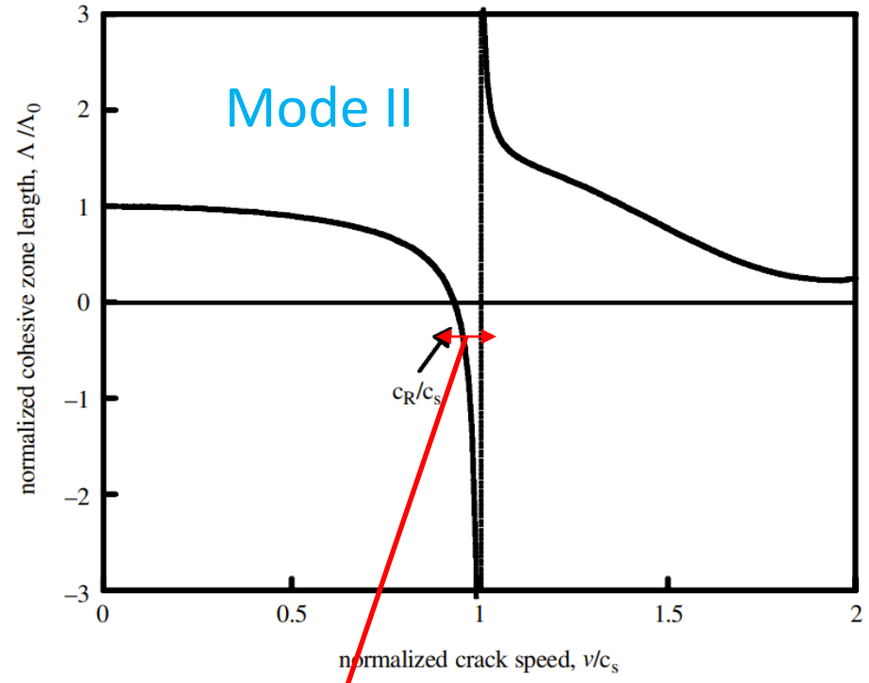

Figure 6. Cohesive zone length as a function of the crack speed for weakly joined identical solids (shear mode).

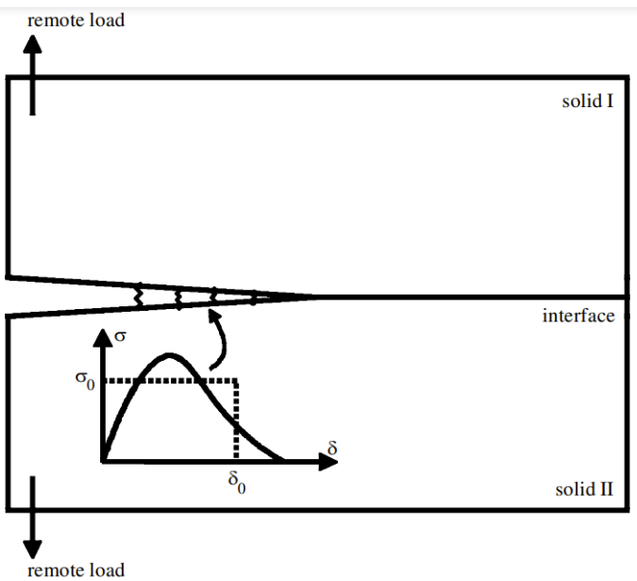

Yu, H.H., Suo, Z., 2000b. Intersonic crack growth on an interface. Proceedings of the Royal Society of London, Series A (Mathematical, Physical and Engineering Sciences) 456, 223–46.

Possibilities of supershear crack propagation

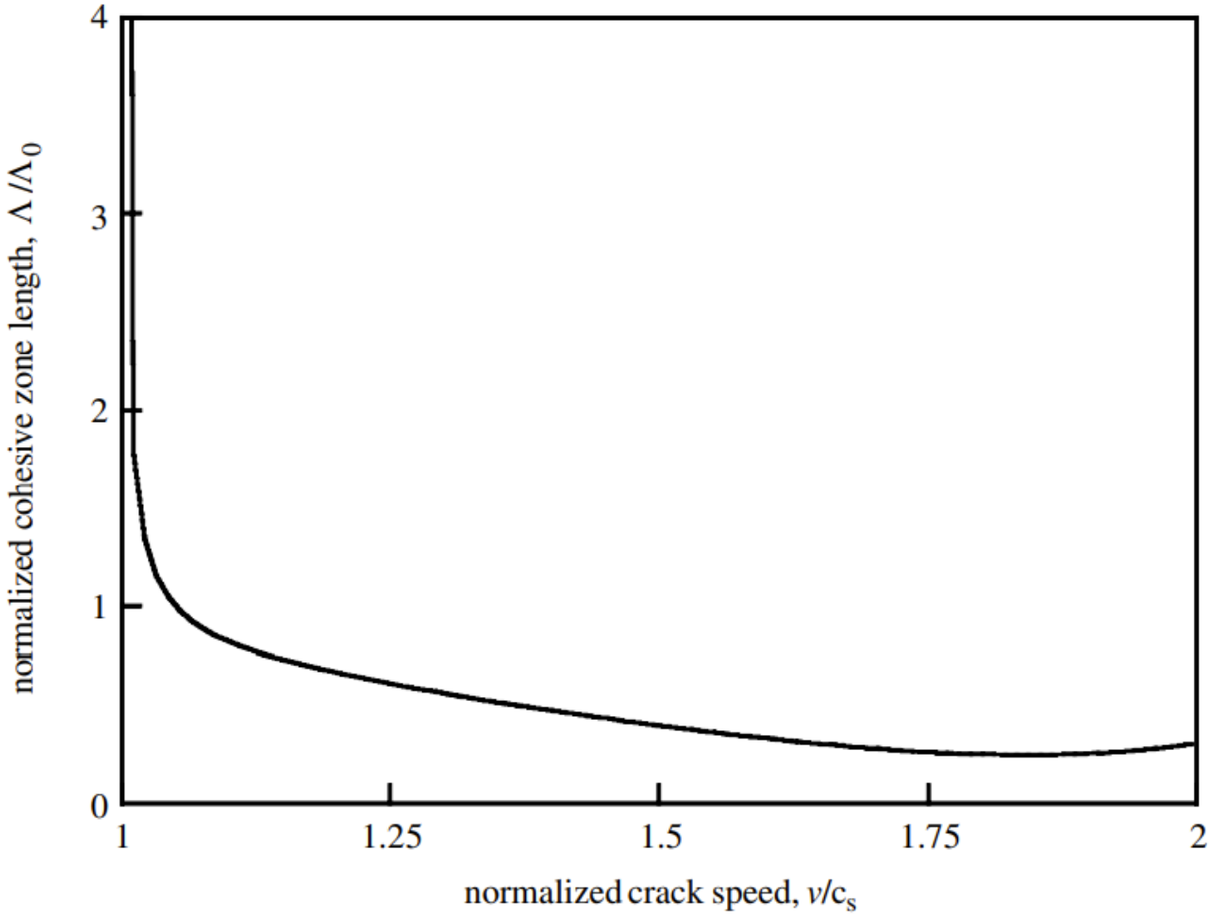

Figure 7. Cohesive zone length as a function of the crack speed for an intersonic crack on the interface between an elastic and a rigid solid.

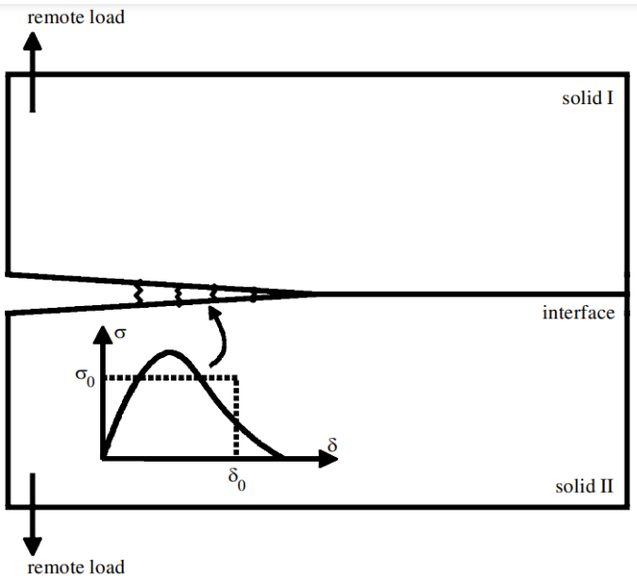

Yu, H.H., Suo, Z., 2000b. Intersonic crack growth on an interface. Proceedings of the Royal Society of London, Series A (Mathematical, Physical and Engineering Sciences) 456, 223–46.

Possibilities of supershear crack propagation

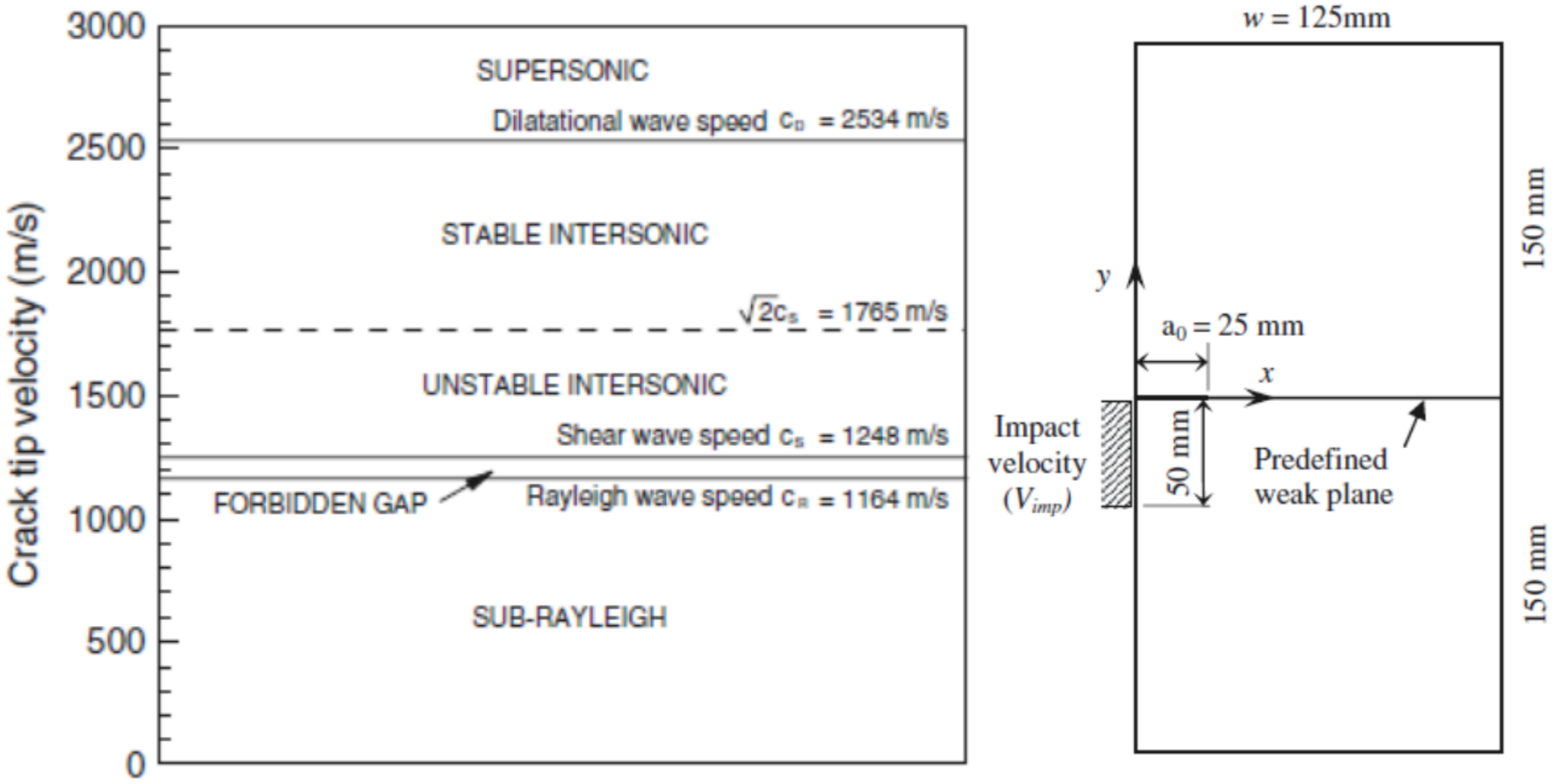

Fig. 5 Representative plot showing wave speeds for Homalite-100 and nomenclature of various regions

Int J Fract (2007) 143:79–102
DOI 10.1007/s10704-007-9051-z

ORIGINAL PAPER

Simulation of dynamic crack growth using the generalized interpolation material point (GIMP) method

Nitin P. Daphalapurkar · Hongbing Lu · Demir Coker · Ranga Komanduri

Possibilities of supershear crack propagation: Burridge–Andrews mechanism

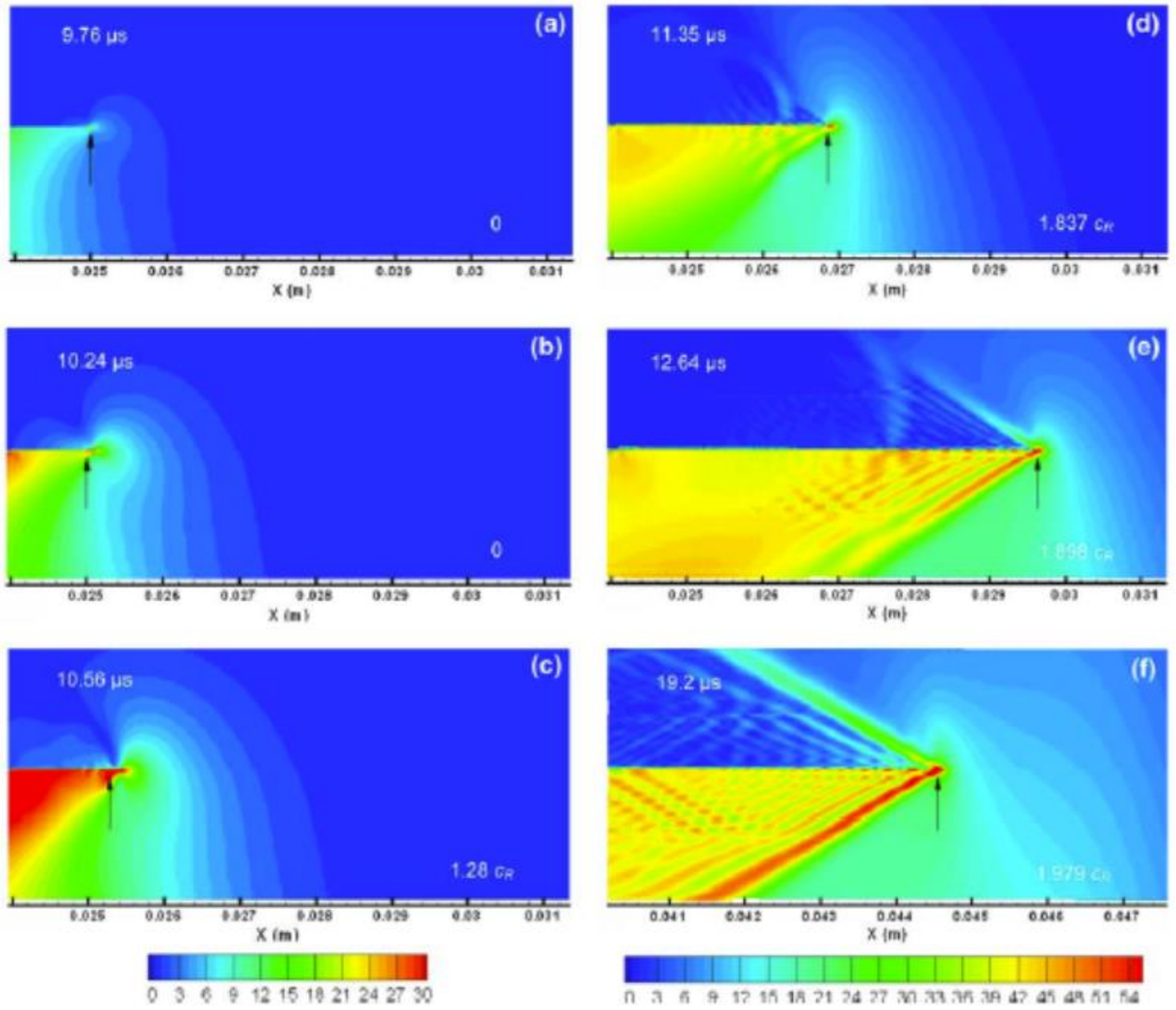

Fig. 7 (Online color) Snapshots of τ_{max} (MPa) for V_{imp} = 30 m/s at various durations (a) Stress wavefront arriving at the initial crack-tip (b) Stress wavefront loading the initial crack in predominantly shear mode (c) Crack has propagated along the interface after initiation at 10.4 μs (d) Maximum shear stress pattern immediately after the transition mechanism (e) Formation of shear shock waves (f) Crack propagation at a sustained crack-tip velocity in intersonic regime (c_R = 1164 m/s)

Int J Fract (2007) 143:79–102
DOI 10.1007/s10704-007-9051-z

ORIGINAL PAPER

Simulation of dynamic crack growth using the generalized interpolation material point (GIMP) method

Nitin P. Daphalapurkar · Hongbing Lu · Demir Coker · Ranga Komanduri

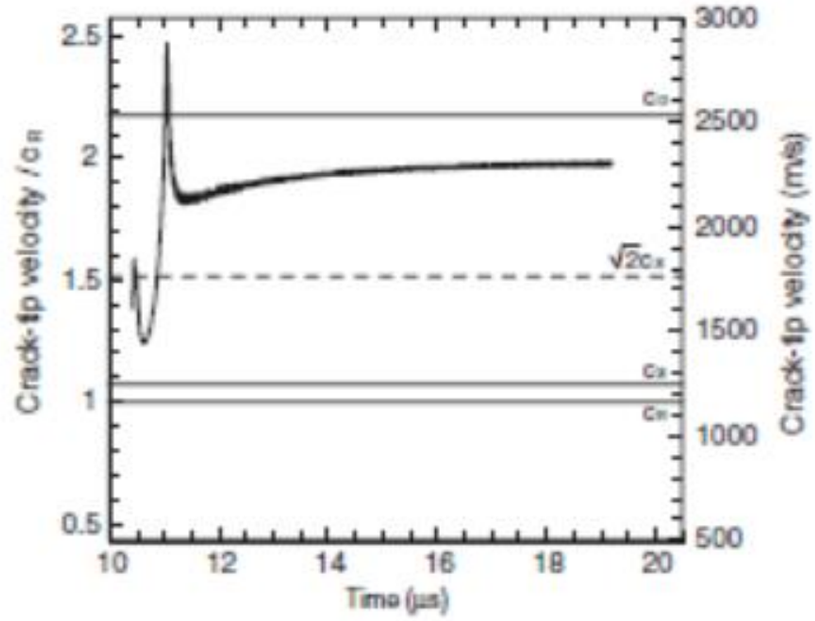

Fig. 9 Plot of normalized (with c_R) crack-tip velocity with time for V_{imp} = 30 m/s

- The sustained crack-tip velocity falls either in the sub-Rayleigh regime or in the region between $\sqrt{2}c_s$ and c_d
- MD simulation: Abraham FF, GaoH(2000) How fast can cracks propagate? Phys Rev Lett 84(40):3113–3116
- Shear dominated crack initially accelerates to c_R
- Followed by the nucleation of a **daughter microcrack ahead of the main crack**
- **Finally coalescence of the mother and daughter-**
- **cracks** with the **crack-tip velocity reaching a**
- **value as high as the longitudinal wave speed**.
- After coalescence, when the far-field loading is relaxed,
- the crack decelerates and propagates at a steady
- rate close to a speed of $\sqrt{2}c_s$.

Possibilities of supershear crack propagation: MACH cones

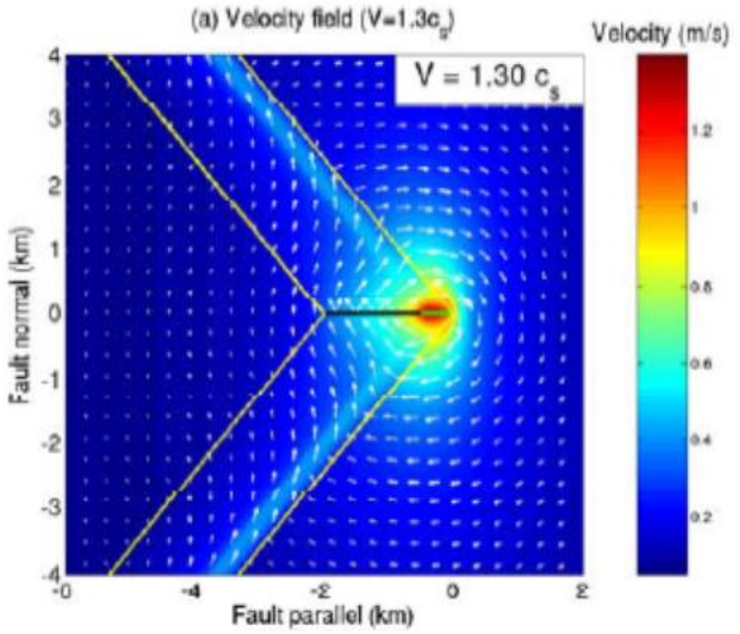

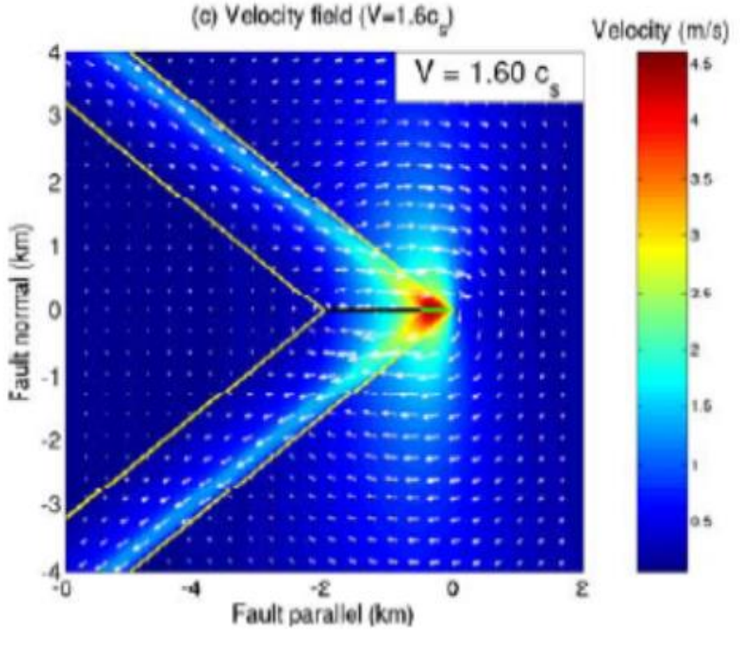

Near-source ground motion from steady state dynamic rupture pulses

Eric M. Dunham
Department of Physics, University of California, Santa Barbara, California, USA

Ralph J. Archuleta
Institute for Crustal Studies and Department of Geological Sciences, University of California, Santa Barbara, California, USA

GEOPHYSICAL RESEARCH LETTERS, VOL. 32, L03302, doi:10.1029/2004GL021793, 2005

Possibilities of supershear crack propagation

Earthquake and wave propagation

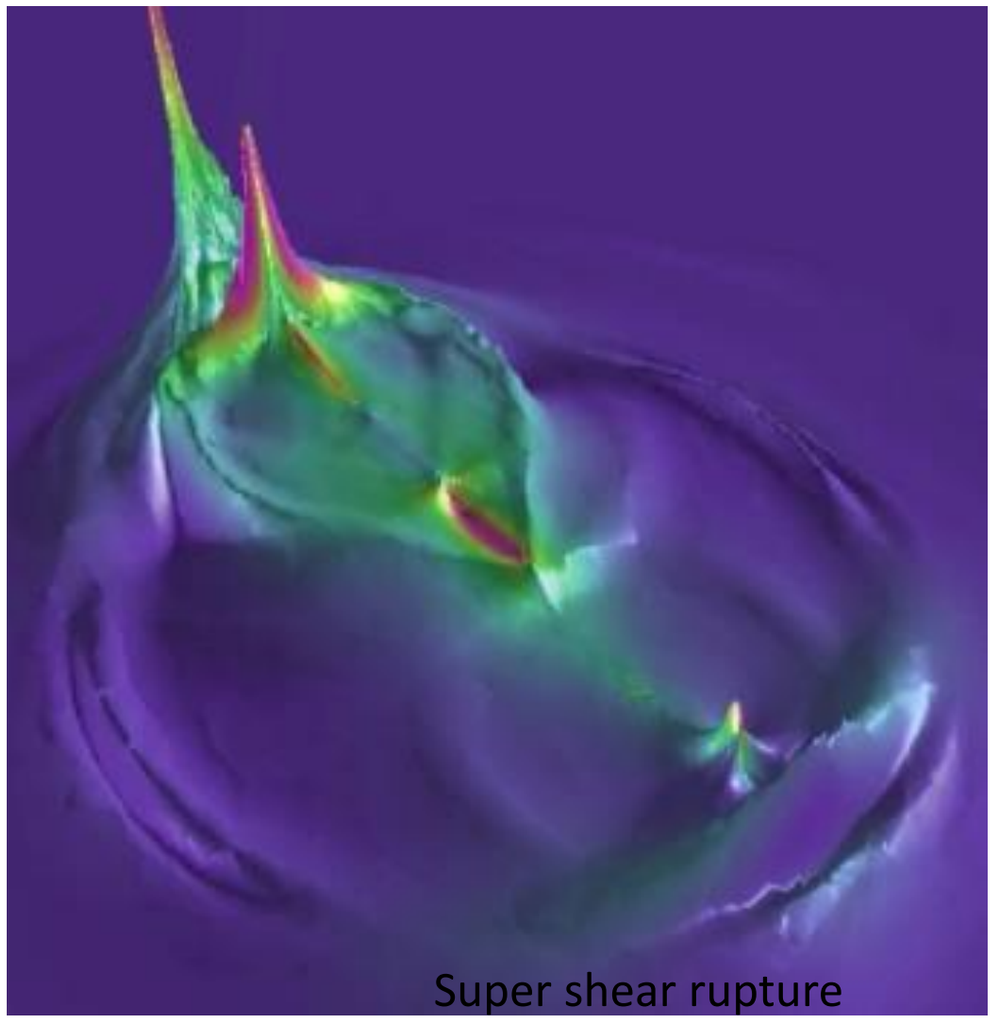

TPV205-2D with Reduced d_c

Supershear Rupture: Mach Cones

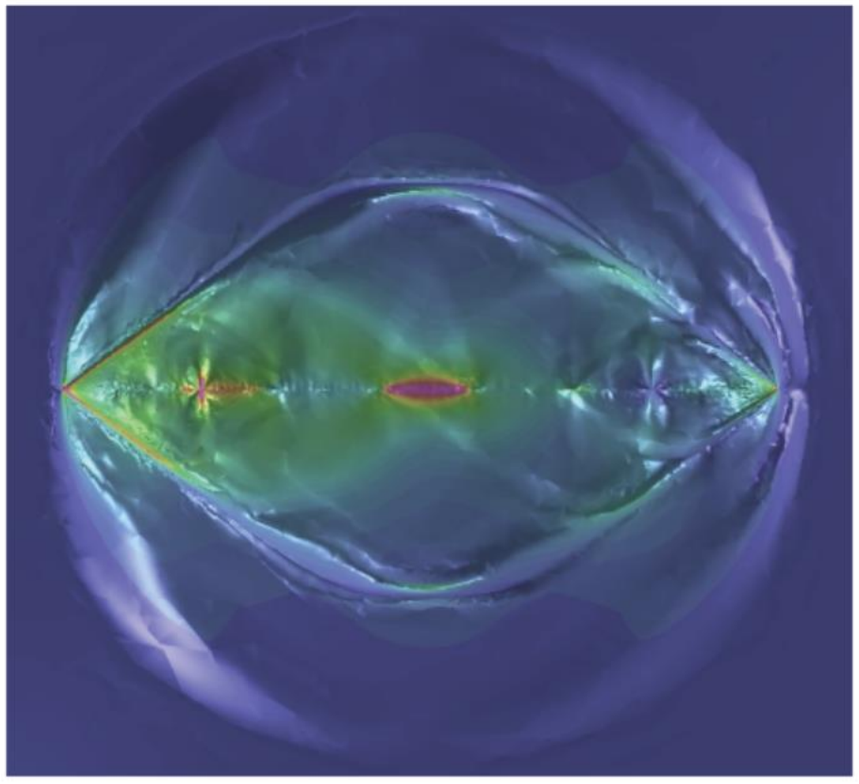

Collaborators: R. Haber, J. Erickson, A. Elbanna (UIUC)

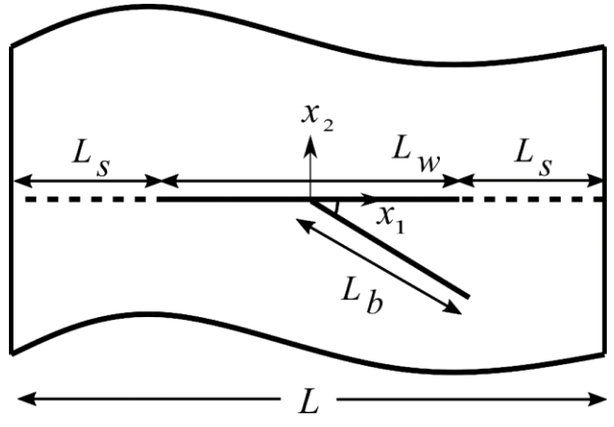

9. Dynamic fracture mechanics and rate effects

9.1. LEFM solution fields

9.2. Dynamics of moving crack tip, process zone size, crack speed

9.3. Crack path instabilities

Do cracks accelerate to Rayleigh speed?

Sharon Fineberg:
mirror, mist, hackle patterns as the crack accelerates

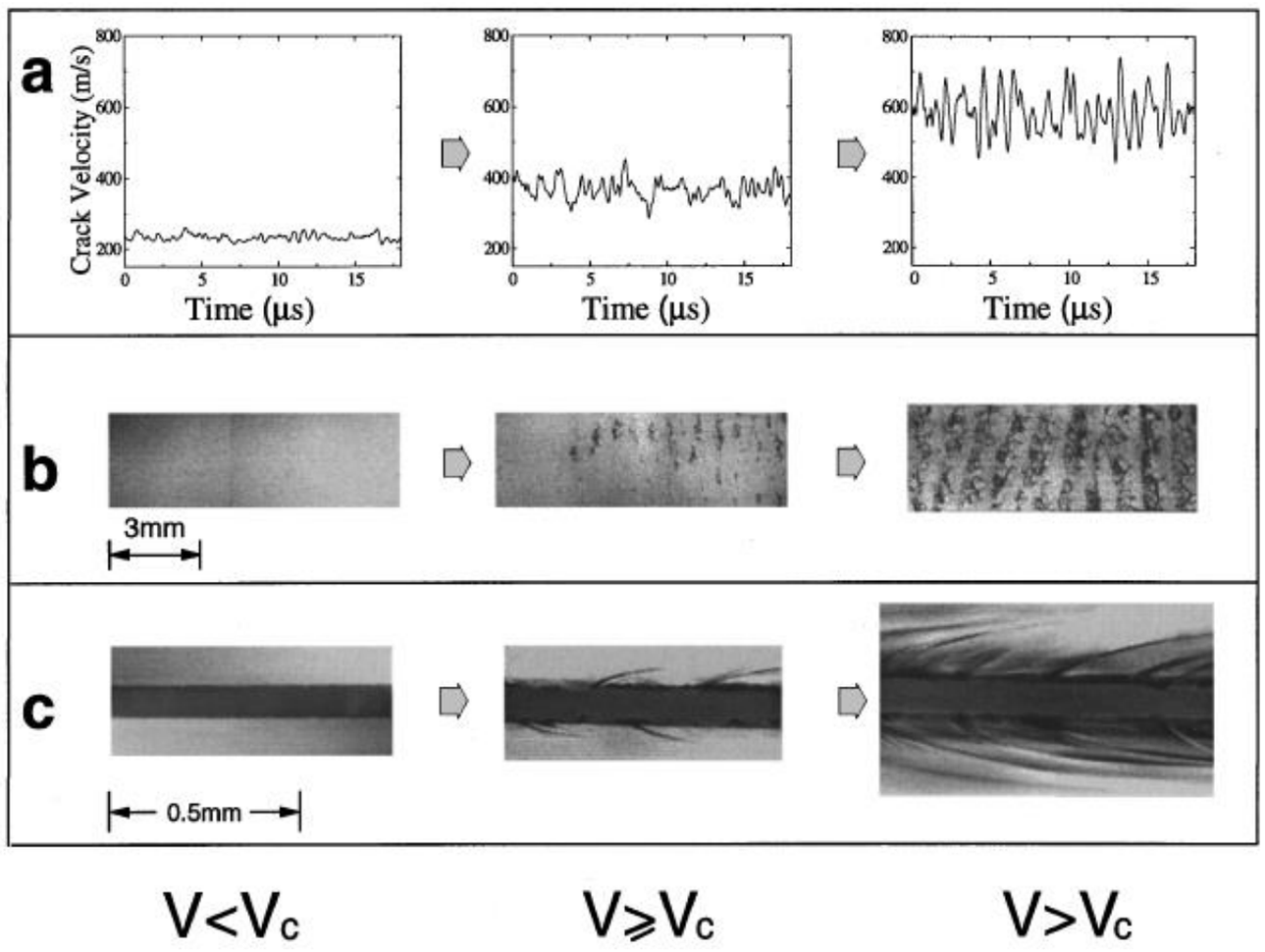

$v_c = 340\text{m/s}$

$(\text{or } 0.36V_R)$

- Crack starts oscillating well before reaching Rayleigh wave speed V_R (c_R)
- Crack speed does not reach V_R (c_R)!
- For this material critical speed $v_c = 0.36\ V_R$

Sample fracture patterns for brittle materials?

Branching only occurred for thicker specimens and very short notch depths

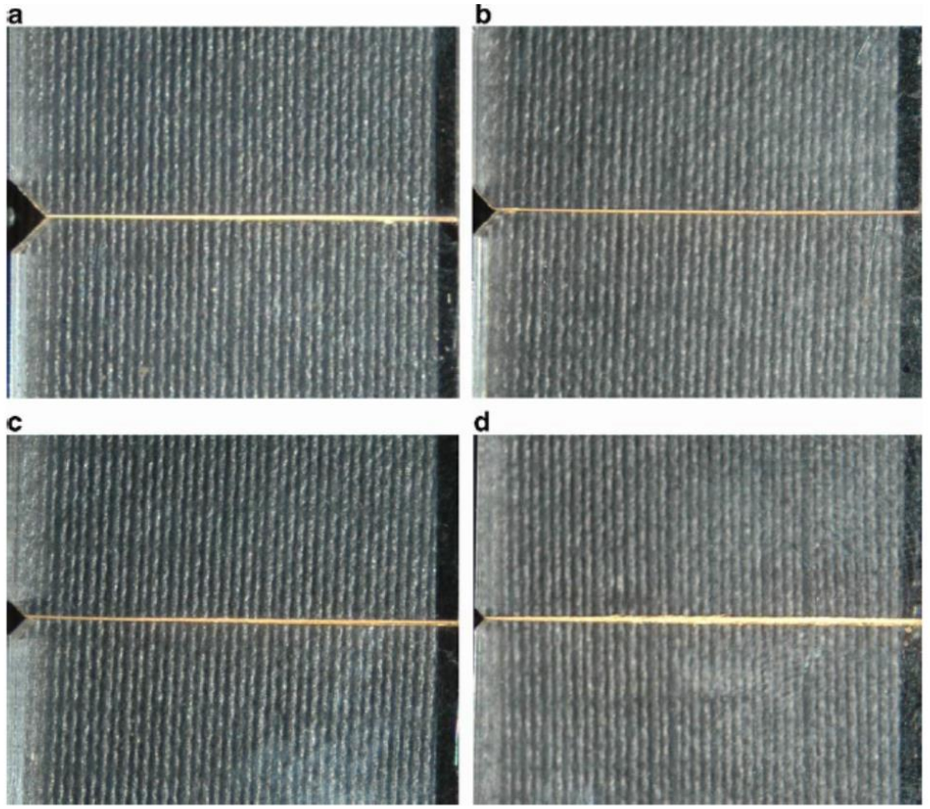

Fig. 5. Macroscopically planar fracture surfaces for the specimens containing the (a) 2.0 mm, (b) 1.4 mm, (c) 1.0 mm and (d) 0.5 mm notches.

Successful branching appears to take place when micro-cracks form a sufficient distance from the main crack tip to allow their subsequent propagation to take place as opposed to being arrested by the arrival of an unloading wave from the main crack.

Murphy 2006, Dynamic crack bifurcation in PMMA

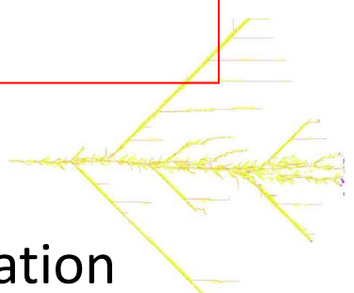

Sample simulation

Sample fracture patterns for brittle materials

1. Too much energy: a single crack cannot dissipate that much energy particularly in brittle materials

- Gao: 1993: Wavy crack path to have a higher energy release rate

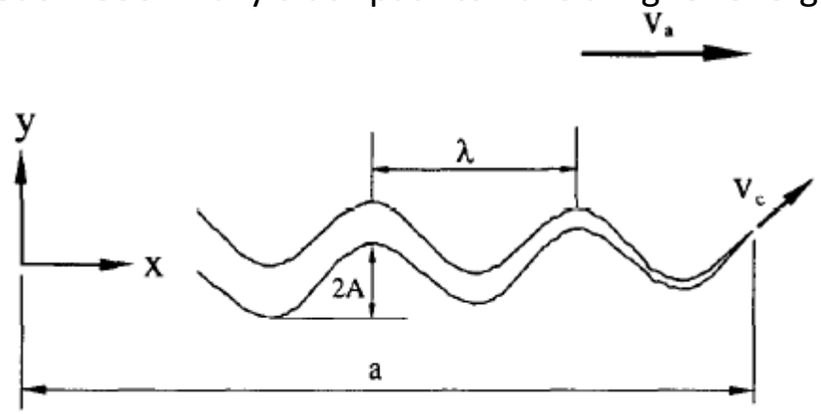

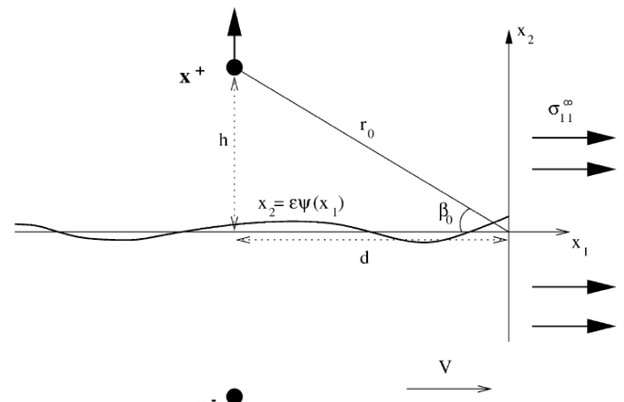

Dynamic stability of a propagating crack

O. Obrezanova[a,*], A.B. Movchan[b], J.R. Willis[c]

2. Yoffe's instability: Angles c ier than 0 degree will have maximum circumferential stress!

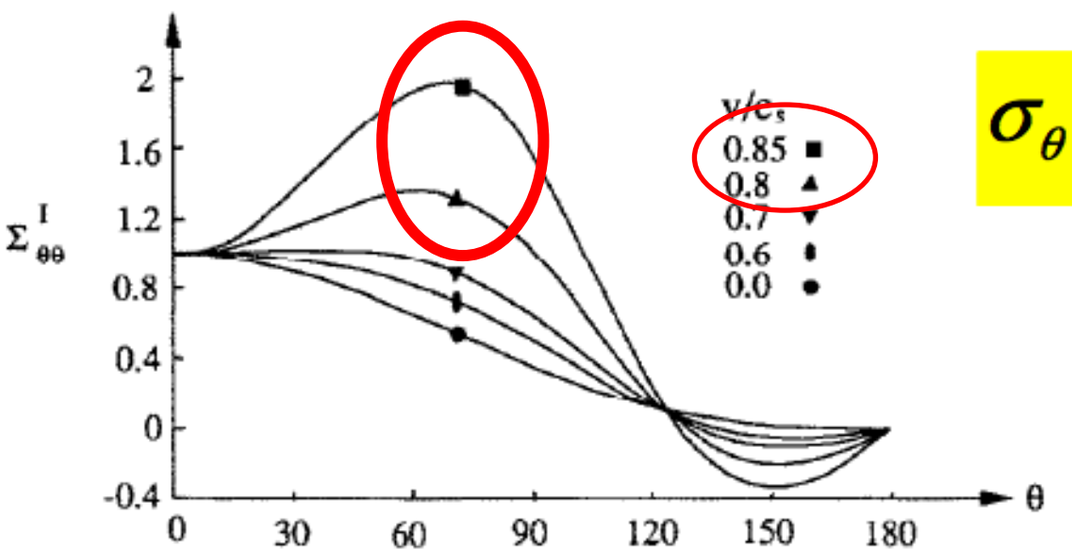

$$\sigma_\theta(r,\theta_c) = \max_{-\pi<\theta<\pi} \sigma_\theta(r,\theta)$$

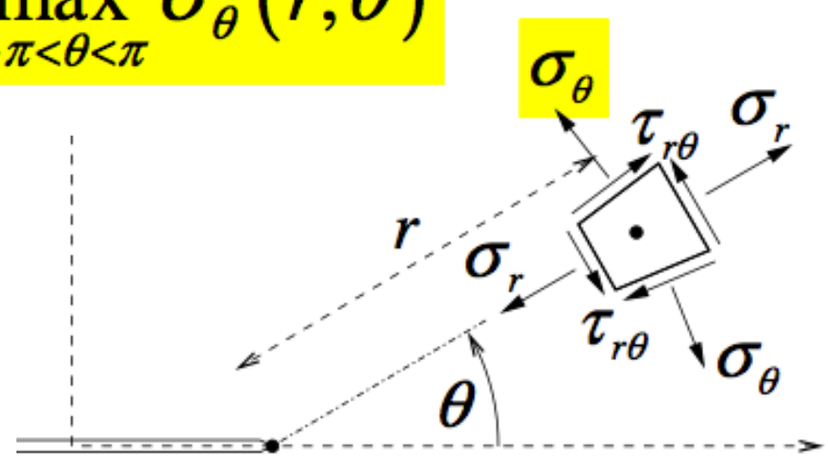

Effect of T-Stress

Murphy 2006, Dynamic crack bifurcation in PMMA

Further developing this theme, Streit and Finnie [6] suggested that the directional stability of a quasi-static crack should be influenced by the state of stress at a finite distance ahead of the crack tip in the location where the micro-cracks or voids are formed. In this case, not only the singular terms in the stress expansions, but also the remote normal stress in the crack propagation direction should be considered. The latter is known as the T-stress, and its influence on crack stability is well known [7]. This concept was applied to dynamic crack curving by Ramulu and Kobayashi [8]. In accordance with previous findings, Ramulu et al. [9] observed that successful branching always took place at a constant value of K_I, which was therefore cited as a necessary

[6] Streit R, Finnie I. An experimental investigation of crack-path directional stability. Exp Mech 1980;20:17–23.

[7] Cotterell B, Rice JR. Slightly curved or kinked cracks. Int J Fracture 1980;16:155–69.

[8] Ramulu M, Kobayashi AS. Dynamic crack curving—a photoelastic evaluation. Exp Mech 1983;23:1–9.

[9] Ramulu M, Kobayashi AS, Kang BSJ, Barker DB. Further studies on dynamic crack branching. Exp Mech 1983;23:431–7.

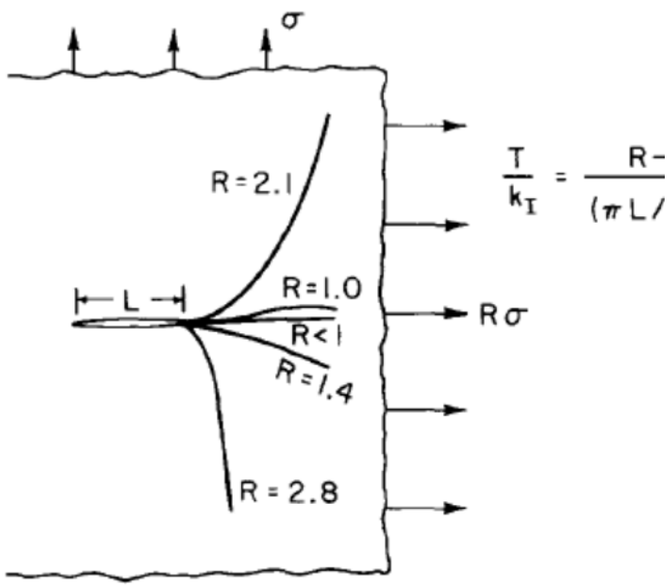

Figure 10. Path of crack growth and dependence on non-singular stress T acting parallel to the initial crack at its tip.

Figure 11. Crack paths observed by Radon *et al.* [29] in experiments on biaxially stressed PMMA sheets.

For small crack growth under nominally Mode I loading, the straight crack path has been shown to be [Cotterell, Rice: 1980]:

- **Stable when T < 0**
- **Unstable when T > 0**

- A critical role of the sign of the T -stress applies only to the situation of single crack growing in a large plate
- Counter examples: Array of collinear cracks, wedge cracks, etc.

Melin, Solveig. "The influence of the T-stress on the directional stability of cracks." International Journal of Fracture 114.3 (2002): 259-265.

Crack branching K-critical value
Relation to T-stress

Ramulu M, Kobayashi AS, Kang BSJ, Barker DB. Further studies on dynamic crack branching. Exp Mech 1983;23:431–7

Branching takes place at a constant value of KI

) A crack-branching stress-intensity factor of K_{Ib} = 3.3 MPa$\sqrt{m}$ and a characteristic radius of r_c = 0.75 mm were determined for this polycarbonate sheet.

T < 0 has suppressing effect

Crack curving of post-branched cracks, attraction and repulsion, depend not only on K_{II}/K_I but more importantly on σ_{ox}. Negative σ_{ox} suppresses crack curving irrespective of the sign of K_{II}/K_I.

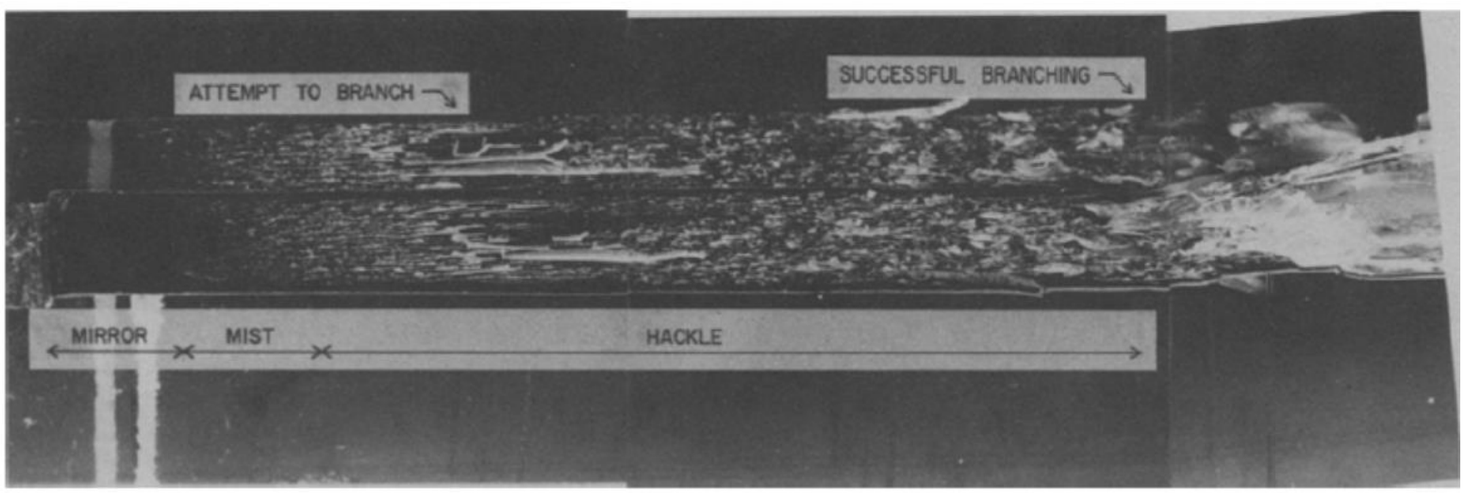

Energetic argument for crack branching

Eshelby JD (1970) Energy relations and the energy–momentum tensor in continuum mechanics. In: Kanninen MF, Adler WF, Rosenfield AR, Jaffee RI (eds) Inelastic behaviour of solids. McGraw-Hill, New York, pp 77–115

Branching takes place when the energy for 1 crack is equal to the energy of 2 bifurcated cracks

In the single crack case, a growth criterion for a branched crack must be based on the equality between the energy flux into the two propagating tips and the energy required to open the material and create new surfaces as a result of this propagation (Eshelby 1970).

Adda-Bedia M (2005) Brittle fracture dynamics with arbitrary paths- III.The branching instability under general loading. J Mech Phys Solids 53:227–248

- The jump in the energy release rate due to branching is maximized when the **branches start to propagate very slowly**.
- The branching of a single propagating crack under tensile loading was found to be energetically possible **when its speed exceeds a certain critical value** (Adda-Bedia 2005).

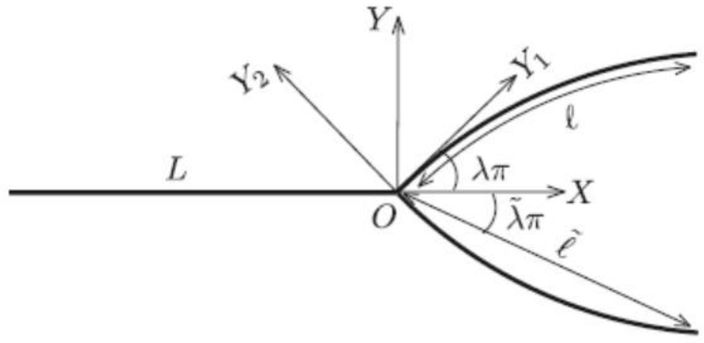

Fig. 12 Schematic representation of a straight crack with symmetrically branched curved extensions. The fictitious straight crack around which the perturbation expansion is performed is drawn on the lower branch

Katzav, E., M. Adda-Bedia, and Rodrigo Arias. "Theory of dynamic crack branching in brittle materials." International Journal of Fracture 143.3 (2007): 245-271.